Using Computer Vision to Identify Objects in an Operating Theatre to Support Safer Working

Okeke Stephen

2023

School of Engineering, Computer and Mathematical Sciences

A thesis submitted to

Auckland University of Technology

in fulfilment of the requirements for the degree of Doctor of Philosophy

Abstract

The accurate selection and identification of drugs in the operating rooms (OR) is a priority for every healthcare institution. During drug preparation and administration in the operating theatre, the anesthetists need to correctly select medications to administer them. Giving the wrong medication can lead to very serious consequences. However, anesthetists can make error cases, especially when they are tired or distracted. This project aims to use computer vision to reduce the likelihood of error and increase patient safety during medication administration in operating theatres. Computer vision methods driven by artificial intelligence have outperformed humans in many tedious tasks involving object identification and recognition. Therefore, in this work, a computer vision-based framework is proposed to identify and extract critical information from medication container labels used during anesthesia in the operating theatres, which can be processed to confirm that the correct medication has been selected. The framework is built to automatically generate voice feedback or raise concerns in the event of a potential drug error. The proposed framework will form part of a front-end to the existing anesthetics medication preparation systems and increase the safety of the whole anesthetic workflow. A number of different approaches have been proposed; currently, the project focuses on automatically recognizing the labels on drug ampules and vials using artificial intelligence-powered computer vision methodologies without the need for QR codes or barcodes on the medication ampoules or vials. The framework is tested for accuracy and compatibility with the anesthetic drug preparation, administration workflow, and efficiency. Also, the research investigated ways to ensure the ampule-to-patient flow is safe – for example, by producing compatible syringe embeddable labels and examining other technologies for recording data around the site of injection for the anesthetic record. After the proof-of-concept development, the framework was rigorously tested and validated for usability using real-time procedures. The reliability, accuracy, and processing speed of critical healthcare products, especially those used in a setting such as the operating theatres, are of utmost importance. The proposed framework achieved remarkable accuracy in identifying the anesthetic drug samples with a rapid processing speed below the maximum threshold (1 second) set for the project while exceeding the originally estimated accuracy threshold.

Contents

List of Figures

List of Tables

List of Appendices

List of Abbreviations

AI - Artificial Intelligence

CV - Computer Vision

SLS - Safe Label System

OCR - Optical Character Recognition

DNN - Deep Neural Network

CNN - Convolutional Neural Network

GPU - Graphics Processing Unit

FCN - Fully connected network

CTC - connectionist temporal classification

TSM - Tree-structured model

ANN - Artificial neural network

VGG - Visual geometry group

ResNet - Residual network

RCNN - Recurrent convolutional neural network

GRCNN - Gated recurrent convolutional neural network

Graph Neural Network (GNN)

CRAFT - Character-Region Awareness for Text detection

CML - Collaborative mutual learning

U-DML - Unified-deep mutual learning

BiSTM - Bidirectional long short-term memory

SIFT - Scale-invariant feature transform

DOG - Difference of Gaussian

SURF - Speeded-up robust features

SSD - Sum of square differences

IFD - Image feature detection

SSD - Single-scale image feature detectors

CRF - Corner response function

FAST - Features from accelerated segment test

SUSAN - Smallest univalue segment assimilating nucleus

USAN - Univalue segment assimilating nucleus

LOG - Laplacian-of-Gaussian

PCA - Principal component analysis

BRISK - Binary robust invariant scalable key points

AGAST - Adaptive corner detection operator

BRIEF - Binary robust independent elementary features

LBP - Local binary pattern

DS - Design science

DSR - Design science research

TSR - Token set ratio

JD - Jaccard Distance

PSNR - Peak signal-to-noise ratio

SSI - Structural similarity index

FSI - Feature similarity index

UIQ - Universal image quality index

DSEDR - Discriminative spatiality embedded dictionary learning representation

DMSDR - Discriminative multi-scale stroke detector-based representation

Attestation of Authorship

I hereby declare that this submission is my own work and that, to the best of my knowledge and belief, it contains no material previously published or written by another person (except where explicitly defined in the acknowledgements), nor material which to a substantial extent has been submitted for the award of any other degree or diploma of a university or other institution of higher learning.

15/03/2023

Signature _____ Date

Co-Authored Works

Please also note in this thesis: it is partially supported by Callaghan Innovation Fund and certain aspects of the project will be subject to a three-year embargo. Consequently, there are limitations on the number of publications that can be produced. You may to note that the publications produced are not directly related to the content of this thesis, but the idea behind the algorithm is the same.

Okeke, Madanian, and Nguyen (2022)

Journal Paper Published in MDPI Sensors.

Title: A Robust Deep Learning Ensemble-Driven Model for Defect and Non-Defect Recognition and Classification Using a Weighted Averaging Sequence-Based Meta-Learning Ensembler.

Authors: Okeke Stephen, Samaneh Madanian, Minh Nguyen.

Year of publication: 2022.

Abstract: The need to overcome the challenges of visual inspections conducted by domain experts drives the recent surge in visual inspection research. Typical manual industrial data analysis and inspection for defects conducted by trained personnel are expensive, time-consuming, and characterized by mistakes. Thus, an efficient intelligent-driven model is needed to eliminate or minimize the challenges of defect identification and elimination in processes to the barest minimum. This paper presents a robust method for recognizing and classifying defects in industrial products using a deep-learning architectural ensemble approach integrated with a weighted sequence meta-learning unification framework. In the proposed method, a unique base model is constructed and fused together with other co-learning pretrained models using a sequence-driven meta-learning ensembler that aggregates the best features learned from the various contributing models for better and superior performance. During experimentation in the study, different publicly available industrial product datasets consisting of the defect and non-defect samples were used to train, validate, and test the introduced model, with remarkable results obtained that demonstrate the viability

of the proposed method in tackling the challenges of the manual visual inspection approach.

Okeke, Madanian, and Nguyen (2022)

Journal Paper Published in MDPI Sensors.

Title: A Hard Voting Policy-Driven Deep Learning Architectural Ensemble Strategy for Industrial Products Defect Recognition and Classification.

Authors: Okeke Stephen, Samaneh Madanian, Minh Nguyen.

Year of publication: 2022.

Abstract: Manual or traditional industrial product inspection and defect-recognition models have some limitations, including process complexity, time-consuming, error-prone, and expensiveness. These issues negatively impact the quality control processes. Therefore, an efficient, rapid, and intelligent model is required to improve industrial products' production fault recognition and classification for optimal visual inspections and quality control. However, intelligent models obtained with a tradeoff of high accuracy for high latency are tedious for real-time implementation and inferencing. This work proposes an ensemble deep-leaning architectural framework based on a deep learning model architectural voting policy to compute and learn the hierarchical and high-level features in industrial artefacts. The voting policy is formulated with respect to three crucial viable model characteristics: model optimality, efficiency, and performance accuracy. In the study, three publicly available industrial produce datasets were used for the proposed model's various experiments and validation process, with remarkable results recorded, demonstrating a significant increase in fault recognition and classification performance in industrial products. In the study, three publicly available industrial produce datasets were used for the proposed model's various experiments and validation process, with remarkable results recorded, demonstrating a significant increase in fault recognition and classification performance in industrial products.

Okeke, Madanian, and Nguyen (2022)

Conference Paper Published in the 19th International Conference on Smart Business Technologies.

Title: An Intrinsic Human Physical Activity Recognition from Fused Motion Sensor Data using Bidirectional Gated Recurrent Neural Network in Healthcare.

Authors: Okeke Stephen, Samaneh Madanian, Minh Nguyen.

Year of publication: 2022.

Abstract: An intrinsic bi-directional gated recurrent neural network for recognizing human physical activities from intelligent sensors is presented in this work. In-depth exploration of human activity data is significant for assisting different groups of people, including healthy, sick, and elderly populations in tracking and monitoring their level of healthcare status and general fitness. The major contributions of this work are the introduction of a bidirectional gated recurrent unit and a state-of-the-art nonlinearity function called rectified adaptive optimizer that boosts the performance accuracy of the proposed model for the classification of human activity signals. The bidirectional gated recurrent unit (Bi-GRU) eliminates the short-term memory problem when training the model with fewer tensor operations, and the nonlinear function, a variant of the classical Adam optimizer provides an instant dynamic adjustment to the adaptive models' learning rate based on the keen observation of the impact of variance and momentum during training. A detailed comparative analysis of the proposed model performance was conducted with long-short-term-memory (LSTM), gated recurrent unit (GRU), and bi-directional LSTM. The proposed method achieved a remarkable landmark result of 99% accuracy on the test samples, outperforming the earlier architectures.

Acknowledgements

First, I would like to express my sincerest gratitude to Dr Minh Nguyen and Dr Samaneh (Sam) Madanian, for their supervision and guidance throughout my PhD journey. Their invaluable insights and feedback have been instrumental in completing this research.

I also acknowledge the examiners and the convenor for their generous investment of time and expertise in examining my thesis. Their constructive feedback and valuable suggestions have greatly improved the quality of my work.

I would also like to thank the DCT community, the Graduate Research School, Department of Computer Science & Software Engineering, including the faculty, staff, and fellow graduate students, for creating a supportive and collaborative environment.

Special thanks go to Dr Rosser Johnson for intervening when it mattered most and resolving issues that arose during the PHD journey. I also acknowledge Dr Alan Merry for facilitating the data samples used in the study and for providing leadership during critical periods of the research. I am also grateful to Callahan Innovative program and SaferSleep for providing financial support during my graduate studies.

Finally, I want to express my deepest gratitude to my family and friends for their unwavering love and support. Their encouragement and belief in me have been a constant source of motivation and strength. I could not have done it without them.

Chapter 1 Introduction

1.1 Anaesthetic Drug Identification System

Anesthetics drug identification system deals with rapid, efficient, and accurate drug identification and recognition in the operating theatre. It provides an avenue for verifying and cross-checking the accuracy; of the drugs used in the operating rooms. Due to the recent advancements in artificial intelligence and computer vision research, the development of an intelligent anesthetics drug recognition system has tremendous potential in solving the anesthetics drug misidentification problems in the OR and thus ensuring patient safety. This thesis investigates the robustness of computer vision and artificial intelligence methodologies for anesthetics drug identification for patient safety. This chapter will present the synopsis of the PhD research activities.

1.2 Background of Anaesthetic Drugs (Agents)

In this section, the antiasthenic agents or medications that serve as the case study and will be identified with the proposed computer vision and artificial intelligence method are investigated in detail.

Anesthesia is a treatment involving the deployment of anesthetic drugs. It is the loss of feeling in the presence or absence of consciousness. The loss of sensation could be attained with various drugs with different chemical compositions housed in containers called ampules and vials (Agency, 2008). Making anesthesia available to patients is an integral part of healthcare services across the globe. It is considered a fundamental human right to grant access to safe anesthesia, and they are global standards that ensure safe anesthetic practices (Bösenberg, 2007). It is thus imperative for healthcare providers to administer effective and safe anesthesia for various surgical procedures when necessary or needed. This work examines ways emerging computer vision and artificial intelligence could contribute to ensuring the efficient and secure administration of anesthetic substances to patients in the operating rooms.

Local and general anesthetics constitute the classic anesthetic agents and other depressants for the central nervous system (CNS), skeletal muscle relaxants, and anticonvulsants (Maher, 2012). The anesthetic drugs are finely grouped into induction

agents such as Propofol and Thiopental; opioids like Fentanyl, Alfentanil, and Morphine; muscle relaxants such as Atracurium, Vecuronium, Rocuronium, Suxamethonium (Smith et al., 2018). They are also muscle relaxants reversal like Neostigmine and Glycopyrronium; local anesthetics such as Bupivacaine and Lidocaine; regularly used emergency drugs like Atropine, Ephedrine, Metaraminol, Adrenaline, Intralipid, and Dantrolene (Hunter, 2020). The containers (vials and ampules) housing these drugs are embedded with labels with rich, diverse semantic information that could be harvested, analyzed, and deployed to identify the drugs.

1.3 Anesthetic Medication Categories

This section presents a summary of the classes and types of drugs used in the operating theatres for anesthesia, whose identification is the study's core focus and are explored in detail in Appendix A. Table *1* shows the list of the commonly used anesthetic drug classes and their varieties of associated drugs.

Table 1: Anaesthetic Drug Categories

Anesthetic Drugs Classes	**Anaesthetic Drug Varieties**
Induction Agents (Tom Lupton, 2008)	Barbiturates, phenols, imidazole, phencyclidines, benzodiazepines
Benzodiazepines and Tranquilizers (Lester et al., 2012)	diazepam, chlordiazepoxide, lorazepam, clorazepate, clonazepam, clobazam, estazolam, temazepam, flurazepam, triazolam, quazepam, alprazolam, oxazepam
Benzodiazephine Antagonists (Penninga et al., 2016)	Flumazenil, fresenius kabi or anexate,
Muscle Relaxants (Vardanyan & Hruby, 2006)	Rocuronium, suxamethonium, atracurium, pancuronium, vecuronium, alcuronium, mivacurium
Relaxant Reversal Agents (Hunter, 2020)	Sugammadex, neostigmine, pyridostigmine, mestinon
Opioids (Ferry & Dhanjal, 2021)	Morphine, fentanyl, hydromorphone, remifentanil, sufentanil, alfentanil, meperidine
Opioid Antagonists (Theriot et al., 2019)	naloxone, methylnaltrexone, nalorphine, nalbuphine, naltrexone, nalmefene
Vasopressors (VanValkinburgh et al., 2018)	Dopamine, epinephrine, norepinephrine, vasopressin, dobutamine, phenylephrine
Hypotensive Agents (Degoute, 2007)	Sodium nitroprusside (SNP), calcium channel antagonists, angiotensin-converting enzyme (ace) inhibitors, nitroglycerin (NTG), *β*-adrenoceptor antagonists, trimethaphan, alprostadil, adenosine, fenoldopam
Local Anesthetics (Butterworth & Lahaye, 2019)	Lidocaine, bupivacaine, cocaine, benzocaine, mepivacaine, procaine, etidocaine, tetracaine, ropivacaine, tetracaine, etc.
Anticholinergic Agents (Lerche, 2015)	Atropine, methscopolamine, scopolamine, trospium, propantheline, tolterodine, orphenadrine, glycopyrrolate, hyoscyamine, homatropine, ipratropium, aclidinium, belladonna alkaloids
Anti-Emetics (Athavale et al., 2020)	Dexamethasone, ondansetron, droperidol, palonosetron, aprepitant, scopolamine, dimenhydrinate, metoclopramide

I. The Induction Anaesthetic Agents

The induction agents (see Figure 1) are anesthetic medications that cause a rapid loss of consciousness when the appropriate dose is administered intravenously to patients (Luciano & Fustinoni, 2014). Their usefulness includes anesthesia inducement before administering other drugs to retain anesthesia. Through intravenous infusion, induction agents keep anesthesia for procedures that take longer and provide sedation during operations in the operating theatres (Pratt, 2008). When administered, the time it takes the drug to move from the injection site to the brain is described as the one-

arm-brain circulation time. The prevalent drugs used as induction agents are categorized depending on the chemical structures that constitute the drugs, and they are Barbiturates, Phenols, Imidazole, Phencyclidines, and Benzodiazepines (Pratt, 2008).

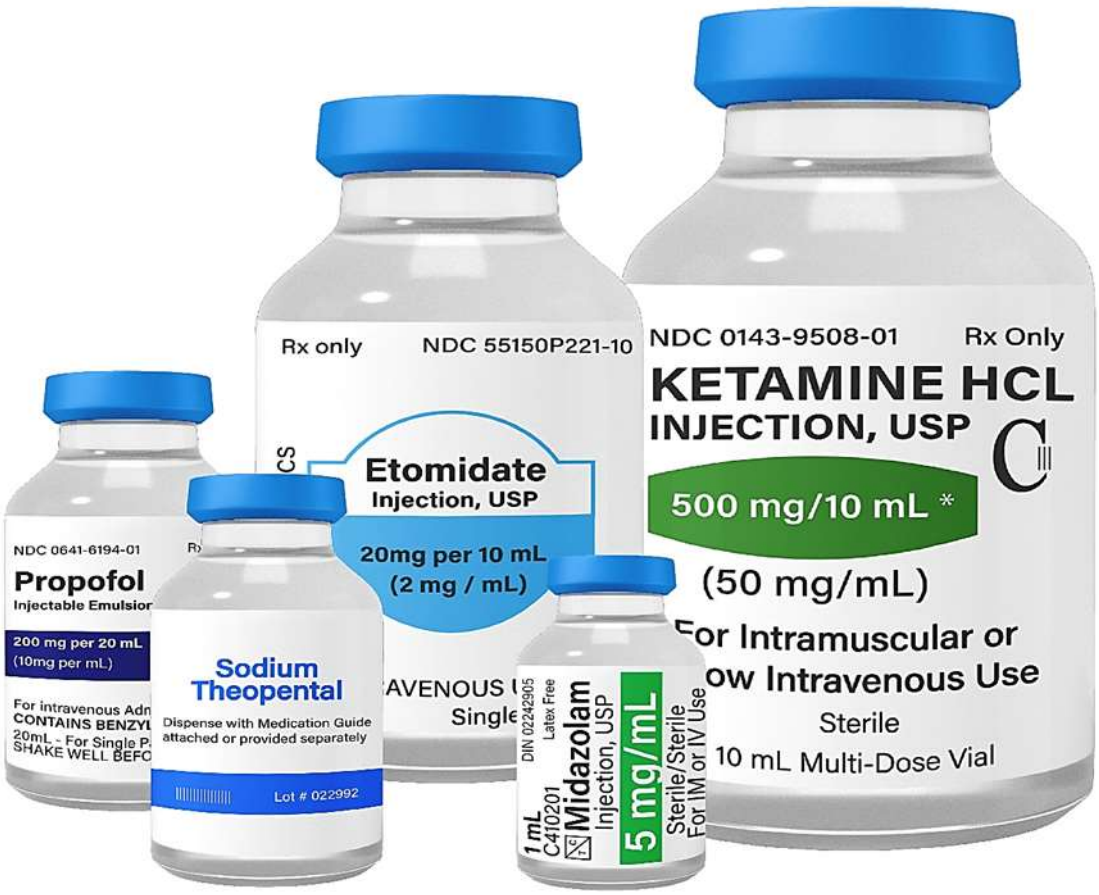

Figure 1: A Cross-section of the Anaesthetic Induction Agents.

They are specific induction agents such as Propofol, Sodium Thiopental, Etomidate, Ketamine, Midazolam, etc., which are commonly used in the operating theatres and whose container contents or inscriptions are among the ampoule containers that will be extracted, analyzed, and deployed to identify the specific drugs (see Appendix A(I)).

II. The Benzodiazepine Anaesthetic Agents

Benzodiazepine is a medication commonly used for anxiety, insomnia treatment (Cloos & Ferreira, 2009), sedation in anesthesia (Cornett et al., 2018), and is also effective in the treatment of other medical conditions. They are often used as a remediation for anxiety reduction pre-anesthesia. Benzodiazepines appear to affect the neurotransmitters found in the brain, although their precise mechanism of action is unknown. Many Benzodiazepines are extensively distributed, adequately absorbed,

and metabolized before their elimination from the body system. Several factors drive the use of the agent: reduced cost, availability, half-life, and route of administration. They are suitable for managing different symptoms that evolve during palliative care (Howard et al., 2014). Some of the commonly used Benzodiazepines are shown in Figure 2.

Figure 2: A Cross-section of the Benzodiazepine Anaesthetic Agents.

Benzodiazepines are split into several classes depending on their pharmacokinetics and chemical structure; however, they share a similar mechanism of action with closely related drugs with various clinical effects generated (see Appendix A(II))

III. The Benzodiazepines Antagonists

These are the class of drugs used for a fractional or total reversal of the sedative impacts produced by various benzodiazepine agents in different clinical settings, like in therapeutic procedures or administered in general anesthesia for diagnostic purposes (Braitberg, 2019). In other words, the antagonists are used to regenerate patients' sensitivity response and prevent the tolerance produced by the benzodiazepine agents (Albaugh et al., 2002). The prevalent and most commonly used benzodiazepine antagonist is flumazenil (Fassoulaki et al., 2010) (see Appendix A(III)).

IV. Anesthetic Muscle Relaxants or Neuromuscular Blocking Agents

These anesthetic agents work to relax or weaken many body muscles without affecting the intestines and heart muscles. This enables surgeons to perform surgeries around the abdomen or other delicate and sensitive body parts. With the administration of muscle relaxants (see Figure 3), patients do not need to be profoundly anesthetized or receive a large number of anesthetic medications, thus minimizing the anesthesia side effects (Flamer & Peng, 2011).

Figure 3: A Cross-section of the Anaesthetic Muscle Relaxing Agents.

The neuromuscular blocking agents greatly facilitate an improved operational process and the enablement of tracheal intubation while ensuring muscle relaxation amid surgery. The patient's recovery from the neuromuscular blocking medications varies among patients because of the pharmacokinetics of a specific patient, the administered adjuvant agents, differences in drug metabolism, and the duration of the medication dose. A standard muscle relaxant agent's duration of action must be controllable from a few minutes of action to hours of action which can be terminated quickly when necessary devoid of any side effects on the patient (Welch, 2017) (see Appendix A(IV)).

V. Opioids Anaesthetic Agents

Narcotic analgesics or opioids are medications generally used in anesthesia as a primary anesthetic agent or pre-anesthetic medication, general anesthetic agent's supplement, or systemic and spinal analgesia (Ferry & Dhanjal, 2018) (see Figure 4). They are mainly used during major surgical procedures, particularly surgical operations that deal with cardiovascular disease patients (Hug Jr, 1992). They are also commonly used in virtually every stage of surgical operations, including chronic pain control during the pre-induction process, anesthesia induction, and maintenance, immediate postoperative pain reduction, and agitation minimization.

Figure 4: A Cross-section of the Opioids Anaesthetic Agents.

Furthermore, opioids (see Figure 4) can be administered to patients intravenously, orally, intrathecal, enteral, subcutaneous, transdermal, aerosolized, and epidural. For the anesthetic use of opioids, the main route of administration is intravenous, which could be continuous infusion or repeat injections. The most commonly used opioids are morphine, fentanyl, hydromorphone, remifentanil, sufentanil, alfentanil, and meperidine (Ferry & Dhanjal, 2021) (see Appendix A(VI)).

1.4 The Structure of Anaesthetic Drug Ampules and Vials

The anesthetic drug ampule and vial containers vary in size, content color, label orientation, and content composition. They are mainly used to preserve and transport medications that are in a liquid state. Although they seem identical, the anesthetic drug ampules and vials are different and perform different functions in terms of drug storage. Ampoules are usually small in size and are used to store single-dose drugs; this implies that ampules are not reusable because they are often sealed in the neck, and once cracked open, they cannot be resealed. Commonly used anesthetic medication containers are made with glass, although some plastic ampoules have recently been available (see Figure 5). The space above the ampule contents may be covered with an inert gas after sealing, and ampule containers are clear or amber and often sufficiently solid for holding the drugs for mobility. The contents, concentration, and sizes of ampoules mirror the regularly available drugs within the region of use, and it is crucial to verify the drugs before use (Pratt, 2008).

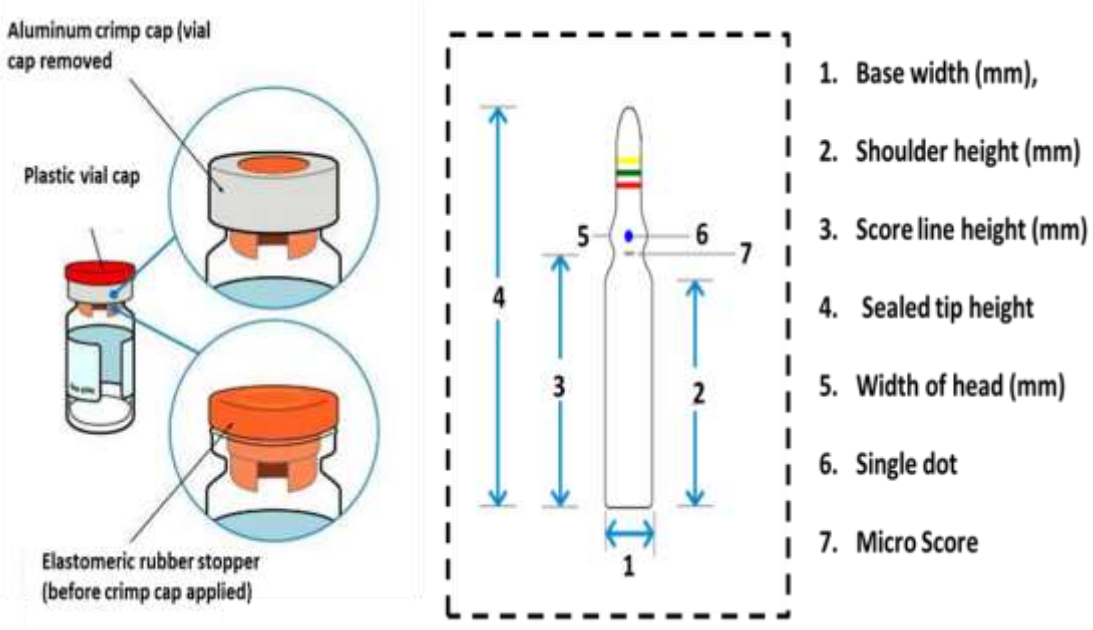

Figure 5: Structural Representation of Anaesthetic Drug Vial and Ampule (Kosmetik, 2017).

The labels on the anesthetic vials and ampules convey critical information about the drugs to the anesthesiologists. The main functions of the anesthetic medication labels are to ensure that drugs with labels used in the operating rooms are visibly and effortlessly identifiable (Lalor, 2011). The likelihood of medication errors increases if the anesthesiologists find reading and understanding the critical safety information on the medication container labels challenging (Wheeler & Wheeler, 2005). Easy

identification of the inscriptions on the anesthetic medication labels enables the anesthesiologists and other healthcare personnel to make rapid but careful, informed decisions during medication preparation and administration in the operating theatres. The anesthetic drug container labels contain diverse text imprints with different font colors, sizes, backgrounds, and orientations for the identification of the drugs. Regular anesthetic medication labels are often inscribed with the medication name, the medication active elements or ingredients, the active ingredients proportion or quantity, and dosage. These imprints on the medication containers can be extracted and transformed into computer-exploitable formats.

These potent anesthetic intravenous drugs housed by the ampules are currently identified and prepared manually by the anesthesiologists for administration to patients during anesthesia. To prepare these drugs, the anesthetics must correctly select the right drug, identify it, and verify it before drawing it into the syringes. In this process, the anesthesiologists often prioritize the patient's safety. Rapid and prompt drug delivery to patients, avoidance and stoppage of medication administration errors, and minimization of the likelihood of drug misidentification and swapping are vital steps to ensure innocuous drug administration in operating theatres. Mistakes from drug delivery in operating theatres are prevalent, and most of them are preventable. Also, according to investigations during onsite visits of operating rooms for this study, the significant causes of medication preparation errors are drug features similarly, tiny textual imprints on the drug labels, and drug swapping. These mistakes concern the anesthesiologists, operating theatre personnel, and healthcare institutions. The provision and adoption of an intelligent computer vision framework will assist the anesthesiologists in promptly identifying and rapidly verifying anesthetic drugs before preparation and administration in the operating theatre and helping to eliminate errors, minimize casualties, and ensure patients' safety.

1.5 Computer and Machine Vision

Computer vision (CV) is a complex and active scientific area. It can be described as a scientific and technical means to allow a machine to acquire and analyze videos and digital images for useful information extraction and utilization (Mulfari et al., 2016). CV deploys several scientific methods that cut across signal processing (Steiglitz, 2020),

digital image processing (Pratt, 2013), pattern recognition (Schalkoff, 2007), statistical optimizations, machine learning (Williams & Hill, 2005), optical character recognition (OCR) (Chaudhuri et al., 2017).

Krishna (2017) said that CV is a field of science that extracts information from digital images and that information obtained from the images can differ in terms of their usage in object identification or other purposes. They further stated that a CV is a collection of algorithms that are capable of understanding image contents and using them for other purposes. According to the study, visions involving humans or machines are categorized into the sensing device and the interpreting mechanism. The sensing device captures as much information as possible from an object or image, and the interpreting system process the information to extract meaning from it (Krishna, 2017).

On the other hand, machine vision is a subset of computer vision, mainly dealing with computer vision use in the industrial domains (Davies, 2012). It enables the conversion of analogue industrial processes into smart processes and the simplification of complex industrial tasks. The visual identification of product defects and the discovery of ineffective processes are the major areas in machine vision that have yielded tremendous achievements. In terms of processing needs and components, machine vision and computer vision systems have a lot in common. For instance, an image acquisition tool consists of a lens and sensors required to feed real-time images into the systems. Also, programs that internally process the acquired images are highly essential in both systems.

1.6 Object Identification and the Anaesthetic Drugs Identification Process Need

Object identification is the process of identifying a particular object from a set of objects that denotes the same object in the real world (Champod, 2015). Object identification becomes necessary when a particular real-world object has little or near attribute distribution over other objects in a set. Despite how high or low objects' similarities could be, each object possesses a special distinguishing property that can be exploited to identify it. Numerous object identification methods have evolved in recent times, but each approach is tailored to the nature and complexity of the objects

to be identified. In object identification tasks, the use of object instances, semantic information, textual information, or other properties plays a vital role in the precise identification of the object. Also, in object identification, there are two major ways of measuring the performance of the object identification process (Karayev et al., 2012). A one-stage process focuses on the identification algorithm's deployment or inference speed, and a two-way process prioritizes the object identification speed and accuracy, respectively. Due to the importance of time and accuracy in the anesthetic drug identification process, this study prioritizes both the processing speed and the accuracy of the working algorithms and the entire proposed anesthetics drug identification framework.

1.7 Real-time Anesthetics Drug Image Processing Requirements

The exploration of physical image features has significantly impacted scientific research and aided innovations in recent times. Numerous innovative and precisive imaging tools have evolved for the acquisition of object structures and other vital information needed for knowledge discovery and fast decision-making from images (L. Wang et al., 2020). In practice, the real-time acquisition of these images is crucial for the algorithmic extraction and processing of the image features. The meaning of real-time in conventional computer vision algorithms is the capacity of an algorithm to process without buffering a certain amount of frames per second. Frame rate is the frequency with which image or video frames are consecutively captured with cameras to meet the needs of visual systems or shown on the screen. It can also be stated as the utmost achievable rate where factors such as the camera exposure time will minimize the capturing frequency to a lower value, and it is expressed in frames per second (FPS).

In anesthesia, the real-time drug label processing time is defined as the time spent capturing a drug container image, detecting and extracting the label content, and matching the extracted features to identify that particular drug. In this project, the maximum set time for the real-time requirement for anesthetic drug label processing is 0.1 seconds. Therefore, certain factors must be considered in the real-time processing of the anesthetic drug labels. These factors include the image scanning time, the lighting condition of the image acquisition environment, the efficiency of the

feature detection and extraction algorithm, and the matching speed of the matching algorithms. Overall, the real-time needs for the anesthetics drug label processing rely on device and algorithmic factors for recognizing and identifying a particular drug. Consequently, the devices and algorithms needed for this study will be explored in detail in the corresponding sections, and their processing methods and impacts will be intuitively described.

1.8 Rationale and Significance of the Study

This section will discuss the rationale and significance of developing this study and why an intelligent computer vision system is desirable for the efficient and accurate identification of anesthetics drugs in operating theatres.

According to a World Health Organization (WHO) report, every year, millions of patients are harmed as a result of medical errors associated with healthcare systems (Reddy, 2015), and these errors cost billions of US dollars. The study further stated that about 500,000 deaths could be prevented globally if the right checks and verifications were put in place. Kohn et al. (2000) stated that errors that lead to harm are known as preventable adverse events. Adverse events are outcomes caused by medical interventions, and not all can be prevented but can be reduced to the barest minimum. For instance, if an operated patient dies from a wrong drug prescription, pneumonia due to the poor instrument cleaning procedure, poor handwashing by theatre personnel, or other avoidable mistakes, these are adverse events that are preventable.

According to Nanji et al. (2016), there are six stages in medication administration: request, dispersion, preparation, administration, documenting, and monitoring, and errors can arise at any point during these processes. Anesthesiologists are usually involved from the drug preparation stage to the monitoring in the operating theatre. According to a study (Khan & Hoda, 2001), most of the critical errors encountered during the anesthetic process result from human and device errors. Other studies have also shown high incidences of drug errors associated with anesthesia (Dhawan et al., 2017; Kothari et al., 2010; Rayan et al., 2019). It is estimated that for every 133 anesthetics administered, there exists one medication error, and 1% of them cause harm to the patient (Webster et al., 2001). In another study by Gordon et al. (2006),

720 anesthetists were surveyed, with 133 questionnaires returned and analyzed. 94% of the respondents admitted that they had unintentionally given the wrong drugs to patients at some point in their careers. Among the 303 wrong drug administrations described, syringe swaps contributed 40% of the errors, drug identification problems contributed 27.1%, fatigue constituted 14.1%, and drug mislabeling and distractions contributed 4.7% each to the errors.

Litman (2018), in his work, stated that there are two points where there is a high chance of error during the administration process in the operating room. The first is when a medication syringe is being prepared from a drug's ampule or vial. It is possible to choose the incorrect medication (i.e., phenylephrine is selected in place of ondansetron) or the wrong concentration (i.e., lidocaine 2% for lidocaine 1%). The possibility of the occurrence of these errors is likely to be high when drug containers are kept in close proximity to each other in the anesthesia drug tray and/or appear similar. The other issue is a result of a syringe swap; the anesthesia provider unknowingly picks the wrong syringe - thinking it contains one drug when in fact, it does not. In addition, medication mismatches in the operating theatres resulting from drug entry for the wrong patient and ambiguous entry of drugs into the drug trays pose a high risk of medication errors.

Other factors, such as work overload, stress, fatigue, or distractions, increase the likelihood of medication misidentification in the operating rooms (Lala et al., 2016). One particular example relates to medication misidentification in anesthesia; in selecting the many medications used intravenously in anesthesia, humans make errors often, in effect, reading what they expect to see on a label rather than what is actually on the drug label.

Without an intelligent automated system to identify the medications used in the operating theatres, patients are left to rely solely on the anesthesiologist’s cognitive effort and attentiveness to make proper drug identification judgments. Unfortunately, humans will always make mistakes. Sydney Dekker, a safety expert, stated that: "adverse medication events cannot be ruled out in every aspect of administering various compositions of volumes, weights, and rates of substances through various

methods" (Dekker, 2012). Intelligent systems may help to assist in reducing and mitigating these errors.

This research focuses on investigating how an intelligent computer vision framework could be made to automatically identify anesthetic drugs during drug preparation by the anesthetists to eliminate completely or reduce to the barest minimum the errors made during drug preparation in the operating rooms. In particular, the detection, extraction, and matching of the semantic features or characters found on ampule and vial containers for automatic anesthetic drug identification. The output of the study is intended to be a framework that could be integrated into the existing anesthetic drug preparation and verification ecosystem to act as a front end to the existing medication safety system. This work concentrates on the process of preparing syringes using medication supplied in vials or ampules and ensuring that the loaded syringe is correctly labeled, and the process recorded.

1.9 Research Objectives

The main goal of this research is to develop and evaluate a novel solution to medication misidentification problems in operating theatres. Therefore, the main Research Question (RQ) is formulated as follows:

Main RQ: Can computer vision be used to automatically identify medications in anesthesia?

To tackle the research question and achieve the research goal, the study is set to investigate the existing operating theatre medication identification system and to develop and evaluate a novel framework for automatic medication identification in the operating theatre. The following specific objectives will guide the research design:

Research objective 1: To investigate and define the requirements for a framework to identify medications as part of the aesthetic workflow.

Research objective 2: To develop a prototype framework to address the requirements identified in (1)

Research objective 3: To test this framework and make suggestions on how to link it to a larger framework that will increase medication safety in anesthesia.

1.10 Main Contributions of this Research

The research work presented in this thesis introduces a novel framework for computer vision and artificial intelligence-driven anesthetic medication identification for rapid, efficient, and reliable drug preparation in operating theatres. In essence, the proposed framework is distinctive because, when preparing this thesis, the work was the first to attempt to use different artificial data processing and computer vision methods to recognize and identify the critical drugs used in the operating rooms. Thus, the key research contributions of this work are:

- The design and development of an efficient and rapid computer vision and intelligent system-based framework to identify anesthetic drugs used in the operating rooms with remarkable accuracies that meet the healthcare sensitivity and confidence needs.
- A demonstration that a single framework could be used to rapidly identify objects with complex structures and tiny text inscriptions (which are extremely difficult to achieve with conventional deep learning approaches) without developing a task-specific framework for different technical field applications. This implies that the capability of the proposed framework is not limited to anesthetic medication identification but can be deployed in other wide range of application areas.
- Developed a feature detection, extraction, and matching strategy for identifying the anesthetic drugs and compared the results with the main proposed framework.
- Developed a mini framework for batch string feature extraction from multiple anesthetic drug containers instead of a single manual procedure for drug label string extraction and storage; this could also be useful in other wide range of application areas.
- Introduced an enhanced Levenshtein Distance computation method using a generalized Ukkonen method, upper bound theorem, and branch pruning algorithms for the rapid anesthetic drugs' rate of substance matching and extraction from the anesthetic drug stream of strings.
- Designed a conceptual strategy for a compact anesthetic drug identification process for standalone or embedded systems.

- Formulated and deployed confidence estimation strategies for the anesthetic drugs identification framework.
- Integrated into the framework, artificial voice feedback and a label processing mechanism using the QRcode technology for efficient and rapid anesthetics medication preparations.
- Results and analysis of the proposed framework's capabilities and limitations.
- Integration of a Laplacian object quality enhancement algorithm for the frameworks' clearer processing of the anesthetic medications in varied processing conditions.

1.11 Thesis Organization

The thesis is partitioned into various chapters, sections, and subsections. Chapter one introduced the concepts of the study. Chapter two contains the research literature review. Chapter three presents and describes the adopted research methodology. Chapter four presents the theoretical background, research findings, and analysis of the findings using conventional computer vision's image feature detection, extraction, and matching for identifying anesthetic drugs. Chapter five will discuss the findings. Chapter six extended the study to address the challenges encountered with adopting the proposed framework. Chapter seven concludes the thesis.

Chapter 1 introduced the anesthetics drug identification concept, the background of the study, the general overview of computer and machine vision, object identification and the anesthetic drugs identification needs, the real-time anesthetics drug image processing requirements, the rationale and significance of the study, and the objectives of the research.

Chapter 2 presents the findings in the existing related literature for the anesthetic drug identification and recognition process. Terms such as the Barcodes or QR codes for ampule identification, color-coding for ampule identification in the operating theatre, scene text detection and recognition, optical character recognition (OCR), and well as OCR engines were explored in detail. The chapter also performed a comparative study of the OCR engines on extracting matchable and analyzable strings from the ampule images.

Chapter 3 examined the usefulness and capabilities of the various object feature detection, extraction, and matching for anesthetics medication identifications. Concepts such as local and global image features for anesthetics medication identifications also were explained in detail. Also, terms such Single-Scale Image Feature Detectors (SSD), Multi-scale Image Feature Detectors (MSD), Speeded-Up Robust Features Descriptor (SURF), and Scale Invariant Feature Transformation (SIFT) for anesthetics medications identification were investigated in the chapter. The chapter ended with concise experiments and results analysis of the aforementioned techniques in identifying the various anesthetic drugs and the merits and demerits associated with adopting them.

Chapter 4 discussed the methodology and the research design strategy adopted in this study. It established the research problems, research questions and sub-questions, methodology and research process, hardware requirements, data collection methods, and the overall results evaluation process.

Chapter 5 presented the general theoretical framework adopted in the study and the research findings. The chapter also established the conceptual workflow of the anesthetic drugs identification framework. In continuation, the adopted string-matching algorithms for the anesthetic's drugs identification framework and as well as the various categories of the strings matching methods suitable for the project were presented in this chapter. An enhanced Levenshtein distance for the anesthetic drug's rate of substance filtering that serves as one of the significant novel contributions of this study was equally presented. Finally, the experimental procedure for the anesthetic drugs identification framework was explained in detail in this chapter with the threshold computation steps as well as the experimental results and analysis process.

Chapter 6 extended the investigation by examining the identification of the anesthetic drugs in varied processing conditions with the anesthetic drugs container stain modeling and the anesthetic drugs container data low-light processing scenario modeling. The anesthetic drugs identification enhancement in varied processing conditions and as well as the establishment of the modeled anesthetic drugs measurement metrics were also done in this chapter. The chapter concluded with

various experiments and analyzing the identification of the anesthetic drugs in varied processing conditions.

Chapter 7 presents the overall summary and conclusion of the thesis. The detailed results extracted from the various experiments run during the study are presented in the appendices.

Chapter 2 Literature Review

2.1 Introduction

In this chapter, a review of related literature that is necessary for the research study is performed. The concept of anesthetic drug ampule identification in the operating theatres and as well as the existing barcodes or QR codes for anesthetic drug ampule identification in the OR are explored. Also, scene text detection and recognition, which formed the basis of the methodology adopted for this project, are investigated in detail. Various object text detection methods from scenes, including the classical and deep learning approaches, are also investigated. The methods for scene text recognition, in particular, deep learning methods, are also presented in this chapter. Finally, the optical character recognition (OCR) system and various engines were studied and analyzed for the best compatible engine for the base project.

2.2 Drug Ampule Identification in the Operating Theatres

Ampule identification poses great challenges because they are often small with tiny text labels and often look similar to one another (see Figure 6). Several publications have proposed different methods for identifying and recognizing drugs in the operating theatre. This includes the barcode/QRcode systems, sensor-based systems, and the color-coded label system.

Figure 6: Anaesthetic Drug Container Samples.

2.2.1 Barcodes or QR Codes for Ampule Identification in the OR

The barcode or QR code systems have the potential to reduce drug maladministration during anesthesia and improve patient safety (Cescon & Etchells, 2008; Merry & Anderson, 2011; Young et al., 2010). Barcode medication administration (BCMA)

technology (Hassink et al., 2012) has witnessed increased adoption by hospitals to enhance patient safety and increase the efficiency of the anesthesiologist in the OR in recent times by aiding drug recognition and verification.

In their work on medication error reduction during anesthesia, Merry et al. (2001) introduced a new safety-oriented system based on barcodes to minimize errors during drug administration in OR. The system comprises a customized drug tray for ensuring a well-structured work environment, the most frequently used anesthetics drug pre-filled syringes, color-coded large legal and approved drug labels, and a computer comprising of barcode reader, visual and auditory devices, and a specialized drug trolley drawer. This system provides a mechanism for well-organized ampoules and syringes, well-labeled syringes, and scanning medication pre drugs administration. The system recorded a high rate of error reduction when compared with a conventional method (Merry et al., 2011).

Another system, the Safe Label System (SLS) (Codonics Inc., Middleburg Heights, OH), is a digitalized drug labeling system (Tribble & Osborne, 2006) made with barcode code systems for anesthesia point-of-care usage. In this system, the drug vial barcode is scanned with the system to generate a corresponding syringe label and color-coded it to comply with standards and regulations. Drug manufacturers were mandated by the United States Food and Drug Administration in 2004 to embed barcodes on drug vials. Numerous anesthesia information management systems (AIMS) can scan medication label barcodes for commercial use (Jelacic et al., 2015).

Despite the impact of these systems in reducing errors during anesthesia, they do not entirely solve the drug preparation problems caused by medication misidentifications in the OR because not all drug containers have barcodes embedded in them.

2.2.2 Color-Coding for Ampules Identification in the Operating Theatre

Several proposals have been made to color-code ampules for easy identification of related drugs to minimize the dangers that arise because ampoules have similar appearances and shapes in operating theatres (Astin et al., 2015). The drug makers perform modern ampule color coding during the medication manufacturing process. The colors on ampules may appear as rings or dots on sealed ampules (see Figure 7). The colors assist anesthesiologists and machines in quickly identifying the content of

the ampule. Color coding can also be used in operating rooms for flow meters, vaporizers, cylinders, lines, pipelines, and syringe stickers to prevent medication errors and ensure patient safety (Jensen et al., 2004).

Figure 7: A Cross-Section of Ampoules with Color Coding.

However, numerous issues have been reported on deploying color-coding to identify and recognize drugs in the operating rooms. Patel et al. (2006) stated that there is no proof that color differentiation can completely eliminate medication errors and that color labels are only viable in drug categorizations and cannot spot an individual drug in a group of drugs. Another work found that events of mix-ups arise because of selection errors between contents in a drug category with dissimilar action and strength (Grissinger, 2012). Filiatrault and Hyland (2009), in their work, stated that the ability to recall multiple complex color-coding models and limited availability of the amount of absolute identifiable colors are other problems associated with using color-coding for drug identification in operating rooms. Finally, color blindness (Janik & Vender, 2019) and negligence of color reading in critical conditions because of lack of

time to identify the colors, shape and size of drugs to be used are other issues associated with the use of color-coding systems.

2.3 A Review of Scene Text Detection and Recognition

Text is often found on objects for conveying information (Lin et al., 2019; Long et al., 2018). Identification of well-structured texts in images (like scanned documents) and complex unstructured texts from scene objects (such as objects with texts from indoor/outdoor buildings, highways, and urban and rural environments) are two major categories of text identification (Raisi et al., 2020). Texts are said to be complex and unstructured if they possess diverse fonts, structures, colors, textures, illuminations, backgrounds, and different geometric distortions. Examples are the anesthetic drug ampules and vials used in this project, as shown in Figure 8.

For text identification or recognition in scanned documents, Optical Character Recognition (OCR) approaches have yielded good performance when compared with the identification of non-scanned images with texts (Chaudhuri et al., 2017; Chen, 2003). However, extracting text from images in an unstructured scene is more complicated than from scanned documents (Long et al., 2018; Shi et al., 2018). The major issues are; text scene complexity, diversity, and distortions (Raisi et al., 2020). Complex texts can be in different orientations, curvatures, fonts, colors, and languages. Text diversity could result from image distortions caused by partial occlusion, capturing angle, motion blurriness, or poor camera resolution during the capturing process (Lin et al., 2019; Long et al., 2018).

Numerous methods of tackling the challenges of identifying and recognizing texts from scene objects have evolved from research over the years, and the prominent amongst them are the classical machine learning approach (Kim et al., 2003; Pan et al., 2009) and deep learning-based methods (J. Baek et al., 2019; Huang et al., 2014). The classical machine learning method often relies on the fusion of feature extraction models to recognize or identify texts from scene imageries (Epshtein et al., 2010; K. Wang et al., 2011). These methods often fail to extract texts from images that contain curved or multiple-oriented texts (Lin et al., 2019; Long et al., 2018) but yield good performance in recognizing scanned texts or horizontally well-aligned texts in scene objects (Lin et al., 2019; Ye & Doermann, 2014). However, deep learning-based models

have demonstrated effectiveness in recognizing texts from objects whose images are captured in adverse conditions (He et al., 2018; Shi et al., 2017), including end-to-end scene object text detection and recognition (Busta et al., 2017; Lyu et al., 2018).

In recent approaches (Epshtein et al., 2010), the text localization process is first performed by spotting regions where text occurs on objects by means of bounding box predictions for each detected region and then recognizing the texts in each of the regions detected. In other words, the task of extracting meaning from text images is broadly split into text detection and text recognition (Figure 8). Text detection strives to locate potions of the scene imagery where text is present. In contrast, the process of preparing the localized text regions into editable words, characters, text lines, or computer-readable format is the responsibility of the text recognition process (Raisi et al., 2020). Deep learning is the principal constituent of the optical character recognition engine used for string extraction in this work.

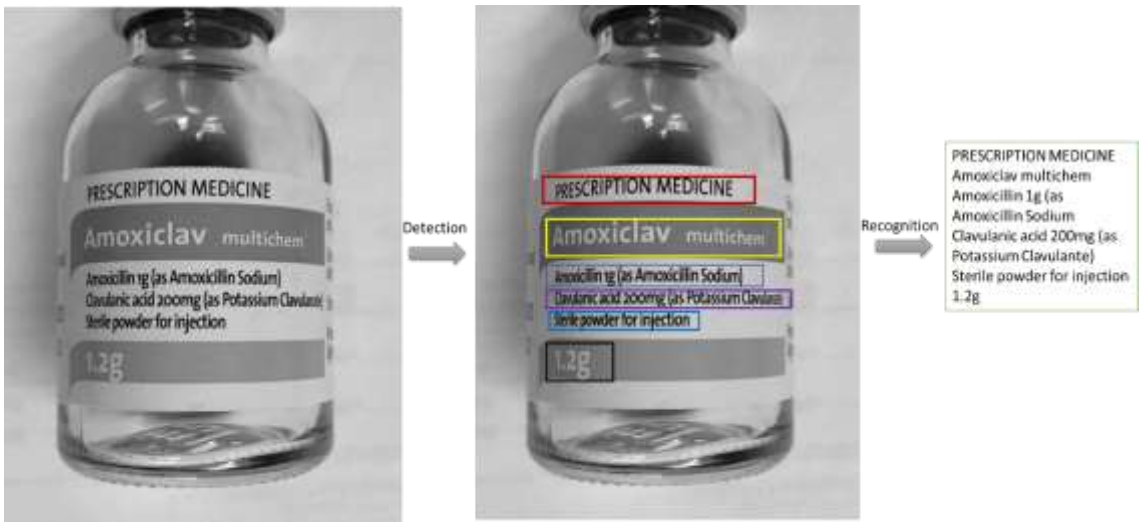

Figure 8: A sketch of scene text detection and recognition.

2.3.1 Objects Text Detection from Scene

Classical machine learning(Neumann & Matas, 2010) and deep learning (Jaderberg et al., 2014a) have been the two main dominant methods for detecting texts embedded in scene objects and have been instrumental in the advancements made in modern text recognition applications. This section offers a detailed review of these two major approaches.

2.3.2 Classical Methods for Scene Text Detection

The classical machine learning approach is subdivided into two main methods; the sliding window and the connected component-based approaches (Raisi et al., 2020). In the sliding-window technique, an image pyramid is built using a given image sample, which rolls over the scene object imagery to discover locations where texts are present, using a specific size of the sliding window (Bissacco et al., 2013; Kim et al., 2003). In each sliding window, image features such as the standard deviation and mean difference (Hanif & Prevost, 2009), histogram of oriented gradients (HOG) (Hanif & Prevost, 2009) and the edge regions (Lee et al., 2011) are extracted. Then, to detect text in each window, a classical classifier such as adaptive boosting (AdaBoost) (Schapire & Singer, 1999) in conjunction with various weak classifiers like the log-likelihood (Chen & Yuille, 2004), decision trees (Lee et al., 2011), likelihood ratio test (Hanif & Prevost, 2009) and random ferns (Bosch et al., 2007) are deployed to classify the derived image features.

On the other hand, connected component-based algorithms extract image regions with comparable features such as textures (Ye et al., 2005), color (Kim & Kim, 2009), corner points (Zhao et al., 2011), and boundaries(Li & Wang, 2008). They use these features to generate texts and non-text categorizable candidate components using conventional classifiers like Nearest neighbor (Neumann & Matas, 2013), support vector machine (SVM) (Neumann & Matas, 2010), and Random Forest (Yao et al., 2012) algorithms. These methods fuse extracted characters from images into text lines (Chen et al., 2011) or words (Epshtein et al., 2010) to detect them. The connected-component-based algorithms are more robust and efficient as they yield fewer false positives, which is a critical condition to consider when dealing with scene text detection compared to the sliding window methods (Liu et al., 2019).

2.3.3 Deep Learning Methods for Scene Text Detection

Recent advancements in deep learning (Krizhevsky et al., 2017) have drastically transformed scene text detection tasks (see Figure 8) and have opened up more research opportunities in the field. In such tasks such as detecting text with varying aspect ratios (Shi et al., 2017), efficient and simpler pipeline (Zhou et al., 2017), and ushering in the possibility of training robust text detection models using synthetic data

(Jaderberg et al., 2016); deep learning-driven text detection models have been more effective than classical machine learning-based techniques in recent times.

Early works on deep learning-driven text detection model architectures were built on many stages (Huang et al., 2014; Jaderberg et al., 2014a). In their work, (Jaderberg et al., 2014a) extended and trained the architecture of an existing convolutional neural network (CNN) to generate text saliency maps and performed filtering and NMS operations at multiple scales to fuse bounding boxes. In another work, deep learning and a traditional connected component technique were combined and deployed to enhance the precisive ability of the text detection model (Huang et al., 2014). A high-contrast-region detector, MSER (Matas et al., 2004), was used to detect each text character candidate in an incoming image sample with texts. A CNN classifier was then deployed to separate non-characters by producing confidence maps which were subsequently used to obtain the outcome of the detections. In another work, text candidates were generated with an aggregate channel feature (ACF) detector (Dollár et al., 2014), and bounding box regressions were produced using a CNN to minimize the occurrence of many false-positive outcomes (Jaderberg et al., 2016). These methods focused primarily on character detections for scene images with less complex backgrounds and exhibited poor performance in detecting texts with varying geometry (Zhang et al., 2016), texts whose color is similar to the background, or other complex text characteristics.

2.3.4 Scene Text Recognition

After texts are detected in scene objects, they need to be transformed into editable and usable characters or words, and scene text recognition models are used for this study (see Figure 8) Several problems are encountered when building scene text recognition models due to the diverse features in scene texts. Furthermore, developing an efficient scene text recognizer based on the classical optical character recognition models is not ideal due to the challenges of scene texts (Bunke & Wang, 1997; Lucas, 2005). These challenges, as aforementioned above, range from extreme lighting (Wang & Belongie, 2010), low resolution (Mishra et al., 2012; Wang & Belongie, 2010), environmental conditions (Karatzas et al., 2015), orientation angles (Risnumawan et al., 2014), diverse fonts and colors (Karatzas et al., 2015), lexicons (Wang & Belongie, 2010) and languages (Iwamura et al., 2017). To address these

problems inherent in scene text recognition, several methods have been proposed, which are grouped into two categories: classical machine learning methods (De Campos et al., 2009; Pan et al., 2009) and deep learning methods (J. Baek et al., 2019; Jaderberg et al., 2014b).

2.3.5 Deep Learning Methods for Scene Text Recognitions

Several deep learning approaches have been proposed to deal with the challenges of recognizing texts in scene objects (Jaderberg et al., 2014b; T. Wang et al., 2012), which leverages the advances made in artificial deep learning architectural research in recent times. For instance, to recognize texts from scene objects, a convolutional neural network-driven model was introduced by (T. Wang et al., 2012) to extract features from image samples with a non-maximal suppression (NMS) algorithm (Neubeck & Van Gool, 2006) employed to perform the actual word predictions.

Furthermore, a fully connected network (FCN) was deployed to extract feature representations from texts, and an n-gram model (Cavnar & Trenkle, 1994) was utilized to recognize the text characters. Multiple SoftMax classifiers deep CNN architecture was built and trained (Jaderberg et al., 2014b) using a synthetically generated dataset to predict each word in a given sample scene image using an independent classifier. However, individual character localization from scene images was the norm in the early deep learning-inspired text recognition models (T. Wang et al., 2012), which posed challenges because of the presence of unnecessary symbols, short gaps among adjacent characters, and complex backgrounds.

In another work, Jaderberg et al. (2016) proposed a convolutional neural network architecture to perform the classification of 90k English words to recognize texts on scene images. However, despite yielding an improved text recognition than the approaches that split characters before recognition (Jaderberg et al., 2014b; T. Wang et al., 2012), the model is unable to recognize words that are not in the training dataset, and the precise word recognition is affected by long word deformations. In several works proposed in recent times (Shi et al., 2016; Yang et al., 2019), each scene text input sequence is mapped into a varying length output sequence, taking into consideration the sequence nature of scene text characters. In continuation, a connectionist temporal classification (CTC) (Graves et al., 2006) was introduced in

many recent works(Lee & Osindero, 2016; Liu et al., 2018) to predict character sequences deriving inspirations from the models' speech recognition prowess. In other studies, conventional convolutional models such as VGG (Simonyan & Zisserman, 2014), ResNet (He et al., 2016), and RCNN (Lee & Osindero, 2016) are combined with CTC to perform scene text recognition tasks (Borisyuk et al., 2018; Yin et al., 2017a). For example, a CNN sliding window is initially deployed to effectively grab contextual information from text lines before a CTC algorithm is utilized to predict the resulting words (Yin et al., 2017b).

In Borisyuk et al. (2018) work, a CNN network was used to extract text features from scene images using ResNet as a base network to predict texts from the feature sequences (Borisyuk et al., 2018). This method suffered drawbacks that impacted its recognition accuracy negatively due to a lack of contextual information despite the drastic reduction of the computational complexity. Further works (He et al., 2015; Shi et al., 2016) utilized a recurrent neural network (RNN) (for improved contextual information extraction) together with a CTC classifier to compute the conditional probability that exists in a target text sequence for text predictions in turn. For instance, a VGG model (Su & Lu, 2014) was employed as a base network to extract features from sample input scene texts. Then a bidirectional long-short-term-memory (BLSTM) (Hochreiter & Schmidhuber, 1997) was deployed to extract contextual information from the text sequences before a CTC loss was finally used to recognize the text character sequence. Wang and Hu (2017) introduced a gated recurrent convolutional neural network (GRCNN) inspired by RCNN to perform recurrent connections modulation emanating from the previous RCNN model using gates. However, irregular texts (Xie et al., 2019) cannot be precisely recognized by these approaches (Cheng et al., 2017; He et al., 2015) due to the 2-dimensional organization of characters in the image planes. This is because CTC classifier are developed for 1-dimensional sequence aligned texts in images, and thus 2D image features are required to be transformed into 1D features. This process could cause vital information loss.

2.4 Optical Character Recognition

According to Zhao et al. (2020), optical character recognition (OCR) is the process of transforming scanned documents and scene images with text or handwritten texts into

a machine-encoded text format that can be manipulated easily by machines (see Figure 9). Islam et al. (2017) stated that machines without an OCR mechanism are less intelligent enough to perceive texts inscribed on images than humans. Humans can easily and repetitively recognize characters many times daily. The target of recent extensive research on OCR is for machines to achieve a reading capability equal to or above that of humans. Due to the increasing demands for the transformation of hard documents into soft or digital formats, OCR has attracted considerable research interest in recent times (Drobac & Lindén, 2020).

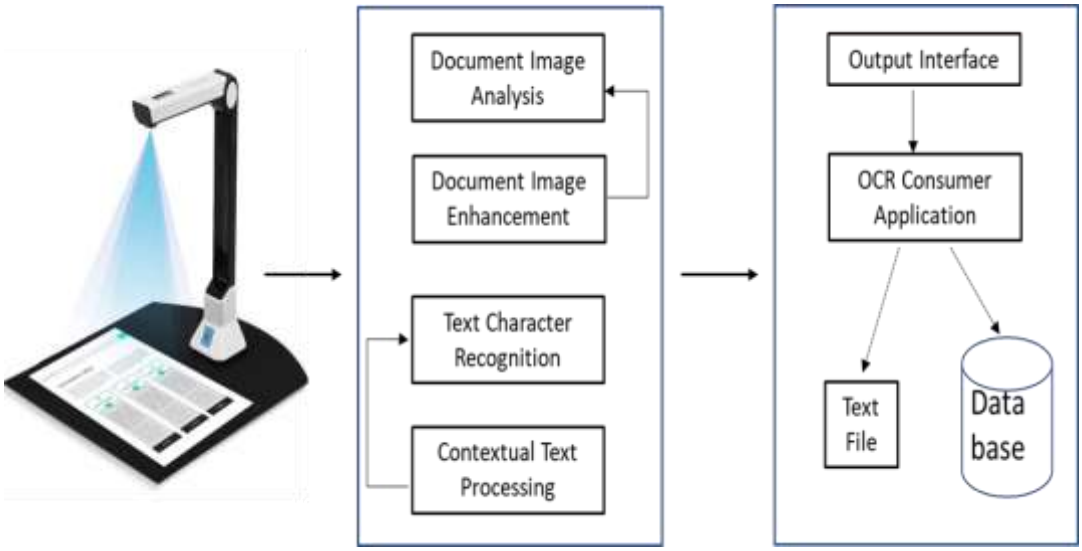

Figure 9: The typical OCR Process.

Clark and Mirmehdi (2000) introduced a real-time scene-image text location system that uses the statistical features present in scene text neighborhoods. In the model, text and non-text regions in images were classified using a neural network trained with measures derived by statistical procedures, extracting text features that are highly invariant to the scene image's color, scale, and orientation. Furthermore, an algorithm to detect and track text regions available in frames of digital videos was introduced in a work done by Li et al. (2000). The proposed model used a text-feature extractor system that is based on a scale-space extraction mechanism together with an artificial neural network processor to extract regions of texts in the videos before tracking their movement. Then the text region extraction output was fed to an OCR to generate indexable keywords. In another similar work, a system that automatically segments texts in digital videos fed to a standard OCR for converting the text segments into ASCII characters was introduced (Lienhart & Effelsberg, 2000). Lienhart and Wernicke (2002)

introduced another model that performs textual localization and segmentation in complex videos and images using a trained multilayer feed-forward network that identifies text lines.

Breuel (2001) proposed a method that adopted a coarse-to-fine method, notably a branch-and-bound search algorithm in conjunction with a geometric model precise least-square matching of text lines to perform text OCR. The proposed algorithm ensured the system's optimal output, considering the least square error model, and the integrated geometric model ensured the algorithm's robustness. A novel system that reads text automatically by deploying an active camera that is fixated on regions of text already spotted in scene images was introduced (Mirmehdi et al., 2001). In the system, the text regions obtained are then analyzed to generate the optimal zoom capable of fitting into them before feeding them to the OCR for recognition. Aiello et al. (2002) introduced an approach that performs logical label alignments in documents and reading order extraction using the documents' spatial relations, content, and textual and geometric features. Similar to our proposed system, this system integrates several mechanisms based on computer vision, natural language processing, and artificial intelligence for document analysis.

Shintani et al. (2006) proposed a neural network comprising four simple layers to recognize text characters. The introduced model, which can recognize text patterns obtained by an affine transformation, used 24 patterns as input patterns which were then divided into 64 local patterns and linked together with the first hidden layer of the neural network. The Alopex algorithm was then used to test the performance of the proposed model. A fast model that is robust to noise and based on an enhanced parallel thinning algorithm was introduced for cursive texts (Shintani et al., 2006). With an improved set of preservation rules through the prearrangement of grid template pixels, the algorithm could handle both cursive and non-cursive texts. A technical report (Maharrey, 2009) introduced the nearest neighbor algorithm for OCR. Maharrey (2009) proposed a novel method for conducting text binarization for precisive OCR using a limited amount of document types. A neural network-based document image clustering, summarization, interpretation, and evaluation was introduced to ease document processing (Rehman & Saba, 2014).

Mohammad et al. (2014) proposed an OCR system that uses a pattern-matching algorithm method to process documents. A fuzzy classify-based optical character recognition algorithm was introduced to classify letters and digits (Fonseca et al., 2011). The study used a semi-automated fuzzy classifier to recognize characters in unstructured environments. To learn the rules that perform regulations on the design of diverse characters and to create rules based on fuzzy methods for the implementation of the fuzzy classifiers, a CART algorithm was deployed, and a fuzzy inference engine was used to conduct the actual classification of characters. A document analysis system that deploys feature descriptors on images with texts was proposed (Ramakrishnan & Bart, 2012). In the system, independent components of text documents were extracted before using the learning descriptor obtained by pooling the components on top of document regions with several overlapping.

In their work, Chattopadhyay et al. (2012) proposed a low-complexity optical recognition system to extract and recognize texts on embedded systems. The method was distinct because of the high text recognition accuracy yield despite the less memory usage and low processing cycle. To tackle the problems of ruptured characters in image documents, a feed-forward neural network model with multiple layers was introduced to improve the recognition accuracy of documents. The enhancement capability of the proposed model was driven by the classification of the text characters that are broken into text documents into groups. These steps were taken in the pre-processing stage of the text document recognition before the OCR recognition and had less impact on the text recognition speed. An OCR based on the combination of a k-nearest neighbor algorithm for process validation and an artificial neural network was proposed to recognize characters in real environments. Instead of the conventional OCR text image pixel processing, their method processes digit angles which made their system less sensitive to digit rotations, diverse condition adaptation, and robust to light variations.

An effort to recognize degraded documents was made in a study (Dutta et al., 2012) by organizing successive components of characters into segments. In this method, character n-grams were deployed as primitives for recognizing characters in documents instead of using them as a postprocessing mechanism. To minimize the ambiguities encountered in the recognition of confusing characters in documents, the

extra contexts available in character n-gram images were rigorously exploited. Then the resulting labels from the constituent n-grams recognitions were combined to form a label of the word that was obtained. Another study involving the recognition of deformed and distorted characters in images, using discriminative spatiality embedded dictionary learning representation (DSEDR) (Shi et al., 2015), was proposed to learn the discriminative strokes in texts automatically. A further comparative study was done on mixtures-of-parts TSM, tree-structured model (TSM), DSEDR and discriminative multi-scale stroke detector-based representation (DMSDR) methods for image character recognition.

In a further study, an InceptionV3-based deep neural network architecture was deployed to train and conduct optical character recognition on image texts (Wei et al., 2018). In the study, about 53,342 noisy character images extracted from newspapers and receipts were used to train and validate the InceptionV3 network, and remarkable text recognition performance was recorded on text images with a reduced quality. In a similar study, a feed-forward neural network was utilized for training and recognizing noise-degraded text images (Afroge et al., 2016). In another work, a backpropagation (BP) based artificial neural network (ANN) algorithm was proposed to recognize noise-degraded image texts of English characters (Kakkar & Dutta, 2014). A text character color and size invariant recognition system that uses a feed-forward neural network was introduced to recognize English alphanumeric characters (Kader & Deb, 2012). In their work, Mollah et al. (2011) proposed a handheld integrated OCR system that acquires inputs from a camera sensor for processing. Xu et al. (2020) proposed a pre-trained approach for image document processing and understanding in their work. The model leverages the relations in scanned document image texts and layout information for document image understanding and, to a larger extent, vital information extraction.

In recent research works on OCR, remarkable improvements have been achieved in performing OCR. Du et al. (2020) introduced a lightweight OCR model to recognize both English and Chinese alphanumeric symbols and characters. In the work, a differentiable binarization (DB) algorithm based on a simple segmentation technique was used as a text detector, and methodologies such as FPGM pruner, light backbone, learning rate warm-up, SE module removal, light head, and learning rate decay were

introduced to enhance the efficiency and effectiveness of the system. Conversely, a convolutional recurrent neural network (Shi et al., 2016) was used to perform the actual text recognition. Significant improvements were obtained in the above-proposed OCR system to balance the trade-off between accuracy and efficiency in the image text recognition process. Through the introduction of techniques such as collaborative mutual learning (CML) algorithm, unified-deep mutual learning (U-DML) algorithm, CopyPaste, enhanced CTCLoss, and a lightweight CPU Network (LCNet), that increased the PP-OCRv2 precision accuracy to 7% from the earlier version.

For entity extraction from images with text, Guo et al. (2019) proposed an attention text extraction model that is based on an Entity-aware mechanism. Without post-processing steps, their introduced entities extraction network uses a trainable end-to-end technique to extract vital information or entities from images with texts. In the network, entity-aware decoders are used to parse each entity, and a state transition system is deployed to enhance the robustness of the proposed entity extraction network. In further works, a non-repetitive multimodal transformer with a confidence-aware scheme (Z. Wang et al., 2020) was introduced to mitigate the inability of the existing model to produce an accurate description of images with texts because of their inability to select essential words from the tokens extracted by OCR, word repetitions in captions predicted and poor reading capabilities of models as shown in Figure 10.

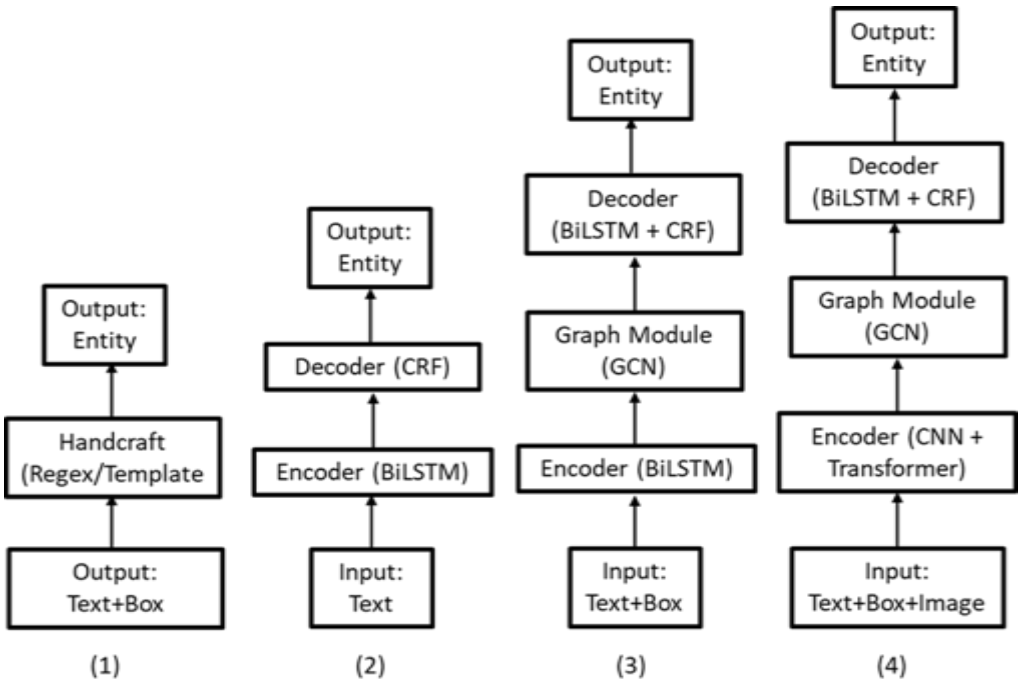

Figure 10: Conventional AI Architectures for Key Information Extraction. (1) Handcrafted-Based Approach. (2) Automated features Extraction Method. (3) & (4) More Complex Feature Extraction Approaches (Yu et al., 2021).

An enhanced graph-based learning convolutional network (Zhang et al., 2019) for extracting vital information from documents was proposed to perform downstream OCR activities (Yu et al., 2021). The study deployed a fussed graph learning model and graph convolution operation to extract rich semantic representations from document images and unambiguous global layout features as shown Figure 11.

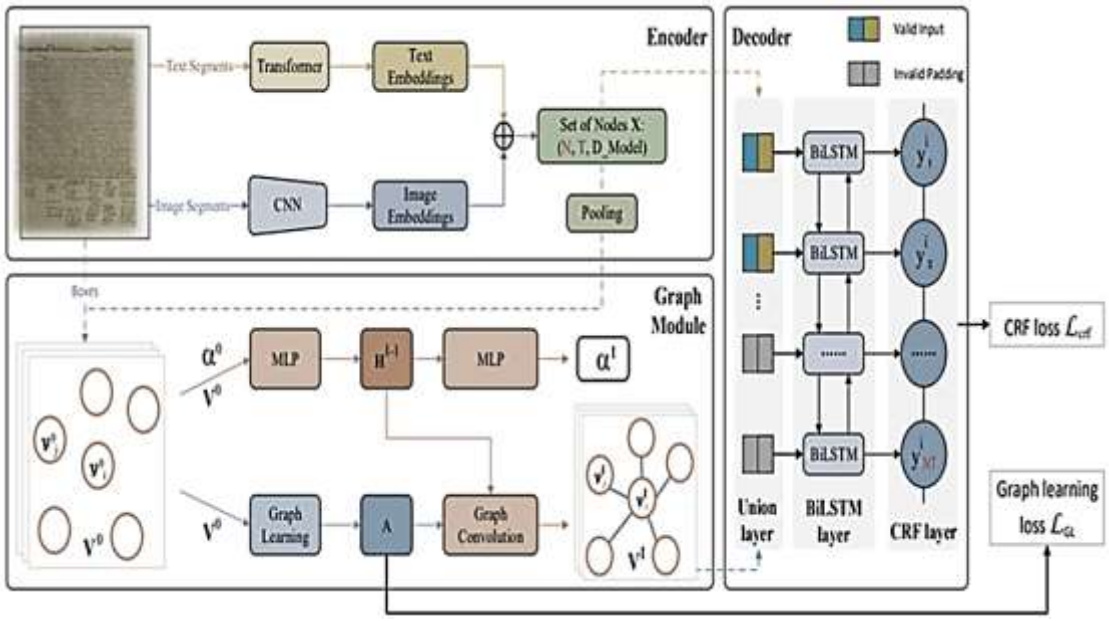

Figure 11: Illustration of the architectural workflow of the enhanced graph-based learning convolutional network for vital documents information extraction (Yu et al., 2021).

The system's architecture is split into three main parts: an encoder, a graph model, and a decoder (see Figure 11). Using a Transformer and a CNN model, text segments are encoded to obtain image segments, text, and image embeddings. The emanating two embeddings are then unified to form a new local representation, serving as an input node to the graph segment. The latent relation that exists in the nodes is derived with the graph module with more useful graph embedding representations using enhanced graph convolutional operation learning. With the aid of BiLSTM and CRF algorithms, sequence tagging is conducted on the character level of the text document in the decoder module. Having done the process above, key information extraction activities are transformed into sequence tagging with both the document layout information and the global information put in perspective.

Their work proposed an end-to-end fused network for reading and extracting key texts from documents (Zhang et al., 2020). To read texts into the network in the study, textual features and multimodal visual information was combined to obtain semantic information that was vital for text reading optimization. Hong et al. (2020) proposed a pre-trained BERT model for spatially distributed text representation and semantic understanding. With the efficient inclusion of the spatial layout information of input visual text, their proposed pre-trained model together with a novel area-masking technique used a graph-based decoder to capture text segment relationships which in turn provide structured outputs for performing different document understanding tasks. For real-world visual-text information extraction, Wang et al. (2021) introduced a combined end-to-end model that simultaneously performs the conventional image text processing tasks using a single text document as input and providing structure information as output. In particular, robust visual and semantic representations of text were obtained from the information extraction stage for multimodal feature fusion tasks that generate higher-level semantic hints for the text spotting optimization process.

Hwang et al. (2020) proposed a model to tackle the complex spatial relationships and high structures that exists in complex real-world image texts. In the model, they treated the information extraction tasks as a spatial dependency parsing process, emphasizing the correlations that exist in text document tokens. The introduced spatial dependency parser can extract hierarchical information without a serializer model from complex structured image documents in end-to-end format. For handling semi-structured documents, Hong et al. (2020) introduced a Graph Neural Network (GNN) architecture in their study to perform entity recognition tasks and extraction of the relationships that exist in semi-structured text image documents. In another work, an attention-based graph neural network was proposed to fuse visual and textual information extraction processes from image documents to tackle the challenging vital information extraction process problems (Hua et al., 2020). In constructing the graph neural network architecture, they introduced a global node that serves as a virtual hub for information gathering among all nodes and edges in the network for the proposed network performance enhancement.

In their study, Lin et al. (2021) concatenated together a BERTgrid architecture and convolutional neural network's intermediate layers to form a multi-modal backbone network for conducting vital information extraction from image documents. In the network, the CNN layers serve as image document receptors and preprocessors, and the BERTgrid serves as a grid of word embedding for document representation generation. In the proposed architecture, the BERT and CNN parameters were mutually trained compared to the BERTgrid method. A pixel-wise field-type classification process was conducted using an auxiliary semantic segmentation head before individual words extracted with an OCR engine were classified using a word-level field-type classification head. A key-value matching method was introduced for multifarious images with ambiguous texts or complex numeric semantic categories extraction (Tang et al., 2021). With the help of the relevancy evaluation process of the key-value matching mechanism, the proposed model circumvents the various semantic recognition stages of image text processing and pays attention to the critical relevant entities. A Num2Vec was incorporated into the architecture to stabilize the encoded values and assist the smooth model convergence in ensuring smooth and effective model processing.

2.5 OCR Engines

The enormous interest in OCR research has yielded remarkable results. It has led to the emergence of many open-source OCR engines such as Tesseract (Smith, 2007), GoogleOCR (Vincent, 2007), PaddleOCR (Du et al., 2020), Calamari (Wick et al., 2018), Ocropy (Miyagawa et al., 2019), easyOCR (Karnawat et al.), KerasOCR, and many others. The Google OCR runs on the Google cloud platform, providing diverse services for secured visual data acquisition, extraction, processing, and analysis.

2.5.1 The GoogleOCR

GoogleOCR consists of five main processing stages and their corresponding subsystems (Mittal & Garg, 2020). Given a document or images with texts, text detection, direction identification, script identification, text recognition, and layout analysis are the main steps GoogleOCR undergoes to yield analyzable useful texts (see Figure 12) successfully.

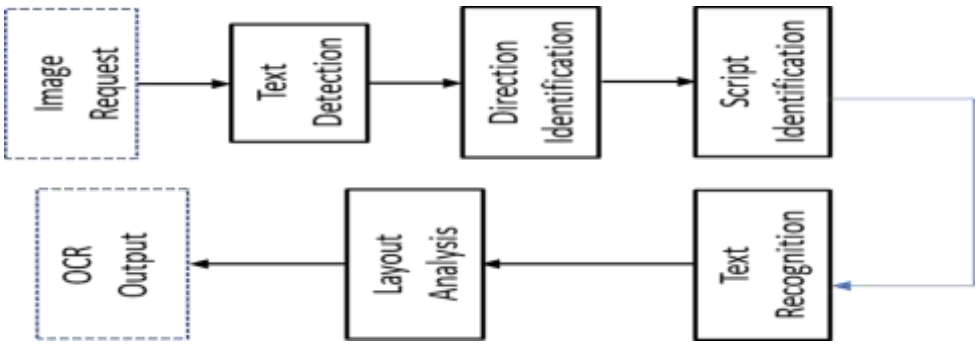

Figure 12: The Processing Stages of Typical GoogleOCR Engine.

GoogleOCR uses a CNN network to detect and locate lines of text in an image through heatmap or pixel-level generation of text likelihood that is then deployed to produce bounding box sets (Walker et al., 2018). Individual line of text detected corresponds to each bounding box. Furthermore, the direction of the text characters in a single line is classified in the direction identification stage, which screens out specific lines that were incorrectly detected as texts. Individual character direction is permitted per line of text, but various lines in a particular document are allowed to have different directions. In the script identification stage, main scripts are identified with the assumption that an individual line possesses an individual dominant script and that multiple lines are permitted in that particular document to have different scripts. To minimize the occurrence of false script classifications, a heuristics scheme was deployed in the direction identification stage to make bias decisions on the detected scripts somewhere else on the document.

In the text recognition stage, lines in images are transformed into codepoints of unicode sequence, which is the actual OCR step. Text characters are made up of single or multiple codepoints. In this stage, a language model based on the N-gram character serves as the primary input. A log-linear approach fuses the optical model as the backbone model with a customized decoding algorithm for the OCR task. Language identification is conducted on individual lines and unveiled as annotation from the previous stage's output. Invariably, an individual model is deployed per script instead of language in the GoogleOCR model. The fusion of the character-based algorithm with the inception-driven CNN (see Figure 13) is highly capable of exploiting the image text contextual information; that is why a combination of bidirectional LSTM and CNN yielded little or negligible performance gains. The inference structure or the layout

analysis determines the reading organization of the generated texts through entity classification and differentiation of titles, headers, footers, and page numbers. The layout analysis functionality is confined to the generation of text blocks and paragraphs by performing segmentation on the texts that were recognized from the previous state. A common bottom-up clustering approach was adopted to identify text blocks, in which each block is positioned as an individual line and neighboring blocks combined recursively until the set heuristic standard is achieved (Fujii et al., 2015).

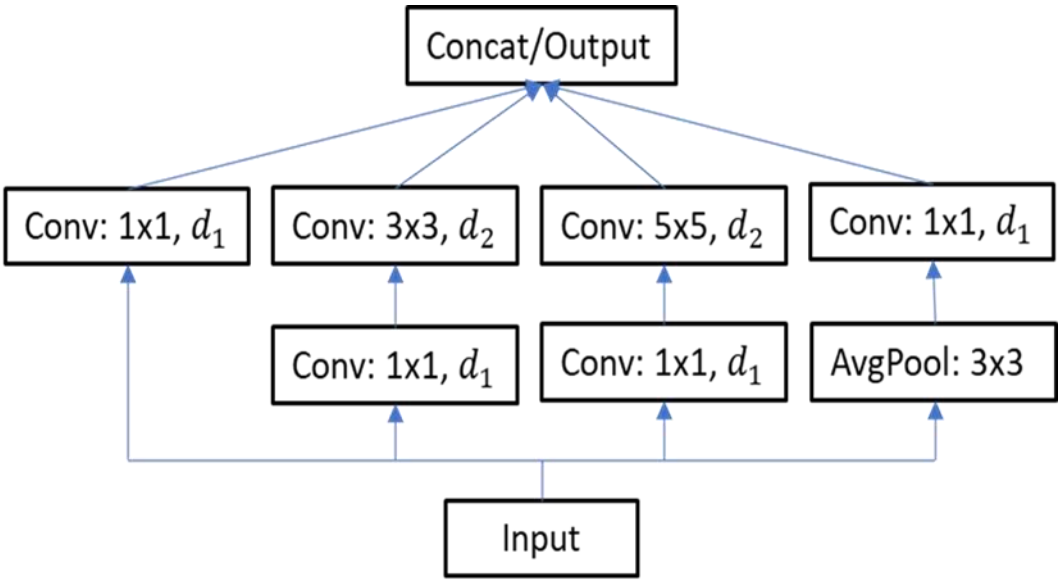

Figure 13: Inception Architecture with Custom Decoders for OCR (Fujii et al., 2017).

2.5.2 The Tesseract OCR engine

Tesseract is undoubtedly one of the most famous open-sourced OCR engines in recent times. The journey of Tesseract started in the HP Labs as a Ph.D. research project before becoming a possible hardware or software add-on. The Tesseract project was motivated because of the abysmal performance of the existing OCR engines at that time. After collaborative work between HP's Colorado scanner division and HP Labs Bristol (Smith, 2007), Tesseract achieved a remarkable lead in performance over other OCR engines. Overtimes, Tesseract has undergone a series of transformations in terms of algorithm and architectural improvements and has improved significantly in accuracy.

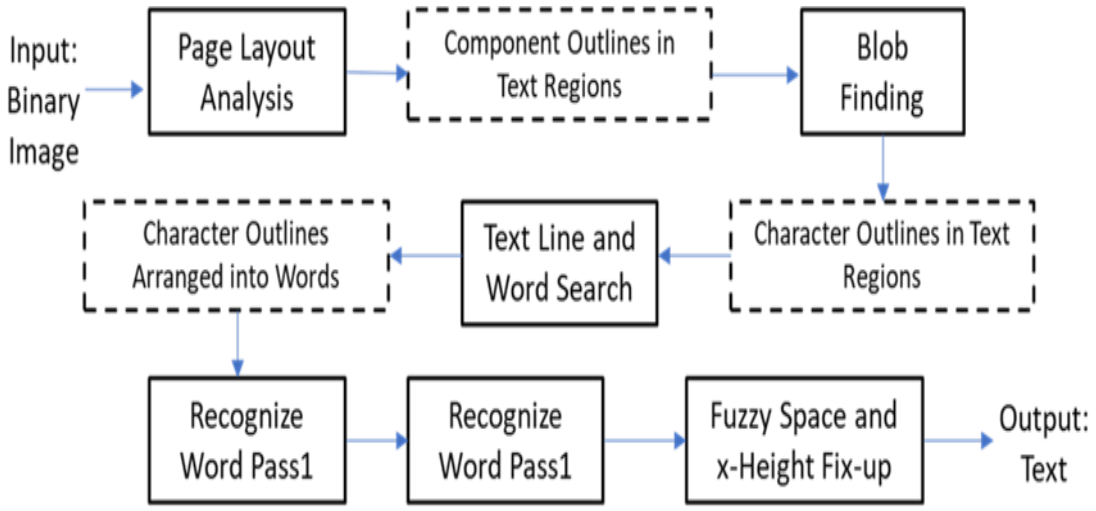

Figure 14: Tesseract Process Top-level Block Diagram (Smith et al., 2009).

Tesseract adheres to the conventional step-by-step image text processing pipeline with some distinctive phases (see Figure 14). Tesseract begins by performing connected component analysis on text images that hold the outlines of the components. This technique was computationally expensive at the inception period of the engine, although with a significant edge. It was easy to detect inversely aligned texts and recognize texts that were in black-on-white format through the nested outline inspections approach. In the early OCR research, Tesseract was perhaps the first optical recognition engine to process at ease white-on-black text formats. By the nesting processing scheme, text outlines are fused to form blobs that are arranged into text lines. The resulting text regions and lines undergo further scrutiny to obtain proportional texts or fixed pitch. With respect to the character spacing, the text lines are split to form words separately, and the fixed pitch texts were sliced using the character cells and the fuzzy spaces together with the definite spaces deployed to slice the proportional texts into words.

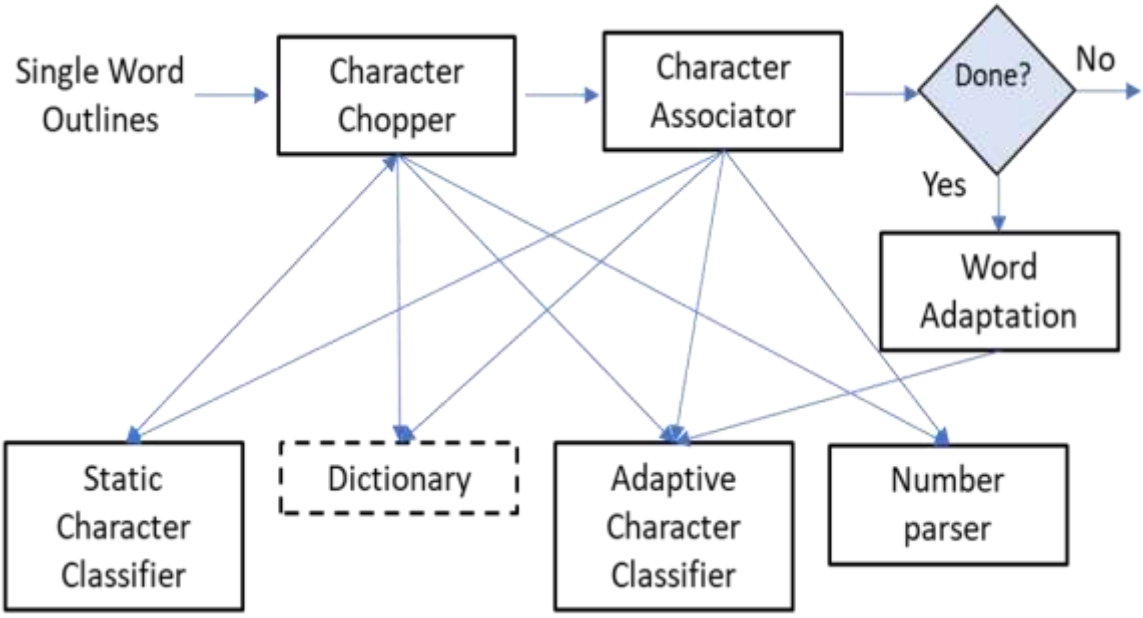

Figure 15: Tesseract Word recognition Block Diagram (Smith et al., 2009).

In the Tesseract text recognition processing phase (see Figure 15), the actual text recognition is performed in a 2-pass processing procedure. An effort is made to recognize individual words in the first pass process, and the emanating satisfactory word is forwarded to the adaptive classifier to constitute the training data. This allows the adaptive classifier to recognize more accurately texts positioned at the lower edge of the page. Then a second pass processing step is performed across the page to recognize accurately the words which were sparingly recognized in the first pass process. Then, alternative hypotheses checks are performed on the x-height to find texts with small caps in the final fuzzy space phase.

2.5.3 The Easy-OCR and Keras-OCR

EasyOCR is an optical character recognition system built with the Python and PyTorch deep learning libraries. It uses the Character-Region Awareness for Text detection (CRAFT) algorithm (Y. Baek et al., 2019) to detect texts from images and the Convolutional Recurrent Neural Network for text recognition tasks. It consists of three main parts, the CRAFT, ResNet+LSTM+CTC architecture, and the greedy decoder (see Figure 16). In the framework, an image having texts is acquired, preprocessed, and parsed to the CRAFT to detect the texts on the image. Intermediate processing is performed, and the learned features are forwarded to the ResNet+LSTM+CTC for text recognition before decoding is performed.

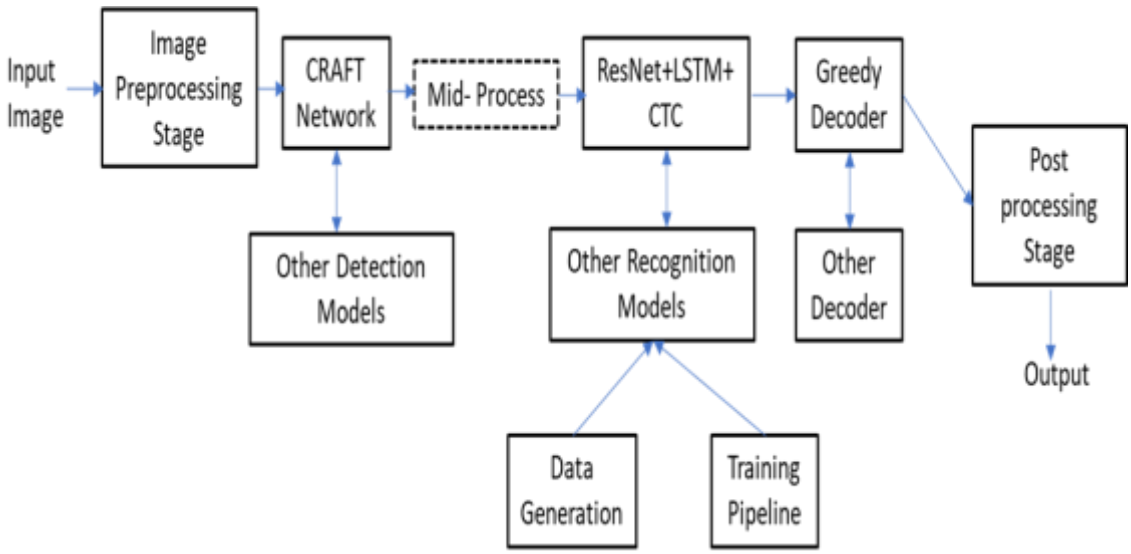

Figure 16: A Cross-Section of the easyOCR Framework.

The CRAFT (Y. Baek et al., 2019) uses a fully convolutional network architecture (Simonyan & Zisserman, 2014) and batch normalization as a backbone network to learn features from text images. In the CRAFT decoder, U-net-like skip connections were used to perform aggregation of tiny left-over features with affinity score and region score as score maps for the final outputs. The ResNet+LSTM+CTC fuses the residual network layers, the long-short-term memory algorithm, and the connectionist temporal classification classifier to recognize texts from the image texts. On the other hand, Keras-OCR is an optical recognition model with an end-to-end training pipeline based on a Keras deep learning framework.

2.5.4 The PaddleOCR

The practical ultra-lightweight OCR (PaddleOCR) is a parallel distributed deep learning-based OCR. It is a lightweight machine learning-based optical character recognition model that strives to strike an equal balance between the accuracy of the optical character recognition system and the computational inference load (Du et al., 2020). The system uses a differentiable binarization network specializing in conventional segmentation networks as a backbone model for text detection (Liao et al., 2020). The differentiable binarization postprocessing activities of the model drastically improved the efficiency of the model, and to assist the differentiable binarization efficiency enhancement drive; six strategies were adopted in the model.

The six approaches adopted for the system efficiency and effectiveness drive include the removal of the SE module, introducing cosine learning rate decay, light backbone,

learning rate warm-up, FPGM pruning, and light head integration. The PaddleOCR uses the convolutional recurrent neural network, which ushers in sequence modeling and feature extraction activity into the model to recognize texts. To eliminate the inconsistencies that arise in-between text prediction and their corresponding labels, the model uses the connectionist temporal classification (CTC) (Graves et al., 2006) loss as a classifier. To enhance the performance of the PaddleOCR, a new version trained with several strategies has been introduced (Du et al., 2021). In the new model, a collection of strategies and tricks were proposed to improve the robustness, accuracy, and processing speed of the previous version of the OCR model.

Despite the recent exploits of the aforementioned OCR engines and others in extracting printed documents, they perform poorly in other text extraction tasks that are outside of the domain of the texts they were trained to recognize (Grieggs et al., 2019), except the GoogleOCR that is robust on different OCR tasks. Other factors contributing to the OCR models' drawbacks are the complexity of the image text to be processed and text variation caused by different sources (Dong et al., 2015). The complexity varies from text background, font size and color, and texture to text character level orientations. These image text complexities abound in the anesthetic drug labels whose strings are to be extracted in this work. Therefore, GoogleOCR, which is robust in extracting texts from different kinds of images, shall be deployed to extract texts from the anesthetic drug labels for processing. A comparison of various OCR engines for extracting matchable and analyzable strings from 52 ampule images is shown in Table 2 below. Table 2 shows the performance of the OCR engines on the horizontally well-aligned texts on the ampule containers.

2.5.5 Comparative Study of the OCR engines on the Extraction of Matchable and Analyzable Strings from the Ampule Images

To achieve the goal of this research project, the adopted computer vision-based anesthetic drugs recognition approach needs to be robust in recognizing the ampule containers, sensitive, accurate, fast, and efficient. The choice of an optical recognition engine plays a critical role in meeting the aforementioned characteristics and, in general, extracting the analyzable strings from drug containers.

In the first OCR engine comparative study, 52 frequently used ampules in the operating theatre were used. The test environment was an anaconda-python environment with a 16GB memory computer that runs on a Windows operating system. In the study, the texts in all the ampule images were extracted using each of the five selected OCR engines (GoogleOCR, KerasOCR, EasyOCR, and PaddleOCR). The original strings from the ampule images were compared with those extracted from each OCR engine, and the outcomes were tabulated (see *Table 2*). Text alignments on the ampule images were not considered in this test.

Table 2: Performance of OCR Engines in the Extraction of Texts from the Selected Anaesthetic Drug Containers.

OCR Engine	**Number of Extracted Images (n)**	**Number of Images not Extracted (n)**
GoogleOCR	52	0
Pytesseract	8	44
EasyOCR	26	26
KerasOCR	22	24
PaddleOCR	26	26

As shown in Table 2, the results obtained from the first study, GoogleOCR successfully extracted analyzable and matchable strings from all 52 ampule sample images. In contrast, Pytesseract successfully extracted only eight samples and failed to extract 44 samples correctly. Meanwhile, EasyOCR successfully extracted analyzable and matchable strings from 26 sample ampule images and was unsuccessful in extracting 26 samples. On the other hand, KerasOCR performed well in extracting 22 ampule image strings and failed 24 samples. Finally, the PaddleOCR extracted correctly matchable strings from 26 ampules and failed to extract 26 samples as EasyOCR.

This second study is similar to the first; however, ten samples of images were used, and an optimal string measurement method was used to measure the difference between the strings extracted from the various OCR engines and the original strings extracted from the ampules. Table 3 shows the performance of the OCR engines on the horizontally well-aligned texts on the ampule containers.

Table 3: Performance of OCR Engines on the Extraction of Analyzable and Matchable Strings on Horizontally Well-Aligned Texts on Sample Ampules.

Drug Name	GoogleOCR	KerasOCR	EasyOCR	PaddleOCR
Paracetamol Cabi	0.98	0.65	0.79	0.83
Hypnomidate	1.00	0.84	0.92	0.96
Suxamethonium	1.00	0.74	0.93	0.96
Solu-Medrol	0.91	0.79	0.85	0.83
Fentanyl	1.00	0.59	0.83	0.88
Pancronium	0.92	0.78	0.89	0.88
Metoprolol	1.00	0.90	0.93	0.89
Remifentanil	0.96	0.81	0.87	0.86
Sodium Chloride	1.00	0.59	0.88	0.92
Glyceryl	0.96	0.75	0.88	0.92

As shown in Table 3, GoogleOCR performed exceptionally well in extracting useable strings from the selected 10 sample ampule containers. It yielded 100% extraction accuracy on five samples, 98% and 96% on three ampule samples, 91% as the least accuracy obtained, and 97.3% overall average. On the other hand, KerasOCR recorded 90% as the highest extraction accuracy, 59% as the least ampules' container string extraction accuracy, and 74.4% as the average ampules' container string extraction accuracy. In continuation, the study revealed that EasyOCR obtained 93% highest extraction accuracy, 79% least extraction accuracy, and 87.7% average ampule contain string extraction accuracy, whereas, PaddleOCR recorded 96% highest ampules' sample string extraction accuracy, 83% lowest, and 89.3% overall average. According to the healthcare usability accuracy threshold, GoogleOCR yielded performance accuracy worthy of adoption in the project.

The processing time is equally an essential factor to consider when selecting an appropriate OCR engine for the drug strings extraction and specific drug identification in the operating theatres. It is the amount of time needed to acquire a drug container label image, extract strings from the captured image, analyze and match the strings, and output the specific drug identified. During the OCR engine comparative studies, the processing speed or the time required to capture and extract strings from the anesthetic drug label images was recorded. GoogleOCR used an average of 0.6 seconds to extract strings from each sample drug image, KerasOCR 8 seconds, PaddleOCR 15 seconds, and EasyOCR 28 seconds. Meanwhile, the set time threshold for each drug

identification cycle is 1 second, and from both studies, GoogleOCR is well suited for the drugs containers' label image string extraction.

In this work, the OCR serves as the character string extractor from the drug ampules; it does not read the labels nor recognize the drugs directly. The OCR will play a vital role in the proposed framework because the conventional deep learning image classification system or object detection models cannot give us the desired accuracy and confidence needed for anesthetic drug identification. This is due to the challenging features of the ampule containers, which include tiny and diverse texts on the drug containers, highly similar drug containers, and the small stature of the ampule containers. Finally, healthcare is critical, and high accuracy and standard are required.

2.6 Research Gaps

Using computer vision methods to identify anesthetic drugs in the operating theatre is a promising approach to reducing drug administration mistakes. However, there are nonetheless significant research gaps in this area. One of the critical challenges is the variability in anesthetic drug labeling and presentation. Different manufacturers use different labeling for their drugs, making it challenging for computer vision systems to recognize and identify them accurately. Therefore, further research is needed to develop more robust computer vision algorithms that recognize anesthetic drugs despite variations in packaging and labeling.

Another research gap is that most existing anesthetic drug identification systems rely on barcodes or QR codes to identify and recognize drugs. This implies that barcodes or QR codes must be embedded on the drug vial or ampule labels for the systems to work efficiently. However, not all anesthetic drug manufacturers append barcodes to the anesthetic drugs. Therefore, for the drugs to be prepared for administration to patients in the operating room, human interventions are still needed to read the content of the drug containers to prepare them; however, this is prone to errors. In continuation, there is no existing accurate way to automatically identify ampules if barcodes are absent. In real-time, no attempt has been made to use computer vision to reliably identify, recognize and extract critical features from anesthetic drug vials and ampules.

Several issues abound regarding the use of the manual color-coding system to identify anesthetics drugs in the operating theatre. These range from the inability of the color-coding system to identify an exact drug to be administered to a patient and the issues of drug mix-ups due to drug selection errors among drug classes. In addition, the forgetfulness of medical personnel to remember multiple complex color codes, color blindness, and negligence of the label reading by healthcare personnel in critical conditions because of lack of time to identify the drug colors, shapes, and sizes.

Lastly, challenges also abound in the use of drug appearance, intensity, and landmarks to identify medications in the operating theater due to the considerable training needed to build different distribution models for the tasks. There are also high computational requirements for feature extractions when using landmark extraction methods to identify drugs in the operating rooms and low sensitivity to light variations. According to findings in this work, drug vials and ampule color, height, width, and weight measurements are not feasible for identifying specific drugs in the operating theater as some drugs have the exact features with only the drug names and rate-of-substance, the differentiable factors among them.

Therefore, the proposed framework will eliminate the gaps above and usher in a rapid drug identification method that meets the real-time requirements for anesthetic drug feature recognition and identification in the operating rooms. This research will also help healthcare organizations make informed decisions about adopting computer vision frameworks for drug identification and improving patient safety.

2.7 Chapter Summary

The purpose of the investigation conducted and reported in this chapter was to explore the existing anesthetic medication identification and verification system in order to understand their working process and identify the existing challenges. The study explored the various existing technologies for anesthetic medication verification, including but not limited to barcode and Qrcode systems and color coding. The existing scene text detection and recognition literature and how they could assist in detecting, recognizing, and identifying anesthetic drugs are also reported. Various object-text scene detection algorithms and models were studied, including the classical conventional and modern scene text detection methods driven by deep learning

models. In addition, several scene text recognition pieces of literature were investigated, spanning from the classical models to the recent deep learning algorithms.

Furthermore, the optical character recognition system was deeply investigated to narrow the search for the best suitable method of identifying anesthetic drugs. In this sub-study, various existing OCR engines were investigated with their corresponding experiments. To obtain the best OCR engine that could rapidly and accurately extract analyzable text characters from the anesthetic labels, a cumulative of 52 anesthetic drug containers that are frequently used in the operating theatres were used to test the selected OCR engines. The performance of the engines was analyzed in terms of text extraction accuracy, processing speed, and reliability. GoogleOCR was more suitable than the KerasOCR, EasyOCR, and PaddleOCR tested during the investigation in this chapter.

Chapter 3 Feature Detection, Extraction, and Matching for Anesthetics Medication Identifications

3.1 Introduction

In this chapter, conventional image feature detection, extraction and matching techniques were thoroughly investigated for the identification of the Anaesthetic medications and the outcome presented. In the study, the relevant algorithms for real-time image frames detection, extraction and analysis were tested, and their results were analyzed for suitability in the identification and recognition of the different kinds of anesthetic drugs used in the operation theatres during procedures.

3.2 Background of Feature Detection, Extraction and Matching

Exploiting images for the detection of the vital features present in them, describing the detected features, and matching the various components of the features for identifying a particular object are the vital computer vision processes that have drawn considerable interest in the past decade. Numerous algorithms for feature detection, description and matching (Chen et al., 2021) have emerged in recent times and have made a considerable impact in various scientific fields involving object identification and recognition (Gupta et al., 2019), image classification and representation (Loussaief & Abdelkrim, 2016), textual classification, and general information retrieval (Salau & Jain, 2019). The identification of a collection of salient points that exist in each image amongst a set of images is vital for establishing relationships between the image set, wherein the correspondences present among the images are required (Burghardt et al., 2015).

In object identification tasks like the anesthetics medication identification, the obtained image feature descriptors and the fixed trained features of other images are matched. The image with the highest relationship is returned as the best match and, in turn, the identified image. This image features description and matching process corresponds to the Mahalanobis or Euclidean distance estimation method (Pushparaj et al., 2013). On the other hand, the spatial alignment of two or more images captured at different times with different camera sensors is needed to perform image registration. The main steps taken to perform image alignment or registration are;

image feature detection, matching of the detected features, deployment of the relationships extracted from the image features for transformation functions derivation and the use of the derived transformation functions to reconstruct the images. For the matching and recognition of a specific anesthetic drug container, the detection of regions of interest and their description is the initial step process, followed by a comparative process that yields the relationship that exists among the drug containers which are needed to conduct the actual recognition tasks. The underlining idea is to initially detect key points which are in tandem with the image class transformations before the feature representations of the invariant features in the drug image are constructed. The extracted features from a given drug image can rely on one or a combination of the coefficients derived from the image transformations, the second-order statistics, or the parametric models.

The global and local features are the main two classes of features extractable from any given anesthetic image feature representation. For instance, the anesthetic image texture and color or, more succinctly, global features provide a description of the image and are said to be the defining characteristics of the image that deal with pixels. On the other hand, interest points or key points present in an anesthetic image sample are detected and described by the local features. More succinctly, if k key points are detected from an anesthetic image by the local feature process, then k vectors that describe the texture, color, shape, orientation and other properties of the anesthetic image are needed. For the anesthetic image similarity estimation tasks, the exploitation of the global texture and color features on the images has yielded remarkable achievements. In determining the presence of the same object in a scene or image classification task, the local structure-oriented features perform well (Zhang et al., 2014). However, the foreground and background that exists in an image cannot be distinguished by the global features and thus mix image properties from various regions of the image together (Mikolajczyk & Tuytelaars, 2008).

As the demand for local descriptors that can run on embedded devices with less memory and computational capabilities grows in recent times, the need for local descriptors that can process images fast with less computational and memory requirements, efficient feature matching with great accuracy and precision has become inevitable. On image feature matching on embedded devices, local feature

descriptors have shown remarkable achievements and are suitable for handling missing objects and occlusion (Valgren & Lilienthal, 2010). Robustness to variation in viewpoints, brightness and image distortions is pertinent for use cases such as object tracking and recognition, image classification, camera calibration and image retrievals (Chen et al., 2009). On the hand, specialized object detectors and descriptors are a requirement for visual recognition problems like detecting and recognizing human faces, the anesthetic drugs, etc. (Viola & Jones, 2004).

Many image feature extraction approaches have been proposed in different literature for reliable image description computations. Most of the researched feature descriptors are specialized in function and utility, like the object shape matcher (Janan & Brady, 2015; Viola & Jones, 2004). An example of the image descriptors is the scale-invariant feature transform (SIFT) (Lowe, 2004) descriptor that deploys local extrema that exists in the diverse Difference of Gaussian (DoG) functions to extract image features. Also, the speeded-up robust features (SURF) (Bay et al., 2008) descriptor driven partly by the SIFT descriptor is another type of image feature descriptor used to process fast, the distinguishing invariant local features inherent in images and are commonly used in different scientific domains. A collection of nonlinear operators and hand-crafted filters are deployed by these image descriptors to represent salient points that exist in a sample image region. In computer vision and image processing, features extracted from images are vital in representing the images during processing. It is quite easy to extract useful information from images by natural eyes, but it is a different scenario when it comes to computer vision algorithms. Local and global feature representations are the main conventional means of representing images by computer vision methods.

3.3 Local Image Features for Anesthetics Medication Identifications

Local image features are often referred to as interest regions or interest points because they possess a set of linked pixels or patches and have related spatial features. The image characteristics that are usually classed as local features are textures, color, and intensity (Mikolajczyk & Tuytelaars, 2009). Any subsection of an image can be an interest point, unlike classical segmentation, and it is not necessary for the boundaries on the image regions to match the image appearance variations like

the texture or color changes. In local image features, overlapping of various regions is possible and homogeneous areas or irrelevant regions can be uncovered. The exploitation of local features in an image is a strategy that has yielded tremendous impact in solving many scientific problems ranging from object recognition tasks and wide baseline object matching to object class recognition (Mikolajczyk & Tuytelaars, 2008). The leverage on object or image local features has reduced the reliance on semantic-level segmentation in handling object identification tasks. Instead of segmenting anesthetic images into background and foreground entities – a difficult and computational expensive process, a collection of overlapping image segment regions can be used to represent the image. Then higher-level processing phases, extract critical information from the image segments.

The local features deliver a collection of highly localized and distinct identifiable and anchorable properties or points, and these have increased the interest in its use in the exploitation of object local features. In local image feature processing, it is irrelevant to determine what individual features represent, provided that each feature location can be accurately determined over time in a stable manner. This can be extremely assistive in image matching, pose estimation, image mosaicking or image alignment. In the absence of conventional image segmentation, robust image representations can be performed for recognizing objects using a collection of local image features in which the precise location of the features is not needed since the individual matching of the features is not the core objective rather than their statistical analysis. Over time, interest points extraction has drawn large scientific interest, and a collection of studies have proposed several ways of extracting them from the extrema of several functions derived from digital shape computations. Local invariant features present in images are useful in finding correspondences in the images even in extreme variations in viewing circumstances, clutter and occlusions. They are also beneficial in describing the content of images needed for performing image retrieval tasks and solving object recognition and identification challenges.

3.4 Global Image Features for Anesthetics Medication Identifications

In the aspect of global image feature representations, a single multidimensional feature vector is used to represent images that provide the information or description

of the entire image. This implies that a single feature vector is generated by the global feature representation having values that measure the diverse properties of the image like the shape, color, or texture. For instance, to differentiate two anesthetic drug images with two different colors, separate vectors for each image are generated from the global color descriptor. The extractable properties using image filters could be specific descriptors or the edges, color histograms or the textures (Oliva & Torralba, 2001). Also, the global feature representation is helpful in solving scientific problems that have the object or image being processed roughly segmented. The derived benefit of global feature representations over the local feature representations is the compactness of the extracted features, less memory consumption and computational efficiency. However, global feature representations suffer from occlusion, sensitivity to clutter, and non-transformational invariant. The choice of image feature representation depends solely on the tasks at hand, and feature representations that have high discriminative tendencies are mostly preferred (Tuytelaars & Mikolajczyk, 2008).

Depending on how they are observed, digital images with objects like the anesthetic containers look differently, and their variations in scale are of utmost significance when they are analyzed. For the detection and extraction of the invariant features on the images, several approaches have been suggested in different pieces of literature. A collection of the methods is built to handle the image scale variations, while others are designed to solve the challenges of the affine transformation. In solving the scale change problems, the variations in scales are assumed to be uniform or the same in all directions by the processing algorithm. During processing, if variations in the image size are encountered, a processing filter is repetitively utilized on it for the successive layers smoothing or by setting the main image untampered with while adjusting the size of the filter only. By deploying attributes such as rotations, translations, shears, flips and scales, affine transformations can be achieved. Any linear mapping that conserves the distance ratios and collinearities that exist in images is said to be affinity or affine transformation.

3.5 Image Feature Detection (IFD) for Anesthetics Medication Identifications

The IFD is the computational approach for abstractions obtained from image data that pioneers decision-making for each point of interest on a given image. The outcome of the feature detection process is a subset of the larger domains in the image, which usually occur as isolated points, connected regions, or continuous curves (Truong & Kim, 2016). Image feature detectors are organized into three main groupings: single-scale detectors (Hassaballah et al., 2016), multi-scale detectors (Fu et al., 2018), and affine invariant detectors (Mikolajczyk & Schmid, 2002). Using the internal parameters of image detectors, only a single object contour representation or features can be found on a single scale paradigm. The single-scale detectors are immune to the image properties variation perturbations such as noise addition, illumination variations, translation and rotations resulting from them. However, single scale detectors suffer from the problems of image scaling. On the other hand, a multiscale detector is necessary in scenarios where it is needed to extract reliable distinctive features from objects or images with changes in scale. For instance, to determine the existence of similar interest points in two anesthetic images captured from the same environmental condition but with different scale variations, a multi-scale detector is required since single-scale detectors have issues processing varying image scales. Intensity-based detectors use first-order or second-order derivatives to determine the availability of corners in an image and the computation of the corner response function (CRF) per pixel in the image (Luo et al., 2020).

3.5.1 Single-Scale Image Feature Detectors (SSD) for Anesthetics Medication Identifications

Many SSDs have emerged from past research over time. These include the Moravec detector, Harris detector, SUSAN detector, FAST detector, and Hessian detector. The Moravec detector is an SSD that performs computations between patches on images to determine the local sum of squared differences (SSD) between the images in four directions (Luo et al., 2020). In other words, distinct regions that exist in an image can be determined using a Moravec detector for the consecutive registration of frames on the image. Moravec detector can also play a vital role in detecting corners with little self-similarities. During processing, the Moravec detector algorithm checks individual

pixels present in an image to determine the presence of corners. Then the sum of square differences (SSD) is used to measure the similarity between the central patch and patches on the other regions of the image. When working with an SSD algorithm, it is assumed that there is a slight variation or neighboring patch similarity if a uniform-intensity image pixel region occurs. The neighboring patches that are directionally parallel to the edge yield slight variations when the pixel is on the edge or significant variations if the edge is in a perpendicular direction to the patches.

However, suppose the pixel is located in regions with considerable variations in all directions. In that case, neighboring patches will be dissimilar, and corner detection can only occur when the resulting variations from any of the changes are significant. Cornerness is measured using the tiniest SSD among the patches and their nearby properties, such as the diagonals and vertical and horizontal leanings. When the SSD attains local maxima, an interest point or a corner is detected. An image must be perpendicular to an edge for a non-maximum suppression operation to be performed on it, and it needs to be scanned in the direction of the gradient. Suppression is performed on any non-local maximal pixel, and the pixel is set to zero. The ability of the Moravec detector to detect many diverse corners is the benefit of its use. However, it is non-isotropic; this implies that changes in intensity are computed as a collection of the discrete set of shifts and edges not found in the direction of the eight neighbors designated to be measured as large cornerness. This invariably means that the Moravec detector outputs a poor repeatability rate because it is non-invariant to rotations.

To solve the aforementioned limitations of Moravec's detector, Harris and Stephens (1988) proposed an algorithm that jointly detects edges and corners in an image. In the study, they obtained a more desirable model with a better repeatability rate and feature detections by determining the intensity variations or autocorrelation changes in all the image orientations. The detector they invented using the auto-correlation matrix technique was extremely useful and has recently been applied in different image-processing domains. In detecting features from images and their local structural description, a critical 2×2 symmetric autocorrelation matrix is illustrated in Equation 3.1.

$$\beta(\alpha 1, \alpha 2) = \sum_{\beta 1, \beta 2} w(\beta 1, \beta 2) * \begin{bmatrix} \theta_{\alpha 1}^2(\alpha 1, \alpha 2) & \theta_{\alpha 1}\theta_{\alpha 2}(\alpha 1, \alpha 2) \\ \theta_{\alpha 1} d_{\alpha 2}(\alpha 1, \alpha 2) & \theta_{\alpha 2}^2(\alpha 1, \alpha 2) \end{bmatrix} \quad 3.1$$

Where $\theta_{p1}\ and\ \theta_{p2}$ represent the derivatives from the local image in the direction of $p1$ and $p2$ pixels, respectively and $w(\beta 1, \beta 2)$ is the sliding window weight over the $(\beta 1, \beta 2)$ region. An isotropic response will occur if a Gaussian window or other circular window is utilized, and a heavier value will be obtained close to the center. Also, eigenvalues of the matrix β are calculated separately for all pixels in order to obtain interest points. A corner is said to be spotted in a particular region if the resulting eigenvalues are large. A response map can be built by computing the cornerness measure $C(\alpha 1, \alpha 2)$ for $\alpha 1\ and\ \alpha 2$ respectively, using

$$\beta(\alpha 1, \alpha 2) = det(\beta) - K(trace(\beta))^2 \quad 3.2$$

where,

$$det(\beta) = e_1 * e_2\ \ and\ \ trace(\beta) = e_1 + e_2$$

In the equation, K is used for parameter alterations and e_1, e_2 represent the eigenvalues of the matrix of autocorrelation. Due to the square root computational requirement, it is highly costly to calculate the distinct eigenvalues. So Harris proposed using the cornerness measure that fuses double eigenvalues in one measure. To determine the local maxima and all the remaining non-zero points in the cornerness map, a non-maximum suppression operation is needed to be conducted.

In their work, Harris and Stephens (1988) proposed a Smallest Univalue Segment Assimilating Nucleus (SUSAN) algorithm that uses a low-level approach to handle image processing without computing image corners with the image derivative technique. This algorithm was useful not only for detecting corners but also for image noise reduction in addition to detecting edges in an image. During processing, a circular mask with a fixated radius is positioned on each pixel found on the image for detecting the corners in the image. The central pixel is regarded as the nucleus that provides a platform for comparing the pixels in the region under the mask with the nucleus to determine their similarity or intensity values' divergence. A combination of pixels that poses relative brightness as the nucleus is unified to yield the term Univalue Segment Assimilating Nucleus (Xingfang et al., 2011) or USAN. A corner is said to be

located in a region if the number of pixels in the univalue segment assimilating nucleus approaches a local minimum and is lower than a set threshold T. The function $S(n, n_0)$, for estimating the similarity among the pixels in a particular mask and its nucleus is represented below in Equation 3.3:

$$S(n, n_0) = \begin{cases} 1, & if |I(n) - I(n_0)| \leq T, \\ 0, & otherwise, \end{cases} \quad 3.3$$

the USAN region size is given as follows:

$$s(n_0) = \sum_{n \in S(n_0)} S(n, n_0) \quad 3.4$$

where $n \; and \; n_0$ represent the coordinates of the nucleus and that of other points found in the mask (see Equation 3.4). The SUSAN is prone to noise and adverse luminance fluctuations because it relies on the comparative similarity function $S(n, n_0)$ to detect corners in images. Despite the shortcomings of the SUSAN detector, it does not utilize derivatives, making it less computationally expensive, and it does not require noise reduction techniques. Also, SUSAN has high repeatability capabilities for detecting image features and is invariant to rotations and translations. However, SUSAN is non-invariant to other image transformations like scaling and requires an adaptive threshold.

In another work, Rosten and Drummond (2005) introduced another algorithm for image feature detection referred to as Features from Accelerated Segment Test (FAST). In this method, a segment test is conducted on each pixel on an image sample using a circle of 16 pixels surrounded by candidate corners as a ground for performing computations which in turn are helpful in detecting candidate points. Despite the high performance recorded from the high-speed test, the FAST algorithm is dented with several drawbacks and weaknesses, as detailed in work by (Rosten & Drummond, 2006). The algorithm was greatly enhanced by using a machine learning approach, and the weaknesses and drawbacks were addressed. In the improvement algorithm, a decision tree algorithm (ID3) was used to learn the question ordering pixel classifier, which helped to enhance the process significantly. In continuation, more criteria are introduced to conduct the non-maximum suppression process as the initial examination generates several adjacent responses nearby the points of interest, which

permits the precisive localization of features in the image. The measure of cornerness is stated as:

$$\beta(\alpha 1, \alpha 2) = max(\sum_{j \in S_b} |\alpha_{l \to j} - \alpha_l| - t, \sum_{j \in S_\theta} |\alpha_l - \alpha_{l \to j}| - t) \quad 3.5$$

where $\alpha_{l \to j}$ represents the pixels that are found on the Bresenham circle and t the threshold value. Given that the second test is only conducted on a section of the image points that scale through the first test, the processing time required is reduced and remains minimal. This implies that a segment test is performed for the corner detection in the initial stage for a specific n value, and the collection of images is thresholded. In continuation, every pixel in the 16 regions on the circle is categorized into similar darker or brighter pixels. Consequently, an ID3 algorithm (Bhardwaj & Vatta, 2013) is ushered into the 16 locations to choose a specific pixel that produces the highest information gain. Then, on the absolute difference sum, a non-maximum suppression is engaged among the pixels found on the contiguous arc in addition to the ones in the central region. Because decision tree models rely on training data that may be limited in all possible corner coverage, the ID3 algorithm may detect vaguely dissimilar corners from those obtained with the segment test detector. The FAST corner detector algorithm is highly suitable for processing videos in real-time due to its high processing speed. Conversely, the FAST algorithm is not robust to noise, threshold dependent, and non-invariant to scale changes.

In another work, Lakemond et al. (2012) introduced a Hessian blob detector that uses a matrix of 2×2 dimension with a second-order derivative, having $I(\alpha 1, \alpha 2)$ image intensity referred to as Hessian matrix. Local image structural analysis could be performed using the proposed matrix, and it is represented in Equation 3.6:

$$H(\alpha 1, \alpha 2, \sigma) = \begin{bmatrix} \theta_{\alpha 1 \alpha 1}(\alpha 1, \alpha 2, \sigma) & \theta(\alpha 1, \alpha 2, \sigma) \\ \theta_{\alpha 1 \alpha 2}(\alpha 1, \alpha 2, \sigma) & \theta_{\alpha 2 \alpha 2}(\alpha 1, \alpha 2, \sigma) \end{bmatrix} \quad 3.6$$

The $\theta_{\alpha 1}\theta_{\alpha 1}$, $\theta_{\alpha 1}\theta_{\alpha 2}$ and $\theta_{\alpha 2}\theta_{\alpha 2}$ denote the second-order derivatives of the image, calculated with the standard deviation σ of a Gaussian function. To detect features of interest, the Hessian detector checks for point subsets with a high concentration of derivative responses in the two orthogonal directions. This implies that the detector

looks for image points that have determinants of the Hessian matrix in the local maxima and is expressed as:

$$det(H) = \theta_{\alpha 1 \alpha 1}\theta_{\alpha 2 \alpha 2} - \theta^2_{\alpha 1 \alpha 2} \quad 3.7$$

During processing, larger structures that possess small signal changes or second derivatives in one direction are penalized by selecting points whose Hessian determinants are maximized. By deploying a non-maximum suppression with a 3×3 window size on the whole image and conserving pixels with larger values than all the eight direct neighbors within the window, the detector will produce all the residual locations with higher values than the threshold T already pre-defined. The detector responses that are produced are generally found on the corners and regions with firm image textures. Furthermore, the Hessian matrix performs the description of the local structure in a region with points. In contrast, the Hessian matrix determinant conducts the detection of structures in the image that show signal variations in double directions. The Hessian matrix determinant is proficient in processing local image patterns that have noticeable changes within any two orthogonal directions compared to other operators like the Laplacian operator (Mikolajczyk et al., 2005). The Hessian detector is noise sensitive due to the introduction of the second-order derivatives, and the local maxima regularly occur close to the straight edges or contours with the signal variations happening in a single direction (Mikolajczyk & Schmid, 2004). By so doing, the localization process is influenced by the little variations in neighboring patterns or noise, thereby making the local maxima stable to a lesser extent.

3.5.2 Multi-scale Image Feature Detectors (MSD) for Anesthetics Medication Identifications

A multi-scale scheme is desirable to perform proper image feature localization and vivid edge detections in an image. The detection and analysis of edges in a given image at multiple scales provide rich information from the image needed to make vital decisions. Investigations on the fine-to-coarse (Halber & Funkhouser, 2017) and coarse-to-fine (Amit et al., 2004; Fleuret & Geman, 2001) methods of merging edges from varied scale ranges have been done. Most of these approaches initially find at each scale, the edge representations before fusing them using a heuristic algorithm. In the case of the fine-to-coarse approach, the tiny scales that detect decent edges are

chosen at nearby regions in the image. The conventional approach for the multi-scale methods involves the fusing of the resultant of each scale edge detector at multiple scales, thereby producing a synthesized edge (Sumengen & Manjunath, 2005).

The commonly used blob detector is the Laplacian-of-Gaussian (LoG) (Cho et al., 2020), a linear combination of second derivatives (Ghosh et al., 2007). Given a sample input image $I(\alpha 1, \alpha 2)$, the representation of the scale space is denoted as $L(\alpha 1, \alpha 2, \sigma)$, which is generated by performing convolution operations on the image using a Gaussian kernel $G(\alpha 1, \alpha 2, \sigma)$ of varying scale, and it is represented in Equation 3.8 as:

$$L(\alpha 1, \alpha 2, \sigma) = G(\alpha 1, \alpha 2, \sigma) * I(\alpha 1, \alpha 2) \quad 3.8$$

where,

$$G(\alpha 1, \alpha 2, \sigma) = \frac{1}{2\pi\sigma^2} e^{\frac{-((\alpha 1)^2 (\alpha 2)^2)}{2\sigma^2}}$$

Then the Laplacian operator is calculated as:

$$\nabla^2 L(\alpha 1, \alpha 2, \sigma) = L_{\alpha 1 \alpha 1}(\alpha 1, \alpha 2, \sigma) + L_{\alpha 2 \alpha 2}(\alpha 1, \alpha 2, \sigma) \quad 3.9$$

The outcome of this expression is a strong positive response for blobs that are found in the image sample and strong negative responses for blobs that are bright in the image with the size of $\sqrt{2\sigma}$. The connection between the blob structure size in the image and the smoothing Gaussian kernel size depend highly on the operator response. The scale is controlled by varying the blurring amount using the standard deviation of the Gaussian process. An automatic scale selection multi-scale method was introduced to grab blobs that have a diverse size in the image regions automatically by performing a search for the scale-space extrema of the scale-normalized Laplacian operator (Lindeberg, 1998) as expressed below:

$$\nabla^2_{norm} L(\alpha 1, \alpha 2, \sigma) = \sigma^2 (L_{\alpha 1 \alpha 1}(\alpha 1, \alpha 2, \sigma) + L_{\alpha 2 \alpha 2}(\alpha 1, \alpha 2, \sigma)) \quad 3.10$$

This is capable of simultaneous points detection in the local minima and maxima of $\nabla^2_{norm} L(\alpha 1, \alpha 2, \sigma)$ in consideration of the scale and space, respectively. The Laplacian-of-Gaussian operator is highly invariant to rotation because it is circularly symmetric and performs exceptionally well in detecting blobs in images because of the circular symmetric property. In addition, LOG is also useful in computing the scale properties

on other image regions, such as the multiple junctions, corners, ridges, and edges. This implies that LoG can be deployed to estimate the scale properties in a specific image region or directly identify the regions with scale-invariant by looking for 3D extrema of the Laplacian-of-Gaussian function. To improve the processing speed of the LoG operators, which suffer from low processing speed, a local 3D extrema-based algorithm that is driven by the Difference-of-Gaussian filters in the image pyramid scale-space was introduced (Lowe, 2004). This algorithm was useful in building the popular scale-invariant feature transform (Lindeberg, 2012) algorithm, which will be explored in detail later in this chapter. Also, it will be used to compare the performance of the proposed string extraction and matching system and the feature extraction and matching methodology. In practice, the Difference-of-Gaussian yields a near approximation term to the LoG and is highly useful in detecting features found in the scale-space extrema of an image sample. By performing a subtraction operation on the adjacent scale stages of a Gaussian pyramid, delaminated by a factor f in the absence of convolution operations, the Difference-of-Gaussian function $D(\alpha 1, \alpha 2, \sigma)$ can be computed as:

$$D(\alpha 1, \alpha 2, \sigma) = (G(\alpha 1, \alpha 2, f\sigma) - G(\alpha 1, \alpha 2, \sigma)) * I(\alpha 1, \alpha 2)$$

$$= L(\alpha 1, \alpha 2, f\sigma) - L(\alpha 1, \alpha 2, \sigma)) \qquad 3.11$$

The LoG operators' extracted feature classes (see Equation 3.11) can be categorized similarly to that of the features extracted using the Difference-of-Gaussian operators. However, the region detectors of the Difference-of-Gaussian look for the scale-space 3D extrema located in the Difference-of-Gaussian function. Consequently, both the DoG and LoG representations suffer from small-scale variations, less stability, and higher noise sensitivity due to the possibility of detecting local maxima in nearby contours available on straight edges (Mikolajczyk & Schmid, 2004).

In another work for multi-scale image feature detections, Mikolajczyk and Schmid (2004) introduced an invariant scale-based corner detector that uses both the Gaussian scale space (Sporring et al., 2013) representation and Harris corner detector (Derpanis, 2004) to detect features from images. Despite the exhibition of invariance to illumination changes and rotation, the Harris-corner points are not invariant to scale. This led to the modification of the second-moment matrix used in the detection

algorithm to be image resolution-independent. In the Harris-Laplace detector algorithm, the second-moment matrix deployed in the scale is expressed as:

$$\beta(\alpha 1, \alpha 2, \sigma_\theta \sigma_{GK}) = \sigma_{GK}^2 g(\sigma_\theta) \begin{bmatrix} \theta_{\alpha 1}^2(\alpha 1, \alpha 2, \sigma_{GK}) & \theta_{\alpha 1}\theta_{\alpha 2}(\alpha 1, \alpha 2, \sigma_{GK}) \\ \theta_{\alpha 1} d_{\alpha 2}(\alpha 1, \alpha 2, \sigma_{GK}) & \theta_{\alpha 2}^2(\alpha 1, \alpha 2, \sigma_{GK}) \end{bmatrix}$$

Where $\theta_{\alpha 1}\ and\ \theta_{\alpha 2}$ represents the derivatives of the images computed with the scale σ_{GK}Of the Gaussian kernel, respectively. In the Gaussian scale-space, the present scale is obtained using the σ_θ parameter for the detection of the Harris corner points. This implies that the size of the gaussian kernels deployed to calculate the derivatives is determined using the scale derivative σ_{GK}. Whereas the weighted average of the derivatives in nearby points is performed using the σ_θ scale. For calculating the measurement of the Harris cornerness of multiple scales, the trace obtained from the second-moment matrix in combination with the determinant is used as:

$$C(\alpha 1, \alpha 2, \sigma_\theta \sigma_{GK}) = det[\beta(\alpha 1, \alpha 2, \sigma_\theta \sigma_{GK})] - \emptyset . trace^2[\beta(\alpha 1, \alpha 2, \sigma_\theta \sigma_{GK})] \qquad 3.12$$

The introduced constant Ø in Equation 3.12 is calibrated between 0.04 and 0.06 values. Interest points are extracted through the detection of local maxima in points $(\alpha 1, \alpha 2)$ within the 8-neighbourhood at each phase of the feature representations. To eliminate cornerness with small maxima that may induce instability in conditions of arbitrary views, a threshold is set which ensures their stability as:

$$C(\alpha 1, \alpha 2, \sigma_\theta \sigma_{GK}) > t_H$$

t_H is the Harris threshold. In continuation, to obtain the scale maxima point, the Laplacian-of-Gaussian is employed to ensure that the responses that are above the set threshold value or the points wherein the Laplacian reaches maxima points are allowed. That is,

$$\sigma_\theta^2 |L_{\alpha 1 \alpha 1}(\alpha 1, \alpha 2, \sigma_\theta) + L_{\alpha 2 \alpha 2}(\alpha 1, \alpha 2, \sigma_\theta)| > t_L \qquad 3.13$$

Where t_L represents the Laplacian threshold in Equation 3.13. A collection of representative points is generated by the Harris-Laplace method that are dominant image characteristics as well as the dimension of the scales. Compared to the Multi-scale Harris method, this approach minimizes to the barest minimum the amounts of redundant interest points, invariant to rotation, illumination, scale variations, and

noise introduction. Since the repeatability of the interest points is high, fewer pints are generated by the Harris-Laplace detector in the advantage when DoG or LoG detectors are used. However, failure in situations where affine transformations occur is the major drawback of this approach.

In another work that is similar to the Harris-Laplace approach, a scale-invariant detector was obtained by applying the same concept used in the Harris-Laplace, to obtain an image feature detector referred to as the Hessian-Laplace detector (Bhatia, 2007). In a Hessian-Laplace detector, DoG filter approximations or Laplacian filters are initially utilized to construct a representation of an image scale space, followed by the extraction of the image scale-invariant features similar to blobs using the Hessian determinants. A large number of image features are extracted by the Hessian-Laplace detector that overshadows the entire image sample with more reduced repeatability, unlike the Harris-Laplace method. Also, because of the close similarity of the filters deployed in the localization of the scale and spatial features, extracted locations using the Hessian-Laplace approach are more suitable for scale estimation tasks, and the second-order Gaussian derivatives are relied upon by the two features. The stability and suitability of the Hessian-driven detectors over the Harris-driven detectors were further validated in work by Bay et al. (2008). To obtain a faster Hessian detector, an integral image approach (Viola & Jones, 2004) was deployed to perform the Hessian determinant approximation (Yang & Niethammer, 2015), similar to the DoG acceleration method through the approximation of the LOG function.

In another work on image features detection, a Gabor wavelets-inspired approach that detects multi-scale interest points was introduced (Yussof & Hitam, 2014). The Gabor wavelets are plane wave-shaped and confined in a Gaussian envelope function. They are also biologically inspired convolution kernels like the 2D receptive field response found in the cortical cell of mammalians. They are controlled by the Gaussian envelope function and are formulated like a complex plane wave. That is,

$$\theta_{o,s}(\alpha) = \frac{\left|\left|K_{o,s}\right|\right|^2}{\sigma^2} e^{\left(\frac{\left|\left|K_{o,s}\right|\right|^2 |\alpha||^2}{2\sigma^2}\right)} \left[e^{i\alpha K_{o,s}} - e^{\frac{\sigma^2}{2}}\right] \quad 3.14$$

Where $K_{o,s} = K_s e^{i\emptyset o}, \alpha = (\alpha 1, \alpha 2),\ o\ = orientation\ of\ the\ Gabor\ wavelets,\ s\ = scale, K_{o,s}\ = K_{max}/f^s$ and $\emptyset o\ = \pi o/8$, the maximum frequency is represented by K_{max} and the space factor that exists between the kernels in the domain of the frequency is denoted by f.

The information found in the local image domain is represented by the convolution coefficient, which is more active when compared to that found in the isolated pixels. Optimal resolutions are generated simultaneously in the domain of the unique frequency and space by the Gabor wavelets, which gives them an edge over the other image feature detectors. Also, the Gabor wavelets can improve low-level image features like ridges, peaks, and valleys. By fusing multiple image orientation responses together, Gabor wavelets can also be used to extract points from an image sample at different scales. The extraction of the interest points at multiple points is made possible by unifying the space orientation homogeneously. Gabor-wavelet-based image feature detector was shown in the study to withstand extreme geometric transformations and yield high accuracy.

3.6 Image Feature Description for Anesthetics Medication Identifications

An appropriate image descriptor is required for image discriminative matching and the deformation of local image regions that are insensitive. This could be performed after the detection of points of interest in a given sample of an image in a $\alpha(\alpha 1, \alpha 2)$ location, s scale and O orientation. Then the structure or content of the image nearby point p requires encoding using the right descriptor. The descriptor needs to be proportional to the scale (s) and well-aligned to the orientation (O). In recent times, numerous image feature descriptors have emerged; however, in this work, the most regularly used image descriptors will be explored, and the appropriate one will be used to detect, describe, and match features from the anesthetic drugs for analysis.

3.6.1 Speeded-Up Robust Features Descriptor (SURF) for Anesthetics Medication Identifications

In another work for image feature description, Bay et al. (2006) developed and introduced an efficient descriptor approach to act as a substitute for SIFT. They claimed that their approach was more robust and processed images faster than other image feature descriptors prior to the introduction of their method. In the algorithm,

instead of deploying conventional Gaussian derivatives for detecting image interest points, the scheme uses 2D box filters to perform image feature descriptions. This implies that the method employs a scale-invariant blob detector that relies on a Hessian matrix determinant to select scales and locations in an image sample. The reason behind this is that, with the use of the set of box filters, the second-order Gaussian derivatives could be approximated efficiently while assisted by the image integrals. In the SURF design, 9 × 9 box filters are the Gaussian approximations with the standard derivative (σ) set at 1.2 and denote the least scale for calculating the maps of the blob response. If the approximations are represented by $A_{\alpha 1\alpha 1}, A_{\alpha 2\alpha 2}\ and\ A_{\alpha 1\alpha 2}$, then the Hessian approximated determinant is expressed as:

$$det(H_{approx}) = A_{\alpha 1\alpha 1}\, A_{\alpha 2\alpha 2} - (wA_{\alpha 1\alpha 2})^2 \qquad 3.15$$

From Equation 3.15 above, the filter responses' relative weight is represented by w, and it is inserted to balance the Hessian determinant (B.-Y. Chen, 2012) expression. The Hessian determinant approximation represents the image feature blob response. During computations, the blob response map serves as a storage point for the responses. The quadratic interpolation is deployed to detect and refine the local maxima, similar to the DoG detector. To obtain a reliable scale of values and interest points, a non-maximum suppression process is performed in 3 × 3 × 3 nearby regions. To perform image description, the SURF initiates the construction of a square region positioned within an interest point that is detected and tilted along the core orientation. SURF deploys wavelet responses along the horizontal and vertical direction for the description of features in images (see Figure 17).

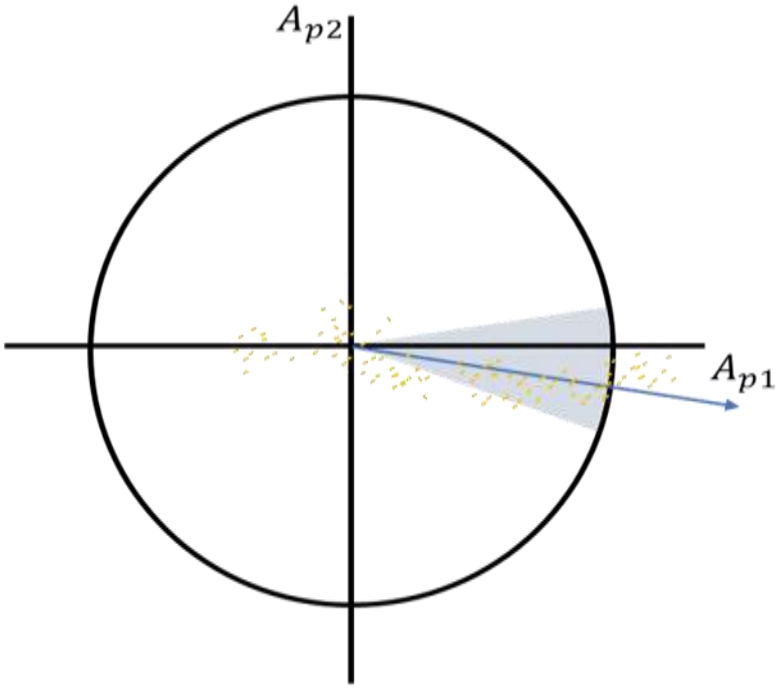

Figure 17: Horizontal and Vertical SURF Wavelet Response Directions.

In the SURF, the window size is set at 20s, wherein the interest points detection scale is represented by s. Furthermore, the region of interest is additionally partitioned into reduced sub-regions of 4 x 4 regions, and the computation of the Harr wavelet responses is performed at the sampled points of 5 × 5 region along with the vertical and horizontal directions for each sub-region. To enhance the detectors' response to localization errors and increase its geometric deformation robustness, the Gaussian window positioned in the interest point is deployed to weigh the responses; then, for each sub-region, the wavelet responses $A_{p1}\ and\ A_{p2}$ are summed and inserted into a feature vector v, having v expressed as:

$$v = (\sum A_{\alpha 1}, \sum |A_{\alpha 1}|, \sum A_{\alpha 2}, \sum |A_{\alpha 2}|) \qquad 3.16$$

Since it uses 64-dimensional feature vectors to perform descriptions of local image features instead of the 128-dimensional feature vectors used by SIFT, SURF performs better in terms of processing speed when compared to SIFT. Notwithstanding, given images with rotation, scale, translation, and other deformations caused by illuminations, SIFT descriptor algorithm has the edge over SURF in processing these kinds of images. The SURF is not entirely immune to affine transformation and has limitations in processing images captured with large view angles or violent rotations. In real-time processing of the anesthetic drug images, the SURF at some point caused the

processing computer to freeze as the number of images logged for the anesthetic drug comparative process became large. However, the SIFT descriptor at no point caused the freezing of the processing computer when the comparing images were increased.

3.6.2 Scale Invariant Feature Transformation (SIFT) for Anesthetics Medication Identifications

In a famous work, Lowe (2004) introduced a scale-invariant-based image feature transformation algorithm, codenamed "SIFT," to detect various interest points from a given image sample by utilizing the Difference-of-Gaussian (DOG) (S. Wang et al., 2012) operator. In the proposed algorithm, the image interest points were chosen in the same way as the DoG functions' local extrema. Feature vectors were extracted in the algorithm for each interest point. The local image orientation was estimated over a couple of scales and interest point neighborhoods by exploiting the local properties found on the image to make the output invariant against rotation. For an individually detected point, a descriptor is calculated by relying on the local information that exists in the image scale or characteristics of the scale. Given a sample point in an image region within a key point, the SIFT algorithm constructs a histogram of gradient orientation. It then computes the peak orientation value and other near values that fall within the 80% mark of the peak value and deploy them to act as the key points' dominant orientations.

For the description of an image features, the SIFT algorithm begins by performing a sampling operation on the image gradient magnitudes and 16 × 16 region orientations within an individual key point by deploying the image scale to choose the degree of Gaussian blur that is suitable for the image. This is followed by the creation of a collection of orientation histograms in which individual histograms consisting of samples generated from a 4×4 subregion that resulted from the main neighborhood region and contains in each region of 8 orientation bins. Furthermore, to allocate weight to the magnitude of a given point and assign greater weights to gradients near the regional center, a Gaussian weighting function that has σ identical to one-half of the region is employed, which is invariably influenced less by the position shifts.

The image feature description is then formulated from a vector consisting of the values from the entire histogram orientation entries. Because in the eight bins, individual 4 ×

4 histograms are found, then 4 × 4 × 8 = 128 elements are formed for the feature vector in each key point. To make the process invariant to affine transformations and illumination, the feature vector is normalized to obtain a unit length. However, non-linear illumination variations happen because of the saturation of the camera used or close factors that induce considerable changes in some of the gradient magnitude. However, the variations can be mitigated or reduced by thresholding the feature vector value to 0.2 highest value, and a normalized vector is obtained.

A typical scale-invariant feature transform descriptors' representation is remarkable in several aspects: the representation in the algorithm is meticulously crafted to evade issues that can arise because of location shifts resulting from boundary smoothing effects, scale, and orientations. This prevents extreme feature vector alterations, and it is inadvertently compact and uses 128 vector elements to represent pixel patches. Also, the SIFT representation is robust to deformations, for instance, the ones triggered by perspective effects but is not obviously affine transformations invariant. These traits exhibited by SIFT make it perform exceptionally well on the anesthetic image feature detections, description, and matching when compared with other feature description algorithms tested with respect to diverse processing conditions such as rotations, lighting, and scale. Furthermore, a typical SIFT algorithm feature vector design is complex, and the decision behind the design selection is not explicitly clear; this causes a high dimensionality problem which affects the computational time adversely during the descriptor process.

Over the years, other variations of SIFT algorithm have been introduced. For instance, Ke and Sukthankar (2004) in their work proposed a SIFT variant that deploys a principal component analysis (PCA) (Jolliffe, 2005) technique to minimize the high dimensionality encountered in the conventional SIFT descriptor. In the introduced algorithm (SIFT-PCA), the gradients from the image patches extracted within key points are normalized with the SIFT descriptor, and their dimension is reduced with the PCA. In a specific image scale, a 41 × 41 patch is extracted along the vertical and horizontal directions; the image gradients are computed before the generation of feature vectors from the gradient concatenations in both directions. In furtherance, a feature vector with 36 elements in length is produced by the projection of the image gradient vector into an already computed feature space. To minimize the effects of illumination

variations, a normalization process is performed on the produced vector resulting in a unit magnitude.

In another work involving SIFT, Morel and Yu (2009) demonstrated that from the six parameters used for the affine transformation, the scale-invariant feature transform algorithm is completely invariant with only a few distinct parameters like the rotations, zoom, and translation. This led them to propose affine-SIFT or ASIFT, which performs simulation on image views grabbed by changing the parameters of the capturing camera axis orientation, such as the angles of the latitude skipped by the SIFT descriptor.

3.6.3 Experiment and Analysis

In this experiment, a set of 25 ampule container images that are frequently used in the operating theatre were selected for this test involving the SIFT algorithm. The test environment was an anaconda-python environment with a 16GB memory computer that runs on a Windows operating system. In the study, the ampule images were captured in different directions, orientations, and scales. Furthermore, four samples of the selected set of image samples were chosen for pairwise comparative studies according to the ampule size and the semantic information embedded in them. The captured image samples were logged in a lookup table, and the four different samples each were used to scan over the images and their similarity scores and the number of extracted features recorded. As explained above, the SIFT algorithm detected, extracted, and computed the features of the image samples. Then, a brute force matching algorithm was deployed to match the computed features, followed by a KNN classifier that classified the distinct image sample. To have a balanced representation of the values extracted from the experiments in charts, the natural logarithm (Ln) of the values where computed and used to plot the various charts in this section. The results of the experiment with the first drug sample (Vecuronium Bromide) were then analyzed as show in Figure *18 and* Table *4* respectively.

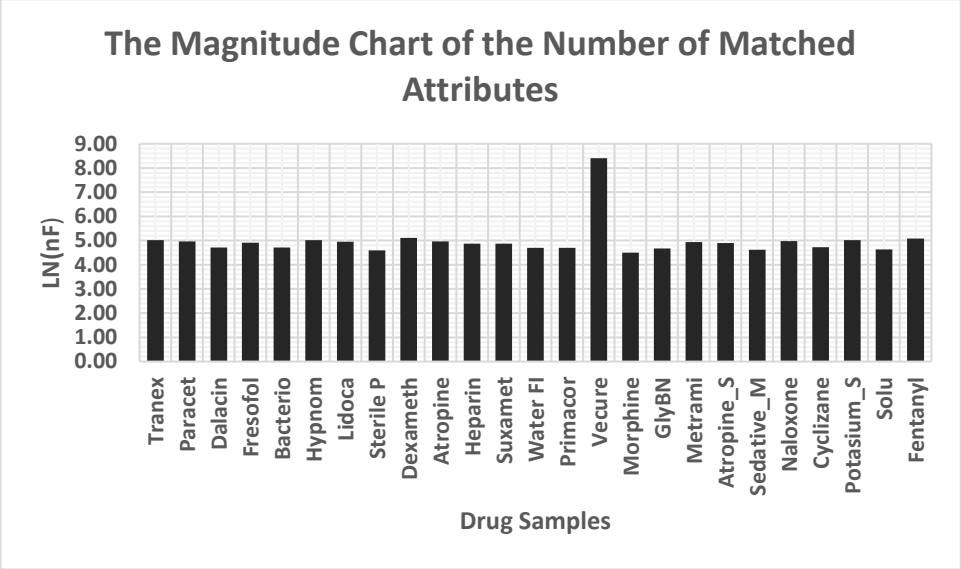

Figure 18: The Matched Attributes with Vecuronium Bromide against other samples using the SIFT Algorithm.

Table 4: The Similarity Scores with Vecuronium Bromide against other samples using the SIFT Algorithm.

	Similarity			
Drug Name	**Sample1**	**Sample2**	**Sample3**	**Sample4**
Atropine	0.03213	0.01914	0.02566	0.02670
Atropine_S	0.02990	0.02059	0.02711	0.03195
Bacterio	0.02499	0.00986	1.00000	0.03447
Cyclizane	0.02521	0.01595	0.03798	0.05138
Dalacin	0.02499	0.01131	0.04161	0.03209
Dexameth	0.03681	0.03827	0.04175	0.03454
Fentanyl	0.03592	0.01334	0.03131	0.04497
Fresofol	0.03034	0.01595	0.03059	0.06606
GlyBN	0.02387	0.02030	0.03044	0.03886
Heparin	0.02923	1.00000	0.02160	0.02727
Hypnom	0.03369	0.00812	0.03668	0.03310
Lidoca	0.03146	0.01305	0.03421	0.04692
Metrami	0.03124	0.01479	0.04335	0.04174
Morphine	0.02008	0.01363	0.02957	0.03418
Naloxone	0.02521	0.00957	0.02378	0.03584
Paracet	0.03213	0.01624	0.02725	1.00000
Potasium_S	0.03369	0.02088	0.02899	0.03584
Primacor	0.02454	0.02146	0.02899	0.02756

Sedative_M	0.02276	0.01972	0.02378	0.02519
Solu	0.02298	0.01566	0.04712	0.03684
Sterile P	0.02209	0.02030	0.02349	0.01921
Suxamet	0.02923	0.01798	0.02218	0.03375
Tranex	0.03391	0.01972	0.03494	0.03735
Vecure	1.00000	0.01914	0.04697	0.05131
Water FI	0.02454	0.01566	0.02493	0.02857

The chart in Figure 18 represents the number of attributes extracted and matched from the first test drug image sample and the similarity scores (Table *4)* obtained from the pairwise comparative process against the other drug images in the set of the selected test drug samples. As can be seen in Figure 18 & Table 4, the distinct image sample used among the four samples is the Vecuronium Bromide drug container with a magnitude of 8.41 or 4482 highest matched attributes when compared with the other logged drug container images and a similarity score of 100%. This was followed by a Dexamethonium medication drug container image with a magnitude of 5.11 or 165 matched attributes and a 0.0368 similarity score. The least extracted and compared features are with a magnitude of 4.50 or 90 attributes with a 0.020 similarity score from the Morphine Sulphate drug. In continuation, the chat in **Error! Reference source not found.**19 represents the features extracted and matched from the second drug sample, i.e., the Heparin Injection.

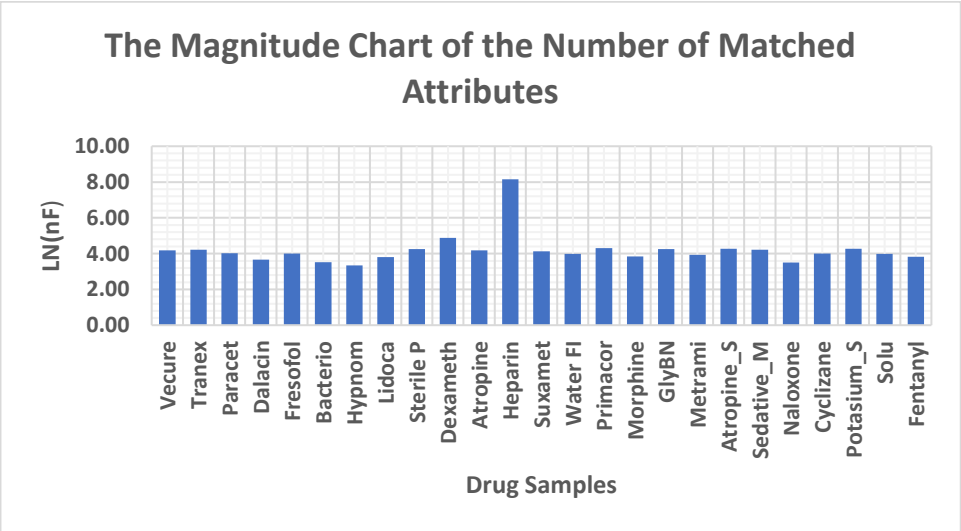

Figure 19: The Matched Attributes with Heparin Injection Against Other Samples Using the SIFT Algorithm.

From the charts above, a magnitude of 8.15 or 3449 attributes represents the highest matched attributes from the collection of features emanating from the test drug samples, indicating that the correctly identified drug is the Heparin Injection container with a similarity score of 100% (see Table 4). This was followed by a Dexamethonium medication drug container image with a magnitude of 4.88 or 132 matched attributes and a 0.038 similarity score. The least extracted and matched features are with a magnitude of 3.33 or 28, with a 0.008 similarity score from the Hypnomidate anesthetic drug sample. On the third anesthetic container image sample, Bacteriostatic Injection was used, and a magnitude of 8.84 or 6898 features were matched, representing the highest matched attributes with a 100% similarity score, as shown in Table 4. This was followed by a Solu-Medrol medication drug container image with a magnitude of 5.78 325 matched attributes and a 0.047 similarity score. The least matched features contain 5.00 magnitude or 149 attributes with a 0.0216 similarity score from the Heparin anesthetics drug sample (see Figure 20*)*.

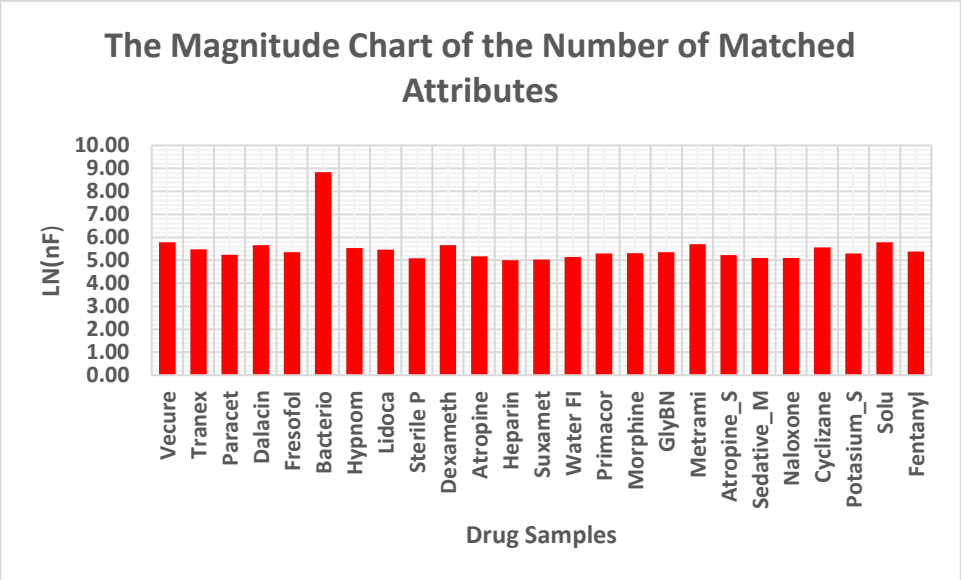

Figure 20: The Matched Attributes with Bacteriostatic Injection Bromide Against Other Samples Using the SIFT Algorithm.

Finally, the Paracetamol Kabi injection image container is the fourth sample used to demonstrate the SIFT algorithm feature pairwise comparative process. During the comparative test process, 9.58 feature magnitude or 13897 attributes representing the highest extracted attributes were correctly matched from the Paracetamol Kabi Injection container. A similarity score of 100% was recorded, as shown in Table . This was followed by a Fresofol medication drug container image with a magnitude of 6.84

or 918 matched attributes and a 0.066 similarity score. The least compared and matched features are with a magnitude of 5.59 or 267 attributes with a 0.019 similarity score from the Sterile Potassium anesthetics drug sample (see Table 4 & Figure 21).

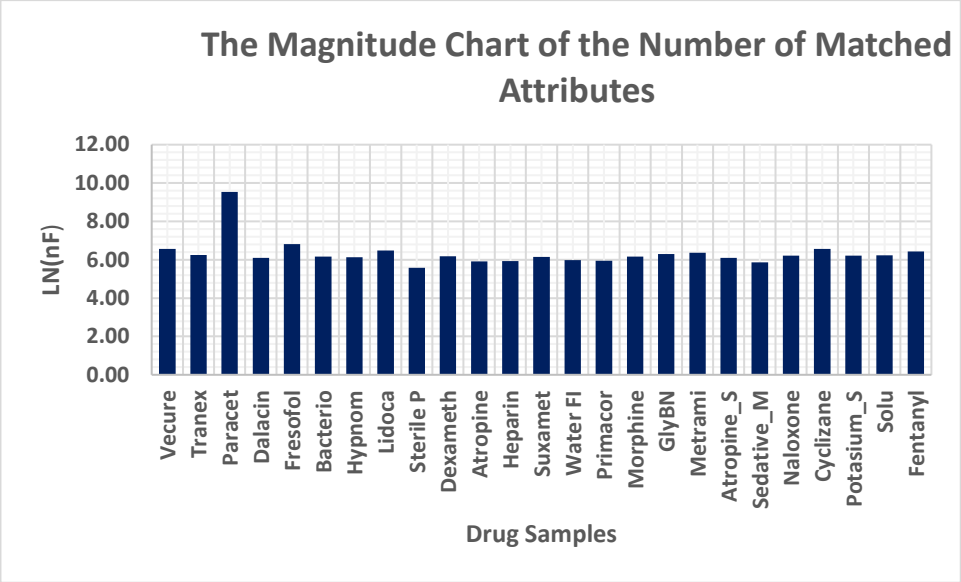

Figure 21: The Matched Attributes with Paracetamol Kabi Bromide Against Other Samples Injection Using the SIFT Algorithm.

3.6.4 Binary robust invariant scalable key points (BRISK) for Anesthetics Medication Identifications

The BRISK (Leutenegger et al., 2011) algorithm, driven by the novel corner detection method that uses a generic method to improve the image feature detection process, was introduced for an enhanced image processing speed. In process, the BRISK algorithm fuses three techniques together to detect essential points in a given image sample, describe the detected points, and match the descriptive points. BRISK initially built a scale-space pyramid before using AGAST (the Adaptive corner detection operator) (Mair et al., 2010) method to extract exceptionally stable points in precisive sub-pixels of the continuous scale space. After this process, the relationship that exists in the pairs of random sample points around the local image is exploited to construct a binary feature descriptor of the local image. Then a Hamming distance method is deployed to match the image features.

In the study, they searched for image maxima using the FAST (Rosten & Drummond, 2006) score s, as a saliency gauge of the scale-space and as well as in the image plane, in order to attain invariance to scale which is extremely crucial for obtaining image

keypoints of high quality. In the continuous scale space, the BRISK detector approximates the real scale that exists in individual keypoint even though it discretizes the scale axis at rougher distances rather than the high-performing detector alternatives. Furthermore, in the BRISK algorithm, n octave c_i with n intra-octaves d_i for $i = 0,1, \ldots, n-1$, which is commonly left at n equal to 4, is the composition of the scale-space pyramid layers. By the gradual and continuous half-sampling of the main image, octaves are formulated during the BRISK process. An individual intra octave d_i, is found amongst layers $c_i \; and \; c_{i+1}$. The initial intra octave d_0 is generated through the process of down sampling the main image c_0 using a factor of 1.5. The remaining intra-octave layers are then obtained by the preceding half-sampling processes. Consequently, if s represents the scale, then $sc_i = 2^i$ and $sd_i = 1.5(2^i)$ respectively.

The BRISK algorithm uses 9-16 detectors on every octave and intra-octave independently but with equal threshold T for the identification of prospective interest regions. This is followed by the conduction of a non-maxima suppression process in the scale space of the points that are found in the same region. The target point needs to meet the maximum condition with regard to the eight FAST neighboring scores s that share the same layer. The beneath and above scores in the layer is also required to be lower. A cross-examination is performed on the patches that have the same square size, and the side length is selected as 2 pixels of the presumed maximum layer. Since different discretization schemes are used to represent layers in a neighborhood, a number of interpolation processes are performed on the patch boundaries. On the other hand, the maxima detection within the axis of scales at the octave c_0 is handled as a unique case. This implies that to generate FAST scores for a d_{-1} virtual intra-octave beneath c_0, a FAST 5-8 mask needs to be applied on c_0.

The key point description has considerable influence on the descriptor-matching process, efficacy, and the entire operation of the algorithm. The BRISK algorithm uses a rigid locality sampling pattern for feature points description rather than the random point pair selection practices of the other binary feature description algorithm like BRIEF. Within a block in the BRISK image feature descriptor, four concentric circles are constructed that have a 40 × 40-pixel size and are positioned on the point of interest. Also, within the four concentric circles, $N(N = 60)$ points that are uniformly distributed with equal spacing are found. When conducting an image intensity

sampling process of a given point p_i, it is necessary to apply a Gaussian smoothing operation that has a standard deviation σ_i, that is relative to the distance in the middle of the points with the respective circle.

In BRISK, the comparative computation of the similarities among the descriptors found on multiple feature points plays a vital role in performing the descriptors matching process. Due to its use of a binary string of bits consisting of 0 and 1 for the extracted feature points description, the computation of the descriptor's Hamming distance is essential in describing the similarity between the descriptors. Furthermore, a bitwise XOR operation computation is required for calculating the Hamming distance; this implies that to perform the operation, two values are needed. Obtaining the same corresponding bits means that the outcome is 0 or else 1. This is followed by performing further examinations by counting the number of the produced 1s and the many the 1s, the higher the dissimilarity between the two descriptors or else the reverse is the case. Taking two given BRISK descriptors as M and N, then

$$M = m_1 m_2 \dots m_i \dots m_N$$

$$N = n_1 n_2 \dots n_i \dots n_N$$

Where 1 and 0 represent the values of m_i and n_i and the Hamming distance is expressed in Equation 3.17 as:

$$HD(M,N) = \sum_{i=1}^{N} m_i \oplus n_i = \sum_{i=1}^{N} k(m_i \oplus n_i) \qquad 3.17$$

Where $k(m_i \oplus n_i)$ denotes the inequality found in the bits and the $i - th$ bits of the descriptors of M and N represented by $m_i \, and \, n_i$.

$$k(m_i \oplus n_i) = \begin{cases} 1 & m \neq n \\ 0 & m = n \end{cases}$$

The XOR operation is represented by $\oplus$, and the Hamming distance value is calculated to obtain the estimation of the extent of the matching process of a given pair of BRISK descriptors. The higher the obtained Hamming distance value, the smaller the degree to which the descriptors are matched.

3.6.5 Experiment and Analysis

In this BRISK experiment, the same setup and variables used for the SIFT algorithm test were deployed, and the results were recorded. The results of the experiment with the first drug sample (Vecuronium Bromide) are shown in Figure 22 and Table below:

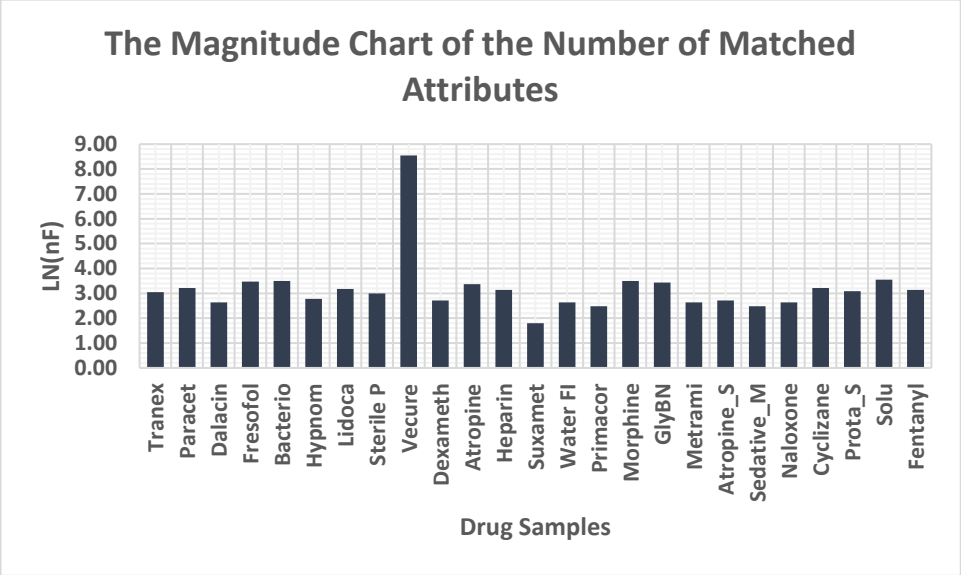

Figure 22: The Matched Attributes with Vecuronium Bromide Injection Bromide Against Other Samples using the BRISK Algorithm.

The total number of attributes extracted from the first tested drug image sample was 5138 attributes, and the close corresponding highest matched attribute was with a magnitude of 8.54 or 5114 attributes after a pairwise comparative test was conducted. In continuation, a 99.5% similarity score was achieved, indicating that the rightly matched and the identified drug is Vecuronium Bromide Injection (see Table 5). This was followed by a Solu-Medrol injection drug container image with a magnitude of 3.57 or 35 extracted attributes and a 0.0068 similarity score. The least extracted and compared features are with a magnitude of 1.78 or 6, with a 0.0012 similarity score from the Suxametonium drug injection. In continuation, a second test with another anesthetic drug sample was conducted.

Table 5: The Similarity Scores with Vecuronium Bromide Injection Bromide Against Other Samples using the BRISK Algorithm.

	Similarity			
Drug Name	**Sample1**	**Sample2**	**Sample3**	**Sample4**
Atropine	0.005644	0.00287	0.002757	0.003381
Atropine_S	0.002919	0.002533	0.003101	0.004491
Bacterio	0.006423	0.001688	0.998392	0.006661
Cyclizane	0.004866	0.003377	0.006547	0.00545
Dalacin	0.002725	0.00152	0.004595	0.004542
Dexameth	0.002919	0.002701	0.003676	0.00323
Fentanyl	0.004476	0.002533	0.005054	0.00762
Fresofol	0.006228	0.001182	0.004595	0.013373
GlyBN	0.006033	0.003039	0.005169	0.005147
Heparin	0.004476	0.998987	0.001838	0.002321
Hypnom	0.003114	0.002533	0.003216	0.00323
Lidoca	0.004671	0.00152	0.005513	0.00545
Metrami	0.002725	0.002701	0.006662	0.00545
Morphine	0.006423	0.003546	0.004939	0.005147
Naloxone	0.002725	0.002195	0.004939	0.002826
Paracet	0.004866	0.002195	0.005169	0.999092
Primacor	0.002336	0.001351	0.005973	0.008579
Prota_S	0.004282	0.001351	0.004595	0.002977
Sedative_M	0.002336	0.00152	0.002757	0.003987
Solu	0.006812	0.00152	0.010682	0.0054
Sterile P	0.003893	0.003208	0.001723	0.001716
Suxamet	0.001168	0.002533	0.001838	0.002321
Tranex	0.004087	0.002701	0.004365	0.004441
Vecure	0.995329	0.004476	0.005973	0.007418
Water FI	0.002725	0.002364	0.003905	0.003078

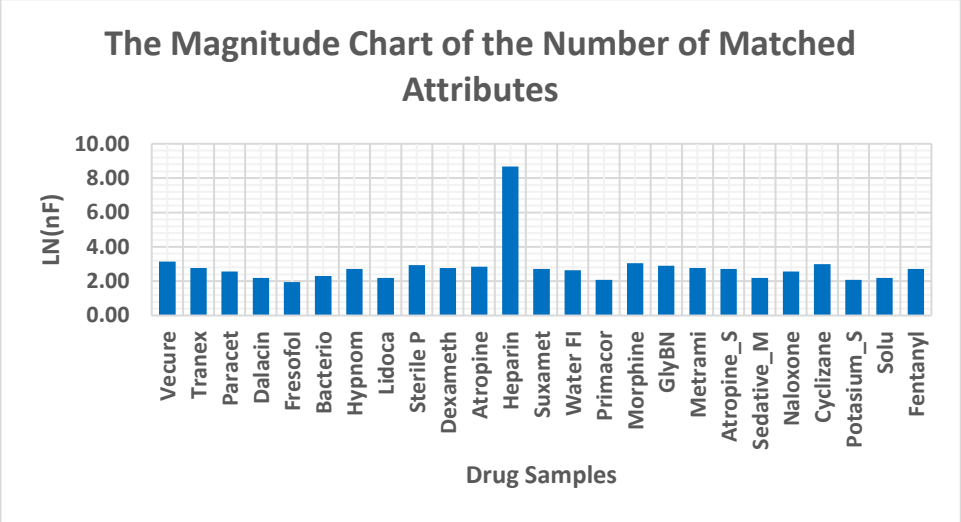

Figure 23: The Matched Attributes with Heparin drug injection Bromide Against Other Samples using the BRISK Algorithm.

In the second sample test involving the BRISK algorithm, a total of 5923 feature attributes was extracted from the second drug image sample, and when a pairwise comparative process was conducted with the other image samples in the set, Heparin drug injection returned with the highest number of related attributes at 8.69 magnitude or 5917 and a similarity score of 99.9%, indicating that Heparin injection is the right drug (see Figure 23). Furthermore, the second-highest matched anesthetic drug from the selected set of drugs was the Vecuronium Bromide Injection, with a magnitude of 3.14 or 23 attributes and a 0.0045 similarity score. On the other hand, the least-matched drug from the set was the Fresofol injection, with seven attributes and a 0.0012 similarity score.

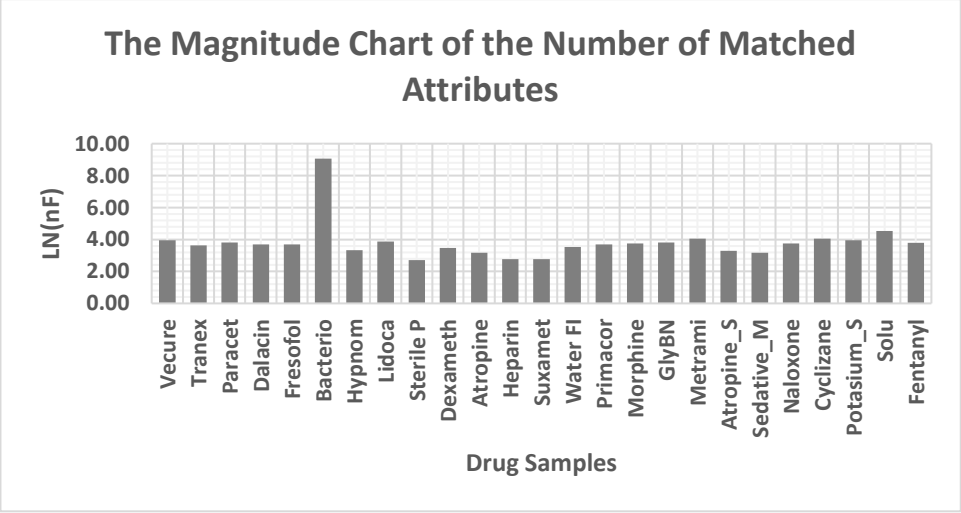

Figure 24: The Matched Attributes with Bacteriostatic Injection Bromide Against Other Samples using the BRISK Algorithm.

On the third test with the third selected anesthetic container image sample, Bacteriostatic Injection was used, and 9.07 a magnitude of features or 8692 attributes were matched from a total of 8706 features extracted from the image sample, representing the highest extracted attributes, with a 99.8% similarity score as shown in Table and Figure 24. This was followed by a Solu-Medrol medication drug container image with a magnitude of 4.53 or 93 extracted attributes and a 0.011 similarity score. The least extracted and compared features are with a magnitude of 2.71 or 15 attributes, with a 0.0017 similarity score from the Sterile Potassium anesthetic drug injection sample.

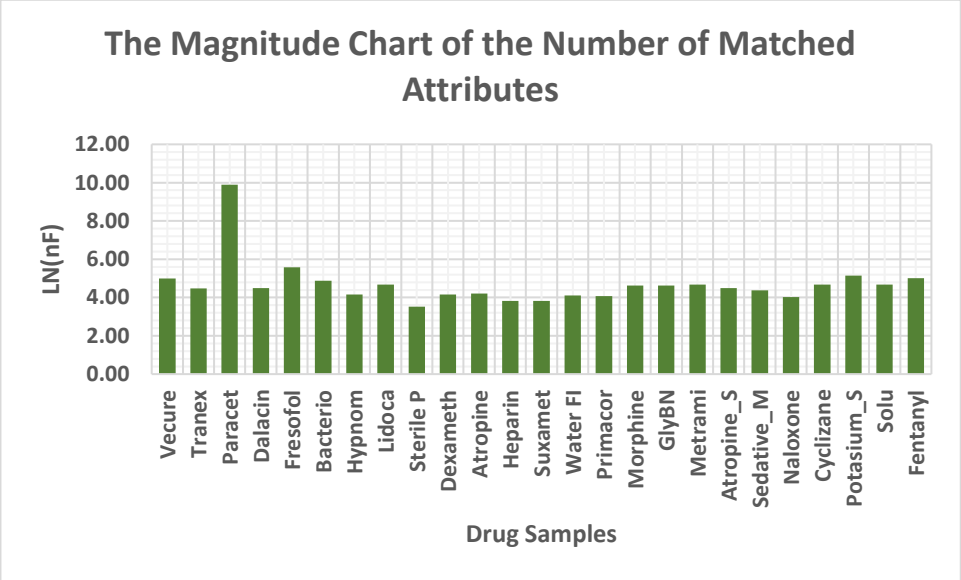

Figure 25: The Matched Attributes with Bromide Against Other Samples Paracetamol Kabi injection using the BRISK Algorithm.

Finally, the fourth sample used for the BRISK algorithm feature's pairwise comparative process was the Paracetamol Kabi injection image container. During the comparative test, 9.89 a magnitude of features or 19798 attributes representing the highest number of attributes were correctly matched from a total of 19816 features extracted from the Paracetamol Kabi Injection container (see Figure 25). A similarity score of approximately 100% was obtained when self-compared, indicating the right-matched drug. This was followed by the Fresofol medication drug container image with a magnitude of 5.58 or 265 matched attributes and a 0.0134 similarity score. The least matched features emanated from the Sterile Potassium anesthetic drug sample with a magnitude of 3.53 or 34 features and a 0.0012 similarity score.

3.6.6 Binary Robust Independent Elementary Features (BRIEF) for Anesthetics Medication Identifications

In another study for image features description and matching, a low-bitrate-based image features descriptor that combines a random forest classification algorithm and a random fern classifier for matching the image features were introduced (Pang et al., 2012). BRIEF is part of the binary image feature descriptors like the Local Binary Pattern (Chen et al., 2009) (LBP) and the Binary robust invariant scalable key points (Leutenegger et al., 2011) (BRISK). BRISK conducts only simple binary comparative tests on images with Hamming distance for image feature descriptions rather than Mahalanobis or Euclidean distance. For the construction of binary descriptors, it is required to run a comparative test between the positions of two pixels found in the detected points of interest. This process permits the generation of descriptive representations at an extremely low computational cost. Also, only the Hamming distance computations that can be speedily processed using the XOR primitives on modern architectures are needed for the binary descriptors matching.

In processing images using BRIEF, only a few intensity difference assessments are depended upon by the BRIEF algorithm for representing image patches in the form of binary strings. In other words, to construct a binary patch for pixel patches with S × S size, the outputs of the test involving the equation below are required to be concatenated

$$T = \begin{cases} 1, if\ I(\alpha 1) > I(\alpha 2), \\ otherwise \\ 0 \end{cases}$$

From the above expression, the smoothed intensity value of the pixel at point $\alpha 2$ is represented by $I(\alpha 2)$ and the process of choosing the location of the entire $\alpha 2$ values is distinctively specified as a collection of binary tests. Gaussian distribution of 0-mean isotropy with $\frac{1}{25}\ \mathrm{S}^2$ variance is where the sampling points are drawn. To enhance the robustness of BRIEF for image feature description, a pre-smoothed patch of pixels and a Gaussian kernel with two variances and a size of 9 × 9 pixels are deployed for the image feature description process.

Furthermore, in a typical BRIEF descriptor algorithm, the binary threshold and the binary pixel pair numbers are the only parameters that can be set. Further experiments involving the algorithm have demonstrated that 128 or 256 bits are commonly suitable for obtaining a sound-matching output. The BRIEF descriptor is highly efficient for both computational cost and memory consumption. However, it is not robust against image rotations that are above 35° and thus could be said not to be invariant to image rotations.

3.6.7 Experiment and Analysis

In furtherance of the image feature detection, extraction, and matching test, more experiments were run with the BRIEF algorithm, and the outcomes were recorded. In this experiment, all physical setup and variables remained the same as with the other anesthetic image feature detection and drug identification algorithms except for the detection algorithm swap. The results of the experiment with the first drug sample (Vecuronium Bromide) are shown in Figure 26 and Table *6 below*:

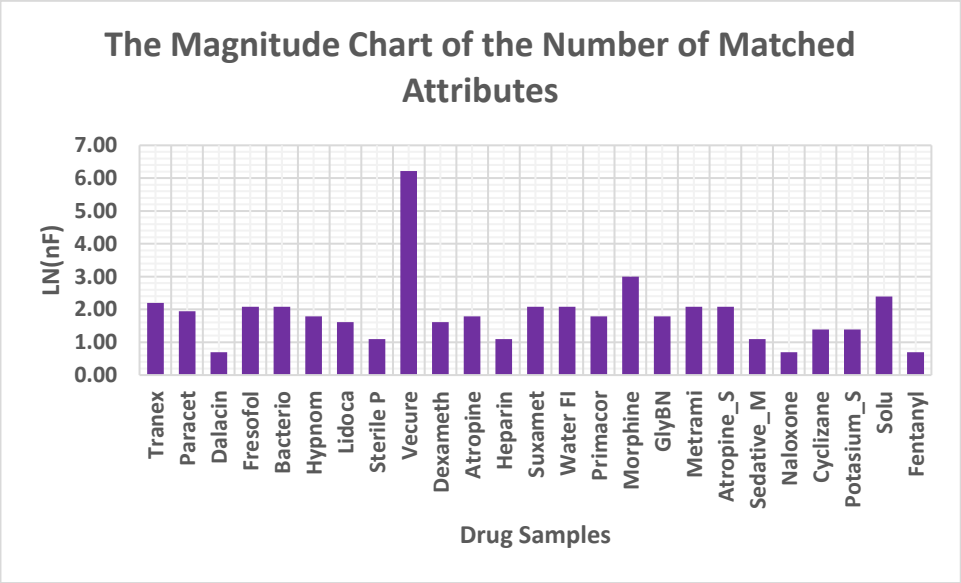

Figure 26: The Matched Attributes with Vecuronium Bromide Injection Against Other Samples using the BRIEF Algorithm.

Table 6: The Similarity Score with Vecuronium Bromide Injection Against Other Samples using the BRIEF Algorithm.

	Similarity			
Drug Name	**Sample1**	**Sample2**	**Sample3**	**Sample4**
Atropine	0.0120	0.0040	0.0120	0.0100
Atropine_S	0.0160	0.0060	0.0180	0.0080
Bacterio	0.0160	0.0080	1.0000	0.0200
Cyclizane	0.0080	0.0060	0.0100	0.0100
Dalacin	0.0040	0.0000	0.0120	0.0060
Dexameth	0.0100	0.0080	0.0100	0.0120
Fentanyl	0.0040	0.0120	0.0220	0.0060
Fresofol	0.0160	0.0040	0.0140	0.0180
GlyBN	0.0120	0.0040	0.0120	0.0060
Heparin	0.0060	1.0000	0.0080	0.0060
Hypnom	0.0120	0.0060	0.0060	0.0160
Lidoca	0.0100	0.0120	0.0080	0.0140
Metrami	0.0160	0.0060	0.0220	0.0160
Morphine	0.0020	0.0040	0.0120	0.0080
Naloxone	0.0040	0.0120	0.0140	0.0060
Paracet	0.0140	0.0100	0.0180	1.0000
Potasium_S	0.0080	0.0120	0.0080	0.0160
Primacor	0.0020	0.0120	0.0120	0.0120
Sedative_M	0.0060	0.0020	0.0060	0.0080
Solu	0.0220	0.0040	0.0300	0.0180
Sterile P	0.0060	0.0100	0.0040	0.0080
Suxamet	0.0160	0.0120	0.0060	0.0040
Tranex	0.0180	0.0120	0.0140	0.0100
Vecure	1.0000	0.0020	0.0280	0.0320
Water FI	0.0160	0.0140	0.0080	0.0080

From the BRIEF experiment, the first anesthetic drug sample, which is the Vecuronium Bromide drug container, matched correctly with itself with a magnitude of 6.21 and 500 attributes when compared with the other logged set of drug container images, and it returned a similarity score of 100%, as shown in Table 6. This was followed by a Solu-Medrol medication drug container image with a magnitude of 2.4 or 11 matched attributes and a 0.022 similarity score. The least extracted and compared feature is

one with a 0.002 similarity score from the Primacor and Morphine Sulphate drug injections, respectively. In continuation, the chat in Figure represents the features extracted and matched from the second drug sample, i.e., the Heparin Injection.

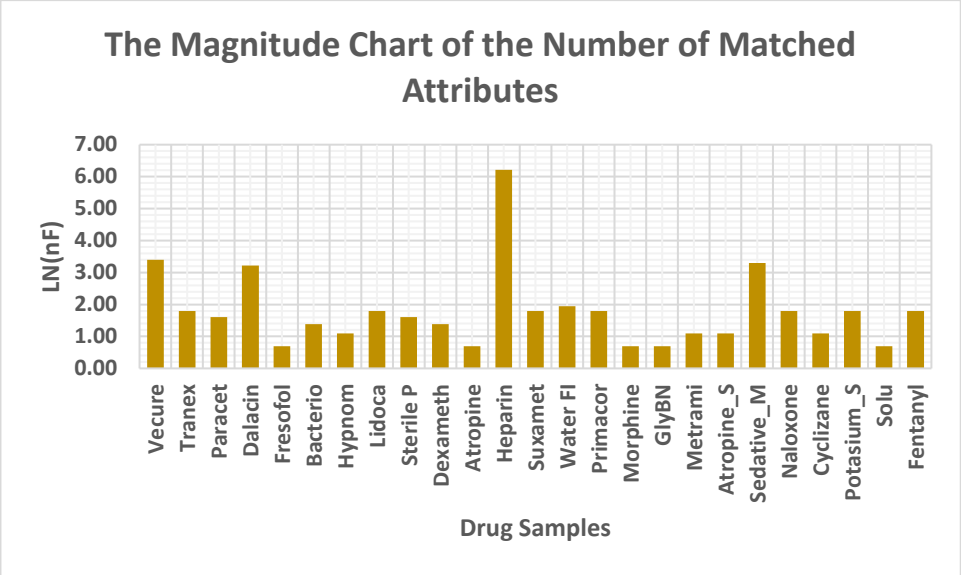

Figure 27: The Matched Attributes with Heparin Injection Against Other Samples using the BRIEF Algorithm.

Furthermore, in the second sample test involving the BRIEF algorithm, a total of 674 feature attributes was extracted from the second drug image sample. When a pairwise comparative process was conducted with the other image samples in the set, Heparin drug injection returned with the highest number of related attributes a magnitude of 6.22 and 503 features and a similarity score of 100%, indicating that Heparin injection is the rightly matched drug. Furthermore, the second-highest matched anesthetic drug from the selected set of drugs was the “Water For Injection” container, with seven attributes and a 0.014 similarity score. On the other hand, the least matched drug from the drug set was the Dalacin injection, with two related attributes and a near zero-similarity score.

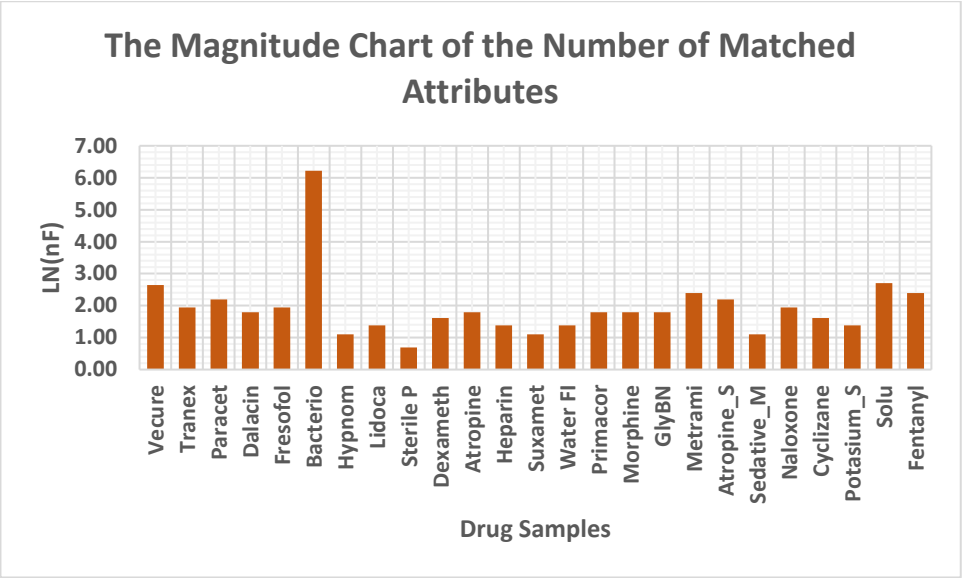

Figure 28: The Matched Attributes with Bacteriostatic Injection Against Other Samples using the BRIEF Algorithm.

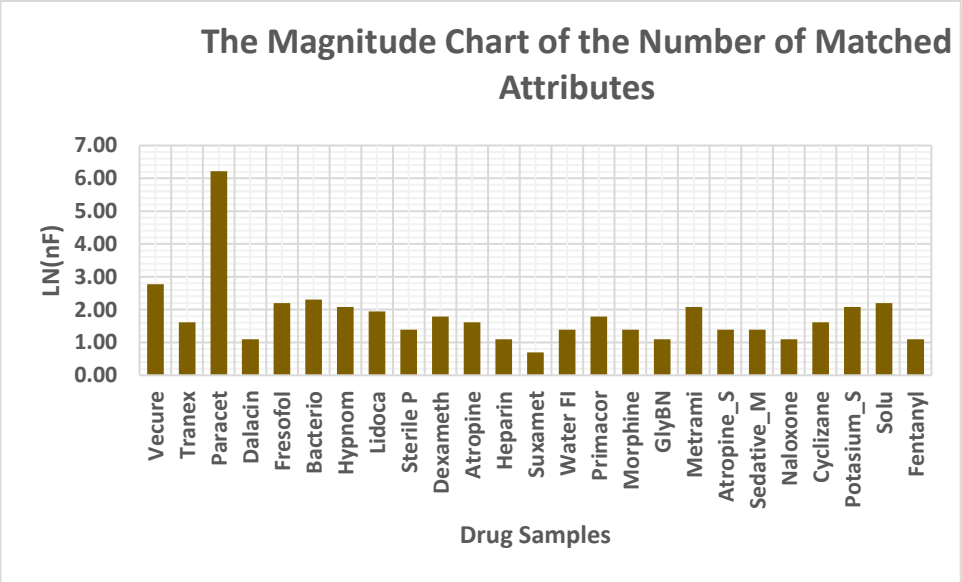

Figure 29: The Matched Attributes and Similarity Scores from Paracetamol Kabi Injection using the BRIEF Algorithm.

In the third selected drug sample test involving the BRIEF algorithm, the Bacteriostatic Injection returned the highest similarity score and, in turn, the rightly matched and identified anesthetic drug from the set of the selected drug samples (see Figure 28 & *Figure 29*). The Bacteriostatic Injection scored a 100% similarity, followed by the Vecuronium Bromide injection with a 0.028 similarity score, and the Sterile Potassium injection as the least similar drug with a 0.004 score. On the other hand, the Paracetamol Kabi injection was the rightly matched and identified anesthetic drug from the 4th drug sample among the set of selected drug samples with a 100%

similarity score. This was followed by the Vecuronium Bromide injection with a 0.032 score, as shown in Table , for the fourth drug test sample involving the BRIEF Algorithm.

3.6.8 Feature Matching Process for Anesthetics Medication Identifications

Image feature matching is an important part of the computer vision processes, as its usefulness expands across many application fields involving object identification, detection, and recognition. It involves the establishment of correspondences between pairs of images located in the same object or scene. The typical dominant method of image matching involves detecting associative interest points, having each interest point linked with a closely related descriptor in a collection of images. In other words, before the establishment of an initial image feature matching process between a set of image samples, image features, and their respective corresponding descriptors are first extracted from the image samples. Having the set of image generality intact, the image feature matching problem can be expressed as follows: Let q represent the detected point by a detector algorithm in a given image sample that has correspondence with a descriptor, then:

$$\varphi(q) \ = \ \{\varphi_c(Q) \mid c \ = \ 1,2,\ldots,C$$

The $c - th$ descriptor generated from the feature vectors for all C is given as

$$\varphi_c(q) \ = \ (f_q^c, f_{2q}^c, \ldots, f_{n_c q}^c)$$

The target is to discover the most suitable correspondence p in a different image from a collection of N points of interest, having $\alpha \ = \ \{\alpha_1, \alpha_2, \ldots, \alpha_N$ through the feature vector $\varphi_c(q)$ Furthermore, comparing with the points found in the set α. After this process, the measure of the distance that exists in the points of interest pair descriptors $\varphi_c(q)$ and $\varphi_c(\alpha)$ can be established as

$$d_c(q, \alpha) \ = \ |\varphi_c(q) \ - \ \varphi_c(\alpha)|$$

With respect to d_c, the points α are independently arranged in ascending order for any individual descriptor that generates the set of points:

$$\omega(q, \alpha) \ = \ \{\omega_c(q, \alpha) \mid c \ = \ 1,2,\ldots,C\} \qquad 3.18$$

having,

$$\omega_c(q,\alpha) = \{\omega_c^1, \omega_c^2, \ldots, \omega_c^N \in \alpha \mid d_c(q,\omega_c^i) \leq d_c(q,\omega_c^j), \forall_i > j\}$$

From the above expression, a match between two points of interest (q,α) is considered if and only if q is the most suitable match for α with respect to all other points in one sample of the image pair and α is the most suitable match for q with respect to other points in the second image pair sample. Therefore, obtaining an efficient image feature matching algorithm is highly desirable to match the features fast and accurately. Furthermore, for matching image feature vectors, a nearest-neighbor matching method can be used to match image features in feature space found in the image descriptors using a normalized Euclidean distance (Bernardin et al., 2017) deployed. In process, however, the characteristics of a data set are highly relied upon by an optimal nearest neighbor algorithm and the factors existing in it. In addition, to match features of high dimensionality, two highly efficient algorithms have emerged: the fast library for approximate nearest neighbors (Muja & Lowe, 2014) (FLANN) and the randomized k-d forest (Hu et al., 2016).

For the binary feature-based methods like BRISK, FREAK, etc., the algorithms are not appropriate because Hamming distance is involved in the computation of the bitwise XOR operation and for performing the bit count of the outcome. The introduction of an approximate matching algorithm as a substitute to the linear search algorithm, which can speedily process features in multiple magnitudes over the linear search, can serve as a resolution to the problem of matching large datasets. This results in the approximation of neighbors caused by the nearest neighbors' algorithm; however, they are normally near in proximity to the actual neighbors.

3.7 Chapter Summary

This chapter investigated the performance of various image frame feature detection, extraction, description, and matching for suitability for the recognition and identification of the anesthetic medications in operating theatres. Experiments were conducted with the available drug samples, and their outcome was analyzed in detail in this chapter. The performance determinant of the various feature-matching

algorithms that use points of interest to match images depends solely on the characteristics of the core interest points and the corresponding image descriptors chosen for the task (Lindeberg, 2015). For a task like anesthetic image identification, a detection algorithm involving blobs is the most appropriate since they are rich information inscribed on the drug labels instead of using corner detector algorithms. The corner detector algorithms are more suitable if the corners of the drug images need to be detected to identify the drugs.

In addition, corner detection algorithms are not suitable for the task since the real-time processing of the medication images induces scale changes. In this case, since they are a high degree of distortions introduced by rotations, scale changes, light variations, and other factors, more robust detectors like the SURF, SIFT, etc., are more suitable for handling the real-time processing and identification of the anesthetic medications. From the various tests run in real-time, the SURF algorithm performed well when few images were involved. However, as the number of images to be matched increased, the SURF algorithm became computationally expensive. On the other, the SIFT algorithm performed exceptionally well even with a more significant number of images. Finally, despite the overall high performance of the detector, description, and matching algorithms, they cannot extract the fine-grained information required to identify the rate of the substance of anesthetic drugs. Also, the drugs with high similarity in semantic features are not distinguishable by the feature exploitative algorithms.

Chapter 4 Research Methodology

4.1 Introduction

A review of the diverse literature that is important in accomplishing this research goal was performed in Chapter 2. The major problems encountered during anesthetics drug preparation were identified, and the methodologies for solving them were explored concisely. Drug misidentifications due to close similarity identification features, medication swapping, and human factors such as negligence in reading the content of drug labels, limited processing time and fatigue, are some of the major problems that induce operating theatre drug preparation errors and pose a threat to patients' safety. In this chapter, the adopted research methodology is presented, which is, by extension, the design science research method. The selection of the design science research approach for this study is driven by the proven and reliable method of information systems investigation and the production of the corresponding framework. The task of the framework development is facilitated by the design science method, and the concise plan for the framework building and evaluation process is presented in this chapter.

4.2 Research Problem Overview

Based on the pieces of literature reviewed and the onsite operating theatre visitation, there is no current system that can automatically identify drug ampules in the operating theatre that does not use barcodes or QR codes on the ampules. In New Zealand and much of the world, ampules do not regularly have barcodes. Therefore, for the anesthetic drugs to be prepared for administration to patients, human interventions are still highly needed to read the content of the drug container labels that do not have barcodes in order to identify them. However, it is highly prone to errors, as outlined in the immediate section.

Also, issues abound in the use of feature detection and description methods that exploit the drugs' appearances, intensity, and landmarks to identify drugs in the operating theatre as a result of the challenging anesthetic drug characteristics, as will be intuitively enumerated in the subsequent section. Also, the feature detection and description approaches cannot filter the fine-grained information needed to

distinguish the drugs' amount of substance and concentration. In addition, according to our findings, drug vials and ampules color, height, and width measurements are not feasible for identifying specific drugs in the operating theatre. This is because some drugs have almost exact features, and only the drug names and rate of substance are distinguishable factors among them. The immediately mentioned approaches are potential candidates for redundancy, efficiency impediment, and low sensitivity if used because of the time required to perform the height computations and weight measurements. For highly similar drugs, filters cannot be applied to them to extract specific drug volume if the feature measurement methods are used without reverting to the proposed OCR method.

Also, for the existing systems to work effectively on new anesthetic drugs, the system must undergo tedious readjustment to accommodate new drugs. Our proposed framework will eliminate the gaps mentioned above and usher in an efficient drug identification framework that meets the real-time requirements for anesthetic drug label extraction and recognition in operating theaters. Therefore, this work will investigate novel computer vision methods that accurately identify specific ampules and vials to reduce the risk of medication errors during anesthesia in the operating rooms.

4.3 The Research Questions

This research aims to concisely examine ways the existing anesthetics drug preparation method could be enhanced through the development of an intelligent computer vision framework. The framework will be capable of detecting, extracting, and recognizing the tiny vital properties embedded in the operating theatre medication container labels and use the extracted features to verify if a selected medication is the right one or not. Thus, the research questions are presented as follows:

Main Research Question: Can computer vision be used to automatically identify medications in anesthesia?

To address the research question and achieve the research goal, the study sets to provide answers to the main research question and frame possible research sub-questions.

RSQ1: Which part of the anesthetic drug administration ecosystem needs improvement to eliminate medication errors?

From the direct interactions I had with anesthesiologists in the operating theatre during the on-site visits for this research, I observed that the two major problems encountered by anesthesiologists in the current anesthetic drug administration cycle were wrong drug selection and drug swapping. These problems mainly occur during the anesthetic drug preparation stage of the drug administration ecosystem. The existing dominant barcoding system does not eliminate drug preparation mistakes entirely, as not all the anesthetic drug containers are embedded with barcodes. Also, there abound numerous issues with the color-coding model, which does not identify specific drugs used by anesthesiologists. So, this proposal intends to address these issues by focusing on the use of an intelligent computer vision system to identify anesthetic drugs by extracting meaningful information from them. Hence, we formulate our second research sub-question as:

RSQ2: What approach can be used to identify anesthetic drugs to solve the problems identified in RSQ1?

In this study, computer vision-driven text recognition systems, particularly optical character recognition systems that undergo text detection, text recognition, and text extraction, shall be deployed to extract useful information from anesthetic drug labels. In addition, advanced sequence matching algorithms will be deployed to comparatively match and estimate the degree of closeness or similarity between streams of string from ampule and vial labels in order to identify specific drugs.

RSQ3: What features are required in the proposed framework to identify and recognize anesthetic drugs to solve the problems identified in RSQ1?

The framework will be able to detect anesthetic drug vials and ampules, extract their features, eliminate irrelevant features, and retain vital features required for performing medication identification and selection in the operating rooms. It tends to identify drugs mismatch or swaps, provide voice feedback and raise concerns when mistakes occur without an initial need for barcodes/QR codes and pre-recorded speeches. The proposed scheme will use an intelligent computer vision optical

character recognition model to capture the label in each drug vial and ampule, pre-process the captured label by eliminating unwanted regions and strings, and automatically convert the useful strings into speech without needing external human interventions. The base identification algorithmic engine will be compared with other algorithms to adapt the most efficient and viable using visual data collected from different anesthetic drug vials and ampules. The proposed framework is meant to enhance the existing anesthetics drugs preparation system to scale up its efficiency in eliminating errors and robustness to new drugs. The experimental platform will be a python programming language with a combination of different python modules.

4.4 Methodology and Research Process

This section provides a detailed discussion of the adopted research methodology and process. The design science (DS) is a detailed framework for coordinating research activities, framework initiation, and building philosophy. In recent times, numerous works have supported the design science research approach (Arazy et al., 2010; Gregor & Jones, 2007; Markus et al., 2002; Walls et al., 2004). The field of computer vision and artificial intelligence are not left out in the adoption of the DSR approach (Neuhauser et al., 2013). In the learning and research context, numerous pieces of evidence have shown the broader acceptance of the DSR methodology, utility, and benefits (Hevner & Chatterjee, 2010). In particular, a detailed investigation can be carried out on a framework and enhanced via consistent repetitions and assessments (Pretorius et al., 2015). The development and creation of frameworks are not only the sole purpose of design science but also to answer pertinent research questions. A researcher can channel the research process into producing a confirmatory outcome or innovation depending on the required outcome or goals of the research process (Johannesson & Perjons, 2014). This is similar to this study in which a verifiable output is expected. As observed from the literature and the onsite visitation during the preliminary investigations of this study, an intelligent framework that can automatically identify the medications used in the operating theatres does not currently exist in New Zealand and the world at large. Therefore, developing such an anesthetic drugs identification framework will require emphasis on the current anesthetic drug preparation flow. Due to the framework-centric facilitation approach of the DSR, it was adopted in this study as the best-suited methodology.

4.5 The Research Process

Despite the acceptability and adoption of the design science research approach in various information system research tasks, the transparency of mixing several research methods in the design science research has been subjected to scrutiny, questions, and improved methods proposed. In their work, Offermann et al. (2009) described design science as “an explicitly organized, rational, and wholly systematic approach to design, not just the utilization of scientific knowledge of artifacts.” They introduced their design science research process adopted for this study (see Figure 30). This method combines different research methods that are well suited for information system research and is partitioned into three major iterative parts or phases. The phases are the problem identification stage, the design of the solution to the identified problems, and the evaluation of the evolved or invented solution. In each phase, many activities are conducted, which are iterative, non-static, and compulsorily non-sequential. This implies that each process in the hierarchy of the adopted method can loop or iterate over each other, and results are produced as the processes progress.

The problem identification stage of the DSR process cycle states the research problem and justifies the research exercise and solution. The core objective of this activity is to motivate researchers and the targets of the research to continue with the research solution. It helps the research target audience to gain adequate knowledge of the researcher’s understanding of the research problem. The relevance of the research problem is revealed after the problem is identified, and it is imperative that the discovered problem must have benefits to the research area and context (Rosemann & Vessey, 2008). Knowledge of the current state of the research problem and the relevance of the solution are the needed resources at this stage.

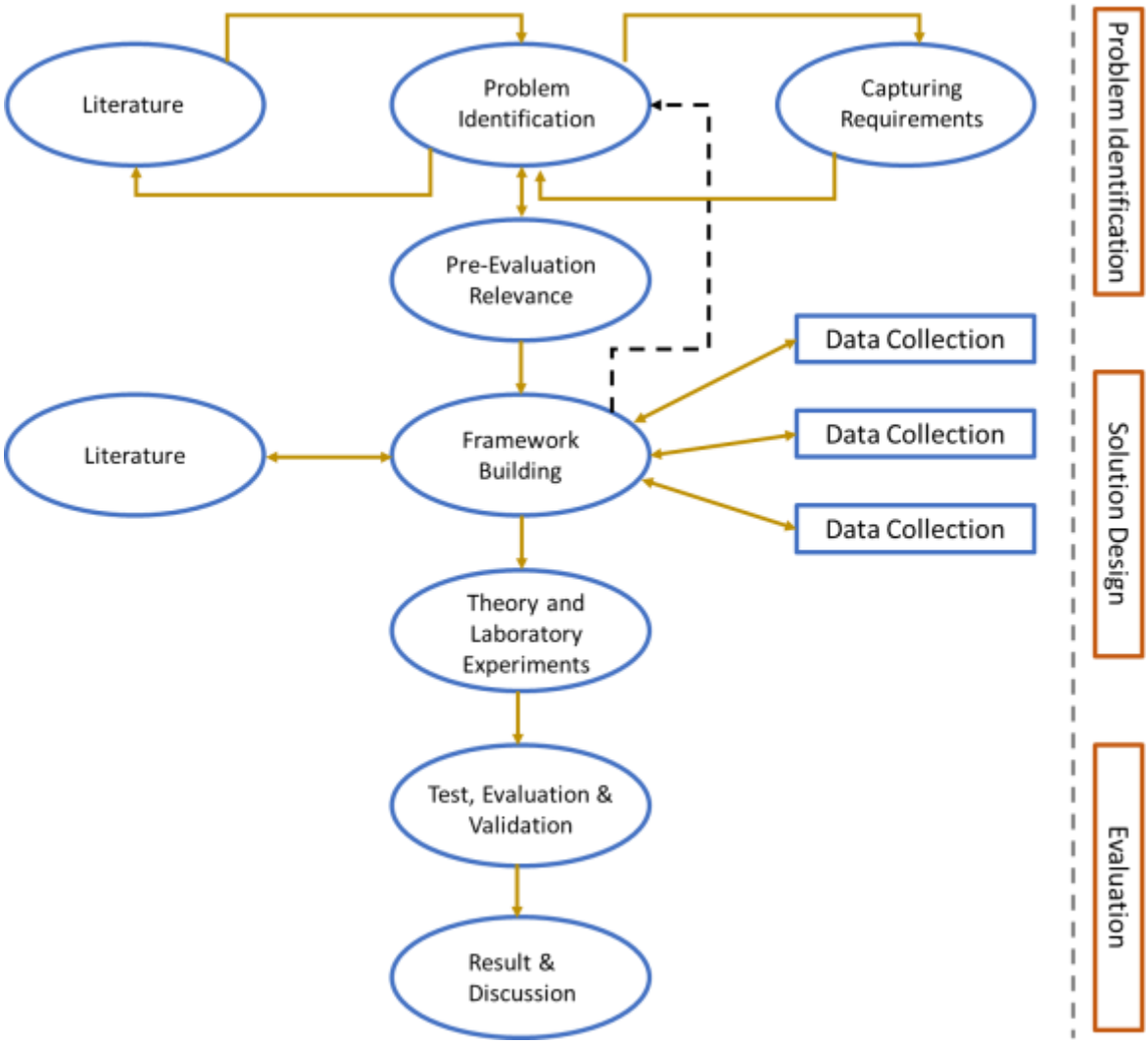

Figure 30: Anesthetics drugs identification DSR flow structure (Offermann et al., 2009).

In this stage of the research, the operating theatres' anesthetic drug misidentification problems were thoroughly investigated through extensive systematic literature reviews and on-site operating room visitations. The existing literature and the on-site visits unveiled the current state of anesthetics drug preparation and the level of technology adoption in the process. An understanding of integrating an intelligent computer vision framework into the anesthetics drug administration workflow was noted in this research stage. Consequently, this research's novelty and scientific contributions were identified in this stage. Figure 31 below illustrates the current anesthetics drugs administration workflow in the operating theatres:

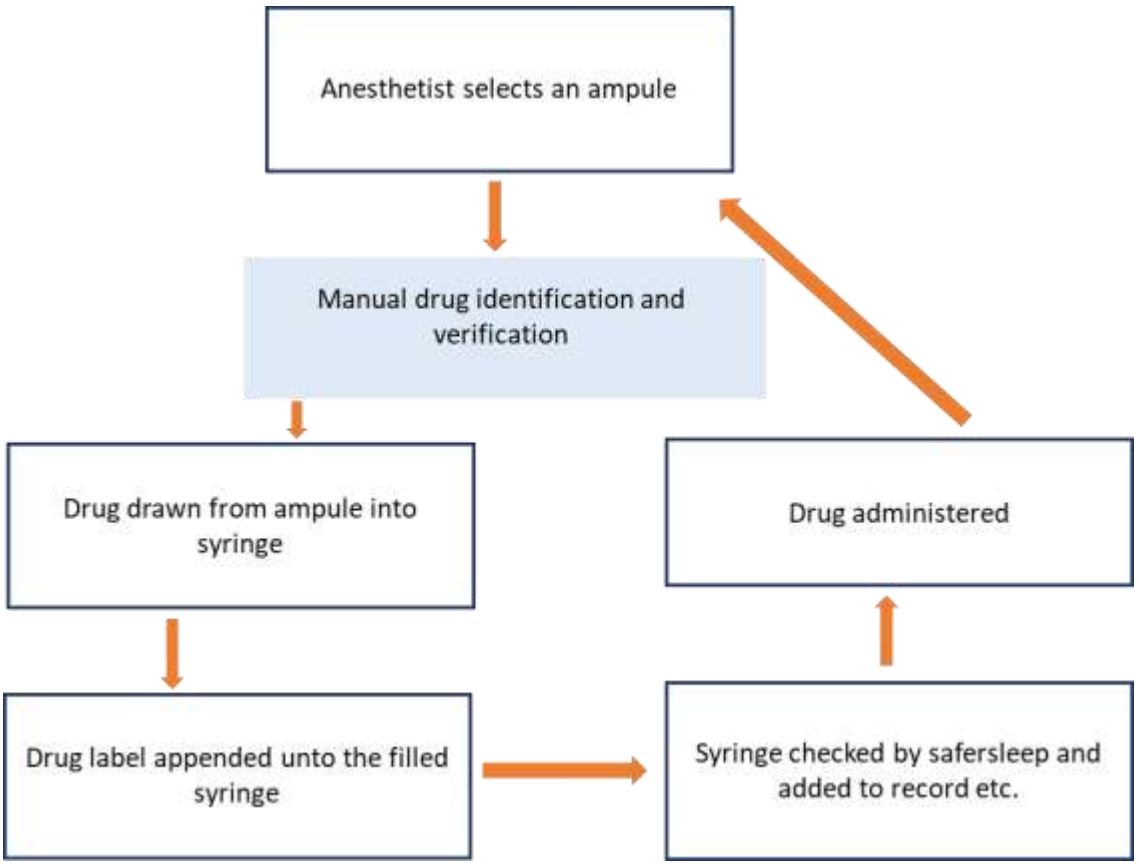

Figure 31: Current anesthetics drugs administration workflow.

From the Figure 31 above, the trained anesthetist selects an anesthetic drug from the drug tray and manually reads the inscription on the drug container label to identify the drug. The content of the drug is then drawn up with the syringe and labeled. Before the administration of the drug to a patient, the prepared and filled syringe is cross-checked with the existing system and recorded. After the cycle, the drug is then administered to the patient.

The framework design is the next phase; it tends to provide the solution design for the study. The selected research methodology emphasizes the importance of the research work in application. Artifacts may be algorithms, languages, computer interfaces, or system design methods. The design phase combines innovative thinking and the knowledge derived from the problem understanding to make assumptions about the required research outcome. This helps to create a new artifact that enhances the existing system and surpasses the performance of the previous method. Thus, the research tends to improve the manual ways of preparing and administering anesthetic medications in the operating theatre, as shown in Figure 31. In the design, the internal

workings of the anesthetics drug administration workflow, the external components, and the necessary interface between these components are considered.

In a nutshell, the design presents the knowledge for the framework implementation solely to satisfy the desired system function. In framework design, a series of questions are asked, providing a base for the framework testing or evaluations. Although the design involving innovation is not wholly systematic, the understanding derived from the design process could be transformed into a systematized process and evaluated until it meets the scientific standard. In addition, the knowledge derived from the design process could form knowledge embeddable into a scientific body of knowledge. Artifacts are not excluded from theories; instead, they depend on the application of kernel theories for evaluation of the artifact, modifications, or extensions. The design process is a complex process and thus requires an understanding of the creative advancements of the domain research area. Thus, during the on-site visitation for the study, the current working ecosystem of the anesthetic drug administration was explained in detail for the design and creation of useful frameworks for the anesthetic drug administration workflow.

The artifact represents a human construct or offers a description of an artificial system. Its' outcome is the target of every research project that adopts the design science process. In broad terms, the project artifact provides a description of the artifact constructs, the models involved, and the methods that deal with algorithmics, instantiations, and better design theories. The design must follow relevant natural theories explaining the research target's work. However, the theories may not be sufficient for developing and integrating the new artifact. On the other hand, scientific theories may assist in one way or the other in describing the artifact. However, they may not be able to wholly account for the human creativity and innovative thinking that produced the qualitative novelty.

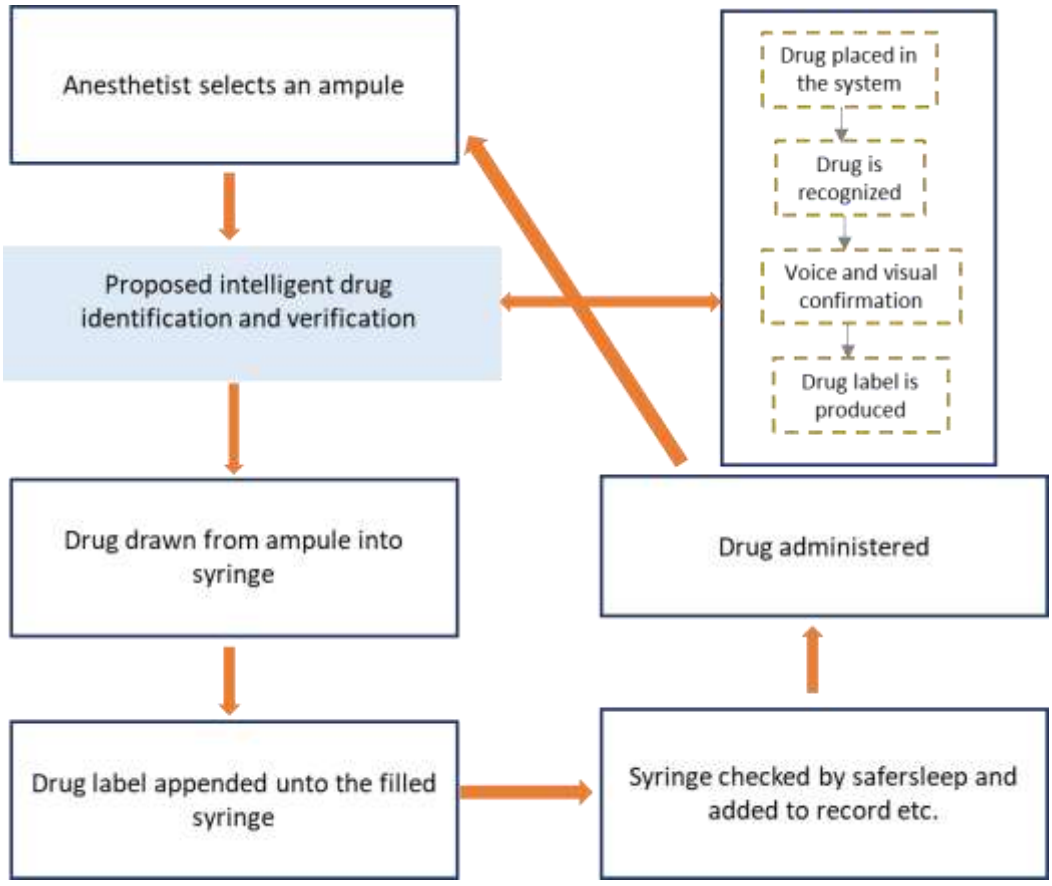

Figure 32: Current anesthetics drugs administration workflow embedded with the proposed intelligent drug recognition system.

The integration of the intelligent vision paradigm will transform the existing anesthetics drug administration ecosystem. Instead of the manual identification and verification of medication after being drawn up from the drug tray by the anesthetics in the operating rooms (see Figure 32), the anesthetist places the drug on the proposed framework, and the proposed framework recognizes the presence of the drug and identifies it. The proposed framework then tells the anesthetics what the medication is through visuals and voice confirmation. After the aforementioned process, the proposed framework prints a corresponding label, as shown in Figure 32.

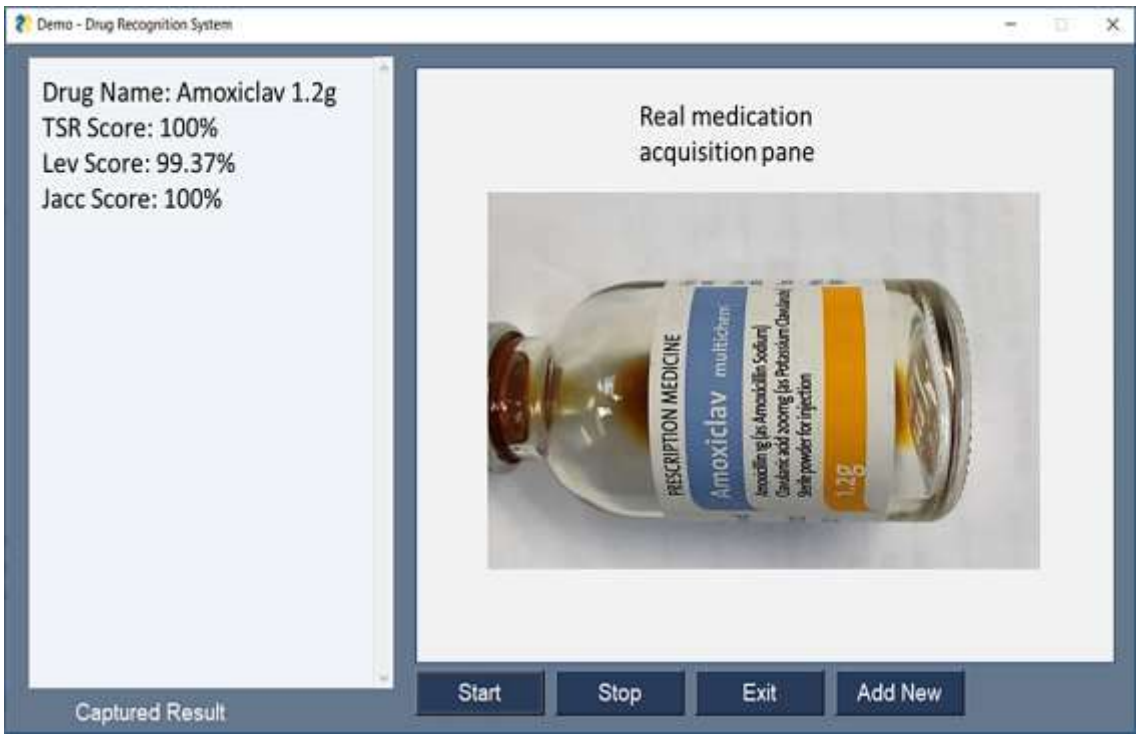

Figure 33: The main interface of the proposed framework.

The proposed framework design is partitioned into two major parts: the drug identification interface and the drug addition part, as shown in Figure 33. In practice, when the start button is pushed, the system gets ready to accept real-time medication objects on the right side of the main interface. After the drug image acquisition, the proposed image text feature detectors, extractors, and matchers (this will be elaborated on in subsequent sections); detects the presence of relevant properties of the drug container label, extract the properties and match the properties with the existing pre-stored features from all the available drug containers. If any incoming drugs' features meet the set requirements for identification, the drugs' vital properties are displayed on the left pane of the main interface. A concern is raised if the matched feature does not meet the set threshold standard. If the stop button is pushed, the system halts processing or waits. With the push of the exit button, the system terminates all process and close the interface. Finally, the add new button, when pushed, enters the frameworks' part where new drugs are acquired and information about them pre-stored.

Figure 34: The expected output of the proposed framework.

The proposed framework is expected to produce confirmatory feedback in the form of artificial voice feedback, display identified drug properties, and then print a corresponding drug label. The voice feedback tells the anesthesiologist the correctly matched drug name and other vital characteristics, such as the drug's rate of substance. Without other critical drug characteristics, the system only tells the anesthesiologist the drug name. If no drug is matched, the system raises a concern and asks the anesthesiologist if she/he may want to add the drug. Then the corresponding label is automatically generated, which the anesthesiologist will append unto the drugs' syringe for onward administration to a patient. The drug label consists of the drug name, the production date, the time, and as well as the QRcode that will enable the anesthesiologist to efficiently verify the drug and record it before administering it to a patient.

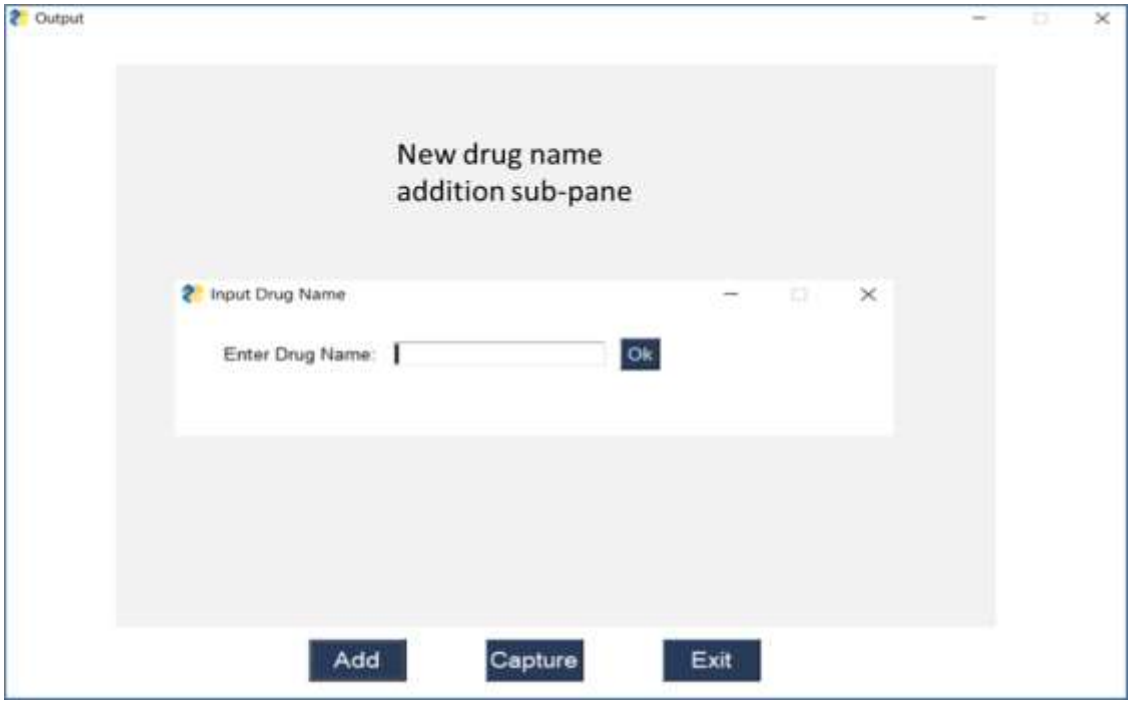

Figure 35: The new drug name acquisition interface of the proposed framework.

After the push of the add new button from the main interface of the proposed framework (see Figure 35), an interface is opened for the acquisition and addition of new drugs. Firstly, the add button is pressed, which will usher in a sub-interface where the new drug's name is expected to be added. After the imputation of the new drug name and the "ok" button is pressed, the framework ushers in the platform for the real-time acquisition of the new drug. At the press of the capture button (see Figure 36), the new drug image is taken, and the framework automatically extracts the features on it and pre-stores it in the existing lookup table in the database. A confirmation message is then displayed to reaffirm that the drug has been added.

Figure 36: The new drug image acquisition interface of the proposed framework.

The need for an on-device standalone framework that is online cloud text processing independent is vital for ensuring the privacy of the users of the proposed framework. Also, a more compact system that can be integrated into embedded devices, android platforms, and other edge processing systems will make integrating the proposed framework into the anesthetic drug preparation and administration workflow easier. This will also reduce the real-time processing cost, memory requirement, and computational cost. Therefore, the proposed system is redesigned to meet the above characteristic, as shown below in Figure 37 and Figure 38.

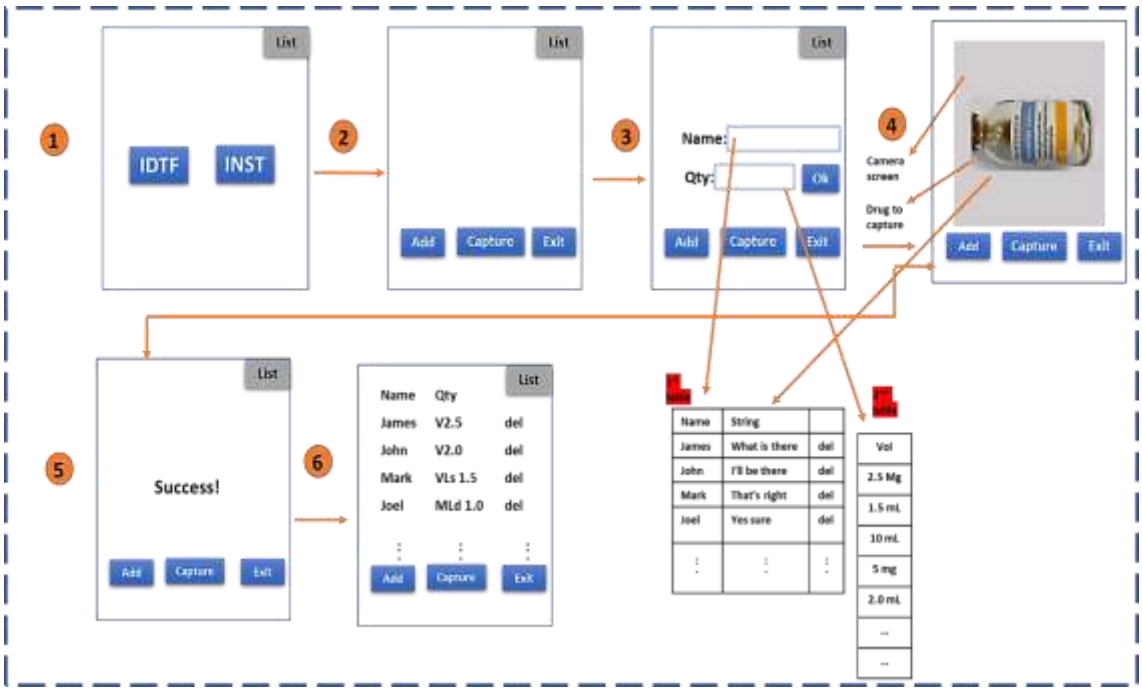

Figure 37: The drug image acquisition interface of the standalone anesthetic drug identifier.

The working principle of the on-device standalone anesthetics drug identification system is similar to the on-the cloud-based anesthetics drug identification system. This approach is equally divided into two major parts: the drug identification interface and the drug addition part, as shown in Figure 37. In practice, when the start button is pressed, the framework gets ready to accept real-time medication containers for processing. The first two main buttons are the IDTF and INST buttons. The IDTF represents the anesthetic drug identification, while the INST represents the new drug insertion. After the INST button is pressed, the main anesthetic drug acquisition interface opens. This interface consists of three primary tabs, the “Add,” “Capture,” and the “Exit” buttons. At the press of the Add button, a third interface opens with fields for capturing a new drug’s information, such as the drug name and volume, and an extra “Ok” button. After the drug Name and Volume are imputed and the Ok button is pressed, then the camera is opened within the platform for real-time drug image acquisitions.

Furthermore, after the Capture button is pressed, the character strings on the captured anesthetic drug image are automatically detected and extracted with the OCR engine, and the extracted character strings are automatically stored in the 1st table with the corresponding drug name. Then the drug volume is subsequently stored

in the 2nd table. Both the 1st and 2nd tables can contain any number of the same drug name and strings; this implies that any drug name and string can be repeated in the 1st table. However, the drug volume is not permitted to be repeated in the 2nd table to avoid the repetition of the drug volumes on the final drug label. This means that a constraint is embedded in the 2nd table, which disallows the addition of any same drug volume data. Confirmation is expected to be displayed when a specific drug name, strings, and volume are successfully updated, and this process can be repeated as many times as possible. In continuation, a “List” tab on the upper right side of the anaesthetic new drug image acquisition platform exists. When the List button is pressed at any time, all the available drugs with their volume are displayed with delete icons on the right-hand side that will enable the deletion of any drug string, but the volume cannot be deleted, as shown in Figure 38.

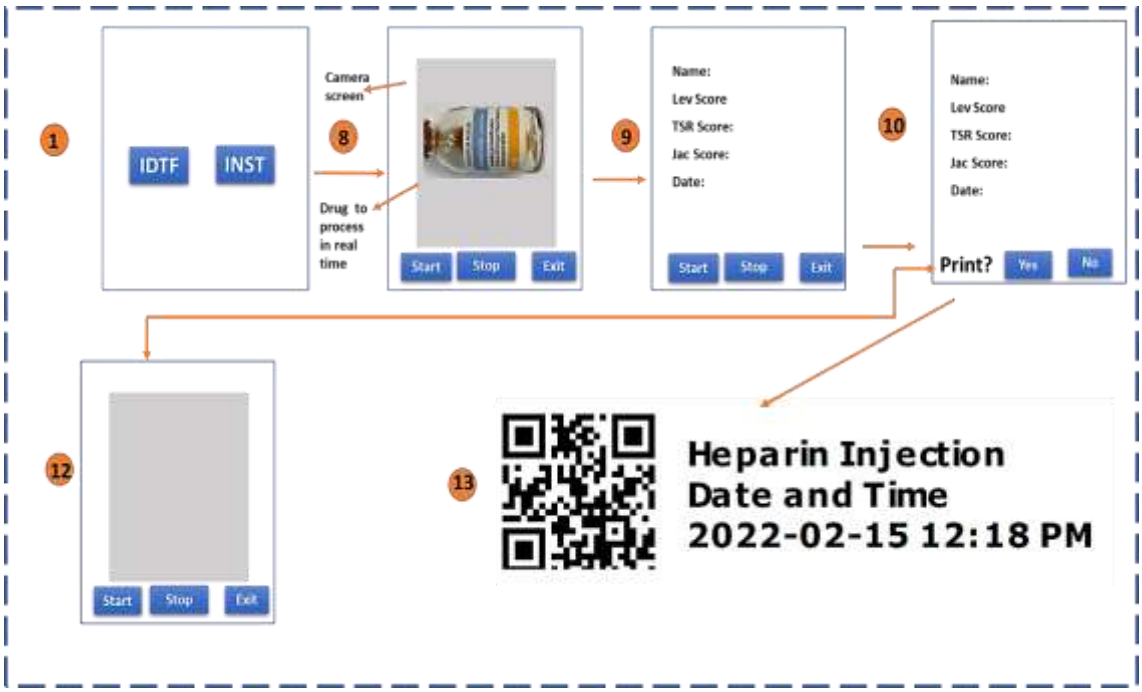

Figure 38: The main interface of the standalone anesthetic drug identifier.

On the other hand, after the IDTF button is pressed, the main anesthetic drug identification interface for real-time medication processing is initiated. This interface consists of three primary tabs, the “Start,” “Stop,” and “Exit” buttons. After the Start button is pressed, an empty real-time screen is initiated to acquire, process, and identify the anesthetic medications. When a drug container with text characters inscribed on it is shown to the camera, the system detects the presence of text,

captures the image containing it, and automatically extracts it. The system then uses the newly extracted texts to perform a pairwise comparative test on the character strings pre-held on the 1st table of step 4 using the Levenstein, Token set Ratio, and Jaccard distance. After the pairwise comparative exercise, the appropriate drug is matched with its' highest score calculated. The calculated scores with each matching algorithm are subjected to further examination through thresholding. A threshold is computed and set. For any given drug to be affirmed as the right drug, the generated scores with each matching scheme must equal or exceed the set threshold. If the character strings from an incoming drug do not meet the set threshold, the drug is returned unavailable. Also, if an image with no text is shown to the camera, no output is returned.

Furthermore, after the highest score is turned in and the threshold is met, the drug name with the highest score is displayed in stage 9 (see Figure 38), together with the matched drug volume in one line. Afterward, the individual Leventein score (Lev Score), Token Set Ratio score (TSR Score), and the Jaccard Distance score (Jac Score), all in percentage, are displayed on the screen, respectively. This is immediately followed by voice feedback that reads the drug's name to the anesthetist. If the presented drug is not available, a confirmatory voice note is also automatically returned to the anesthetist indicating that the drug is not available and whether the anesthetist would like to add the drug. Afterward, the system asks the anesthetist if the matched drug label should be printed; if the anesthetist indicates "yes," the matched drug label will then be printed on the physical printer, but if the anesthetist indicates "no," the printing process is bypassed. The anesthetics drug confirmatory process cycle continues.

4.6 Hardware Requirements

The proposed anesthetic drug identification hardware requirements will be divided and examined into two types. The standalone setup with a controlled environment and a handheld approach. The standalone setup will consist of a stand with a controlled light source. The controlled system is due to the tiny or small nature of the string character inscriptions on the anesthetic drug container labels and the natural scene instability caused by the varying natural lighting conditions. Thus, a controlled

environment for the real-time acquisition and processing of drug container images is desirable. The setup will also contain a camera for real-time anesthetic drug capturing. This device will have a high-definition or HD camera for clear real-time drug acquisition and processing. It is projected that the portable device implementation of the proposed system will offer easy integration of the proposed system into the anesthetic drug preparation and administration workflow.

4.7 Data Collection Methods

The data used in this study were collected in two stages: during the pre-evaluation stage and the experimental stage of the study. The data were sourced and selected by on-site anesthesiologists and submitted for the study. It consists of various empty anesthetic drug containers used intravenously in operating theatres. It includes different ampules and vials of various sizes, shapes, colors, and weights. In most of the experiments, the entire data was used at once. In other experiments, a set of samples were selected according to the medication containers' physical properties, such as size, color, and the number of texts inscribed on them.

4.8 Formal Evaluation Approach as a Tool for Evaluation

Within the context of the design science research methodology, the formal evaluation methods are deployed as tools for validating a proposed system. System checking through the utility of formal methods is integral to the validation method. The extensive use of the approach in past research works drives the deployment of formal methods for validating a proposed system. For instance, Easterbrook et al. (1998), in their work, validated their proposed modeled spacecraft fault protection systems using the formal validation method as a tool. They opined that formal methods usher in a variety of ways that are assistive in validating a system, and system checking is one such method. In another work involving a formal method, Antoni and Ammad (2011) used a formal method to validate their proposed system.

4.8.1 Evaluation Process

The performance of the proposed framework will be evaluated through the laboratory evaluation process. The laboratory evaluation will be presented in the form of visual plots with charts and other formats. Before the commencement of the evaluation

process, matrices need to be well defined as they are critical to the success of the evaluation process.

4.8.2 Statistical Results Evaluation

The statistical evaluations will rely on the in-lab experiments and the real-world domain evaluation outcome. The result will demonstrate the degree of robustness and practicality of the proposed system in the operating theatres. The approach deployed to evaluate the framework has been concisely explained in the preliminary research progress of the development of the framework.

4.9 Other Research Methodologies

This section introduces other research approaches that were explored in addition to design science research to determine the most suitable approach for this research project. As stated above, the design science research method was selected for this project because of the artifact-centric drive of the method. During the preliminary study, other research methodologies like the grounded theory (Dey, 2004), the standard quantitative model (Chih-Pei & Chang, 2017), and the phenomenology approach (McCance & Mcilfatrick, 2008) were investigated for suitability.

4.9.1 The Grounded Theory and Phenomenology Approach

In this research approach, theories are formulated by studying concepts that are hidden in a given research data, and the end objective of this methodology is to construct a social process (Starks & Brown Trinidad, 2007). In practice, participants who have had experience in a particular phenomenon under diverse situations are needed in the study (Corbin & Strauss, 2006). Interviews are veritable tools required for this research method wherein partakers of the research are needed to share their experiences. In a nutshell, grounded theory is best suited for research studies where the core objective of the study is to produce a theory from experience harvested from the research partakers (Bowen, 2006).

On the other hand, the phenomenology approach is a research method that is based on qualitative study (Eberle, 2014). It is a research philosophy that advocates for the analysis of issues themselves. The phenomenology approach is not limited to the interpretation of research data alone; instead, it starts prior to the collection of

empirical research data (Khan, 2014). Also, this research approach plays a vital role in describing the phenomenon of real experience. In other words, to conduct research on a field, the researcher needs the experience of those who are domain experts in the area of research interest. Therefore, the research output of the phenomenology research method is the thematic explanation of the pre-specified construct of acquired experience over time (Starks & Brown Trinidad, 2007).

4.9.2 The Standard Quantitative Research Model

In this approach, statistical tools are used to conduct an analysis of the collected research data. The main focus of this method is to use the vast research data collected across multiple research participants to formulate generalizations or to offer an explanation of a specific phenomenon (Chih-Pei & Chang, 2017). In continuation, data is collected using designed study tools such as questionnaires in this research method, and the data could be in number or statistical formats. Interviews or historical archives can serve as sources of data gathering. During the study, research participants are asked questions, and the data gathered from the exercise are analyzed to establish correlations between the resulting variables obtained from the research design phase. In other words, this research method is used to construct relationships among variables emanating from a population.

The proposed anesthetics drug identification research will not involve a high degree of participants since it is artifact-driven research, as stated in the previous section. This study deals with the deployment of conceptual models and the development of a framework in the form of an artifact which will be investigated for validity. The anesthetics drug identification research investigates suitable computer vision approaches for improving patient safety in the operating theatre. At the same time, domain experts will observe and examine the proposed system, but it does not deal with social process construct. Thus, since this research is not focused on explaining a specific phenomenon or obtaining generalizations on collected research data, the grounded theory, phenomenology, and quantitative research models are not suitable for the research, which is why the design science research method was adopted.

4.10 Chapter Summary

In this chapter, the adopted research methodology for the anesthetic drug identification framework was explored in detail. The chapter started with an overview of the core problems the proposed framework seeks to solve, including the current manual anesthetic drug preparation method and the issues involving the deployment of the feature extraction strategy in identifying anesthetic drugs. Also, the design science research approach adopted in the study was presented in detail, including the workflow of the existing anesthetics drugs administration and the proposed intelligent drug recognition framework embedded into the current anesthetics' drugs administration ecosystem. The chapter also presented a conceptual standalone anesthetic drug identifier embeddable into edge systems and other portable devices. Furthermore, the hardware requirements, the data collection method, and the formal evaluation approach used for the frameworks' evaluation are presented. Finally, also presented in this chapter are other research methodologies, such as the Grounded Theory and Phenomenology and the Standard Quantitative research model examined for suitability for the project.

Chapter 5 Theoretical Framework and Research Findings

This chapter presents the core foundational theoretical framework and the research findings. The theoretical framework is a critical component of this thesis, as it presents the theoretical concepts, algorithms, and models that guide and support the development of the anesthetic drug identification framework. It provides the conceptual framework for the study, assisting in explaining the relationships between various conceptual components, identifying gaps in the adopted algorithms, and providing a new idea to fill the gap identified. The theoretical framework chart is developed early in the research process and guided the flow of the remaining part of the research.

On the other hand, the research findings contain the outcome of the investigations presented in this thesis and experiments conducted in the study. This subsection of the thesis presents the data obtained from the various experiments conducted during the study and analyzes them with respect to the research questions and problems. The findings are concisely organized, logical, and presented with charts, graphs, and tables for accessibility and understating of readers.

5.1 Conceptual Workflow of The Anaesthetic Drugs Identification Framework

The schematic workflow of the proposed framework provides a flow guideline for the development of the anesthetic drug identification system. Each stage of the workflow is critical to the success of the framework development process and the thesis overall. The proposed framework is divided into five parts, as shown in the schematic workflow diagram in Figure 39.

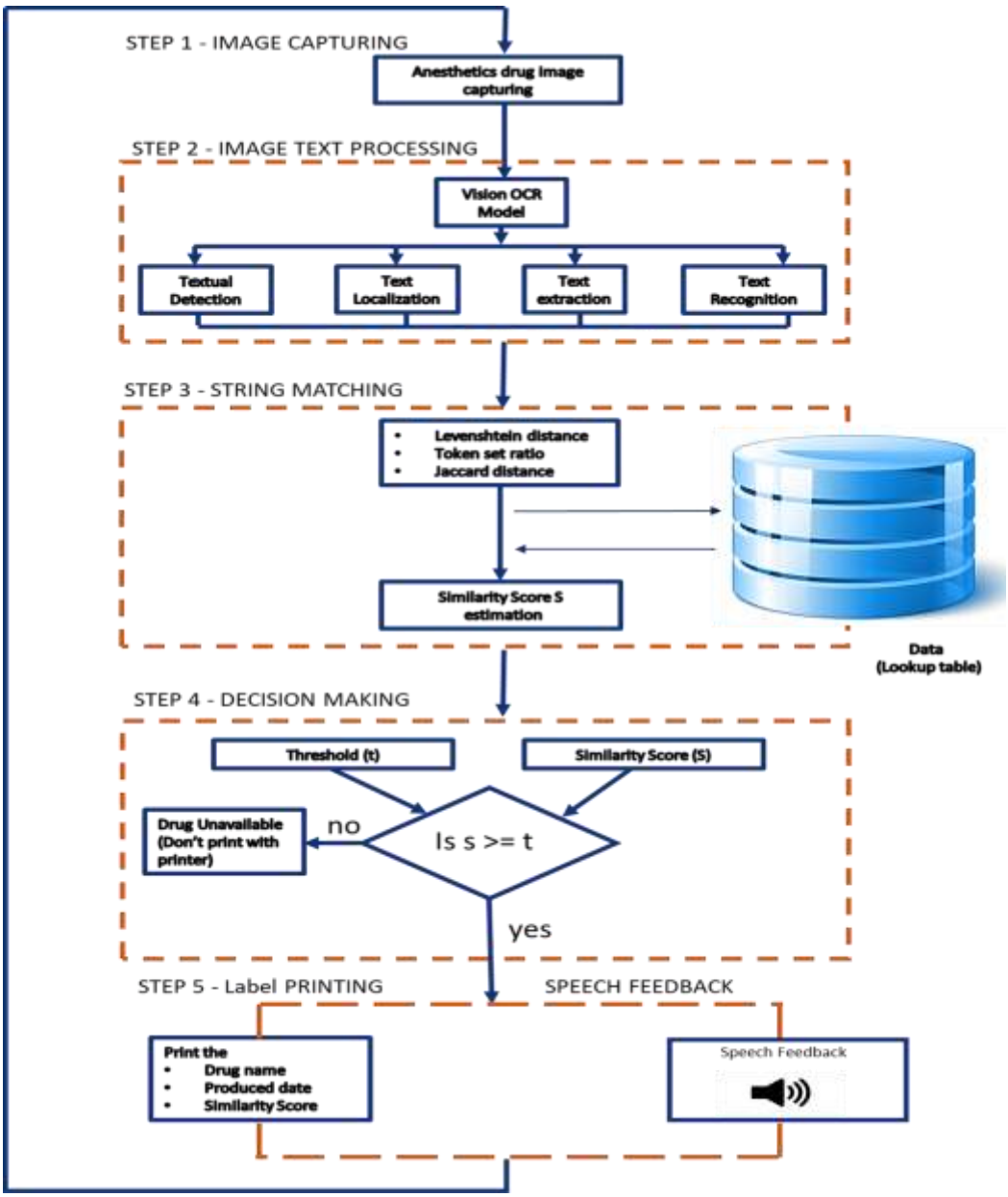

Figure 39: The cross-section of the schematic workflow of the proposed framework.

The schematic workflow sketch in Figure 39 consists of the image frame capturing section (for anesthetic drug image frame acquisitions) and the image-text processor, with the OCR responsible for the anesthetic drug label strings extraction and the string-matching component. It also contains the decision-making and label-processing sections, completing the parts that conceptually build up the proposed framework. Upon the reception of an input image frame with texts, the OCR performs text detection, localization, recognition, and extraction tasks before passing the extracted strings down to the matching algorithm to distinguish and identify the drug. The strings on each drug ampule are extracted using the OCR engine and compared to a lookup table, including the strings extracted from the known ampules for the string-matching

tasks. The framework only compares the test ampule with sample types already stored in the lookup – a “new” or unmatched ampule is reported as an error.

This fits with the inaesthetic workflow because it is known in advance which ampules should be present in the anesthetic tray. The Levenshtein distance, Token set ratio, and Jaccard distance methods are used to estimate the closeness or similarity between the incoming strings from the image-text processor and the ones held in the lookup table. Furthermore, the estimated similarity score is compared with a set threshold value to validate the matched drug from the decision-making stage before the final label is processed. After related texts are matched, the matched drug information is displayed on the screen and printed on a physical printer. However, in the event of discovering drugs that are not prescribed or drug swapped, the framework raises concerns.

5.2 String Matching for Anesthetics Drugs Identification

After strings are extracted from the vials and ampoules using the OCR, there is the need to match the strings against each other in order to precisely identify an incoming new drug. In this work, string-matching algorithms will be deployed to estimate the closeness or similarity between the strings to distinguish one drug from another appropriately. Three algorithms that fit into this task are the Levenshtein Distance (Haldar & Mukhopadhyay, 2011), the Token Set Ratio (an extension of the Levenshtein Distance), and the Jaccard Distance (Levandowsky & Winter, 1971).

String matching is a crucial pattern-matching process whereby the patterns are treated as symbols of a finite sequence. It deals with the search and discovery of one or all the occurrences of a specific pattern $p = p_0, p_1 \ldots p_{x-1}$ with a length x, in a text $t = t_0, t_1 \ldots t_{y-1}$ with a length y, where $y \geq x$. Both $p \; and \; t$ are incorporated into the same alphabet denoted as $\sum$. In simpler terms, string matching deals with scanning a given pair of text corpus and computing the relationship or similarities between the scanned texts. A string-matching algorithm compares a pattern or short string with a larger string, referred to as text, to determine if the string is a substring of the text. The string-matching process produces a location in a situation of finding a pattern in the text or generates a signal that indicates a mismatch in a case in which the desired pattern is not found.

In further description, a string S with length L can be said to have an array of infinite number $S[0\,..\,L-1]$ provided that $L \geq 0$. More succinctly, for $L = 0$, an empty string is obtained and can be represented as ε. The $(m+1)-st$ character of S can be represented as $S[m]$, for $0 \leq m < l$. Also, the substring of S found among the characters $(m+1)-st$ and $(n+1)-st$ can be represented as $S[m\,..n]$, for $0 \leq m \leq n < L$. In addition, for any $m,n \in \mathbb{Z}$, $S[m\,..n] = \varepsilon$ is inserted if $m > n\ and\ S[m\,..n] = S[max(m,0), min(n, L-1)]\ if\ m \leq n$ (Faro & Lecroq, 2013).

A substring of a particular string S is also known as a $factor$ of S and is represented as $Fact(S)$. In other words, $Fact(S)$ is a collection of the whole factors found in the string S. A substring that is of the arrangement $S[0\,..m]$ is referred to as a prefix of S, and a substring that is presented as $S[m\,..L-1]$ is referred to as the suffix of S given that $0 \leq m \leq L-1$. The collection of suffixes that exist in the string S is represented by $Suff(s)$ and that of prefixes of S as $Priff(S)$ with $n+1\ length$, i.e., $Priff(S) = S[0\,..n]$. If a substring δ of S is both a $Priff(S)$ and a $Suff(s)$, then δ is a border. If for m, $0 \leq m < L - k$, $z[m] = z[m+k]$ of any given two strings z and q, then an integer k represents a period of the word z. The least period found in z denotes the period of z, which is represented as $per(z)$. If a given word z cannot be expressed as the power of another word, then the word is regarded as $basic$. This implies that a word v does not exist and also an integer k does not exist that could yield $z = v^k$. The reverse of $S[0\,..L-1]$ string is represented by $\bar{S}$. Furthermore, it is obtained by joining its characters beginning from the last letter to the first, i.e., $S[L-1]\,S[L-2]\ldots S[1]\,S[0]$.

Given a text t with a length L and a pattern p of $L0$ length, then a shift s is said to be of the pattern p in t if a given character $c[0]$ is aligned with another character $c[1]$ of the text being processed, given that the character $c[m]$ is aligned with the character $c[s+m]$, for $m = 0,\ldots,L-1$. Then, a current substring is taken as $c[s\,..s+L-1]$, and in a situation where $c[s\,..s+L-1] = p$, then a shift is regarded as valid. In the text scanning process for string matching, an attempt is said to have occurred if patterns in the text are compared to match a specific string character.

5.2.1 Categories of String Matching for Anesthetics Drugs Identification

String matching is generally categorized into exact and inexact or approximate string matching. The exact string-matching methods do not permit any tolerance or mismatch. For instance, the section of the proposed framework that deals with the precisive matching of the rate of substance of the anesthetic drugs do not tolerate any mismatch and, thus, an exact matching problem. On the other hand, the inexact string-matching approach permits to some extent, mismatches, provided that the set threshold is not exceeded. The more significant part of the proposed framework uses inexact string-matching methods to identify a particular drug before the identification of the medication rate of substance by the exact method.

- Exact String Matching

In continuation, the exact string matching is defined as the process of scanning for a pattern $P = [1..x]$ in a long string text $T = [1..y]$ with all the occurrence of the exact match maintaining $y >> x$ (Patel & Thakkar, 2014). In other words, all the occurrences of a particular string pattern P from a specific text T must be found. The exact string-matching algorithm is classified into software and hardware-based approaches. In this work, however, the software-based approaches are developed and used for the anesthetic drugs identification, and the work focuses mainly on the software framework methodology. The exact string-matching approach is further grouped into single and multiple-pattern methods. The single exact string matching method is subdivided into character comparison, hybrid, hashing, and bit-parallel approaches (Hakak et al., 2019).

In the fixed or exact string-matching task, initially, it is appropriate to consider a window for the text scanning process. During the comparative process, both character strings' window lengths need to be equal. The window demarcates the text factors and is often the text pattern length. The window slides through the text rightward from the left, and the window periodically shifts depending on the rules that govern the specific algorithm during the scanning process. At a particular position on the text during the search process, the algorithm checks if a string pattern occurs there or not by performing a comparative test of the characters found in the window with the corresponding aligned characters of the string. When a whole match is detected, the position where the match occurred is reported. While performing the scanning

operation, the algorithm notes vital information from the text that can be used to obtain the next shift length of the window. To obtain an efficient exact string-matching algorithm, it is necessary to shift characters in situations of string mismatch occurrence. To conserve time for the next scan operation, the matching algorithm can memorize some valuable parts of the noted information (Navarro & Raffinot, 2002). The exact string-matching strategy is employed in matching the amount of substance found in the various anesthetic drug ampules in this work.

- Inexact String Matching

The inexact or approximate string matching (Cinti et al., 2020) deals with the matching of a collection of generic strings delineated on the same alphabet and permits a degree of inexactness compared to the exact string-matching counterpart. In the approximate string-matching process, a pair of strings match if their dissimilarity does not exceed a set threshold value. The inexact string-matching strategy is a special case of the subgraph matching process that is highly useful in many technology and scientific fields. The strings to be matched in this work are mainly inexact, with different levels of inexactness and variations.

The inexact string-matching algorithms adopted in this study offer us the ability to determine the similarities between the set of strings extracted from the various anesthetic drug ampule labels for the prompt and rapid identification of a specific drug with respect to the set string metrics. In the process of finding the right drug among the collection of drug samples, an approximate substring is matched from a given drug sample's corpus of strings and determining the string pattern that matches approximately the specific drug string to be identified by the proposed framework. The nearness of match between an incoming new string from an anesthetic drug and the collection of already held strings from other known anesthetic drugs is measured with respect to the number of primitive operations required to transform the string from the new incoming drug to an exact match in the held stream of strings.

5.2.2 Levenshtein Distance for Anesthetics Drug Label String Matching

The Levenshtein Distance, also called Edit Distance, is one of the three anesthetic string-matching algorithms selected for this study. It is defined as a similarity gauge between pairs of strings (Haldar & Mukhopadhyay, 2011). The distance between a

source string (S) and a target string (Z) is described as the least amount of edit tasks (deletions, insertions, or substitutions) needed to convert the source string (S) into the target string (Z) (Backurs & Indyk, 2015). The lesser the distance between the strings, the higher the similarity between them. The Levenshtein distance performs well on a stream of strings of unequal length, like the strings extracted from the anesthetic drug labels. The higher the Levenshtein distance, the higher the difference between strings (Andoni et al., 2010). Given two strings, S = $s_1 \dots s_n$ and Z = $z_1 \dots z_n$, the distance between them is the minimum edit operations required to convert S into Z (Trevisan, 2001), where likely operations are:

- Insertion operation

  Insert (s, i, c) = $s_1 s_2 \dots s_i c s_{i+1} \dots s_n$.
- Deletion operation

  Delete (s, i) = $s_i s_2 \dots s_{i-1} s_{i+1} \dots s_n$.
- Substitute operation

  Substitute (s, i, c) = $s_1 s_2 \dots s_{i-1} c s_{i+1} \dots s_n$.

More succinctly, the Levenshtein Distance of two given strings, m, and n, having length |m| and |n| respectively, can be expressed as $L_{m,n}\,(|m|, |n|)$. Where:

$$L_{m,n}\,(i,j) = \begin{cases} \max(i,j) & if\ min(i,j) = 0, \\ min \begin{cases} L_{m,n}(i-1,j) + 1 \\ L_{m,n}(j-1,i) + 1 \\ L_{m,n}(i-1,j-1) + 1_{\left(m_i \neq n_j\right)} \end{cases} & otherwise \end{cases}$$

Where, $1_{\left(m_i \neq n_j\right)}$ represents an indication function that is equal to 0 if $m_i = n_i$ otherwise equal to 1 and $L_{m,n}\,(i,j)$ is the distance between the initial i character of m and the initial j character of m. i and j represent the 1-base indices. It is a dynamic programming problem because it computes the distance between strings step by step.

- The Minimum Edit Distance

According to (Trevisan, 2001), the minimum edit distance is the least amount of tasks (insertion, deletion, and substitution) needed to be done to convert a stream of strings into another. Let the concatenation of δ_{P} and $\delta_{\mathrm{Ş}}$ pair of symbols with a finite alphabet represented as ∑ define a pattern $\mathrm{P} = \langle \mathrm{P}^0, \mathrm{P}^1, \dots, \mathrm{P}^{(\delta_{\mathrm{P}}-1)} \rangle$ and a string $\mathrm{Ş} = \langle \mathrm{Ş}^0, \mathrm{Ş}^1, \dots, \mathrm{Ş}^{(\delta_{\mathrm{Ş}}-1)} \rangle$, respectively. Also, let the contiguous symbol subset of δ found in Ş

beginning from i position be represented by $\hat{\mathrm{S}} = \langle \hat{\mathrm{S}}^0, \hat{\mathrm{S}}^1, \ldots, \hat{\mathrm{S}}^{(\delta_{\hat{\mathrm{S}}}-1)} \rangle = \langle \mathrm{Ş}^{(i)}, \mathrm{Ş}^{(i+1)}, \ldots, \mathrm{Ş}^{(i+\delta)-1)} \rangle = \mathrm{Ş}[i, \delta]$ generic substring. Then, the Levenshtein distance $\mathrm{lev}(\mathcal{P}, \hat{\mathrm{S}}) \in \mathbb{N}_0$ serves as a measure of the dissimilarity that exists between the pair of strings $\mathcal{P}$ and $\hat{\mathrm{S}}$, which is the smallest amount of single character edit operations needed to convert $\mathcal{P}$ into $\hat{\mathrm{S}}$. For instance, the minimum edit operation required to transform the substance "Bromide" into "Chloride" is 4, as shown in the memorization matrix process table presented in Figure 40 below:

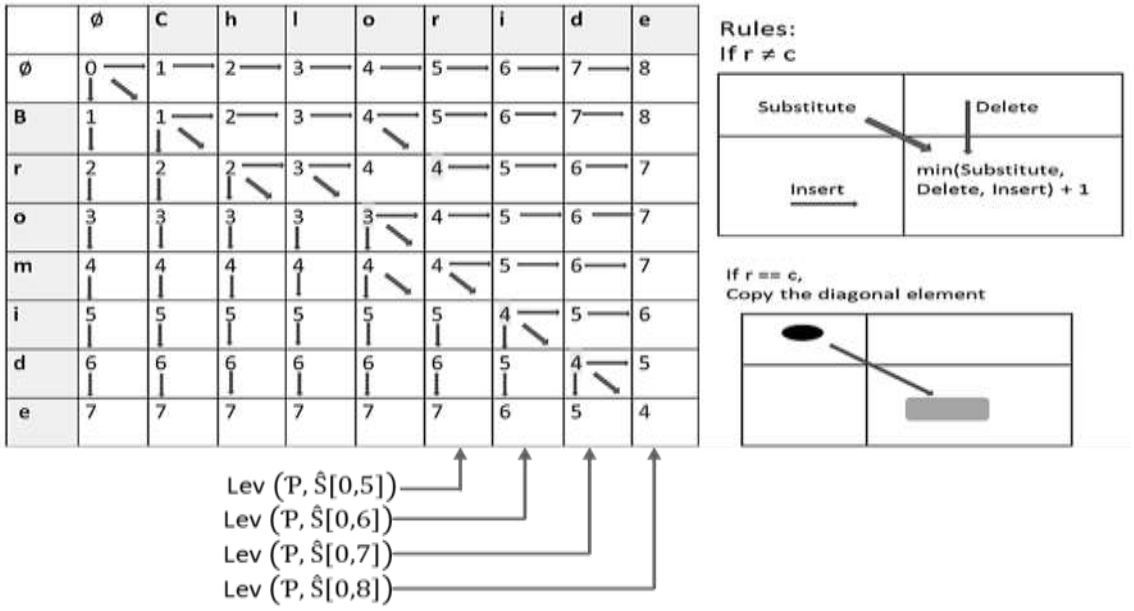

	∅	C	h	l	o	r	i	d	e
∅	0	1	2	3	4	5	6	7	8
B	1	1	2	3	4	5	6	7	8
r	2	2	2	3	4	4	5	6	7
o	3	3	3	3	3	4	5	6	7
m	4	4	4	4	4	4	5	6	7
i	5	5	5	5	5	5	4	5	6
d	6	6	6	6	6	6	5	4	5
e	7	7	7	7	7	7	6	5	4

Figure 40: Memorization matrix process to convert Bromide to Chloride.

The procedures taken to obtain the memorization matrix tables above are as follows (H. Chen, 2012):

$$Let\ the\ source\ string\ be\ denoted\ as\ S,$$

$$target\ string\ as\ T,$$

$$C\ as\ the\ length\ of\ the\ source\ string\ S,$$

$$R\ as\ the\ length\ of\ target\ the\ string\ T,$$

a) $Sketch\ a\ memorization\ matrix\ M\ consisting\ of\ R\ rows\ and\ C\ columns$
b) $Set\ the\ first\ row\ from\ 0\ to\ R\ and\ first\ column\ from\ 0\ to\ C$
c) $Inspect\ individual\ characters\ in\ S\ (i\ from\ 1\ to\ R)\ and$
d) $individual\ characters\ in\ T\ (j\ from\ 1\ to\ C)$
e) $If\ S[i] = T[j], then\ the\ cost\ is\ 0. Else, the\ cost\ is\ 1.$
f) $Set\ cell\ m[i,j]\ of\ the\ memorization\ matrix\ equal\ to\ the\ minimum\ of:$
   I. $The\ immediate\ cell\ up\ plus\ 1: m[i-1,j] + 1.$
   II. $The\ immediate\ cell\ to\ the\ left\ plus\ 1: m[i,j-1] + 1.$
   III. $The\ diagonal\ cell\ to\ the\ left\ and\ above\ plus\ cost: m[i-1,j-1] + cost.$

The distance is then obtained in cell $m[R, C]$ *after the completion of steps* 3,4 *and* 5 *iterations*.

The pseudocode for minimum edit distance

```
for(i=0; i<len(S) + 1; i++)
  {
    for (j=0; j<len(T) + 1; j++)
      {
        If (i==0 && j==0)
           T[i][j] = 0;
        elseif (i==0)
              T[i][j] = T[i][j-1] + 1;
        elseif (j==0)
              T[i][j] = T[i-1][j] + 1;
         else {if(str1[i-1]==str2[j-1])
                  T[i][j] = T[i-1][j-1];
                else
                    T[i][j] = 1 + min  [T[i][j − 1], insert
                                        T[i − 1][j], delete
                                        T[i − 1][j − 1], substitute]
  }
     }
          }
```

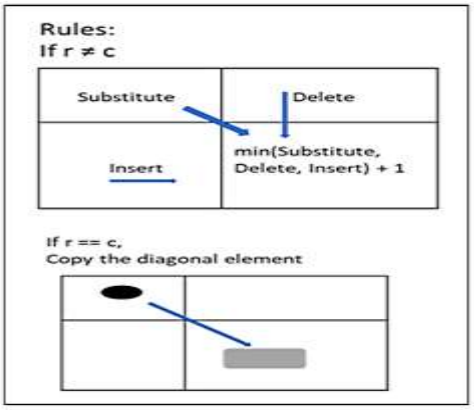

5.2.3 Enhanced Levenshtein Distance for Anesthetic Drugs Rate of Substance Filtering

The fast and accurate extraction and matching of the fine-grained character entities, like the rates of substances from the anesthetics drug containers, play a vital role in the efficient precisive identification of the anesthetic drugs. After a given drug is rightly matched and identified from the previously presented methods, there is the need to correctly extract more low-level or specific character features from the given drug. This is to facilitate the appropriate administration of the drug's desired quantity, volume, weight, or concentration to the patient (see Figure 41). Also, given two drugs with the same text character embedding but having different concentrations or volumes, this proposed method tends to help to distinguish the drugs and efficiently identify them accurately.

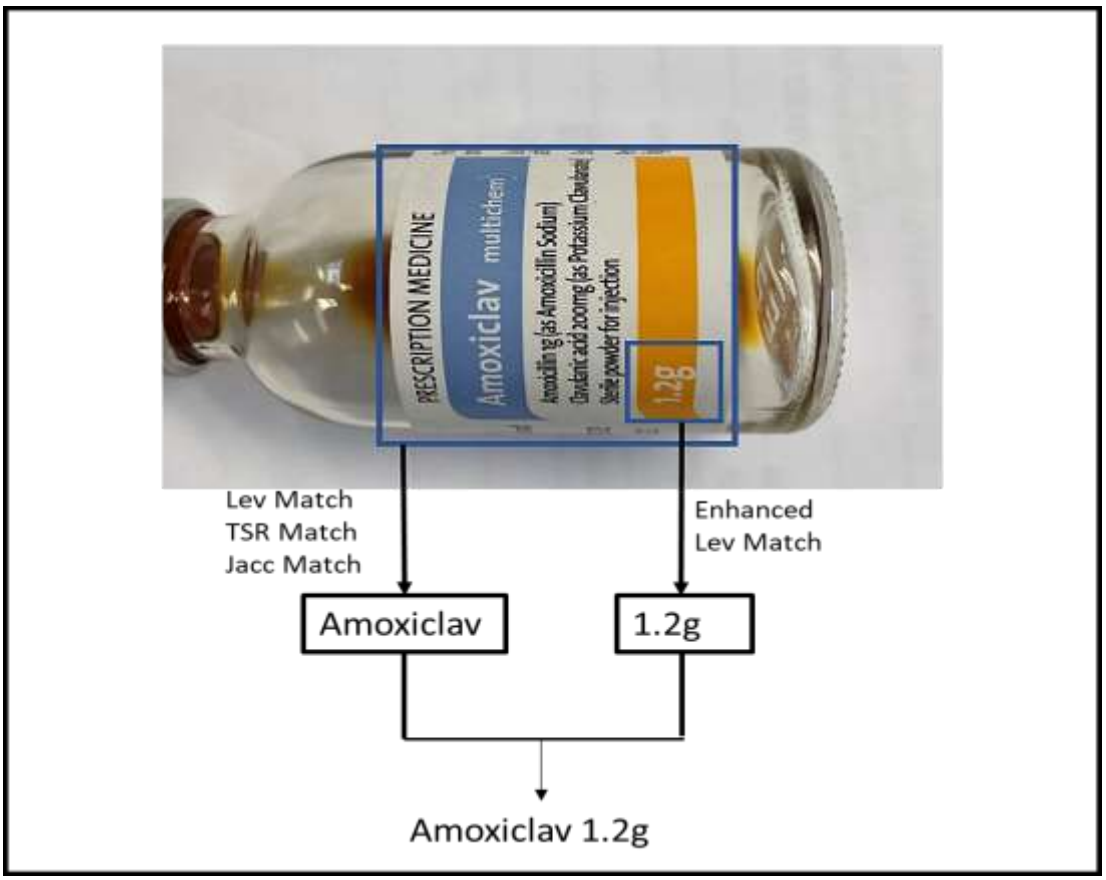

Figure 41: Process flow with the introduced enhanced Levenshtein Matching Algorithm.

As illustrated in Figure 41, after the entire characters extracted from a drug container label are used to identify the specific drug, the proposed enhanced Levenshtein distance algorithm is then employed to extract the exact rate of substance from the given medication. In this section, the illustration of the faster and memory-conservative string-matching approach obtained through the optimization of the Levenshtein distance algorithm is performed. To achieve this, a generalized Ukkonen method (Papamichail & Papamichail, 2009), an upper bound theorem (Bille et al., 2012), and branch pruning algorithms (Morrison et al., 2016) are explored, combined, and employed to optimize the Levenshtein distance. This enables us to achieve efficient precisive and specific anesthetic drug feature extraction and enhance the overall anesthetic drug identification process.

- Set of Character Patterns for the Exact Substance Rate Match Process

The finding of the presence of all the text characters C of any pattern in a collection of patterns $P = \{p_1, p_2, \ldots, p_n\}$ plays an essential role in the immediate exact match problem generalization. For instance, let q represent the overall length of the entire

patterns in P and r denotes the T length; then, the time required to perform the exact set matching process can be represented as $O(q + zr)$. This is because of the use of any linear time approach separately for the individual z patterns. However, the exact set matching issue can be done quicker than $O(q + zr)$ in $O(q + r + k)$ time, where k represents the number of appearances in T of the patterns found in P.

- Set of strings using Generalized Suffix Tree

The more convenient way of constructing a well-generalized suffix tree is to attach a distinct end string marker to every string held in the string set and join together all the strings before constructing a suffix tree for the strings that were concatenated. It is ideal to utilize symbols not used in any of the strings at the end of the marker. A one leaf for each individual suffix of the joined string must be contained in the suffix tree outcome, and it is constructed in time that is proportionate to the summation of the entire string lengths. Then the transition of the leaf numbers into two numbers can be easily performed so that one will identify a string S_i. Furthermore, the remaining serves as a starting spot in S.

Using Ukkonen's algorithm, the concatenation process can be eliminated by constructing a suffix tree for a given two-string samples S_1 and S_2 with the assumption that the strings are distinct. In doing so, a suffix tree for S_1 is initially built with the assumption that it is a terminal character and then match S_2 at the beginning of the root of the tree with another assumption that the character terminal has to be added contrary to a path obtained in the tree until the occurrence of a mismatch. All the suffixes of S_1 are encoded in the tree at this point if the initial character i of S_2 match and continue to subtly encode each suffix of the string $S_2[1 \ldots i]$. This implies that the initial stage i of the Ukkonen's algorithm for S_2 has been successfully implemented on top of the tree for S_1. Continually, the resulting tree is used to perform Ukkonen's algorithm process on string S_2 in the proceeding stage $i + 1$. At the completion of S_2 processing, the entire suffixes of S_1 and S_2 will be encoded, but the suffixes of S_2 will be devoid of synthetic suffixes.

The continued repeat of this process for any of the strings in the string set will produce a generalized suffix tree in time that is proportionate to the summation of the length of the entire strings contained in the string set. For the generalized optimization of

Ukkonen's algorithm, if the modification or editing of the string matching steps that cost more than Q is not considered, then the compute, at most, the $Z \times (2Q + 1)$.

Given two strings U and V that have lengths q and r, respectively, with $q \leq r$. Using the upper bound theorem, it is inevitable that the Levenshtein distance cannot be above q. Thus,

$$LevDist(U,V) \leq q$$

Where LevDist is the Levenshtein Distance between U and V. For instance, let $i - th$ character of a given string L be denoted with L_i. Then applying this notation, U and V can be represented below:

$$\mathrm{U} = U_1, U_2, U_3 \ldots U_{q-1}\, U_q$$

$$V = V_1, V_2, V_3, \ldots V_{r-1}\, V_r$$

Since $q \leq r$, V can be transformed into

$$\mathrm{U} = U_1, U_2, U_3 \ldots U_{q-1}\, U_q$$

$$V = V_1, V_2, V_3, \ldots V_{q-1}\, V_q \ldots V_r$$

From the above equation, V can be transformed into U by substituting the $V_1, \ldots V_r$ sequence to $U_1 \ldots U_q$ and deleting $V_{q+1} \ldots V_r$. From this demonstration, it is proven that the cost of undergoing this operation can only be less than or equal to r because q substitutions and $(r - q)$ deletions are required.

- Levenshtein Distance Optimization Process

In this demonstration, the above-established theorem is employed to optimize and enhance the Levenshtein distance algorithm for the precisive anesthetic string-matching tasks. At the beginning of the process, emphasis is placed on the cells located in the upper-right corner of the memorization matrix table. For instance, given a pair of anesthetic medications with the rate of substances as "50mL" and "1.2g", respectively, let $\mathrm{U} = 50\mathrm{mL}$ and $V = 1.2\mathrm{g}$, then the cell can be constructed as shown in Table 8a below:

Table 7: Memorization matrix table showing the Levenshtein Distance Optimization Process.

		1	.	2	G
	~	~	~	~	-
5	~	~	~	~	~
0	~	~	~	~	~
m	~	~	~	~	~
L	~	~	~	~	~

A

		1	.	2	g
	0	1	2	3	4
5	~	~	~	~	5
0	~	~	~	~	6
m	~	~	~	~	7
L	~	~	~	~	8

b

		1	.	2	g
	~	~	~	-	
5	~	~	~	~	-
0	~	~	~	~	~
m	~	~	~	~	~
L	~	~	~	~	~

c

From Table 7a above, an exact single path that traverses through the cell exists, which is the r deletions + q insertions edit path. The path is shown in Table 7b. This is indeed the costlier method of transforming U to V. Since $(q + r)$ steps are required, the cost along the path will continue to remain $(q + r)$. Since it is established that the edit distance between U and V remain below r, a path that costs $q + r$ is not necessary and should not be considered. Therefore, when computing the edit distance, the corner cell is unnecessary and can always be discarded while the outcome of the edit operation remains correct. This method can also be extended to the other cells in the memorization matrix table. In another example, taking the cells that are adjacent to the cell in the corner, as shown in Table 7c, although they are many edit paths that traverse one or both of them, the following steps are always contained in the path: $(q - 1)$ insertions + $(r - 1)$ deletions.

Following the above theory, if the $r \leq (r-1) + (q-1)$ inequality stands, then these cells can be confidently overlooked. Conducting the inequality condition simplification process, the expression yields $2 \leq q$. This implies that the computation of these cells is unnecessary, provided that U's length remains greater than one. In general, the observation above can be further demonstrated by selecting a cell S from the memorization matrix table and representing the Manhattan distance obtained from it to the closer corner cell by C_s(i.e., the corner at the upper-right or the corner at the lower-left side). Given that any operation path that traverses through the matrix needs $(q - C_s)$ insertions + $(r - C_s)$ deletions steps, a cell can be left behind if the $r \leq (q - C_s) + (r - C_s)$ condition occurs. So, any cell that satisfies the $2C_s \leq q$ condition can be safely left behind, and the edit operation will still be correct.

For instance, with the rate of substances as “50mL” and “1.2g”, respectively, let $\mathrm{U} = 50\mathrm{mL}$ and $V = 1.2\mathrm{g}$. Then the conventional Levenshtein Distance computation that produces the edit distance is shown below in Table 8.

Table 8: Memorization matrix table for the drug rate samples.

		1	.	2	g
	0	1	2	3	4
5	1				
0	2				
m	3				
L	4				

a

		1	.	2	g
	0	1	2	3	4
5	1	1	2	3	4
0	2	2	2	3	4
m	3	3	3	3	4
L	4	4	4	4	

b

		1	.	2	g
	0	1	2	3	4
5	1	1	2	3	4
0	2	2	2	3	4
m	3	3	3	3	4
L	4	4	4	4	4

c

Table 8a, b & c illustrate the step-by-step method of computing the edit distance between the chosen drug rates of substance samples. The process begins by initializing the distance matrix between the two strings, as shown in Table 8a. The size of the memorization matrix is 5×5, excluding the row and column designated for the labels. The five rows in the matrix table are equal to the character numbers in the first four-character strings + 1, which is the same as the number of string characters in the column. The actual Levenshtein distance value between the two drug rates of substance is the last value found at the bottom-right corner of the memorization matrix table that is contained in the 5^{th} row (i.e., index four, beginning from zero) and the 5^{th} column on index five. The additional initialization row and column contain values that begin from zero and increment by one; this assists the dynamic programming process in the edit distance computation.

The Levenshtein distance computation process adheres to the dynamic programming paradigm, which breaks down complex tasks into smaller units of problems for easy solution provision. The filling up of the memorization matrix table is a complex task, and the counterpart smaller problem involves picking a 2×2 matrix from the larger matrix and solving it in a single step until the best edit distance is obtained, as shown in Table 8b. Because the initialization process involves the column at the extreme left corner of the matrix table and the first top row with numbers beginning with zero, three outstanding elements will always exist with only one element missing. The

missing element is the element to be found, and it usually corresponds to the element at the bottom-right corner of the smaller 2×2 matrix that requires a solution.

The missing element of the smaller matrix can be obtained using one of these two options depending on the similarity of the pair of the prefixes to be compared. That is, the least element of the three initialized elements, i.e., $min(0, 1, 1) = 0$, if the two compared prefixes are identical or the least element of the three initialized elements + 1, i.e., $min(0, 1, 1) + 1 = 0 + 1 = 1$ if the prefixes are not identical as can be obtained in Table 8c. If the prefixes are identical or the same, no computations are performed as the closest top diagonal element is copied with no extra cost. On the other hand, if the prefixes are non-identical, the full edit distance operation is performed with an added cost of 1. By following these principles, all the distance matrices are obtained. In a nutshell, three known elements must exist by adhering to the dynamic programming process, with one missing element in the subproblem to be solved. The remaining unknown value is obtained by performing the outlined comparative process above. However, in the absence of the first additional initialization row and column, then there will be four unknown elements, and the dynamic programming process will not be applicable in solving the problem.

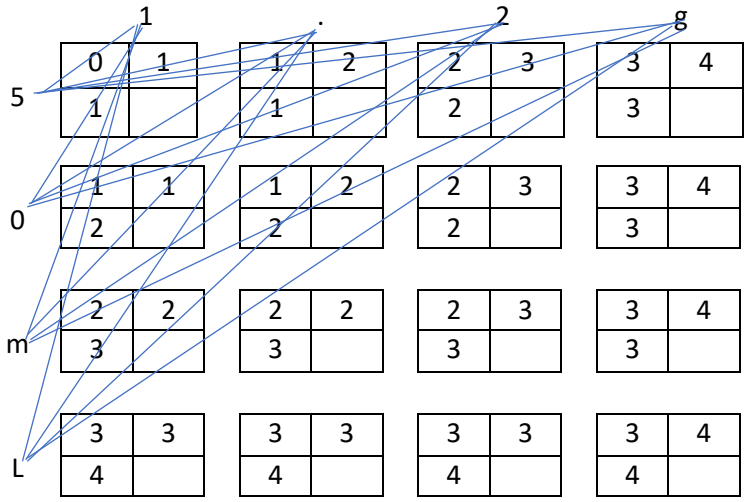

Figure 42: The Sub-tasks of the Edit Distance Computation between string U and V.

- The Levenshtein Distance Sub-Tasks Computation Procedure

In this section, the step-by-step procedure followed in obtaining the edit distances between the two drug rate samples presented in Figure 42 is explained in detail. The distance between the first two prefixes of the drug rates is computed first. The initial prefixes are 5 and 1, and they are found in the first 2×2 matrix located in the upper

left corner of the sub-task table in Figure 42. Because the two prefixes are unidentical, the distance between them is computed by adding 1 to the least value among the three values, i.e., $min(0, 1, 1) + 1$, which is equal to 1. The memorization matrix table is then updated accordingly. The next step is to compute the distance between the first prefix of the drug rate against the second prefix of the second drug rate, that is $min(1, 1, 2) + 1$, which is equal to 2. This process continues until the entire row is filled with the resulting distances of 3 and 4, respectively.

In continuation, the second row, which corresponds to the second prefix, is to be filled. The first missing value to be found in the second row represents the distance required to transform 50 into 1, the second missing value represents the distance needed to transform 50 into 1., and the third missing value represents the distance required to transform 50 into 1.2, until the last value. This is due to the dependence of the computation of the distance between 0 and the prefixes in the second drug's rate sample "1.2g" on the distance obtained for the prefix 5. In computing the distance between 0 and 1, the first 2×2 sub-task matrix in the second row is used. As earlier observed, since the two prefixes 0 and 1 are unidentical, the distance between them is $min(1, 1, 2) + 1$, which equals 2. The next move is to obtain the distance between 0 from the first drug rate and (.) from the second drug rate, as shown in the second 2×2 sub-task matrix of the second row. Because 0 and (.) are not identical, the distance between them is $min(1, 2, 2) + 1$, which is equal to 2. The procedure continues until all the missing values in the second row that corresponds to 0 are obtained.

This process persists until all the missing values are found and a complete memorization matrix table, as shown in Table 9c, is obtained. The least distance between the two complete drug rates, 50mL, and 1.2g, is found at the bottom-right corner of the memorization matrix table, and the path to the least distance value follows the middle diagonal path of the matrix table. The last bottom-right cell number is equal to 4, which invariably means that 4 is the least value required to transform 50mL into 1.2g.

- The Improved Levenshtein Distance Sub-Tasks Computation Procedure

In this section, the step-by-step process followed in calculating the edit distances between the two drug rate samples using the improved Levenshtein distance algorithm presented in Table 9 is explained in detail.

Table 9: Enhanced Memorization matrix table for the drug rate samples.

		1	.	2	g
	~	~	-	-	-
5	~	~	~	-	-
0	-	~	~	~	-
m	-	-	~	~	~
L	-	-	-	~	~

a

		1	.	2	g
	~	E	-	-	-
5	~	F	G	-	-
0	-	~	~	~	-
m	-	-	~	~	~
L	-	-	-	~	~

b

		1	.	2	g
	0	1	-	-	-
5	1	1	2	-	-
0	-	2	2	3	-
m	-	-	3	3	4
L	-	-	-	4	4

c

In calculating the edit distance of the two drug rate samples using the enhanced method, the sub-task is partitioned as shown in Table 9a, b, and c. The distance computation focuses only on the relevant cells. As with the typical Levenshtein process, the distance between the first two prefixes of the drug rates is computed first. The initial prefixes are 5 and 1, and they are found in the first 2×2 matrix located in the upper left corner of the sub-task table in Table 9a. Because the two prefixes are not identical, the distance between them is computed by adding 1 to the least value among the three values, i.e., $min(0, 1, 1) + 1$, which is equal to 1. The enhanced memorization matrix table is then updated accordingly. The next step is to calculate the distance between the first prefix of the drug rate against the second prefix of the second drug rate, that is $min(1, 1) + 1$, which is equal to 2. Since the remaining cells met the $r \leq (r-1) + (q-1)$ inequality, it is safe to move to the next row.

Furthermore, the second row corresponding to the second prefix must be filled. The first missing value to be found in the second row denotes the distance needed to convert 50 into 1. The second missing value denotes the distance needed to transform 50 into 1(.), and the third missing number denotes the distance needed to transform 50 into 1.2, which is the last value to be found in the row. In calculating the distance between 0 and 1, the first 2×2 sub-task matrix in the second row is utilized. As stated earlier, since the two prefixes 0 and 1 are unidentical, the distance between them is $min(1, 1) + 1$, which is equal to 2. The next move is to obtain the distance between 0 from the first drug rate and (.) from the second drug rate, as shown in the second 2×2 sub-task matrix of the second row. Because 0 and (.) are not identical, the

distance between them is $min(1, 2, 2) + 1$, which is equal to 2. The process is also performed for the next missing values in the second row that corresponds to 0, which is $min(2, 2) + 1$ = 3.

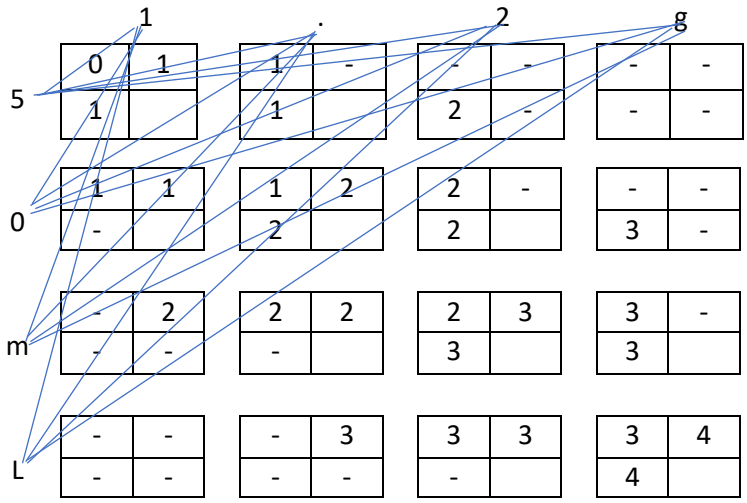

Figure 43: The Sub-tasks of the Edit Distance Computation between string U and V using the Enhanced Memorization matrix table.

The third row is the row in which the missing values are to be computed. The first cell is ignored since it met the inequality criteria, and the second cell's missing value is calculated as $min(2, 2) + 1$ = 3. The third cell's missing value is calculated as $min(2, 3,3) + 1$ = 2, and the missing value in the last cell is obtained using $min(3, 3) + 1 = 4$. In the final row of the enhanced matrix table, only the last two cell's missing values are to be found since the first two initial cells met the inequality criteria. The second to the last cell's missing number is computed as $min(3, 3) + 1 = 4$ and the missing value of the last cell of the last row is calculated as $min(3, 4,4) + 1 = 4$. The least distance between the two drug rates, "50mL" and "1.2g", is found at the bottom-right corner of the memorization matrix table as with the conventional Levenshtein distance matrix table. It is equal to 4, which invariably means that 4 is the minimum value required to transform 50mL into 1.2g (see Figure 43).

As can be observed in the two processes above, i.e., the typical Levenshtein distance and the improved Levenshtein distance computation processes, the improved Levenshtein distance computation process is faster since it does not traverse the whole memorization matrix table in order to find the proper minimum edit distance. In processing larger volumes of strings, the typical Levenshtein computation approach

calculates all the missing values in the memorization matrix table by traversing all the cells in the matrix table. This includes the cells with high values located at the upper-right and bottom-left corners of the matrix table that have less or no impact in obtaining the least edit distance. Therefore, the need for an enhanced method through optimization with threshold infusion and having all the distances beyond a set boundary treated as being out of range. With the improved method, only the values in the right diagonal positions need to be computed. In so doing, the improved method yields better time efficiency and complexity and enhances the processing speed of a large corpus of strings.

- Anesthetics Drug Similarity Score Estimation Using Levenshtein Distance

After the distance between the anesthetic drug strings is computed, there is the need to obtain the confidence or similarity score, which is used as a yardstick to identify a specific drug among other drugs. The similarity scores (Lev Scores) are computed using the Levenshtein string similarity estimation technique shown in Equation 5.1. This is achieved by performing pairwise comparisons with the stream of strings from an incoming anesthetic drug against all other drugs whose strings are pre-stored in the look-up table. The string with the highest similarity score will be returned as the matched and recognized drug. A perfect match yields a score of 1.0 or 100%, and an utterly dissimilar stream of strings will result in a 0.0 score (Sarkar et al., 2016). Mathematically, the Levenshtein ratio or similarity score between string $S_1$from a particular anasthetic drug sample and string S_2 from another anesthetic drug sample is expressed as:

$$\text{LevRatio}(S_1, S_2) = \frac{(|S_1|+|S_2|)-lev_{S_1,S_2}(i,j)}{(|S_1|+|S_2|)}$$

$$= 1 - \frac{lev_{S_1,S_2}(i,j)}{(|S_1| + |S_2|)} \qquad 5.1$$

Where, $|S_1|$and $|S_2|$ are the lengths of string from the S_1drug sample and S_2 from the second drug sample respectively. Here, when the similarity ratio of the two drug samples is computed with the Levenshtein ratio, the cost of substitution operation is two but has a cost of 1 in computing the distance. For instance,

let S_1 = Bromide

S_2 = Chloride

Then the minimum edit distance $lev_{S_1,S_2}(i,j)$, required to transform S_1 to S_2 = 4, as demonstrated in the memorization matrix table above (see Figure 43). Then Levenshtein ratio or similarity score,

$$\text{LevRatio}\,(S_1, S_2) = 1 - \frac{lev_{S_1,S_2}(i,j)}{|\text{Bromide}| + |\text{Chloride}|} = 1 - \frac{4}{|7| + |8|}$$

$$= 1 - \frac{4}{15} \approx 0.73$$

Therefore, the similarity score between the two samples (Bromine and Chloride) is approximately 73%.

5.3 Token Set Ratio for Anesthetics Drug Similarity Estimation

To reaffirm the confidence score obtained using the Levenshtein similarity score estimation strategy, a Token Set Ratio method for the anesthetics drug similarity computation is adopted. This approach also performs a pairwise comparison using the stream of strings from an incoming anesthetic drug against all other drugs whose strings are pre-stored in the look-up table. However, it undergoes further preprocessing tasks by tokenizing, sorting, and grouping common tokens or intersections between the strings together before performing the pairwise comparisons between the strings, which in turn boosts the similarity score of the string similarity estimation (Rao et al., 2018; J. Wang et al., 2011). Tokenization is the process of fragmenting words or strings into smaller potions, known as tokens (Rai & Borah, 2020). For instance, given a pair of strings from two anesthetic drugs:

S_1 = “prescription only medicine keep out of the reach of children 500 mg/50 mL fresofol 1% mct/lct propofol 500 mg/50 mL injection produced in New Zealand”

S_2 = “prescription only medicine keep out of the reach of children 500 mg/50 mL fresofol 1% mct/lct propofol 500 mg/50 mL injection made in new zealand”

Performing tokenization on both strings, then we have:

S_1^t = “prescription” “only” “medicine” “out” “of” “the” “reach” “of”
“Children” “mg/50” “mL” “fresofol” “1%” “mct/lct” “propofol” “500”
“mg/50” “mL” ‘injection” “produced” “in” ‘new” ‘Zealand”

S_2^t = “prescription” ‘only” “medicine” ‘keep” ‘out” “of” “the” “reach” ‘of” “children”

“500” “mg/50” “mL” “fresofol” “1%” “mct/lct” “propofol”

“500” “mg/50” ‘mL” “injection” “made” “in” “new” “Zealand”

After tokenization, S_1 yields 23 tokens and S_2 yields 26 tokens. Eliminating duplicates, string S_1 reduces to 20 tokens while S_2 reduces 21 tokens, respectively.

5.4 Jaccard Distance for Anesthetics Drug Similarity Estimation

A third similarity score computation method is employed for further validation of the obtained anesthetic drugs’ confidence score. The Jaccard similarity or Jacc Score is another string-similarity estimation method used to compute the similarity between the stream of strings from the ampule containers. It is calibrated between 0 and 1 (i.e., $0 \leq J(S_1, S_2) \leq 1$), represented mathematically as stated in Equation 5.2, and the higher the score, the more similar the compared strings. Mathematically (Kosub, 2019),

$$J(S_1, S_2) = \frac{(S_1 \cap S_2)}{(S_1 \cup S_2} = \frac{(S_1 \cap S_2)}{|S_1| + |S_2| - |S_1 \cap S_2|} \quad 5.2$$

Again, give two sets of strings:

S_1 = {“prescription”, “only”, “medicine”, “keep”, “out”, “of”, “the”, “reach”, “children”, “mg/50”, “fresofol”, “1%”, “mct/lct”, “propofol”, “mL”, “injection”, “produced”, “in”, “new”, “zealand”}

S_2 = {“prescription”, “only”, “keep”, “out”, “the”, “reach”, “children”, “500”, “mg/50”, “fresofol”, “1%”, “mct/lct”, “propofol”, “mL”, “injection”, “made”, “in”, “new”}, Then the Jaccard similarity or Jacc Score between the two string is:

$$J(S_1, S_2) = \frac{16}{22} \approx 0.73$$

Therefore, the Jaccard similarity between the two strings is about 73%.

5.5 Experimental Procedure for the Anaesthetic Drugs Identification Framework

This section describes how the data used in this work was collected, captured, and applied to the proposed anesthetic medication identification framework. It also describes the experimental procedure and the evaluation of the capabilities of the proposed framework in identifying the drugs used in the operating theatres. The insight into the threshold search process for a suitable threshold value computation by comparing different threshold calibrations is also performed. The section first describes the dataset's source, content, and nature and provides a concise explanation of the experimental setup. Finally, the results of the experiments are presented with a detailed analysis of the experimental outcome.

5.5.1 Dataset Description

The research on the automatic identification of anesthetic drugs using artificial intelligence and computer vision is new research without publicly available datasets. The dataset used in this work was collected during visitations to the real anesthetic operating rooms at Auckland University Hospital. A total of 30 empty anesthetic drug containers, which are the actual dataset, were collected in the first onsite visit. Then, on the second operating room visit, the remaining dataset of about 23 used empty anesthetic drugs were received for the experiments. The data comprises different empty drug containers used in the operating rooms. The containers appear in the form of ampoules and vials with different shapes, sizes, structures, and orientations. Of utmost importance are the labels embedded on the drug containers as they are extracted and made use of in this work. The labels on the drug containers appear in different shapes, color, and the text inscriptions on them are of different font colors, curvatures, and sizes.

5.5.2 Experimental Setup

The visual acquisition and feeding of data into the proposed framework were handled using the OpenCV-python module and a Logitech 1080p HD camera which can capture the about 180 degrees view of the anesthetic drug containers. The hardware components and their corresponding measurements used in performing this experiment are shown in Figure 44.

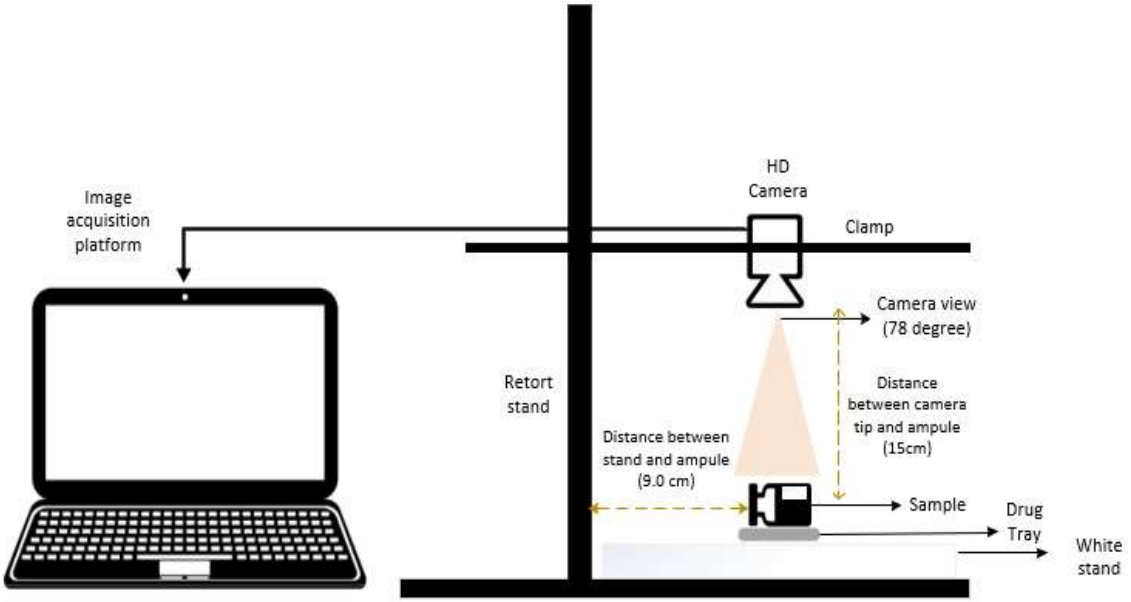

Figure 44: The experimental setup for the anesthetic drug image acquisition.

The experimental set consists of a personal computer, a retort stand, a 1080p HD camera, and a drug tray, as shown in Figure 44. The distance between the camera and the anesthetic drug ampoule positioned to be captured is 15cm, and the length between the positioned drug ampoule and the retort stand is 9.0cm. A total of 52 empty anesthetic drug images were captured for the experiments performed throughout the work. During the experiments, a python programming language, the dominant language for computer vision application research, Anaconda jupyter notebook, and a pycharm development environment or editor were used for the frameworks' development process. Google Vision OCR was deployed for the anesthetic drugs text inscription detection and vital information extraction. Also, the Fuzzywuzzy-python module is used to compute the token set ratio for similarity estimation, Python-Levenshtein (a tool for the Levenshtein string similarity measurement), and the Win32printing python module for the experimental physical printing tasks. For the artificial voice feedback generation, the pyttsx3x python module was used to convert the relevant extracted features from text to speech.

5.5.3 Experimental Process

The strings on each drug ampule were extracted using the OCR engine to create a lookup table (an excel document containing each string extracted from each drug container) for the string-matching task. We build a mini framework to automate the string extraction and lookup table construction process. No formatting of any kind is

needed on the strings in the lookup table. Any form of formatting may induce errors or adversely affect the similarity scores between the strings. After the character strings are extracted from the drug containers, there is the need to match them in order to recognize an incoming drug by estimating the string closeness, similarity, or dissimilarity between the strings extracted from the drug labels in real-time. In real-time processing and identification of the anesthetic drug samples, the strings on each drug ampule are extracted using the OCR engine and compared to a lookup table, including the strings extracted from the known ampules for the drug identification task. The framework only compares the test ampule with sample types already stored in the lookup – a "new" or unmatched ampule is reported as an error. This fits in the anesthetic workflow because it is known in advance which ampules should be present in the anesthetic tray.

The Levenshtein distance, token set ratio, and Jaccard distance methods explained above are used to estimate the closeness or similarity between the incoming strings from the image-text processor and the ones held in the lookup table. Furthermore, each estimated similarity score is compared with a set threshold value to validate the matched drug from the decision-making stage before the final label is printed. After related texts are matched, the matched drug information is displayed on the screen and printed on a physical printer. However, the system raises concerns when discovering drugs that are not prescribed or drug swapped. We chose these two methods because of their ability to match strings of uneven or unequal lengths. The distance between a source string and a target string is the minimum number of edit operations (deletions, insertions, or substitutions) required to transform the source into the target (Backurs & Indyk, 2015). The lower the distance, the more similar the strings become.

5.6 Threshold Computation for Anesthetics Drug Identification Process

Anesthetic drugs are powerful drugs that require absolute care during preparation and administration. A single mistake can lead to fatal and severe complications; that is why several standards are put in place to ensure zero medication misidentification in the proposed framework. One such standard is the thresholding strategy. A threshold in the proposed framework context is a specific confidence value that an incoming

anaesthetic drug string similarity must attain to be considered the right drug. The thresholding strategy assists the proposed framework in achieving the critical healthcare sensitivity level, medication recognition accuracy, and standard. This section describes the process involved in the computation of the appropriate threshold value used in the proposed framework and the analysis of the various threshold calibrations considered during the experiments.

During the experiments, the threshold target value was computed by running tests on all the available drug containers, and pairwise comparison was performed on the resulting similarity scores. That is, each drug ampule image is compared to every other image, including itself. A similarity threshold is calculated by identifying the second-highest similarity (the highest is when the image is compared to itself). When an unknown image with texts is used, it is compared to each of the images in the lookup table, and the closest match drug image from the database is used to identify the drug in the new image unless the similarity score is below the threshold (i.e., it cannot be distinguished from a false match).

Furthermore, in selecting the appropriate threshold for the proposed framework, the threshold value was split or calibrated between T10 and T100 in the range of ten. Then, tests run iteratively on each drug sample, observations are recorded, and the outcome is analyzed. For the first drug sample, the plot of similarity scores obtained is shown below in Figure 45. At each threshold, the number of false drug identification is denoted as No_False, and true identification is represented as No_True. The complete and summarized results of the threshold computation experiment are attached in Appendix B and C.

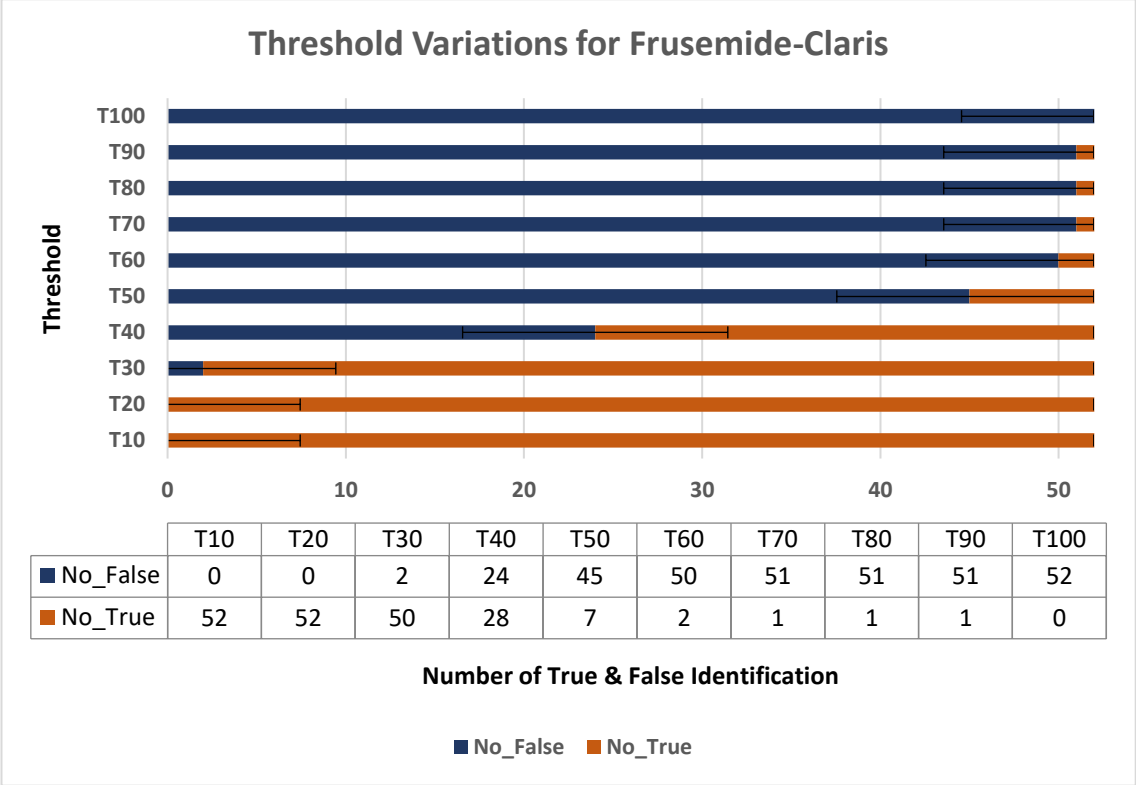

	T10	T20	T30	T40	T50	T60	T70	T80	T90	T100
No_False	0	0	2	24	45	50	51	51	51	52
No_True	52	52	50	28	7	2	1	1	1	0

Figure 45: Threshold variation and observation using Frusemide-Claris drug sample.

From Figure 45, at thresholds 10 (T10) & 20 (T20), the total number of drugs returned as false by the proposed framework is 0, while the total number of drugs returned as true is 52. This implies that the framework recognized all the drug samples as right at these thresholds, making 10 and 20 unsuitable candidates for the standard threshold. At T30, the overall drug samples returned as false by the framework is 2, while 50 samples were identified as true, knocking T30 out as the potential threshold candidate. Furthermore, a cumulative total of 24 drug samples were identified as false, and 28 were identified as true at T40, giving T40 no hope as the right threshold value. In continuation, a total of 45 and 50 drug samples each were identified as false at T50 and T60; respectively, 7 and 2 samples returned as true, drawing nearer to the right threshold candidate for the sample under analysis. Between T70 and T90, all the drug samples (51) except the right drug (1) were returned as false, while only the Frusemide-Claris drug sample was returned as true. This gives us hope that any value between 70 and 90 can serve as a threshold for the framework depending on the required sensitivity level and the analysis outcome of the remaining drug samples. At T100, all the drug samples were identified as false, making 100 unsuitable for the threshold value. The next drug sample analyzed for the appropriate threshold selection is the Morphine Sulphate injection, as illustrated in Figure 46.

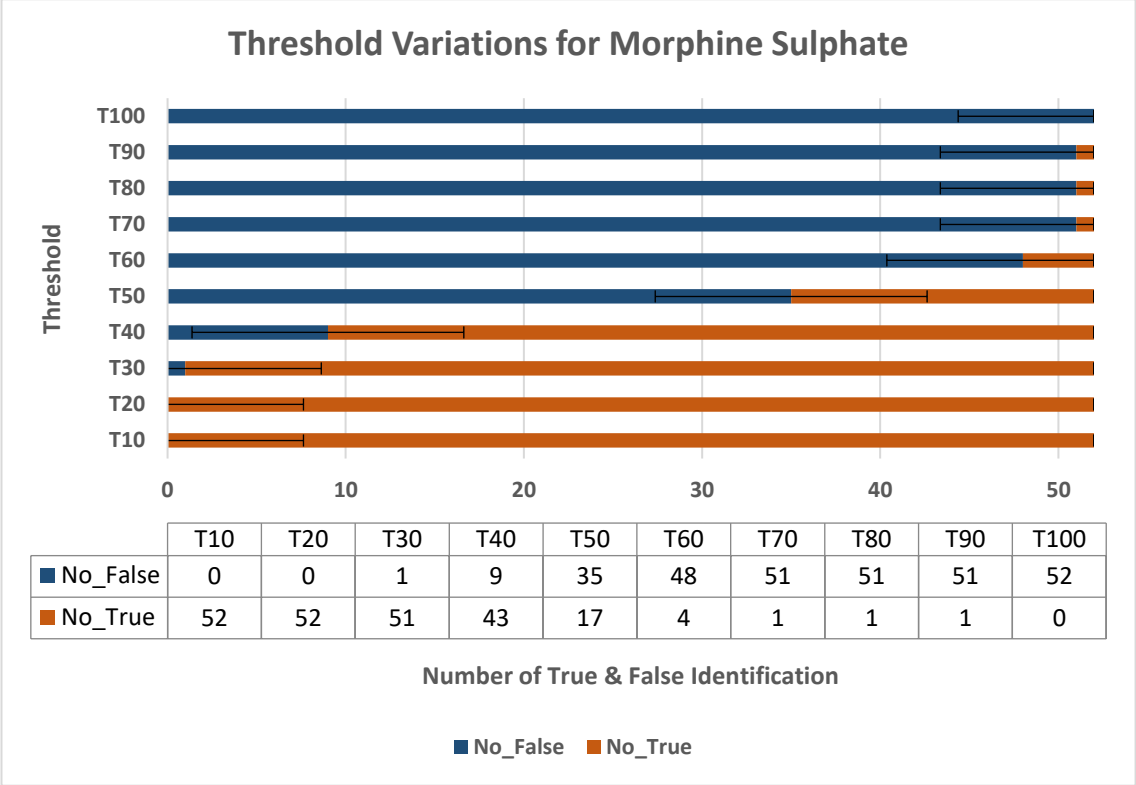

	T10	T20	T30	T40	T50	T60	T70	T80	T90	T100
No_False	0	0	1	9	35	48	51	51	51	52
No_True	52	52	51	43	17	4	1	1	1	0

Figure 46: Threshold variation and observation using Morphine Sulphate drug sample.

Like the previous sample in Figure 46, at T10 & T20, the total number of drugs returned by the framework as false is 0, while the total number of drugs returned as true is 52 (Figure 46). This means that the framework identified all the drug samples as appropriate at these thresholds, making 10 and 20 unsuitable candidates for the standard threshold. In continuation, the framework recognized only one drug sample as false at T30; unlike the immediately analyzed sample, the framework returned two drug samples as false when the threshold value was set at 30. The overall drug samples returned as true were 50, knocking T30 out as the potential threshold candidate. Furthermore, a cumulative total of 9 drug samples were identified as false, and 43 were recognized as true at T40, giving T40 no hope as the right threshold value. Also, at T50 and T60, a total of 35 and 48 drug samples each were identified as false, while 17 and 4 drug samples each returned as true, respectively, drawing closer to the right threshold candidate for the sample under analysis. Similar to the sample in Figure 46, between T70 and T90, all the drug samples (51) except the right drug (1) were identified as false, while only the Morphine Sulphate drug sample was returned as true. Again, this gives us confidence that any value between 70 and 90 can be selected as a threshold for the framework subject to the sensitivity requirement level of the

user and the analysis outcome of the remaining drug samples. At T100, all the drug samples were returned as false, making 100 unsuitable for the threshold value.

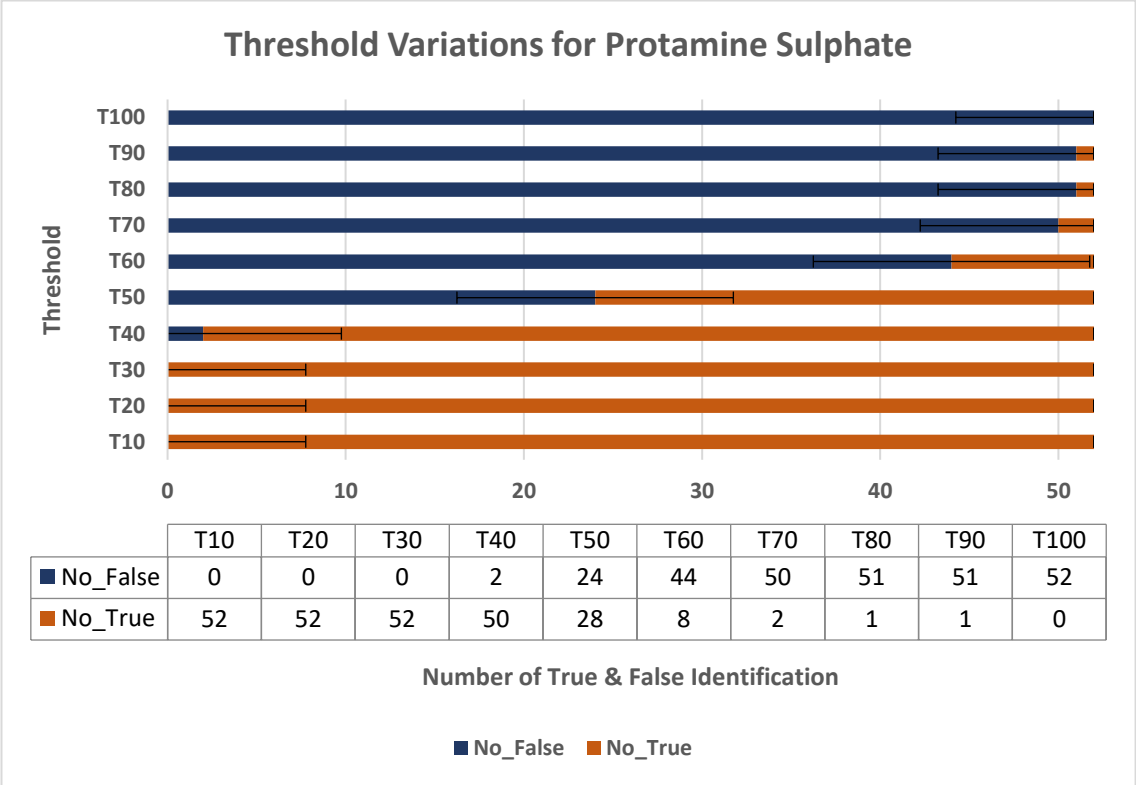

	T10	T20	T30	T40	T50	T60	T70	T80	T90	T100
No_False	0	0	0	2	24	44	50	51	51	52
No_True	52	52	52	50	28	8	2	1	1	0

Figure 47: Threshold variation and observation using Protamine Sulphate drug sample.

The third randomly selected sample for review for the threshold computation is the Protamine Sulphate anesthetic medication, as shown in 47. In this sample, the first three threshold calibrations, T10, T20, and T30, the framework identified all the medication samples as false while returning all the drug samples (52) as true, unlike the two previously analyzed samples that the framework returned the first two samples as false. At T40, a cumulative total of 2 anesthetic medication samples were identified by the framework as false, while 50 medication samples were recognized as true, making 40 an unsuitable candidate value for the threshold setting for the proposed framework. Furthermore, at T50, the number of medication samples identified as false was 24, and 28 returned as true. At T60, a total of 44 anesthetic drug samples were identified by the introduced framework as false and eight as true, drawing closer to the appropriate threshold value. Different from the two previously analyzed samples in Figure 45 and Figure 46, at T70, 50 drug samples were identified as false instead of 51 samples, drawing the appropriate threshold value closer. Between T80 and T90, all the drug samples (51) except the right drug (1) were identified as

false, while only Protamine Sulphate, the drug sample under analysis, was returned as true. This, in turn, gives confidence that any value between 80 and 90 can be chosen as a threshold for the framework subject to the degree of sensitivity requirement by the user and the analysis outcome of the remaining drug samples. At T100, all the drug samples were returned as false, making 100 unsuitable for the threshold value.

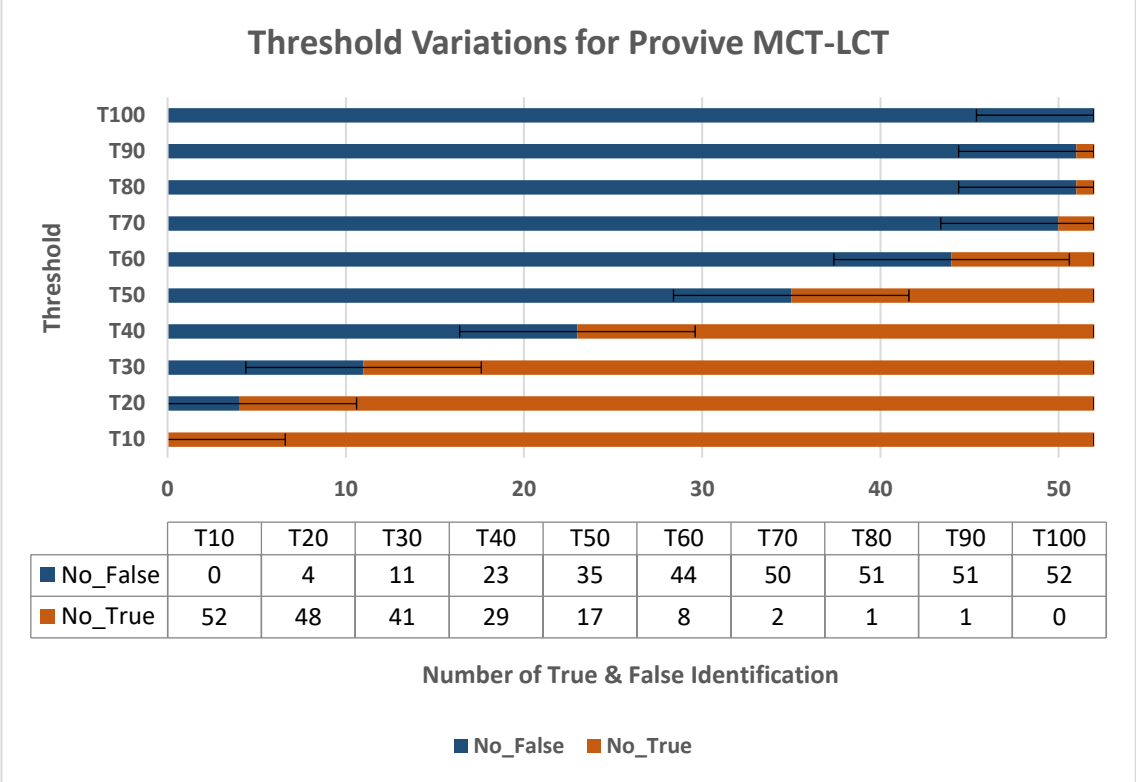

	T10	T20	T30	T40	T50	T60	T70	T80	T90	T100
No_False	0	4	11	23	35	44	50	51	51	52
No_True	52	48	41	29	17	8	2	1	1	0

Figure 48: Threshold variation and observation using Provive MCT-LCT drug sample.

The following drug sample used for the threshold search operation was the Provive MCT-LCT anesthetic medication. Unlike the three previously investigated samples, the framework returned 0 false number of drugs at T10 and T20 for the first two samples and 0 false number of drugs at T10, T20, and T30 for the third sample. With the Provive MCT-LCT medication sample, the framework returned zero false value and identified all 52 drug samples as true at T10, as shown in Figure 48. At T20 and T30, the proposed framework identified 4 and 11 medications as false and 48 and 41 as true. Furthermore, at T40 and T50, the framework classified 23 and 35 numbers of the anesthetic medications as false, respectively, and 29 and 17 numbers of drugs as true. Also, at T60 and T70, the cumulative total number of the drug samples classified as false were 44 and 50, respectively, while only 8 and 2 drug samples were identified as true. Between T80 and T90, all the anesthetic drug samples were identified as false by

the framework except the right drug, which is the Provive MCT-LCT. This signifies that any value from 80 to 90 could be set as the appropriate threshold value, depending on the degree of sensitivity required by the user and the outcome of the analysis of the remaining drugs. At T100, all the drug samples were identified as false, and no drugs were returned as true, indicating that 100 cannot serve as the proper threshold value.

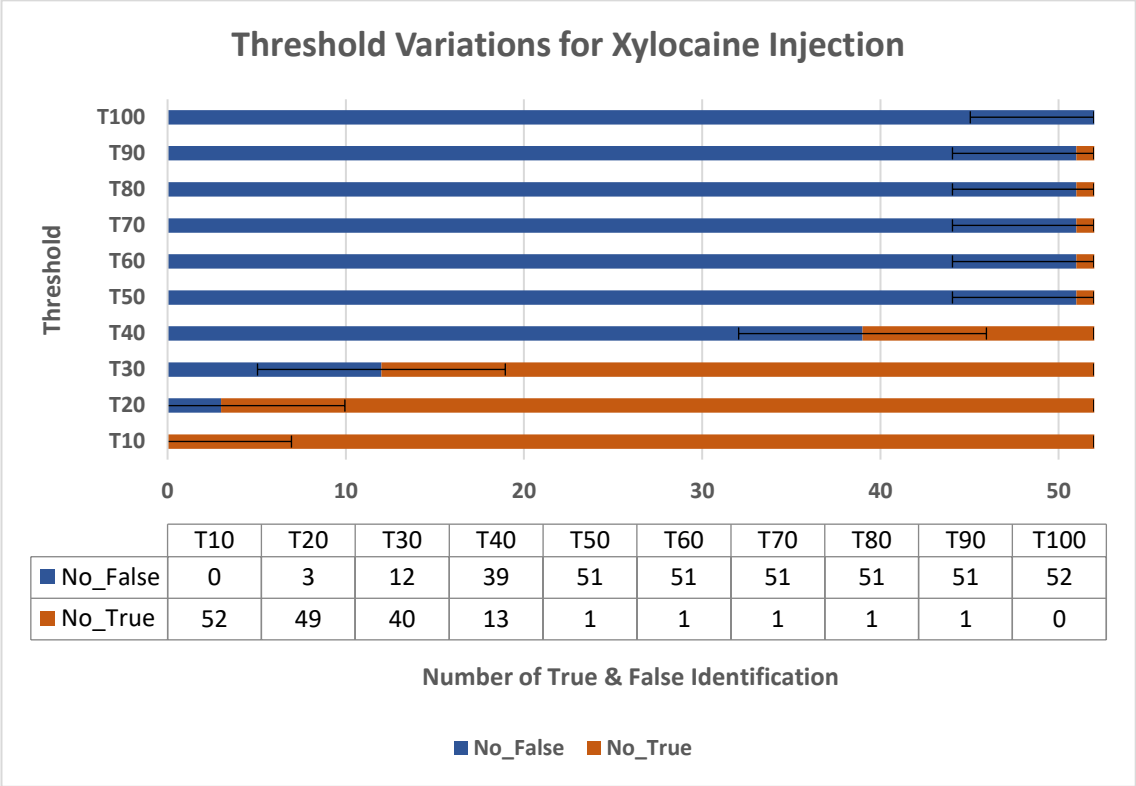

	T10	T20	T30	T40	T50	T60	T70	T80	T90	T100
No_False	0	3	12	39	51	51	51	51	51	52
No_True	52	49	40	13	1	1	1	1	1	0

Figure 49: Threshold variation and observation using Xylocaine Injection drug sample.

The next anesthetic drug sample selected for the threshold search and analysis operation is the Xylocaine Injection drug. Starting from T10, all the tested drug samples were returned true by the proposed framework (see Figure 49), similar to the result obtained with the Provive MCT-LCT drug sample analysis. Then at T20 and T30, when the test iteration was performed, 3 and 12 drug samples were identified as false, respectively, while 49 and 40 drug samples were classed as true. In continuation, when the threshold was set at T40, the framework classified 39 of the anaesthetic medications as false, while 13 of the drug samples were identified as true. Between T50 and T90, all the anesthetic drug samples were identified as false by the framework except the right drug, which is Xylocaine Injection. This signifies that any value from 50 to 90 could be set as the appropriate threshold value subject to the degree of confidence required by the user and the outcome of the analysis of the remaining

drugs. Unlike the previously analyzed samples with their lowest thresholds at T70 and T80, the Xylocaine Injection sample returned the lowest threshold at T50. At T100, all the drug samples were identified as false, and no drugs were returned as true, indicating that 100 cannot serve as the right threshold value.

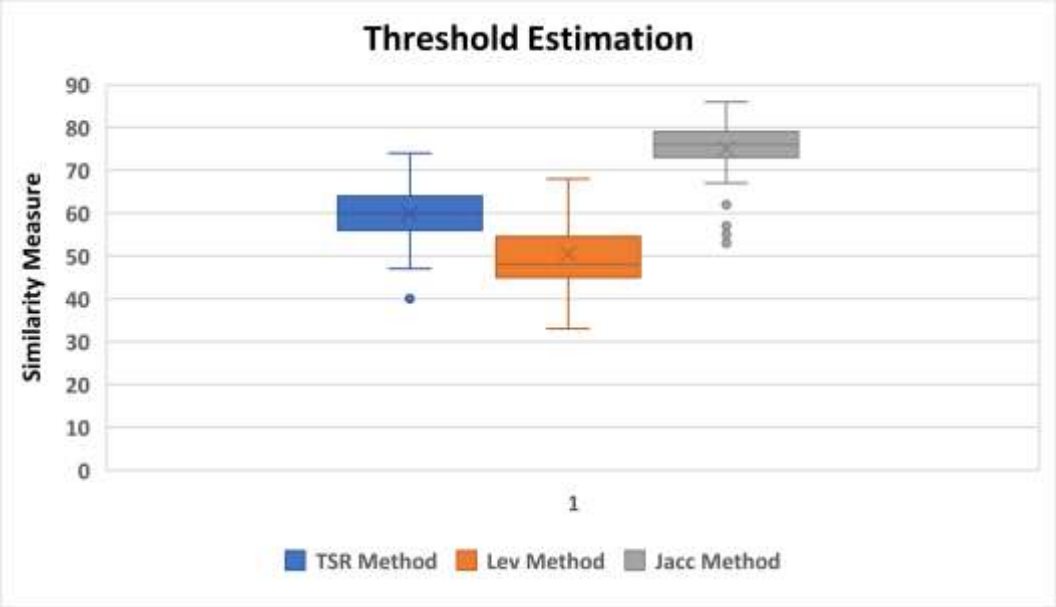

Figure 50: The summary of the outcomes of the threshold computation process.

Furthermore, the proper threshold search operation continued until all the drug samples were each compared with others until the overall average best threshold was obtained with the proposed framework, as shown in Figure 50. As can be seen in the summary chat in Figure 50, the second-highest values extracted from the pool of the computed similarity scores are illustrated, and the chart shows variation because some drug labels are more similar to each other than others. The different anesthetic drugs analyzed returned different minimum threshold values. At T50, a total number of 6 drug samples returned 50 as their minimum threshold, 13 drug samples returned 60 as the minimum threshold, 20 anesthetic medication samples returned 70 as the minimum threshold value, 12 anesthetic drug samples returned 80 as the minimum threshold while no drug sample returned 10 to 40 and 90 to 100 threshold values as the minimum threshold value. Therefore, a threshold value set at 85 can ensure that no drug can be misidentified, no matter how similar they seem to be. The threshold restores confidence in an identified drug and prevents the closely related medication from being identified as another.

5.7 Experimental Results and Analysis

The outcome of the experimental processes and procedures described in Section 5, in which different sets of results from several experimental iterations were obtained, are presented in this section. This section precedes the earlier established threshold computation strategy required for reliable and rapid anesthetic drug identification tasks. In this result analysis and demonstration, 5 to 6 results from different randomly selected anesthetic medication samples shall be presented in charts. The overall compact outcome of the experimental iterations involving all the used drug samples will be presented in a tabular form. The Rocuronium Bromide Injection is the first randomly selected drug to be analyzed in this section.

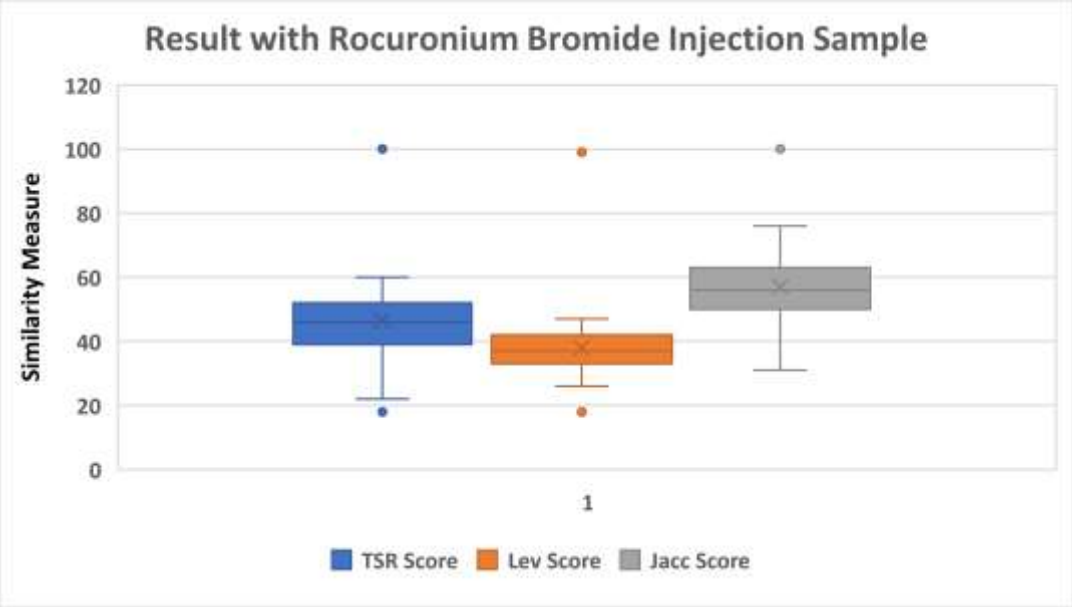

Figure 51: Result obtained from the Rocuronium Bromide Injection sample iterative test.

During the pairwise comparative iterative process, the Rocuronium Bromide Injection produced a similarity confidence score of about 99% with the Levenshtein similarity estimation algorithm (Lev Score). In contrast, the Token Set Ratio (TSR Score) and Jaccard distances (Jacc Score) returned a 100% score each; these positioned the Rocuronium Bromide Injection as the rightly identified drug shown in Figure 51. The framework also generated an edit distance of 1 (see Table 10), implying that the algorithm correctly matched all the characters from the test ampule image with its corresponding ampule string in the lookup table and needed only one edit operation to transform both strings.

Table 10: The extracted results using the Rocuronium Bromide Injection sample.

Drug Name	Edit Distance	TSR Scores (%)	Lev Scores (%)	Jacc Scores (%)
Primacor Injection	70	47	43	47
Cefazolin Sodium 1g	111	43	37	44
NALOXONE HCl 400mg in 1mL	60	47	38	57
Calcium Chloride 1g in 10mL	98	43	38	52
Actrapid Penfill 3ml	65	50	30	50
Vecuronium bromide	58	53	46	60
Sugammadex 200mg/2ml	69	53	35	65
Amiodarone Hydrochloride	67	51	36	60
Protamine Sulphate 50mg in 5ml	69	52	43	57
Summethonium Chloride 100mg in 2mL	53	54	47	68
Protamine Sulfate 10mg/ml	72	50	37	63
Glyceryl Trinitrate 1 mg/ml	80	45	33	58
Tranexamic acid	68	38	32	50
Heparin Injection 25000IU in 5 mL	63	54	45	55
Sterile Potassium Chloride	84	39	40	57
Metaraminol 10mg/ml	62	56	36	65
Cyclizine lactate	72	22	18	31
PITRESSIN argipressin	59	48	37	64
Dexamethasone phosphate 4 mg/ml	59	54	38	56
Ephedrine Hydrochloride	62	46	36	59
Ondansetron Solution	72	36	34	50
FRUSEMIDE	66	32	29	44
DALACINC PHOSPHATE	62	39	33	52
METOPROLOL Mylan	77	51	36	62
WATER FOR INJECTIONS BP	82	43	34	53
MORPHINE SULFATE	52	57	44	67
Glycopyrronium Bromide and Neostigmine	65	6	41	72
Clonidine HCl	59	54	39	76
Rocuronium Bromide Injection	1	100	99	100
Fresofol 1% MCT/LCT	315	52	26	44
Sedative Midazolam 5mg	65	43	33	47
Adrenaline Injection	58	48	43	67
Paracetamol Kabi	522	18	18	40
Provive MCT-LCT 1%	259	46	29	47
Adrenaline Injection 1mg in 10mL	58	48	43	67
Amoxicillin Sodium	121	39	32	44
Lidocain Injection	61	39	35	57
SODIUM CHLORIDE	103	36	37	53
Remifentanil-Act Injection	73	42	39	54
Sterile Dopamine	55	38	43	58
Hypnomida Etomidate 2mg	65	44	38	52
Xylocaine 1%	63	44	33	48
Fentanyl Injection	107	46	39	56
Noradrenaline acid	72	35	34	62
Magnesium Sulfate 2.47g in 5mL	58	56	47	55
Sugammadex Injection	60	55	42	71
Dynastat Powder	75	47	40	63
Hydrocortisone sodium	80	45	39	55
Atracurium Besylate	64	42	37	64
Atropine	62	38	33	54
PancuroInresa	72	51	43	55

The Rocuronium Bromide Injection sample score is closely followed by three drug samples with scores ranging from 71% to 76% using the Jaccard confidence computation matric, 44% to 47% using the Lev similarity computation metric, and 56% to 60% with the TSR string estimation method. Then, followed by another six sets of drug samples with a range of scores from 65% to 68% scores with the Jaccard matric, seven samples scoring between 43% to 45% with the Lev similarity computation algorithm, and 53% to 56% scores by the TSR string similarity computation strategy. In continuation, another set of six drug samples scored between 62% and 64% with the Jaccard matric, eight sets of the drug samples scored between 39% and 42% using the Lev method, and the TSR polled 50% to 52% on seven drug samples. Also, another set of nine drug samples scored between 46% and 48% using the TSR method, 37% to 38% by the Lev method, and 57% to 60% similarity confidence scores with the Jacc estimation method. Returning lower similarity confidence scores are set of about 23 drug samples ranging from 18% to 45% scores using the TSR similarity confidence computation method, 18% to 36% using the Lev method, and finally, 31% to 56% scores using the Jacc similarity confidence score computation algorithm. This whole computation process costs 0.3593s, which is within the desired processing time for the anesthetic workflow.

The next drug sample randomly picked for analysis is the Atropine anesthetic drug injection. After the first pairwise comparative iterative process, the Atropine Injection returned a similarity confidence score of 98% with the Levenshtein similarity estimation algorithm, while the TSR Score and Jaccard distance, respectively, returned a 100% score each, as shown in Figure 51. These scores affirm the Atropine Injection as the rightly identified drug. Also, similar to the first analyzed drug sample (Rocuronium Bromide Injection), the framework also produced an edit distance of 1 (see Table 11), implying that the algorithm correctly matched all the characters from the Atropine Injection ampule image with its corresponding ampule string in the lookup table and needed only one edit operation to transform both strings and with a 0.4063s computational cost. Furthermore, close to the Atropine Injection similarity confidence score is a four-set of drug samples with scores ranging from 67% to 70% applying the Jaccard confidence computation strategy, 46% to 48% using the TSR similarity computation algorithm, and 42% to 49% with the Lev string estimation method.

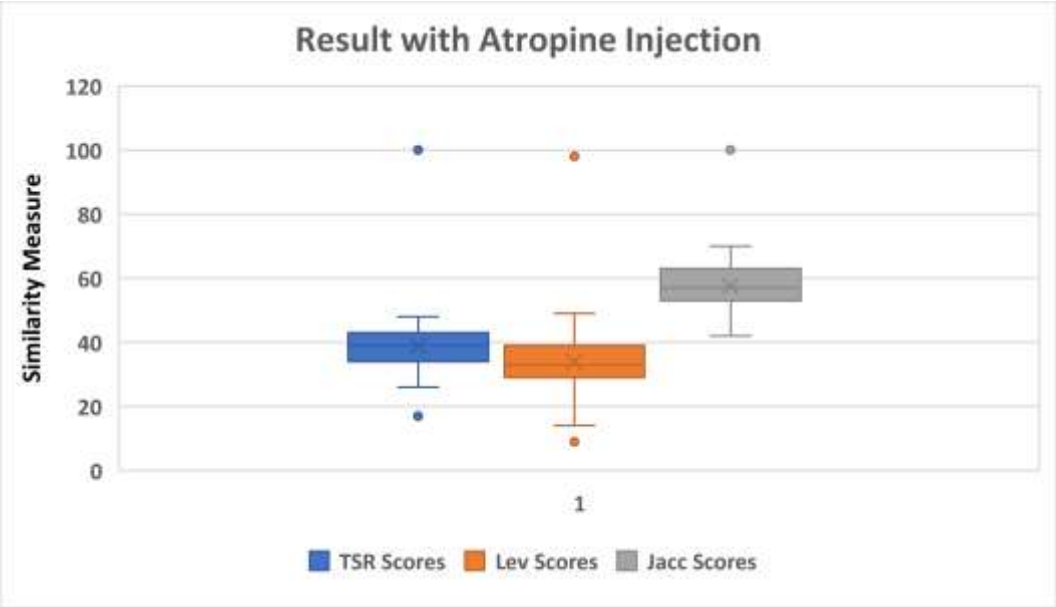

Figure 52: Results obtained from the Atropine Injection sample iterative test.

In another set of six drug samples, scores ranging from 64% to 67% were obtained using the Jaccard string closeness computation algorithm, 43% to 45% with the TRS similarity computation algorithm, and 40% to 41% scores with the TSR string similarity computation strategy as shown in Figure 52. Also, another set of five drug samples scored between 61% and 64% with the Jaccard confidence estimator, 42% and 43% using the TSR similarity confidence estimator, while the TSR scored between 37% to 39% on the set of drug samples under analysis. Furthermore, another set of six drug samples scored between 59% and 61% using the Jaccard method, 40% to 42% by the TRS method, and 34% to 37% similarity confidence scores with the Lev estimation method.

On the other hand, another five-set of the drug samples scored against the main sample with scores ranging from 57% to 59% deploying the Jaccard confidence computation algorithm, 39% to 49% using the TRS method, and 33% to 34% with the Lev confidence similarity estimator. Closely followed by the last set of drug samples are another set of 10 drugs that scored between 54% and 56% using the Jaccard method, 36% to 39% with the TSR confidence scoring method, and 31% to 33% using the Lev similarity computation algorithm. However, another set of nine samples was closer to the last sample with a 50% to 53% score range using the Jaccard similarity estimator, a 31% to 35% score range with the TSR algorithm, and 26% to 31% using the Lev strategy.

Table 11: The extracted results using the Atropine Injection sample.

Drug Name	Edit Distance	TSR Scores (%)	Lev Scores (%)	Jacc Scores (%)
Primacor Injection	70	42	40	60
Cefazolin Sodium 1g	121	33	26	52
NALOXONE HCl 400mg in 1mL	26	40	42	42
Calcium Chloride 1g in 10mL	107	38	29	60
Actrapid Penfill 3ml	53	40	31	59
Vecuronium bromide	45	0.4	33	58
Sugammadex 200mg/2ml	62	43	31	63
Amiodarone Hydrochloride	67	41	32	58
Protamine Sulphate 50mg in 5ml	75	43	36	60
Summethonium Chloride 100mg in 2mL	39	42	40	65
Protamine Sulfate 10mg/ml	64	40	35	67
Glyceryl Trinitrate 1 mg/ml	86	30	26	56
Tranexamic acid	61	39	32	53
Heparin Injection 25000IU in 5 mL	64	38	34	53
Sterile Potassium Chloride	101	32	26	55
Metaraminol 10mg/ml	41	43	43	70
Cyclizine lactate	25	31	27	46
PITRESSIN argipressin	36	46	41	68
Dexamethasone phosphate 4 mg/ml	52	47	39	59
Ephedrine Hydrochloride	37	43	35	57
Ondansetron Solution	66	39	33	53
FRUSEMIDE	49	34	26	54
DALACINC PHOSPHATE	46	40	40	61
METOPROLOL Mylan	75	35	29	67
WATER FOR INJECTIONS BP	77	40	34	56
MORPHINE SULFATE	29	45	49	64
Glycopyrronium Bromide and Neostigmine	68	40	31	63
Clonidine HCl	25	48	44	46
Rocuronium Bromide Injection	61	38	33	54
Fresofol 1% MCT/LCT	345	46	14	50
Sedative Midazolam 5mg	50	34	31	45
Adrenaline Injection	56	39	34	57
Paracetamol Kabi	551	18	9.0	45
Provive MCT-LCT 1%	282	17	17	54
Adrenaline Injection 1mg in 10mL	56	39	34	57
Amoxicillin Sodium	134	26	22	52
Lidocain Injection	28	45	40	54
SODIUM CHLORIDE	123	28	23	51
Remifentanil-Act Injection	76	43	37	63
Sterile Dopamine	33	34	39	56
Hypnomida Etomidate 2mg	65	42	32	61
Xylocaine 1%	30	39	39	52
Fentanyl Injection	120	37	31	50
Noradrenaline acid	69	27	28	54
Magnesium Sulfate 2.47g in 5mL	68	38	31	44
Sugammadex Injection	56	44	35	68
Dynastat Powder	72	36	37	61
Hydrocortisone sodium	80	34	36	64
Atracurium Besylate	45	38	28	54
Atropine	1	100	98	100
PancuroInresa	78	31	31	64

Outputting lower similarity confidence scores are a set of six drug samples ranging from 42% to 46% scores using the Jaccard similarity confidence computation method, 17% to 31% using the TRS method, and finally, 0.09% to 26% scores using the Lev similarity confidence score computation algorithm.

The third drug sample randomly selected for analysis is the Remifentanil-Act Injection which produced similarity confidence scores of about 100% each of the Levenshtein similarity estimation algorithm, Token Set Ratio, and Jaccard distances, respectively, during the pairwise comparative iterative process. These scores placed the Remifentanil-Act Injection as the appropriately identified drug, as shown in Figure 53. The framework also generated an edit distance of 1 (see Table 12), similar to the two previously analyzed samples. This shows that the matching algorithm correctly matched all the characters from the test ampule image with its corresponding string in the lookup table and required only one edit operation to convert both strings.

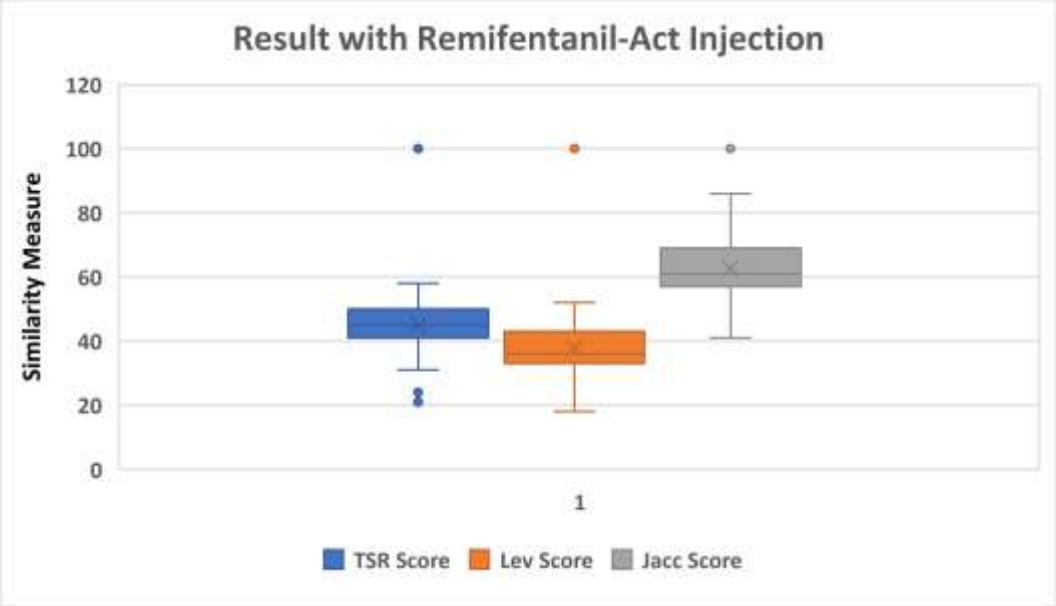

Figure 53: Result obtained from the Remifentanil-Act Injection sample iterative test.

In continuation, similarity confidence scores ranging from 53% to 58% from five drug sample sets using the TSR similarity computation algorithm, 46% to 52% using the Lev string estimation method, and 74% to 86% with the Jaccard similarity metric estimation algorithm were observed closer to the main drug sample under analysis (see Figure 53).

Table 12: The extracted results using the Remifentanil-Act Injection sample.

Drug Name	Edit Distance	TSR Scores (%)	Lev Scores (%)	Jacc Scores (%)
Primacor Injection	79	53	44	59
Cefazolin Sodium 1g	95	54	47	71
NALOXONE HCl 400mg in 1mL	83	32	29	43
Calcium Chloride 1g in 10mL	96	45	40	59
Actrapid Penfill 3ml	84	45	30	62
Vecuronium bromide	69	51	46	74
Sugammadex 200mg/2ml	82	49	39	67
Amiodarone Hydrochloride	82	48	38	74
Protamine Sulphate 50mg in 5ml	85	51	38	69
Summethonium Chloride 100mg in 2mL	77	42	36	69
Protamine Sulfate 10mg/ml	74	48	44	59
Glyceryl Trinitrate 1 mg/ml	89	44	35	60
Tranexamic acid	81	46	37	58
Heparin Injection 25000IU in 5 mL	80	46	36	62
Sterile Potassium Chloride	97	46	37	64
Metaraminol 10mg/ml	76	44	36	61
Cyclizine lactate	90	21	18	41
PITRESSIN argipressin	75	42	38	59
Dexamethasone phosphate 4 mg/ml	81	50	37	69
Ephedrine Hydrochloride	68	58	45	68
Ondansetron Solution	74	44	43	73
FRUSEMIDE	83	34	30	53
DALACINC PHOSPHATE	83	34	28	55
METOPROLOL Mylan	85	50	44	70
WATER FOR INJECTIONS BP	88	47	36	60
MORPHINE SULFATE	79	42	33	68
Glycopyrronium Bromide and Neostigmine	81	47	38	61
Clonidine HCl	82	44	30	52
Rocuronium Bromide Injection 50 mg in 5 ml	74	42	39	54
Fresofol 1% MCT/LCT	311	34	28	62
Sedative Midazolam 5mg	83	31	26	46
Adrenaline Injection	70	51	43	56
Paracetamol Kabi	501	24	23	56
Provive MCT-LCT 1%	247	34	33	67
Adrenaline Injection 1mg in 10mL	70	51	43	56
Amoxicillin Sodium	121	48	03	70
Lidocain Injection	83	35	28	59
SODIUM CHLORIDE	111	41	35	59
Remifentanil-Act Injection	1	100	100	100
Sterile Dopamine	82	34	30	50
Hypnomida Etomidate 2mg	78	42	36	76
Xylocaine 1%	83	34	29	47
Fentanyl Injection	99	57	50	63
Noradrenaline acid	79	45	35	59
Magnesium Sulfate 2.47g in 5mL	79	49	36	57
Sugammadex Injection	69	50	43	66
Dynastat Powder	64	57	52	76
Hydrocortisone sodium	73	51	47	86
Atracurium Besylate	78	39	36	65
Atropine	78	43	35	63
PancuroInresa	81	44	38	58

Furthermore, in another set of five drug samples, uniform scores of 51% were obtained using the TRS string closeness computation algorithm, 43% to 46% with the Lev similarity computation algorithm, and 74% to 86% scores with the Jaccard string similarity computation strategy as shown in Table 12. In addition, another set of six drug samples scored between 48% and 50% with the TSR confidence estimator, 39% and 43% using the Lev similarity confidence estimator, while the Jaccard algorithm scored between 69% to 73% on the set of drug samples under analysis. Also, another set of seven anesthetic drug samples scored between 46% and 48% using the TRS method, 37% to 38% by the Lev method, and 62% to 66% similarity confidence scores with the Jaccard estimation method. Then again, another eight sets of the drug samples scored against the main sample with scores ranging from 44% (five samples) to 45% (three samples) using the TSR confidence computation algorithm. All 36% scores except one sample that returned 47% using the Lev method and 59% to 62% with the Jaccard confidence similarity estimator.

In the continued similarity confidence estimation process, another set of six drug samples closely followed the last set of drug samples scoring between 42% (five samples) and the remaining sample scoring 43% using the TSR method. A 33% (two samples) and 35% (four samples) with the Lev confidence scoring method and 58% to 59% using the Jaccard similarity computation algorithm. On the other hand, another set of nine samples was closer to the last sample with a score range from 34% to 41% using the TSR similarity estimator, a 28% to 33% score range with the Lev algorithm, and a 50% to 57% using the Jaccard string closeness computation strategy. Producing the least range of similarity confidence scores are the last set of four drug samples ranging from 21% to 32% scores using the TSR similarity confidence computation method and 18% to 28% using the Lev method. Finally, 41% to 47% scores using the Jaccard similarity confidence score calculation algorithm.

In continuation of the iterative similarity pairwise comparative process, the Clonidine HCI injection was randomly picked as the fourth drug sample for analysis. The Clonidine HCI injection produced similarity confidence scores of about 97% with the Levenshtein similarity estimation algorithm, 98% with Token Set Ratio, and about 100% with the Jaccard distances, respectively, during the pairwise comparative iterative process, as shown in Figure 54.

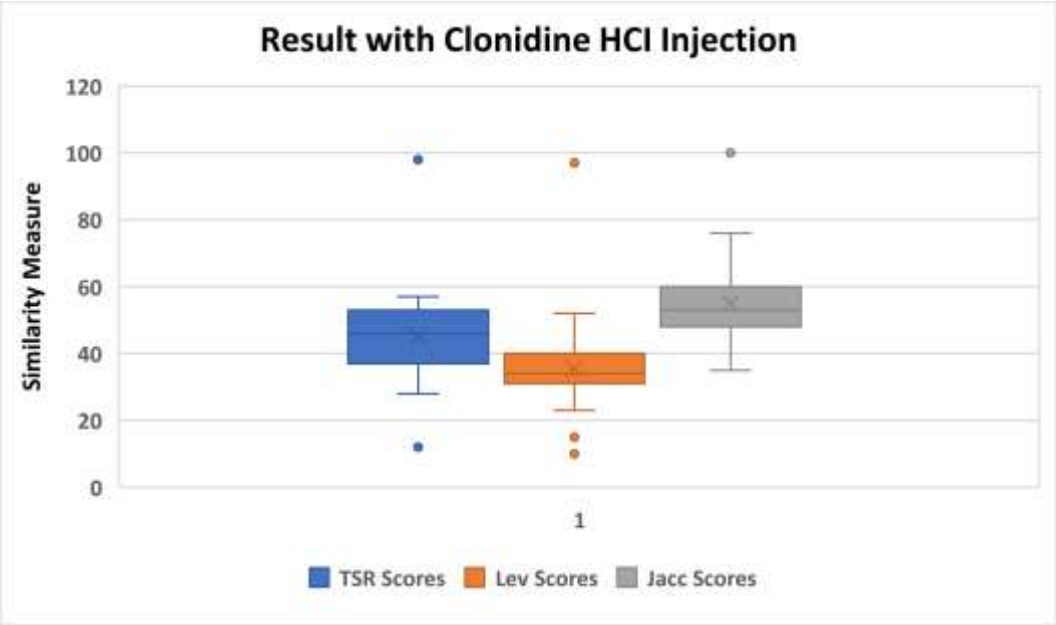

Figure 54: Result obtained from the Clonidine HCl Injection sample iterative test.

These scores affirm the Clonidine HCl injection as the appropriately identified drug, as shown in 54. The framework produced an edit distance of 2 (see Table 13), slightly different from the three previously analyzed samples. This implies that the matching algorithms correctly matched all the characters from the test ampule image with its corresponding string except a few strings in the lookup table and required only two edit operations to convert the strings. Furthermore, closely following Clonidine HCl injection in terms of similarity scores are the similarity confidence scores ranging from 65% to 76% from four drug sample sets using the Jaccard similarity computation algorithm, 48% to 52% using the Lev string estimation method, and 55% to 57% with the TSR similarity metric estimation algorithm (see Figure 54).

In continuation of the iterative analysis process with the fourth sample, another set of six drug samples produced scores ranging from 62 to 65% using the Jaccard string closeness computation algorithm, 42% to 47% with the Lev similarity computation algorithm, and 55% to 57% scores with the TSR string similarity computation strategy as shown in Table 13. Also, another set of six drug samples scored between 57% and 61% with the Jaccard confidence estimator, 37% and 42% using the Lev similarity confidence estimator, while the TSR algorithm scored all through 53% on the set of drug samples under analysis.

Table 13: The extracted results using the Clonidine HCI Injection sample.

Drug Name	Edit Distance	TSR Scores (%)	Lev Scores (%)	Jacc Scores (%)
Primacor Injection	75	53	33	50
Cefazolin Sodium 1g	117	43	30	52
NALOXONE HCI 400mg in 1mL	20	57	52	54
Calcium Chloride 1g in 10mL	104	43	32	50
Actrapid Penfill 3ml	54	54	34	53
Vecuronium bromide	39	37	40	46
Sugammadex 200mg/2ml	60	46	36	57
Amiodarone Hydrochloride	64	53	36	64
Protamine Sulphate 50mg in 5ml	75	54	37	55
Summethonium Chloride 100mg in 2mL	44	48	34	65
Protamine Sulfate 10mg/ml	64	44	33	61
Glyceryl Trinitrate 1 mg/ml	84	36	31	62
Tranexamic acid	61	38	31	53
Heparin Injection 25000IU in 5 mL	61	53	37	59
Sterile Potassium Chloride	97	37	31	55
Metaraminol 10mg/ml	42	55	39	70
Cyclizine lactate	28	30	25	35
PITRESSIN argipressin	38	49	42	54
Dexamethasone phosphate 4 mg/ml	49	53	42	65
Ephedrine Hydrochloride	40	51	48	57
Ondansetron Solution	70	29	29	44
FRUSEMIDE	51	33	23	48
DALACINC PHOSPHATE	45	35	37	55
METOPROLOL Mylan	74	53	32	60
WATER FOR INJECTIONS BP	80	39	29	47
MORPHINE SULFATE	28	56	50	64
Glycopyrronium Bromide and Neostigmine	68	43	32	63
Clonidine HCI	2	98	97	100
Rocuronium Bromide Injection	56	56	42	76
Fresofol 1% MCT/LCT	343	53	15	50
Sedative Midazolam 5mg	48	35	34	50
Adrenaline Injection	58	47	35	50
Paracetamol Kabi	550	12	10	42
Provive MCT-LCT 1%	282	53	17	46
Adrenaline Injection 1mg in 10mL	58	47	35	50
Amoxicillin Sodium	132	43	24	47
Lidocain Injection	27	46	47	68
SODIUM CHLORIDE	121	31	24	51
Remifentanil-Act Injection	81	43	31	52
Sterile Dopamine	33	41	42	56
Hypnomida Etomidate 2mg	62	51	37	55
Xylocaine 1%	28	44	49	46
Fentanyl Injection	125	53	27	55
Noradrenaline acid	65	28	31	48
Magnesium Sulfate 2.47g in 5mL	67	53	35	48
Sugammadex Injection	52	53	42	62
Dynastat Powder	74	43	33	50
Hydrocortisone sodium	80	43	35	59
Atracurium Besylate	43	36	34	48
Atropine	24	48	47	46
PancuroInresa	79	34	30	48

In addition, another set of six anesthetic drug samples scored all through 55% except one sample that scored 56% against the main sample using the Jaccard method, 35% to 37% by the Lev method, and 47% to 51% similarity confidence scores with the TSR estimation method. Also, another six sets of the drug samples scored against the main sample with scores ranging from 52% to 54% utilizing the Jaccard confidence computation algorithm, 33% to 35% scores using the Lev method, and 43% to 47% scores with the TRS confidence similarity estimator. Continuing with the similarity confidence estimation process, another set of eight drug samples closely followed the previous set of drug samples scoring between 50% (seven samples) and the remaining one sample scoring 51% using the Jaccard method. A 31% score (three samples), 32% (three samples), and 33% (two samples) returned with the Lev confidence scoring method and 41% to 43% using the TSR similarity computation algorithm.

In addition, another set of five of the drug samples was closer to the last sample with a score of 48% all through the samples using the Jaccard similarity estimator, a 29% to 31% score range with the Lev algorithm, and 36% to 38% using the TSR string closeness computation strategy. Also, with another set of six of the drug samples, a score range of 46% (four samples) and 47% (two samples) were recorded using the Jaccard similarity estimator, 23% to 29% with the Lev Jaccard similarity estimator, and 30% to 35% with the TSR similarity computation algorithm. At the bottom of the similarity confidence scores against the main drug sample under analysis is the last set of three drug samples ranging from 35% to 44% scores using the Jaccard similarity confidence computation method, 10% to 17% using the Lev method. Furthermore, 12% to 29% scores using the TSR similarity confidence score calculation algorithm.

The last drug sample selected for detailed analysis is the Paracetamol Kabi which generated similarity confidence scores of about 100% with the Jaccard similarity estimation algorithm, 82% with the Lev method, and about 100% with the TSR string distance computation strategy during the fifth pairwise comparative iterative process as shown in Figure 55. These scores imply that the Paracetamol Kabi medication is the appropriately identified drug among the other drugs held in the lookup table. The framework generated an edit distance of 205 (see Table 14 and Figure 55), which is highly different from the other previously analyzed samples connoting that the matching algorithms required 205 edit operations to convert the strings.

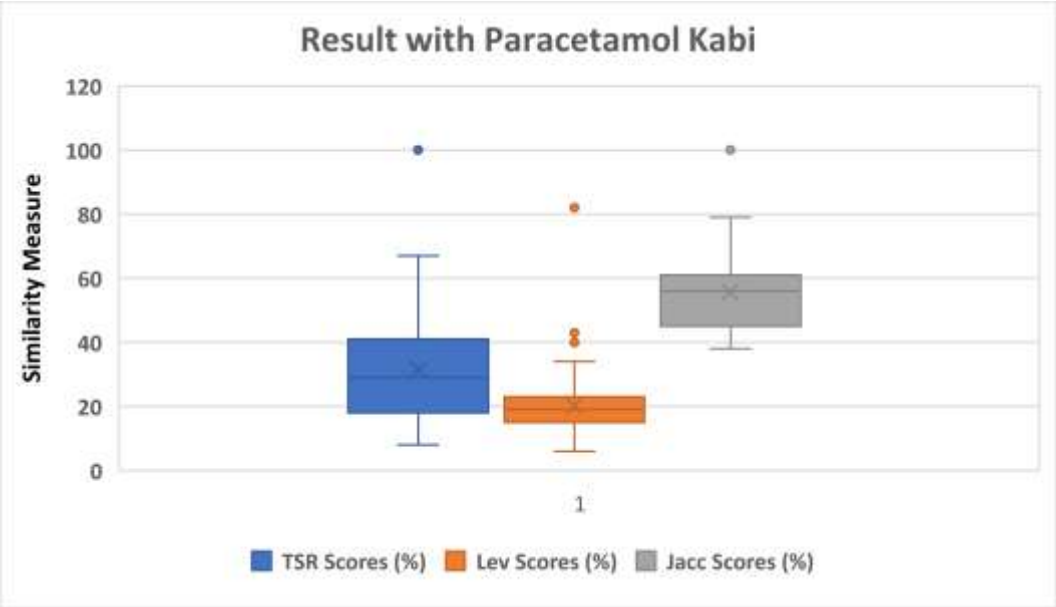

Figure 55: Results obtained from the Paracetamol Kabi sample iterative test.

Furthermore, closely followed the Paracetamol Kabi medication in terms of similarity scores are the similarity confidence scores ranging from 70% to 79% from five drug sample sets using the Jaccard similarity computation algorithm, 27% to 43% using the Lev string estimation method and 54% to 67% with the TSR similarity metric estimation algorithm (see Figure 55). Also, as the iterative analysis process continued with another set of six drug samples, scores ranging from 64 to 69% were generated using the Jaccard string closeness computation algorithm. Also, 23% to 26% scores were outputted with the Lev similarity computation algorithm, and 41% to 53% scores using the TSR string similarity computation strategy, as shown in Table 14. Additionally, another set of four drug samples scored between 60% and 61% with the Jaccard confidence estimator, 21% to 23% using the Lev similarity confidence estimator, while the TSR algorithm scored between 37% to 41% on the set of drug samples under analysis.

In continuation, another set of the six anesthetic drug samples scored all 58% against the main sample under evaluation using the Jaccard method, 20% all through by the Lev method, and 33% to 36% similarity confidence scores with the TSR estimation method. Also, another six sets of the drug samples scored against the main sample with scores ranging from 56% to 57% with the Jaccard confidence computation algorithm, 18% to 20% scores using the Lev method, and 25% to 30% scores with the TRS confidence similarity estimator.

Table 14: The extracted results using the Paracetamol Kabi medication sample.

Drug Name	Edit Distance	TSR Scores (%)	Lev Scores (%)	Jacc Scores (%)
Primacor Injection	508	41	21	69
Cefazolin Sodium 1g	454	67	34	67
NALOXONE HCl 400mg in 1mL	547	12	9	43
Calcium Chloride 1g in 10mL	487	29	25	61
Actrapid Penfill 3ml	525	20	16	60
Vecuronium bromide	529	36	15	52
Sugammadex 200mg/2ml	515	22	18	56
Amiodarone Hydrochloride	514	48	19	52
Protamine Sulphate 50mg in 5ml	508	20	20	58
Summethonium Chloride 100mg in 2mL	531	33	14	57
Protamine Sulfate 10mg/ml	509	40	20	58
Glyceryl Trinitrate 1 mg/ml	504	30	21	55
Tranexamic acid	522	41	16	64
Heparin Injection 25000IU in 5 mL	517	22	18	57
Sterile Potassium Chloride	496	25	23	58
Metaraminol 10mg/ml	523	53	16	48
Cyclizine lactate	557	8	6	38
PITRESSIN argipressin	527	19	15	43
Dexamethasone phosphate 4 mg/ml	523	47	16	57
Ephedrine Hydrochloride	533	15	13	40
Ondansetron Solution	511	36	20	60
FRUSEMIDE	526	19	15	50
DALACINC PHOSPHATE	534	16	13	55
METOPROLOL Mylan	499	54	23	47
WATER FOR INJECTIONS BP	509	45	20	70
MORPHINE SULFATE	536	20	13	52
Glycopyrronium Bromide and Neostigmine	517	37	18	56
Clonidine HCl	547	11	9	42
Rocuronium Bromide Injection	517	18	18	40
Fresofol 1% MCT/LCT	400	59	43	78
Sedative Midazolam 5mg	533	16	13	58
Adrenaline Injection	510	17	20	40
Paracetamol Kabi	205	100	82	100
Provive MCT-LCT 1%	431	56	40	79
Adrenaline Injection 1mg in 10mL	510	17	20	40
Amoxicillin Sodium	474	33	29	70
Lidocain Injection	545	11	10	43
SODIUM CHLORIDE	484	34	26	73
Remifentanil-Act Injection	497	24	23	56
Sterile Dopamine	540	15	11	44
Hypnomida Etomidate 2mg	512	47	19	58
Xylocaine 1%	545	11	10	39
Fentanyl Injection	480	30	27	64
Noradrenaline acid	508	24	20	47
Magnesium Sulfate 2.47g in 5mL	516	20	18	60
Sugammadex Injection	513	29	19	55
Dynastat Powder	492	41	25	58
Hydrocortisone sodium	491	35	25	64
Atracurium Besylate	521	64	17	43
Atropine	547	18	9	45
PancuroInresa	502	25	22	64

On the other hand, another six sets of the drug samples closely followed the previous set of drug samples scoring between 52% (three samples) and 55% (three samples) using the Jaccard method, 16% (two samples), 17% (one sample), and 18% (three samples) with the Lev confidence scoring method. Scores ranging from 20% to 24% were returned using the TSR similarity computation algorithm. Continuing, another set of ten of the drug samples scored against the main sample with a score range of 43% to 50% using the Jaccard similarity estimator, a 13% to 16% score range with the Lev algorithm, and a 16% to 20% using the TSR string closeness computation strategy. Closer to the least scores is another set of five of the drug samples, with a score range of 40% (four samples) and the remaining one sample polling 42% using the Jaccard similarity estimator, 9% to 11% with the Lev similarity estimator and 11% to 15% with the TSR similarity computation algorithm. Finally, the lowest scores at the bottom of the similarity confidence scores against the main drug sample under analysis are the last set of two drug samples ranging from 38% to 39%, using the Jaccard similarity confidence computation method. Also, 0.6% to 0.9% scores were also produced using the Lev method, and 0.8% to 11% scores using the TSR similarity confidence score calculation algorithm.

Despite the high edit score (205) outputted by the Paracetamol Kabi medication in the match with itself, the time required to comparatively perform the similarity estimations process with the rest of the drug samples fell within the required threshold for the real-time anesthetic integration workflow. The overall computation or processing time used by the proposed framework to process the Paracetamol Kabi similarity computation against the other drug samples is 0.5709s, which is below the 1-second set maximum threshold.

Table *1*5 shows the overall similarity confidence scores or accuracies generated by each drug sample against the other drug samples used for the experiments and the processing time required to compute the similarity of each of the drug samples against the other drug samples. The proposed framework performed exceptionally in matching and identifying the drug samples, as almost all the drug samples were accurately recognized with high confidence scores. Only a few drug samples returned slightly low accuracies with one of the matching algorithms adopted for the work.

Table 15: Summary of the highest overall scores by each drug sample used.

Drug Name	Edit Distance	TSR Scores (%)	Lev Scores (%)	Jacc Scores (%)	Time(s)
Summethonium Chloride 100mg in 2mL	1	100	99	100	0.62
Dynastat Powder	1	100	99	100	0.46
Protamine Sulfate 10mg/ml	1	100	99	100	0.51
Fresofol 1% MCT/LCT	2	100	100	97	0.52
Tranexamic acid	1	100	99	100	0.47
Paracetamol Kabi	3	100	82	100	0.57
MORPHINE SULFATE	1	100	99	100	0.51
Sugammadex 200mg/2ml	1	100	99	100	0.35
Ephedrine Hydrochloride	1	100	99	100	0.38
Protamine Sulphate 50mg in 5ml	1	100	99	100	0.43
Atracurium Besylate	1	100	99	100	0.53
DALACINC PHOSPHATE	1	100	99	100	0.37
Dexamethasone phosphate 4 mg/ml	1	100	99	100	0.41
Sterile Dopamine	1	100	99	100	0.38
Calcium Chloride 1g in 10mL	1	100	100	100	0.45
Cefazolin Sodium 1g	1	100	100	100	0.40
Magnesium Sulfate 2.47g in 5mL	1	100	99	100	0.36
Amiodarone Hydrochloride	1	100	99	100	0.36
Amoxicillin Sodium	1	100	100	100	0.41
Primacor Injection	1	100	99	100	0.40
Xylocaine 1%	1	100	99	100	0.42
Ondansetron Solution	1	100	99	100	0.42
Actrapid Penfill 3ml	1	100	99	100	0.55
METOPROLOL Mylan	1	100	99	100	0.37
Sterile Potassium Chloride	3	100	99	97	0.48
Sugammadex Injection	1	100	99	100	0.45
Lidocain Injection	2	100	97	95	0.37
WATER FOR INJECTIONS BP	2	100	99	97	0.49
Remifentanil-Act Injection	1	100	100	100	0.50
Cyclizine lactate	1	100	98	100	0.42
Noradrenaline acid	1	100	99	100	0.47
Vecuronium bromide	1	100	99	100	0.52
SODIUM CHLORIDE	2	96	89	93	0.57
Provive MCT-LCT 1%	1	100	100	100	0.49
Adrenaline Injection	1	100	99	100	0.47
Hydrocortisone sodium	1	100	100	100	0.36
Glycopyrronium and Neostigmine	1	100	99	100	0.48
Metaraminol 10mg/ml	1	100	99	100	0.63
PITRESSIN argipressin	1	100	99	100	0.41
Clonidine HCl	2	98	97	100	0.47
Sedative Midazolam 5mg	1	100	99	100	0.45
NALOXONE HCl 400mg in 1mL	1	100	98	100	0.30
Atropine	1	100	98	100	0.41
Hypnomida Etomidate 2mg	1	100	99	100	0.52
Fentanyl Injection	1	100	100	100	0.51
Ondansetron Solution	3	91	98	89	0.35
PancuroInresa	1	100	99	100	0.48
Rocuronium Bromide Injection	1	100	99	100	0.36
Cefazolin Sodium 1g	2	86	91	93	0.39
Heparin Injection 25000IU in 5 mL	1	100	99	100	0.28

Anaesthetic drug samples such as the Sodium Chloride injection and Paracetamol Kabi recorded confidence scores slightly below 90% but above the set threshold with the Levenshtein similarity estimation algorithm. On the other hand, the Cefazolin Sodium injection recorded the least confidence score (86%) against the other drug samples by the framework using the TSR algorithm. In contrast, on the part of the Jaccard similarity estimation strategy, only the Ondansetron Solution medication scored the least, with an 89% score.

Furthermore, in processing time management and efficiency, the proposed framework demonstrated high time management, as shown in Table 15. The Time(s) column in the table shows the maximum time required by each incoming drug sample to appropriately match and identify the right drug amongst all the other drug samples. As can be observed from the table, no drug samples' processing time exceeded the threshold (one second) required in the real-time anesthetic drug identification for medication preparation in the operating theatre. Drug samples such as Metaraminol injection and Summethonium Chloride injection recorded the highest processing time (about 0.6 seconds) due to the number of features embedded in their label and the efforts required by the proposed framework to process, match and pairwise compare them with the other drug samples in order to identify the right drug. The complete results obtained from the confidence computation experiment are attached in Appendix D.

5.8 Chapter Summary

This chapter presented the core theoretical and conceptual workflow of the proposed novel intelligent anesthetic drug identification framework. The string-matching techniques were equally presented, such as the exact and inexact string-matching approaches that played a vital role in the optimal identification of anesthetic drugs. Also found in the chapter are the adopted and crafted anesthetic drug similarity score estimation methodologies, including the Levenshtein (Lev scores), Token Set Ratio (TSR scores), Jaccard distance scores (Jacc Scores) and as well as the optimized Levenshtein algorithm. In the chapter, the generalized Ukkonen and upper bound theorems were adopted to optimize the conventional Levenshtein algorithm, which significantly improved the computation speed of the extraction of the rate-of-substance of the

anesthetic drugs. In the sub-sections of the chapter, the detailed optimization process of the Levenshtein distance, the Levenshtein distance sub-tasks computation procedure, and as well as the enhanced Levenshtein distance sub-tasks computation steps were presented. In addition, the experimental procedure, the dataset description, the experimental setup and process, and as well as the threshold computation procedure for efficient and rapid anesthetic drug identification were presented. Finally, the detailed outcome of the experiments was presented in the form of charts and tabulation with a detailed analysis of selected samples of the anesthetic medications.

Chapter 6 Anesthetic Drugs Identification in Varied Processing Conditions

The last set of experiments performed for the study presented in this thesis deals with examining various scenarios that could affect the processing performance of the proposed anesthetic drug identification framework. Poor lighting conditions and stains are two significant factors that could adversely influence the drug's recognition accuracy and confidence scores and are thus considered for further investigation in this chapter. In this investigation, ten different anesthetic drug samples were randomly selected. The real-life anesthetic drug container label stain and low-light conditions were modeled using various advanced image processing techniques. Such strategies include noise-inducing strategies and different real-life image quality reduction methods, such as the image blurring and filtering stages. The Laplacian object quality enhancement scheme was deployed to demonstrate the restoration and recoverability of the badly affected anesthetic drugs, and remarkable improvements were recorded.

6.1 The Anesthetic Drugs Container Stain Modelling

Anesthetic drug image noising is one of the ways used in this work to model the real-time factors that affect the performance of the proposed framework. It is the degradation of the quality of the acquired anesthetic drug image signals induced by external environmental sources such as stains, dust particles in the acquisition sensors, interference in the transmission channel, and low lighting conditions. In other words, the anesthetic container stain is the random variation of the drug containers' label color information or brightness during the acquisition process. Noise in anesthetic drug containers plays a vital role in determining a recognized medication's accuracy and confidence level. Noise in the acquired anesthetic drug container can be multiplicative or additive, but most of the noise encountered in the anesthetic identification process is additive. The additive signal contaminates the original signal to generate a bad input or noisy signal that is expressed (*Topic 5: Noise in Images*)z as follows:

$$\varphi(i,j) = \omega(i,j) + \delta(i,j) \qquad 6.1$$

Where, $\varphi(i,j)$ denotes the generated corrupted signal, $\omega(i,j)$ represents the intensity of the original drug image and $\delta(i,j)$, the noise added to create the corrupted signal at

(i, j). On the other hand, the multiplicative factor linked with each of the image pixels is expressed as:

$$\varphi(i,j) = \sigma(i,j)\omega(i,j) + \delta(i,j) \quad 6.2$$

Where, $\sigma(i,j)$ represents the multiplicative factor achieved in each of the image signals. In the experiments, the impulse-valued noise model, also referred to as the salt and pepper noise model, was used to corrupt the original anesthetic image data values statistically. The image data were not fully corrupted as obtainable in real life, but some pixels in them are sparingly altered to depict stained drug containers. During the process, about 255-pixel values of random bright pixels and 0-pixel values of random dark pixel values were added to the image data to model the stained anesthetic drug containers.

6.2 The Anaesthetic Drugs Container Data Low-light Modelling

An image-blurring technique with different kernel filtering sizes was deployed to erode some details in the anesthetic drug samples and create the low-light operating scenario. In the investigation, the Gaussian blurring algorithm that uses the weighted mean strategy to induce blurring into image data was used to naturally model situations where the introduced framework operates in low-light conditions. The Gaussian blurring method uses weighted mean computation in which the nearby pixels nearer to the central pixels of the anesthetic drug samples contribute more weight than the average blurring scheme. Based on the Gaussian blurring algorithm, the anesthetic data blurring process uses convolution operations with kernels. The convolution functions use different methods to induce blur (low light) on the data sample by replacing the weighted sum in the image data samples with pixels that are closer to them and do not have any effects on the image data sizes. Mathematically, the convolution operation is generally expressed as:

$$\varphi(i,j) = \omega * \delta(i,j) = \sum_{di=-a}^{a} \sum_{dj=-b}^{b} \omega(di,dj)\,\delta(i-di, j-dj\ ) \quad 6.3$$

Where the filtered image is represented by $\varphi(i,j)$, ω = the filter kernel and $\delta(i,j)$ denotes the original image sample. In the filter kernel, each element is considered by $-a \leq di \leq a$ and $-b \leq dj \leq b$. In the blurring process involving convolutions, convolution kernels are required in the convolution function to determine how neighboring pixel values are utilized in calculating the destination pixel values. They are 1D or 2D grids of numerals that point out the impact of the neighbors of a pixel on its last value. In the computation of the value of an individual transformed pixel, the products of individual neighboring pixel values are added to the resulting kernel value. While performing a convolution operation, each pixel in the image sample is repeatedly scanned over by the kernel function, and the process's effects are applied to the whole image sample. The kernels do not need to have the same height and width; the height or width can be equal to 1 (1D), or the height and width can be greater than 1 (2D). However, the dimensions of the kernel must be odd numbers to centrally position the kernel over the pixel during a pixel transformation process.

The identity kernel is the simplest form of a kernel with a single value: 1. The output of a kernel operation applied centrally to the nine grid values is shown in the formula below. It first performs a multiplication operation of the pixel with the central value found in the convolution kernel before multiplying the neighboring pixel values by 9, resulting in a sum of 0.5 value. The image sample stays unaltered during the identity kernel convolution operation. In a box blur or 2D kernel, the nearby pixels' average value is returned. To model the real-life scenarios of environments with low-lights or poor quality of the anesthetic image acquisition in the experiments, three kernel sizes of the Gaussian blurring algorithm were used, namely, the 3×3, 5×5, and 7×7 sizes. Each of the kernel sizes exerted some degree of modifications on the selected image data samples depicting the levels of low lights or poor quality of the anesthetic image data samples.

In process, the origin of the convolution process is typically the initial location of the kernel that is overhead the current pixel output. The 3×3 kernel-sized convolutions exerted a lesser degree of low light scenario or blurring compared to the 5×5 and 7×7 kernels, respectively, as illustrated in the result section of this chapter. This implies that the increase in complexity of the blurring kernel raises the influence of the pixel in the image dataset with respect to the distance of the kernel's processing center.

6.3 Anesthetic Drugs Identification Enhancement in Varied Processing Conditions

The color constant-driven object sample improvement strategy is an image-centered visual effect-boosting technique obtained from the performance of computations and transformations on the image sample to yield the authentic image. The Laplacian operator is specifically fitted in the enhancement of blurring orchestrated by diffusion effects such as low light influence, environment, and other factors. The Laplacian operator is typically not deployed to detect edges in object samples due to its significant influence and high sensitivity to noise. The major impact of the Laplacian method on the recovery of an original image sample resolves around the deployment of its zero-crossing attributes for the localization of edges in the samples and the determination of the side in which pixels in the image samples (bright or dark side) belongs (Tian et al., 2018).

To demonstrate the adaptability of the proposed framework in various working environments and conditions modeled above, the Laplacian image frames enhancement algorithm is deployed to recover the low-light and stained anesthetic drug container labels modeled above. The Laplacian operation on a given object sample highlights areas in the object with rapid intensity alterations, and it belongs to the second derivative technique or second order of object enhancement (Bhairannawar, 2018). The Laplacian strategy is remarkably great in obtaining fine details on a given sample of an object, and features that possess sharp discontinuity from the rest of the components are enhanced through the Laplacian operator. This is demonstrated in the various experiments performed to recover the anesthetic drugs acquired in low light processing conditions or those with stains. The Laplacian is a popular linear differential operator that approximates the second-order derivatives as isotropic, and the operation does not depend on the direction of the image samples' feature discontinuities. For a given sample of the anesthetic drug container image, the function $f(i, j)$ can be mathematically expressed as:

$$\nabla^2\varphi \approx \frac{\partial^2\varphi}{\partial^2 i^2} + \frac{\partial^2\varphi}{\partial^2 j^2} \qquad 6.4$$

Since the derivative above has a linear operation, the Laplacian is said to be a linear operator. Putting into consideration of a given pixel's horizontal and vertical neighbors, then the Laplacian can be found in the i and j directions as expressed below:

$$\frac{\partial^2 \varphi}{\partial^2 i^2} \approx \varphi(i+1,j) + \varphi(i-1,j) - 2\varphi(i,j), \quad 6.5$$

$$\frac{\partial^2 \varphi}{\partial^2 j^2} \approx \varphi(i,j+1) + \varphi(i,j-1) - 2\varphi(i,j) \quad 6.6$$

By combining the two equations above, the 2D Laplacian can then be expressed as:

$$\nabla^2 \varphi \approx [\varphi(i+1,j) + \varphi(i-1,j) + \varphi(i,j+1) + \varphi(i,j-1) - 4\varphi(i,j) \quad 6.7$$

The Laplacian operator's template coefficients are computed in Equation 6.7, which possesses a normalization function that ensures that the template coefficient's injection is uniform so that the enhancement process does not erode critical information in the given drug container samples. The Laplacian operator inhibits the influence of distant pixels away from the template center and obtains the difference in the pixels nearer to the center of the pixels. During the Laplacian computation process, the pixel intensity range is pegged between 0–255, the minimum pixel is found first, and the maximum is then obtained and multiplied by 255/max using each element in the image sample.

6.4 Modeled Anaesthetic Drugs Measurement Metrics

To compute the differences in the original drug samples, the modeled low-light and poor-quality anesthetic drugs processing conditions and the enhanced samples using the Laplacian algorithm, the peak signal-to-noise ratio (PSNR), structural similarity index (SSI), feature similarity indexing (FSI) and the universal image quality index (UIQ) metrics were deployed.

6.4.1 The peak signal-to-noise ratio (PSNR)

The PSNR measures the ratio between the anesthetic drug sample signal's maximum possible power and the corrupting noise power influencing the fidelity of the representations in the drug sample. In other words, the PSNR measures the difference between the anesthetic drug sample pairs, including the noisy/stained versus the original sample, the low-light samples versus the original sample, the restored sample

versus the actual sample, and the restoration algorithmic performance evaluation etc. The PSNR is typically represented in logarithmic decibel scale, and its value in video compression and the noisy image is 8 bits around 30 and 50 dB. The higher the values, the more suitable the images are. The PSNR standard values for 16-bit data fall between 60 and 80 dB (Korhonen & You, 2012). To compute the PSNR, the mean-squared error (MSE) between the two drug pairs is first calculated as follows:

$$MSE = \frac{\sum_{i,j}[C_1(i,j) - C_2(i,j)]^2}{i * j} \quad 6.8$$

Where $i\ and\ j$ represent the number of rows and columns in the matrix of the input image data sample. Then the PSNR is expressed as:

$$\text{PSNR} = 10log_{10}\left(\frac{R^2}{MSE}\right) \quad 6.9$$

R denotes the highest possible pixel values available in the drug image samples.

6.4.2 The structural similarity index (SSI)

The SSIM, on the other hand, measures the quality of degradation of the drug image samples due to the noising and the blurring activities that created the low-light and poor processing environmental conditions. SSIM operates on the visual structure of a given image sample pair and thus estimates the difference in perception of the related image pairs (Bakurov et al., 2022). In process, the SSI does not determine the superiority amongst given image samples; instead, it infers the difference between the altered anesthetic drug container images and the original ones. The SSIM values are calibrated between −1 and 1, with 1 signifying a perfect structural similarity. Given $i\ and\ j$ as the input of two anaesthetic drug sample image pair, then SSIM is represented mathematically as:

$$SSIM(i,j) = [C(i,j)]^{\alpha}[Q(i,j)]^{\beta}[Z(i,j)]^{\gamma} \quad 6.10$$

Where $C(i,j)$ represents the brightness between the two-image pair, $Q(i,j)$ the comparison of the contrast between them with $Z(i,j)$, representing the comparison of the structure of the image pairs. Furthermore, $C(i,j)$, $Q(i,j)$ and $Z(i,j)$ are obtained individually as expressed below:

$$C(i,j) = \frac{2\mu_i\mu_j + q_1}{\mu i^2 + \mu j^2 + q_1}$$

$$Q(i,j) = \frac{2\sigma_{ij} + q_2}{\sigma i^2 + \sigma j^2 + q_2}$$

$$Z(i,j) = \frac{\sigma_{ij} + q_3}{\sigma_i\sigma_j + q_3}$$

Where, μ_i and μ_j denote the average value of the given image pairs, respectively, σ_i and σ_j denote the standard deviations of the given image pairs, while the covariance of the pair of the image samples is represented by $\sigma_i\sigma_j$. Finally, the q_1, q_2 and q_3 are constants.

6.4.3 The feature similarity index (FSI)

The FSI measures and compares the feature and structural similarities between the enhanced or restored anesthetic drugs and the original. The FSI adheres to the phase congruency and gradient magnitude principle with values ranging from 0 to 1. A comparison process that yields 1 signifies a perfect match, and those close to 0 imply that the drugs' features differ highly. The FSI computation process follows two phases; the local similarity map computation process constitutes the first stage, and the aggregation of the similarity maps into a unified similarity score makes up the second stage (Zhang et al., 2011). To measure the similarities between two drug sample features, i.e., $f_1(i)$ and $f_2(i)$ of a given anaesthetic drug samples, the feature similarity measurement is first separated into two parts, each representing eighter the phase congruency (PC) or the gradient magnitude (GM). The similarity computation for the phase congruency, $PC_1(i)$ and $PC_2(i)$ is first computed with:

$$SM_{PC}(i) = \frac{2PC_1(i).PC_2(i) + Q_1}{PC_1^2(i) + PC_2^2(i) + Q_1} \qquad 6.11$$

Where Q_1represents a constant positive value to boost the $SM_{PC}(i)$ stability. The choice of Q_1relies on the dynamic range of the phase congruency values and the outcome of $SM_{PC}(i)$ is typically in the range of 0 and 1. On the other hand, the

gradient magnitude (GM) with $GM_1(i)$ and $GM_2(i)$ values are compared, and their similarities are computed using:

$$SM_{GM}(i) = \frac{2GM_1(i).GM_2(i) + Q_1}{GM_1^2(i) + GM_2^2(i) + Q_1} \quad 6.12$$

Where Q_1represents a constant positive value that depends on the range of dynamics of the values of the GM. Combining $SM_{PC}(i)$ and $SM_{GM}(i)$ yield the similarity $S_I(i)$ of $f_1(i)$ and $f_2(i)$ defined as:

$$S_I(i) = [SM_{PC}(i)]^{\alpha}.[SM_{PC}(i)]^{\beta} \quad 6.13$$

Where α and β denote the factors that vary the relative importance of PC and GM features. Setting α = β =1 for ease of computation, Equation 6.13 yields $S_I(i) = SM_{PC}(i).SM_{PC}(i)$. To determine the relevance of $S_I(i)$, $PC_{max}(i) = \max(PC_1(i), PC_2(i))$ is used across the similarity between $f_1(i)$ and $f_2(i)$. Then the overall similarity between $f_1(i)$ and $f_2(i)$ can be stated as:

$$FSI = \frac{\sum_{i\in\emptyset} S_I(i).PC_{max}(i)}{\sum_{i\in\emptyset} PC_{max}(i)} \quad 6.14$$

Where Ø represents the entirety of the spatial domain of the images.

6.4.4 The universal image quality index (UIQ)

The UIQ models the anesthetic drug image distortion as a blend of three factors: correlation loss, luminance, and contrast distortion (Wang & Bovik, 2002) and can be computed using the expression below:

$$I_q = \frac{\sigma_{ij}}{\sigma_i\sigma_j} * \frac{2\bar{i}\bar{j}}{(\bar{i})^2(\bar{j})^2} * \frac{2\sigma_i\sigma_j}{\sigma_i^2 + \sigma_j^2} \quad 6.15$$

The $\frac{\sigma_{ij}}{\sigma_i\sigma_j}$ component of the equation represents the correlation coefficient between i and j pair of images and measures the linear correlation between them. The $\frac{2\bar{i}\bar{j}}{(\bar{i})^2(\bar{j})^2}$ section of the equation computes the closeness of the mean luminance between i and j and has a value range of [0.1]. Furthermore, the $\frac{2\sigma_i\sigma_j}{\sigma_i^2+\sigma_j^2}$ part of the equation computes the similarity in contrast of the pair of the image samples and the index I_q range of values is between [-1,1]. The optimal value is 1, obtainable only if the pair of compared

images are identical, and the minimum value is -1 for extremely unidentical image pairs.

6.5 Experimental Procedure

The key objective of the investigation performed in this chapter is to model and proffer solutions to the real-life scenarios that affect the proposed anesthetic drug identification framework's performance. The study used scene object distortion modalities like artificial data noising and blurring to depict the real-life stain on the anesthetic drug container labels and low-light operating environments. After the modeling, solutions using an object visual quality enhancement strategy known as the Laplacian algorithm was deployed to demonstrate the feasibility of the adaptability of the proposed anesthetic drugs identification framework in diverse processing conditions.

The experiment conducted in this section is an extension of the experimental setups in the previous chapters, together with the introduction of the artificial noise(stain) and blurring (low light) to the selected anesthetic drug sample data. As described above, various degrees of distortions were introduced to the chosen anesthetic drug samples using the noising strategy and different object distortions kernel sizes, including 3×3, 5×5, and 7×7 kernel sizes. After a series of experimental iterations using the chosen drug samples, different results were obtained for both the distortion process and the enhancement counterpart. Furthermore, the original anesthetic drug containers and the resultant distorted and improved samples were subjected to testing using various image object quality measures described in Section 6.0. Also, the various selected original drug samples, the resultant distorted and enhanced samples, were subjected to a further test using the proposed drug string extraction, matching, and confidence computation methods. The results showed that the proposed framework could withstand the variations in processing conditions with the integration of the Laplacian object quality enhancement strategy introduced in this chapter.

6.6 Results and Analysis

The investigation results involving the real-world modeling of the stained anesthetic drug label using the noise inducement method are shown in Table 16. The rows of the

table correspond to the selected drug samples, i.e., s1 = Paracetamol Kabi, s2 = Amoxicillin Sodium, s3 = Vecuronium Bromide, s4 = Sterile Potassium Chloride, s5 = Heparin Sodium, s6 = Cefazolin Sodium, s7 = Parecoxib Injection, s8 = Calcium Chloride, s9 = Sugammadex Injection and s10 = Rocuronium Bromide. The columns show the different results obtained using the four metrics deployed to measure the quality gains between the noisy/stained drugs and the improved drug data. The metrics are the peak signal-to-noise ratio (PSNR), feature similarity index (FSI), structural similarity index (SSI), and universal image quality index (UIQ), explained in Section 6.0.

Table 16: Quality comparison of the original data samples, noisy and noise-recovered data sample.

	Original Vs Noise				**Original Vs Noise Recovered**				**Change in Quality**			
Samples	**PSNR**	**FSI**	**SSI**	**UIQ**	**PSNR**	**FSI**	**SSI**	**UIQ**	**ΔPSNR**	**ΔFSI**	**ΔSSI**	**ΔUIQ**
s1	20.98	0.49	0.97	0.24	23.37	0.55	0.99	0.29	2.39	0.06	0.02	0.05
s2	15.82	0.48	0.93	0.16	16.49	0.53	0.95	0.23	0.67	0.05	0.02	0.07
s3	18.73	0.46	0.96	0.12	20.21	0.51	0.98	0.18	1.48	0.05	0.02	0.06
s4	19.21	0.37	0.96	0.1	20.96	0.41	0.98	0.15	1.75	0.04	0.02	0.05
s5	22.46	0.36	0.98	0.07	28.05	0.41	0.99	0.13	5.59	0.05	0.01	0.06
s6	19.73	0.51	0.97	0.17	21.33	0.54	0.99	0.21	1.6	0.03	0.02	0.04
s7	19.04	0.45	0.97	0.1	20.62	0.5	0.99	0.16	1.58	0.05	0.02	0.06
s8	18.86	0.46	0.97	0.14	20.33	0.51	0.98	0.2	1.47	0.05	0.01	0.06
s9	17.51	0.57	0.96	0.19	18.46	0.61	0.98	0.26	0.95	0.04	0.02	0.07
s10	14.98	0.57	0.94	0.25	15.47	0.62	0.96	0.33	0.49	0.05	0.02	0.08

As illustrated in Table 16, there is a significant data quality gain between the noise-induced sample data and the quality-enhanced data samples. For the s1 drug sample, the PSNR between the original drug sample and the stained drug sample is 20.98, and the PSNR between the original drug sample and the stain-recovered drug sample is 23.37, showing a 2.39-decibel quality gain. Also, the universal image quality index between the s1 original sample and the stained sample is 0.24, and the UIQ between the s1 original sample and the recovered sample stood at 0.99, showing a significant gain in the quality of the sample due to the introduction of the Laplacian enhancement technique. For sample s2, the quality gain through the PSNR measure stands at 0.67 decibels and 0.07 of UIQ; the s3 sample gained 1.48-decibel PSNR and 0.06 UIQ, sample s4 gained 1.75-decibel PSNR and 0.05 UIQ, s5 sample gained 5.59-decibel PSNR and 0.06 UIQ. Furthermore, s6 to s10 samples also gained remarkable quality improvements using the various measuring metrics, as illustrated in Table 16 and Figure 56. The improved S6 sample gained 1.6-decibel PSNR, 0.03 FSI, 0.02 SSI, and 0.04 UIQ; s7 gained 1.58 PSNR, 0.05 FSI, 0.02 SSI, and 0.06 UIQ; the s8 sample earned 1.47-

decibel PSNR, 0.05 FSI, 0.01 SSI, and 0.06 UIQ. On the other hand, the s9 drug sample gained 0.95-decibel PSNR, 0.04 FSI, 0.02 SSI, and 0.07 UIQ, whereas the s10 achieved a 0.49-decibel PSNR, 0.05 FSI, 0.02 SSI, and 0.08 UIQ quality improvement respectively.

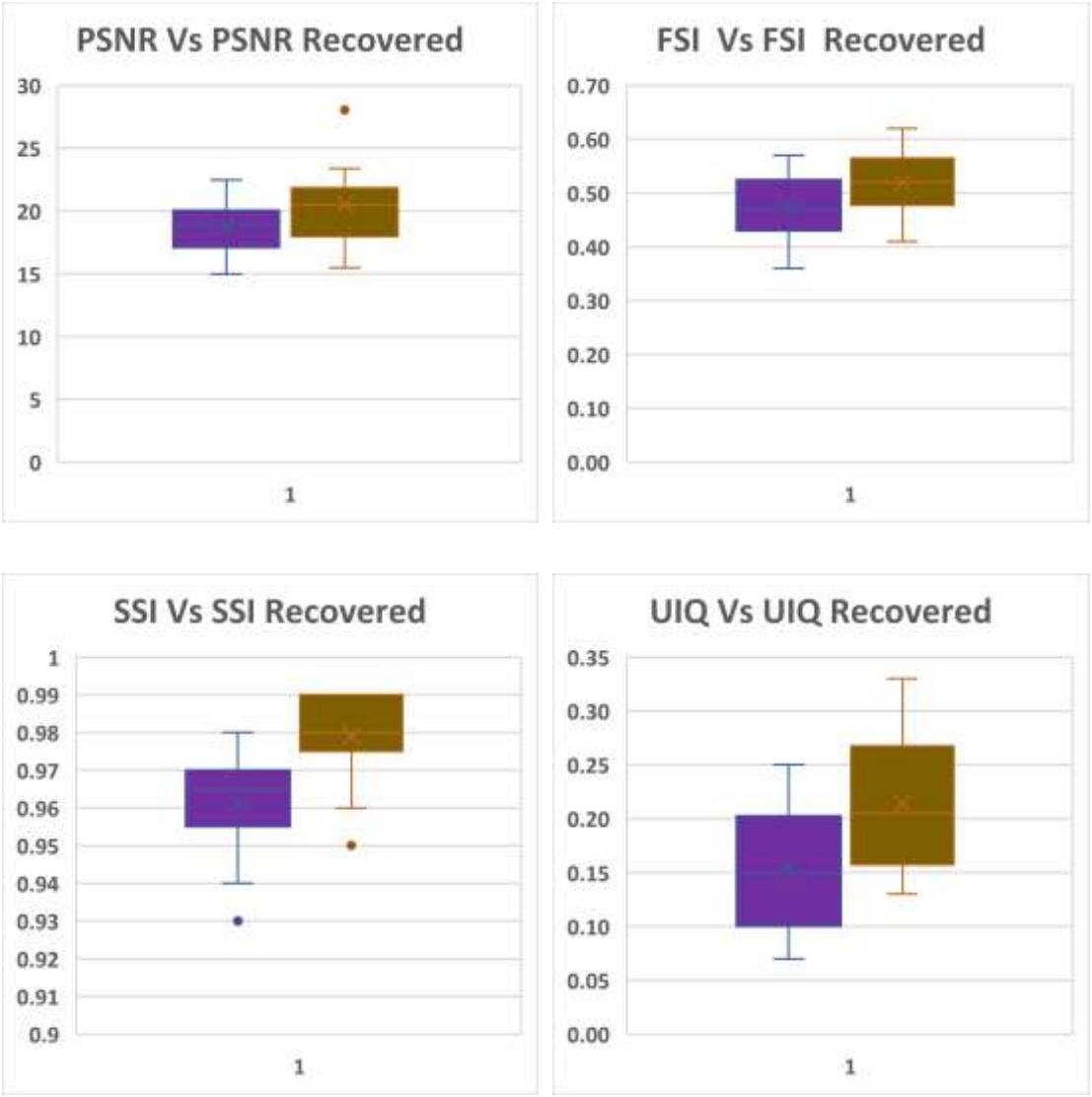

Figure 56: Quality metric between the original data samples, noise, and noise-recovered sample data for noise inducement.

In continuation, the comparative results obtained from the 3x3 kernel size blur-induced low light processing condition are presented in Table 17. The s1 data sample produced a PSNR score of 20.96 decibels between the original s1 data sample and the 3x3 kernel size-induced low-light condition. Furthermore, a 23.35-decibel PSNR score between the original s1 data sample and the recovered data sample showed a significant quality improvement of 2.39-decibel PSNR, 0.06 FSI, 0.02 FSI, and 0.05 UIQ, respectively. Also, the s2 data sample showed a remarkable quality gain, recording a

PSNR score of 15.8 decibels between the original s2 data sample and the 3x3 kernel size-induced low light condition. It also obtained a 16.47-decibel PSNR score between the original s2 data sample and the recovered data sample, showing a substantial quality gain of 0.67-decibel PSNR, 0.04 FSI, 0.02 FSI, and 0.07 UIQ, respectively.

Table 17: Quality comparison of the original data samples, kernel size 3x3 blur-induced low light and recovered data sample.

	Original Vs Average Blur (kernel Sizes (3,3))				**Original Vs Average Blur Recovered (kernel Sizes (3,3))**				**Change in Quality**			
Samples	PSNR	FSI	**SSI**	**UIQ**	**PSNR**	**FSI**	**SSI**	**UIQ**	**ΔPSNR**	**ΔFSI**	**ΔSSI**	**ΔUIQ**
s1	20.96	0.47	0.95	0.22	23.35	0.53	0.97	0.27	2.39	0.06	0.02	0.05
s2	15.8	0.46	0.91	0.14	16.47	0.5	0.93	0.21	0.67	0.04	0.02	0.07
s3	18.71	0.44	0.94	0.1	20.19	0.49	0.96	0.16	1.48	0.05	0.02	0.06
s4	19.2	0.36	0.95	0.09	20.95	0.4	0.97	0.14	1.75	0.04	0.02	0.05
s5	22.42	0.34	0.96	0.07	28.03	0.39	0.97	0.12	5.61	0.05	0.01	0.05
s6	19.71	0.49	0.95	0.15	21.31	0.52	0.97	0.19	1.6	0.03	0.02	0.04
s7	19.02	0.42	0.95	0.1	20.49	0.47	0.96	0.13	1.47	0.05	0.01	0.03
s8	18.84	0.44	0.95	0.12	20.31	0.49	0.96	0.19	1.47	0.05	0.01	0.07
s9	17.48	0.55	0.94	0.17	18.44	0.59	0.95	0.24	0.96	0.04	0.01	0.07
s10	14.96	0.55	0.91	0.21	15.44	0.61	0.94	0.31	0.48	0.06	0.03	0.1

On the other hand, the s3 data sample showed a notable quality gain as it recorded a PSNR score of 18.71 decibels between the original s3 data sample and the 3x3 kernel size-induced low light condition. Furthermore, a 20.19-decibel PSNR score between the original s2 data sample and the recovered data sample showed a considerable quality gain of 1.48-decibel PSNR, 0.05 FSI, 0.02 FSI, and 0.06 UIQ, respectively. As shown in Table 17 and Figure 57, all the remaining stained, enhanced, and tested selected data samples achieved notable performance quality improvement using the quality estimation matrices for the introduced Laplacian object quality improvement algorithm. That is, a 1.75-decibel PSNR, 0.04 FSI, 0.02 SSI, and 0.05 UIQ improvements were recorded between the low-light s4 drug data and the improved, 5.61 PSNR, 0.05 FSI, 0.01 SSI and 0.05 UIQ between the low-light s5 drug data and the improved, 1.6 PSNR, 0.03 FSI, 0.02 SSI and 0.04 UIQ between the low-light s6 drug data and the improved sample and relatively similar quality improvements on the remaining drug samples.

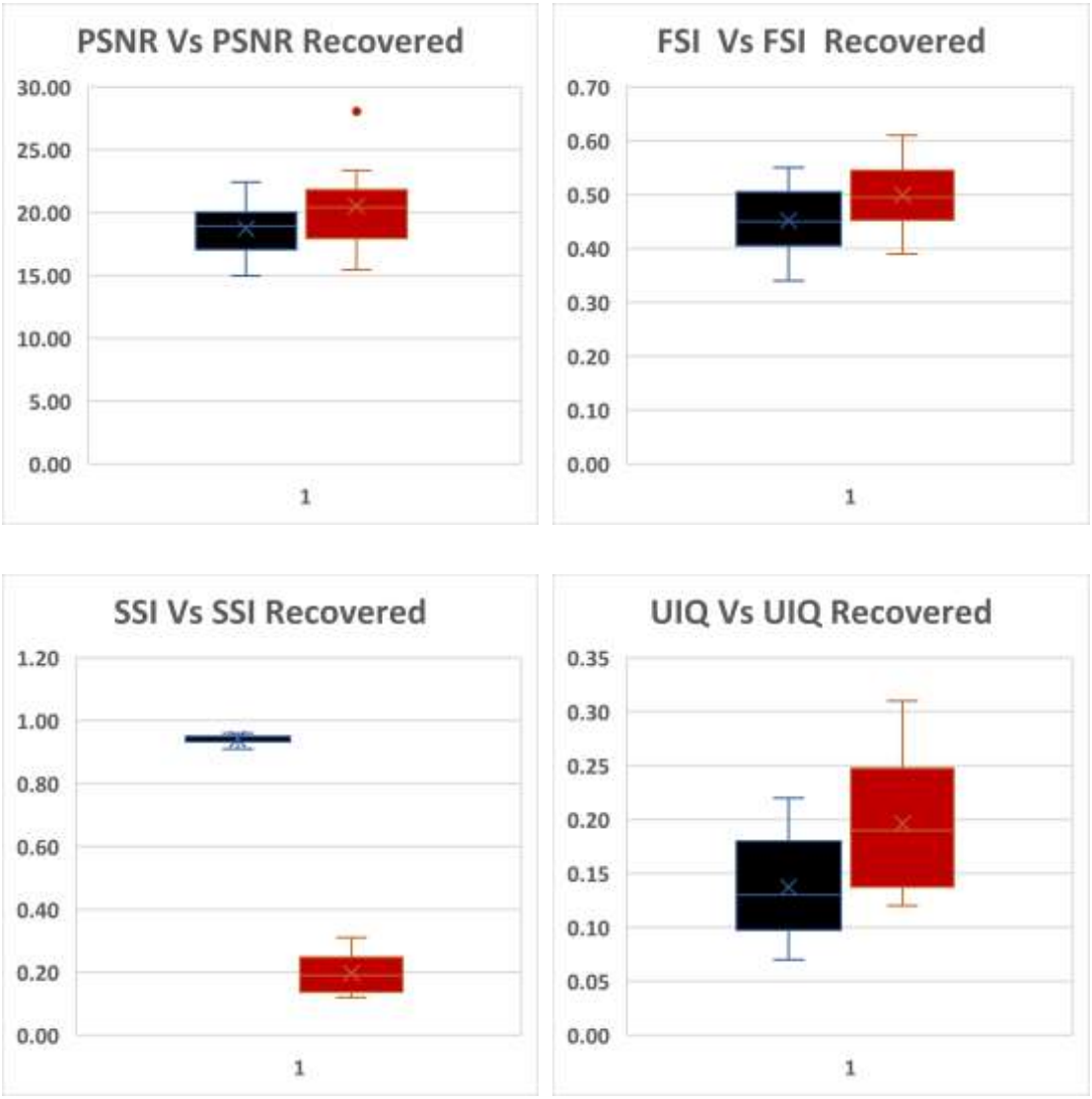

Figure 57: Quality metric between the original data samples, kernel size (3,3) blur induced low light and recovered data sample.

Furthermore, more quality-reduced anesthetic drug samples were obtained using a 5x5 kernel-sized induced low light condition, improved with Laplacian's algorithm, and tested with the various quality metrics. From the results recorded in Table 18, a PSNR score of 20.94 decibels between the original s1 data sample and the 5x5 kernel size-induced low light condition was produced, and a 23.21decibel PSNR score between the original s1 data sample and the recovered data sample, showing a substantial quality enhancement of 2.27-decibel PSNR, 0.06 FSI, 0.02 FSI, and 0.03 UIQ respectively. Also, the s2 data sample showed a notable quality gain as a PSNR score of 15.72 decibels between the original s2 sample and the 5x5 kernel size-induced low light condition and a 16.41-decibel PSNR score between the original s2 data sample and the recovered

data sample was recorded, showing a substantial quality gain of 0.69-decibel PSNR, 0.04 FSI, 0.02 FSI, and 0.06 UIQ respectively.

Table 18: Quality comparison of the original data samples, 5x5 kernel-size blur induced low-light and recovered data sample.

	Original Vs Median Blur (kernel Sizes (5,5))				**Original Vs Median Blur Recovered (kernel Sizes (5,5))**				**Change in Quality**			
Samples	PSNR	FSI	SSI	UIQ	PSNR	FSI	SSI	UIQ	ΔPSNR	ΔFSI	ΔSSI	ΔUIQ
s1	20.94	0.45	0.93	0.21	23.21	0.51	0.95	0.24	2.27	0.06	0.02	0.03
s2	15.72	0.44	0.89	0.12	16.41	0.48	0.91	0.18	0.69	0.04	0.02	0.06
s3	18.69	0.42	0.92	0.13	20.17	0.48	0.93	0.18	1.48	0.06	0.01	0.05
s4	19.17	0.1	0.92	0.07	20.79	0.34	0.93	0.11	1.62	0.24	0.01	0.04
s5	22.42	0.2	0.94	0.03	27.34	0.32	0.95	0.09	4.92	0.12	0.01	0.06
s6	19.69	0.2	0.93	0.14	21.19	0.47	0.95	0.2	1.5	0.27	0.02	0.06
s7	19.04	0.2	0.93	0.1	20.62	0.45	0.95	0.14	1.58	0.25	0.02	0.04
s8	18.82	0.32	0.93	0.11	20.21	0.35	0.94	0.12	1.39	0.03	0.01	0.01
s9	17.48	0.23	0.92	0.15	18.38	0.3	0.93	0.21	0.9	0.07	0.01	0.06
s10	14.94	0.52	0.89	0.21	15.41	0.57	0.92	0.29	0.47	0.05	0.03	0.08

Also, in the experiment, the s3 data sample showed a notable quality gain as a PSNR score of 18.69 decibels between the original s3 data sample and the 5x5 kernel-size induced low light condition was obtained and a 20.17-decibel PSNR score between the original s2 data sample and the recovered data sample, showing a substantial quality gain of 1.47-decibel PSNR, 0.05 FSI, 0.01 FSI, and 0.05 UIQ respectively. As shown in Table 18 and Figure 58, all the remaining low-light modeled data, enhanced and tested selected data samples achieved notable performance quality improvement using the quality estimation matrices for the introduced Laplacian object quality improvement algorithm. This implies that a 1.62-decibel PSNR, 0.24 FSI, 0.01 SSI, and 0.04 UIQ improvements were obtained between the low-light s4 drug data and the improved, 4.92 PSNR, 0.12 FSI, 0.01 SSI and 0.06 UIQ between the low-light s5 drug data and the enhanced, 1.5 PSNR, 0.27 FSI, 0.02 SSI and 0.06 UIQ between the low-light s6 drug data and the improved sample and fairly similar quality improvements on the remaining drug samples.

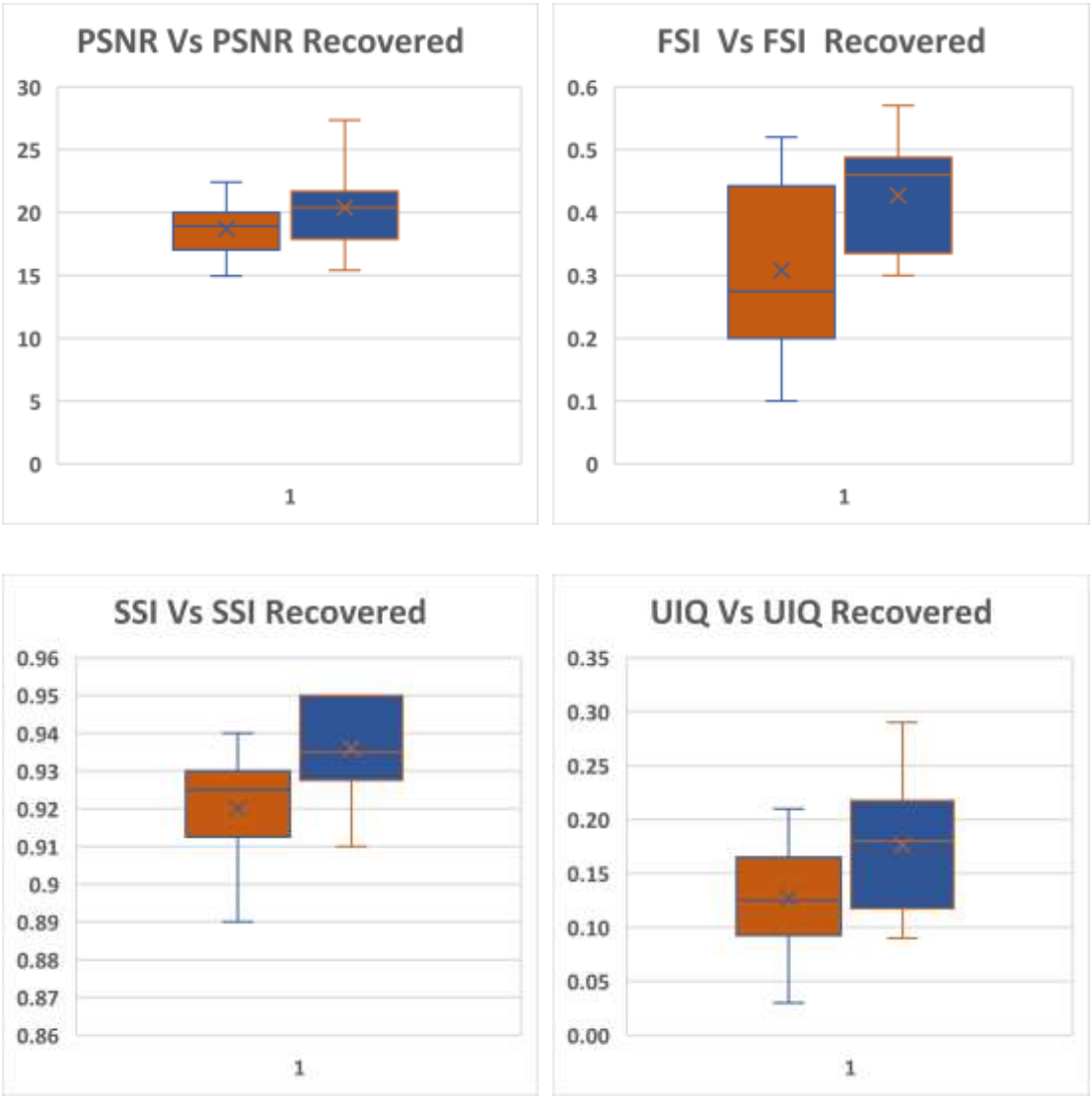

Figure 58: Quality metric between the original data samples, kernel size (5,5) blur-induced low-light and recovered data sample.

The final demonstrated low-quality anesthetic drug samples were performed using a 7x7 kernel-sized induced low light condition, enhanced with the Laplacian's algorithm, and tested with the various quality matrices. According to the results obtained and presented in Table 19, a PSNR score of 20.28 decibels between the original s1 data sample and the 7x7 kernel size-induced low-light condition was produced, and a 20.33-decibel PSNR score between the original s1 data sample and the recovered data sample, showing a quality enhancement of about 0.05-decibel PSNR, 0.02 FSI, 0.02 FSI, and 0.02 UIQ respectively. Also, the s2 data sample showed a negligible quality gain as a PSNR score of 16.07 decibels between the original s2 sample and the 7x7 kernel size-induced low-light condition and a 16.08-decibel PSNR score between the original s2 data sample and the recovered data sample was recorded, showing a small margin in

the quality gain of 0.01-decibel PSNR, 0.02 FSI, 0.01 FSI, and 0.02 UIQ respectively. The low-quality gain is a result of the high kernel-size induced low-light condition that produced very low-quality anesthetic drug label features.

Table 19: Quality comparison of the original data samples, 7x7 kernel-size blur induced low-light and recovered data sample.

	Original Vs Bilateral Blur (kernel Sizes (7,7))				Original Vs Bilateral Blur Recovered (kernel Sizes (7,7))				Change in Quality			
Samples	**PSNR**	**FSI**	**SSI**	**UIQ**	**PSNR**	**FSI**	**SSI**	**UIQ**	**ΔPSNR**	**ΔFSI**	**ΔSSI**	**ΔUIQ**
s1	20.28	0.57	0.97	0.48	20.33	0.59	0.99	0.5	0.05	0.02	0.02	0.02
s2	16.07	0.57	0.94	0.42	16.08	0.59	0.95	0.44	0.01	0.02	0.01	0.02
s3	20.03	0.59	0.97	0.45	20.07	0.61	0.98	0.47	0.04	0.02	0.01	0.02
s4	21.36	0.5	0.98	0.34	21.37	0.5	0.98	0.34	0.01	0	0	0
s5	31.79	0.55	0.99	0.27	31.82	0.55	0.99	0.21	0.03	0	0	-0.06
s6	20.43	0.57	0.98	0.47	20.46	0.57	0.98	0.46	0.03	0	0	-0.01
s7	20.22	0.57	0.98	0.43	20.23	0.59	0.99	0.45	0.01	0.02	0.01	0.02
s8	19.88	0.59	0.98	0.46	19.9	0.59	0.98	0.47	0.02	0	0	0.01
s9	17.68	0.59	0.97	0.43	17.71	0.6	0.98	0.45	0.03	0.01	0.01	0.02
s10	15.1	0.59	0.94	0.43	15.13	0.61	0.95	0.44	0.03	0.02	0.01	0.01

In continuation with the experiments, the s3 data sample showed a slight quality gain as a PSNR score of 20.03 decibels between the original s3 data sample and the 7x7 kernel-size induced low-light condition was obtained, and a 20.07-decibel PSNR score between the original s3 data sample and the recovered data sample, showing a little quality gain of 0.04-decibel PSNR, 0.02 FSI, 0.01 FSI, and 0.02 UIQ respectively. As shown in both Table 19 and Figure 59, all the tested selected data samples achieved slight performance quality improvement using the quality estimation matrices for the introduced Laplacian object improvement algorithm due to the high-level kernel size used in the low-light inducement process. Some other samples, like the s4, s5, s6, and s8, recorded no change in FSI and SSI metrics.

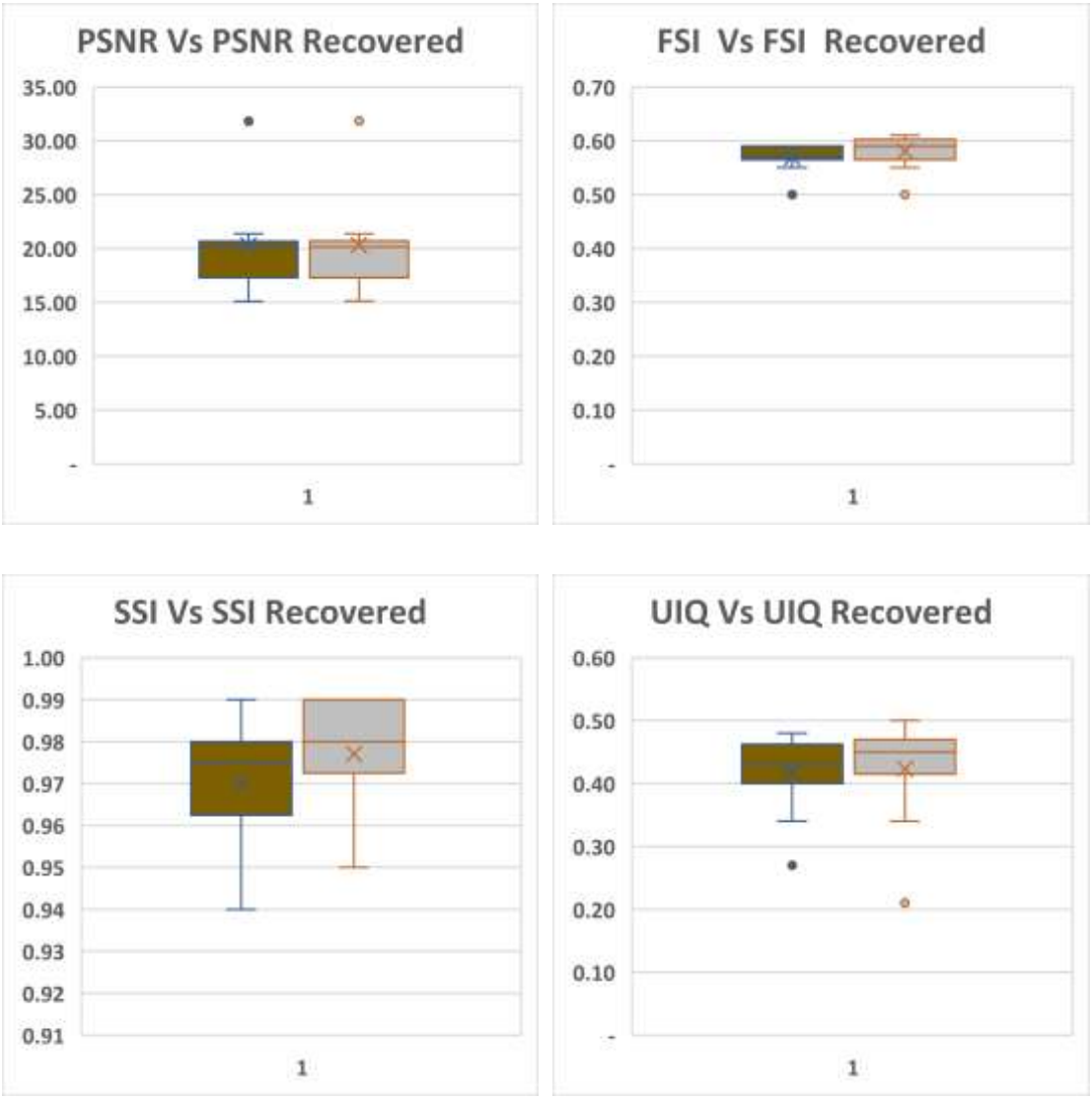

Figure 59: Quality metric between the original data samples, kernel size (7,7) blur induced low-light and recovered data sample.

In furtherance of the investigation in this chapter, the stained modeled drug samples, the low-light samples, the enhanced samples, and the actual samples were utilized to test the proposed anesthetic drugs identification framework. The observation of the experiments conducted using one of the samples (s1) are shown in Table 20. The results in the table are split into sections, i.e., the s1 stain-modeled sample Vs. other samples, the s1 enhanced stain-modeled sample Vs. other samples, the s1 low-light modeled sample with a 3x3 filter Vs. others, the s1 improved low-light modeled sample with a 3x3 filter Vs. others, the s1 low-light modeled sample with a 5x5 filter Vs. others, the improved s1 low-light modeled sample with a 5x5 filter Vs. others, the s1 low-light modeled sample with a 7x7 filter Vs. others and the improved s1 low-light modeled sample with a 7x7 filter Vs. others.

Table 20: Comparative results obtained using the proposed framework with the s1 data sample, the modelled stained sample, low-light and enhanced samples.

s1_noisy Vs others					**s1_noisy enhanced Vs others**				
Drug Name	Edit Distance	TSR Scores	Lev Scores	Jacc Scores	Drug Name	Edit Distance	TSR Scores	Lev Scores	Jacc Scores
s1	60	0.98	0.94	1.00	s1	141	0.97	0.86	1.00
s1_noisy	**0**	**1.0**	**1.00**	**1.00**	s1_noisy	86	0.98	0.92	1.00
s1_noisy_en	86	0.98	0.92	1.00	**s1_noisy_en**	**0**	**1.0**	**1.00**	**1.00**
s1_3x3	85	0.99	0.92	1.00	s1_3x3	15	0.97	0.99	1.00
s1_3x3_en	86	0.98	0.92	1.00	s1_3x3_en	0	1.0	1.00	1.00
s1_5x5	93	0.97	0.91	0.97	s1_5x5	19	0.97	0.98	0.97
s1_5x5_en	482	0.35	0.29	0.64	s1_5x5_en	476	0.34	0.29	0.64
s1_7x7	133	0.95	0.86	0.97	s1_7x7	63	0.94	0.94	0.97
s1_7x7_en	122	1.0	0.88	1.00	s1_7x7_en	51	0.99	0.95	1.00
s1_3x3 Vs others					s1_3x3_enhanced Vs Vs others				
s1	132	0.98	0.87	1.00	s1_3x3_enhanced	141	0.97	0.86	1.00
s1_noisy	85	0.99	0.92	1.00	s1	86	0.98	0.92	1.00
s1_noisy_en	15	0.97	0.99	1.00	s1_noisy	0	1.0	1.00	1.00
s1_3x3	**0**	**1.0**	**1.00**	**1.00**	s1_noisy_en	15	0.97	0.99	1.00
s1_3x3_en	15	0.97	0.99	1.00	s1_3x3	19	0.97	0.98	0.97
s1_5x5	24	0.97	0.98	0.97	**s1_3x3_en**	**0**	**1.0**	**1.0**	**1.0**
s1_5x5_en	483	0.35	0.28	0.64	s1_5x5	476	0.34	0.29	0.64
s1_7x7	68	0.95	0.93	0.97	s1_5x5_en	63	0.94	0.94	0.97
s1_7x7_en	54	0.98	0.95	1.00	s1_7x7	51	0.99	0.95	1.00
s1_5x5 Vs others					s1_5x5_enhanced Vs others				
s1	145	0.96	0.86	0.97	s1	499	0.35	0.29	0.64
s1_noisy	93	0.97	0.91	0.97	s1_noisy	482	0.35	0.29	0.64
s1_noisy_en	19	0.97	0.98	0.97	s1_noisy_en	476	0.34	0.29	0.64
s1_3x3	24	0.97	0.98	0.97	s1_3x3	483	0.35	0.28	0.64
s1_3x3_en	19	0.97	0.98	0.97	s1_3x3_en	476	0.34	0.29	0.64
s1_5x5	**0**	**1.0**	**1.00**	**1.00**	s1_5x5	467	0.35	0.29	0.66
s1_5x5_en	467	0.35	0.29	0.66	**s1_5x5_en**	**0**	**1.0**	**1.00**	**1.00**
s1_7x7	53	0.95	0.94	1.00	s1_7x7	427	0.37	0.30	0.66
s1_7x7_en	59	0.97	0.94	0.97	s1_7x7_en	482	0.35	0.28	0.64
s1_7x7 Vs others					s1_7x7_enhanced Vs others				
s1	178	0.93	0.81	0.97	s1	96	0.97	0.91	1.00
s1_noisy	133	0.95	0.86	0.97	s1_noisy	122	1.0	0.88	1.00
s1_noisy_en	63	0.94	0.94	0.97	s1_noisy_en	51	0.99	0.95	1.00
s1_3x3	68	0.95	0.93	0.97	s1_3x3	54	0.98	0.95	1.00
s1_3x3_en	63	0.94	0.94	0.97	s1_3x3_en	51	0.99	0.95	1.00
s1_5x5	53	0.95	0.94	1.00	s1_5x5	59	0.97	0.94	0.97
s1_5x5_en	427	0.37	0.30	0.66	s1_5x5_en	482	0.35	0.28	0.64
s1_7x7	**0**	**1.0**	**1.00**	**1.00**	s1_7x7	101	0.95	0.89	0.97
s1_7x7_en	101	0.95	0.89	0.97	**s1_7x7_en**	**0**	**1.0**	**1.00**	**1.00**

The rows in the table correspond to the original drug sample, the variant-modeled stained and low-light samples, and the s1-enhanced samples. The columns show the various confidence scores obtained from the experiments with the aforementioned

samples. The proposed anesthetic drugs identification framework showed a remarkable performance in handling both the normal drug samples, the stained samples, and the low-light samples, as evidenced in the results tabulated in Table 20. The framework returned an edit distance of zero for each of the samples, signifying that it could correctly match the various drug samples in the various processing conditions modeled. Recall that the edit distance is the number of operations required to correctly match a given pair of string samples. The lower the Edith distance, the higher the similar strings being matched. Also, the TSR, Lev, and Jacc scores highlighted in the table show that the framework accurately matched the various sample with 100% confidence scores.

Furthermore, as highlighted in the table, the framework returned remarkable results using the other matching algorithms. This proves that with the integrated Laplacian object quality improvement strategy, the proposed anesthetic drug identification framework can process and identify the various drugs used in the operating rooms in different operating conditions. Finally, the results obtained from the other samples selected for the investigation can be found in Appendix E; the proposed framework yielded tremendous performance in all the drug samples signifying the high processing diversity of the framework.

6.7 Chapter Summary

In this chapter, the diverse operating conditions that can impact the performance of the proposed anesthetic drug identification framework were modeled using the artificial digital object noise inducement method. The modeling depicts the stained drug samples and low-light processing conditions induced by the digital image blurring kernels. In the study, different object blurring kernel filter sizes such as 3x3, 5x5, and 7x7 filters were deployed to model the different levels of low-light operating situations and their impacts measured using the various object quality estimation algorithm. Laplacian digital image enhancement algorithm was deployed to enhance the low-quality drug containers to improve the modeled stained and low-light drug conditions. The adoption of the Laplacian algorithm significantly improved the quality of the drug samples and enhanced the confidence of the proposed framework in different conditions order than the typically controlled processing environment. The rapid

processing and enhancement of bad-quality digital images of the Laplacian theory motivated its adoption in this study. There were significant quality improvements in the peak-signal-to-noise ratio between the modeled stained and low-light drug samples and the enhanced drug samples. The other quality measures adopted in this chapter also validated the gains recorded in the drug container improvement tasks.

Chapter 7 Conclusion

7.1 Thesis Summary

This thesis described the introduced computer vision and artificial intelligence-driven framework that identify the medications used in the operating theaters to eliminate the errors occasionally occurring during drug selection and administration in the operating rooms. Chapter 1 introduced the synopsis of the study, including a brief background of the anesthetic agents, the structure of ampules and vials, the rationale and significance of the study, the research objective, the contributions of the research, and the thesis organization.

Chapter 2 x-rayed the existing efforts in the minimization or complete elimination of the anesthetic drugs selection and administration errors in operating theaters, a review of relevant topics of interest such as scene text detection and recognition, optical character recognition, and comparative performance study of the OCR engines for the recognition of the characters inscribed on the anesthetic medications. Chapter 3 examined the capability of the various conventional object feature detection, extraction, and matching for anesthetics medication identification. In this chapter, different prominent algorithms were investigated and deployed to identify anesthetic drugs. Their performance was recorded, analyzed, and compared.

Chapter 4 dealt with the research method adopted in the study. The research problem and questions, methodology and research process, hardware requirements, data collection methods, and results evaluation process were presented in this chapter. Chapter 5, on the other hand, presented the theoretical framework and the research findings. In this chapter, one of the major novel contributions of the work was established in detail. Also, the data used in the study was concisely described, and the experimental setup, processes, results, and analysis were presented in this chapter. Finally, Chapter 6 examined the various ways the problems that could occur during the real-time use of the proposed framework could be mitigated or eliminated completely. The problems were modeled, investigated, and solutions proffered in this chapter.

7.2 Future Research Direction

One potential future research direction for using computer vision to identify and recognize anesthetic drugs in operating theatres is developing an efficient and portable OCR engine that can accurately detect and recognize the complex texts inscribed on the various anesthetic drugs. This engine could then be used to substitute the current engine used in the proposed framework and make the framework more cost-effective.

Also, the structures and labeling of the containers housing the anesthetic drugs play a vital role in the ease or complexity of identifying the drugs using computer vision methods. This was notable during the study because the medications on flat containers or with distinct labels were easier to identify and process than those housed in round containers with complex labels. An investigation into a synergy between drug manufacturers and technology experts will significantly assist in the further improvement and performance of the proposed framework.

Another potential future research direction in this area could be to explore other techniques, such as rule-based systems or expert systems, for identifying anesthetic drugs based on their visual appearance. These systems rely on pre-defined rules or expert knowledge to make decisions rather than learning from data.

Finally, it may also be helpful to investigate the use of other modalities, such as 3D imaging or spectroscopy, to aid the real-time anesthetic drug image acquisitions; to improve the performance and robustness of the drug identification framework. Combining the information from these different modalities may achieve even higher levels of performance and reliability in identifying anesthetic drugs in operating theaters.

7.3 Concluding Remarks

In conclusion, this work was inspired by the efforts to solve the problem of anesthetic drug selection and administration errors often encountered in operating theatres.

In the study, we have been able to establish that the use of computer vision to classify and identify anesthetic drugs in operating theatres has the potential to improve

patient safety and efficiency in the operating room. By accurately identifying the specific drugs being used, healthcare professionals can ensure that the correct medication and dosage are being administered to patients and that potential drug errors are avoided. The novel results obtained in the various experiments run during the study provide hope for completely eliminating the errors encountered during drug selection and administration ecosystem in the operating rooms.

Overall, the outcomes of this study demonstrate the effectiveness of using computer vision for the classification and identification of anesthetic drugs in operating theaters. With further development, refinement, and integration, this technology has the potential to become a valuable tool for healthcare professionals in the operating rooms. Finally, the use of computer vision for the classification and identification of anesthetic drugs has the potential to improve patient safety and efficiency in the operating room. It is a promising area of research that warrants further exploration and development.

References

Abi-Aad, K. R., & Derian, A. (2017). Hydromorphone.

Afroge, S., Ahmed, B., & Mahmud, F. (2016). Optical character recognition using back propagation neural network. 2016 2nd International Conference on Electrical, Computer & Telecommunication Engineering (ICECTE),

Aiello, M., Monz, C., Todoran, L., & Worring, M. (2002). Document understanding for a broad class of documents. *International Journal on Document Analysis and Recognition, 5*(1), 1-16.

Albaugh, P. A., Marshall, L., Gregory, J., White, G., Hutchison, A., Ross, P. C., Gallagher, D. W., Tallman, J. F., Crago, M., & Cassella, J. V. (2002). Synthesis and Biological Evaluation of 7, 8, 9, 10-Tetrahydroimidazo [1, 2-c] pyrido [3, 4-e] pyrimdin-5 (6H)-ones as Functionally Selective Ligands of the Benzodiazepine Receptor Site on the GABAA Receptor. *Journal of medicinal chemistry, 45*(23), 5043-5051.

Amit, Y., Geman, D., & Fan, X. (2004). A coarse-to-fine strategy for multiclass shape detection. *IEEE transactions on pattern analysis and machine intelligence, 26*(12), 1606-1621.

Andoni, A., Krauthgamer, R., & Onak, K. (2010). Polylogarithmic approximation for edit distance and the asymmetric query complexity. 2010 IEEE 51st Annual Symposium on Foundations of Computer Science,

Antoni, M., & Ammad, N. (2011). Practical formal validation method of interlocking systems. *Practical formal validation method for interlocking systems*, 1-15.

Arazy, O., Kumar, N., & Shapira, B. (2010). A theory-driven design framework for social recommender systems. *Journal of the Association for Information Systems, 11*(9), 2.

Armenian, P., Vo, K. T., Barr-Walker, J., & Lynch, K. L. (2018). Fentanyl, fentanyl analogs and novel synthetic opioids: a comprehensive review. *Neuropharmacology, 134*, 121-132.

Astin, J., Steynberg, S., & Cook, T. (2015). Time for mandatory colour coding of drug ampoules and packaging–yet again. *Anaesthesia, 70*(4), 502-502.

Athavale, A., Athavale, T., & Roberts, D. M. (2020). Antiemetic drugs: what to prescribe and when. *Australian Prescriber, 43*(2), 49.

Backurs, A., & Indyk, P. (2015). Edit distance cannot be computed in strongly subquadratic time (unless SETH is false). Proceedings of the forty-seventh annual ACM symposium on Theory of computing,

Baek, J., Kim, G., Lee, J., Park, S., Han, D., Yun, S., Oh, S. J., & Lee, H. (2019). What is wrong with scene text recognition model comparisons? dataset and model analysis. Proceedings of the IEEE International Conference on Computer Vision,

Baek, Y., Lee, B., Han, D., Yun, S., & Lee, H. (2019). Character region awareness for text detection. Proceedings of the IEEE Conference on Computer Vision and Pattern Recognition,

Bakurov, I., Buzzelli, M., Schettini, R., Castelli, M., & Vanneschi, L. (2022). Structural similarity index (SSIM) revisited: A data-driven approach. *Expert Systems with Applications, 189*, 116087.

Baldwin, D. S., Aitchison, K., Bateson, A., Curran, H. V., Davies, S., Leonard, B., Nutt, D. J., Stephens, D. N., & Wilson, S. (2013). Benzodiazepines: risks and benefits. A reconsideration. *Journal of psychopharmacology, 27*(11), 967-971.

Barak, M., Yoav, L., & Abu el-Naaj, I. (2015). Hypotensive anesthesia versus normotensive anesthesia during major maxillofacial surgery: a review of the literature. *The Scientific World Journal, 2015*.

Barnett, V., Twycross, R., Mihalyo, M., & Wilcock, A. (2014). Opioid antagonists. *Journal of pain and symptom management, 47*(2), 341-352.

Basit, H., & Kahwaji, C. I. (2021). Clonazepam. In *StatPearls [Internet]*. StatPearls Publishing.

Battershill, A. J., & Keating, G. M. (2006). Remifentanil. *Drugs, 66*(3), 365-385.

Bay, H., Tuytelaars, T., & Van Gool, L. (2006). Surf: Speeded up robust features. European conference on computer vision,

Beers, R., & Camporesi, E. (2004). Remifentanil update. *CNS drugs, 18*(15), 1085-1104.

Bhairannawar, S. S. (2018). Efficient medical image enhancement technique using transform HSV space and adaptive histogram equalization. In *Soft Computing Based Medical Image Analysis* (pp. 51-60). Elsevier.

Bhardwaj, R., & Vatta, S. (2013). Implementation of ID3 algorithm. *International Journal of Advanced Research in Computer Science and Software Engineering, 3*(6).

Bhatia, A. (2007). *Hessian-Laplace feature detector and Haar descriptor for image matching* University of Ottawa (Canada)].

Bille, P., Gørtz, I. L., Vildhøj, H. W., & Wind, D. K. (2012). String matching with variable length gaps. *Theoretical Computer Science, 443*, 25-34.

Bissacco, A., Cummins, M., Netzer, Y., & Neven, H. (2013). Photoocr: Reading text in uncontrolled conditions. Proceedings of the IEEE International Conference on Computer Vision,

Bock, M., Klippel, K., Nitsche, B., Bach, A., Martin, E., & Motsch, J. (2000). Rocuronium potency and recovery characteristics during steady-state desflurane, sevoflurane, isoflurane or propofol anaesthesia. *British journal of anaesthesia, 84*(1), 43-47.

Borisyuk, F., Gordo, A., & Sivakumar, V. (2018). Rosetta: Large scale system for text detection and recognition in images. Proceedings of the 24th ACM SIGKDD International Conference on Knowledge Discovery & Data Mining,

Bosch, A., Zisserman, A., & Munoz, X. (2007). Image classification using random forests and ferns. 2007 IEEE 11th international conference on computer vision,

Bösenberg, A. T. (2007). Pediatric anesthesia in developing countries. *Current Opinion in Anesthesiology, 20*(3), 204-210.

Bowen, G. A. (2006). Grounded theory and sensitizing concepts. *International journal of qualitative methods, 5*(3), 12-23.

Braitberg, G. (2019). Drugs and antidotes in acute intoxication. In *Critical Care Nephrology* (pp. 574-588. e573). Elsevier.

Breuel, T. M. (2001). Robust least-square-baseline finding using a branch and bound algorithm. Document Recognition and Retrieval IX,

Bunke, H., & Wang, P. S.-p. (1997). *Handbook of character recognition and document image analysis*. World scientific.

Burghardt, T., Damen, D., Mayol-Cuevas, W., & Mirmehdi, M. (2015). Correspondence, matching and recognition. *International journal of computer vision, 113*(3), 161-162.

Busta, M., Neumann, L., & Matas, J. (2017). Deep textspotter: An end-to-end trainable scene text localization and recognition framework. Proceedings of the IEEE International Conference on Computer Vision,

Butterworth, J. F., & Lahaye, L. (2019). Clinical use of local anesthetics in anesthesia. *UpToDate. Available online: https://www. uptodate. com/contents/clinical-use-of-local-anesthetics-in-anesthesia (accessed on 29 November 2018)*.

Cadavid-Puentes, A., Bermúdez-Guerrero, F. J., Giraldo-Salazar, O., Muñoz-Zapata, F., Otálvaro-Henao, J., Ruíz-Sierra, J., Alvarado-Ramírez, J., Hernández-Herrera, G., & Aguirre-Acevedo, D. C. (2017). Comparison of the effectiveness of fentanyl versus morphine for severe postoperative pain management. A randomized, double blind, clinical trial. *Colombian Journal of Anesthesiology, 45*(2), 100-107.

Caillat, C. (2017). *Prémédication sédative per os: état actuel des connaissances, enquête de pratique en Lorraine auprès des chirurgiens-dentistes* Université de Lorraine].

Çakırtekin, V., Yıldırım, A., Bakan, N., Çelebi, N., & Bozkurt, Ö. (2015). Comparison of the effects of thiopental sodium and propofol on haemodynamics, awareness and newborns during caesarean section under general anaesthesia. *Turkish journal of anaesthesiology and reanimation, 43*(2), 106.

Catterall, W. A., & Mackie, K. (2011). Local anesthetics. *Goodman & Gilman's the pharmacological basis of therapeutics, 12th ed McGraw-Hill, Medical Publishing Division, New York, NY*, 565-582.

Cavnar, W. B., & Trenkle, J. M. (1994). N-gram-based text categorization. Proceedings of SDAIR-94, 3rd annual symposium on document analysis and information retrieval,

Cescon, D. W., & Etchells, E. (2008). Barcoded medication administration: a last line of defense. *JAMA, 299*(18), 2200-2202.

Champod, C. (2015). Overview and meaning of identification/individualization. In *Professional Issues in Forensic Science* (pp. 95-103). Academic Press Oxford/San Diego, CA, USA.

Chaudhuri, A., Mandaviya, K., Badelia, P., & Ghosh, S. K. (2017). Optical character recognition systems. In *Optical Character Recognition Systems for Different Languages with Soft Computing* (pp. 9-41). Springer.

Chen, B.-Y. (2012). An explicit formula of Hessian determinants of composite functions and its applications. *Kragujevac Journal of Mathematics, 36*(1), 27-39.

Chen, D. (2003). *Text detection and recognition in images and video sequences*.

Chen, H. (2012). String Metrics and Word Similarity applied to Information Retrieval. *University of Eastern Finland*.

Chen, H., Tsai, S. S., Schroth, G., Chen, D. M., Grzeszczuk, R., & Girod, B. (2011). Robust text detection in natural images with edge-enhanced maximally stable extremal regions. 2011 18th IEEE International Conference on Image Processing,

Chen, J., Shan, S., He, C., Zhao, G., Pietikäinen, M., Chen, X., & Gao, W. (2009). WLD: A robust local image descriptor. *IEEE transactions on pattern analysis and machine intelligence, 32*(9), 1705-1720.

Chen, L., Rottensteiner, F., & Heipke, C. (2021). Feature detection and description for image matching: from hand-crafted design to deep learning. *Geo-spatial Information Science, 24*(1), 58-74.

Chen, X., & Yuille, A. L. (2004). Detecting and reading text in natural scenes. Proceedings of the 2004 IEEE Computer Society Conference on Computer Vision and Pattern Recognition, 2004. CVPR 2004.,

Cheng, Z., Bai, F., Xu, Y., Zheng, G., Pu, S., & Zhou, S. (2017). Focusing attention: Towards accurate text recognition in natural images. Proceedings of the IEEE international conference on computer vision,

Chih-Pei, H., & Chang, Y.-Y. (2017). John W. Creswell, research design: Qualitative, quantitative, and mixed methods approaches. *Journal of Social and Administrative Sciences, 4*(2), 205-207.

Cho, Y., Kim, D., Saeed, S., Kakli, M. U., Jung, S.-H., Seo, J., & Park, U. (2020). Keypoint detection using higher order Laplacian of Gaussian. *IEEE Access, 8*, 10416-10425.

Chung, J. Y., Cho, J. Y., Yu, K. S., Kim, J. R., Lim, K., Sohn, D. R., Shin, S. G., & Jang, I. J. (2008). Pharmacokinetic and pharmacodynamic interaction of lorazepam and valproic acid in relation to UGT2B7 genetic polymorphism in healthy subjects. *Clinical pharmacology & therapeutics, 83*(4), 595-600.

Cinti, A., Bianchi, F. M., Martino, A., & Rizzi, A. (2020). A novel algorithm for online inexact string matching and its FPGA implementation. *Cognitive Computation, 12*(2), 369-387.

Cloos, J.-M., & Ferreira, V. (2009). Current use of benzodiazepines in anxiety disorders. *Current opinion in psychiatry, 22*(1), 90-95.

Cook, D., & Simons, D. J. (2021). Neuromuscular blockade. In *StatPearls [Internet]*. StatPearls Publishing.

Corbin, J., & Strauss, A. (2006). Grounded Theory Research: Procedures, Canons and Evaluative.

Cornett, E. M., Novitch, M. B., Brunk, A. J., Davidson, K. S., Menard, B. L., Urman, R. D., & Kaye, A. D. (2018). New benzodiazepines for sedation. *Best Practice & Research Clinical Anaesthesiology, 32*(2), 149-164.

Das, G. N., Sharma, P., & Maani, C. V. (2021). Pancuronium. *StatPearls [Internet]*.

Davies, E. R. (2012). *Computer and machine vision: theory, algorithms, practicalities*. Academic Press.

De Campos, T. E., Babu, B. R., & Varma, M. (2009). Character recognition in natural images. *VISAPP (2), 7*.

Degoute, C.-S. (2007). Controlled hypotension: a guide to drug choice. *Drugs, 67*, 1053-1076.

Dekker, S. (2012). *Just culture: Balancing safety and accountability*. Ashgate Publishing, Ltd.

Derpanis, K. G. (2004). The harris corner detector. *York University, 2*.

Dey, I. (2004). Grounded theory. *Qualitative research practice*, 80-93.

Dhaliwal, J. S., Rosani, A., & Saadabadi, A. (2020). Diazepam. *StatPearls [Internet]*.

Dhaliwal, J. S., Rosani, A., & Saadabadi, A. (2021). Diazepam. In *StatPearls [Internet]*. StatPearls Publishing.

Dhawan, I., Tewari, A., Sehgal, S., & Sinha, A. C. (2017). Medication errors in anesthesia: unacceptable or unavoidable? *Revista Brasileira de Anestesiologia, 67*, 184-192.

Dollár, P., Appel, R., Belongie, S., & Perona, P. (2014). Fast feature pyramids for object detection. *IEEE transactions on pattern analysis and machine intelligence, 36*(8), 1532-1545.

Dong, C., Zhu, X., Deng, Y., Loy, C. C., & Qiao, Y. (2015). Boosting optical character recognition: A super-resolution approach. *arXiv preprint arXiv:1506.02211*.

Drobac, S., & Lindén, K. (2020). Optical character recognition with neural networks and post-correction with finite state methods. *International Journal on Document Analysis and Recognition (IJDAR), 23*(4), 279-295.

Du, Y., Li, C., Guo, R., Cui, C., Liu, W., Zhou, J., Lu, B., Yang, Y., Liu, Q., & Hu, X. (2021). PP-OCRv2: Bag of Tricks for Ultra Lightweight OCR System. *arXiv preprint arXiv:2109.03144*.

Du, Y., Li, C., Guo, R., Yin, X., Liu, W., Zhou, J., Bai, Y., Yu, Z., Yang, Y., & Dang, Q. (2020). PP-OCR: A Practical Ultra Lightweight OCR System. *arXiv preprint arXiv:2009.09941*.

Dutta, S., Sankaran, N., Sankar, K. P., & Jawahar, C. (2012). Robust recognition of degraded documents using character n-grams. 2012 10th IAPR International Workshop on Document Analysis Systems,

Easterbrook, S., Lutz, R., Covington, R., Kelly, J., Ampo, Y., & Hamilton, D. (1998). Experiences using lightweight formal methods for requirements modeling. *IEEE Transactions on Software Engineering, 24*(1), 4-14.

Eberle, T. S. (2014). Phenomenology as a research method. *The SAGE handbook of qualitative data analysis*, 184-202.

Eger, E. I. (2004). Characteristics of anesthetic agents used for induction and maintenance of general anesthesia. *American Journal of Health-System Pharmacy, 61*(suppl_4), S3-S10.

Epshtein, B., Ofek, E., & Wexler, Y. (2010). Detecting text in natural scenes with stroke width transform. 2010 IEEE Computer Society Conference on Computer Vision and Pattern Recognition,

Faro, S., & Lecroq, T. (2013). The exact online string matching problem: A review of the most recent results. *ACM Computing Surveys (CSUR), 45*(2), 1-42.

Fassoulaki, A., Theodoraki, K., & Melemeni, A. (2010). Pharmacology of sedation agents and reversal agents. *Digestion, 82*(2), 80-83.

Ferry, N., & Dhanjal, S. (2018). Opioid Anesthesia.

Ferry, N., & Dhanjal, S. (2021). Opioid Anesthesia. *StatPearls [Internet]*.

Filiatrault, P., & Hyland, S. (2009). Does colour-coded labelling reduce the risk of medication errors? *The Canadian Journal of Hospital Pharmacy, 62*(2).

Flamer, D., & Peng, P. W. (2011). Intravenous regional anesthesia: a review of common local anesthetic options and the use of opioids and muscle relaxants as adjuncts. *Local and regional anesthesia, 4*, 57.

Fleuret, F., & Geman, D. (2001). Coarse-to-fine face detection. *International journal of computer vision, 41*(1), 85-107.

Folino, T. B., Muco, E., Safadi, A. O., & Parks, L. J. (2022). Propofol. In *StatPearls [Internet]*. StatPearls Publishing.

Fonseca, J. M., Rodrigues, N. M., Mora, A. D., & Ribeiro, R. A. (2011). Optical character recognition using automatically generated Fuzzy classifiers. 2011 Eighth International Conference on Fuzzy Systems and Knowledge Discovery (FSKD),

Forman, S. A., & Warner, D. S. (2011). Clinical and molecular pharmacology of etomidate. *The Journal of the American Society of Anesthesiologists, 114*(3), 695-707.

Fu, Z., Jin, Z., Qi, G.-J., Shen, C., Jiang, R., Chen, Y., & Hua, X.-S. (2018). Previewer for multi-scale object detector. Proceedings of the 26th ACM international conference on Multimedia,

Fuchs-Buder, T., Meistelman, C., & Raft, J. (2013). Sugammadex: clinical development and practical use. *Korean journal of anesthesiology, 65*(6), 495.

Fujii, Y., Driesen, K., Baccash, J., Hurst, A., & Popat, A. C. (2017). Sequence-to-label script identification for multilingual ocr. 2017 14th IAPR International Conference on Document Analysis and Recognition (ICDAR),

Fujii, Y., Genzel, D., Popat, A. C., & Teunen, R. (2015). Label transition and selection pruning and automatic decoding parameter optimization for time-synchronous viterbi decoding. 2015 13th International Conference on Document Analysis and Recognition (ICDAR),

Gales, A., & Maxwell, S. (2018). Ketamine: Recent evidence and current uses. *ATOTW, 381*, 1-7.

Garnock-Jones, K. P., & McKeage, K. (2010). Methylnaltrexone. *Drugs, 70*(7), 919-928.

Ghiasi, N., Bhansali, R. K., & Marwaha, R. (2021). Lorazepam. In *StatPearls [Internet]*. StatPearls Publishing.

Ghosh, K., Sarkar, S., & Bhaumik, K. (2007). Understanding image structure from a new multi-scale representation of higher order derivative filters. *Image and vision computing, 25*(8), 1228-1238.

Gordon, P., Llewellyn, R., & James, M. (2006). Drug administration errors by South African anaesthetists-a survey. *South African Medical Journal, 96*(7), 630-632.

Graves, A., Fernández, S., Gomez, F., & Schmidhuber, J. (2006). Connectionist temporal classification: labelling unsegmented sequence data with recurrent neural networks. Proceedings of the 23rd international conference on Machine learning,

Gray, J., & Ray, S. (2014). Anticholinergics.

Gregor, S., & Jones, D. (2007). The anatomy of a design theory.

Grieggs, S., Shen, B., Li, P., Short, C., Ma, J., McKenny, M., Wauke, M., Price, B., & Scheirer, W. (2019). Measuring Human Perception to Improve Handwritten Document Transcription. *arXiv preprint arXiv:1904.03734*.

Grissinger, M. (2012). Color-coded syringes for anesthesia drugs—use with care. *Pharmacy and Therapeutics, 37*(4), 199.

Gropper, M. A., Miller, R. D., Eriksson, L. I., Fleisher, L. A., Wiener-Kronish, J. P., Cohen, N. H., & Leslie, K. (2019). *Miller's anesthesia, 2-volume set E-book*. Elsevier Health Sciences.

Gündüz, M., Sakalli, Ş., Güneş, Y., Kesiktaş, E., Özcengiz, D., & Işik, G. (2011). Comparison of effects of ketamine, ketamine-dexmedetomidine and ketamine-midazolam on dressing changes of burn patients. *Journal of anaesthesiology, clinical pharmacology, 27*(2), 220.

Guo, H., Qin, X., Liu, J., Han, J., Liu, J., & Ding, E. (2019). Eaten: Entity-aware attention for single shot visual text extraction. 2019 International Conference on Document Analysis and Recognition (ICDAR),

Gupta, S., Kumar, M., & Garg, A. (2019). Improved object recognition results using SIFT and ORB feature detector. *Multimedia tools and applications, 78*, 34157-34171.

Hakak, S. I., Kamsin, A., Shivakumara, P., Gilkar, G. A., Khan, W. Z., & Imran, M. (2019). Exact string matching algorithms: Survey, issues, and future research directions. *IEEE Access, 7*, 69614-69637.

Halber, M., & Funkhouser, T. (2017). Fine-to-coarse global registration of rgb-d scans. Proceedings of the IEEE Conference on Computer Vision and Pattern Recognition,

Haldar, R., & Mukhopadhyay, D. (2011). Levenshtein distance technique in dictionary lookup methods: An improved approach. *arXiv preprint arXiv:1101.1232*.

Hanif, S. M., & Prevost, L. (2009). Text detection and localization in complex scene images using constrained adaboost algorithm. 2009 10th international conference on document analysis and recognition,

Harris, C., & Stephens, M. (1988). A combined corner and edge detector. Alvey vision conference,

[Record #700 is using a reference type undefined in this output style.]

Hassink, J. J. M., Jansen, M. M. P. M., & Helmons, P. J. (2012). Effects of bar code-assisted medication administration (BCMA) on frequency, type and severity of medication administration errors: a review of the literature. *European Journal of Hospital Pharmacy: Science and Practice, 19*(5), 489-494.

He, K., Zhang, X., Ren, S., & Sun, J. (2016). Deep residual learning for image recognition. Proceedings of the IEEE conference on computer vision and pattern recognition,

He, P., Huang, W., Qiao, Y., Loy, C. C., & Tang, X. (2015). Reading scene text in deep convolutional sequences. *arXiv preprint arXiv:1506.04395*.

He, T., Tian, Z., Huang, W., Shen, C., Qiao, Y., & Sun, C. (2018). An end-to-end textspotter with explicit alignment and attention. Proceedings of the IEEE Conference on Computer Vision and Pattern Recognition,

Health, W. D. (2016). *Clonazepam – Palliative Care (Adults)*. https://www.waitematadhb.govt.nz/assets/Documents/health-professionals/palliative-care/Clonazepam-PalliativeCareJun16.pdf

Hevner, A., & Chatterjee, S. (2010). Design science research in information systems. In *Design research in information systems* (pp. 9-22). Springer.

Hill, R., Santhakumar, R., Dewey, W., Kelly, E., & Henderson, G. (2020). Fentanyl depression of respiration: comparison with heroin and morphine. *British journal of pharmacology, 177*(2), 254-265.

Hochreiter, S., & Schmidhuber, J. (1997). Long short-term memory. *Neural computation, 9*(8), 1735-1780.

Hong, T., Kim, D., Ji, M., Hwang, W., Nam, D., & Park, S. (2020). BROS: A Pre-trained Language Model for Understanding Texts in Document.

Hottinger, D. G., Beebe, D. S., Kozhimannil, T., Prielipp, R. C., & Belani, K. G. (2014). Sodium nitroprusside in 2014: A clinical concepts review. *Journal of anaesthesiology, clinical pharmacology, 30*(4), 462.

Howard, P., Twycross, R., Shuster, J., Mihalyo, M., & Wilcock, A. (2014). Benzodiazepines. *Journal of pain and symptom management, 47*(5), 955-964.

Hu, L., Nooshabadi, S., & Ahmadi, M. (2016). Parallel randomized KD-tree forest on GPU cluster for image descriptor matching. 2016 IEEE International Symposium on Circuits and Systems (ISCAS),

Hua, Y., Huang, Z., Guo, J., & Qiu, W. (2020). Attention-Based Graph Neural Network with Global Context Awareness for Document Understanding. China National Conference on Chinese Computational Linguistics,

Huang, W., Qiao, Y., & Tang, X. (2014). Robust scene text detection with convolution neural network induced mser trees. European conference on computer vision,

Hug Jr, C. C. (1992). Opioids: Clinical use as anesthetic agents. *Journal of pain and symptom management, 7*(6), 350-355.

Hunter, J. (2020). Reversal of neuromuscular block. *BJA education, 20*(8), 259.

Hwang, W., Yim, J., Park, S., Yang, S., & Seo, M. (2020). Spatial Dependency Parsing for Semi-Structured Document Information Extraction. *arXiv preprint arXiv:2005.00642*.

Islam, N., Islam, Z., & Noor, N. (2017). A survey on optical character recognition system. *arXiv preprint arXiv:1710.05703*.

Iwamura, M., Morimoto, N., Tainaka, K., Bazazian, D., Gomez, L., & Karatzas, D. (2017). ICDAR2017 robust reading challenge on omnidirectional video. 2017 14th IAPR International Conference on Document Analysis and Recognition (ICDAR),

Jaderberg, M., Simonyan, K., Vedaldi, A., & Zisserman, A. (2014a). Deep structured output learning for unconstrained text recognition. *arXiv preprint arXiv:1412.5903*.

Jaderberg, M., Simonyan, K., Vedaldi, A., & Zisserman, A. (2014b). Synthetic Data and Artificial Neural Networks for Natural Scene Text Recognition. arXiv:1406.2227. Retrieved June 01, 2014, from https://ui.adsabs.harvard.edu/abs/2014arXiv1406.2227J

Jaderberg, M., Simonyan, K., Vedaldi, A., & Zisserman, A. (2016). Reading text in the wild with convolutional neural networks. *International journal of computer vision, 116*(1), 1-20.

Jain, A., Wermuth, H. R., Dua, A., Singh, K., & Maani, C. V. (2019). Rocuronium.

Janan, F., & Brady, M. (2015). Shape description and matching using integral invariants on eccentricity transformed images. *International journal of computer vision, 113*(2), 92-112.

Janik, L. S., & Vender, J. S. (2019). Pro/Con Debate: Color-Coded Medication Labels. *Pro: Color-coded medication labels improve patient safety. APSF Newsletter, 33*, 72-73.

Jelacic, S., Bowdle, A., Nair, B. G., Kusulos, D., Bower, L., & Togashi, K. (2015). A system for anesthesia drug administration using barcode technology: the Codonics Safe Label System and Smart Anesthesia Manager™. *Anesthesia & Analgesia, 121*(2), 410-421.

Jensen, L., Merry, A., Webster, C., Weller, J., & Larsson, L. (2004). Evidence-based strategies for preventing drug administration errors during anaesthesia. *Anaesthesia, 59*(5), 493-504.

Johannesson, P., & Perjons, E. (2014). *An introduction to design science*. Springer.

Jolliffe, I. (2005). Principal component analysis. *Encyclopedia of statistics in behavioral science*.

Kader, M. F., & Deb, K. (2012). Neural network-based English Alphanumeric character recognition. *International Journal of Computer Science, Engineering and Applications, 2*(4), 1.

Kakkar, P., & Dutta, U. (2014). A novel Approach to Recognition of English Characters Using Artificial Neural Networks. *International Journal of Advanced Research in Electrical, Electronics and Instrumentation Engineering, 3*(6).

Kandasamy, J., & Carlo IV, W. (2016). Pharmacologic therapies IV: other medications. *Assisted Ventilation of the Neonate: An Evidence-Based Approach to Newborn Respiratory Care. 6th ed. Philadelphia: Elsevier*, 366-379.

Karatzas, D., Gomez-Bigorda, L., Nicolaou, A., Ghosh, S., Bagdanov, A., Iwamura, M., Matas, J., Neumann, L., Chandrasekhar, V. R., & Lu, S. (2015). ICDAR 2015 competition on robust reading. 2015 13th International Conference on Document Analysis and Recognition (ICDAR),

Karayev, S., Baumgartner, T., Fritz, M., & Darrell, T. (2012). Timely object recognition. *Advances in Neural Information Processing Systems, 25*.

Karnawat, A., More, K., Rade, T., Rane, B., & Mulik, M. A Survey on Easy OCR Techniques used to build Systems for Visually Impaired People.

Ke, Y., & Sukthankar, R. (2004). PCA-SIFT: A more distinctive representation for local image descriptors. Proceedings of the 2004 IEEE Computer Society Conference on Computer Vision and Pattern Recognition, 2004. CVPR 2004.,

Kellum, J. A., & Pinsky, M. R. (2002). Use of vasopressor agents in critically ill patients. *Current opinion in critical care, 8*(3), 236-241.

Khan, F., & Hoda, M. (2001). A prospective survey of intra-operative critical incidents in a teaching hospital in a developing country. *Anaesthesia, 56*(2), 177-182.

Khan, S. N. (2014). Qualitative research method-phenomenology. *Asian Social Science, 10*(21), 298.

Kim, K. I., Jung, K., & Kim, J. H. (2003). Texture-based approach for text detection in images using support vector machines and continuously adaptive mean shift algorithm. *IEEE transactions on pattern analysis and machine intelligence, 25*(12), 1631-1639.

Kim, W., & Kim, C. (2009, February 01, 2009). A New Approach for Overlay Text Detection and Extraction From Complex Video Scene. *IEEE Transactions on Image Processing, 18*, 401. https://doi.org/10.1109/tip.2008.2008225

Kohn, L. T., Corrigan, J., & Donaldson, M. S. (2000). *To err is human: building a safer health system* (Vol. 6). National academy press Washington, DC.

Korhonen, J., & You, J. (2012). Peak signal-to-noise ratio revisited: Is simple beautiful? 2012 Fourth International Workshop on Quality of Multimedia Experience,

Kosmetik, G. (2017). *Active concentrate in glass ampoules*. Medsafe New Zealand. https://timesofmalta.com/articles/view/Active-concentrate-in-glass-ampoules.643610

Kosub, S. (2019). A note on the triangle inequality for the Jaccard distance. *Pattern Recognition Letters, 120*, 36-38.

Kothari, D., Gupta, S., Sharma, C., & Kothari, S. (2010). Medication error in anaesthesia and critical care: A cause for concern. *Indian journal of anaesthesia, 54*(3), 187.

[Record #427 is using a reference type undefined in this output style.]

Krizhevsky, A., Sutskever, I., & Hinton, G. E. (2017). Imagenet classification with deep convolutional neural networks. *Communications of the ACM, 60*(6), 84-90.

Kunøe, N., Lobmaier, P., Ngo, H., & Hulse, G. (2014). Injectable and implantable sustained release naltrexone in the treatment of opioid addiction. *British journal of clinical pharmacology, 77*(2), 264-271.

Kurdi, M. S., Theerth, K. A., & Deva, R. S. (2014). Ketamine: Current applications in anesthesia, pain, and critical care. *Anesthesia, essays and researches, 8*(3), 283.

Lakemond, R., Sridharan, S., & Fookes, C. (2012). Hessian-based affine adaptation of salient local image features. *Journal of Mathematical Imaging and Vision, 44*(2), 150-167.

Lala, A. I., Sturzu, L., Picard, J., Druot, F., Grama, F., & Bobirnac, G. (2016). Coping behavior and risk and resilience stress factors in French regional emergency medicine unit workers: a cross-sectional survey. *Journal of medicine and life, 9*(4), 363.

Lalor, D. (2011). Medicines labelling.

Lee, C.-Y., & Osindero, S. (2016). Recursive recurrent nets with attention modeling for ocr in the wild. Proceedings of the IEEE Conference on Computer Vision and Pattern Recognition,

Lee, J.-J., Lee, P.-H., Lee, S.-W., Yuille, A., & Koch, C. (2011). Adaboost for text detection in natural scene. 2011 International Conference on Document Analysis and Recognition,

Lerche, P. (2015). Anticholinergics. *Veterinary Anesthesia and Analgesia: The Fifth Edition of Lumb and Jones*, 178-182.

Lester, P. A., Moore, R. M., Shuster, K. A., & Myers, D. D. (2012). Anesthesia and analgesia. In *The laboratory rabbit, guinea pig, hamster, and other rodents* (pp. 33-56). Elsevier.

Leutenegger, S., Chli, M., & Siegwart, R. Y. (2011). BRISK: Binary robust invariant scalable keypoints. 2011 International conference on computer vision,

Levandowsky, M., & Winter, D. (1971). Distance between sets. *Nature, 234*(5323), 34-35.

Li, H., Doermann, D., & Kia, O. (2000). Automatic text detection and tracking in digital video. *IEEE Transactions on Image Processing, 9*(1), 147-156.

Li, M., & Wang, C. (2008). An adaptive text detection approach in images and video frames. 2008 IEEE International Joint Conference on Neural Networks (IEEE World Congress on Computational Intelligence),

Liao, M., Wan, Z., Yao, C., Chen, K., & Bai, X. (2020). Real-time scene text detection with differentiable binarization. Proceedings of the AAAI Conference on Artificial Intelligence,

Lienhart, R., & Effelsberg, W. (2000). Automatic text segmentation and text recognition for video indexing. *Multimedia systems, 8*(1), 69-81.

Lienhart, R., & Wernicke, A. (2002). Localizing and segmenting text in images and videos. *IEEE Transactions on circuits and systems for video technology, 12*(4), 256-268.

Lin, H., Yang, P., & Zhang, F. (2019). Review of scene text detection and recognition. *Archives of Computational Methods in Engineering*, 1-22.

Lindeberg, T. (1998). Feature detection with automatic scale selection. *International journal of computer vision, 30*(2), 79-116.

Lindeberg, T. (2012). Scale invariant feature transform.

Lindeberg, T. (2015). Image matching using generalized scale-space interest points. *Journal of Mathematical Imaging and Vision, 52*(1), 3-36.

Lingamchetty, T. N., Hosseini, S. A., & Saadabadi, A. (2021). Midazolam. In *StatPearls [Internet]*. StatPearls Publishing.

Litman, R. (2018). How to prevent medication errors in the operating room? Take away the human factor. *British journal of anaesthesia, 120*(3), 438-440.

Liu, X., Meng, G., & Pan, C. (2019). Scene text detection and recognition with advances in deep learning: a survey. *International Journal on Document Analysis and Recognition (IJDAR), 22*(2), 143-162.

Liu, Y., Wang, Z., Jin, H., & Wassell, I. (2018). Synthetically supervised feature learning for scene text recognition. Proceedings of the European Conference on Computer Vision (ECCV),

Long, S., He, X., & Yao, C. (2018). Scene Text Detection and Recognition: The Deep Learning Era. arXiv:1811.04256. Retrieved November 01, 2018, from https://ui.adsabs.harvard.edu/abs/2018arXiv181104256L

Loussaief, S., & Abdelkrim, A. (2016). Machine learning framework for image classification. 2016 7th International Conference on Sciences of Electronics, Technologies of Information and Telecommunications (SETIT),

Lowe, D. G. (2004). Distinctive image features from scale-invariant keypoints. *International journal of computer vision, 60*(2), 91-110.

Lucas, S. M. (2005). ICDAR 2005 text locating competition results. Eighth International Conference on Document Analysis and Recognition (ICDAR'05),

Luciano, A., & Fustinoni, O. (2014). Neurologic aspects of systemic disease part III. *Handbook of Clinical Neurology*.

Luo, T., Shi, Z., & Wang, P. (2020). Robust and efficient corner detector using non-corners exclusion. *Applied Sciences, 10*(2), 443.

Lyu, P., Liao, M., Yao, C., Wu, W., & Bai, X. (2018). Mask textspotter: An end-to-end trainable neural network for spotting text with arbitrary shapes. Proceedings of the European Conference on Computer Vision (ECCV),

Maharrey, B. (2009). *A Neural Network Implementation of Optical Character Recognition*.

Maher, T. J. (2012). Anesthetic agents: general and local anesthetics. *Foye's Princ. Med. Chem., 7th ed., Lippincott Williams & Wilkins*, 508-539.

Mair, E., Hager, G. D., Burschka, D., Suppa, M., & Hirzinger, G. (2010). Adaptive and generic corner detection based on the accelerated segment test. European conference on Computer vision,

Markus, M. L., Majchrzak, A., & Gasser, L. (2002). A design theory for systems that support emergent knowledge processes. *MIS quarterly*, 179-212.

McCance, T., & Mcilfatrick, S. (2008). Phenomenology. *Watson, R., Mckenna, H., Cowman, S., & Keady, J.(Ed.) Nursing research: Designs and methods*, 231-242.

McKeage, K., & Perry, C. M. (2003). Propofol. *CNS drugs, 17*(4), 235-272.

Medsafe. (2019a). *Aspen Adrenaline Injection*. New Zealand Medicines and Medical Devices Safety Authority. https://www.medsafe.govt.nz/profs/datasheet/a/aspenadrenalineinj.pdf

Medsafe. (2019b). *Atracurium Besylate Injection*. New Zealand Medicines and Medical Devices Safety Authority. Retrieved 2021 from https://www.medsafe.govt.nz/profs/datasheet/a/Atracuriumbesylateinj.pdf

Medsafe. (2019c). *Fentanyl Injection*. New Zealand Medicines and Medical Devices Safety Authority. https://www.medsafe.govt.nz/profs/datasheet/f/fentanylinj.pdf

Medsafe. (2019d). *midazolam*. New Zealand Medicines and Medical Devices Safety Authority. https://www.medsafe.govt.nz/profs/datasheet/m/midazolaminjpfizer.pdf

Medsafe. (2019e). *Neostigmine Methylsulfate Injection*. New Zealand Medicines and Medical Devices Safety Authority. https://www.medsafe.govt.nz/profs/datasheet/n/Neostigmineinj.pdf

Medsafe. (2020). *Flumazenil Injection*. New Zealand Medicines and Medical Devices Safety Authority. https://www.medsafe.govt.nz/profs/datasheet/d/DBLFlumazenilinj.pdf

Medsafe. (2021a). *Morphine Sulphate*. New Zealand Medicines and Medical Devices Safety Authority. https://www.medsafe.govt.nz/profs/datasheet/m/morphinesulphateinjbiomed.pdf

Medsafe. (2021b). *Rocuronium bromide*. New Zealand Medicines and Medical Devices Safety Authority. Retrieved 2022 from https://www.medsafe.govt.nz/profs/datasheet/r/rocuroniumbromideinj.pdf

Medsafe. (2021c). *Sterile Dopamine Concentrate BP*. New Zealand Medicines and Medical Devices Safety Authority. https://www.medsafe.govt.nz/profs/Datasheet/s/steriledopamineinj.pdf

Medsafe. (2022a). *Diazepam*. New Zealand Medicines and Medical Devices Safety Authority. https://www.medsafe.govt.nz/profs/datasheet/a/arrowdiazepamtab.pdf

Medsafe. (2022b). *NORMISON (temazepam)*. New Zealand Medicines and Medical Devices Safety Authority. Retrieved 2022 from https://www.medsafe.govt.nz/profs/datasheet/n/normisontab.pdf

Merry, A. F., & Anderson, B. J. (2011). Medication errors–new approaches to prevention. *Pediatric Anesthesia, 21*(7), 743-753.

Merry, A. F., & Peck, D. J. (1995). Anaesthetists, errors in drug administration and the law. *The New Zealand medical journal, 108*(1000), 185-187.

Merry, A. F., Webster, C. S., Hannam, J., Mitchell, S. J., Henderson, R., Reid, P., Edwards, K.-E., Jardim, A., Pak, N., & Cooper, J. (2011). Multimodal system designed to reduce errors in recording and administration of drugs in anaesthesia: prospective randomised clinical evaluation. *Bmj, 343*.

Merry, A. F., Webster, C. S., & Mathew, D. J. (2001). A new, safety-oriented, integrated drug administration and automated anesthesia record system. *Anesthesia & Analgesia, 93*(2), 385-390.

Mikolajczyk, K., & Schmid, C. (2002). An affine invariant interest point detector. European conference on computer vision,

Mikolajczyk, K., & Schmid, C. (2004). Scale & affine invariant interest point detectors. *International journal of computer vision, 60*(1), 63-86.

Mikolajczyk, K., & Tuytelaars, T. (2008). Local invariant feature detectors: a survey. *Foundations and trends in computer graphics and vision, 3*(3), 177-280.

Mikolajczyk, K., & Tuytelaars, T. (2009). Local Image Features. *Encyclopedia of Biometrics, 939*.

Mikolajczyk, K., Tuytelaars, T., Schmid, C., Zisserman, A., Matas, J., Schaffalitzky, F., Kadir, T., & Van Gool, L. (2005). A comparison of affine region detectors. *International journal of computer vision, 65*(1), 43-72.

Mirakhur, R. (2009). Sugammadex in clinical practice. *Anaesthesia, 64*, 45-54.

Mirmehdi, M., Clark, P., & Lam, J. (2001). Extracting low resolution text with an active camera for OCR. In *Unknown* (pp. 43-48). U Juame I.

Mishra, A., Alahari, K., & Jawahar, C. (2012). Scene text recognition using higher order language priors.

Mittal, R., & Garg, A. (2020). Text extraction using OCR: a systematic review. 2020 Second International Conference on Inventive Research in Computing Applications (ICIRCA),

Miyagawa, S., Bulert, K., Büchler, M., & Behlmer, H. (2019). Optical character recognition of typeset Coptic text with neural networks. *Digital Scholarship in the Humanities, 34*(Supplement_1), i135-i141.

Mohammad, F., Anarase, J., Shingote, M., & Ghanwat, P. (2014). Optical character recognition implementation using pattern matching. *International Journal of Computer Science and Information Technologies, 5*(2), 2088-2090.

Moore, P. (2004). Sedative-hypnotics, antianxiety drugs, and centrally acting muscle relaxants. *Pharmacology and Therapeutics in Dentistry, 5th edn. Oxford: Elsevier Mosby*, 193-218.

Morel, J.-M., & Yu, G. (2009). ASIFT: A new framework for fully affine invariant image comparison. *SIAM journal on imaging sciences, 2*(2), 438-469.

Morrison, D. R., Jacobson, S. H., Sauppe, J. J., & Sewell, E. C. (2016). Branch-and-bound algorithms: A survey of recent advances in searching, branching, and pruning. *Discrete Optimization, 19*, 79-102.

Muja, M., & Lowe, D. G. (2014). Scalable nearest neighbor algorithms for high dimensional data. *IEEE transactions on pattern analysis and machine intelligence, 36*(11), 2227-2240.

Mulfari, D., Celesti, A., Fazio, M., Villari, M., & Puliafito, A. (2016). Using Google Cloud Vision in assistive technology scenarios. 2016 IEEE symposium on computers and communication (ISCC),

Murray, A., & Hagen, N. A. (2005). Hydromorphone. *Journal of pain and symptom management, 29*(5), 57-66.

Nag, D. S., Samaddar, D. P., Chatterjee, A., Kumar, H., & Dembla, A. (2015). Vasopressors in obstetric anesthesia: A current perspective. *World Journal of Clinical Cases: WJCC, 3*(1), 58.

Nanji, K. C., Patel, A., Shaikh, S., Seger, D. L., & Bates, D. W. (2016). Evaluation of perioperative medication errors and adverse drug events. *Anesthesiology: The Journal of the American Society of Anesthesiologists, 124*(1), 25-34.

Navarro, G., & Raffinot, M. (2002). *Flexible pattern matching in strings: practical on-line search algorithms for texts and biological sequences*. Cambridge university press.

Neely, G. A., Sabir, S., & Kohli, A. (2021). Neostigmine. *StatPearls [Internet]*.

Neubeck, A., & Van Gool, L. (2006). Efficient non-maximum suppression. 18th International Conference on Pattern Recognition (ICPR'06),

Neuhauser, L., Kreps, G. L., Morrison, K., Athanasoulis, M., Kirienko, N., & Van Brunt, D. (2013). Using design science and artificial intelligence to improve health communication: ChronologyMD case example. *Patient education and counseling, 92*(2), 211-217.

Neumann, L., & Matas, J. (2010). A method for text localization and recognition in real-world images. Asian Conference on Computer Vision,

Neumann, L., & Matas, J. (2013). Scene text localization and recognition with oriented stroke detection. Proceedings of the ieee international conference on computer vision,

Nunes, E. V., Gordon, M., Friedmann, P. D., Fishman, M. J., Lee, J. D., Chen, D. T., Hu, M. C., Boney, T. Y., Wilson, D., & O'Brien, C. P. (2018). Relapse to opioid use disorder after inpatient treatment: Protective effect of injection naltrexone. *Journal of substance abuse treatment, 85*, 49-55.

Oliva, A., & Torralba, A. (2001). Modeling the shape of the scene: A holistic representation of the spatial envelope. *International journal of computer vision, 42*(3), 145-175.

Pan, Y.-F., Hou, X., & Liu, C.-L. (2009). Text localization in natural scene images based on conditional random field. 2009 10th International Conference on Document Analysis and Recognition,

Pang, Y., Li, W., Yuan, Y., & Pan, J. (2012). Fully affine invariant SURF for image matching. *Neurocomputing, 85*, 6-10.

Pani, N., Dongare, P. A., & Mishra, R. K. (2015). Reversal agents in anaesthesia and critical care. *Indian journal of anaesthesia, 59*(10), 664.

Papamichail, D., & Papamichail, G. (2009). Improved algorithms for approximate string matching. *BMC bioinformatics, 10*(1), 1-11.

Patel, B., Holland, C., Pook, J., Barker*, G., & Baba, R. (2006). Near misses with prefilled syringes. *British journal of anaesthesia, 96*(2), 270-271.

Patel, U., & Thakkar, M. (2014). An Efficient Exact Single Pattern Matching Algorithm. *vol, 3*, 1955-1958.

Penninga, E. I., Graudal, N., Ladekarl, M. B., & Jürgens, G. (2016). Adverse events associated with flumazenil treatment for the management of suspected benzodiazepine intoxication–a systematic review with meta-analyses of randomised trials. *Basic & clinical pharmacology & toxicology, 118*(1), 37-44.

Persson, J. (2010). Wherefore ketamine? *Current Opinion in Anesthesiology, 23*(4), 455-460.

Pierre, S., & Whelan, R. (2013). Nausea and vomiting after surgery. *Continuing Education in Anaesthesia, Critical Care & Pain, 13*(1), 28-32.

Pratt, O. Intravenous drugs used for the induction of anaesthesia.

Pratt, O. (2008). INTRAVENOUS DRUGS USED FOR THE INDUCTION OF ANAESTHESIA ANAESTHESIA TUTORIAL OF THE WEEK 107 4TH AUGUST 2008.

Pratt, W. K. (2013). *Introduction to digital image processing*. CRC press.

Pretorius, D.-L., Goede, R., & Terblanche, J. (2015). Action Research or Design Science Research as Methodology for the Development of a Historical Digital Graphical Novel? A Critical Systems Perspective. Proceedings of the 59th Annual Meeting of the ISSS-2015 Berlin, Germany,

Prommer, E. (2020). Midazolam: an essential palliative care drug. *Palliative care and social practice, 14*, 2632352419895527.

Pushparaj, V., Gurunathan, U., & Arumugam, B. (2013). An effective dental shape extraction algorithm using contour information and matching by mahalanobis distance. *Journal of digital imaging, 26*, 259-268.

Rai, A., & Borah, S. (2020). Study of Various Methods for Tokenization. In *Applications of Internet of Things* (pp. 193-200). Springer.

Raisi, Z., Naiel, M. A., Fieguth, P., Wardell, S., & Zelek, J. (2020). Text Detection and Recognition in the Wild: A Review. *arXiv preprint arXiv:2006.04305*.

Ramakrishnan, K., & Bart, E. (2012). Learning domain-specific feature descriptors for document images. 2012 10th IAPR International Workshop on Document Analysis Systems,

Ramzy, M., & McAllister, R. K. (2021). Vecuronium. *StatPearls [Internet]*.

Ranadive, S. M., Eugene, A. R., Dillon, G., Nicholson, W. T., & Joyner, M. J. (2017). Comparison of the vasodilatory effects of sodium nitroprusside vs. nitroglycerin. *Journal of Applied Physiology, 123*(2), 402-406.

Rao, G. A., Srinivas, G., VenkataRao, K., & Prasad Reddy, P. (2018). A partial ratio and ratio based fuzzy-wuzzy procedure for characteristic mining of mathematical formulas from documents. *IJSC—ICTACT J Soft Comput, 8*(4), 1728-1732.

Rayan, A. A., Hemdan, S. E., & Shetaia, A. M. (2019). Root cause analysis of blunders in anesthesia. *Anesthesia, essays and researches, 13*(2), 193.

Reddy, N. G. (2015). Medication errors in anesthesia and critical care. *Journal of Evolution of Medical and Dental Sciences, 4*(15), 2586-2595.

Rehman, A., & Saba, T. (2014). Neural networks for document image preprocessing: state of the art. *Artificial Intelligence Review, 42*(2), 253-273.

Reves, J., Glass, P., Lubarsky, D. A., McEvoy, M., & Martinez-Ruiz, R. (2010). Miller's anesthesia. *Churchill Livingstone*.

Richards, E., Lopez, M. J., & Maani, C. V. (2021). Phenylephrine. *StatPearls [Internet]*.

Risnumawan, A., Shivakumara, P., Chan, C. S., & Tan, C. L. (2014). A robust arbitrary text detection system for natural scene images. *Expert Systems with Applications, 41*(18), 8027-8048.

Ritz, M. L., & Derian, A. (2018). Atracurium.

Roberts, J. R. (2017). *Roberts and Hedges' clinical procedures in emergency medicine and acute care e-book*. Elsevier Health Sciences.

Rosemann, M., & Vessey, I. (2008). Toward improving the relevance of information systems research to practice: the role of applicability checks. *MIS quarterly*, 1-22.

Rosten, E., & Drummond, T. (2005). Fusing points and lines for high performance tracking. Tenth IEEE International Conference on Computer Vision (ICCV'05) Volume 1,

Rosten, E., & Drummond, T. (2006). Machine learning for high-speed corner detection. European conference on computer vision,

Rushton, A., & Sneyd, J. (2003). Clinical pharmacology and anesthetic techniques. *Wylie and Churchill-Davidson's A practice of Anesthesia. 7th ed. London: Arnold*, 565-582.

Salau, A. O., & Jain, S. (2019). Feature extraction: a survey of the types, techniques, applications. 2019 international conference on signal processing and communication (ICSC),

Sarkar, S., Das, D., Pakray, P., & Gelbukh, A. (2016). JUNITMZ at SemEval-2016 task 1: Identifying semantic similarity using Levenshtein ratio. Proceedings of the 10th International Workshop on Semantic Evaluation (SemEval-2016),

Schalkoff, R. J. (2007). Pattern recognition. *Wiley Encyclopedia of Computer Science and Engineering*.

Schapire, R. E., & Singer, Y. (1999). Improved boosting algorithms using confidence-rated predictions. *Machine learning, 37*(3), 297-336.

Schwerthöffer, D., & Pajonk, F. (2018). Comparison of sublingual and intravenous administration of lorazepam in psychiatric emergencies in emergency medical services. *Der Anaesthesist, 68*(2), 83-89.

Scott, L. J., & Perry, C. M. (2005). Remifentanil: a review of its use during the induction and maintenance of general anaesthesia. *Drugs, 65*, 1793-1823.

Shi, B., Bai, X., & Belongie, S. (2017). Detecting oriented text in natural images by linking segments. Proceedings of the IEEE Conference on Computer Vision and Pattern Recognition,

Shi, B., Bai, X., & Yao, C. (2016). An end-to-end trainable neural network for image-based sequence recognition and its application to scene text recognition. *IEEE transactions on pattern analysis and machine intelligence, 39*(11), 2298-2304.

Shi, B., Yang, M., Wang, X., Lyu, P., Yao, C., & Bai, X. (2018). Aster: An attentional scene text recognizer with flexible rectification. *IEEE transactions on pattern analysis and machine intelligence, 41*(9), 2035-2048.

Shi, C.-Z., Gao, S., Liu, M.-T., Qi, C.-Z., Wang, C.-H., & Xiao, B.-H. (2015). Stroke detector and structure based models for character recognition: a comparative study. *IEEE Transactions on Image Processing, 24*(12), 4952-4964.

Shintani, H., Akutagawa, M., Nagashino, H., & Kinouchi, Y. (2006). Recognition mechanism of a neural network for character recognition. 2005 IEEE Engineering in Medicine and Biology 27th Annual Conference,

Short, T. G., & Hannam, J. A. (2019). Pharmacodynamic drug interactions. In *Pharmacology and Physiology for Anesthesia* (pp. 113-129). Elsevier.

Simons, R., Koerhuis, C. L., Valk, P. J., & Van den Oord, M. H. (2006). Usefulness of temazepam and zaleplon to induce afternoon sleep. *Military medicine, 171*(10), 998-1001.

Simonyan, K., & Zisserman, A. (2014). Very Deep Convolutional Networks for Large-Scale Image Recognition. arXiv:1409.1556. Retrieved September 01, 2014, from https://ui.adsabs.harvard.edu/abs/2014arXiv1409.1556S

Slatkin, N., Thomas, J., Lipman, A. G., Wilson, G., Boatwright, M. L., Wellman, C., Zhukovsky, D. S., Stephenson, R., Portenoy, R., & Stambler, N. (2009). Methylnaltrexone for treatment of opioid-induced constipation in advanced illness patients. *The journal of supportive oncology, 7*(1), 39-46.

Smith, G., D'Cruz, J. R., Rondeau, B., & Goldman, J. (2018). General anesthesia for surgeons.

Smith, R. (2007). An overview of the Tesseract OCR engine. Ninth international conference on document analysis and recognition (ICDAR 2007),

Smith, R., Antonova, D., & Lee, D.-S. (2009). Adapting the Tesseract open source OCR engine for multilingual OCR. Proceedings of the International Workshop on Multilingual OCR,

Sporring, J., Nielsen, M., Florack, L., & Johansen, P. (2013). *Gaussian scale-space theory* (Vol. 8). Springer Science & Business Media.

Srivastava, A., & Hunter, J. (2009). Reversal of neuromuscular block. *British journal of anaesthesia, 103*(1), 115-129.

Starks, H., & Brown Trinidad, S. (2007). Choose your method: A comparison of phenomenology, discourse analysis, and grounded theory. *Qualitative health research, 17*(10), 1372-1380.

Steiglitz, K. (2020). *Digital Signal Processing Primer*. Courier Dover Publications.

Su, B., & Lu, S. (2014). Accurate scene text recognition based on recurrent neural network. Asian Conference on Computer Vision,

Sumengen, B., & Manjunath, B. (2005). Multi-scale edge detection and image segmentation. 2005 13th European Signal Processing Conference,

Tang, G., Xie, L., Jin, L., Wang, J., Chen, J., Xu, Z., Wang, Q., Wu, Y., & Li, H. (2021). MatchVIE: Exploiting Match Relevancy between Entities for Visual Information Extraction. *arXiv preprint arXiv:2106.12940*.

Theriot, J., Sabir, S., & Azadfard, M. (2019). Opioid antagonists.

Tian, Q., Xie, G., Wang, Y., & Zhang, Y. (2018). Pedestrian detection based on laplace operator image enhancement algorithm and faster R-CNN. 2018 11th International Congress on Image and Signal Processing, BioMedical Engineering and Informatics (CISP-BMEI),

Tom Lupton, O. P. (2008). *Intravenous Drugs Used For The Induction*. https://resources.wfsahq.org/atotw/intravenous-drugs-used-for-the-induction-of-anaesthesia-tutorial-of-the-week-107/

Topic 5: Noise in Images. Retrieved 19/10 from https://www2.ph.ed.ac.uk/~wjh/teaching/dia/documents/noise.pdf

Trapani, G., Altomare, C., Sanna, E., Biggio, G., & Liso, G. (2000). Propofol in anesthesia. Mechanism of action, structure-activity relationships, and drug delivery. *Current medicinal chemistry, 7*(2), 249-271.

Trizotti, J. P. S. d. S., Braga, A. d. F. d. A., Carvalho, V. H., & Braga, F. S. d. S. (2020). Influence of different local anesthetics on atracurium neuromuscular blockade on rats. *Revista Brasileira de Anestesiologia, 70*, 220-224.

Truong, M. T. N., & Kim, S. (2016). A Review on Image Feature Detection and Description. Proceedings of the Korea Information Processing Society Conference,

Tschopp, C., Tramèr, M. R., Schneider, A., Zaarour, M., & Elia, N. (2018). Benefit and harm of adding epinephrine to a local anesthetic for neuraxial and locoregional anesthesia: a meta-analysis of randomized controlled trials with trial sequential analyses. *Anesthesia & Analgesia, 127*(1), 228-239.

Tuytelaars, T., & Mikolajczyk, K. (2008). A survey on local invariant features. *Foundations and trends in computer graphics and vision, 3*(3), 176-280.

Valgren, C., & Lilienthal, A. J. (2010). SIFT, SURF & seasons: Appearance-based long-term localization in outdoor environments. *Robotics and Autonomous Systems, 58*(2), 149-156.

VanValkinburgh, D., Kerndt, C. C., & Hashmi, M. F. (2018). Inotropes and vasopressors.

Vardanyan, R., & Hruby, V. (2006). Muscle relaxants. *Synthesis of essential drugs*, 209-218.

Vincent, L. (2007). Google book search: Document understanding on a massive scale. Ninth International Conference on Document Analysis and Recognition (ICDAR 2007),

Viola, P., & Jones, M. J. (2004). Robust real-time face detection. *International journal of computer vision, 57*(2), 137-154.

Walker, J., Fujii, Y., & Popat, A. C. (2018). A web-based ocr service for documents. Proceedings of the 13th IAPR International Workshop on Document Analysis Systems (DAS), Vienna, Austria,

Walls, J. G., Widermeyer, G. R., & El Sawy, O. A. (2004). Assessing information system design theory in perspective: how useful was our 1992 initial rendition? *Journal of Information Technology Theory and Application (JITTA), 6*(2), 6.

Wang, J., & Hu, X. (2017). Gated recurrent convolution neural network for ocr. *Advances in Neural Information Processing Systems, 30*, 335-344.

Wang, J., Li, G., & Fe, J. (2011). Fast-join: An efficient method for fuzzy token matching based string similarity join. 2011 IEEE 27th International Conference on Data Engineering,

Wang, J., Liu, C., Jin, L., Tang, G., Zhang, J., Zhang, S., Wang, Q., Wu, Y., & Cai, M. (2021). Towards Robust Visual Information Extraction in Real World: New Dataset and Novel Solution. Proceedings of the AAAI Conference on Artificial Intelligence,

Wang, K., Babenko, B., & Belongie, S. (2011). End-to-end scene text recognition. 2011 International Conference on Computer Vision,

Wang, K., & Belongie, S. (2010). Word spotting in the wild. European Conference on Computer Vision,

Wang, L., Yan, J., Mu, L., & Huang, L. (2020). Knowledge discovery from remote sensing images: A review. *Wiley Interdisciplinary Reviews: Data Mining and Knowledge Discovery, 10*(5), e1371.

Wang, S., Li, W., Wang, Y., Jiang, Y., Jiang, S., & Zhao, R. (2012). An Improved Difference of Gaussian Filter in Face Recognition. *J. Multim., 7*(6), 429-433.

Wang, T., Wu, D. J., Coates, A., & Ng, A. Y. (2012). End-to-end text recognition with convolutional neural networks. Proceedings of the 21st international conference on pattern recognition (ICPR2012),

Wang, Z., Bao, R., Wu, Q., & Liu, S. (2020). Confidence-aware Non-repetitive Multimodal Transformers for TextCaps. *arXiv preprint arXiv:2012.03662*.

Wang, Z., & Bovik, A. C. (2002). A universal image quality index. *IEEE Signal Processing Letters, 9*(3), 81-84.

Webster, C., Merry, A., Larsson, L., McGrath, K., & Weller, J. (2001). The frequency and nature of drug administration error during anaesthesia. *Anaesthesia and intensive care, 29*(5), 494-500.

Wegman, A., Van der Windt, D., Bongers, M., Twisk, J., Stalman, W., & De Vries, T. (2005). Efficacy of temazepam in frequent users: a series of N-of-1 trials. *Family practice, 22*(2), 152-159.

Wei, T. C., Sheikh, U., & Ab Rahman, A. A.-H. (2018). Improved optical character recognition with deep neural network. 2018 IEEE 14th International Colloquium on Signal Processing & Its Applications (CSPA),

Welch, E. (2017). Neuromuscular blocking agents and their reversal.

Wheeler, S., & Wheeler, D. (2005). Medication errors in anaesthesia and critical care. *Anaesthesia, 60*(3), 257-273.

Wick, C., Reul, C., & Puppe, F. (2018). Calamari-a high-performance tensorflow-based deep learning package for optical character recognition. *arXiv preprint arXiv:1807.02004*.

Williams, L. M., Boyd, K. L., & Fitzgerald, B. M. (2021). Etomidate. In *StatPearls [Internet]*. StatPearls Publishing.

Xie, Z., Huang, Y., Zhu, Y., Jin, L., Liu, Y., & Xie, L. (2019). Aggregation cross-entropy for sequence recognition. Proceedings of the IEEE Conference on Computer Vision and Pattern Recognition,

Xingfang, Y., Yumei, H., Yan, L., & Feng, G. (2011). An Algorithm for Feature Points Detection Based on Univalue Segment Assimilating Nucleus. *Mechanical Science and Technology for Aerospace Engineering*, 07.

Yang, L., Wang, P., Li, H., Gao, Y., Zhang, L., Shen, C., & Zhang, Y. (2019). A Simple and Strong Convolutional-Attention Network for Irregular Text Recognition. *arXiv preprint arXiv:1904.01375*.

Yang, X., & Niethammer, M. (2015). Uncertainty quantification for LDDMM using a low-rank Hessian approximation. International Conference on Medical Image Computing and Computer-Assisted Intervention,

Yao, C., Bai, X., Liu, W., Ma, Y., & Tu, Z. (2012). Detecting texts of arbitrary orientations in natural images. 2012 IEEE conference on computer vision and pattern recognition,

Ye, Q., & Doermann, D. (2014). Text detection and recognition in imagery: A survey. *IEEE transactions on pattern analysis and machine intelligence, 37*(7), 1480-1500.

Ye, Q., Huang, Q., Gao, W., & Zhao, D. (2005). Fast and robust text detection in images and video frames. *Image and vision computing, 23*(6), 565-576.

Yin, F., Wu, Y.-C., Zhang, X.-Y., & Liu, C.-L. (2017a). Scene Text Recognition with Sliding Convolutional Character Models. arXiv:1709.01727. Retrieved September 01, 2017, from https://ui.adsabs.harvard.edu/abs/2017arXiv170901727Y

Yin, F., Wu, Y.-C., Zhang, X.-Y., & Liu, C.-L. (2017b). Scene text recognition with sliding convolutional character models. *arXiv preprint arXiv:1709.01727*.

Young, J., Slebodnik, M., & Sands, L. (2010). Bar code technology and medication administration error. *Journal of patient safety, 6*(2), 115-120.

Yu, W., Lu, N., Qi, X., Gong, P., & Xiao, R. (2021). Pick: Processing key information extraction from documents using improved graph learning-convolutional networks. 2020 25th International Conference on Pattern Recognition (ICPR),

Yussof, W. N. J. H. W., & Hitam, M. S. (2014). Invariant Gabor-based interest points detector under geometric transformation. *Digital Signal Processing, 25*, 190-197.

Zamiri, B., Eftekharian, H., & Arasteh, N. (2012). Clonazepam for the management of anxiety associated with oral surgery: a randomized double-blind controlled trial.

Zhang, L., Zhang, L., Mou, X., & Zhang, D. (2011). FSIM: A feature similarity index for image quality assessment. *IEEE Transactions on Image Processing, 20*(8), 2378-2386.

Zhang, P., Xu, Y., Cheng, Z., Pu, S., Lu, J., Qiao, L., Niu, Y., & Wu, F. (2020). Trie: End-to-end text reading and information extraction for document understanding. Proceedings of the 28th ACM International Conference on Multimedia,

Zhang, S., Tian, Q., Huang, Q., Gao, W., & Rui, Y. (2014). USB: Ultrashort binary descriptor for fast visual matching and retrieval. *IEEE Transactions on Image Processing, 23*(8), 3671-3683.

Zhang, S., Tong, H., Xu, J., & Maciejewski, R. (2019). Graph convolutional networks: a comprehensive review. *Computational Social Networks, 6*(1), 1-23.

Zhang, Z., Zhang, C., Shen, W., Yao, C., Liu, W., & Bai, X. (2016). Multi-oriented text detection with fully convolutional networks. Proceedings of the IEEE Conference on Computer Vision and Pattern Recognition,

Zhao, X., Lin, K.-H., Fu, Y., Hu, Y., Liu, Y., & Huang, T. S. (2011, March 01, 2011). Text From Corners: A Novel Approach to Detect Text and Caption in Videos. *IEEE Transactions on Image Processing, 20*, 790. https://doi.org/10.1109/tip.2010.2068553

Zhao, Z., Jiang, M., Guo, S., Wang, Z., Chao, F., & Tan, K. C. (2020). Improving deep learning based optical character recognition via neural architecture search. 2020 IEEE Congress on Evolutionary Computation (CEC),

Zhou, Y., Ye, Q., Qiu, Q., & Jiao, J. (2017). Oriented response networks. Proceedings of the IEEE Conference on Computer Vision and Pattern Recognition,

Appendices

Appendix A -- Anaesthetic Drug Categories

The appendix contains the anaesthetic drug categories.

Appendix B: Threshold Computation

This appendix consists of all the results used in calculating the threshold.

Appendix C: Threshold Computation Data Summary

The appendix contains the summary of the results used in obtaining the threshold.

Appendix D: Drug Identification

The appendix is made up of the complete results of the confidence score computation.

Appendix E: Drug Identification in Varied Conditions

This appendix contains the complete results of modeling the anesthetic drug identification in varied processing conditions.

Appendix A -- Anaesthetic Drug Categories

I. The Induction Anaesthetic Agents

The induction agents are anesthetic medications that cause a rapid loss of consciousness when the appropriate dose is administered intravenously to patients (Luciano & Fustinoni, 2014). Their usefulness includes anesthesia inducement before administering other drugs to retain anesthesia. Through intravenous infusion, induction agents keep anesthesia for procedures that take longer and provide sedation during operations in the operating theatres (Pratt, 2008). When administered, the time it takes the drug to move from the injection site to the brain is described as the one-arm-brain circulation time. The prevalent drugs used as induction agents are categorized depending on the chemical structures that constitute the drugs, and they are Barbiturates, Phenols, Imidazole, Phencyclidines, and Benzodiazepines (Pratt, 2008).

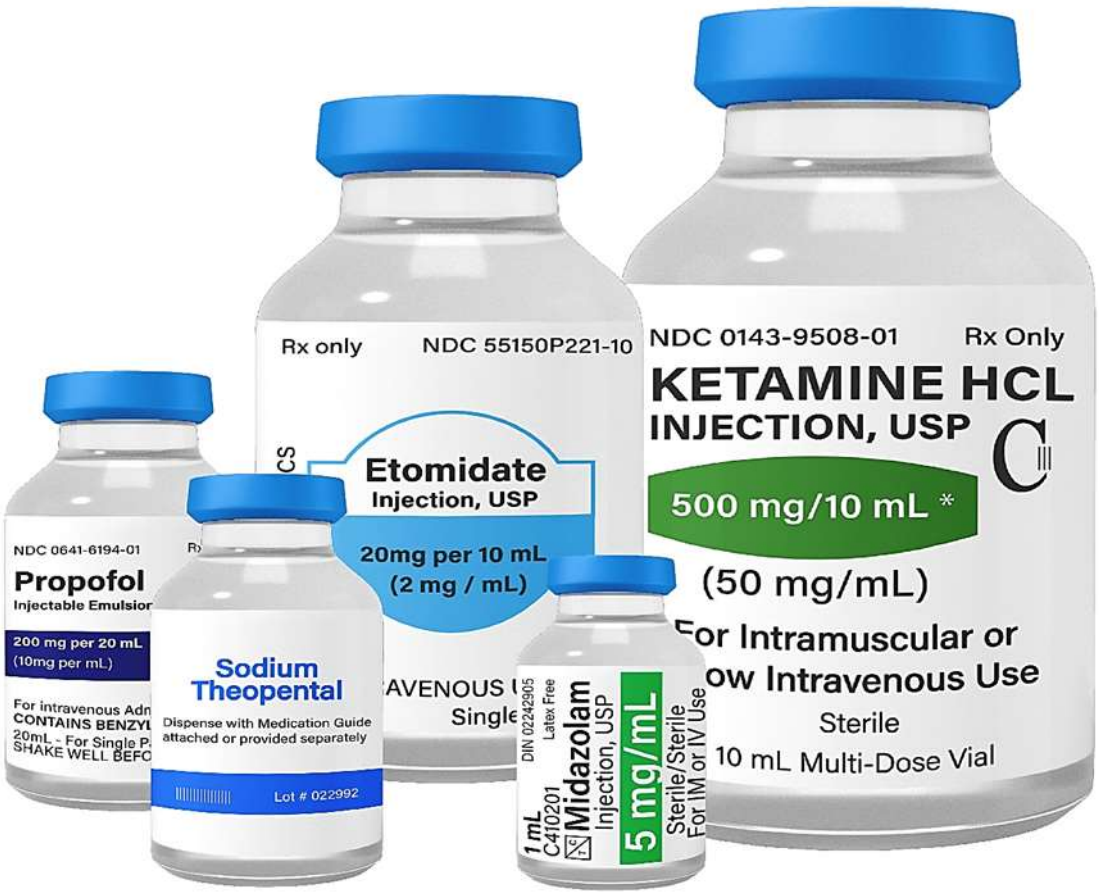

A Cross-section of the Anaesthetic Induction Agents.

The pharmacokinetic and pharmacodynamic characteristics of the induction agents are enormous, and they play vital roles in the intravenous anesthetic drug design process

(Pratt). The main pharmacokinetic characteristics of the induction agents are that their circulation time from the site of injection to the brain is rapid (Eger, 2004). They are quick in vessel-rich tissue redistribution, have a fast metabolism and clearance activities, and do not contain active metabolites. On the other hand, the pharmacodynamic characteristics of the induction agents are that they are high in therapeutic ratio, have low effects on cardiovascular and respiratory activities, absent of hypersensitivity reactions or histamine release (Short & Hannam, 2019). They are specific induction agents such as Propofol, Sodium Thiopental, Etomidate, Ketamine, Midazolam, etc., which are commonly used in the operating theatres and whose container contents or inscriptions are among the ampoule containers that will be extracted, analyzed, and deployed to identify the specific drugs.

- The Propofol Agent

Propofol is derived from phenolics and possesses sedative and hypnotic characteristics (Folino et al., 2022). They are highly lipophilic and rapidly infiltrate the barrier between the blood and brain, which causes the speedy onset of action (McKeage & Perry, 2003). Propofol is often given as a 1 or 2% aqueous emulsion with egg phosphatide, soya oil, and glycerol as its constituents. It has a pH of 7.0 - 8.5 and is isotonic to plasma. The propofols' action is short and lasts approximately 30 seconds, and its recovery is generally rapid. A dose of 2-2.5mg/kg of propofol ensures smooth anesthesia induction, and its notable endpoint is verbal contact loss by the patient in the operating theatre (Trapani et al., 2000).

Except for the ketamine anesthetic agent, all the induction drugs work on the center of respiration to induce respiratory depression. This action is most familiar with the propofol anesthetic drug, whose apnea period is often visible. Propofol is also ideal for a laryngeal mask because of its ability to minimize airway and pharyngeal reflexes. In addition, it also minimizes metabolic rate, cerebral blood flow, and intracranial pressure (Merry & Peck, 1995). The use of propofol provides sedation for matured patients admitted to the intensive care unit and for performing minor procedures.

- The Sodium Thiopental Agent

Also known as Pentothal or thiopentone, it is a barbiturate provided as a hygroscopic pale-yellow powder. A thiopental ampoule typically holds sodium thiopental of 500mg

in volume, in conjunction with a sodium carbonate of 6% in an inert nitrogen surrounding. When diluted with 20 ml of water, a 25mg/ml solution is obtained with a 10.8 pH value. A smooth onset of hypnosis with tremendous and perfect endpoints in a 30-second intravenous injection can be obtained with a 4-5mg/kg dose of thiopental. After a single dose, recovery from thiopental is rapid because of the redistributive properties of the drug (Çakırtekin et al., 2015).

The metabolism of the thiopental anesthetic agent is slow and occurs in the liver, and the metabolites are removed through the urine. Its constituent is 65-85% protein that is protein bound. If administered repeatedly, the metabolism of thiopental adheres to the zero-kinetics order; this inevitably implies that irrespective of the plasma concentration, a constant amount of the agent is removed in each unit of time. The contractile force in the heart is unswervingly depressed by the Thiopental agent, thereby minimizing blood pressure and cardiac output. When used, the rate of oxygen demand, cerebral metabolic rate, and cerebral blood flow decrease by the thiopental agent (McKeage & Perry, 2003).

- The Ketamine Agent

Ketamine is a water-soluble anesthetic agent derived from phencyclidine, a dissociative drug previously deployed as an anesthetic agent for inducing neurotoxic and hallucinogenic reactions (Gales & Maxwell, 2018). It is a special anesthetic intravenous agent that induces a wide range of pharmacological reactions like sympathetic nervous system stimulation, sedation, somatic analgesia, and catalepsy (Kurdi et al., 2014). In peripheral body tissues, Ketamine breakdown and redistributes rapidly and extensively undergoes metabolism in the liver through ring hydroxylation and N-demethylation pathways (Reves et al., 2010). It is expelled from the body system through faces and urine as a hydroxylated derivative and Norketamine.

Ketamine reacts with opioid receptors, purinergic, adrenoreceptor systems, cholinergic, monoamine and possesses local anesthetic effects (Persson, 2010). They are used in the emergency setting as an intravenous induction agent for hypotensive or shocked patients, children with congenital heart disease, and for burn dressing changes when performing grafting and excision (Gündüz et al., 2011). In addition,

Ketamine is also used for sedation and prehospital and battlefield medication (Rushton & Sneyd, 2003).

- The Etomidate Agent

The etomidate is in the form of a clear solution or lipid emulsion that contains propylene glycol of 2mg/ml concentration (Williams et al., 2021). A typical dose of etomidate is 0.3mg/k,g, and recuperation from the drug is rapid because of the fast redistribution in fat and muscles (Pratt, 2008). It is an exceptional agent used for sedation and general anesthetic induction. Initially created as an antifungal agent, several compounds of etomidate that have hypnotic potential were discovered when tested with animals. The observed compounds emerged to be meaningfully safer when compared with Barbiturates.

Several studies and investigations of etomidate existed but rapidly doubled when it was discovered to have adrenal toxicity. Afterward, the number of annual scientific publications on etomidate decreased but later resurged. The widening use of etomidate during intubations in intensive care units and the emergency departments pioneered renewed and resurgent research interests. Concerns exist about the consequences of adrenal toxicity induced by etomidate in critically ill patients. The quest to understand more about the molecular pharmacologic features of etomidate also spiked the recent rise in article publications on the drug. This, in turn, signifies the scientific progress being recorded on etomidate (Forman & Warner, 2011; Persson, 2010). From early clinical investigations, it is established that hypnosis of about 5–10 minutes can be achieved with a 0.2–0.4 mg/kg intravenous bolus dose of etomidate. A continuous etomidate infusion at 30–100 μg · kg−1· min−1 can ensure general anesthesia maintenance after a bolus. Oral transmucosal etomidate can also be used to induce sedation. In pediatric patients, rectal administration has been deployed for available anesthetic inducements (Forman & Warner, 2011).

- The Midazolam Agent

Midazolam is a clear water-soluble solution, often at a 2mg/ml concentration (Prommer, 2020). As an acidic solution, in an ampoule container, the molecules present in the drug occur in an ionized form. These molecules in midazolam transform into a highly lipid-soluble unionized ring at a physiological pH responsible for its fast

onset of action. In continuation, some factors such as patients' medical condition, weight, current medication intake, and response to therapy determine the dose that could be administered to a patient. However, it is usually used to perform sedation at a 0.05-0.1mg/kg intravenous dose range. It is advantageous in situations where a short span of action is required and has amnesic properties (Lingamchetty et al., 2021).

According to data extracted from New Zealand's Medsafe medication datasheet, a single milliliter (mL) dose of midazolam injection has 1 milligram (mg) and 5 milligrams of midazolam (Medsafe, 2019d). A single vial of midazolam injection of 1 milligram/milliliter (mg/mL) consists of 8 mg/mL sodium, and a single vial of midazolam injection of 5 milligram/milliliter (mg/mL) consists of 8 mg/mL sodium. Midazolam is a preoperative premedication in infants at a 0.5mg/kg oral dose for 30 minutes. It can serve as a sole intravenous induction agent at a 0.3mg/kg dose. However, it has a significant drawback of slow-onset duration that limits its utility. Flumazenil, a potent benzodiazepine antagonist, can be used to reverse the effects of midazolam.

II. The Benzodiazepine Anaesthetic Agents

Benzodiazepine is a medication commonly used for anxiety, insomnia treatment (Cloos & Ferreira, 2009), sedation in anesthesia (Cornett et al., 2018), and is also effective in the treatment of other medical conditions. They are often used as a remediation for anxiety reduction pre-anesthesia. Benzodiazepines appear to affect the neurotransmitters found in the brain, although their precise mechanism of action is unknown. Many Benzodiazepines are extensively distributed, adequately absorbed, and metabolized before their elimination from the body system. Several factors drive the use of the agent: reduced cost, availability, half-life, and route of administration. They are suitable for managing different symptoms that evolve during palliative care (Howard et al., 2014). Some of the commonly used Benzodiazepines are shown in Figure 3 and Table 2, respectively.

A Cross-section of the Benzodiazepine Anaesthetic Agents.

Benzodiazepines are split into several classes depending on their pharmacokinetics and chemical structure; however, they share a similar mechanism of action with closely related drugs with various clinical effects generated. In addition, the Benzodiazepine agents have different duration of action, times of impact, and potency. To obtain the desired clinical effect, some Benzodiazepine agents require repeated daily doses, while others need only a dose daily to function optimally. Also, numerous Benzodiazepine agents possess long-term active metabolites that can be amassed with repeated doses, particularly in patients with physical health issues, elderly patients, or those with genetic variants that cause low or no actions of crucial cytochrome P450 enzymes (Baldwin et al., 2013).

Approximate Equivalent PO Anxiolytic-Sedative Doses (Howard et al., 2014).

Drug	Dose (PO)
Diazepam	5mg
Lorazepam	500microgram
Clonazepam	250microgram
Temazepam	10mg
Nitrazepam	5mg
Alprazolam	0.5mg
Chlordiazepoxide	15mg
Oxazepam	15mg

- The Diazepam Agent

Diazepam is a popular rapid-action and potent anxiolytic drug with low toxicity, a broad therapeutic index, and an improved safety profile that can be used on pregnant, breastfeeding women, and elderly patients (Dhaliwal et al., 2021). It has sedation capabilities and can appear in different forms, such as intravenous, intramuscular injections (IM), oral tablets, or rectal gel. When intravenously administered, it has an onset of action between one to three minutes or 15 to 60 minutes if administered orally. The diazepam effect can last up to 12 hours (Dhaliwal et al., 2020).

It is an FDA-approved medication that can be used to manage spasticity caused by upper motor neuron disorders, anxiety disorders, and muscle spasms. It can also be used in adjunct therapy, relief of preoperative anxiety, and brief anxiety symptoms relief. Additionally, it can act as an adjunct in status epilepticus relief, severe recurrent convulsive seizure management, and some refractory epilepsy patients' management. They are also used in temporary spasticity treatment for children with cerebral palsy and for sedation in intensive care units. According to the New Zealand Medsafe datasheet, each 2mL of Diazepam ampoule comprises 10 mg of diazepam. It is colorless to a pale-yellow solution with a pH of 6.2 – 7.0 (Medsafe, 2022a). The usual adult dosage is 2-10 mg I.M., but for intravenous use, it can be repeated every three to four hours, depending on demand. Conventionally, the highest dosage recommended to be administered to an adult patient should not exceed 30 mg for eight hours (Dhaliwal et al., 2021).

- Lorazepam Agent

Lorazepam, also known as Ativan, is derived from ortho-chloro-phenyl. It is a pre-anesthetic agent administered through the mouth, intravenously, or through intramuscular injections (Ghiasi et al., 2021). For anti-recall and antianxiety use, a 0.04 to 0.06 mg/kg parental dosage of Lorazepam has recorded the utmost effectiveness in pre-anesthetic medication (Chung et al., 2008). The capability of Lorazepam to produce reliable anterograde amnesia and long duration of action gives it a predominant upper hand against other benzodiazepine agents. The drug can also be used as an adjuvant agent (i.e., delivered before the induction period) to reduce a patient's tendency to remember unpleasant experiences during anesthesia and surgery.

This agent is quite suitable in situations where a patient is intolerant of the appropriate depth of anesthesia to produce the required amnesic effect that relies solely on the anesthetic agent. This usually occurs in critically ill patients whose cardiovascular mechanisms are intolerant or inadaptability to a reasonable or deep concentration of inhaled anesthetic agents from the physiologic standpoint. It is not advisable to use the medication on outpatients due to its duration of action, although the metabolic activities of the drug are inactive. The administration of physostigmine can reverse the agent's adverse central nervous system actions (Schwerthöffer & Pajonk, 2018).

- Clonazepam Agent

Clonazepam is an integral part of the benzodiazepine family of drugs used as an anticonvulsant agent for panic attacks and seizure control. The drug's mechanism of action is to calm the overreactive chemicals found in the brain. It is used in pre-anesthesia to minimize anxiety before surgery or assist patients' post-surgery recovery (Zamiri et al., 2012). Surgery-induced stress can produce devastating fear in people, even in emergency cases. Events that lead to the emergency can cause patients-agitation and panic feelings. Thus, a calming agent like Clonazepam is needed to sedate patients and help prepare them for surgery.

Furthermore, since clonazepam is to slow down the brain's activities and reinforce the brain's neurotransmitters, it helps fade body tension by putting the patient's body in a relaxation mode. At the same time, the mind returns to a calmer mode. Consequently, anesthesia becomes more effective, and sedation occurs faster. After remaining still

and quiet for many days, Clonazepam assists the patient in healing and recovering quickly. According to the Waitemata District Health Board palliative care protocols, Clonazepam is presented in 1mg/ml ampoules, 2.5mg/ml oral drops with one drop equal to 0.1mg of the active ingredient, and 0.5mg or 2mg tablets (Health, 2016). Clonazepam's actions on patients last long and can be administered one dose a day of the bolus injection. The table below shows the amount of substance or dosage administered to patients depending on the medical condition, as extracted from the Waitemata District Health Board palliative care protocols document.

The Adult dosage of Clonazepam Agent (Basit & Kahwaji, 2021).

Indication	**Route**	**Stat & Starting PRN doses**	**Maximum dose Recommended**	**Range**
Terminal restlessness	Subcut	0.5mg q2hr	3mg	2 – 8mg in 24 hours duration
	Syringe driver (CSCI)	1mg	3mg	2 – 8mg over 24 hours
Neuropathic pain	PO	0.3 – 0.5mg (3 to 5 drops) q12hr or 0.25 – 0.5mg (tablets)	2mg	0.5 – 8mg/day divided doses
Restless legs	PO	0.3mg (3drops) q12hr or 0.25mg (tablets)	2mg	0.5 – 2mg nocte
Seizures	PO/Subcut	0.5 – 1mg	4mg	1 – 8mg/day divided doses
Panic disorder	PO	0.3mg (3drops) q12hr or 0.25mg (tablets)	2mg	0.5 – 4mg nocte

- Temazepam Agent

Temazepam is a short-action hypnotic agent used commonly to treat severe anxiety, panic disorders, and insomnia (Wegman et al., 2005). It is another class of benzodiazepine medication used for pre-anesthetic restlessness or anxiety treatment and post-surgery night's optimal quality sleep and quantity sleep aid (Simons et al., 2006). The night before surgery, it is administered as a single 20mg oral dose sedative agent that ensures quality night sleep devoid of significant residual effects. The short duration of action of temazepam enables fast postoperative recovery in adults, the elderly, and children. It is thus essential for performing short-duration surgery procedures that require quick recovery and immediate return to fitness (Caillat, 2017).

According to the New Zealand datasheet on temazepam (Medsafe, 2022b), the drug is also known as Normison. Each tablet of temazepam consists of 10mg of temazepam and is round, white, and biconvex with a stylized "S" embedded on one side of the drug and plain on the remaining side (Medsafe, 2022b). According to the document, it is administered 30-60 minutes before surgery or other procedures. As a hypnotic agent, temazepam 20mg is commonly administered to adults 1 hour and 30 minutes before retirement. A 10mg dose of Normison is recommended to be initially issued to critically ill patients or the elderly. The dosage is usually individualized to the least effective dose. However, a 10 to 30mg dose is the recommended range for adults. As a pre-mendicant, a 20-30mg dose administered within 30-60 minutes before the surgical operation or some other procedures is recommended.

III. The Benzodiazepines Antagonists

These are the class of drugs used for a fractional or total reversal of the sedative impacts produced by various benzodiazepine agents in different clinical settings, like in therapeutic procedures or administered in general anesthesia for diagnostic purposes (Braitberg, 2019). In other words, the antagonists are used to regenerate patients' sensitivity response and prevent the tolerance produced by the benzodiazepine agents (Albaugh et al., 2002). The prevalent and most commonly used benzodiazepine antagonist is flumazenil (Fassoulaki et al., 2010).

Flumazenil is a famous benzodiazepine antagonist with the clinical ability to reverse benzodiazepine overdose and fasten anesthesia or sedations driven by the benzodiazepine agents (Moore, 2004). Flumazenil functions by replacing the benzodiazepine receptor and reacting with the receptor. It is a competitive antagonist that competes with the benzodiazepine receptors and generates antagonist agents that are surmountable and reversible (Gropper et al., 2019). According to New Zealand's Medsafe datasheet, each 5mL ampoule of flumazenil consists of 0.5mg of flumazenil (Medsafe, 2020). And each 10mL ampoule of flumazenil consists of 1.0mg of flumazenil with a solution of flumazenil-Baxter prepared for injection consisting of approximately 3.5mg of sodium.

The flumazenil-Baxter is a sterile, colorless, almost-colorless clear solution used in anesthesia to terminate the general anesthesia driven or maintained by

benzodiazepines for patients in the operating rooms. They are also used to reverse paradoxical reactions caused by benzodiazepines, short-term diagnostic sedations, and therapeutic procedures for inpatients and outpatients. In intensive care units, they are vital in managing accidental overdose or self-poisoning of benzodiazepine. It is advised that the antagonist be administered intravenously by an experienced physician or anesthesiologist.

IV. Anesthetic Muscle Relaxants or Neuromuscular Blocking Agents

These anesthetic agents work to relax or weaken many body muscles without affecting the intestines and heart muscles. This enables surgeons to perform surgeries around the abdomen or other delicate and sensitive body parts. With the administration of muscle relaxants (see Figure), patients do not need to be profoundly anesthetized or receive a large number of anesthetic medications, thus minimizing the anesthesia side effects (Flamer & Peng, 2011).

A Cross-section of the Anaesthetic Muscle Relaxing Agents.

The neuromuscular blocking agents greatly facilitate an improved operational process and the enablement of tracheal intubation while ensuring muscle relaxation amid surgery. The patient's recovery from the neuromuscular blocking medications varies among patients because of the pharmacokinetics of a specific patient, the

administered adjuvant agents, differences in drug metabolism, and the duration of the medication dose. A standard muscle relaxant agent's duration of action must be controllable from a few minutes of action to hours of action which can be terminated quickly when necessary devoid of any side effects on the patient (Welch, 2017). The Table below is the summary of the neuromuscular blocking agents and their clinical properties.

Summary of the Neuromuscular Blocking Agents (Cook & Simons, 2021).

Drug	2 x ED mg/kg	Onset (min)	Offset (25% recovery) min
Amino steroids			
Rocuronium	0.6	1.0	43
Pancuronium	0.1	2.9	86
Vecuronium	0.1	2.4	44
Benzylisoquinolium diesters			
Mivacurium	0.15	1.8	16
Atracurium	0.4	2.5	38
Cis-atracurium	0.1	7.7	46
Quaternary amines			
Succinylcholine	1.0	0.75	7.6

- Rocuronium Neuromuscular Blocking Agent

This is a non-depolarizing muscle relaxant or neuromuscular blocker utilized in modern anesthesia to cause skeletal muscle relaxation and induce endotracheal intubation in mechanical ventilation or during surgical procedures (Jain et al., 2019). Rocuronium agent has a rapid to an intermediate period of action in operating theatres and is specified as a general anesthesia adjunct. The agent is given to patients by experienced clinicians or highly trained personnel overseen by qualified clinicians who are conversant with the utilization, characteristics, actions, and issues resulting from neuromuscular blocking agents (Bock et al., 2000).

Rocuronium is a solution for injection with a clear, colorless-to-pale brownish-yellow color of 3.8 to 4.2 pH value and 270 – 310 mosmol/kg osmolality (Medsafe, 2021b). Every vial with 2.5 mL solution consists of 50mg rocuronium bromide, and every vial with 10 mL solution consists of 100mg of the substance. The dose to be administered to a patient depends on that particular patient. However, a 0.6 mg/kg initial dose is required in tracheal intubation, while a dose range between 0.6 and 1.2 mg/kg is needed for rapid sequence intubation. On the other hand, the response to the initial

dose drives the administration of maintenance doses. The maintenance doses are not given to a patient until there is recovery evidence. In continuous infusion, an initial 10 to 12 mcg/kg/min rate is administered, beginning with evidence of intubation dose recovery, according to the FDA Accessdata on rocuronium bromide.

- Pancuronium Neuromuscular Blocking Agent

Pancuronium bromide is a non-depolarizing, long-action, and bis-quaternary aminosteroid neuromuscular blocking agent. In recent times, the use of pancuronium for neuromuscular blocking activities has drastically reduced due to the discovery of other intermediate-acting neuromuscular blocking agents like atracurium, rocuronium, vecuronium, cisatracurium and as well as its extended elimination period and context-sensitive half time (Das et al., 2021). On the Pharmacokinetic of pancuronium, it is a water-soluble compound and highly ionized at a physiologic pH. Pancuronium bromide cannot infiltrate the blood-brain barrier to affect the central nervous system due to its poor lipid solubility.

Pancuronium is usually administered to patients by intravenous bolus; however, in the management of critically ill patients, it may be administered through continuous intravenous infusion. A dose of 0.1 mg/kg of the substance is the usual intubation dosage with a three to five-minute onset to utmost muscle relaxation. A 0.07 mg/kg dose of the agent is required to attain a 95% effective dose, and the duration of action of the medication ranges from 60- to 90 minutes with a standard intubation dose. A 0.02 mg/kg dose of the agent titrated to the blockade level can be used to possibly maintain a neuromuscular blockade (Das et al., 2021).

- Vecuronium Neuromuscular Blocking Agent

Vecuronium Bromide is peripherally acting, steroidal, nonquaternary, nondepolarizing neuromuscular blocking medication with an intermediate duration of action (Kandasamy & Carlo IV, 2016). It is utilized during general anesthesia to enable endotracheal intubation to achieve surgical relaxation. The agent is used sparingly in intensive care units to induce paralysis in mechanical ventilation to achieve adequate patient sedation (Ramzy & McAllister, 2021). The agent is provided as a sterile nonpyrogenic freeze-dried protected cake of very fine tiny crystalline substances exclusively for intravenous injection.

A single vial of the agent consists of 10mg or 20mg of vecuronium bromide. Also, a single 10mg vial of the agent comprises 20.75mg citric acid anhydrous, 97 mg mannitol, sodium phosphate dibasic anhydrous of 16.25mg, phosphoric acid, and sodium hydroxide for buffering and adjusting to a 3.5 to 4.5 pH range. Due to the poor stability in the solution of the agent, it is prepared as a lyophilized powder. Thus, it has a very little shelf life in this state and requires reconstitution before administration. In a controlled setting prior to surgery, the endotracheal intubation dose ranges between 0.08 mg/kg - 0.1 mg/kg, or if succinylcholine is used before the administration of the agent, then the amount is between 0.04 mg/kg to 0.06 mg/kg intravenous (Ramzy & McAllister, 2021).

A dose range between 0.1 mg/kg to 0.2 mg/kg intravenous is required for rapid sequence intubation. In contrast, a dose range of 0.01 mg/kg - 0.015 mg/kg IV is needed for continued surgical relaxation maintenance, and it is administered between 20 – 45 minutes before the first dose and each 12 – 15 minutes as required. Furthermore, for continuous infusion maintenance, a bolus dose range from 0.08 mg/kg to 0.1 mg/kg IV is initially administered to the patient beginning from 20 minutes after recovery from bolus, and then 0.05 mg/kg/hour to 0.07 mg/kg/hour intravenous (IV) ((Ramzy & McAllister, 2021).

- Atracurium Neuromuscular Blocking Agent

Like the other aforementioned muscle-relaxing agents, Atracurium is a neuromuscular blocking medication that produces effective surgical paralysis (Trizotti et al., 2020). It is used in general anesthesia to induce endotracheal intubation that aids the relation of the skeletal muscle during mechanical ventilation or surgery in operating theatres. It is administered to patients intravenously through infusion or bolus and is not given to the patients intramuscularly because of the excessive irritation of the tissues (Ritz & Derian, 2018).

According to New Zealand's Medsafe datasheet, Atracurium is provided as an "Atracurium Besylate 10 mg/mL solution for injection", and each mL contains atracurium besylate 10mg (Medsafe, 2019b). It appears clear, faintly yellow, or colorless with an adjusted pH value between 3.2 to 7.7. For the initial dose, a 0.4 to 0.5 mg/kg dose range is recommended to be administered to most patients as an

intravenous bolus injection. After administration, an utmost neuromuscular blockade is expected to be achieved within 3 to 5 minutes. The initial dose often yields complete neuromuscular blockade within 20 to 35 minutes under balanced anesthesia.

A dose range of atracurium besylate between 0.08 to 0.10 mg/kg can be used to maintain neuromuscular blockade for prolonged surgical procedures. A duration of 20 to 45 minutes is usually needed to administer the first maintenance dose after the first primary atracurium dose. However, individual patients' responses and needs are determinants of the maintenance doses.

V. Relaxant Reversal Agents

These are neuromuscular blocking agents' antagonists. They are used to reverse the actions of the neuromuscular blocking medications with fast onset maximum effects devoid of cardiovascular and muscarinic adverse effects (Pani et al., 2015). A typical neuromuscular blocking antagonist could be administered to patients at any time after administering the muscular relaxing agent without causing muscarinic side effects (Srivastava & Hunter, 2009).

A Cross-section of the Relaxant Reversal Agents.

- Sugammadex Neuromuscular Blocking Agents Antagonist

Sugammadex is a selective relaxant binding class of agents that can undo residual paralysis by encapsulating the free circulation of the non-depolarizing muscle relaxants (Mirakhur, 2009). During surgery and general anesthesia in operating theatres, the availability of sugammadex gives clinicians better flexibility than using vecuronium and rocuronium anesthetic agents. The primary edge sugammadex has over other neuromuscular blocking antagonists is its patient rapid recovery time and its ability to efficiently reverse high levels of neuromuscular blockade in its initial dose (Fuchs-Buder et al., 2013).

An approximate 2mg.kg−1 dose of sugammadex is needed to reverse a shallow neuromuscular blockade induced by the neuromuscular blocking agents. A 4mg.kg−1 dose is required to reverse profound neuromuscular blockade. For the quick reversal of a neuromuscular blockade produced by a 1–1.2mg.kg^{-1} dosage of rocuronium, 16mg.kg^{-1} larger dose of sugammadex is administered three minutes post-rocuronium agent administration (Mirakhur, 2009).

- Neostigmine Neuromuscular Blocking Agents Antagonist

Neostigmine is a non-depolarizing neuromuscular blocking agent's antagonist that is used to reverse the neuromuscular blockade after surgery (Gropper et al., 2019). Also, Neostigmine can be used to treat after-operation urinary retention, intestinal atony, and myasthenia gravis treatment during severe exacerbations. It can be administered as an intravenous (IV), subcutaneous (SC), or intramuscular (IM) injection to patients in the operating rooms (Neely et al., 2021).

According to the New Zealand MedSafe documentation, for an adult patient, a dose between 0.5 to 2.5mg of Neostigmine should be simultaneously administered together with a 0.6-1.2mg of atropine sulphate in separate syringes through slow intravenous injection over one minute (Medsafe, 2019e). In children, a 0.05 mg/kg/dose of Neostigmine in conjunction with a 0.02 mg/kg/dose of atropine sulphate is suggested to be administered through intravenous injection in over one minute.

VI. Opioids Anaesthetic Agents

Narcotic analgesics or opioids are medications generally used in anesthesia as a primary anesthetic agent or pre-anesthetic medication, general anesthetic agent's

supplement, or systemic and spinal analgesia (Ferry & Dhanjal, 2018). They are mainly used during major surgical procedures, particularly surgical operations that deal with cardiovascular disease patients (Hug Jr, 1992). They are also commonly used in virtually every stage of surgical operations, including chronic pain control during the pre-induction process, anesthesia induction, and maintenance, immediate postoperative pain reduction, and agitation minimization.

A Cross-section of the Opioids Anaesthetic Agents.

Furthermore, opioids can be administered to patients intravenously, orally, intrathecal, enteral, subcutaneous, transdermal, aerosolized, and epidural. For the anesthetic use of opioids, the main route of administration is intravenous, which could be continuous infusion or repeat injections. The most commonly used opioids are morphine, fentanyl, hydromorphone, remifentanil, sufentanil, alfentanil, and meperidine (Ferry & Dhanjal, 2021).

- Fentanyl Opioid Anaesthetic Agent

Fentanyl belongs to the class of narcotic analgesics used for pre-and post-surgery pain relief in operating theatres (Armenian et al., 2018). Fentanyl has the edge over other agents that belong to the same category as it possesses rapid serum clearance abilities,

the least histamine release, and high potency. It can rapidly permeate the blood-brain barrier and induce analgesia within one to two minutes of administration (Roberts, 2017).

According to the New Zealand's MedSafe data sheet, a single 2ml ampoule of fentanyl injection consists as fentanyl citrate, 100mg of fentanyl and a single 10ml ampoule of fentanyl injection contains as fentanyl citrate, 500mg of fentanyl (Medsafe, 2019c). It appears as a particle-free, colorless, and clear solution with a 4.0-7.5 pH range. It is administered to patients according to an individual requirement with respect to body weight, fundamental pathological condition, age, physical status, use of other prescriptions, the surgical procedure involved, and the type of anesthesia to be utilized.

- Morphine Opioid Anaesthetic Agent

Morphine agent is a highly efficacious medication for treating mild to acute pain and serves as a yardstick for measuring other similar agents (Cadavid-Puentes et al., 2017). Also, morphine is used for preoperative anxiety reduction, sedation inducement, and reduction of anesthetic dose in operating theatres. It is also effective in the treatment of pulmonary oedema and myocardial infarction due to the bradycardic and vasodilatory effects of the agent (Hill et al., 2020).

It appears as a colorless, clear, or almost colorless solution for injection. For slow intravenous use, morphine is administered to adults when rapid action of onset is required. A range of 2.5 to 15mg dosage is normally administered to adult patients slowly over four to five minutes. For a continuous intravenous infusion, morphine is administered according to the analgesic needs of a patient and the prior opiate experience of the patient. For severe pain management through intravenous infusion, a dose range of 0.5 to 2.0 mg/hour can be continued on a majority of adults without prior history of opioid consumption after the establishment of adequate analgesia, according to the New Zealand MedSafe data sheet on Morphine Sulphate (Medsafe, 2021a).

- Remifentanil Opioid Anaesthetic Agent

Remifentanil is a member of the opioid family that is clinically flexible and can be used in sedation for naturally inhaling patients undergoing painful operations and for

intravenous analgesia (Scott & Perry, 2005). With remifentanil, deep analgesia can be obtained with negligible effects on cognitive function and can also facilitate analgesia and sedation during regional anesthetic block placement together with topical anesthesia and as well as airway nerve blocks (Beers & Camporesi, 2004).

Furthermore, sedation through analgesia, having remifentanil as the opioid agent, is an essential choice in the ICU settings for mechanically ventilated patients. The distinct properties of remifentanil, such as rapid offset of action, absence of accumulation, and organ-independent metabolism, make it unique from other similar competing opioid agents (Battershill & Keating, 2006). A single vial of remifentanil-AFT 1mg consists of 1mg of remifentanil, single vial of remifentanil-AFT 2mg consists of 2mg of remifentanil and single vial of remifentanil-AFT 5mg consists of 5mg of remifentanil. Remifentanil-AFT appears as a powder for injection or as a white to off-white freeze-dried powder. In general anesthesia, remifentanil-AFT must be administered by an experienced clinician according to an individual patient's needs and response and is not recommended as the only agent in general anesthesia.

- Hydromorphone Opioid Anaesthetic Agent

Hydromorphone agent is a semi-synthetic opioid class of medication used to treat or manage mild to chronic pain. It can be administered to patients orally, subcutaneously, intramuscular, intrathecal, epidural, intravenously, or through other means. It appears as a solution, powder, modified-release tablet, and immediate-release tablet. Hydromorphone is extremely similar to morphine structurally, except for the presence of some substances that are not found in morphine (Murray & Hagen, 2005).

Due to the high potency, overdose risk, and potential for abuse of hydromorphone, it is prescribed only when treatments with other first-line agents fail. Hydromorphone has an onset of action at a range of 15 to 30 minutes for immediate-release oral formulations, peaks between 30 to 60 minutes, and lasts between three to four hours. On the other hand, hydromorphone has an onset of action at 6 hours for extended-release formulations with 9 hours peak and lasts up to 13 hours (Abi-Aad & Derian, 2017).

VII. Opioid Antagonists

These agents reverse the actions of the opioid drugs used in operating theatres. Opioid reversal drugs play essential roles in the reversal of acute opioid overdose, respiratory depression, alcohol, and opioid relapse prevention, constipation caused by opioids or pruritus induced by cholestasis, and perhaps, chronic renal failure (Theriot et al., 2019). In the operating rooms, the postoperative administration of a shallow dose of opioid antagonists like Nalmefene and Naloxone potentiates the actions of opioids such as morphine or minimizes the detrimental actions of the opioid drugs (Barnett et al., 2014). Figure 4 below shows commonly used opioid antagonist agents.

A Cross-section of the Opioid Antagonists.

- The Naloxone Opioid Antagonist

Naloxone is an opioid antagonist that reverses the respiratory depression induced by the use of opioids. It acts by blocking the opioid agents from attacking the opioid receptors found in the brain. It is useful in operating theatres to reverse the actions of anesthetic medications such as fentanyl, heroin, and carfentanil. The agent can be delivered by medical professionals or trained paramedics through intramuscular injection by means of ampoules, subcutaneously, intranasal spray, or pre-filled syringes.

In New Zealand, the drug appears as a solution for injection with 400 micrograms/mL of Naloxone Hydrochloride (Kosmetik, 2017). Each mL solution of naloxone hydrochloride infusion or injection consists of 3.54mg of sodium. In terms of color, it appears as a colorless and clear solution devoid of observable particles. The utmost fast onset of action of naloxone is obtainable through intravenous infusion, and it is ideal for emergencies. In adult opioid overdose, a range of 0.4mg to 2mg of naloxone hydrochloride dose may be intravenously administered initially and can be repeated at a 2-to-3-minute gap if the required amount of improvement and counteraction is not achieved.

On the other hand, naltrexone blocks the actions of narcotic agents, and it is used to prevent the relapse of adults under the influence of opioid medications. In addition, naltrexone injection plays a vital role in the reduction of the urge for alcohol consumption and the treatment of alcoholism, although not a permanent cure for alcoholism or drug addictions (Nunes et al., 2018). When compared with naloxone, naltrexone is well suited for prolonged antagonism, while naloxone is better for sedation reversals induced with opioids (Kunøe et al., 2014).

- Methylnaltrexone Opioid Antagonist

Methylnaltrexone is another type of opioid antagonist used to manage and treat peripheral effects like constipation caused by opioids without having any effect on the core functions of opioid analgesia, such as pain relief (Garnock-Jones & McKeage, 2010). In other words, without inducing precipitating withdrawal of opioids in patients that have complex medical problems or interfering with the actions of the core anesthesia, methylnaltrexone acts by blocking the opioid peripheral activities that occur within intestinal smooth muscle.

Methylnaltrexone is administered to patients in the form of a subcutaneous injection through the abdomen, upper arm, or thigh. A single dose of the opioid antagonist is provided in a single-use vial that consists of 0.6mL water and 12mg methylnaltrexone. The medication is administered according to a specific patient's weight. It is recommended to administer 0.15 mg/kg dose to patients under 38kg, 8mg dose to patients in the weight range of 38 – 61 kg, 12mg dose to patients whose weights are

between 62 – 114 kg, and 0.15mg/kg dose to patients above 114 kg weight (Slatkin et al., 2009).

VIII. Vasopressor Anaesthetic Agents

The vasopressors are vasoactive agents or categories of medications used to generate or elevate vasoconstriction, which causes systemic vascular resistance (SVR) increment in patients. The increase of systemic vascular resistance in patients causes the mean arterial pressure (MAP) to increment, and the body organs' perfusion increases (VanValkinburgh et al., 2018). The drugs can be administered through an intravenous route, and a continuous infusion is the primary method of choice that permits instant titration for the required action. The medications under this class can be used in obstetrics for post-neuraxial anesthesia hypotension counteraction (Nag et al., 2015). The most commonly used vasopressor agents(Kellum & Pinsky, 2002) are Dopamine, Epinephrine, Norepinephrine, Vasopressin, Dobutamine, and Phenylephrine which will be examined separately below.

Cross-section of the Vasopressors Anaesthetic Agents.

- Dopamine Agent

Dopamine belongs to the many endogenous catecholamines that work as neurotransmitters inside the autonomic and central nervous systems. Dopamine synthesis occurs in the central nervous system neurons and, specifically, the ventral tegmental region, substantia nigra, and adrenal medulla (Freeman & Berger, 2014).

Dopamine medication appears as a solution for injection with sterile dopamine concentrate BP as the identifier with 200mg/5ml amount of substance. To prevent the accidental administration of an unintended bolus of dopamine substance, the amount of dopamine given to patients is controlled, and regular therapy evaluation is conducted. The drug is delivered to patients through veins to minimize the extravasation risk into nearby tissues that can trigger necrosis. Also, the drug is intravenously administered to patients via needles or intravenous catheter after dilution, and it is necessary to control the quantity of the drug flow per minute into the patient's vein using an intravenous drip chamber or other appropriate metering tools according to the New Zealand Medsafe datasheet (Medsafe, 2021c).

- Epinephrine Agent

Epinephrine is a vasopressor anesthetic agent that is used as an adjuvant medication to local anesthetics (LAs) for sensory nerve blockade elongation and systemic LA uptake delay, thereby minimizing anesthetic toxicity risk. From investigations, a combination of epinephrine and intrathecal LAs extends analgesia duration for about 30 minutes, and the combination of epinephrine and locoregional LAs prolongs analgesia duration for about 60 minutes (Tschopp et al., 2018).

Epinephrine, also known as adrenaline, is a colorless, clear solution for injection that can be delivered to patients intramuscularly in an auto-injector, i.e., automatic injection devices that can be disposed of or pre-filled injectors. A patient's body weight determines the appropriate dosage strength of epinephrine that can be administered to the patient. For adult patients greater than or equal to 30kg, an EpiPen auto-injector that consists of 0.3mg of adrenaline injection delivered intramuscularly is required. For infants between the weight range of 15 to 30kg, EPIPEN JR, which consists of 0.15mg of adrenaline injection delivered intramuscularly, is required according to the New Zealand Medsafe datasheet (Medsafe, 2019a).

- Phenylephrine Agent

The phenylephrine appears as phenylephrine hydrochloride and is used intravenously to increase blood pressure in adult patients with significant clinical hypotension, resulting primarily from vasodilation in anesthetic or septic shock settings. Phenylephrine is a preferred vasopressor in the spinal anesthetic setting as it has demonstrated effectiveness in counterbalancing the hypotension that is commonly encountered by obstetric patients (Richards et al., 2021).

Phenylephrine is administered to patients commonly through intranasal, intravenous, ophthalmic, topical, rectal, or oral routes. Less often, phenylephrine is given to patients as an adjunct to peripheral nerve blockade in the epidural space, in the intravenous space, subcutaneously, and intramuscularly. In the intravenous administration of phenylephrine, a dose range of 50 to 100 mcg of aliquots is normally required, and redosing is frequently needed due to the short onset action and brief action duration of the drug (Richards et al., 2021).

IX. Hypotensive Anaesthetic Agents

Hypotensive anesthesia is a strategy for controlling or lowering patients' blood pressure during anesthesia. The patients' blood pressure reduction in anesthesia can be accomplished in different ways. An ideal hypotensive reduction agent in anesthesia should be administered easily with a reduced onset time and be meticulously controllable. Its action can rapidly vanish when discontinued without adverse or undesirable effects (Barak et al., 2015).

Cross-section of the Hypotensive Anaesthetic Agents.

In recent times, several hypotensive medications (see Figure 5) that have different working mechanisms and lengths of action for hypotensive anesthesia have emerged. These hypotensive agents can be combined with other medications to minimize the dosage of each drug or reduce the other drugs' adverse effects. The agents can also be used alone, and they are sodium nitroprusside (SNP), calcium channel antagonists, nitroglycerin (NTG), β-adrenoceptor antagonists, trimethaphan, α2-adrenoceptor agonists and angiotensin-converting enzyme (ACE) inhibitors (Barak et al., 2015).

- The Sodium Nitroprusside Hypotensive Agent

Sodium nitroprusside (SNP) is an agent used to control and manage severe hypertension. It is an active vasodilator and can be given to patients through the intravenous drip or infusion route with rigorous monitoring. The evanescent activity of the agent makes it appropriate for hypotension control in general anesthesia (Ranadive et al., 2017).

Sodium nitroprusside is commonly administered via intravenous infusion with a 0.5µg/kg/min initial dose titrated to the desired effect with a 10µg/kg/min maximum dose to induce blood pressure control for a short period. SNP effect is required in clinician conditions where it is urgent to reduce a patient's blood pressure, and the

action of the agent is felt within minutes. This implies that the agent is keenly monitored when administered to patients in order to circumvent the hypo-perfusion rapid onset or potential hypotension that is life-threatening. These characteristics of SNP typically restrict its use to therapies with a short duration in the ICU, operating rooms, cardiac care unit, or other units where experienced clinicians can provide continuous close monitoring (Hottinger et al., 2014).

- The Nitroglycerin Hypotensive Agent

The hypotensive mechanism of action of nitroglycerin (NTG) is similar to that of SNP as both agents have rapid and vigorous onset of vasodilatation that is driven by nitric oxide. However, the NTG and SNP have different effects on coronary blood flow, and NTG is mainly a vasodilator, while SNP is both an arteria and vasodilator. When administered intravenously, NTG causes blood pressure reduction by cutting down the sum of peripheral venous return or resistance (Barak et al., 2015).

Furthermore, other hypotensive agents, such as the β-adrenoceptor antagonists, are used to effectively induce hypotensive anesthesia during maxillofacial procedures. They can be given to patients as a standalone agent or combined with SNP. Different β-antagonists are in clinical use; however, their selectivity for β-adrenoreceptors and duration of action differs. On the other hand, calcium channel antagonist hypotensive agents like nicardipine or nifedipine are commonly used to induce hypotension (Barak et al., 2015).

X. Local Anaesthetic Agents

Local anesthetics (LAs) are medications (see

) that are used to inhibit pain sensation in the body parts where they are administered. In recent times, there are several procedures that can be painlessly and safely carried out while a patient remains awake. Local anesthesia is typically a one-time medical injection that eliminates feelings from a section of the body. It is essential for procedures involving breast biopsy, skin biopsy, broken bone repair, or deep-cut stitching. In these procedures, the patient is usually awake and alert and may experience some pressure but will not feel pains in the body part being treated (Catterall & Mackie, 2011).

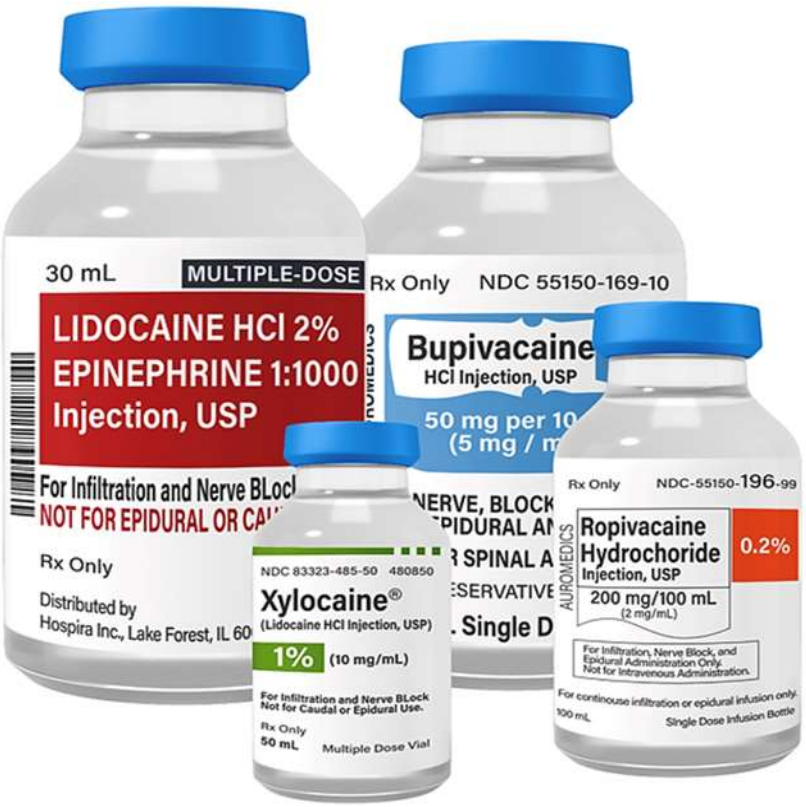

A Cross-section of Local Anesthetics Agents.

XI. The Anticholinergic Agents

Anticholinergics are widely used in operating theatres prior to anesthesia or Parkinson's disease symptomatic control; prophylactic for motion sickness prevention; atypical heart slowing when poisoned with organophosphates or other cholinergic medications; peptic ulcer treatment and irritable bowel syndrome. Anticholinergic agents are typically used to inhibit the activation of muscarinic acetylcholine receptors or nicotinic mediated by the acetylcholine (Gray & Ray, 2014). A collection of anticholinergics is shown below:

A Cross-section of Anticholinergic Agents.

XII. The Anti-Emetics

The antiemetic agents are used to prevent postoperative nausea and vomiting (PONV), which is among the typical and main issues encountered by patients after surgical operations. Patients suffer PONV during the initial 24 hours postoperative, with the peak encountered immediately after procedures (Weibel et al., 2020). PONV is one of the main post-anesthesia patient dissatisfaction inducers, and three main classes of antiemetic medication have similar potency used to treat PONV. The agent's categories are corticosteroids (e.g., dexamethasone), serotonin antagonists (e.g., ondansetron), and dopamine antagonists (e.g., droperidol). The Figure below shows a set of antiemetics, and the Table shows the antiemetic drug classes, their mode of administration, dose, and timing (Pierre & Whelan, 2013).

A Cross-section of Anti-Emetics.

The Dose Recommendation of Antiemetic Agents for Prophylaxis in Matured Patients (Athavale et al., 2020).

	Generic name	Administered Route	Dose (mg)	Timing of administration
First-class	Dexamethasone	I.V.	4–8	Induction
	Ondansetron	I.V.	4	Induction
	Droperidol	I.V.	0.625–1.25	End of surgery
	Palonosetron	I.V.	0.075	Induction
	Aprepitant	Oral	40	Before induction
Second-class	Dimenhydrinate	I.V.	50	Induction
	Metoclopramide	I.V.	25–50	Induction
	Scopolamine	Transdermal	1	The night before/day of surgery

Appendix B -- Threshold: Sodium Chloride against other samples

Drug Name	Similarity Score	T10	T20	T30	T40	T50	T60	T70	T80	T90	T100
Frusemide-Claris 20mg	38%	T	T	T	F	F	F	F	F	F	F
Water For Injections 10mL	34%	T	T	T	F	F	F	F	F	F	F
Paracetamol 1000mg/100mL	34%	T	T	T	F	F	F	F	F	F	F
Fresofol 1% MCT/LCT	37%	T	T	T	F	F	F	F	F	F	F
Amoxicillin 1g	40%	T	T	T	F	F	F	F	F	F	F
Hydrocortisone sodium 100mg	39%	T	T	T	F	F	F	F	F	F	F
Cefazolin Sodium 1g	42%	T	T	T	T	F	F	F	F	F	F
Atracurium Besylate 50mg	35%	T	T	T	F	F	F	F	F	F	F
Naloxone HCl 400mg in 1mL	42%	T	T	T	T	F	F	F	F	F	F
Morphine Sulfate Injection 10mg	34%	T	T	T	F	F	F	F	F	F	F
Ondansetron Solution	37%	T	T	T	F	F	F	F	F	F	F
Protamine Sulfate 10mg/ml	37%	T	T	T	F	F	F	F	F	F	F
Vecuronium Bromide	25%	T	T	F	F	F	F	F	F	F	F
Potassium Chloride 10mmol	45%	T	T	T	T	F	F	F	F	F	F
Heparin Injection 25000IU	35%	T	T	T	F	F	F	F	F	F	F
Sugammadex 200mg/2ml	33%	T	T	T	F	F	F	F	F	F	F
Protamine Sulphate 50mg in 5ml	35%	T	T	T	F	F	F	F	F	F	F
Sodium Chloride 10ml	46%	T	T	T	T	F	F	F	F	F	F
Remifentanil-AFT 2g	39%	T	T	T	F	F	F	F	F	F	F
Sedative Midazolam 5mg	29%	T	T	F	F	F	F	F	F	F	F
Glyceryl Trinitrate 10mg in 10ml	35%	T	T	T	F	F	F	F	F	F	F
Fentanyl Citrate 785 micrograms	40%	T	T	T	F	F	F	F	F	F	F
Cefazolin-AFT 1g	42%	T	T	T	T	F	F	F	F	F	F
Dynastat 40 mg	34%	T	T	T	F	F	F	F	F	F	F
Tranexamic-AFT	39%	T	T	T	F	F	F	F	F	F	F
Calcium Chloride 1g in 10mL	39%	T	T	T	F	F	F	F	F	F	F
Provive MCT-LCT 1%	40%	T	T	T	F	F	F	F	F	F	F
METOPROLOL Mylan 5mg	32%	T	T	T	F	F	F	F	F	F	F
Noradrenaline 4mL	34%	T	T	T	F	F	F	F	F	F	F
Lidocaine-Claris 5ml	36%	T	T	T	F	F	F	F	F	F	F
Atropine Injection 600Ug	25%	T	T	F	F	F	F	F	F	F	F
Xylocaine 1%	19%	T	F	F	F	F	F	F	F	F	F
Sodium Chloride 0.9%	**100%**	**T**	**T**	**T**	**T**	**T**	**T**	**T**	**T**	**T**	**F**
Hypnomidate 10mL	39%	T	T	T	F	F	F	F	F	F	F
Adrenaline Injection 1mg	27%	T	T	F	F	F	F	F	F	F	F
Sterile Dopamine 200mg/5ml	36%	T	T	T	F	F	F	F	F	F	F
Suxamethonium 100mg in 2 ml	46%	T	T	T	T	F	F	F	F	F	F
Amiodarone HCL 50 mg/ml	40%	T	T	T	F	F	F	F	F	F	F
Primacor Injection 10mL	37%	T	T	T	F	F	F	F	F	F	F
Sugammadex 200 mg/2ml	36%	T	T	T	F	F	F	F	F	F	F
Rocuronium Bromide 50 mg	31%	T	T	T	F	F	F	F	F	F	F
Clonidine HCl 150 ug/1mL	29%	T	T	F	F	F	F	F	F	F	F
Cyclizine Lactate 50	35%	T	T	T	F	F	F	F	F	F	F
PITRESSIN 20 Units in 1 mL	31%	T	T	T	F	F	F	F	F	F	F
Magnesium Sulfate 2.47g	40%	T	T	T	F	F	F	F	F	F	F
Metaraminol 10mg/mL	33%	T	T	T	F	F	F	F	F	F	F
Dalacin Phosphate 600 mg/4 mL	28%	T	T	F	F	F	F	F	F	F	F
Pancuronium Inresa 4mg/2ml	35%	T	T	T	F	F	F	F	F	F	F
Ephedrine Hydrochloride 30mg	32%	T	T	T	F	F	F	F	F	F	F
Dexamethasone Phosphate 4mg	32%	T	T	T	F	F	F	F	F	F	F
Glycopyrronium and Neostigmine	38%	T	T	T	F	F	F	F	F	F	F
Actrapid Penfill 3mL	33%	T	T	T	F	F	F	F	F	F	F

Threshold: Frusemide-Claris against other samples

Drug Name	Similarity Score	T10	T20	T30	T40	T50	T60	T70	T80	T90	T100
Frusemide-Claris 20mg	**100%**	**T**	**T**	**T**	**T**	**T**	**T**	**T**	**T**	**T**	**F**
Water For Injections 10mL	41%	T	T	T	T	F	F	F	F	F	F
Paracetamol 1000mg/100mL	55%	T	T	T	T	T	F	F	F	F	F
Fresofol 1% MCT/LCT	40%	T	T	T	F	F	F	F	F	F	F
Amoxicillin 1g	44%	T	T	T	T	F	F	F	F	F	F
Hydrocortisone sodium 100mg	47%	T	T	T	T	F	F	F	F	F	F
Cefazolin Sodium 1g	51%	T	T	T	T	T	F	F	F	F	F
Atracurium Besylate 50mg	46%	T	T	T	T	F	F	F	F	F	F
Naloxone HCl 400mg in 1mL	30%	T	T	F	F	F	F	F	F	F	F
Morphine Sulfate Injection 10mg	34%	T	T	T	F	F	F	F	F	F	F
Ondansetron Solution	61%	T	T	T	T	T	T	F	F	F	F
Protamine Sulfate 10mg/ml	48%	T	T	T	T	F	F	F	F	F	F
Vecuronium Bromide	38%	T	T	T	F	F	F	F	F	F	F
Potassium Chloride 10mmol	40%	T	T	T	F	F	F	F	F	F	F
Heparin Injection 25000IU	40%	T	T	T	F	F	F	F	F	F	F
Sugammadex 200mg/2ml	45%	T	T	T	T	F	F	F	F	F	F
Protamine Sulphate 50mg in 5ml	47%	T	T	T	T	F	F	F	F	F	F
Sodium Chloride 10ml	51%	T	T	T	T	T	F	F	F	F	F
Remifentanil-AFT 2g	38%	T	T	T	F	F	F	F	F	F	F
Sedative Midazolam 5mg	39%	T	T	T	F	F	F	F	F	F	F
Glyceryl Trinitrate 10mg in 10ml	41%	T	T	T	T	F	F	F	F	F	F
Fentanyl Citrate 785 micrograms	38%	T	T	T	F	F	F	F	F	F	F
Cefazolin-AFT 1g	42%	T	T	T	T	F	F	F	F	F	F
Dynastat 40 mg	48%	T	T	T	T	F	F	F	F	F	F
Tranexamic-AFT	54%	T	T	T	T	T	F	F	F	F	F
Calcium Chloride 1g in 10mL	44%	T	T	T	T	F	F	F	F	F	F
Provive MCT-LCT 1%	40%	T	T	T	F	F	F	F	F	F	F
METOPROLOL Mylan 5mg	47%	T	T	T	T	F	F	F	F	F	F
Noradrenaline 4mL	36%	T	T	T	F	F	F	F	F	F	F
Lidocaine-Claris 5ml	48%	T	T	T	T	F	F	F	F	F	F
Atropine Injection 600Ug	35%	T	T	T	F	F	F	F	F	F	F
Xylocaine 1%	27%	T	T	F	F	F	F	F	F	F	F
Sodium Chloride 0.9%	43%	T	T	T	T	F	F	F	F	F	F
Hypnomidate 10mL	43%	T	T	T	T	F	F	F	F	F	F
Adrenaline Injection 1mg	32%	T	T	T	F	F	F	F	F	F	F
Sterile Dopamine 200mg/5ml	36%	T	T	T	F	F	F	F	F	F	F
Suxamethonium 100mg in 2 ml	46%	T	T	T	T	F	F	F	F	F	F
Amiodarone HCL 50 mg/ml	53%	T	T	T	T	T	F	F	F	F	F
Primacor Injection 10mL	43%	T	T	T	T	F	F	F	F	F	F
Sugammadex 200 mg/2ml	39%	T	T	T	F	F	F	F	F	F	F
Rocuronium Bromide 50 mg	34%	T	T	T	F	F	F	F	F	F	F
Clonidine HCl 150 ug/1mL	37%	T	T	T	F	F	F	F	F	F	F
Cyclizine Lactate 50	43%	T	T	T	T	F	F	F	F	F	F
PITRESSIN 20 Units in 1 mL	40%	T	T	T	F	F	F	F	F	F	F
Magnesium Sulfate 2.47g	39%	T	T	T	F	F	F	F	F	F	F
Metaraminol 10mg/mL	46%	T	T	T	T	F	F	F	F	F	F
Dalacin Phosphate 600 mg/4 mL	35%	T	T	T	F	F	F	F	F	F	F
Pancuronium Inresa 4mg/2ml	40%	T	T	T	F	F	F	F	F	F	F
Ephedrine Hydrochloride 30mg	35%	T	T	T	F	F	F	F	F	F	F
Dexamethasone Phosphate 4mg	48%	T	T	T	T	F	F	F	F	F	F
Glycopyrronium and Neostigmine	49%	T	T	T	T	F	F	F	F	F	F
Actrapid Penfill 3mL	39%	T	T	T	F	F	F	F	F	F	F

Threshold: Morphine Sulphate against other samples

Drug Name	Similarity Score	T10	T20	T30	T40	T50	T60	T70	T80	T90	T100
Frusemide-Claris 20mg	34%	T	T	T	F	F	F	F	F	F	F
Water For Injections 10mL	53%	T	T	T	T	T	F	F	F	F	F
Paracetamol 1000mg/100mL	24%	T	T	F	F	F	F	F	F	F	F
Fresofol 1% MCT/LCT	51%	T	T	T	T	T	F	F	F	F	F
Amoxicillin 1g	35%	T	T	T	F	F	F	F	F	F	F
Hydrocortisone sodium 100mg	42%	T	T	T	T	F	F	F	F	F	F
Cefazolin Sodium 1g	37%	T	T	T	F	F	F	F	F	F	F
Atracurium Besylate 50mg	51%	T	T	T	T	T	F	F	F	F	F
Naloxone HCl 400mg in 1mL	49%	T	T	T	T	F	F	F	F	F	F
Morphine Sulphate Injection 10mg	**100%**	**T**	**T**	**T**	**T**	**T**	**T**	**T**	**T**	**T**	**F**
Ondansetron Solution	38%	T	T	T	F	F	F	F	F	F	F
Protamine Sulfate 10mg/ml	61%	T	T	T	T	T	T	F	F	F	F
Vecuronium Bromide	39%	T	T	T	F	F	F	F	F	F	F
Potassium Chloride 10mmol	41%	T	T	T	T	F	F	F	F	F	F
Heparin Injection 25000IU	54%	T	T	T	T	T	F	F	F	F	F
Sugammadex 200mg/2ml	52%	T	T	T	T	T	F	F	F	F	F
Protamine Sulphate 50mg in 5ml	55%	T	T	T	T	T	F	F	F	F	F
Sodium Chloride 10ml	58%	T	T	T	T	T	F	F	F	F	F
Remifentanil-AFT 2g	41%	T	T	T	T	F	F	F	F	F	F
Sedative Midazolam 5mg	53%	T	T	T	T	T	F	F	F	F	F
Glyceryl Trinitrate 10mg in 10ml	46%	T	T	T	T	F	F	F	F	F	F
Fentanyl Citrate 785 micrograms	45%	T	T	T	T	F	F	F	F	F	F
Cefazolin-AFT 1g	41%	T	T	T	T	F	F	F	F	F	F
Dynastat 40 mg	47%	T	T	T	T	F	F	F	F	F	F
Tranexamic-AFT	44%	T	T	T	T	F	F	F	F	F	F
Calcium Chloride 1g in 10mL	49%	T	T	T	T	F	F	F	F	F	F
Provive MCT-LCT 1%	51%	T	T	T	T	T	F	F	F	F	F
METOPROLOL Mylan 5mg	48%	T	T	T	T	F	F	F	F	F	F
Noradrenaline 4mL	36%	T	T	T	F	F	F	F	F	F	F
Lidocaine-Claris 5ml	49%	T	T	T	T	F	F	F	F	F	F
Atropine Injection 600Ug	42%	T	T	T	T	F	F	F	F	F	F
Xylocaine 1%	44%	T	T	T	T	F	F	F	F	F	F
Sodium Chloride 0.9%	40%	T	T	T	F	F	F	F	F	F	F
Hypnomidate 10mL	50%	T	T	T	T	F	F	F	F	F	F
Adrenaline Injection 1mg	47%	T	T	T	T	F	F	F	F	F	F
Sterile Dopamine 200mg/5ml	44%	T	T	T	T	F	F	F	F	F	F
Suxamethonium 100mg in 2 ml	53%	T	T	T	T	T	F	F	F	F	F
Amiodarone HCL 50 mg/ml	47%	T	T	T	T	F	F	F	F	F	F
Primacor Injection 10mL	50%	T	T	T	T	F	F	F	F	F	F
Sugammadex 200 mg/2ml	47%	T	T	T	T	F	F	F	F	F	F
Rocuronium Bromide 50 mg	65%	T	T	T	T	T	T	F	F	F	F
Clonidine HCl 150 ug/1mL	51%	T	T	T	T	T	F	F	F	F	F
Cyclizine Lactate 50	45%	T	T	T	T	F	F	F	F	F	F
PITRESSIN 20 Units in 1 mL	56%	T	T	T	T	T	F	F	F	F	F
Magnesium Sulfate 2.47g	63%	T	T	T	T	T	T	F	F	F	F
Metaraminol 10mg/mL	48%	T	T	T	T	F	F	F	F	F	F
Dalacin Phosphate 600 mg/4 mL	46%	T	T	T	T	F	F	F	F	F	F
Pancuronium Inresa 4mg/2ml	37%	T	T	T	F	F	F	F	F	F	F
Ephedrine Hydrochloride 30mg	46%	T	T	T	T	F	F	F	F	F	F
Dexamethasone Phosphate 4mg	58%	T	T	T	T	T	F	F	F	F	F
Glycopyrronium and Neostigmine	45%	T	T	T	T	F	F	F	F	F	F
Actrapid Penfill 3mL	49%	T	T	T	T	F	F	F	F	F	F

Threshold: Ondansetron Solution against other samples

Drug Name	Similarity Score	T10	T20	T30	T40	T50	T60	T70	T80	T90	T100
Frusemide-Claris 20mg	61%	T	T	T	T	T	T	F	F	F	F
Water For Injections 10mL	41%	T	T	T	T	F	F	F	F	F	F
Paracetamol 1000mg/100mL	33%	T	T	T	F	F	F	F	F	F	F
Fresofol 1% MCT/LCT	38%	T	T	T	F	F	F	F	F	F	F
Amoxicillin 1g	47%	T	T	T	T	F	F	F	F	F	F
Hydrocortisone sodium 100mg	43%	T	T	T	T	F	F	F	F	F	F
Cefazolin Sodium 1g	40%	T	T	T	F	F	F	F	F	F	F
Atracurium Besylate 50mg	38%	T	T	T	F	F	F	F	F	F	F
Naloxone HCl 400mg in 1mL	37%	T	T	T	F	F	F	F	F	F	F
Morphine Sulfate Injection 10mg	38%	T	T	T	F	F	F	F	F	F	F
Ondansetron Solution	**100%**	**T**	**T**	**T**	**T**	**T**	**T**	**T**	**T**	**T**	**F**
Protamine Sulfate 10mg/ml	51%	T	T	T	T	T	F	F	F	F	F
Vecuronium Bromide	35%	T	T	T	F	F	F	F	F	F	F
Potassium Chloride 10mmol	39%	T	T	T	F	F	F	F	F	F	F
Heparin Injection 25000IU	42%	T	T	T	T	F	F	F	F	F	F
Sugammadex 200mg/2ml	46%	T	T	T	T	F	F	F	F	F	F
Protamine Sulphate 50mg in 5ml	49%	T	T	T	T	F	F	F	F	F	F
Sodium Chloride 10ml	46%	T	T	T	T	F	F	F	F	F	F
Remifentanil-AFT 2g	42%	T	T	T	T	F	F	F	F	F	F
Sedative Midazolam 5mg	37%	T	T	T	F	F	F	F	F	F	F
Glyceryl Trinitrate 10mg in 10ml	46%	T	T	T	T	F	F	F	F	F	F
Fentanyl Citrate 785 micrograms	44%	T	T	T	T	F	F	F	F	F	F
Cefazolin-AFT 1g	39%	T	T	T	F	F	F	F	F	F	F
Dynastat 40 mg	42%	T	T	T	T	F	F	F	F	F	F
Tranexamic-AFT	50%	T	T	T	T	F	F	F	F	F	F
Calcium Chloride 1g in 10mL	45%	T	T	T	T	F	F	F	F	F	F
Provive MCT-LCT 1%	34%	T	T	T	F	F	F	F	F	F	F
METOPROLOL Mylan 5mg	46%	T	T	T	T	F	F	F	F	F	F
Noradrenaline 4mL	41%	T	T	T	T	F	F	F	F	F	F
Lidocaine-Claris 5ml	53%	T	T	T	T	T	F	F	F	F	F
Atropine Injection 600Ug	34%	T	T	T	F	F	F	F	F	F	F
Xylocaine 1%	30%	T	T	F	F	F	F	F	F	F	F
Sodium Chloride 0.9%	43%	T	T	T	T	F	F	F	F	F	F
Hypnomidate 10mL	45%	T	T	T	T	F	F	F	F	F	F
Adrenaline Injection 1mg	34%	T	T	T	F	F	F	F	F	F	F
Sterile Dopamine 200mg/5ml	41%	T	T	T	T	F	F	F	F	F	F
Suxamethonium 100mg in 2 ml	44%	T	T	T	T	F	F	F	F	F	F
Amiodarone HCL 50 mg/ml	53%	T	T	T	T	T	F	F	F	F	F
Primacor Injection 10mL	41%	T	T	T	T	F	F	F	F	F	F
Sugammadex 200 mg/2ml	43%	T	T	T	T	F	F	F	F	F	F
Rocuronium Bromide 50 mg	34%	T	T	T	F	F	F	F	F	F	F
Clonidine HCl 150 ug/1mL	43%	T	T	T	T	F	F	F	F	F	F
Cyclizine Lactate 50	42%	T	T	T	T	F	F	F	F	F	F
PITRESSIN 20 Units in 1 mL	37%	T	T	T	F	F	F	F	F	F	F
Magnesium Sulfate 2.47g	40%	T	T	T	F	F	F	F	F	F	F
Metaraminol 10mg/mL	49%	T	T	T	T	F	F	F	F	F	F
Dalacin Phosphate 600 mg/4 mL	33%	T	T	T	F	F	F	F	F	F	F
Pancuronium Inresa 4mg/2ml	41%	T	T	T	T	F	F	F	F	F	F
Ephedrine Hydrochloride 30mg	39%	T	T	T	F	F	F	F	F	F	F
Dexamethasone Phosphate 4mg	48%	T	T	T	T	F	F	F	F	F	F
Glycopyrronium and Neostigmine	53%	T	T	T	T	T	F	F	F	F	F
Actrapid Penfill 3mL	38%	T	T	T	F	F	F	F	F	F	F

Threshold: Protamine Sulphate against other samples

Drug Name	Similarity Score	T10	T20	T30	T40	T50	T60	T70	T80	T90	T100
Frusemide-Claris 20mg	48%	T	T	T	T	F	F	F	F	F	F
Water For Injections 10mL	54%	T	T	T	T	T	F	F	F	F	F
Paracetamol 1000mg/100mL	39%	T	T	T	F	F	F	F	F	F	F
Fresofol 1% MCT/LCT	46%	T	T	T	T	F	F	F	F	F	F
Amoxicillin 1g	48%	T	T	T	T	F	F	F	F	F	F
Hydrocortisone sodium 100mg	47%	T	T	T	T	F	F	F	F	F	F
Cefazolin Sodium 1g	49%	T	T	T	T	F	F	F	F	F	F
Atracurium Besylate 50mg	52%	T	T	T	T	T	F	F	F	F	F
Naloxone HCl 400mg in 1mL	43%	T	T	T	T	F	F	F	F	F	F
Morphine Sulfate Injection 10mg	61%	T	T	T	T	T	T	F	F	F	F
Ondansetron Solution	51%	T	T	T	T	T	F	F	F	F	F
Protamine Sulphate 10mg/ml	**100%**	**T**	**T**	**T**	**T**	**T**	**T**	**T**	**T**	**T**	**F**
Vecuronium Bromide	51%	T	T	T	T	T	F	F	F	F	F
Potassium Chloride 10mmol	56%	T	T	T	T	T	F	F	F	F	F
Heparin Injection 25000IU	59%	T	T	T	T	T	F	F	F	F	F
Sugammadex 200mg/2ml	64%	T	T	T	T	T	T	F	F	F	F
Protamine Sulphate 50mg in 5ml	75%	T	T	T	T	T	T	T	F	F	F
Sodium Chloride 10ml	62%	T	T	T	T	T	T	F	F	F	F
Remifentanil-AFT 2g	49%	T	T	T	T	F	F	F	F	F	F
Sedative Midazolam 5mg	45%	T	T	T	T	F	F	F	F	F	F
Glyceryl Trinitrate 10mg in 10ml	44%	T	T	T	T	F	F	F	F	F	F
Fentanyl Citrate 785 micrograms	47%	T	T	T	T	F	F	F	F	F	F
Cefazolin-AFT 1g	56%	T	T	T	T	T	F	F	F	F	F
Dynastat 40 mg	55%	T	T	T	T	T	F	F	F	F	F
Tranexamic-AFT	57%	T	T	T	T	T	F	F	F	F	F
Calcium Chloride 1g in 10mL	55%	T	T	T	T	T	F	F	F	F	F
Provive MCT-LCT 1%	46%	T	T	T	T	F	F	F	F	F	F
METOPROLOL Mylan 5mg	60%	T	T	T	T	T	F	F	F	F	F
Noradrenaline 4mL	42%	T	T	T	T	F	F	F	F	F	F
Lidocaine-Claris 5ml	46%	T	T	T	T	F	F	F	F	F	F
Atropine Injection 600Ug	47%	T	T	T	T	F	F	F	F	F	F
Xylocaine 1%	42%	T	T	T	T	F	F	F	F	F	F
Sodium Chloride 0.9%	43%	T	T	T	T	F	F	F	F	F	F
Hypnomidate 10mL	45%	T	T	T	T	F	F	F	F	F	F
Adrenaline Injection 1mg	43%	T	T	T	T	F	F	F	F	F	F
Sterile Dopamine 200mg/5ml	53%	T	T	T	T	T	F	F	F	F	F
Suxamethonium 100mg in 2 ml	58%	T	T	T	T	T	F	F	F	F	F
Amiodarone HCL 50 mg/ml	56%	T	T	T	T	T	F	F	F	F	F
Primacor Injection 10mL	52%	T	T	T	T	T	F	F	F	F	F
Sugammadex 200 mg/2ml	58%	T	T	T	T	T	F	F	F	F	F
Rocuronium Bromide 50 mg	52%	T	T	T	T	T	F	F	F	F	F
Clonidine HCl 150 ug/1mL	53%	T	T	T	T	T	F	F	F	F	F
Cyclizine Lactate 50	44%	T	T	T	T	F	F	F	F	F	F
PITRESSIN 20 Units in 1 mL	56%	T	T	T	T	T	F	F	F	F	F
Magnesium Sulfate 2.47g	57%	T	T	T	T	T	F	F	F	F	F
Metaraminol 10mg/mL	66%	T	T	T	T	T	T	F	F	F	F
Dalacin Phosphate 600 mg/4 mL	38%	T	T	T	F	F	F	F	F	F	F
Pancuronium Inresa 4mg/2ml	44%	T	T	T	T	F	F	F	F	F	F
Ephedrine Hydrochloride 30mg	44%	T	T	T	T	F	F	F	F	F	F
Dexamethasone Phosphate 4mg	64%	T	T	T	T	T	T	F	F	F	F
Glycopyrronium and Neostigmine	63%	T	T	T	T	T	T	F	F	F	F
Actrapid Penfill 3mL	50%	T	T	T	T	F	F	F	F	F	F

Threshold: Vecuronium Bromide against other samples

Drug Name	Similarity Score	T10	T20	T30	T40	T50	T60	T70	T80	T90	T100
Frusemide-Claris 20mg	38%	T	T	T	F	F	F	F	F	F	F
Water For Injections 10mL	46%	T	T	T	T	F	F	F	F	F	F
Paracetamol 1000mg/100mL	34%	T	T	T	F	F	F	F	F	F	F
Fresofol 1% MCT/LCT	54%	T	T	T	T	T	F	F	F	F	F
Amoxicillin 1g	51%	T	T	T	T	T	F	F	F	F	F
Hydrocortisone sodium 100mg	60%	T	T	T	T	T	F	F	F	F	F
Cefazolin Sodium 1g	58%	T	T	T	T	T	F	F	F	F	F
Atracurium Besylate 50mg	51%	T	T	T	T	T	F	F	F	F	F
Naloxone HCl 400mg in 1mL	32%	T	T	T	F	F	F	F	F	F	F
Morphine Sulfate Injection 10mg	39%	T	T	T	F	F	F	F	F	F	F
Ondansetron Solution	35%	T	T	T	F	F	F	F	F	F	F
Protamine Sulfate 10mg/ml	51%	T	T	T	T	T	F	F	F	F	F
Vecuronium Bromide	**100%**	**T**	**T**	**T**	**T**	**T**	**T**	**T**	**T**	**T**	**F**
Potassium Chloride 10mmol	40%	T	T	T	F	F	F	F	F	F	F
Heparin Injection 25000IU	48%	T	T	T	T	F	F	F	F	F	F
Sugammadex 200mg/2ml	53%	T	T	T	T	T	F	F	F	F	F
Protamine Sulphate 50mg in 5ml	52%	T	T	T	T	T	F	F	F	F	F
Sodium Chloride 10ml	47%	T	T	T	T	F	F	F	F	F	F
Remifentanil-AFT 2g	58%	T	T	T	T	T	F	F	F	F	F
Sedative Midazolam 5mg	29%	T	T	F	F	F	F	F	F	F	F
Glyceryl Trinitrate 10mg in 10ml	35%	T	T	T	F	F	F	F	F	F	F
Fentanyl Citrate 785 micrograms	45%	T	T	T	T	F	F	F	F	F	F
Cefazolin-AFT 1g	58%	T	T	T	T	T	F	F	F	F	F
Dynastat 40 mg	66%	T	T	T	T	T	T	F	F	F	F
Tranexamic-AFT	34%	T	T	T	F	F	F	F	F	F	F
Calcium Chloride 1g in 10mL	44%	T	T	T	T	F	F	F	F	F	F
Provive MCT-LCT 1%	45%	T	T	T	T	F	F	F	F	F	F
METOPROLOL Mylan 5mg	48%	T	T	T	T	F	F	F	F	F	F
Noradrenaline 4mL	34%	T	T	T	F	F	F	F	F	F	F
Lidocaine-Claris 5ml	39%	T	T	T	F	F	F	F	F	F	F
Atropine Injection 600Ug	48%	T	T	T	T	F	F	F	F	F	F
Xylocaine 1%	40%	T	T	T	F	F	F	F	F	F	F
Sodium Chloride 0.9%	30%	T	T	F	F	F	F	F	F	F	F
Hypnomidate 10mL	37%	T	T	T	F	F	F	F	F	F	F
Adrenaline Injection 1mg	47%	T	T	T	T	F	F	F	F	F	F
Sterile Dopamine 200mg/5ml	30%	T	T	F	F	F	F	F	F	F	F
Suxamethonium 100mg in 2 ml	53%	T	T	T	T	T	F	F	F	F	F
Amiodarone HCL 50 mg/ml	46%	T	T	T	T	F	F	F	F	F	F
Primacor Injection 10mL	40%	T	T	T	F	F	F	F	F	F	F
Sugammadex 200 mg/2ml	53%	T	T	T	T	T	F	F	F	F	F
Rocuronium Bromide 50 mg	65%	T	T	T	T	T	T	F	F	F	F
Clonidine HCl 150 ug/1mL	50%	T	T	T	T	F	F	F	F	F	F
Cyclizine Lactate 50	35%	T	T	T	F	F	F	F	F	F	F
PITRESSIN 20 Units in 1 mL	49%	T	T	T	T	F	F	F	F	F	F
Magnesium Sulfate 2.47g	47%	T	T	T	T	F	F	F	F	F	F
Metaraminol 10mg/mL	47%	T	T	T	T	F	F	F	F	F	F
Dalacin Phosphate 600 mg/4 mL	29%	T	T	F	F	F	F	F	F	F	F
Pancuronium Inresa 4mg/2ml	43%	T	T	T	T	F	F	F	F	F	F
Ephedrine Hydrochloride 30mg	46%	T	T	T	T	F	F	F	F	F	F
Dexamethasone Phosphate 4mg	47%	T	T	T	T	F	F	F	F	F	F
Glycopyrronium and Neostigmine	67%	T	T	T	T	T	T	F	F	F	F
Actrapid Penfill 3mL	46%	T	T	T	T	F	F	F	F	F	F

Threshold: Potassium Chloride against other samples

Drug Name	Similarity Score	T10	T20	T30	T40	T50	T60	T70	T80	T90	T100
Frusemide-Claris 20mg	39%	T	T	T	F	F	F	F	F	F	F
Water For Injections 10mL	46%	T	T	T	T	F	F	F	F	F	F
Paracetamol 1000mg/100mL	26%	T	T	F	F	F	F	F	F	F	F
Fresofol 1% MCT/LCT	34%	T	T	T	F	F	F	F	F	F	F
Amoxicillin 1g	46%	T	T	T	T	F	F	F	F	F	F
Hydrocortisone sodium 100mg	43%	T	T	T	T	F	F	F	F	F	F
Cefazolin Sodium 1g	43%	T	T	T	T	F	F	F	F	F	F
Atracurium Besylate 50mg	42%	T	T	T	T	F	F	F	F	F	F
Naloxone HCl 400mg in 1mL	33%	T	T	T	F	F	F	F	F	F	F
Morphine Sulfate Injection 10mg	41%	T	T	T	T	F	F	F	F	F	F
Ondansetron Solution	39%	T	T	T	F	F	F	F	F	F	F
Protamine Sulfate 10mg/ml	55%	T	T	T	T	T	F	F	F	F	F
Vecuronium Bromide	39%	T	T	T	F	F	F	F	F	F	F
Potassium Chloride 10mmol	**100%**	**T**	**T**	**T**	**T**	**T**	**T**	**T**	**T**	**T**	**F**
Heparin Injection 25000IU	53%	T	T	T	T	T	F	F	F	F	F
Sugammadex 200mg/2ml	43%	T	T	T	T	F	F	F	F	F	F
Protamine Sulphate 50mg in 5ml	46%	T	T	T	T	F	F	F	F	F	F
Sodium Chloride 10ml	47%	T	T	T	T	F	F	F	F	F	F
Remifentanil-AFT 2g	46%	T	T	T	T	F	F	F	F	F	F
Sedative Midazolam 5mg	36%	T	T	T	F	F	F	F	F	F	F
Glyceryl Trinitrate 10mg in 10ml	39%	T	T	T	F	F	F	F	F	F	F
Fentanyl Citrate 785 micrograms	45%	T	T	T	T	F	F	F	F	F	F
Cefazolin-AFT 1g	45%	T	T	T	T	F	F	F	F	F	F
Dynastat 40 mg	40%	T	T	T	F	F	F	F	F	F	F
Tranexamic-AFT	42%	T	T	T	T	F	F	F	F	F	F
Calcium Chloride 1g in 10mL	51%	T	T	T	T	T	F	F	F	F	F
Provive MCT-LCT 1%	32%	T	T	T	F	F	F	F	F	F	F
METOPROLOL Mylan 5mg	38%	T	T	T	F	F	F	F	F	F	F
Noradrenaline 4mL	40%	T	T	T	F	F	F	F	F	F	F
Lidocaine-Claris 5ml	40%	T	T	T	F	F	F	F	F	F	F
Atropine Injection 600Ug	40%	T	T	T	F	F	F	F	F	F	F
Xylocaine 1%	33%	T	T	T	F	F	F	F	F	F	F
Sodium Chloride 0.9%	52%	T	T	T	T	T	F	F	F	F	F
Hypnomidate 10mL	40%	T	T	T	F	F	F	F	F	F	F
Adrenaline Injection 1mg	34%	T	T	T	F	F	F	F	F	F	F
Sterile Dopamine 200mg/5ml	58%	T	T	T	T	T	F	F	F	F	F
Suxamethonium 100mg in 2 ml	53%	T	T	T	T	T	F	F	F	F	F
Amiodarone HCL 50 mg/ml	52%	T	T	T	T	T	F	F	F	F	F
Primacor Injection 10mL	47%	T	T	T	T	F	F	F	F	F	F
Sugammadex 200 mg/2ml	50%	T	T	T	T	F	F	F	F	F	F
Rocuronium Bromide 50 mg	37%	T	T	T	F	F	F	F	F	F	F
Clonidine HCl 150 ug/1mL	44%	T	T	T	T	F	F	F	F	F	F
Cyclizine Lactate 50	44%	T	T	T	T	F	F	F	F	F	F
PITRESSIN 20 Units in 1 mL	43%	T	T	T	T	F	F	F	F	F	F
Magnesium Sulfate 2.47g	59%	T	T	T	T	T	F	F	F	F	F
Metaraminol 10mg/mL	45%	T	T	T	T	F	F	F	F	F	F
Dalacin Phosphate 600 mg/4 mL	38%	T	T	T	F	F	F	F	F	F	F
Pancuronium Inresa 4mg/2ml	37%	T	T	T	F	F	F	F	F	F	F
Ephedrine Hydrochloride 30mg	39%	T	T	T	F	F	F	F	F	F	F
Dexamethasone Phosphate 4mg	36%	T	T	T	F	F	F	F	F	F	F
Glycopyrronium and Neostigmine	50%	T	T	T	T	F	F	F	F	F	F
Actrapid Penfill 3mL	42%	T	T	T	T	F	F	F	F	F	F

Threshold: Heparin Injection against other samples

Drug Name	Similarity Score	T10	T20	T30	T40	T50	T60	T70	T80	T90	T100
Frusemide-Claris 20mg	40%	T	T	T	F	F	F	F	F	F	F
Water For Injections 10mL	51%	T	T	T	T	T	F	F	F	F	F
Paracetamol 1000mg/100mL	23%	T	T	F	F	F	F	F	F	F	F
Fresofol 1% MCT/LCT	43%	T	T	T	T	F	F	F	F	F	F
Amoxicillin 1g	45%	T	T	T	T	F	F	F	F	F	F
Hydrocortisone sodium 100mg	47%	T	T	T	T	F	F	F	F	F	F
Cefazolin Sodium 1g	49%	T	T	T	T	F	F	F	F	F	F
Atracurium Besylate 50mg	54%	T	T	T	T	T	F	F	F	F	F
Naloxone HCl 400mg in 1mL	38%	T	T	T	F	F	F	F	F	F	F
Morphine Sulfate Injection 10mg	54%	T	T	T	T	T	F	F	F	F	F
Ondansetron Solution	42%	T	T	T	T	F	F	F	F	F	F
Protamine Sulfate 10mg/ml	59%	T	T	T	T	T	F	F	F	F	F
Vecuronium Bromide	48%	T	T	T	T	F	F	F	F	F	F
Potassium Chloride 10mmol	52%	T	T	T	T	T	F	F	F	F	F
Heparin Injection 25000IU	**100%**	**T**	**T**	**T**	**T**	**T**	**T**	**T**	**T**	**T**	**F**
Sugammadex 200mg/2ml	56%	T	T	T	T	T	F	F	F	F	F
Protamine Sulphate 50mg in 5ml	55%	T	T	T	T	T	F	F	F	F	F
Sodium Chloride 10ml	52%	T	T	T	T	T	F	F	F	F	F
Remifentanil-AFT 2g	46%	T	T	T	T	F	F	F	F	F	F
Sedative Midazolam 5mg	38%	T	T	T	F	F	F	F	F	F	F
Glyceryl Trinitrate 10mg in 10ml	37%	T	T	T	F	F	F	F	F	F	F
Fentanyl Citrate 785 micrograms	45%	T	T	T	T	F	F	F	F	F	F
Cefazolin-AFT 1g	51%	T	T	T	T	T	F	F	F	F	F
Dynastat 40 mg	54%	T	T	T	T	T	F	F	F	F	F
Tranexamic-AFT	41%	T	T	T	T	F	F	F	F	F	F
Calcium Chloride 1g in 10mL	47%	T	T	T	T	F	F	F	F	F	F
Provive MCT-LCT 1%	43%	T	T	T	T	F	F	F	F	F	F
METOPROLOL Mylan 5mg	47%	T	T	T	T	F	F	F	F	F	F
Noradrenaline 4mL	38%	T	T	T	F	F	F	F	F	F	F
Lidocaine-Claris 5ml	45%	T	T	T	T	F	F	F	F	F	F
Atropine Injection 600Ug	49%	T	T	T	T	F	F	F	F	F	F
Xylocaine 1%	41%	T	T	T	T	F	F	F	F	F	F
Sodium Chloride 0.9%	41%	T	T	T	T	F	F	F	F	F	F
Hypnomidate 10mL	38%	T	T	T	F	F	F	F	F	F	F
Adrenaline Injection 1mg	44%	T	T	T	T	F	F	F	F	F	F
Sterile Dopamine 200mg/5ml	41%	T	T	T	T	F	F	F	F	F	F
Suxamethonium 100mg in 2 ml	50%	T	T	T	T	F	F	F	F	F	F
Amiodarone HCL 50 mg/ml	49%	T	T	T	T	F	F	F	F	F	F
Primacor Injection 10mL	47%	T	T	T	T	F	F	F	F	F	F
Sugammadex 200 mg/2ml	55%	T	T	T	T	T	F	F	F	F	F
Rocuronium Bromide 50 mg	55%	T	T	T	T	T	F	F	F	F	F
Clonidine HCl 150 ug/1mL	52%	T	T	T	T	T	F	F	F	F	F
Cyclizine Lactate 50	39%	T	T	T	F	F	F	F	F	F	F
PITRESSIN 20 Units in 1 mL	61%	T	T	T	T	T	T	F	F	F	F
Magnesium Sulfate 2.47g	50%	T	T	T	T	F	F	F	F	F	F
Metaraminol 10mg/mL	50%	T	T	T	T	F	F	F	F	F	F
Dalacin Phosphate 600 mg/4 mL	46%	T	T	T	T	F	F	F	F	F	F
Pancuronium Inresa 4mg/2ml	43%	T	T	T	T	F	F	F	F	F	F
Ephedrine Hydrochloride 30mg	48%	T	T	T	T	F	F	F	F	F	F
Dexamethasone Phosphate 4mg	51%	T	T	T	T	T	F	F	F	F	F
Glycopyrronium and Neostigmine	51%	T	T	T	T	T	F	F	F	F	F
Actrapid Penfill 3mL	53%	T	T	T	T	T	F	F	F	F	F

Threshold: Sugammadex against other samples

Drug Name	Similarity Score	T10	T20	T30	T40	T50	T60	T70	T80	T90	T100
Frusemide-Claris 20mg	45%	T	T	T	T	F	F	F	F	F	F
Water For Injections 10mL	47%	T	T	T	T	F	F	F	F	F	F
Paracetamol 1000mg/100mL	62%	T	T	T	T	T	T	F	F	F	F
Fresofol 1% MCT/LCT	67%	T	T	T	T	T	T	F	F	F	F
Amoxicillin 1g	46%	T	T	T	T	F	F	F	F	F	F
Hydrocortisone sodium 100mg	52%	T	T	T	T	T	F	F	F	F	F
Cefazolin Sodium 1g	46%	T	T	T	T	F	F	F	F	F	F
Atracurium Besylate 50mg	50%	T	T	T	T	F	F	F	F	F	F
Naloxone HCl 400mg in 1mL	39%	T	T	T	F	F	F	F	F	F	F
Morphine Sulfate Injection 10mg	52%	T	T	T	T	T	F	F	F	F	F
Ondansetron Solution	46%	T	T	T	T	F	F	F	F	F	F
Protamine Sulfate 10mg/ml	64%	T	T	T	T	T	T	F	F	F	F
Vecuronium Bromide	53%	T	T	T	T	T	F	F	F	F	F
Potassium Chloride 10mmol	44%	T	T	T	T	F	F	F	F	F	F
Heparin Injection 25000IU	56%	T	T	T	T	T	F	F	F	F	F
Sugammadex 200mg/2ml	**100%**	**T**	**T**	**T**	**T**	**T**	**T**	**T**	**T**	**T**	**F**
Protamine Sulphate 50mg in 5ml	53%	T	T	T	T	T	F	F	F	F	F
Sodium Chloride 10ml	55%	T	T	T	T	T	F	F	F	F	F
Remifentanil-AFT 2g	47%	T	T	T	T	F	F	F	F	F	F
Sedative Midazolam 5mg	41%	T	T	T	T	F	F	F	F	F	F
Glyceryl Trinitrate 10mg in 10ml	42%	T	T	T	T	F	F	F	F	F	F
Fentanyl Citrate 785 micrograms	44%	T	T	T	T	F	F	F	F	F	F
Cefazolin-AFT 1g	54%	T	T	T	T	T	F	F	F	F	F
Dynastat 40 mg	54%	T	T	T	T	T	F	F	F	F	F
Tranexamic-AFT	48%	T	T	T	T	F	F	F	F	F	F
Calcium Chloride 1g in 10mL	54%	T	T	T	T	T	F	F	F	F	F
Provive MCT-LCT 1%	70%	T	T	T	T	T	T	F	F	F	F
METOPROLOL Mylan 5mg	57%	T	T	T	T	T	F	F	F	F	F
Noradrenaline 4mL	35%	T	T	T	F	F	F	F	F	F	F
Lidocaine-Claris 5ml	46%	T	T	T	T	F	F	F	F	F	F
Atropine Injection 600Ug	49%	T	T	T	T	F	F	F	F	F	F
Xylocaine 1%	38%	T	T	T	F	F	F	F	F	F	F
Sodium Chloride 0.9%	39%	T	T	T	F	F	F	F	F	F	F
Hypnomidate 10mL	47%	T	T	T	T	F	F	F	F	F	F
Adrenaline Injection 1mg	45%	T	T	T	T	F	F	F	F	F	F
Sterile Dopamine 200mg/5ml	44%	T	T	T	T	F	F	F	F	F	F
Suxamethonium 100mg in 2 ml	61%	T	T	T	T	T	T	F	F	F	F
Amiodarone HCL 50 mg/ml	55%	T	T	T	T	T	F	F	F	F	F
Primacor Injection 10mL	46%	T	T	T	T	F	F	F	F	F	F
Sugammadex 200 mg/2ml	91%	T	T	T	T	T	T	T	T	T	F
Rocuronium Bromide 50 mg	57%	T	T	T	T	T	F	F	F	F	F
Clonidine HCl 150 ug/1mL	49%	T	T	T	T	F	F	F	F	F	F
Cyclizine Lactate 50	40%	T	T	T	F	F	F	F	F	F	F
PITRESSIN 20 Units in 1 mL	59%	T	T	T	T	T	F	F	F	F	F
Magnesium Sulfate 2.47g	55%	T	T	T	T	T	F	F	F	F	F
Metaraminol 10mg/mL	60%	T	T	T	T	T	F	F	F	F	F
Dalacin Phosphate 600 mg/4 mL	40%	T	T	T	F	F	F	F	F	F	F
Pancuronium Inresa 4mg/2ml	45%	T	T	T	T	F	F	F	F	F	F
Ephedrine Hydrochloride 30mg	45%	T	T	T	T	F	F	F	F	F	F
Dexamethasone Phosphate 4mg	64%	T	T	T	T	T	T	F	F	F	F
Glycopyrronium and Neostigmine	60%	T	T	T	T	T	F	F	F	F	F
Actrapid Penfill 3mL	46%	T	T	T	T	F	F	F	F	F	F

Threshold: Protamine Sulphate against other samples

Drug Name	Similarity Score	T10	T20	T30	T40	T50	T60	T70	T80	T90	T100
Frusemide-Claris 20mg	47%	T	T	T	T	F	F	F	F	F	F
Water For Injections 10mL	52%	T	T	T	T	T	F	F	F	F	F
Paracetamol 1000mg/100mL	24%	T	T	F	F	F	F	F	F	F	F
Fresofol 1% MCT/LCT	51%	T	T	T	T	T	F	F	F	F	F
Amoxicillin 1g	49%	T	T	T	T	F	F	F	F	F	F
Hydrocortisone sodium 100mg	49%	T	T	T	T	F	F	F	F	F	F
Cefazolin Sodium 1g	48%	T	T	T	T	F	F	F	F	F	F
Atracurium Besylate 50mg	56%	T	T	T	T	T	F	F	F	F	F
Naloxone HCl 400mg in 1mL	41%	T	T	T	T	F	F	F	F	F	F
Morphine Sulfate Injection 10mg	55%	T	T	T	T	T	F	F	F	F	F
Ondansetron Solution	49%	T	T	T	T	F	F	F	F	F	F
Protamine Sulfate 10mg/ml	75%	T	T	T	T	T	T	T	F	F	F
Vecuronium Bromide	52%	T	T	T	T	T	F	F	F	F	F
Potassium Chloride 10mmol	46%	T	T	T	T	F	F	F	F	F	F
Heparin Injection 25000IU	55%	T	T	T	T	T	F	F	F	F	F
Sugammadex 200mg/2ml	53%	T	T	T	T	T	F	F	F	F	F
Protamine Sulphate 50mg in 5ml	**100%**	**T**	**T**	**T**	**T**	**T**	**T**	**T**	**T**	**T**	**F**
Sodium Chloride 10ml	51%	T	T	T	T	T	F	F	F	F	F
Remifentanil-AFT 2g	47%	T	T	T	T	F	F	F	F	F	F
Sedative Midazolam 5mg	40%	T	T	T	F	F	F	F	F	F	F
Glyceryl Trinitrate 10mg in 10ml	43%	T	T	T	T	F	F	F	F	F	F
Fentanyl Citrate 785 micrograms	41%	T	T	T	T	F	F	F	F	F	F
Cefazolin-AFT 1g	51%	T	T	T	T	T	F	F	F	F	F
Dynastat 40 mg	49%	T	T	T	T	F	F	F	F	F	F
Tranexamic-AFT	43%	T	T	T	T	F	F	F	F	F	F
Calcium Chloride 1g in 10mL	54%	T	T	T	T	T	F	F	F	F	F
Provive MCT-LCT 1%	51%	T	T	T	T	T	F	F	F	F	F
METOPROLOL Mylan 5mg	59%	T	T	T	T	T	F	F	F	F	F
Noradrenaline 4mL	39%	T	T	T	F	F	F	F	F	F	F
Lidocaine-Claris 5ml	44%	T	T	T	T	F	F	F	F	F	F
Atropine Injection 600Ug	43%	T	T	T	T	F	F	F	F	F	F
Xylocaine 1%	41%	T	T	T	T	F	F	F	F	F	F
Sodium Chloride 0.9%	40%	T	T	T	F	F	F	F	F	F	F
Hypnomidate 10mL	44%	T	T	T	T	F	F	F	F	F	F
Adrenaline Injection 1mg	44%	T	T	T	T	F	F	F	F	F	F
Sterile Dopamine 200mg/5ml	48%	T	T	T	T	F	F	F	F	F	F
Suxamethonium 100mg in 2 ml	53%	T	T	T	T	T	F	F	F	F	F
Amiodarone HCL 50 mg/ml	58%	T	T	T	T	T	F	F	F	F	F
Primacor Injection 10mL	47%	T	T	T	T	F	F	F	F	F	F
Sugammadex 200 mg/2ml	54%	T	T	T	T	T	F	F	F	F	F
Rocuronium Bromide 50 mg	51%	T	T	T	T	T	F	F	F	F	F
Clonidine HCl 150 ug/1mL	56%	T	T	T	T	T	F	F	F	F	F
Cyclizine Lactate 50	40%	T	T	T	F	F	F	F	F	F	F
PITRESSIN 20 Units in 1 mL	51%	T	T	T	T	T	F	F	F	F	F
Magnesium Sulfate 2.47g	53%	T	T	T	T	T	F	F	F	F	F
Metaraminol 10mg/mL	61%	T	T	T	T	T	T	F	F	F	F
Dalacin Phosphate 600 mg/4 mL	35%	T	T	T	F	F	F	F	F	F	F
Pancuronium Inresa 4mg/2ml	42%	T	T	T	T	F	F	F	F	F	F
Ephedrine Hydrochloride 30mg	43%	T	T	T	T	F	F	F	F	F	F
Dexamethasone Phosphate 4mg	61%	T	T	T	T	T	T	F	F	F	F
Glycopyrronium and Neostigmine	55%	T	T	T	T	T	F	F	F	F	F
Actrapid Penfill 3mL	48%	T	T	T	T	F	F	F	F	F	F

Threshold: Sodium Chloride against other samples

Drug Name	Similarity Score	T10	T20	T30	T40	T50	T60	T70	T80	T90	T100
Frusemide-Claris 20mg	51%	T	T	T	T	T	F	F	F	F	F
Water For Injections 10mL	48%	T	T	T	T	F	F	F	F	F	F
Paracetamol 1000mg/100mL	46%	T	T	T	T	F	F	F	F	F	F
Fresofol 1% MCT/LCT	41%	T	T	T	T	F	F	F	F	F	F
Amoxicillin 1g	46%	T	T	T	T	F	F	F	F	F	F
Hydrocortisone sodium 100mg	54%	T	T	T	T	T	F	F	F	F	F
Cefazolin Sodium 1g	48%	T	T	T	T	F	F	F	F	F	F
Atracurium Besylate 50mg	48%	T	T	T	T	F	F	F	F	F	F
Naloxone HCl 400mg in 1mL	42%	T	T	T	T	F	F	F	F	F	F
Morphine Sulfate Injection 10mg	58%	T	T	T	T	T	F	F	F	F	F
Ondansetron Solution	46%	T	T	T	T	F	F	F	F	F	F
Protamine Sulfate 10mg/ml	62%	T	T	T	T	T	T	F	F	F	F
Vecuronium Bromide	47%	T	T	T	T	F	F	F	F	F	F
Potassium Chloride 10mmol	48%	T	T	T	T	F	F	F	F	F	F
Heparin Injection 25000IU	52%	T	T	T	T	T	F	F	F	F	F
Sugammadex 200mg/2ml	55%	T	T	T	T	T	F	F	F	F	F
Protamine Sulphate 50mg in 5ml	51%	T	T	T	T	T	F	F	F	F	F
Sodium Chloride 10ml	**100%**	**T**	**T**	**T**	**T**	**T**	**T**	**T**	**T**	**T**	**F**
Remifentanil-AFT 2g	44%	T	T	T	T	F	F	F	F	F	F
Sedative Midazolam 5mg	41%	T	T	T	T	F	F	F	F	F	F
Glyceryl Trinitrate 10mg in 10ml	40%	T	T	T	F	F	F	F	F	F	F
Fentanyl Citrate 785 micrograms	49%	T	T	T	T	F	F	F	F	F	F
Cefazolin-AFT 1g	48%	T	T	T	T	F	F	F	F	F	F
Dynastat 40 mg	52%	T	T	T	T	T	F	F	F	F	F
Tranexamic-AFT	52%	T	T	T	T	T	F	F	F	F	F
Calcium Chloride 1g in 10mL	50%	T	T	T	T	F	F	F	F	F	F
Provive MCT-LCT 1%	42%	T	T	T	T	F	F	F	F	F	F
METOPROLOL Mylan 5mg	55%	T	T	T	T	T	F	F	F	F	F
Noradrenaline 4mL	36%	T	T	T	F	F	F	F	F	F	F
Lidocaine-Claris 5ml	47%	T	T	T	T	F	F	F	F	F	F
Atropine Injection 600Ug	39%	T	T	T	F	F	F	F	F	F	F
Xylocaine 1%	28%	T	T	F	F	F	F	F	F	F	F
Sodium Chloride 0.9%	53%	T	T	T	T	T	F	F	F	F	F
Hypnomidate 10mL	48%	T	T	T	T	F	F	F	F	F	F
Adrenaline Injection 1mg	35%	T	T	T	F	F	F	F	F	F	F
Sterile Dopamine 200mg/5ml	30%	T	T	F	F	F	F	F	F	F	F
Suxamethonium 100mg in 2 ml	72%	T	T	T	T	T	T	T	F	F	F
Amiodarone HCL 50 mg/ml	54%	T	T	T	T	T	F	F	F	F	F
Primacor Injection 10mL	44%	T	T	T	T	F	F	F	F	F	F
Sugammadex 200 mg/2ml	51%	T	T	T	T	T	F	F	F	F	F
Rocuronium Bromide 50 mg	56%	T	T	T	T	T	F	F	F	F	F
Clonidine HCl 150 ug/1mL	52%	T	T	T	T	T	F	F	F	F	F
Cyclizine Lactate 50	36%	T	T	T	F	F	F	F	F	F	F
PITRESSIN 20 Units in 1 mL	55%	T	T	T	T	T	F	F	F	F	F
Magnesium Sulfate 2.47g	49%	T	T	T	T	F	F	F	F	F	F
Metaraminol 10mg/mL	51%	T	T	T	T	T	F	F	F	F	F
Dalacin Phosphate 600 mg/4 mL	31%	T	T	T	F	F	F	F	F	F	F
Pancuronium Inresa 4mg/2ml	46%	T	T	T	T	F	F	F	F	F	F
Ephedrine Hydrochloride 30mg	42%	T	T	T	T	F	F	F	F	F	F
Dexamethasone Phosphate 4mg	69%	T	T	T	T	T	T	F	F	F	F
Glycopyrronium and Neostigmine	59%	T	T	T	T	T	F	F	F	F	F
Actrapid Penfill 3mL	51%	T	T	T	T	T	F	F	F	F	F

Threshold: Remifentanil-AFT against other samples

Drug Name	Similarity Score	T10	T20	T30	T40	T50	T60	T70	T80	T90	T100
Frusemide-Claris 20mg	38%	T	T	T	F	F	F	F	F	F	F
Water For Injections 10mL	44%	T	T	T	T	F	F	F	F	F	F
Paracetamol 1000mg/100mL	29%	T	T	F	F	F	F	F	F	F	F
Fresofol 1% MCT/LCT	36%	T	T	T	F	F	F	F	F	F	F
Amoxicillin 1g	47%	T	T	T	T	F	F	F	F	F	F
Hydrocortisone sodium 100mg	52%	T	T	T	T	T	F	F	F	F	F
Cefazolin Sodium 1g	68%	T	T	T	T	T	T	F	F	F	F
Atracurium Besylate 50mg	45%	T	T	T	T	F	F	F	F	F	F
Naloxone HCl 400mg in 1mL	33%	T	T	T	F	F	F	F	F	F	F
Morphine Sulfate Injection 10mg	41%	T	T	T	T	F	F	F	F	F	F
Ondansetron Solution	42%	T	T	T	T	F	F	F	F	F	F
Protamine Sulfate 10mg/ml	49%	T	T	T	T	F	F	F	F	F	F
Vecuronium Bromide	58%	T	T	T	T	T	F	F	F	F	F
Potassium Chloride 10mmol	46%	T	T	T	T	F	F	F	F	F	F
Heparin Injection 25000IU	46%	T	T	T	T	F	F	F	F	F	F
Sugammadex 200mg/2ml	47%	T	T	T	T	F	F	F	F	F	F
Protamine Sulphate 50mg in 5ml	47%	T	T	T	T	F	F	F	F	F	F
Sodium Chloride 10ml	44%	T	T	T	T	F	F	F	F	F	F
Remifentanil-AFT 2g	**100%**	**T**	**T**	**T**	**T**	**T**	**T**	**T**	**T**	**T**	**F**
Sedative Midazolam 5mg	28%	T	T	F	F	F	F	F	F	F	F
Glyceryl Trinitrate 10mg in 10ml	38%	T	T	T	F	F	F	F	F	F	F
Fentanyl Citrate 785 micrograms	57%	T	T	T	T	T	F	F	F	F	F
Cefazolin-AFT 1g	74%	T	T	T	T	T	T	T	F	F	F
Dynastat 40 mg	56%	T	T	T	T	T	F	F	F	F	F
Tranexamic-AFT	42%	T	T	T	T	F	F	F	F	F	F
Calcium Chloride 1g in 10mL	48%	T	T	T	T	F	F	F	F	F	F
Provive MCT-LCT 1%	34%	T	T	T	F	F	F	F	F	F	F
METOPROLOL Mylan 5mg	46%	T	T	T	T	F	F	F	F	F	F
Noradrenaline 4mL	46%	T	T	T	T	F	F	F	F	F	F
Lidocaine-Claris 5ml	44%	T	T	T	T	F	F	F	F	F	F
Atropine Injection 600Ug	43%	T	T	T	T	F	F	F	F	F	F
Xylocaine 1%	29%	T	T	F	F	F	F	F	F	F	F
Sodium Chloride 0.9%	45%	T	T	T	T	F	F	F	F	F	F
Hypnomidate 10mL	39%	T	T	T	F	F	F	F	F	F	F
Adrenaline Injection 1mg	44%	T	T	T	T	F	F	F	F	F	F
Sterile Dopamine 200mg/5ml	33%	T	T	T	F	F	F	F	F	F	F
Suxamethonium 100mg in 2 ml	45%	T	T	T	T	F	F	F	F	F	F
Amiodarone HCL 50 mg/ml	50%	T	T	T	T	F	F	F	F	F	F
Primacor Injection 10mL	46%	T	T	T	T	F	F	F	F	F	F
Sugammadex 200 mg/2ml	49%	T	T	T	T	F	F	F	F	F	F
Rocuronium Bromide 50 mg	43%	T	T	T	T	F	F	F	F	F	F
Clonidine HCl 150 ug/1mL	44%	T	T	T	T	F	F	F	F	F	F
Cyclizine Lactate 50	40%	T	T	T	F	F	F	F	F	F	F
PITRESSIN 20 Units in 1 mL	42%	T	T	T	T	F	F	F	F	F	F
Magnesium Sulfate 2.47g	45%	T	T	T	T	F	F	F	F	F	F
Metaraminol 10mg/mL	47%	T	T	T	T	F	F	F	F	F	F
Dalacin Phosphate 600 mg/4 mL	30%	T	T	F	F	F	F	F	F	F	F
Pancuronium Inresa 4mg/2ml	40%	T	T	T	F	F	F	F	F	F	F
Ephedrine Hydrochloride 30mg	58%	T	T	T	T	T	F	F	F	F	F
Dexamethasone Phosphate 4mg	46%	T	T	T	T	F	F	F	F	F	F
Glycopyrronium and Neostigmine	50%	T	T	T	T	F	F	F	F	F	F
Actrapid Penfill 3mL	46%	T	T	T	T	F	F	F	F	F	F

Threshold: Water for Injections against other samples

Drug Name	Similarity Score	T10	T20	T30	T40	T50	T60	T70	T80	T90	T100
Frusemide-Claris 20mg	41%	T	T	T	T	F	F	F	F	F	F
Water For Injections 10mL	**100%**	**T**	**T**	**T**	**T**	**T**	**T**	**T**	**T**	**T**	**F**
Paracetamol 1000mg/100mL	45%	T	T	T	T	F	F	F	F	F	F
Fresofol 1% MCT/LCT	45%	T	T	T	T	F	F	F	F	F	F
Amoxicillin 1g	39%	T	T	T	F	F	F	F	F	F	F
Hydrocortisone sodium 100mg	43%	T	T	T	T	F	F	F	F	F	F
Cefazolin Sodium 1g	41%	T	T	T	T	F	F	F	F	F	F
Atracurium Besylate 50mg	45%	T	T	T	T	F	F	F	F	F	F
Naloxone HCl 400mg in 1mL	39%	T	T	T	F	F	F	F	F	F	F
Morphine Sulfate Injection 10mg	53%	T	T	T	T	T	F	F	F	F	F
Ondansetron Solution	41%	T	T	T	T	F	F	F	F	F	F
Protamine Sulfate 10mg/ml	54%	T	T	T	T	T	F	F	F	F	F
Vecuronium Bromide	46%	T	T	T	T	F	F	F	F	F	F
Potassium Chloride 10mmol	46%	T	T	T	T	F	F	F	F	F	F
Heparin Injection 25000IU	51%	T	T	T	T	T	F	F	F	F	F
Sugammadex 200mg/2ml	47%	T	T	T	T	F	F	F	F	F	F
Protamine Sulphate 50mg in 5ml	52%	T	T	T	T	T	F	F	F	F	F
Sodium Chloride 10ml	48%	T	T	T	T	F	F	F	F	F	F
Remifentanil-AFT 2g	44%	T	T	T	T	F	F	F	F	F	F
Sedative Midazolam 5mg	43%	T	T	T	T	F	F	F	F	F	F
Glyceryl Trinitrate 10mg in 10ml	44%	T	T	T	T	F	F	F	F	F	F
Fentanyl Citrate 785 micrograms	43%	T	T	T	T	F	F	F	F	F	F
Cefazolin-AFT 1g	47%	T	T	T	T	F	F	F	F	F	F
Dynastat 40 mg	48%	T	T	T	T	F	F	F	F	F	F
Tranexamic-AFT	42%	T	T	T	T	F	F	F	F	F	F
Calcium Chloride 1g in 10mL	45%	T	T	T	T	F	F	F	F	F	F
Provive MCT-LCT 1%	29%	T	T	F	F	F	F	F	F	F	F
METOPROLOL Mylan 5mg	42%	T	T	T	T	F	F	F	F	F	F
Noradrenaline 4mL	43%	T	T	T	T	F	F	F	F	F	F
Lidocaine-Claris 5ml	46%	T	T	T	T	F	F	F	F	F	F
Atropine Injection 600Ug	41%	T	T	T	T	F	F	F	F	F	F
Xylocaine 1%	36%	T	T	T	F	F	F	F	F	F	F
Sodium Chloride 0.9%	40%	T	T	T	F	F	F	F	F	F	F
Hypnomidate 10mL	52%	T	T	T	T	T	F	F	F	F	F
Adrenaline Injection 1mg	44%	T	T	T	T	F	F	F	F	F	F
Sterile Dopamine 200mg/5ml	40%	T	T	T	F	F	F	F	F	F	F
Suxamethonium 100mg in 2 ml	47%	T	T	T	T	F	F	F	F	F	F
Amiodarone HCL 50 mg/ml	43%	T	T	T	T	F	F	F	F	F	F
Primacor Injection 10mL	44%	T	T	T	T	F	F	F	F	F	F
Sugammadex 200 mg/2ml	44%	T	T	T	T	F	F	F	F	F	F
Rocuronium Bromide 50 mg	41%	T	T	T	T	F	F	F	F	F	F
Clonidine HCl 150 ug/1mL	41%	T	T	T	T	F	F	F	F	F	F
Cyclizine Lactate 50	41%	T	T	T	T	F	F	F	F	F	F
PITRESSIN 20 Units in 1 mL	47%	T	T	T	T	F	F	F	F	F	F
Magnesium Sulfate 2.47g	45%	T	T	T	T	F	F	F	F	F	F
Metaraminol 10mg/mL	49%	T	T	T	T	F	F	F	F	F	F
Dalacin Phosphate 600 mg/4 mL	47%	T	T	T	T	F	F	F	F	F	F
Pancuronium Inresa 4mg/2ml	39%	T	T	T	F	F	F	F	F	F	F
Ephedrine Hydrochloride 30mg	39%	T	T	T	F	F	F	F	F	F	F
Dexamethasone Phosphate 4mg	47%	T	T	T	T	F	F	F	F	F	F
Glycopyrronium and Neostigmine	48%	T	T	T	T	F	F	F	F	F	F
Actrapid Penfill 3mL	46%	T	T	T	T	F	F	F	F	F	F

Threshold: Sedative Midazolam against other samples

Drug Name	Similarity Score	T10	T20	T30	T40	T50	T60	T70	T80	T90	T100
Frusemide-Claris 20mg	39%	T	T	T	F	F	F	F	F	F	F
Water For Injections 10mL	43%	T	T	T	T	F	F	F	F	F	F
Paracetamol 1000mg/100mL	16%	T	F	F	F	F	F	F	F	F	F
Fresofol 1% MCT/LCT	25%	T	T	F	F	F	F	F	F	F	F
Amoxicillin 1g	30%	T	T	F	F	F	F	F	F	F	F
Hydrocortisone sodium 100mg	30%	T	T	F	F	F	F	F	F	F	F
Cefazolin Sodium 1g	27%	T	T	F	F	F	F	F	F	F	F
Atracurium Besylate 50mg	39%	T	T	T	F	F	F	F	F	F	F
Naloxone HCl 400mg in 1mL	43%	T	T	T	T	F	F	F	F	F	F
Morphine Sulfate Injection 10mg	53%	T	T	T	T	T	F	F	F	F	F
Ondansetron Solution	37%	T	T	T	F	F	F	F	F	F	F
Protamine Sulfate 10mg/ml	45%	T	T	T	T	F	F	F	F	F	F
Vecuronium Bromide	29%	T	T	F	F	F	F	F	F	F	F
Potassium Chloride 10mmol	36%	T	T	T	F	F	F	F	F	F	F
Heparin Injection 25000IU	38%	T	T	T	F	F	F	F	F	F	F
Sugammadex 200mg/2ml	41%	T	T	T	T	F	F	F	F	F	F
Protamine Sulphate 50mg in 5ml	40%	T	T	T	F	F	F	F	F	F	F
Sodium Chloride 10ml	41%	T	T	T	T	F	F	F	F	F	F
Remifentanil-AFT 2g	28%	T	T	F	F	F	F	F	F	F	F
Sedative Midazolam 5mg	**100%**	**T**	**T**	**T**	**T**	**T**	**T**	**T**	**T**	**T**	**F**
Glyceryl Trinitrate 10mg in 10ml	39%	T	T	T	F	F	F	F	F	F	F
Fentanyl Citrate 785 micrograms	35%	T	T	T	F	F	F	F	F	F	F
Cefazolin-AFT 1g	35%	T	T	T	F	F	F	F	F	F	F
Dynastat 40 mg	35%	T	T	T	F	F	F	F	F	F	F
Tranexamic-AFT	44%	T	T	T	T	F	F	F	F	F	F
Calcium Chloride 1g in 10mL	35%	T	T	T	F	F	F	F	F	F	F
Provive MCT-LCT 1%	25%	T	T	F	F	F	F	F	F	F	F
METOPROLOL Mylan 5mg	40%	T	T	T	F	F	F	F	F	F	F
Noradrenaline 4mL	32%	T	T	T	F	F	F	F	F	F	F
Lidocaine-Claris 5ml	37%	T	T	T	F	F	F	F	F	F	F
Atropine Injection 600Ug	34%	T	T	T	F	F	F	F	F	F	F
Xylocaine 1%	34%	T	T	T	F	F	F	F	F	F	F
Sodium Chloride 0.9%	35%	T	T	T	F	F	F	F	F	F	F
Hypnomidate 10mL	50%	T	T	T	T	F	F	F	F	F	F
Adrenaline Injection 1mg	29%	T	T	F	F	F	F	F	F	F	F
Sterile Dopamine 200mg/5ml	48%	T	T	T	T	F	F	F	F	F	F
Suxamethonium 100mg in 2 ml	50%	T	T	T	T	F	F	F	F	F	F
Amiodarone HCL 50 mg/ml	35%	T	T	T	F	F	F	F	F	F	F
Primacor Injection 10mL	41%	T	T	T	T	F	F	F	F	F	F
Sugammadex 200 mg/2ml	38%	T	T	T	F	F	F	F	F	F	F
Rocuronium Bromide 50 mg	44%	T	T	T	T	F	F	F	F	F	F
Clonidine HCl 150 ug/1mL	35%	T	T	T	F	F	F	F	F	F	F
Cyclizine Lactate 50	48%	T	T	T	T	F	F	F	F	F	F
PITRESSIN 20 Units in 1 mL	40%	T	T	T	F	F	F	F	F	F	F
Magnesium Sulfate 2.47g	38%	T	T	T	F	F	F	F	F	F	F
Metaraminol 10mg/mL	35%	T	T	T	F	F	F	F	F	F	F
Dalacin Phosphate 600 mg/4 mL	47%	T	T	T	T	F	F	F	F	F	F
Pancuronium Inresa 4mg/2ml	36%	T	T	T	F	F	F	F	F	F	F
Ephedrine Hydrochloride 30mg	32%	T	T	T	F	F	F	F	F	F	F
Dexamethasone Phosphate 4mg	44%	T	T	T	T	F	F	F	F	F	F
Glycopyrronium and Neostigmine	38%	T	T	T	F	F	F	F	F	F	F
Actrapid Penfill 3mL	34%	T	T	T	F	F	F	F	F	F	F

Threshold: Glyceryl Trinitrate against other samples

Drug Name	Similarity Score	T10	T20	T30	T40	T50	T60	T70	T80	T90	T100
Frusemide-Claris 20mg	41%	T	T	T	T	F	F	F	F	F	F
Water For Injections 10mL	44%	T	T	T	T	F	F	F	F	F	F
Paracetamol 1000mg/100mL	26%	T	T	F	F	F	F	F	F	F	F
Fresofol 1% MCT/LCT	36%	T	T	T	F	F	F	F	F	F	F
Amoxicillin 1g	39%	T	T	T	F	F	F	F	F	F	F
Hydrocortisone sodium 100mg	42%	T	T	T	T	F	F	F	F	F	F
Cefazolin Sodium 1g	40%	T	T	T	F	F	F	F	F	F	F
Atracurium Besylate 50mg	47%	T	T	T	T	F	F	F	F	F	F
Naloxone HCl 400mg in 1mL	41%	T	T	T	T	F	F	F	F	F	F
Morphine Sulfate Injection 10mg	46%	T	T	T	T	F	F	F	F	F	F
Ondansetron Solution	46%	T	T	T	T	F	F	F	F	F	F
Protamine Sulfate 10mg/ml	44%	T	T	T	T	F	F	F	F	F	F
Vecuronium Bromide	35%	T	T	T	F	F	F	F	F	F	F
Potassium Chloride 10mmol	40%	T	T	T	F	F	F	F	F	F	F
Heparin Injection 25000IU	37%	T	T	T	F	F	F	F	F	F	F
Sugammadex 200mg/2ml	42%	T	T	T	T	F	F	F	F	F	F
Protamine Sulphate 50mg in 5ml	43%	T	T	T	T	F	F	F	F	F	F
Sodium Chloride 10ml	40%	T	T	T	F	F	F	F	F	F	F
Remifentanil-AFT 2g	38%	T	T	T	F	F	F	F	F	F	F
Sedative Midazolam 5mg	39%	T	T	T	F	F	F	F	F	F	F
Glyceryl Trinitrate 10mg in 10ml	**100%**	**T**	**T**	**T**	**T**	**T**	**T**	**T**	**T**	**T**	**F**
Fentanyl Citrate 785 micrograms	38%	T	T	T	F	F	F	F	F	F	F
Cefazolin-AFT 1g	42%	T	T	T	T	F	F	F	F	F	F
Dynastat 40 mg	41%	T	T	T	T	F	F	F	F	F	F
Tranexamic-AFT	43%	T	T	T	T	F	F	F	F	F	F
Calcium Chloride 1g in 10mL	41%	T	T	T	T	F	F	F	F	F	F
Provive MCT-LCT 1%	32%	T	T	T	F	F	F	F	F	F	F
METOPROLOL Mylan 5mg	47%	T	T	T	T	F	F	F	F	F	F
Noradrenaline 4mL	40%	T	T	T	F	F	F	F	F	F	F
Lidocaine-Claris 5ml	43%	T	T	T	T	F	F	F	F	F	F
Atropine Injection 600Ug	31%	T	T	T	F	F	F	F	F	F	F
Xylocaine 1%	33%	T	T	T	F	F	F	F	F	F	F
Sodium Chloride 0.9%	41%	T	T	T	T	F	F	F	F	F	F
Hypnomidate 10mL	45%	T	T	T	T	F	F	F	F	F	F
Adrenaline Injection 1mg	41%	T	T	T	T	F	F	F	F	F	F
Sterile Dopamine 200mg/5ml	39%	T	T	T	F	F	F	F	F	F	F
Suxamethonium 100mg in 2 ml	48%	T	T	T	T	F	F	F	F	F	F
Amiodarone HCL 50 mg/ml	49%	T	T	T	T	F	F	F	F	F	F
Primacor Injection 10mL	44%	T	T	T	T	F	F	F	F	F	F
Sugammadex 200 mg/2ml	40%	T	T	T	F	F	F	F	F	F	F
Rocuronium Bromide 50 mg	43%	T	T	T	T	F	F	F	F	F	F
Clonidine HCl 150 ug/1mL	36%	T	T	T	F	F	F	F	F	F	F
Cyclizine Lactate 50	41%	T	T	T	T	F	F	F	F	F	F
PITRESSIN 20 Units in 1 mL	42%	T	T	T	T	F	F	F	F	F	F
Magnesium Sulfate 2.47g	41%	T	T	T	T	F	F	F	F	F	F
Metaraminol 10mg/mL	49%	T	T	T	T	F	F	F	F	F	F
Dalacin Phosphate 600 mg/4 mL	41%	T	T	T	T	F	F	F	F	F	F
Pancuronium Inresa 4mg/2ml	43%	T	T	T	T	F	F	F	F	F	F
Ephedrine Hydrochloride 30mg	35%	T	T	T	F	F	F	F	F	F	F
Dexamethasone Phosphate 4mg	46%	T	T	T	T	F	F	F	F	F	F
Glycopyrronium and Neostigmine	42%	T	T	T	T	F	F	F	F	F	F
Actrapid Penfill 3mL	42%	T	T	T	T	F	F	F	F	F	F

Threshold: Fentanyl Citrate against other samples

Drug Name	Similarity Score	T10	T20	T30	T40	T50	T60	T70	T80	T90	T100
Frusemide-Claris 20mg	38%	T	T	T	F	F	F	F	F	F	F
Water For Injections 10mL	43%	T	T	T	T	F	F	F	F	F	F
Paracetamol 1000mg/100mL	32%	T	T	T	F	F	F	F	F	F	F
Fresofol 1% MCT/LCT	41%	T	T	T	T	F	F	F	F	F	F
Amoxicillin 1g	42%	T	T	T	T	F	F	F	F	F	F
Hydrocortisone sodium 100mg	48%	T	T	T	T	F	F	F	F	F	F
Cefazolin Sodium 1g	51%	T	T	T	T	T	F	F	F	F	F
Atracurium Besylate 50mg	38%	T	T	T	F	F	F	F	F	F	F
Naloxone HCl 400mg in 1mL	31%	T	T	T	F	F	F	F	F	F	F
Morphine Sulfate Injection 10mg	45%	T	T	T	T	F	F	F	F	F	F
Ondansetron Solution	44%	T	T	T	T	F	F	F	F	F	F
Protamine Sulfate 10mg/ml	47%	T	T	T	T	F	F	F	F	F	F
Vecuronium Bromide	45%	T	T	T	T	F	F	F	F	F	F
Potassium Chloride 10mmol	45%	T	T	T	T	F	F	F	F	F	F
Heparin Injection 25000IU	45%	T	T	T	T	F	F	F	F	F	F
Sugammadex 200mg/2ml	44%	T	T	T	T	F	F	F	F	F	F
Protamine Sulphate 50mg in 5ml	41%	T	T	T	T	F	F	F	F	F	F
Sodium Chloride 10ml	49%	T	T	T	T	F	F	F	F	F	F
Remifentanil-AFT 2g	57%	T	T	T	T	T	F	F	F	F	F
Sedative Midazolam 5mg	35%	T	T	T	F	F	F	F	F	F	F
Glyceryl Trinitrate 10mg in 10ml	38%	T	T	T	F	F	F	F	F	F	F
Fentanyl Citrate 785 micrograms	**100%**	**T**	**T**	**T**	**T**	**T**	**T**	**T**	**T**	**T**	**F**
Cefazolin-AFT 1g	62%	T	T	T	T	T	T	F	F	F	F
Dynastat 40 mg	41%	T	T	T	T	F	F	F	F	F	F
Tranexamic-AFT	43%	T	T	T	T	F	F	F	F	F	F
Calcium Chloride 1g in 10mL	49%	T	T	T	T	F	F	F	F	F	F
Provive MCT-LCT 1%	41%	T	T	T	T	F	F	F	F	F	F
METOPROLOL Mylan 5mg	42%	T	T	T	T	F	F	F	F	F	F
Noradrenaline 4mL	36%	T	T	T	F	F	F	F	F	F	F
Lidocaine-Claris 5ml	45%	T	T	T	T	F	F	F	F	F	F
Atropine Injection 600Ug	40%	T	T	T	F	F	F	F	F	F	F
Xylocaine 1%	24%	T	T	F	F	F	F	F	F	F	F
Sodium Chloride 0.9%	46%	T	T	T	T	F	F	F	F	F	F
Hypnomidate 10mL	45%	T	T	T	T	F	F	F	F	F	F
Adrenaline Injection 1mg	61%	T	T	T	T	T	T	F	F	F	F
Sterile Dopamine 200mg/5ml	33%	T	T	T	F	F	F	F	F	F	F
Suxamethonium 100mg in 2 ml	45%	T	T	T	T	F	F	F	F	F	F
Amiodarone HCL 50 mg/ml	46%	T	T	T	T	F	F	F	F	F	F
Primacor Injection 10mL	42%	T	T	T	T	F	F	F	F	F	F
Sugammadex 200 mg/2ml	45%	T	T	T	T	F	F	F	F	F	F
Rocuronium Bromide 50 mg	41%	T	T	T	T	F	F	F	F	F	F
Clonidine HCl 150 ug/1mL	52%	T	T	T	T	T	F	F	F	F	F
Cyclizine Lactate 50	40%	T	T	T	F	F	F	F	F	F	F
PITRESSIN 20 Units in 1 mL	41%	T	T	T	T	F	F	F	F	F	F
Magnesium Sulfate 2.47g	48%	T	T	T	T	F	F	F	F	F	F
Metaraminol 10mg/mL	44%	T	T	T	T	F	F	F	F	F	F
Dalacin Phosphate 600 mg/4 mL	31%	T	T	T	F	F	F	F	F	F	F
Pancuronium Inresa 4mg/2ml	40%	T	T	T	F	F	F	F	F	F	F
Ephedrine Hydrochloride 30mg	61%	T	T	T	T	T	T	F	F	F	F
Dexamethasone Phosphate 4mg	47%	T	T	T	T	F	F	F	F	F	F
Glycopyrronium and Neostigmine	51%	T	T	T	T	T	F	F	F	F	F
Actrapid Penfill 3mL	40%	T	T	T	F	F	F	F	F	F	F

Threshold: Cefazolin-AFT against other samples

Drug Name	Similarity Score	T10	T20	T30	T40	T50	T60	T70	T80	T90	T100
Frusemide-Claris 20mg	42%	T	T	T	T	F	F	F	F	F	F
Water For Injections 10mL	47%	T	T	T	T	F	F	F	F	F	F
Paracetamol 1000mg/100mL	25%	T	T	F	F	F	F	F	F	F	F
Fresofol 1% MCT/LCT	40%	T	T	T	F	F	F	F	F	F	F
Amoxicillin 1g	51%	T	T	T	T	T	F	F	F	F	F
Hydrocortisone sodium 100mg	64%	T	T	T	T	T	T	F	F	F	F
Cefazolin Sodium 1g	99%	T	T	T	T	T	T	T	T	T	F
Atracurium Besylate 50mg	49%	T	T	T	T	F	F	F	F	F	F
Naloxone HCl 400mg in 1mL	31%	T	T	T	F	F	F	F	F	F	F
Morphine Sulfate Injection 10mg	41%	T	T	T	T	F	F	F	F	F	F
Ondansetron Solution	39%	T	T	T	F	F	F	F	F	F	F
Protamine Sulfate 10mg/ml	56%	T	T	T	T	T	F	F	F	F	F
Vecuronium Bromide	58%	T	T	T	T	T	F	F	F	F	F
Potassium Chloride 10mmol	46%	T	T	T	T	F	F	F	F	F	F
Heparin Injection 25000IU	51%	T	T	T	T	T	F	F	F	F	F
Sugammadex 200mg/2ml	54%	T	T	T	T	T	F	F	F	F	F
Protamine Sulphate 50mg in 5ml	51%	T	T	T	T	T	F	F	F	F	F
Sodium Chloride 10ml	48%	T	T	T	T	F	F	F	F	F	F
Remifentanil-AFT 2g	74%	T	T	T	T	T	T	T	F	F	F
Sedative Midazolam 5mg	35%	T	T	T	F	F	F	F	F	F	F
Glyceryl Trinitrate 10mg in 10ml	42%	T	T	T	T	F	F	F	F	F	F
Fentanyl Citrate 785 micrograms	62%	T	T	T	T	T	T	F	F	F	F
Cefazolin-AFT 1g	**100%**	**T**	**T**	**T**	**T**	**T**	**T**	**T**	**T**	**T**	**F**
Dynastat 40 mg	57%	T	T	T	T	T	F	F	F	F	F
Tranexamic-AFT	47%	T	T	T	T	F	F	F	F	F	F
Calcium Chloride 1g in 10mL	46%	T	T	T	T	F	F	F	F	F	F
Provive MCT-LCT 1%	46%	T	T	T	T	F	F	F	F	F	F
METOPROLOL Mylan 5mg	47%	T	T	T	T	F	F	F	F	F	F
Noradrenaline 4mL	38%	T	T	T	F	F	F	F	F	F	F
Lidocaine-Claris 5ml	44%	T	T	T	T	F	F	F	F	F	F
Atropine Injection 600Ug	50%	T	T	T	T	F	F	F	F	F	F
Xylocaine 1%	35%	T	T	T	F	F	F	F	F	F	F
Sodium Chloride 0.9%	49%	T	T	T	T	F	F	F	F	F	F
Hypnomidate 10mL	40%	T	T	T	F	F	F	F	F	F	F
Adrenaline Injection 1mg	61%	T	T	T	T	T	T	F	F	F	F
Sterile Dopamine 200mg/5ml	35%	T	T	T	F	F	F	F	F	F	F
Suxamethonium 100mg in 2 ml	53%	T	T	T	T	T	F	F	F	F	F
Amiodarone HCL 50 mg/ml	47%	T	T	T	T	F	F	F	F	F	F
Primacor Injection 10mL	50%	T	T	T	T	F	F	F	F	F	F
Sugammadex 200 mg/2ml	55%	T	T	T	T	T	F	F	F	F	F
Rocuronium Bromide 50 mg	42%	T	T	T	T	F	F	F	F	F	F
Clonidine HCl 150 ug/1mL	52%	T	T	T	T	T	F	F	F	F	F
Cyclizine Lactate 50	40%	T	T	T	F	F	F	F	F	F	F
PITRESSIN 20 Units in 1 mL	49%	T	T	T	T	F	F	F	F	F	F
Magnesium Sulfate 2.47g	45%	T	T	T	T	F	F	F	F	F	F
Metaraminol 10mg/mL	55%	T	T	T	T	T	F	F	F	F	F
Dalacin Phosphate 600 mg/4 mL	36%	T	T	T	F	F	F	F	F	F	F
Pancuronium Inresa 4mg/2ml	41%	T	T	T	T	F	F	F	F	F	F
Ephedrine Hydrochloride 30mg	41%	T	T	T	T	F	F	F	F	F	F
Dexamethasone Phosphate 4mg	53%	T	T	T	T	T	F	F	F	F	F
Glycopyrronium and Neostigmine	51%	T	T	T	T	T	F	F	F	F	F
Actrapid Penfill 3mL	48%	T	T	T	T	F	F	F	F	F	F

Threshold: Dynastat against other samples

Drug Name	Similarity Score	T10	T20	T30	T40	T50	T60	T70	T80	T90	T100
Frusemide-Claris 20mg	48%	T	T	T	T	F	F	F	F	F	F
Water For Injections 10mL	48%	T	T	T	T	F	F	F	F	F	F
Paracetamol 1000mg/100mL	49%	T	T	T	T	F	F	F	F	F	F
Fresofol 1% MCT/LCT	61%	T	T	T	T	T	T	F	F	F	F
Amoxicillin 1g	59%	T	T	T	T	T	F	F	F	F	F
Hydrocortisone sodium 100mg	68%	T	T	T	T	T	T	F	F	F	F
Cefazolin Sodium 1g	63%	T	T	T	T	T	T	F	F	F	F
Atracurium Besylate 50mg	61%	T	T	T	T	T	T	F	F	F	F
Naloxone HCl 400mg in 1mL	35%	T	T	T	F	F	F	F	F	F	F
Morphine Sulfate Injection 10mg	47%	T	T	T	T	F	F	F	F	F	F
Ondansetron Solution	42%	T	T	T	T	F	F	F	F	F	F
Protamine Sulfate 10mg/ml	55%	T	T	T	T	T	F	F	F	F	F
Vecuronium Bromide	66%	T	T	T	T	T	T	F	F	F	F
Potassium Chloride 10mmol	40%	T	T	T	F	F	F	F	F	F	F
Heparin Injection 25000IU	54%	T	T	T	T	T	F	F	F	F	F
Sugammadex 200mg/2ml	54%	T	T	T	T	T	F	F	F	F	F
Protamine Sulphate 50mg in 5ml	49%	T	T	T	T	F	F	F	F	F	F
Sodium Chloride 10ml	52%	T	T	T	T	T	F	F	F	F	F
Remifentanil-AFT 2g	56%	T	T	T	T	T	F	F	F	F	F
Sedative Midazolam 5mg	35%	T	T	T	F	F	F	F	F	F	F
Glyceryl Trinitrate 10mg in 10ml	41%	T	T	T	T	F	F	F	F	F	F
Fentanyl Citrate 785 micrograms	41%	T	T	T	T	F	F	F	F	F	F
Cefazolin-AFT 1g	57%	T	T	T	T	T	F	F	F	F	F
Dynastat 40 mg	**100%**	**T**	**T**	**T**	**T**	**T**	**T**	**T**	**T**	**T**	**F**
Tranexamic-AFT	40%	T	T	T	F	F	F	F	F	F	F
Calcium Chloride 1g in 10mL	47%	T	T	T	T	F	F	F	F	F	F
Provive MCT-LCT 1%	59%	T	T	T	T	T	F	F	F	F	F
METOPROLOL Mylan 5mg	60%	T	T	T	T	T	F	F	F	F	F
Noradrenaline 4mL	41%	T	T	T	T	F	F	F	F	F	F
Lidocaine-Claris 5ml	43%	T	T	T	T	F	F	F	F	F	F
Atropine Injection 600Ug	44%	T	T	T	T	F	F	F	F	F	F
Xylocaine 1%	35%	T	T	T	F	F	F	F	F	F	F
Sodium Chloride 0.9%	40%	T	T	T	F	F	F	F	F	F	F
Hypnomidate 10mL	39%	T	T	T	F	F	F	F	F	F	F
Adrenaline Injection 1mg	42%	T	T	T	T	F	F	F	F	F	F
Sterile Dopamine 200mg/5ml	33%	T	T	T	F	F	F	F	F	F	F
Suxamethonium 100mg in 2 ml	50%	T	T	T	T	F	F	F	F	F	F
Amiodarone HCL 50 mg/ml	57%	T	T	T	T	T	F	F	F	F	F
Primacor Injection 10mL	49%	T	T	T	T	F	F	F	F	F	F
Sugammadex 200 mg/2ml	56%	T	T	T	T	T	F	F	F	F	F
Rocuronium Bromide 50 mg	48%	T	T	T	T	F	F	F	F	F	F
Clonidine HCl 150 ug/1mL	52%	T	T	T	T	T	F	F	F	F	F
Cyclizine Lactate 50	34%	T	T	T	F	F	F	F	F	F	F
PITRESSIN 20 Units in 1 mL	51%	T	T	T	T	T	F	F	F	F	F
Magnesium Sulfate 2.47g	44%	T	T	T	T	F	F	F	F	F	F
Metaraminol 10mg/mL	52%	T	T	T	T	T	F	F	F	F	F
Dalacin Phosphate 600 mg/4 mL	44%	T	T	T	T	F	F	F	F	F	F
Pancuronium Inresa 4mg/2ml	48%	T	T	T	T	F	F	F	F	F	F
Ephedrine Hydrochloride 30mg	44%	T	T	T	T	F	F	F	F	F	F
Dexamethasone Phosphate 4mg	53%	T	T	T	T	T	F	F	F	F	F
Glycopyrronium and Neostigmine	54%	T	T	T	T	T	F	F	F	F	F
Actrapid Penfill 3mL	45%	T	T	T	T	F	F	F	F	F	F

Threshold: Tranexamic-AFT against other samples

Drug Name	Similarity Score	T10	T20	T30	T40	T50	T60	T70	T80	T90	T100
Frusemide-Claris 20mg	54%	T	T	T	T	T	F	F	F	F	F
Water For Injections 10mL	42%	T	T	T	T	F	F	F	F	F	F
Paracetamol 1000mg/100mL	30%	T	T	F	F	F	F	F	F	F	F
Fresofol 1% MCT/LCT	34%	T	T	T	F	F	F	F	F	F	F
Amoxicillin 1g	41%	T	T	T	T	F	F	F	F	F	F
Hydrocortisone sodium 100mg	34%	T	T	T	F	F	F	F	F	F	F
Cefazolin Sodium 1g	42%	T	T	T	T	F	F	F	F	F	F
Atracurium Besylate 50mg	44%	T	T	T	T	F	F	F	F	F	F
Naloxone HCl 400mg in 1mL	39%	T	T	T	F	F	F	F	F	F	F
Morphine Sulfate Injection 10mg	44%	T	T	T	T	F	F	F	F	F	F
Ondansetron Solution	50%	T	T	T	T	F	F	F	F	F	F
Protamine Sulfate 10mg/ml	57%	T	T	T	T	T	F	F	F	F	F
Vecuronium Bromide	34%	T	T	T	F	F	F	F	F	F	F
Potassium Chloride 10mmol	43%	T	T	T	T	F	F	F	F	F	F
Heparin Injection 25000IU	41%	T	T	T	T	F	F	F	F	F	F
Sugammadex 200mg/2ml	48%	T	T	T	T	F	F	F	F	F	F
Protamine Sulphate 50mg in 5ml	43%	T	T	T	T	F	F	F	F	F	F
Sodium Chloride 10ml	52%	T	T	T	T	T	F	F	F	F	F
Remifentanil-AFT 2g	42%	T	T	T	T	F	F	F	F	F	F
Sedative Midazolam 5mg	44%	T	T	T	T	F	F	F	F	F	F
Glyceryl Trinitrate 10mg in 10ml	43%	T	T	T	T	F	F	F	F	F	F
Fentanyl Citrate 785 micrograms	43%	T	T	T	T	F	F	F	F	F	F
Cefazolin-AFT 1g	47%	T	T	T	T	F	F	F	F	F	F
Dynastat 40 mg	40%	T	T	T	F	F	F	F	F	F	F
Tranexamic-AFT	**100%**	**T**	**T**	**T**	**T**	**T**	**T**	**T**	**T**	**T**	**F**
Calcium Chloride 1g in 10mL	45%	T	T	T	T	F	F	F	F	F	F
Provive MCT-LCT 1%	32%	T	T	T	F	F	F	F	F	F	F
METOPROLOL Mylan 5mg	44%	T	T	T	T	F	F	F	F	F	F
Noradrenaline 4mL	45%	T	T	T	T	F	F	F	F	F	F
Lidocaine-Claris 5ml	44%	T	T	T	T	F	F	F	F	F	F
Atropine Injection 600Ug	39%	T	T	T	F	F	F	F	F	F	F
Xylocaine 1%	33%	T	T	T	F	F	F	F	F	F	F
Sodium Chloride 0.9%	46%	T	T	T	T	F	F	F	F	F	F
Hypnomidate 10mL	49%	T	T	T	T	F	F	F	F	F	F
Adrenaline Injection 1mg	44%	T	T	T	T	F	F	F	F	F	F
Sterile Dopamine 200mg/5ml	35%	T	T	T	F	F	F	F	F	F	F
Suxamethonium 100mg in 2 ml	46%	T	T	T	T	F	F	F	F	F	F
Amiodarone HCL 50 mg/ml	46%	T	T	T	T	F	F	F	F	F	F
Primacor Injection 10mL	44%	T	T	T	T	F	F	F	F	F	F
Sugammadex 200 mg/2ml	41%	T	T	T	T	F	F	F	F	F	F
Rocuronium Bromide 50 mg	38%	T	T	T	F	F	F	F	F	F	F
Clonidine HCl 150 ug/1mL	41%	T	T	T	T	F	F	F	F	F	F
Cyclizine Lactate 50	42%	T	T	T	T	F	F	F	F	F	F
PITRESSIN 20 Units in 1 mL	44%	T	T	T	T	F	F	F	F	F	F
Magnesium Sulfate 2.47g	41%	T	T	T	T	F	F	F	F	F	F
Metaraminol 10mg/mL	46%	T	T	T	T	F	F	F	F	F	F
Dalacin Phosphate 600 mg/4 mL	41%	T	T	T	T	F	F	F	F	F	F
Pancuronium Inresa 4mg/2ml	38%	T	T	T	F	F	F	F	F	F	F
Ephedrine Hydrochloride 30mg	42%	T	T	T	T	F	F	F	F	F	F
Dexamethasone Phosphate 4mg	50%	T	T	T	T	F	F	F	F	F	F
Glycopyrronium and Neostigmine	48%	T	T	T	T	F	F	F	F	F	F
Actrapid Penfill 3mL	42%	T	T	T	T	F	F	F	F	F	F

Threshold: Calcium Chloride against other samples

Drug Name	Similarity Score	T10	T20	T30	T40	T50	T60	T70	T80	T90	T100
Frusemide-Claris 20mg	44%	T	T	T	T	F	F	F	F	F	F
Water For Injections 10mL	45%	T	T	T	T	F	F	F	F	F	F
Paracetamol 1000mg/100mL	50%	T	T	T	T	F	F	F	F	F	F
Fresofol 1% MCT/LCT	57%	T	T	T	T	T	F	F	F	F	F
Amoxicillin 1g	47%	T	T	T	T	F	F	F	F	F	F
Hydrocortisone sodium 100mg	45%	T	T	T	T	F	F	F	F	F	F
Cefazolin Sodium 1g	46%	T	T	T	T	F	F	F	F	F	F
Atracurium Besylate 50mg	46%	T	T	T	T	F	F	F	F	F	F
Naloxone HCl 400mg in 1mL	33%	T	T	T	F	F	F	F	F	F	F
Morphine Sulfate Injection 10mg	49%	T	T	T	T	F	F	F	F	F	F
Ondansetron Solution	45%	T	T	T	T	F	F	F	F	F	F
Protamine Sulfate 10mg/ml	55%	T	T	T	T	T	F	F	F	F	F
Vecuronium Bromide	44%	T	T	T	T	F	F	F	F	F	F
Potassium Chloride 10mmol	51%	T	T	T	T	T	F	F	F	F	F
Heparin Injection 25000IU	47%	T	T	T	T	F	F	F	F	F	F
Sugammadex 200mg/2ml	54%	T	T	T	T	T	F	F	F	F	F
Protamine Sulphate 50mg in 5ml	54%	T	T	T	T	T	F	F	F	F	F
Sodium Chloride 10ml	50%	T	T	T	T	F	F	F	F	F	F
Remifentanil-AFT 2g	48%	T	T	T	T	F	F	F	F	F	F
Sedative Midazolam 5mg	35%	T	T	T	F	F	F	F	F	F	F
Glyceryl Trinitrate 10mg in 10ml	41%	T	T	T	T	F	F	F	F	F	F
Fentanyl Citrate 785 micrograms	49%	T	T	T	T	F	F	F	F	F	F
Cefazolin-AFT 1g	46%	T	T	T	T	F	F	F	F	F	F
Dynastat 40 mg	47%	T	T	T	T	F	F	F	F	F	F
Tranexamic-AFT	45%	T	T	T	T	F	F	F	F	F	F
Calcium Chloride 1g in 10mL	**100%**	**T**	**T**	**T**	**T**	**T**	**T**	**T**	**T**	**T**	**F**
Provive MCT-LCT 1%	52%	T	T	T	T	T	F	F	F	F	F
METOPROLOL Mylan 5mg	48%	T	T	T	T	F	F	F	F	F	F
Noradrenaline 4mL	39%	T	T	T	F	F	F	F	F	F	F
Lidocaine-Claris 5ml	46%	T	T	T	T	F	F	F	F	F	F
Atropine Injection 600Ug	42%	T	T	T	T	F	F	F	F	F	F
Xylocaine 1%	32%	T	T	T	F	F	F	F	F	F	F
Sodium Chloride 0.9%	45%	T	T	T	T	F	F	F	F	F	F
Hypnomidate 10mL	46%	T	T	T	T	F	F	F	F	F	F
Adrenaline Injection 1mg	41%	T	T	T	T	F	F	F	F	F	F
Sterile Dopamine 200mg/5ml	36%	T	T	T	F	F	F	F	F	F	F
Suxamethonium 100mg in 2 ml	48%	T	T	T	T	F	F	F	F	F	F
Amiodarone HCL 50 mg/ml	55%	T	T	T	T	T	F	F	F	F	F
Primacor Injection 10mL	49%	T	T	T	T	F	F	F	F	F	F
Sugammadex 200 mg/2ml	55%	T	T	T	T	T	F	F	F	F	F
Rocuronium Bromide 50 mg	41%	T	T	T	T	F	F	F	F	F	F
Clonidine HCl 150 ug/1mL	50%	T	T	T	T	F	F	F	F	F	F
Cyclizine Lactate 50	40%	T	T	T	F	F	F	F	F	F	F
PITRESSIN 20 Units in 1 mL	49%	T	T	T	T	F	F	F	F	F	F
Magnesium Sulfate 2.47g	44%	T	T	T	T	F	F	F	F	F	F
Metaraminol 10mg/mL	50%	T	T	T	T	F	F	F	F	F	F
Dalacin Phosphate 600 mg/4 mL	32%	T	T	T	F	F	F	F	F	F	F
Pancuronium Inresa 4mg/2ml	38%	T	T	T	F	F	F	F	F	F	F
Ephedrine Hydrochloride 30mg	43%	T	T	T	T	F	F	F	F	F	F
Dexamethasone Phosphate 4mg	46%	T	T	T	T	F	F	F	F	F	F
Glycopyrronium and Neostigmine	50%	T	T	T	T	F	F	F	F	F	F
Actrapid Penfill 3mL	49%	T	T	T	T	F	F	F	F	F	F

Threshold: Provive MCT-LCT against other samples

Drug Name	Similarity Score	T10	T20	T30	T40	T50	T60	T70	T80	T90	T100
Frusemide-Claris 20mg	40%	T	T	T	F	F	F	F	F	F	F
Water For Injections 10mL	29%	T	T	F	F	F	F	F	F	F	F
Paracetamol 1000mg/100mL	59%	T	T	T	T	T	F	F	F	F	F
Fresofol 1% MCT/LCT	68%	T	T	T	T	T	T	F	F	F	F
Amoxicillin 1g	46%	T	T	T	T	F	F	F	F	F	F
Hydrocortisone sodium 100mg	49%	T	T	T	T	F	F	F	F	F	F
Cefazolin Sodium 1g	70%	T	T	T	T	T	T	F	F	F	F
Atracurium Besylate 50mg	67%	T	T	T	T	T	T	F	F	F	F
Naloxone HCl 400mg in 1mL	34%	T	T	T	F	F	F	F	F	F	F
Morphine Sulfate Injection 10mg	51%	T	T	T	T	T	F	F	F	F	F
Ondansetron Solution	34%	T	T	T	F	F	F	F	F	F	F
Protamine Sulfate 10mg/ml	46%	T	T	T	T	F	F	F	F	F	F
Vecuronium Bromide	45%	T	T	T	T	F	F	F	F	F	F
Potassium Chloride 10mmol	31%	T	T	T	F	F	F	F	F	F	F
Heparin Injection 25000IU	43%	T	T	T	T	F	F	F	F	F	F
Sugammadex 200mg/2ml	70%	T	T	T	T	T	T	F	F	F	F
Protamine Sulphate 50mg in 5ml	51%	T	T	T	T	T	F	F	F	F	F
Sodium Chloride 10ml	42%	T	T	T	T	F	F	F	F	F	F
Remifentanil-AFT 2g	34%	T	T	T	F	F	F	F	F	F	F
Sedative Midazolam 5mg	25%	T	T	F	F	F	F	F	F	F	F
Glyceryl Trinitrate 10mg in 10ml	32%	T	T	T	F	F	F	F	F	F	F
Fentanyl Citrate 785 micrograms	41%	T	T	T	T	F	F	F	F	F	F
Cefazolin-AFT 1g	46%	T	T	T	T	F	F	F	F	F	F
Dynastat 40 mg	59%	T	T	T	T	T	F	F	F	F	F
Tranexamic-AFT	32%	T	T	T	F	F	F	F	F	F	F
Calcium Chloride 1g in 10mL	52%	T	T	T	T	T	F	F	F	F	F
Provive MCT-LCT 1%	**100%**	**T**	**T**	**T**	**T**	**T**	**T**	**T**	**T**	**T**	**F**
METOPROLOL Mylan 5mg	65%	T	T	T	T	T	T	F	F	F	F
Noradrenaline 4mL	30%	T	T	F	F	F	F	F	F	F	F
Lidocaine-Claris 5ml	35%	T	T	T	F	F	F	F	F	F	F
Atropine Injection 600Ug	19%	T	F	F	F	F	F	F	F	F	F
Xylocaine 1%	16%	T	F	F	F	F	F	F	F	F	F
Sodium Chloride 0.9%	43%	T	T	T	T	F	F	F	F	F	F
Hypnomidate 10mL	40%	T	T	T	F	F	F	F	F	F	F
Adrenaline Injection 1mg	30%	T	T	F	F	F	F	F	F	F	F
Sterile Dopamine 200mg/5ml	19%	T	F	F	F	F	F	F	F	F	F
Suxamethonium 100mg in 2 ml	48%	T	T	T	T	F	F	F	F	F	F
Amiodarone HCL 50 mg/ml	65%	T	T	T	T	T	T	F	F	F	F
Primacor Injection 10mL	45%	T	T	T	T	F	F	F	F	F	F
Sugammadex 200 mg/2ml	75%	T	T	T	T	T	T	T	F	F	F
Rocuronium Bromide 50 mg	56%	T	T	T	T	T	F	F	F	F	F
Clonidine HCl 150 ug/1mL	44%	T	T	T	T	F	F	F	F	F	F
Cyclizine Lactate 50	25%	T	T	F	F	F	F	F	F	F	F
PITRESSIN 20 Units in 1 mL	53%	T	T	T	T	T	F	F	F	F	F
Magnesium Sulfate 2.47g	36%	T	T	T	F	F	F	F	F	F	F
Metaraminol 10mg/mL	55%	T	T	T	T	T	F	F	F	F	F
Dalacin Phosphate 600 mg/4 mL	20%	T	F	F	F	F	F	F	F	F	F
Pancuronium Inresa 4mg/2ml	34%	T	T	T	F	F	F	F	F	F	F
Ephedrine Hydrochloride 30mg	26%	T	T	F	F	F	F	F	F	F	F
Dexamethasone Phosphate 4mg	58%	T	T	T	T	T	F	F	F	F	F
Glycopyrronium and Neostigmine	36%	T	T	T	F	F	F	F	F	F	F
Actrapid Penfill 3mL	27%	T	T	F	F	F	F	F	F	F	F

Threshold: Noradrenaline against other samples

Drug Name	Similarity Score	T10	T20	T30	T40	T50	T60	T70	T80	T90	T100
Frusemide-Claris 20mg	36%	T	T	T	F	F	F	F	F	F	F
Water For Injections 10mL	43%	T	T	T	T	F	F	F	F	F	F
Paracetamol 1000mg/100mL	25%	T	T	F	F	F	F	F	F	F	F
Fresofol 1% MCT/LCT	32%	T	T	T	F	F	F	F	F	F	F
Amoxicillin 1g	39%	T	T	T	F	F	F	F	F	F	F
Hydrocortisone sodium 100mg	35%	T	T	T	F	F	F	F	F	F	F
Cefazolin Sodium 1g	38%	T	T	T	F	F	F	F	F	F	F
Atracurium Besylate 50mg	37%	T	T	T	F	F	F	F	F	F	F
Naloxone HCl 400mg in 1mL	30%	T	T	F	F	F	F	F	F	F	F
Morphine Sulfate Injection 10mg	36%	T	T	T	F	F	F	F	F	F	F
Ondansetron Solution	41%	T	T	T	T	F	F	F	F	F	F
Protamine Sulfate 10mg/ml	42%	T	T	T	T	F	F	F	F	F	F
Vecuronium Bromide	34%	T	T	T	F	F	F	F	F	F	F
Potassium Chloride 10mmol	39%	T	T	T	F	F	F	F	F	F	F
Heparin Injection 25000IU	38%	T	T	T	F	F	F	F	F	F	F
Sugammadex 200mg/2ml	35%	T	T	T	F	F	F	F	F	F	F
Protamine Sulphate 50mg in 5ml	39%	T	T	T	F	F	F	F	F	F	F
Sodium Chloride 10ml	36%	T	T	T	F	F	F	F	F	F	F
Remifentanil-AFT 2g	46%	T	T	T	T	F	F	F	F	F	F
Sedative Midazolam 5mg	32%	T	T	T	F	F	F	F	F	F	F
Glyceryl Trinitrate 10mg in 10ml	40%	T	T	T	F	F	F	F	F	F	F
Fentanyl Citrate 785 micrograms	36%	T	T	T	F	F	F	F	F	F	F
Cefazolin-AFT 1g	38%	T	T	T	F	F	F	F	F	F	F
Dynastat 40 mg	41%	T	T	T	T	F	F	F	F	F	F
Tranexamic-AFT	45%	T	T	T	T	F	F	F	F	F	F
Calcium Chloride 1g in 10mL	39%	T	T	T	F	F	F	F	F	F	F
Provive MCT-LCT 1%	30%	T	T	F	F	F	F	F	F	F	F
METOPROLOL Mylan 5mg	42%	T	T	T	T	F	F	F	F	F	F
Noradrenaline 4mL	**100%**	**T**	**T**	**T**	**T**	**T**	**T**	**T**	**T**	**T**	**F**
Lidocaine-Claris 5ml	43%	T	T	T	T	F	F	F	F	F	F
Atropine Injection 600Ug	29%	T	T	F	F	F	F	F	F	F	F
Xylocaine 1%	32%	T	T	T	F	F	F	F	F	F	F
Sodium Chloride 0.9%	40%	T	T	T	F	F	F	F	F	F	F
Hypnomidate 10mL	35%	T	T	T	F	F	F	F	F	F	F
Adrenaline Injection 1mg	47%	T	T	T	T	F	F	F	F	F	F
Sterile Dopamine 200mg/5ml	42%	T	T	T	T	F	F	F	F	F	F
Suxamethonium 100mg in 2 ml	34%	T	T	T	F	F	F	F	F	F	F
Amiodarone HCL 50 mg/ml	43%	T	T	T	T	F	F	F	F	F	F
Primacor Injection 10mL	41%	T	T	T	T	F	F	F	F	F	F
Sugammadex 200 mg/2ml	38%	T	T	T	F	F	F	F	F	F	F
Rocuronium Bromide 50 mg	35%	T	T	T	F	F	F	F	F	F	F
Clonidine HCl 150 ug/1mL	33%	T	T	T	F	F	F	F	F	F	F
Cyclizine Lactate 50	31%	T	T	T	F	F	F	F	F	F	F
PITRESSIN 20 Units in 1 mL	37%	T	T	T	F	F	F	F	F	F	F
Magnesium Sulfate 2.47g	45%	T	T	T	T	F	F	F	F	F	F
Metaraminol 10mg/mL	37%	T	T	T	F	F	F	F	F	F	F
Dalacin Phosphate 600 mg/4 mL	31%	T	T	T	F	F	F	F	F	F	F
Pancuronium Inresa 4mg/2ml	34%	T	T	T	F	F	F	F	F	F	F
Ephedrine Hydrochloride 30mg	44%	T	T	T	T	F	F	F	F	F	F
Dexamethasone Phosphate 4mg	37%	T	T	T	F	F	F	F	F	F	F
Glycopyrronium and Neostigmine	35%	T	T	T	F	F	F	F	F	F	F
Actrapid Penfill 3mL	37%	T	T	T	F	F	F	F	F	F	F

Threshold: METOPROLOL Mylan against other samples

Drug Name	Similarity Score	T10	T20	T30	T40	T50	T60	T70	T80	T90	T100
Frusemide-Claris 20mg	47%	T	T	T	T	F	F	F	F	F	F
Water For Injections 10mL	42%	T	T	T	T	F	F	F	F	F	F
Paracetamol 1000mg/100mL	55%	T	T	T	T	T	F	F	F	F	F
Fresofol 1% MCT/LCT	70%	T	T	T	T	T	T	F	F	F	F
Amoxicillin 1g	58%	T	T	T	T	T	F	F	F	F	F
Hydrocortisone sodium 100mg	60%	T	T	T	T	T	F	F	F	F	F
Cefazolin Sodium 1g	58%	T	T	T	T	T	F	F	F	F	F
Atracurium Besylate 50mg	73%	T	T	T	T	T	T	T	F	F	F
Naloxone HCl 400mg in 1mL	35%	T	T	T	F	F	F	F	F	F	F
Morphine Sulfate Injection 10mg	48%	T	T	T	T	F	F	F	F	F	F
Ondansetron Solution	46%	T	T	T	T	F	F	F	F	F	F
Protamine Sulfate 10mg/ml	60%	T	T	T	T	T	F	F	F	F	F
Vecuronium Bromide	48%	T	T	T	T	F	F	F	F	F	F
Potassium Chloride 10mmol	38%	T	T	T	F	F	F	F	F	F	F
Heparin Injection 25000IU	47%	T	T	T	T	F	F	F	F	F	F
Sugammadex 200mg/2ml	57%	T	T	T	T	T	F	F	F	F	F
Protamine Sulphate 50mg in 5ml	59%	T	T	T	T	T	F	F	F	F	F
Sodium Chloride 10ml	55%	T	T	T	T	T	F	F	F	F	F
Remifentanil-AFT 2g	46%	T	T	T	T	F	F	F	F	F	F
Sedative Midazolam 5mg	40%	T	T	T	F	F	F	F	F	F	F
Glyceryl Trinitrate 10mg in 10ml	47%	T	T	T	T	F	F	F	F	F	F
Fentanyl Citrate 785 micrograms	42%	T	T	T	T	F	F	F	F	F	F
Cefazolin-AFT 1g	47%	T	T	T	T	F	F	F	F	F	F
Dynastat 40 mg	60%	T	T	T	T	T	F	F	F	F	F
Tranexamic-AFT	44%	T	T	T	T	F	F	F	F	F	F
Calcium Chloride 1g in 10mL	48%	T	T	T	T	F	F	F	F	F	F
Provive MCT-LCT 1%	65%	T	T	T	T	T	T	F	F	F	F
METOPROLOL Mylan 5mg	**100%**	**T**	**T**	**T**	**T**	**T**	**T**	**T**	**T**	**T**	**F**
Noradrenaline 4mL	42%	T	T	T	T	F	F	F	F	F	F
Lidocaine-Claris 5ml	41%	T	T	T	T	F	F	F	F	F	F
Atropine Injection 600Ug	36%	T	T	T	F	F	F	F	F	F	F
Xylocaine 1%	39%	T	T	T	F	F	F	F	F	F	F
Sodium Chloride 0.9%	37%	T	T	T	F	F	F	F	F	F	F
Hypnomidate 10mL	43%	T	T	T	T	F	F	F	F	F	F
Adrenaline Injection 1mg	51%	T	T	T	T	T	F	F	F	F	F
Sterile Dopamine 200mg/5ml	36%	T	T	T	F	F	F	F	F	F	F
Suxamethonium 100mg in 2 ml	44%	T	T	T	T	F	F	F	F	F	F
Amiodarone HCL 50 mg/ml	74%	T	T	T	T	T	T	T	F	F	F
Primacor Injection 10mL	43%	T	T	T	T	F	F	F	F	F	F
Sugammadex 200 mg/2ml	51%	T	T	T	T	T	F	F	F	F	F
Rocuronium Bromide 50 mg	54%	T	T	T	T	T	F	F	F	F	F
Clonidine HCl 150 ug/1mL	45%	T	T	T	T	F	F	F	F	F	F
Cyclizine Lactate 50	36%	T	T	T	F	F	F	F	F	F	F
PITRESSIN 20 Units in 1 mL	50%	T	T	T	T	F	F	F	F	F	F
Magnesium Sulfate 2.47g	49%	T	T	T	T	F	F	F	F	F	F
Metaraminol 10mg/mL	59%	T	T	T	T	T	F	F	F	F	F
Dalacin Phosphate 600 mg/4 mL	42%	T	T	T	T	F	F	F	F	F	F
Pancuronium Inresa 4mg/2ml	43%	T	T	T	T	F	F	F	F	F	F
Ephedrine Hydrochloride 30mg	44%	T	T	T	T	F	F	F	F	F	F
Dexamethasone Phosphate 4mg	64%	T	T	T	T	T	T	F	F	F	F
Glycopyrronium and Neostigmine	59%	T	T	T	T	T	F	F	F	F	F
Actrapid Penfill 3mL	42%	T	T	T	T	F	F	F	F	F	F

Threshold: Paracetamol against other samples

Drug Name	Similarity Score	T10	T20	T30	T40	T50	T60	T70	T80	T90	T100
Frusemide-Claris 20mg	55%	T	T	T	T	T	F	F	F	F	F
Water For Injections 10mL	45%	T	T	T	T	F	F	F	F	F	F
Paracetamol 1000mg/100mL	**100%**	**T**	**T**	**T**	**T**	**T**	**T**	**T**	**T**	**T**	**F**
Fresofol 1% MCT/LCT	61%	T	T	T	T	T	T	F	F	F	F
Amoxicillin 1g	35%	T	T	T	F	F	F	F	F	F	F
Hydrocortisone sodium 100mg	39%	T	T	T	F	F	F	F	F	F	F
Cefazolin Sodium 1g	46%	T	T	T	T	F	F	F	F	F	F
Atracurium Besylate 50mg	45%	T	T	T	T	F	F	F	F	F	F
Naloxone HCl 400mg in 1mL	12%	T	F	F	F	F	F	F	F	F	F
Morphine Sulfate Injection 10mg	24%	T	T	F	F	F	F	F	F	F	F
Ondansetron Solution	33%	T	T	T	F	F	F	F	F	F	F
Protamine Sulfate 10mg/ml	39%	T	T	T	F	F	F	F	F	F	F
Vecuronium Bromide	34%	T	T	T	F	F	F	F	F	F	F
Potassium Chloride 10mmol	26%	T	T	F	F	F	F	F	F	F	F
Heparin Injection 25000IU	23%	T	T	F	F	F	F	F	F	F	F
Sugammadex 200mg/2ml	62%	T	T	T	T	T	T	F	F	F	F
Protamine Sulphate 50mg in 5ml	24%	T	T	F	F	F	F	F	F	F	F
Sodium Chloride 10ml	46%	T	T	T	T	F	F	F	F	F	F
Remifentanil-AFT 2g	29%	T	T	F	F	F	F	F	F	F	F
Sedative Midazolam 5mg	16%	T	F	F	F	F	F	F	F	F	F
Glyceryl Trinitrate 10mg in 10ml	26%	T	T	F	F	F	F	F	F	F	F
Fentanyl Citrate 785 micrograms	32%	T	T	T	F	F	F	F	F	F	F
Cefazolin-AFT 1g	25%	T	T	F	F	F	F	F	F	F	F
Dynastat 40 mg	49%	T	T	T	T	F	F	F	F	F	F
Tranexamic-AFT	30%	T	T	F	F	F	F	F	F	F	F
Calcium Chloride 1g in 10mL	50%	T	T	T	T	F	F	F	F	F	F
Provive MCT-LCT 1%	59%	T	T	T	T	T	F	F	F	F	F
METOPROLOL Mylan 5mg	55%	T	T	T	T	T	F	F	F	F	F
Noradrenaline 4mL	25%	T	T	F	F	F	F	F	F	F	F
Lidocaine-Claris 5ml	24%	T	T	F	F	F	F	F	F	F	F
Atropine Injection 600Ug	15%	T	F	F	F	F	F	F	F	F	F
Xylocaine 1%	12%	T	F	F	F	F	F	F	F	F	F
Sodium Chloride 0.9%	35%	T	T	T	F	F	F	F	F	F	F
Hypnomidate 10mL	35%	T	T	T	F	F	F	F	F	F	F
Adrenaline Injection 1mg	18%	T	F	F	F	F	F	F	F	F	F
Sterile Dopamine 200mg/5ml	16%	T	F	F	F	F	F	F	F	F	F
Suxamethonium 100mg in 2 ml	39%	T	T	T	F	F	F	F	F	F	F
Amiodarone HCL 50 mg/ml	65%	T	T	T	T	T	T	F	F	F	F
Primacor Injection 10mL	47%	T	T	T	T	F	F	F	F	F	F
Sugammadex 200 mg/2ml	45%	T	T	T	T	F	F	F	F	F	F
Rocuronium Bromide 50 mg	20%	T	F	F	F	F	F	F	F	F	F
Clonidine HCl 150 ug/1mL	17%	T	F	F	F	F	F	F	F	F	F
Cyclizine Lactate 50	19%	T	F	F	F	F	F	F	F	F	F
PITRESSIN 20 Units in 1 mL	19%	T	F	F	F	F	F	F	F	F	F
Magnesium Sulfate 2.47g	24%	T	T	F	F	F	F	F	F	F	F
Metaraminol 10mg/mL	44%	T	T	T	T	F	F	F	F	F	F
Dalacin Phosphate 600 mg/4 mL	16%	T	F	F	F	F	F	F	F	F	F
Pancuronium Inresa 4mg/2ml	29%	T	T	F	F	F	F	F	F	F	F
Ephedrine Hydrochloride 30mg	40%	T	T	T	F	F	F	F	F	F	F
Dexamethasone Phosphate 4mg	47%	T	T	T	T	F	F	F	F	F	F
Glycopyrronium and Neostigmine	41%	T	T	T	T	F	F	F	F	F	F
Actrapid Penfill 3mL	22%	T	T	F	F	F	F	F	F	F	F

Threshold: Lidocaine-Claris against other samples

Drug Name	Similarity Score	T10	T20	T30	T40	T50	T60	T70	T80	T90	T100
Frusemide-Claris 20mg	48%	T	T	T	T	F	F	F	F	F	F
Water For Injections 10mL	46%	T	T	T	T	F	F	F	F	F	F
Paracetamol 1000mg/100mL	24%	T	T	F	F	F	F	F	F	F	F
Fresofol 1% MCT/LCT	32%	T	T	T	F	F	F	F	F	F	F
Amoxicillin 1g	39%	T	T	T	F	F	F	F	F	F	F
Hydrocortisone sodium 100mg	43%	T	T	T	T	F	F	F	F	F	F
Cefazolin Sodium 1g	40%	T	T	T	F	F	F	F	F	F	F
Atracurium Besylate 50mg	47%	T	T	T	T	F	F	F	F	F	F
Naloxone HCl 400mg in 1mL	37%	T	T	T	F	F	F	F	F	F	F
Morphine Sulfate Injection 10mg	49%	T	T	T	T	F	F	F	F	F	F
Ondansetron Solution	53%	T	T	T	T	T	F	F	F	F	F
Protamine Sulfate 10mg/ml	46%	T	T	T	T	F	F	F	F	F	F
Vecuronium Bromide	39%	T	T	T	F	F	F	F	F	F	F
Potassium Chloride 10mmol	41%	T	T	T	T	F	F	F	F	F	F
Heparin Injection 25000IU	45%	T	T	T	T	F	F	F	F	F	F
Sugammadex 200mg/2ml	46%	T	T	T	T	F	F	F	F	F	F
Protamine Sulphate 50mg in 5ml	44%	T	T	T	T	F	F	F	F	F	F
Sodium Chloride 10ml	47%	T	T	T	T	F	F	F	F	F	F
Remifentanil-AFT 2g	44%	T	T	T	T	F	F	F	F	F	F
Sedative Midazolam 5mg	37%	T	T	T	F	F	F	F	F	F	F
Glyceryl Trinitrate 10mg in 10ml	43%	T	T	T	T	F	F	F	F	F	F
Fentanyl Citrate 785 micrograms	45%	T	T	T	T	F	F	F	F	F	F
Cefazolin-AFT 1g	44%	T	T	T	T	F	F	F	F	F	F
Dynastat 40 mg	43%	T	T	T	T	F	F	F	F	F	F
Tranexamic-AFT	44%	T	T	T	T	F	F	F	F	F	F
Calcium Chloride 1g in 10mL	46%	T	T	T	T	F	F	F	F	F	F
Provive MCT-LCT 1%	35%	T	T	T	F	F	F	F	F	F	F
METOPROLOL Mylan 5mg	41%	T	T	T	T	F	F	F	F	F	F
Noradrenaline 4mL	43%	T	T	T	T	F	F	F	F	F	F
Lidocaine-Claris 5ml	**100%**	**T**	**T**	**T**	**T**	**T**	**T**	**T**	**T**	**T**	**F**
Atropine Injection 600Ug	43%	T	T	T	T	F	F	F	F	F	F
Xylocaine 1%	45%	T	T	T	T	F	F	F	F	F	F
Sodium Chloride 0.9%	43%	T	T	T	T	F	F	F	F	F	F
Hypnomidate 10mL	47%	T	T	T	T	F	F	F	F	F	F
Adrenaline Injection 1mg	44%	T	T	T	T	F	F	F	F	F	F
Sterile Dopamine 200mg/5ml	35%	T	T	T	F	F	F	F	F	F	F
Suxamethonium 100mg in 2 ml	41%	T	T	T	T	F	F	F	F	F	F
Amiodarone HCL 50 mg/ml	47%	T	T	T	T	F	F	F	F	F	F
Primacor Injection 10mL	42%	T	T	T	T	F	F	F	F	F	F
Sugammadex 200 mg/2ml	45%	T	T	T	T	F	F	F	F	F	F
Rocuronium Bromide 50 mg	46%	T	T	T	T	F	F	F	F	F	F
Clonidine HCl 150 ug/1mL	44%	T	T	T	T	F	F	F	F	F	F
Cyclizine Lactate 50	41%	T	T	T	T	F	F	F	F	F	F
PITRESSIN 20 Units in 1 mL	46%	T	T	T	T	F	F	F	F	F	F
Magnesium Sulfate 2.47g	47%	T	T	T	T	F	F	F	F	F	F
Metaraminol 10mg/mL	43%	T	T	T	T	F	F	F	F	F	F
Dalacin Phosphate 600 mg/4 mL	32%	T	T	T	F	F	F	F	F	F	F
Pancuronium Inresa 4mg/2ml	38%	T	T	T	F	F	F	F	F	F	F
Ephedrine Hydrochloride 30mg	54%	T	T	T	T	T	F	F	F	F	F
Dexamethasone Phosphate 4mg	47%	T	T	T	T	F	F	F	F	F	F
Glycopyrronium and Neostigmine	45%	T	T	T	T	F	F	F	F	F	F
Actrapid Penfill 3mL	43%	T	T	T	T	F	F	F	F	F	F

Threshold: Atropine Injection against other samples

Drug Name	Similarity Score	T10	T20	T30	T40	T50	T60	T70	T80	T90	T100
Frusemide-Claris 20mg	35%	T	T	T	F	F	F	F	F	F	F
Water For Injections 10mL	41%	T	T	T	T	F	F	F	F	F	F
Paracetamol 1000mg/100mL	15%	T	F	F	F	F	F	F	F	F	F
Fresofol 1% MCT/LCT	32%	T	T	T	F	F	F	F	F	F	F
Amoxicillin 1g	31%	T	T	T	F	F	F	F	F	F	F
Hydrocortisone sodium 100mg	40%	T	T	T	F	F	F	F	F	F	F
Cefazolin Sodium 1g	39%	T	T	T	F	F	F	F	F	F	F
Atracurium Besylate 50mg	41%	T	T	T	T	F	F	F	F	F	F
Naloxone HCl 400mg in 1mL	34%	T	T	T	F	F	F	F	F	F	F
Morphine Sulfate Injection 10mg	42%	T	T	T	T	F	F	F	F	F	F
Ondansetron Solution	34%	T	T	T	F	F	F	F	F	F	F
Protamine Sulfate 10mg/ml	47%	T	T	T	T	F	F	F	F	F	F
Vecuronium Bromide	48%	T	T	T	T	F	F	F	F	F	F
Potassium Chloride 10mmol	40%	T	T	T	F	F	F	F	F	F	F
Heparin Injection 25000IU	49%	T	T	T	T	F	F	F	F	F	F
Sugammadex 200mg/2ml	49%	T	T	T	T	F	F	F	F	F	F
Protamine Sulphate 50mg in 5ml	43%	T	T	T	T	F	F	F	F	F	F
Sodium Chloride 10ml	39%	T	T	T	F	F	F	F	F	F	F
Remifentanil-AFT 2g	43%	T	T	T	T	F	F	F	F	F	F
Sedative Midazolam 5mg	34%	T	T	T	F	F	F	F	F	F	F
Glyceryl Trinitrate 10mg in 10ml	31%	T	T	T	F	F	F	F	F	F	F
Fentanyl Citrate 785 micrograms	40%	T	T	T	F	F	F	F	F	F	F
Cefazolin-AFT 1g	50%	T	T	T	T	F	F	F	F	F	F
Dynastat 40 mg	44%	T	T	T	T	F	F	F	F	F	F
Tranexamic-AFT	39%	T	T	T	F	F	F	F	F	F	F
Calcium Chloride 1g in 10mL	42%	T	T	T	T	F	F	F	F	F	F
Provive MCT-LCT 1%	19%	T	F	F	F	F	F	F	F	F	F
METOPROLOL Mylan 5mg	36%	T	T	T	F	F	F	F	F	F	F
Noradrenaline 4mL	29%	T	T	F	F	F	F	F	F	F	F
Lidocaine-Claris 5ml	43%	T	T	T	T	F	F	F	F	F	F
Atropine Injection 600Ug	**100%**	**T**	**T**	**T**	**T**	**T**	**T**	**T**	**T**	**T**	**F**
Xylocaine 1%	41%	T	T	T	T	F	F	F	F	F	F
Sodium Chloride 0.9%	30%	T	T	F	F	F	F	F	F	F	F
Hypnomidate 10mL	42%	T	T	T	T	F	F	F	F	F	F
Adrenaline Injection 1mg	47%	T	T	T	T	F	F	F	F	F	F
Sterile Dopamine 200mg/5ml	39%	T	T	T	F	F	F	F	F	F	F
Suxamethonium 100mg in 2 ml	53%	T	T	T	T	T	F	F	F	F	F
Amiodarone HCL 50 mg/ml	41%	T	T	T	T	F	F	F	F	F	F
Primacor Injection 10mL	45%	T	T	T	T	F	F	F	F	F	F
Sugammadex 200 mg/2ml	50%	T	T	T	T	F	F	F	F	F	F
Rocuronium Bromide 50 mg	53%	T	T	T	T	T	F	F	F	F	F
Clonidine HCl 150 ug/1mL	63%	T	T	T	T	T	T	F	F	F	F
Cyclizine Lactate 50	40%	T	T	T	F	F	F	F	F	F	F
PITRESSIN 20 Units in 1 mL	52%	T	T	T	T	T	F	F	F	F	F
Magnesium Sulfate 2.47g	36%	T	T	T	F	F	F	F	F	F	F
Metaraminol 10mg/mL	45%	T	T	T	T	F	F	F	F	F	F
Dalacin Phosphate 600 mg/4 mL	36%	T	T	T	F	F	F	F	F	F	F
Pancuronium Inresa 4mg/2ml	35%	T	T	T	F	F	F	F	F	F	F
Ephedrine Hydrochloride 30mg	50%	T	T	T	T	F	F	F	F	F	F
Dexamethasone Phosphate 4mg	52%	T	T	T	T	T	F	F	F	F	F
Glycopyrronium and Neostigmine	43%	T	T	T	T	F	F	F	F	F	F
Actrapid Penfill 3mL	48%	T	T	T	T	F	F	F	F	F	F

Threshold: Xylocaine against other samples

Drug Name	Similarity Score	T10	T20	T30	T40	T50	T60	T70	T80	T90	T100
Frusemide-Claris 20mg	27%	T	T	F	F	F	F	F	F	F	F
Water For Injections 10mL	36%	T	T	T	F	F	F	F	F	F	F
Paracetamol 1000mg/100mL	12%	T	F	F	F	F	F	F	F	F	F
Fresofol 1% MCT/LCT	17%	T	F	F	F	F	F	F	F	F	F
Amoxicillin 1g	24%	T	T	F	F	F	F	F	F	F	F
Hydrocortisone sodium 100mg	31%	T	T	T	F	F	F	F	F	F	F
Cefazolin Sodium 1g	27%	T	T	F	F	F	F	F	F	F	F
Atracurium Besylate 50mg	38%	T	T	T	F	F	F	F	F	F	F
Naloxone HCl 400mg in 1mL	42%	T	T	T	T	F	F	F	F	F	F
Morphine Sulfate Injection 10mg	44%	T	T	T	T	F	F	F	F	F	F
Ondansetron Solution	30%	T	T	F	F	F	F	F	F	F	F
Protamine Sulfate 10mg/ml	42%	T	T	T	T	F	F	F	F	F	F
Vecuronium Bromide	40%	T	T	T	F	F	F	F	F	F	F
Potassium Chloride 10mmol	34%	T	T	T	F	F	F	F	F	F	F
Heparin Injection 25000IU	41%	T	T	T	T	F	F	F	F	F	F
Sugammadex 200mg/2ml	38%	T	T	T	F	F	F	F	F	F	F
Protamine Sulphate 50mg in 5ml	41%	T	T	T	T	F	F	F	F	F	F
Sodium Chloride 10ml	28%	T	T	F	F	F	F	F	F	F	F
Remifentanil-AFT 2g	29%	T	T	F	F	F	F	F	F	F	F
Sedative Midazolam 5mg	34%	T	T	T	F	F	F	F	F	F	F
Glyceryl Trinitrate 10mg in 10ml	33%	T	T	T	F	F	F	F	F	F	F
Fentanyl Citrate 785 micrograms	24%	T	T	F	F	F	F	F	F	F	F
Cefazolin-AFT 1g	35%	T	T	T	F	F	F	F	F	F	F
Dynastat 40 mg	35%	T	T	T	F	F	F	F	F	F	F
Tranexamic-AFT	33%	T	T	T	F	F	F	F	F	F	F
Calcium Chloride 1g in 10mL	32%	T	T	T	F	F	F	F	F	F	F
Provive MCT-LCT 1%	16%	T	F	F	F	F	F	F	F	F	F
METOPROLOL Mylan 5mg	39%	T	T	T	F	F	F	F	F	F	F
Noradrenaline 4mL	32%	T	T	T	F	F	F	F	F	F	F
Lidocaine-Claris 5ml	45%	T	T	T	T	F	F	F	F	F	F
Atropine Injection 600Ug	41%	T	T	T	T	F	F	F	F	F	F
Xylocaine 1%	**100%**	**T**	**T**	**T**	**T**	**T**	**T**	**T**	**T**	**T**	**F**
Sodium Chloride 0.9%	24%	T	T	F	F	F	F	F	F	F	F
Hypnomidate 10mL	35%	T	T	T	F	F	F	F	F	F	F
Adrenaline Injection 1mg	36%	T	T	T	F	F	F	F	F	F	F
Sterile Dopamine 200mg/5ml	36%	T	T	T	F	F	F	F	F	F	F
Suxamethonium 100mg in 2 ml	39%	T	T	T	F	F	F	F	F	F	F
Amiodarone HCL 50 mg/ml	32%	T	T	T	F	F	F	F	F	F	F
Primacor Injection 10mL	33%	T	T	T	F	F	F	F	F	F	F
Sugammadex 200 mg/2ml	35%	T	T	T	F	F	F	F	F	F	F
Rocuronium Bromide 50 mg	41%	T	T	T	T	F	F	F	F	F	F
Clonidine HCl 150 ug/1mL	41%	T	T	T	T	F	F	F	F	F	F
Cyclizine Lactate 50	34%	T	T	T	F	F	F	F	F	F	F
PITRESSIN 20 Units in 1 mL	41%	T	T	T	T	F	F	F	F	F	F
Magnesium Sulfate 2.47g	32%	T	T	T	F	F	F	F	F	F	F
Metaraminol 10mg/mL	38%	T	T	T	F	F	F	F	F	F	F
Dalacin Phosphate 600 mg/4 mL	33%	T	T	T	F	F	F	F	F	F	F
Pancuronium Inresa 4mg/2ml	27%	T	T	F	F	F	F	F	F	F	F
Ephedrine Hydrochloride 30mg	38%	T	T	T	F	F	F	F	F	F	F
Dexamethasone Phosphate 4mg	42%	T	T	T	T	F	F	F	F	F	F
Glycopyrronium and Neostigmine	33%	T	T	T	F	F	F	F	F	F	F
Actrapid Penfill 3mL	42%	T	T	T	T	F	F	F	F	F	F

Threshold: Hypnomidate against other samples

Drug Name	Similarity Score	T10	T20	T30	T40	T50	T60	T70	T80	T90	T100
Frusemide-Claris 20mg	43%	T	T	T	T	F	F	F	F	F	F
Water For Injections 10mL	53%	T	T	T	T	T	F	F	F	F	F
Paracetamol 1000mg/100mL	34%	T	T	T	F	F	F	F	F	F	F
Fresofol 1% MCT/LCT	37%	T	T	T	F	F	F	F	F	F	F
Amoxicillin 1g	40%	T	T	T	F	F	F	F	F	F	F
Hydrocortisone sodium 100mg	44%	T	T	T	T	F	F	F	F	F	F
Cefazolin Sodium 1g	36%	T	T	T	F	F	F	F	F	F	F
Atracurium Besylate 50mg	42%	T	T	T	T	F	F	F	F	F	F
Naloxone HCl 400mg in 1mL	39%	T	T	T	F	F	F	F	F	F	F
Morphine Sulfate Injection 10mg	49%	T	T	T	T	F	F	F	F	F	F
Ondansetron Solution	44%	T	T	T	T	F	F	F	F	F	F
Protamine Sulfate 10mg/ml	46%	T	T	T	T	F	F	F	F	F	F
Vecuronium Bromide	37%	T	T	T	F	F	F	F	F	F	F
Potassium Chloride 10mmol	41%	T	T	T	T	F	F	F	F	F	F
Heparin Injection 25000IU	38%	T	T	T	F	F	F	F	F	F	F
Sugammadex 200mg/2ml	47%	T	T	T	T	F	F	F	F	F	F
Protamine Sulphate 50mg in 5ml	44%	T	T	T	T	F	F	F	F	F	F
Sodium Chloride 10ml	48%	T	T	T	T	F	F	F	F	F	F
Remifentanil-AFT 2g	38%	T	T	T	F	F	F	F	F	F	F
Sedative Midazolam 5mg	50%	T	T	T	T	F	F	F	F	F	F
Glyceryl Trinitrate 10mg in 10ml	44%	T	T	T	T	F	F	F	F	F	F
Fentanyl Citrate 785 micrograms	45%	T	T	T	T	F	F	F	F	F	F
Cefazolin-AFT 1g	40%	T	T	T	F	F	F	F	F	F	F
Dynastat 40 mg	40%	T	T	T	F	F	F	F	F	F	F
Tranexamic-AFT	49%	T	T	T	T	F	F	F	F	F	F
Calcium Chloride 1g in 10mL	46%	T	T	T	T	F	F	F	F	F	F
Provive MCT-LCT 1%	39%	T	T	T	F	F	F	F	F	F	F
METOPROLOL Mylan 5mg	43%	T	T	T	T	F	F	F	F	F	F
Noradrenaline 4mL	34%	T	T	T	F	F	F	F	F	F	F
Lidocaine-Claris 5ml	48%	T	T	T	T	F	F	F	F	F	F
Atropine Injection 600Ug	42%	T	T	T	T	F	F	F	F	F	F
Xylocaine 1%	35%	T	T	T	F	F	F	F	F	F	F
Sodium Chloride 0.9%	46%	T	T	T	T	F	F	F	F	F	F
Hypnomidate 10mL	**100%**	**T**	**T**	**T**	**T**	**T**	**T**	**T**	**T**	**T**	**F**
Adrenaline Injection 1mg	37%	T	T	T	F	F	F	F	F	F	F
Sterile Dopamine 200mg/5ml	42%	T	T	T	T	F	F	F	F	F	F
Suxamethonium 100mg in 2 ml	51%	T	T	T	T	T	F	F	F	F	F
Amiodarone HCL 50 mg/ml	47%	T	T	T	T	F	F	F	F	F	F
Primacor Injection 10mL	47%	T	T	T	T	F	F	F	F	F	F
Sugammadex 200 mg/2ml	45%	T	T	T	T	F	F	F	F	F	F
Rocuronium Bromide 50 mg	43%	T	T	T	T	F	F	F	F	F	F
Clonidine HCl 150 ug/1mL	48%	T	T	T	T	F	F	F	F	F	F
Cyclizine Lactate 50	46%	T	T	T	T	F	F	F	F	F	F
PITRESSIN 20 Units in 1 mL	42%	T	T	T	T	F	F	F	F	F	F
Magnesium Sulfate 2.47g	45%	T	T	T	T	F	F	F	F	F	F
Metaraminol 10mg/mL	42%	T	T	T	T	F	F	F	F	F	F
Dalacin Phosphate 600 mg/4 mL	41%	T	T	T	T	F	F	F	F	F	F
Pancuronium Inresa 4mg/2ml	40%	T	T	T	F	F	F	F	F	F	F
Ephedrine Hydrochloride 30mg	45%	T	T	T	T	F	F	F	F	F	F
Dexamethasone Phosphate 4mg	48%	T	T	T	T	F	F	F	F	F	F
Glycopyrronium and Neostigmine	48%	T	T	T	T	F	F	F	F	F	F
Actrapid Penfill 3mL	44%	T	T	T	T	F	F	F	F	F	F

Threshold: Adrenaline Injection against other samples

Drug Name	Similarity Score	T10	T20	T30	T40	T50	T60	T70	T80	T90	T100
Frusemide-Claris 20mg	32%	T	T	T	F	F	F	F	F	F	F
Water For Injections 10mL	44%	T	T	T	T	F	F	F	F	F	F
Paracetamol 1000mg/100mL	18%	T	F	F	F	F	F	F	F	F	F
Fresofol 1% MCT/LCT	49%	T	T	T	T	F	F	F	F	F	F
Amoxicillin 1g	42%	T	T	T	T	F	F	F	F	F	F
Hydrocortisone sodium 100mg	61%	T	T	T	T	T	T	F	F	F	F
Cefazolin Sodium 1g	61%	T	T	T	T	T	T	F	F	F	F
Atracurium Besylate 50mg	46%	T	T	T	T	F	F	F	F	F	F
Naloxone HCl 400mg in 1mL	37%	T	T	T	F	F	F	F	F	F	F
Morphine Sulfate Injection 10mg	47%	T	T	T	T	F	F	F	F	F	F
Ondansetron Solution	34%	T	T	T	F	F	F	F	F	F	F
Protamine Sulfate 10mg/ml	43%	T	T	T	T	F	F	F	F	F	F
Vecuronium Bromide	47%	T	T	T	T	F	F	F	F	F	F
Potassium Chloride 10mmol	35%	T	T	T	F	F	F	F	F	F	F
Heparin Injection 25000IU	44%	T	T	T	T	F	F	F	F	F	F
Sugammadex 200mg/2ml	45%	T	T	T	T	F	F	F	F	F	F
Protamine Sulphate 50mg in 5ml	44%	T	T	T	T	F	F	F	F	F	F
Sodium Chloride 10ml	35%	T	T	T	F	F	F	F	F	F	F
Remifentanil-AFT 2g	44%	T	T	T	T	F	F	F	F	F	F
Sedative Midazolam 5mg	29%	T	T	F	F	F	F	F	F	F	F
Glyceryl Trinitrate 10mg in 10ml	41%	T	T	T	T	F	F	F	F	F	F
Fentanyl Citrate 785 micrograms	61%	T	T	T	T	T	T	F	F	F	F
Cefazolin-AFT 1g	61%	T	T	T	T	T	T	F	F	F	F
Dynastat 40 mg	42%	T	T	T	T	F	F	F	F	F	F
Tranexamic-AFT	44%	T	T	T	T	F	F	F	F	F	F
Calcium Chloride 1g in 10mL	41%	T	T	T	T	F	F	F	F	F	F
Provive MCT-LCT 1%	30%	T	T	F	F	F	F	F	F	F	F
METOPROLOL Mylan 5mg	51%	T	T	T	T	T	F	F	F	F	F
Noradrenaline 4mL	47%	T	T	T	T	F	F	F	F	F	F
Lidocaine-Claris 5ml	44%	T	T	T	T	F	F	F	F	F	F
Atropine Injection 600Ug	47%	T	T	T	T	F	F	F	F	F	F
Xylocaine 1%	36%	T	T	T	F	F	F	F	F	F	F
Sodium Chloride 0.9%	32%	T	T	T	F	F	F	F	F	F	F
Hypnomidate 10mL	36%	T	T	T	F	F	F	F	F	F	F
Adrenaline Injection 1mg	**100%**	**T**	**T**	**T**	**T**	**T**	**T**	**T**	**T**	**T**	**F**
Sterile Dopamine 200mg/5ml	31%	T	T	T	F	F	F	F	F	F	F
Suxamethonium 100mg in 2 ml	35%	T	T	T	F	F	F	F	F	F	F
Amiodarone HCL 50 mg/ml	42%	T	T	T	T	F	F	F	F	F	F
Primacor Injection 10mL	42%	T	T	T	T	F	F	F	F	F	F
Sugammadex 200 mg/2ml	44%	T	T	T	T	F	F	F	F	F	F
Rocuronium Bromide 50 mg	51%	T	T	T	T	T	F	F	F	F	F
Clonidine HCl 150 ug/1mL	43%	T	T	T	T	F	F	F	F	F	F
Cyclizine Lactate 50	35%	T	T	T	F	F	F	F	F	F	F
PITRESSIN 20 Units in 1 mL	49%	T	T	T	T	F	F	F	F	F	F
Magnesium Sulfate 2.47g	45%	T	T	T	T	F	F	F	F	F	F
Metaraminol 10mg/mL	48%	T	T	T	T	F	F	F	F	F	F
Dalacin Phosphate 600 mg/4 mL	36%	T	T	T	F	F	F	F	F	F	F
Pancuronium Inresa 4mg/2ml	34%	T	T	T	F	F	F	F	F	F	F
Ephedrine Hydrochloride 30mg	45%	T	T	T	T	F	F	F	F	F	F
Dexamethasone Phosphate 4mg	49%	T	T	T	T	F	F	F	F	F	F
Glycopyrronium and Neostigmine	38%	T	T	T	F	F	F	F	F	F	F
Actrapid Penfill 3mL	50%	T	T	T	T	F	F	F	F	F	F

Threshold: Sterile Dopamine against other samples

Drug Name	Similarity Score	T10	T20	T30	T40	T50	T60	T70	T80	T90	T100
Frusemide-Claris 20mg	36%	T	T	T	F	F	F	F	F	F	F
Water For Injections 10mL	40%	T	T	T	F	F	F	F	F	F	F
Paracetamol 1000mg/100mL	16%	T	F	F	F	F	F	F	F	F	F
Fresofol 1% MCT/LCT	23%	T	T	F	F	F	F	F	F	F	F
Amoxicillin 1g	44%	T	T	T	T	F	F	F	F	F	F
Hydrocortisone sodium 100mg	32%	T	T	T	F	F	F	F	F	F	F
Cefazolin Sodium 1g	32%	T	T	T	F	F	F	F	F	F	F
Atracurium Besylate 50mg	38%	T	T	T	F	F	F	F	F	F	F
Naloxone HCl 400mg in 1mL	42%	T	T	T	T	F	F	F	F	F	F
Morphine Sulfate Injection 10mg	44%	T	T	T	T	F	F	F	F	F	F
Ondansetron Solution	41%	T	T	T	T	F	F	F	F	F	F
Protamine Sulfate 10mg/ml	53%	T	T	T	T	T	F	F	F	F	F
Vecuronium Bromide	30%	T	T	F	F	F	F	F	F	F	F
Potassium Chloride 10mmol	58%	T	T	T	T	T	F	F	F	F	F
Heparin Injection 25000IU	41%	T	T	T	T	F	F	F	F	F	F
Sugammadex 200mg/2ml	44%	T	T	T	T	F	F	F	F	F	F
Protamine Sulphate 50mg in 5ml	48%	T	T	T	T	F	F	F	F	F	F
Sodium Chloride 10ml	30%	T	T	F	F	F	F	F	F	F	F
Remifentanil-AFT 2g	33%	T	T	T	F	F	F	F	F	F	F
Sedative Midazolam 5mg	48%	T	T	T	T	F	F	F	F	F	F
Glyceryl Trinitrate 10mg in 10ml	39%	T	T	T	F	F	F	F	F	F	F
Fentanyl Citrate 785 micrograms	33%	T	T	T	F	F	F	F	F	F	F
Cefazolin-AFT 1g	35%	T	T	T	F	F	F	F	F	F	F
Dynastat 40 mg	33%	T	T	T	F	F	F	F	F	F	F
Tranexamic-AFT	35%	T	T	T	F	F	F	F	F	F	F
Calcium Chloride 1g in 10mL	36%	T	T	T	F	F	F	F	F	F	F
Provive MCT-LCT 1%	19%	T	F	F	F	F	F	F	F	F	F
METOPROLOL Mylan 5mg	36%	T	T	T	F	F	F	F	F	F	F
Noradrenaline 4mL	42%	T	T	T	T	F	F	F	F	F	F
Lidocaine-Claris 5ml	35%	T	T	T	F	F	F	F	F	F	F
Atropine Injection 600Ug	39%	T	T	T	F	F	F	F	F	F	F
Xylocaine 1%	36%	T	T	T	F	F	F	F	F	F	F
Sodium Chloride 0.9%	37%	T	T	T	F	F	F	F	F	F	F
Hypnomidate 10mL	43%	T	T	T	T	F	F	F	F	F	F
Adrenaline Injection 1mg	31%	T	T	T	F	F	F	F	F	F	F
Sterile Dopamine 200mg/5ml	**100%**	**T**	**T**	**T**	**T**	**T**	**T**	**T**	**T**	**T**	**F**
Suxamethonium 100mg in 2 ml	41%	T	T	T	T	F	F	F	F	F	F
Amiodarone HCL 50 mg/ml	47%	T	T	T	T	F	F	F	F	F	F
Primacor Injection 10mL	42%	T	T	T	T	F	F	F	F	F	F
Sugammadex 200 mg/2ml	39%	T	T	T	F	F	F	F	F	F	F
Rocuronium Bromide 50 mg	37%	T	T	T	F	F	F	F	F	F	F
Clonidine HCl 150 ug/1mL	39%	T	T	T	F	F	F	F	F	F	F
Cyclizine Lactate 50	46%	T	T	T	T	F	F	F	F	F	F
PITRESSIN 20 Units in 1 mL	40%	T	T	T	F	F	F	F	F	F	F
Magnesium Sulfate 2.47g	47%	T	T	T	T	F	F	F	F	F	F
Metaraminol 10mg/mL	42%	T	T	T	T	F	F	F	F	F	F
Dalacin Phosphate 600 mg/4 mL	42%	T	T	T	T	F	F	F	F	F	F
Pancuronium Inresa 4mg/2ml	32%	T	T	T	F	F	F	F	F	F	F
Ephedrine Hydrochloride 30mg	42%	T	T	T	T	F	F	F	F	F	F
Dexamethasone Phosphate 4mg	40%	T	T	T	F	F	F	F	F	F	F
Glycopyrronium and Neostigmine	39%	T	T	T	F	F	F	F	F	F	F
Actrapid Penfill 3mL	40%	T	T	T	F	F	F	F	F	F	F

Threshold: Suxamethonium against other samples

Drug Name	Similarity Score	T10	T20	T30	T40	T50	T60	T70	T80	T90	T100
Frusemide-Claris 20mg	46%	T	T	T	T	F	F	F	F	F	F
Water For Injections 10mL	47%	T	T	T	T	F	F	F	F	F	F
Paracetamol 1000mg/100mL	39%	T	T	T	F	F	F	F	F	F	F
Fresofol 1% MCT/LCT	46%	T	T	T	T	F	F	F	F	F	F
Amoxicillin 1g	41%	T	T	T	T	F	F	F	F	F	F
Hydrocortisone sodium 100mg	49%	T	T	T	T	F	F	F	F	F	F
Cefazolin Sodium 1g	44%	T	T	T	T	F	F	F	F	F	F
Atracurium Besylate 50mg	44%	T	T	T	T	F	F	F	F	F	F
Naloxone HCl 400mg in 1mL	51%	T	T	T	T	T	F	F	F	F	F
Morphine Sulfate Injection 10mg	53%	T	T	T	T	T	F	F	F	F	F
Ondansetron Solution	44%	T	T	T	T	F	F	F	F	F	F
Protamine Sulfate 10mg/ml	58%	T	T	T	T	T	F	F	F	F	F
Vecuronium Bromide	53%	T	T	T	T	T	F	F	F	F	F
Potassium Chloride 10mmol	54%	T	T	T	T	T	F	F	F	F	F
Heparin Injection 25000IU	50%	T	T	T	T	F	F	F	F	F	F
Sugammadex 200mg/2ml	61%	T	T	T	T	T	T	F	F	F	F
Protamine Sulphate 50mg in 5ml	53%	T	T	T	T	T	F	F	F	F	F
Sodium Chloride 10ml	72%	T	T	T	T	T	T	T	F	F	F
Remifentanil-AFT 2g	45%	T	T	T	T	F	F	F	F	F	F
Sedative Midazolam 5mg	50%	T	T	T	T	F	F	F	F	F	F
Glyceryl Trinitrate 10mg in 10ml	48%	T	T	T	T	F	F	F	F	F	F
Fentanyl Citrate 785 micrograms	45%	T	T	T	T	F	F	F	F	F	F
Cefazolin-AFT 1g	53%	T	T	T	T	T	F	F	F	F	F
Dynastat 40 mg	50%	T	T	T	T	F	F	F	F	F	F
Tranexamic-AFT	46%	T	T	T	T	F	F	F	F	F	F
Calcium Chloride 1g in 10mL	48%	T	T	T	T	F	F	F	F	F	F
Provive MCT-LCT 1%	48%	T	T	T	T	F	F	F	F	F	F
METOPROLOL Mylan 5mg	44%	T	T	T	T	F	F	F	F	F	F
Noradrenaline 4mL	34%	T	T	T	F	F	F	F	F	F	F
Lidocaine-Claris 5ml	41%	T	T	T	T	F	F	F	F	F	F
Atropine Injection 600Ug	53%	T	T	T	T	T	F	F	F	F	F
Xylocaine 1%	39%	T	T	T	F	F	F	F	F	F	F
Sodium Chloride 0.9%	47%	T	T	T	T	F	F	F	F	F	F
Hypnomidate 10mL	52%	T	T	T	T	T	F	F	F	F	F
Adrenaline Injection 1mg	35%	T	T	T	F	F	F	F	F	F	F
Sterile Dopamine 200mg/5ml	41%	T	T	T	T	F	F	F	F	F	F
Suxamethonium 100mg in 2 ml	**100%**	**T**	**T**	**T**	**T**	**T**	**T**	**T**	**T**	**T**	**F**
Amiodarone HCL 50 mg/ml	51%	T	T	T	T	T	F	F	F	F	F
Primacor Injection 10mL	52%	T	T	T	T	T	F	F	F	F	F
Sugammadex 200 mg/2ml	57%	T	T	T	T	T	F	F	F	F	F
Rocuronium Bromide 50 mg	56%	T	T	T	T	T	F	F	F	F	F
Clonidine HCl 150 ug/1mL	56%	T	T	T	T	T	F	F	F	F	F
Cyclizine Lactate 50	41%	T	T	T	T	F	F	F	F	F	F
PITRESSIN 20 Units in 1 mL	50%	T	T	T	T	F	F	F	F	F	F
Magnesium Sulfate 2.47g	48%	T	T	T	T	F	F	F	F	F	F
Metaraminol 10mg/mL	50%	T	T	T	T	F	F	F	F	F	F
Dalacin Phosphate 600 mg/4 mL	40%	T	T	T	F	F	F	F	F	F	F
Pancuronium Inresa 4mg/2ml	45%	T	T	T	T	F	F	F	F	F	F
Ephedrine Hydrochloride 30mg	40%	T	T	T	F	F	F	F	F	F	F
Dexamethasone Phosphate 4mg	53%	T	T	T	T	T	F	F	F	F	F
Glycopyrronium and Neostigmine	51%	T	T	T	T	T	F	F	F	F	F
Actrapid Penfill 3mL	47%	T	T	T	T	F	F	F	F	F	F

Threshold: Amiodarone HCL against other samples

Drug Name	Similarity Score	T10	T20	T30	T40	T50	T60	T70	T80	T90	T100
Frusemide-Claris 20mg	53%	T	T	T	T	T	F	F	F	F	F
Water For Injections 10mL	43%	T	T	T	T	F	F	F	F	F	F
Paracetamol 1000mg/100mL	65%	T	T	T	T	T	T	F	F	F	F
Fresofol 1% MCT/LCT	59%	T	T	T	T	T	F	F	F	F	F
Amoxicillin 1g	54%	T	T	T	T	T	F	F	F	F	F
Hydrocortisone sodium 100mg	62%	T	T	T	T	T	T	F	F	F	F
Cefazolin Sodium 1g	55%	T	T	T	T	T	F	F	F	F	F
Atracurium Besylate 50mg	70%	T	T	T	T	T	T	F	F	F	F
Naloxone HCl 400mg in 1mL	34%	T	T	T	F	F	F	F	F	F	F
Morphine Sulfate Injection 10mg	47%	T	T	T	T	F	F	F	F	F	F
Ondansetron Solution	53%	T	T	T	T	T	F	F	F	F	F
Protamine Sulfate 10mg/ml	56%	T	T	T	T	T	F	F	F	F	F
Vecuronium Bromide	46%	T	T	T	T	F	F	F	F	F	F
Potassium Chloride 10mmol	53%	T	T	T	T	T	F	F	F	F	F
Heparin Injection 25000IU	49%	T	T	T	T	F	F	F	F	F	F
Sugammadex 200mg/2ml	55%	T	T	T	T	T	F	F	F	F	F
Protamine Sulphate 50mg in 5ml	58%	T	T	T	T	T	F	F	F	F	F
Sodium Chloride 10ml	54%	T	T	T	T	T	F	F	F	F	F
Remifentanil-AFT 2g	50%	T	T	T	T	F	F	F	F	F	F
Sedative Midazolam 5mg	35%	T	T	T	F	F	F	F	F	F	F
Glyceryl Trinitrate 10mg in 10ml	49%	T	T	T	T	F	F	F	F	F	F
Fentanyl Citrate 785 micrograms	46%	T	T	T	T	F	F	F	F	F	F
Cefazolin-AFT 1g	47%	T	T	T	T	F	F	F	F	F	F
Dynastat 40 mg	57%	T	T	T	T	T	F	F	F	F	F
Tranexamic-AFT	46%	T	T	T	T	F	F	F	F	F	F
Calcium Chloride 1g in 10mL	55%	T	T	T	T	T	F	F	F	F	F
Provive MCT-LCT 1%	65%	T	T	T	T	T	T	F	F	F	F
METOPROLOL Mylan 5mg	74%	T	T	T	T	T	T	T	F	F	F
Noradrenaline 4mL	43%	T	T	T	T	F	F	F	F	F	F
Lidocaine-Claris 5ml	47%	T	T	T	T	F	F	F	F	F	F
Atropine Injection 600Ug	41%	T	T	T	T	F	F	F	F	F	F
Xylocaine 1%	32%	T	T	T	F	F	F	F	F	F	F
Sodium Chloride 0.9%	46%	T	T	T	T	F	F	F	F	F	F
Hypnomidate 10mL	48%	T	T	T	T	F	F	F	F	F	F
Adrenaline Injection 1mg	42%	T	T	T	T	F	F	F	F	F	F
Sterile Dopamine 200mg/5ml	47%	T	T	T	T	F	F	F	F	F	F
Suxamethonium 100mg in 2 ml	51%	T	T	T	T	T	F	F	F	F	F
Amiodarone HCL 50 mg/ml	**100%**	**T**	**T**	**T**	**T**	**T**	**T**	**T**	**T**	**T**	**F**
Primacor Injection 10mL	52%	T	T	T	T	T	F	F	F	F	F
Sugammadex 200 mg/2ml	48%	T	T	T	T	F	F	F	F	F	F
Rocuronium Bromide 50 mg	63%	T	T	T	T	T	T	F	F	F	F
Clonidine HCl 150 ug/1mL	54%	T	T	T	T	T	F	F	F	F	F
Cyclizine Lactate 50	43%	T	T	T	T	F	F	F	F	F	F
PITRESSIN 20 Units in 1 mL	49%	T	T	T	T	F	F	F	F	F	F
Magnesium Sulfate 2.47g	55%	T	T	T	T	T	F	F	F	F	F
Metaraminol 10mg/mL	63%	T	T	T	T	T	T	F	F	F	F
Dalacin Phosphate 600 mg/4 mL	33%	T	T	T	F	F	F	F	F	F	F
Pancuronium Inresa 4mg/2ml	47%	T	T	T	T	F	F	F	F	F	F
Ephedrine Hydrochloride 30mg	53%	T	T	T	T	T	F	F	F	F	F
Dexamethasone Phosphate 4mg	69%	T	T	T	T	T	T	F	F	F	F
Glycopyrronium and Neostigmine	56%	T	T	T	T	T	F	F	F	F	F
Actrapid Penfill 3mL	48%	T	T	T	T	F	F	F	F	F	F

Threshold: Primacor Injection against other samples

Drug Name	Similarity Score	T10	T20	T30	T40	T50	T60	T70	T80	T90	T100
Frusemide-Claris 20mg	43%	T	T	T	T	F	F	F	F	F	F
Water For Injections 10mL	44%	T	T	T	T	F	F	F	F	F	F
Paracetamol 1000mg/100mL	47%	T	T	T	T	F	F	F	F	F	F
Fresofol 1% MCT/LCT	47%	T	T	T	T	F	F	F	F	F	F
Amoxicillin 1g	42%	T	T	T	T	F	F	F	F	F	F
Hydrocortisone sodium 100mg	46%	T	T	T	T	F	F	F	F	F	F
Cefazolin Sodium 1g	44%	T	T	T	T	F	F	F	F	F	F
Atracurium Besylate 50mg	48%	T	T	T	T	F	F	F	F	F	F
Naloxone HCl 400mg in 1mL	38%	T	T	T	F	F	F	F	F	F	F
Morphine Sulfate Injection 10mg	50%	T	T	T	T	F	F	F	F	F	F
Ondansetron Solution	41%	T	T	T	T	F	F	F	F	F	F
Protamine Sulfate 10mg/ml	52%	T	T	T	T	T	F	F	F	F	F
Vecuronium Bromide	40%	T	T	T	F	F	F	F	F	F	F
Potassium Chloride 10mmol	46%	T	T	T	T	F	F	F	F	F	F
Heparin Injection 25000IU	47%	T	T	T	T	F	F	F	F	F	F
Sugammadex 200mg/2ml	46%	T	T	T	T	F	F	F	F	F	F
Protamine Sulphate 50mg in 5ml	47%	T	T	T	T	F	F	F	F	F	F
Sodium Chloride 10ml	44%	T	T	T	T	F	F	F	F	F	F
Remifentanil-AFT 2g	46%	T	T	T	T	F	F	F	F	F	F
Sedative Midazolam 5mg	41%	T	T	T	T	F	F	F	F	F	F
Glyceryl Trinitrate 10mg in 10ml	44%	T	T	T	T	F	F	F	F	F	F
Fentanyl Citrate 785 micrograms	42%	T	T	T	T	F	F	F	F	F	F
Cefazolin-AFT 1g	50%	T	T	T	T	F	F	F	F	F	F
Dynastat 40 mg	49%	T	T	T	T	F	F	F	F	F	F
Tranexamic-AFT	44%	T	T	T	T	F	F	F	F	F	F
Calcium Chloride 1g in 10mL	49%	T	T	T	T	F	F	F	F	F	F
Provive MCT-LCT 1%	45%	T	T	T	T	F	F	F	F	F	F
METOPROLOL Mylan 5mg	43%	T	T	T	T	F	F	F	F	F	F
Noradrenaline 4mL	41%	T	T	T	T	F	F	F	F	F	F
Lidocaine-Claris 5ml	42%	T	T	T	T	F	F	F	F	F	F
Atropine Injection 600Ug	45%	T	T	T	T	F	F	F	F	F	F
Xylocaine 1%	33%	T	T	T	F	F	F	F	F	F	F
Sodium Chloride 0.9%	41%	T	T	T	T	F	F	F	F	F	F
Hypnomidate 10mL	47%	T	T	T	T	F	F	F	F	F	F
Adrenaline Injection 1mg	42%	T	T	T	T	F	F	F	F	F	F
Sterile Dopamine 200mg/5ml	42%	T	T	T	T	F	F	F	F	F	F
Suxamethonium 100mg in 2 ml	52%	T	T	T	T	T	F	F	F	F	F
Amiodarone HCL 50 mg/ml	52%	T	T	T	T	T	F	F	F	F	F
Primacor Injection 10mL	**100%**	**T**	**T**	**T**	**T**	**T**	**T**	**T**	**T**	**T**	**F**
Sugammadex 200 mg/2ml	52%	T	T	T	T	T	F	F	F	F	F
Rocuronium Bromide 50 mg	47%	T	T	T	T	F	F	F	F	F	F
Clonidine HCl 150 ug/1mL	53%	T	T	T	T	T	F	F	F	F	F
Cyclizine Lactate 50	51%	T	T	T	T	T	F	F	F	F	F
PITRESSIN 20 Units in 1 mL	51%	T	T	T	T	T	F	F	F	F	F
Magnesium Sulfate 2.47g	57%	T	T	T	T	T	F	F	F	F	F
Metaraminol 10mg/mL	49%	T	T	T	T	F	F	F	F	F	F
Dalacin Phosphate 600 mg/4 mL	41%	T	T	T	T	F	F	F	F	F	F
Pancuronium Inresa 4mg/2ml	47%	T	T	T	T	F	F	F	F	F	F
Ephedrine Hydrochloride 30mg	40%	T	T	T	F	F	F	F	F	F	F
Dexamethasone Phosphate 4mg	55%	T	T	T	T	T	F	F	F	F	F
Glycopyrronium and Neostigmine	47%	T	T	T	T	F	F	F	F	F	F
Actrapid Penfill 3mL	48%	T	T	T	T	F	F	F	F	F	F

Threshold: Fresofol 1% MCT/LCT against other samples

Drug Name	Similarity Score	T10	T20	T30	T40	T50	T60	T70	T80	T90	T100
Frusemide-Claris 20mg	40%	T	T	T	F	F	F	F	F	F	F
Water For Injections 10mL	45%	T	T	T	T	F	F	F	F	F	F
Paracetamol 1000mg/100mL	61%	T	T	T	T	T	T	F	F	F	F
Fresofol 1% MCT/LCT	**100%**	**T**	**T**	**T**	**T**	**T**	**T**	**T**	**T**	**T**	**F**
Amoxicillin 1g	48%	T	T	T	T	F	F	F	F	F	F
Hydrocortisone sodium 100mg	50%	T	T	T	T	F	F	F	F	F	F
Cefazolin Sodium 1g	67%	T	T	T	T	T	T	F	F	F	F
Atracurium Besylate 50mg	76%	T	T	T	T	T	T	T	F	F	F
Naloxone HCl 400mg in 1mL	42%	T	T	T	T	F	F	F	F	F	F
Morphine Sulfate Injection 10mg	51%	T	T	T	T	T	F	F	F	F	F
Ondansetron Solution	38%	T	T	T	F	F	F	F	F	F	F
Protamine Sulfate 10mg/ml	46%	T	T	T	T	F	F	F	F	F	F
Vecuronium Bromide	54%	T	T	T	T	T	F	F	F	F	F
Potassium Chloride 10mmol	34%	T	T	T	F	F	F	F	F	F	F
Heparin Injection 25000IU	43%	T	T	T	T	F	F	F	F	F	F
Sugammadex 200mg/2ml	67%	T	T	T	T	T	T	F	F	F	F
Protamine Sulphate 50mg in 5ml	51%	T	T	T	T	T	F	F	F	F	F
Sodium Chloride 10ml	41%	T	T	T	T	F	F	F	F	F	F
Remifentanil-AFT 2g	36%	T	T	T	F	F	F	F	F	F	F
Sedative Midazolam 5mg	25%	T	T	F	F	F	F	F	F	F	F
Glyceryl Trinitrate 10mg in 10ml	36%	T	T	T	F	F	F	F	F	F	F
Fentanyl Citrate 785 micrograms	41%	T	T	T	T	F	F	F	F	F	F
Cefazolin-AFT 1g	40%	T	T	T	F	F	F	F	F	F	F
Dynastat 40 mg	61%	T	T	T	T	T	T	F	F	F	F
Tranexamic-AFT	34%	T	T	T	F	F	F	F	F	F	F
Calcium Chloride 1g in 10mL	57%	T	T	T	T	T	F	F	F	F	F
Provive MCT-LCT 1%	68%	T	T	T	T	T	T	F	F	F	F
METOPROLOL Mylan 5mg	70%	T	T	T	T	T	T	F	F	F	F
Noradrenaline 4mL	32%	T	T	T	F	F	F	F	F	F	F
Lidocaine-Claris 5ml	32%	T	T	T	F	F	F	F	F	F	F
Atropine Injection 600Ug	32%	T	T	T	F	F	F	F	F	F	F
Xylocaine 1%	17%	T	F	F	F	F	F	F	F	F	F
Sodium Chloride 0.9%	40%	T	T	T	F	F	F	F	F	F	F
Hypnomidate 10mL	38%	T	T	T	F	F	F	F	F	F	F
Adrenaline Injection 1mg	49%	T	T	T	T	F	F	F	F	F	F
Sterile Dopamine 200mg/5ml	23%	T	T	F	F	F	F	F	F	F	F
Suxamethonium 100mg in 2 ml	46%	T	T	T	T	F	F	F	F	F	F
Amiodarone HCL 50 mg/ml	59%	T	T	T	T	T	F	F	F	F	F
Primacor Injection 10mL	47%	T	T	T	T	F	F	F	F	F	F
Sugammadex 200 mg/2ml	59%	T	T	T	T	T	F	F	F	F	F
Rocuronium Bromide 50 mg	63%	T	T	T	T	T	T	F	F	F	F
Clonidine HCl 150 ug/1mL	44%	T	T	T	T	F	F	F	F	F	F
Cyclizine Lactate 50	28%	T	T	F	F	F	F	F	F	F	F
PITRESSIN 20 Units in 1 mL	47%	T	T	T	T	F	F	F	F	F	F
Magnesium Sulfate 2.47g	42%	T	T	T	T	F	F	F	F	F	F
Metaraminol 10mg/mL	36%	T	T	T	F	F	F	F	F	F	F
Dalacin Phosphate 600 mg/4 mL	29%	T	T	F	F	F	F	F	F	F	F
Pancuronium Inresa 4mg/2ml	37%	T	T	T	F	F	F	F	F	F	F
Ephedrine Hydrochloride 30mg	28%	T	T	F	F	F	F	F	F	F	F
Dexamethasone Phosphate 4mg	58%	T	T	T	T	T	F	F	F	F	F
Glycopyrronium and Neostigmine	45%	T	T	T	T	F	F	F	F	F	F
Actrapid Penfill 3mL	28%	T	T	F	F	F	F	F	F	F	F

Threshold: Sugammadex against other samples

Drug Name	Similarity Score	T10	T20	T30	T40	T50	T60	T70	T80	T90	T100
Frusemide-Claris 20mg	39%	T	T	T	F	F	F	F	F	F	F
Water For Injections 10mL	44%	T	T	T	T	F	F	F	F	F	F
Paracetamol 1000mg/100mL	45%	T	T	T	T	F	F	F	F	F	F
Fresofol 1% MCT/LCT	59%	T	T	T	T	T	F	F	F	F	F
Amoxicillin 1g	50%	T	T	T	T	F	F	F	F	F	F
Hydrocortisone sodium 100mg	52%	T	T	T	T	T	F	F	F	F	F
Cefazolin Sodium 1g	49%	T	T	T	T	F	F	F	F	F	F
Atracurium Besylate 50mg	48%	T	T	T	T	F	F	F	F	F	F
Naloxone HCl 400mg in 1mL	35%	T	T	T	F	F	F	F	F	F	F
Morphine Sulfate Injection 10mg	47%	T	T	T	T	F	F	F	F	F	F
Ondansetron Solution	43%	T	T	T	T	F	F	F	F	F	F
Protamine Sulfate 10mg/ml	58%	T	T	T	T	T	F	F	F	F	F
Vecuronium Bromide	53%	T	T	T	T	T	F	F	F	F	F
Potassium Chloride 10mmol	50%	T	T	T	T	F	F	F	F	F	F
Heparin Injection 25000IU	55%	T	T	T	T	T	F	F	F	F	F
Sugammadex 200mg/2ml	91%	T	T	T	T	T	T	T	T	T	F
Protamine Sulphate 50mg in 5ml	54%	T	T	T	T	T	F	F	F	F	F
Sodium Chloride 10ml	51%	T	T	T	T	T	F	F	F	F	F
Remifentanil-AFT 2g	49%	T	T	T	T	F	F	F	F	F	F
Sedative Midazolam 5mg	38%	T	T	T	F	F	F	F	F	F	F
Glyceryl Trinitrate 10mg in 10ml	40%	T	T	T	F	F	F	F	F	F	F
Fentanyl Citrate 785 micrograms	45%	T	T	T	T	F	F	F	F	F	F
Cefazolin-AFT 1g	55%	T	T	T	T	T	F	F	F	F	F
Dynastat 40 mg	56%	T	T	T	T	T	F	F	F	F	F
Tranexamic-AFT	41%	T	T	T	T	F	F	F	F	F	F
Calcium Chloride 1g in 10mL	55%	T	T	T	T	T	F	F	F	F	F
Provive MCT-LCT 1%	75%	T	T	T	T	T	T	T	F	F	F
METOPROLOL Mylan 5mg	51%	T	T	T	T	T	F	F	F	F	F
Noradrenaline 4mL	38%	T	T	T	F	F	F	F	F	F	F
Lidocaine-Claris 5ml	45%	T	T	T	T	F	F	F	F	F	F
Atropine Injection 600Ug	50%	T	T	T	T	F	F	F	F	F	F
Xylocaine 1%	35%	T	T	T	F	F	F	F	F	F	F
Sodium Chloride 0.9%	43%	T	T	T	T	F	F	F	F	F	F
Hypnomidate 10mL	45%	T	T	T	T	F	F	F	F	F	F
Adrenaline Injection 1mg	44%	T	T	T	T	F	F	F	F	F	F
Sterile Dopamine 200mg/5ml	39%	T	T	T	F	F	F	F	F	F	F
Suxamethonium 100mg in 2 ml	57%	T	T	T	T	T	F	F	F	F	F
Amiodarone HCL 50 mg/ml	48%	T	T	T	T	F	F	F	F	F	F
Primacor Injection 10mL	52%	T	T	T	T	T	F	F	F	F	F
Sugammadex 200 mg/2ml	**100%**	**T**	**T**	**T**	**T**	**T**	**T**	**T**	**T**	**T**	**F**
Rocuronium Bromide 50 mg	51%	T	T	T	T	T	F	F	F	F	F
Clonidine HCl 150 ug/1mL	56%	T	T	T	T	T	F	F	F	F	F
Cyclizine Lactate 50	39%	T	T	T	F	F	F	F	F	F	F
PITRESSIN 20 Units in 1 mL	52%	T	T	T	T	T	F	F	F	F	F
Magnesium Sulfate 2.47g	57%	T	T	T	T	T	F	F	F	F	F
Metaraminol 10mg/mL	56%	T	T	T	T	T	F	F	F	F	F
Dalacin Phosphate 600 mg/4 mL	37%	T	T	T	F	F	F	F	F	F	F
Pancuronium Inresa 4mg/2ml	46%	T	T	T	T	F	F	F	F	F	F
Ephedrine Hydrochloride 30mg	44%	T	T	T	T	F	F	F	F	F	F
Dexamethasone Phosphate 4mg	52%	T	T	T	T	T	F	F	F	F	F
Glycopyrronium and Neostigmine	53%	T	T	T	T	T	F	F	F	F	F
Actrapid Penfill 3mL	55%	T	T	T	T	T	F	F	F	F	F

Threshold: Rocuronium Bromide against other samples

Drug Name	Similarity Score	T10	T20	T30	T40	T50	T60	T70	T80	T90	T100
Frusemide-Claris 20mg	34%	T	T	T	F	F	F	F	F	F	F
Water For Injections 10mL	41%	T	T	T	T	F	F	F	F	F	F
Paracetamol 1000mg/100mL	20%	T	F	F	F	F	F	F	F	F	F
Fresofol 1% MCT/LCT	63%	T	T	T	T	T	T	F	F	F	F
Amoxicillin 1g	35%	T	T	T	F	F	F	F	F	F	F
Hydrocortisone sodium 100mg	43%	T	T	T	T	F	F	F	F	F	F
Cefazolin Sodium 1g	35%	T	T	T	F	F	F	F	F	F	F
Atracurium Besylate 50mg	67%	T	T	T	T	T	T	F	F	F	F
Naloxone HCl 400mg in 1mL	52%	T	T	T	T	T	F	F	F	F	F
Morphine Sulfate Injection 10mg	65%	T	T	T	T	T	T	F	F	F	F
Ondansetron Solution	34%	T	T	T	F	F	F	F	F	F	F
Protamine Sulfate 10mg/ml	52%	T	T	T	T	T	F	F	F	F	F
Vecuronium Bromide	65%	T	T	T	T	T	T	F	F	F	F
Potassium Chloride 10mmol	38%	T	T	T	F	F	F	F	F	F	F
Heparin Injection 25000IU	55%	T	T	T	T	T	F	F	F	F	F
Sugammadex 200mg/2ml	57%	T	T	T	T	T	F	F	F	F	F
Protamine Sulphate 50mg in 5ml	51%	T	T	T	T	T	F	F	F	F	F
Sodium Chloride 10ml	56%	T	T	T	T	T	F	F	F	F	F
Remifentanil-AFT 2g	43%	T	T	T	T	F	F	F	F	F	F
Sedative Midazolam 5mg	44%	T	T	T	T	F	F	F	F	F	F
Glyceryl Trinitrate 10mg in 10ml	43%	T	T	T	T	F	F	F	F	F	F
Fentanyl Citrate 785 micrograms	41%	T	T	T	T	F	F	F	F	F	F
Cefazolin-AFT 1g	42%	T	T	T	T	F	F	F	F	F	F
Dynastat 40 mg	48%	T	T	T	T	F	F	F	F	F	F
Tranexamic-AFT	38%	T	T	T	F	F	F	F	F	F	F
Calcium Chloride 1g in 10mL	41%	T	T	T	T	F	F	F	F	F	F
Provive MCT-LCT 1%	56%	T	T	T	T	T	F	F	F	F	F
METOPROLOL Mylan 5mg	54%	T	T	T	T	T	F	F	F	F	F
Noradrenaline 4mL	35%	T	T	T	F	F	F	F	F	F	F
Lidocaine-Claris 5ml	46%	T	T	T	T	F	F	F	F	F	F
Atropine Injection 600Ug	53%	T	T	T	T	T	F	F	F	F	F
Xylocaine 1%	41%	T	T	T	T	F	F	F	F	F	F
Sodium Chloride 0.9%	38%	T	T	T	F	F	F	F	F	F	F
Hypnomidate 10mL	44%	T	T	T	T	F	F	F	F	F	F
Adrenaline Injection 1mg	51%	T	T	T	T	T	F	F	F	F	F
Sterile Dopamine 200mg/5ml	37%	T	T	T	F	F	F	F	F	F	F
Suxamethonium 100mg in 2 ml	56%	T	T	T	T	T	F	F	F	F	F
Amiodarone HCL 50 mg/ml	63%	T	T	T	T	T	T	F	F	F	F
Primacor Injection 10mL	47%	T	T	T	T	F	F	F	F	F	F
Sugammadex 200 mg/2ml	51%	T	T	T	T	T	F	F	F	F	F
Rocuronium Bromide 50 mg	**100%**	**T**	**T**	**T**	**T**	**T**	**T**	**T**	**T**	**T**	**F**
Clonidine HCl 150 ug/1mL	54%	T	T	T	T	T	F	F	F	F	F
Cyclizine Lactate 50	43%	T	T	T	T	F	F	F	F	F	F
PITRESSIN 20 Units in 1 mL	59%	T	T	T	T	T	F	F	F	F	F
Magnesium Sulfate 2.47g	63%	T	T	T	T	T	T	F	F	F	F
Metaraminol 10mg/mL	48%	T	T	T	T	F	F	F	F	F	F
Dalacin Phosphate 600 mg/4 mL	38%	T	T	T	F	F	F	F	F	F	F
Pancuronium Inresa 4mg/2ml	45%	T	T	T	T	F	F	F	F	F	F
Ephedrine Hydrochloride 30mg	51%	T	T	T	T	T	F	F	F	F	F
Dexamethasone Phosphate 4mg	56%	T	T	T	T	T	F	F	F	F	F
Glycopyrronium and Neostigmine	61%	T	T	T	T	T	T	F	F	F	F
Actrapid Penfill 3mL	51%	T	T	T	T	T	F	F	F	F	F

Threshold: Clonidine HCl against other samples

Drug Name	Similarity Score	T10	T20	T30	T40	T50	T60	T70	T80	T90	T100
Frusemide-Claris 20mg	37%	T	T	T	F	F	F	F	F	F	F
Water For Injections 10mL	41%	T	T	T	T	F	F	F	F	F	F
Paracetamol 1000mg/100mL	17%	T	F	F	F	F	F	F	F	F	F
Fresofol 1% MCT/LCT	44%	T	T	T	T	F	F	F	F	F	F
Amoxicillin 1g	44%	T	T	T	T	F	F	F	F	F	F
Hydrocortisone sodium 100mg	46%	T	T	T	T	F	F	F	F	F	F
Cefazolin Sodium 1g	52%	T	T	T	T	T	F	F	F	F	F
Atracurium Besylate 50mg	46%	T	T	T	T	F	F	F	F	F	F
Naloxone HCl 400mg in 1mL	45%	T	T	T	T	F	F	F	F	F	F
Morphine Sulfate Injection 10mg	51%	T	T	T	T	T	F	F	F	F	F
Ondansetron Solution	43%	T	T	T	T	F	F	F	F	F	F
Protamine Sulfate 10mg/ml	53%	T	T	T	T	T	F	F	F	F	F
Vecuronium Bromide	50%	T	T	T	T	F	F	F	F	F	F
Potassium Chloride 10mmol	45%	T	T	T	T	F	F	F	F	F	F
Heparin Injection 25000IU	52%	T	T	T	T	T	F	F	F	F	F
Sugammadex 200mg/2ml	49%	T	T	T	T	F	F	F	F	F	F
Protamine Sulphate 50mg in 5ml	56%	T	T	T	T	T	F	F	F	F	F
Sodium Chloride 10ml	52%	T	T	T	T	T	F	F	F	F	F
Remifentanil-AFT 2g	44%	T	T	T	T	F	F	F	F	F	F
Sedative Midazolam 5mg	35%	T	T	T	F	F	F	F	F	F	F
Glyceryl Trinitrate 10mg in 10ml	36%	T	T	T	F	F	F	F	F	F	F
Fentanyl Citrate 785 micrograms	52%	T	T	T	T	T	F	F	F	F	F
Cefazolin-AFT 1g	52%	T	T	T	T	T	F	F	F	F	F
Dynastat 40 mg	52%	T	T	T	T	T	F	F	F	F	F
Tranexamic-AFT	41%	T	T	T	T	F	F	F	F	F	F
Calcium Chloride 1g in 10mL	50%	T	T	T	T	F	F	F	F	F	F
Provive MCT-LCT 1%	44%	T	T	T	T	F	F	F	F	F	F
METOPROLOL Mylan 5mg	45%	T	T	T	T	F	F	F	F	F	F
Noradrenaline 4mL	33%	T	T	T	F	F	F	F	F	F	F
Lidocaine-Claris 5ml	44%	T	T	T	T	F	F	F	F	F	F
Atropine Injection 600Ug	63%	T	T	T	T	T	T	F	F	F	F
Xylocaine 1%	41%	T	T	T	T	F	F	F	F	F	F
Sodium Chloride 0.9%	36%	T	T	T	F	F	F	F	F	F	F
Hypnomidate 10mL	49%	T	T	T	T	F	F	F	F	F	F
Adrenaline Injection 1mg	43%	T	T	T	T	F	F	F	F	F	F
Sterile Dopamine 200mg/5ml	39%	T	T	T	F	F	F	F	F	F	F
Suxamethonium 100mg in 2 ml	56%	T	T	T	T	T	F	F	F	F	F
Amiodarone HCL 50 mg/ml	54%	T	T	T	T	T	F	F	F	F	F
Primacor Injection 10mL	53%	T	T	T	T	T	F	F	F	F	F
Sugammadex 200 mg/2ml	56%	T	T	T	T	T	F	F	F	F	F
Rocuronium Bromide 50 mg	54%	T	T	T	T	T	F	F	F	F	F
Clonidine HCl 150 ug/1mL	**100%**	**T**	**T**	**T**	**T**	**T**	**T**	**T**	**T**	**T**	**F**
Cyclizine Lactate 50	44%	T	T	T	T	F	F	F	F	F	F
PITRESSIN 20 Units in 1 mL	51%	T	T	T	T	T	F	F	F	F	F
Magnesium Sulfate 2.47g	44%	T	T	T	T	F	F	F	F	F	F
Metaraminol 10mg/mL	54%	T	T	T	T	T	F	F	F	F	F
Dalacin Phosphate 600 mg/4 mL	36%	T	T	T	F	F	F	F	F	F	F
Pancuronium Inresa 4mg/2ml	34%	T	T	T	F	F	F	F	F	F	F
Ephedrine Hydrochloride 30mg	49%	T	T	T	T	F	F	F	F	F	F
Dexamethasone Phosphate 4mg	53%	T	T	T	T	T	F	F	F	F	F
Glycopyrronium and Neostigmine	45%	T	T	T	T	F	F	F	F	F	F
Actrapid Penfill 3mL	53%	T	T	T	T	T	F	F	F	F	F

Threshold: Cyclizine Lactate against other samples

Drug Name	Similarity Score	T10	T20	T30	T40	T50	T60	T70	T80	T90	T100
Frusemide-Claris 20mg	40%	T	T	T	F	F	F	F	F	F	F
Water For Injections 10mL	41%	T	T	T	T	F	F	F	F	F	F
Paracetamol 1000mg/100mL	19%	T	F	F	F	F	F	F	F	F	F
Fresofol 1% MCT/LCT	27%	T	T	F	F	F	F	F	F	F	F
Amoxicillin 1g	36%	T	T	T	F	F	F	F	F	F	F
Hydrocortisone sodium 100mg	34%	T	T	T	F	F	F	F	F	F	F
Cefazolin Sodium 1g	33%	T	T	T	F	F	F	F	F	F	F
Atracurium Besylate 50mg	39%	T	T	T	F	F	F	F	F	F	F
Naloxone HCl 400mg in 1mL	41%	T	T	T	T	F	F	F	F	F	F
Morphine Sulfate Injection 10mg	43%	T	T	T	T	F	F	F	F	F	F
Ondansetron Solution	41%	T	T	T	T	F	F	F	F	F	F
Protamine Sulfate 10mg/ml	44%	T	T	T	T	F	F	F	F	F	F
Vecuronium Bromide	31%	T	T	T	F	F	F	F	F	F	F
Potassium Chloride 10mmol	40%	T	T	T	F	F	F	F	F	F	F
Heparin Injection 25000IU	38%	T	T	T	F	F	F	F	F	F	F
Sugammadex 200mg/2ml	40%	T	T	T	F	F	F	F	F	F	F
Protamine Sulphate 50mg in 5ml	41%	T	T	T	T	F	F	F	F	F	F
Sodium Chloride 10ml	36%	T	T	T	F	F	F	F	F	F	F
Remifentanil-AFT 2g	38%	T	T	T	F	F	F	F	F	F	F
Sedative Midazolam 5mg	48%	T	T	T	T	F	F	F	F	F	F
Glyceryl Trinitrate 10mg in 10ml	42%	T	T	T	T	F	F	F	F	F	F
Fentanyl Citrate 785 micrograms	38%	T	T	T	F	F	F	F	F	F	F
Cefazolin-AFT 1g	39%	T	T	T	F	F	F	F	F	F	F
Dynastat 40 mg	31%	T	T	T	F	F	F	F	F	F	F
Tranexamic-AFT	42%	T	T	T	T	F	F	F	F	F	F
Calcium Chloride 1g in 10mL	42%	T	T	T	T	F	F	F	F	F	F
Provive MCT-LCT 1%	26%	T	T	F	F	F	F	F	F	F	F
METOPROLOL Mylan 5mg	36%	T	T	T	F	F	F	F	F	F	F
Noradrenaline 4mL	31%	T	T	T	F	F	F	F	F	F	F
Lidocaine-Claris 5ml	42%	T	T	T	T	F	F	F	F	F	F
Atropine Injection 600Ug	38%	T	T	T	F	F	F	F	F	F	F
Xylocaine 1%	36%	T	T	T	F	F	F	F	F	F	F
Sodium Chloride 0.9%	42%	T	T	T	T	F	F	F	F	F	F
Hypnomidate 10mL	46%	T	T	T	T	F	F	F	F	F	F
Adrenaline Injection 1mg	35%	T	T	T	F	F	F	F	F	F	F
Sterile Dopamine 200mg/5ml	42%	T	T	T	T	F	F	F	F	F	F
Suxamethonium 100mg in 2 ml	39%	T	T	T	F	F	F	F	F	F	F
Amiodarone HCL 50 mg/ml	43%	T	T	T	T	F	F	F	F	F	F
Primacor Injection 10mL	51%	T	T	T	T	T	F	F	F	F	F
Sugammadex 200 mg/2ml	39%	T	T	T	F	F	F	F	F	F	F
Rocuronium Bromide 50 mg	40%	T	T	T	F	F	F	F	F	F	F
Clonidine HCl 150 ug/1mL	44%	T	T	T	T	F	F	F	F	F	F
Cyclizine Lactate 50	**99%**	**T**	**T**	**T**	**T**	**T**	**T**	**T**	**T**	**T**	**F**
PITRESSIN 20 Units in 1 mL	42%	T	T	T	T	F	F	F	F	F	F
Magnesium Sulfate 2.47g	40%	T	T	T	F	F	F	F	F	F	F
Metaraminol 10mg/mL	38%	T	T	T	F	F	F	F	F	F	F
Dalacin Phosphate 600 mg/4 mL	38%	T	T	T	F	F	F	F	F	F	F
Pancuronium Inresa 4mg/2ml	35%	T	T	T	F	F	F	F	F	F	F
Ephedrine Hydrochloride 30mg	35%	T	T	T	F	F	F	F	F	F	F
Dexamethasone Phosphate 4mg	43%	T	T	T	T	F	F	F	F	F	F
Glycopyrronium and Neostigmine	43%	T	T	T	T	F	F	F	F	F	F
Actrapid Penfill 3mL	40%	T	T	T	F	F	F	F	F	F	F

Threshold: PITRESSIN against other samples

Drug Name	Similarity Score	T10	T20	T30	T40	T50	T60	T70	T80	T90	T100
Frusemide-Claris 20mg	40%	T	T	T	F	F	F	F	F	F	F
Water For Injections 10mL	47%	T	T	T	T	F	F	F	F	F	F
Paracetamol 1000mg/100mL	19%	T	F	F	F	F	F	F	F	F	F
Fresofol 1% MCT/LCT	47%	T	T	T	T	F	F	F	F	F	F
Amoxicillin 1g	39%	T	T	T	F	F	F	F	F	F	F
Hydrocortisone sodium 100mg	46%	T	T	T	T	F	F	F	F	F	F
Cefazolin Sodium 1g	42%	T	T	T	T	F	F	F	F	F	F
Atracurium Besylate 50mg	58%	T	T	T	T	T	F	F	F	F	F
Naloxone HCl 400mg in 1mL	40%	T	T	T	F	F	F	F	F	F	F
Morphine Sulfate Injection 10mg	56%	T	T	T	T	T	F	F	F	F	F
Ondansetron Solution	37%	T	T	T	F	F	F	F	F	F	F
Protamine Sulfate 10mg/ml	56%	T	T	T	T	T	F	F	F	F	F
Vecuronium Bromide	49%	T	T	T	T	F	F	F	F	F	F
Potassium Chloride 10mmol	44%	T	T	T	T	F	F	F	F	F	F
Heparin Injection 25000IU	61%	T	T	T	T	T	T	F	F	F	F
Sugammadex 200mg/2ml	59%	T	T	T	T	T	F	F	F	F	F
Protamine Sulphate 50mg in 5ml	51%	T	T	T	T	T	F	F	F	F	F
Sodium Chloride 10ml	55%	T	T	T	T	T	F	F	F	F	F
Remifentanil-AFT 2g	42%	T	T	T	T	F	F	F	F	F	F
Sedative Midazolam 5mg	40%	T	T	T	F	F	F	F	F	F	F
Glyceryl Trinitrate 10mg in 10ml	42%	T	T	T	T	F	F	F	F	F	F
Fentanyl Citrate 785 micrograms	41%	T	T	T	T	F	F	F	F	F	F
Cefazolin-AFT 1g	49%	T	T	T	T	F	F	F	F	F	F
Dynastat 40 mg	51%	T	T	T	T	T	F	F	F	F	F
Tranexamic-AFT	44%	T	T	T	T	F	F	F	F	F	F
Calcium Chloride 1g in 10mL	49%	T	T	T	T	F	F	F	F	F	F
Provive MCT-LCT 1%	53%	T	T	T	T	T	F	F	F	F	F
METOPROLOL Mylan 5mg	50%	T	T	T	T	F	F	F	F	F	F
Noradrenaline 4mL	37%	T	T	T	F	F	F	F	F	F	F
Lidocaine-Claris 5ml	46%	T	T	T	T	F	F	F	F	F	F
Atropine Injection 600Ug	52%	T	T	T	T	T	F	F	F	F	F
Xylocaine 1%	41%	T	T	T	T	F	F	F	F	F	F
Sodium Chloride 0.9%	37%	T	T	T	F	F	F	F	F	F	F
Hypnomidate 10mL	43%	T	T	T	T	F	F	F	F	F	F
Adrenaline Injection 1mg	49%	T	T	T	T	F	F	F	F	F	F
Sterile Dopamine 200mg/5ml	40%	T	T	T	F	F	F	F	F	F	F
Suxamethonium 100mg in 2 ml	50%	T	T	T	T	F	F	F	F	F	F
Amiodarone HCL 50 mg/ml	49%	T	T	T	T	F	F	F	F	F	F
Primacor Injection 10mL	51%	T	T	T	T	T	F	F	F	F	F
Sugammadex 200 mg/2ml	52%	T	T	T	T	T	F	F	F	F	F
Rocuronium Bromide 50 mg	59%	T	T	T	T	T	F	F	F	F	F
Clonidine HCl 150 ug/1mL	51%	T	T	T	T	T	F	F	F	F	F
Cyclizine Lactate 50	43%	T	T	T	T	F	F	F	F	F	F
PITRESSIN 20 Units in 1 mL	**100%**	**T**	**T**	**T**	**T**	**T**	**T**	**T**	**T**	**T**	**F**
Magnesium Sulfate 2.47g	48%	T	T	T	T	F	F	F	F	F	F
Metaraminol 10mg/mL	56%	T	T	T	T	T	F	F	F	F	F
Dalacin Phosphate 600 mg/4 mL	39%	T	T	T	F	F	F	F	F	F	F
Pancuronium Inresa 4mg/2ml	43%	T	T	T	T	F	F	F	F	F	F
Ephedrine Hydrochloride 30mg	45%	T	T	T	T	F	F	F	F	F	F
Dexamethasone Phosphate 4mg	60%	T	T	T	T	T	F	F	F	F	F
Glycopyrronium and Neostigmine	48%	T	T	T	T	F	F	F	F	F	F
Actrapid Penfill 3mL	59%	T	T	T	T	T	F	F	F	F	F

Threshold: Magnesium Sulphate against other samples

Drug Name	Similarity Score	T10	T20	T30	T40	T50	T60	T70	T80	T90	T100
Frusemide-Claris 20mg	39%	T	T	T	F	F	F	F	F	F	F
Water For Injections 10mL	45%	T	T	T	T	F	F	F	F	F	F
Paracetamol 1000mg/100mL	24%	T	T	F	F	F	F	F	F	F	F
Fresofol 1% MCT/LCT	42%	T	T	T	T	F	F	F	F	F	F
Amoxicillin 1g	40%	T	T	T	F	F	F	F	F	F	F
Hydrocortisone sodium 100mg	44%	T	T	T	T	F	F	F	F	F	F
Cefazolin Sodium 1g	42%	T	T	T	T	F	F	F	F	F	F
Atracurium Besylate 50mg	47%	T	T	T	T	F	F	F	F	F	F
Naloxone HCl 400mg in 1mL	49%	T	T	T	T	F	F	F	F	F	F
Morphine Sulfate Injection 10mg	63%	T	T	T	T	T	T	F	F	F	F
Ondansetron Solution	40%	T	T	T	F	F	F	F	F	F	F
Protamine Sulfate 10mg/ml	57%	T	T	T	T	T	F	F	F	F	F
Vecuronium Bromide	47%	T	T	T	T	F	F	F	F	F	F
Potassium Chloride 10mmol	59%	T	T	T	T	T	F	F	F	F	F
Heparin Injection 25000IU	50%	T	T	T	T	F	F	F	F	F	F
Sugammadex 200mg/2ml	55%	T	T	T	T	T	F	F	F	F	F
Protamine Sulphate 50mg in 5ml	53%	T	T	T	T	T	F	F	F	F	F
Sodium Chloride 10ml	49%	T	T	T	T	F	F	F	F	F	F
Remifentanil-AFT 2g	45%	T	T	T	T	F	F	F	F	F	F
Sedative Midazolam 5mg	38%	T	T	T	F	F	F	F	F	F	F
Glyceryl Trinitrate 10mg in 10ml	41%	T	T	T	T	F	F	F	F	F	F
Fentanyl Citrate 785 micrograms	48%	T	T	T	T	F	F	F	F	F	F
Cefazolin-AFT 1g	45%	T	T	T	T	F	F	F	F	F	F
Dynastat 40 mg	44%	T	T	T	T	F	F	F	F	F	F
Tranexamic-AFT	41%	T	T	T	T	F	F	F	F	F	F
Calcium Chloride 1g in 10mL	44%	T	T	T	T	F	F	F	F	F	F
Provive MCT-LCT 1%	36%	T	T	T	F	F	F	F	F	F	F
METOPROLOL Mylan 5mg	49%	T	T	T	T	F	F	F	F	F	F
Noradrenaline 4mL	45%	T	T	T	T	F	F	F	F	F	F
Lidocaine-Claris 5ml	47%	T	T	T	T	F	F	F	F	F	F
Atropine Injection 600Ug	36%	T	T	T	F	F	F	F	F	F	F
Xylocaine 1%	32%	T	T	T	F	F	F	F	F	F	F
Sodium Chloride 0.9%	45%	T	T	T	T	F	F	F	F	F	F
Hypnomidate 10mL	44%	T	T	T	T	F	F	F	F	F	F
Adrenaline Injection 1mg	45%	T	T	T	T	F	F	F	F	F	F
Sterile Dopamine 200mg/5ml	47%	T	T	T	T	F	F	F	F	F	F
Suxamethonium 100mg in 2 ml	48%	T	T	T	T	F	F	F	F	F	F
Amiodarone HCL 50 mg/ml	55%	T	T	T	T	T	F	F	F	F	F
Primacor Injection 10mL	57%	T	T	T	T	T	F	F	F	F	F
Sugammadex 200 mg/2ml	57%	T	T	T	T	T	F	F	F	F	F
Rocuronium Bromide 50 mg	63%	T	T	T	T	T	T	F	F	F	F
Clonidine HCl 150 ug/1mL	44%	T	T	T	T	F	F	F	F	F	F
Cyclizine Lactate 50	39%	T	T	T	F	F	F	F	F	F	F
PITRESSIN 20 Units in 1 mL	48%	T	T	T	T	F	F	F	F	F	F
Magnesium Sulphate 2.47g	**100%**	**T**	**T**	**T**	**T**	**T**	**T**	**T**	**T**	**T**	**F**
Metaraminol 10mg/mL	48%	T	T	T	T	F	F	F	F	F	F
Dalacin Phosphate 600 mg/4 mL	35%	T	T	T	F	F	F	F	F	F	F
Pancuronium Inresa 4mg/2ml	43%	T	T	T	T	F	F	F	F	F	F
Ephedrine Hydrochloride 30mg	44%	T	T	T	T	F	F	F	F	F	F
Dexamethasone Phosphate 4mg	48%	T	T	T	T	F	F	F	F	F	F
Glycopyrronium and Neostigmine	52%	T	T	T	T	T	F	F	F	F	F
Actrapid Penfill 3mL	47%	T	T	T	T	F	F	F	F	F	F

Threshold: Metaraminol against other samples

Drug Name	Similarity Score	T10	T20	T30	T40	T50	T60	T70	T80	T90	T100
Frusemide-Claris 20mg	46%	T	T	T	T	F	F	F	F	F	F
Water For Injections 10mL	49%	T	T	T	T	F	F	F	F	F	F
Paracetamol 1000mg/100mL	44%	T	T	T	T	F	F	F	F	F	F
Fresofol 1% MCT/LCT	36%	T	T	T	F	F	F	F	F	F	F
Amoxicillin 1g	43%	T	T	T	T	F	F	F	F	F	F
Hydrocortisone sodium 100mg	47%	T	T	T	T	F	F	F	F	F	F
Cefazolin Sodium 1g	48%	T	T	T	T	F	F	F	F	F	F
Atracurium Besylate 50mg	52%	T	T	T	T	T	F	F	F	F	F
Naloxone HCl 400mg in 1mL	39%	T	T	T	F	F	F	F	F	F	F
Morphine Sulfate Injection 10mg	48%	T	T	T	T	F	F	F	F	F	F
Ondansetron Solution	49%	T	T	T	T	F	F	F	F	F	F
Protamine Sulfate 10mg/ml	66%	T	T	T	T	T	T	F	F	F	F
Vecuronium Bromide	47%	T	T	T	T	F	F	F	F	F	F
Potassium Chloride 10mmol	46%	T	T	T	T	F	F	F	F	F	F
Heparin Injection 25000IU	50%	T	T	T	T	F	F	F	F	F	F
Sugammadex 200mg/2ml	60%	T	T	T	T	T	F	F	F	F	F
Protamine Sulphate 50mg in 5ml	61%	T	T	T	T	T	T	F	F	F	F
Sodium Chloride 10ml	51%	T	T	T	T	T	F	F	F	F	F
Remifentanil-AFT 2g	47%	T	T	T	T	F	F	F	F	F	F
Sedative Midazolam 5mg	35%	T	T	T	F	F	F	F	F	F	F
Glyceryl Trinitrate 10mg in 10ml	49%	T	T	T	T	F	F	F	F	F	F
Fentanyl Citrate 785 micrograms	44%	T	T	T	T	F	F	F	F	F	F
Cefazolin-AFT 1g	55%	T	T	T	T	T	F	F	F	F	F
Dynastat 40 mg	52%	T	T	T	T	T	F	F	F	F	F
Tranexamic-AFT	46%	T	T	T	T	F	F	F	F	F	F
Calcium Chloride 1g in 10mL	50%	T	T	T	T	F	F	F	F	F	F
Provive MCT-LCT 1%	55%	T	T	T	T	T	F	F	F	F	F
METOPROLOL Mylan 5mg	59%	T	T	T	T	T	F	F	F	F	F
Noradrenaline 4mL	37%	T	T	T	F	F	F	F	F	F	F
Lidocaine-Claris 5ml	43%	T	T	T	T	F	F	F	F	F	F
Atropine Injection 600Ug	45%	T	T	T	T	F	F	F	F	F	F
Xylocaine 1%	38%	T	T	T	F	F	F	F	F	F	F
Sodium Chloride 0.9%	38%	T	T	T	F	F	F	F	F	F	F
Hypnomidate 10mL	41%	T	T	T	T	F	F	F	F	F	F
Adrenaline Injection 1mg	48%	T	T	T	T	F	F	F	F	F	F
Sterile Dopamine 200mg/5ml	42%	T	T	T	T	F	F	F	F	F	F
Suxamethonium 100mg in 2 ml	50%	T	T	T	T	F	F	F	F	F	F
Amiodarone HCL 50 mg/ml	63%	T	T	T	T	T	T	F	F	F	F
Primacor Injection 10mL	49%	T	T	T	T	F	F	F	F	F	F
Sugammadex 200 mg/2ml	56%	T	T	T	T	T	F	F	F	F	F
Rocuronium Bromide 50 mg	48%	T	T	T	T	F	F	F	F	F	F
Clonidine HCl 150 ug/1mL	54%	T	T	T	T	T	F	F	F	F	F
Cyclizine Lactate 50	40%	T	T	T	F	F	F	F	F	F	F
PITRESSIN 20 Units in 1 mL	56%	T	T	T	T	T	F	F	F	F	F
Magnesium Sulfate 2.47g	48%	T	T	T	T	F	F	F	F	F	F
Metaraminol 10mg/mL	**100%**	**T**	**T**	**T**	**T**	**T**	**T**	**T**	**T**	**T**	**F**
Dalacin Phosphate 600 mg/4 mL	33%	T	T	T	F	F	F	F	F	F	F
Pancuronium Inresa 4mg/2ml	43%	T	T	T	T	F	F	F	F	F	F
Ephedrine Hydrochloride 30mg	45%	T	T	T	T	F	F	F	F	F	F
Dexamethasone Phosphate 4mg	62%	T	T	T	T	T	T	F	F	F	F
Glycopyrronium and Neostigmine	56%	T	T	T	T	T	F	F	F	F	F
Actrapid Penfill 3mL	54%	T	T	T	T	T	F	F	F	F	F

Threshold: Dalacin Phosphate against other samples

Drug Name	Similarity Score	T10	T20	T30	T40	T50	T60	T70	T80	T90	T100
Frusemide-Claris 20mg	35%	T	T	T	F	F	F	F	F	F	F
Water For Injections 10mL	47%	T	T	T	T	F	F	F	F	F	F
Paracetamol 1000mg/100mL	16%	T	F	F	F	F	F	F	F	F	F
Fresofol 1% MCT/LCT	29%	T	T	F	F	F	F	F	F	F	F
Amoxicillin 1g	32%	T	T	T	F	F	F	F	F	F	F
Hydrocortisone sodium 100mg	35%	T	T	T	F	F	F	F	F	F	F
Cefazolin Sodium 1g	32%	T	T	T	F	F	F	F	F	F	F
Atracurium Besylate 50mg	41%	T	T	T	T	F	F	F	F	F	F
Naloxone HCl 400mg in 1mL	39%	T	T	T	F	F	F	F	F	F	F
Morphine Sulfate Injection 10mg	46%	T	T	T	T	F	F	F	F	F	F
Ondansetron Solution	33%	T	T	T	F	F	F	F	F	F	F
Protamine Sulfate 10mg/ml	38%	T	T	T	F	F	F	F	F	F	F
Vecuronium Bromide	29%	T	T	F	F	F	F	F	F	F	F
Potassium Chloride 10mmol	39%	T	T	T	F	F	F	F	F	F	F
Heparin Injection 25000IU	46%	T	T	T	T	F	F	F	F	F	F
Sugammadex 200mg/2ml	40%	T	T	T	F	F	F	F	F	F	F
Protamine Sulphate 50mg in 5ml	35%	T	T	T	F	F	F	F	F	F	F
Sodium Chloride 10ml	31%	T	T	T	F	F	F	F	F	F	F
Remifentanil-AFT 2g	30%	T	T	F	F	F	F	F	F	F	F
Sedative Midazolam 5mg	47%	T	T	T	T	F	F	F	F	F	F
Glyceryl Trinitrate 10mg in 10ml	41%	T	T	T	T	F	F	F	F	F	F
Fentanyl Citrate 785 micrograms	31%	T	T	T	F	F	F	F	F	F	F
Cefazolin-AFT 1g	36%	T	T	T	F	F	F	F	F	F	F
Dynastat 40 mg	44%	T	T	T	T	F	F	F	F	F	F
Tranexamic-AFT	41%	T	T	T	T	F	F	F	F	F	F
Calcium Chloride 1g in 10mL	32%	T	T	T	F	F	F	F	F	F	F
Provive MCT-LCT 1%	20%	T	F	F	F	F	F	F	F	F	F
METOPROLOL Mylan 5mg	42%	T	T	T	T	F	F	F	F	F	F
Noradrenaline 4mL	31%	T	T	T	F	F	F	F	F	F	F
Lidocaine-Claris 5ml	32%	T	T	T	F	F	F	F	F	F	F
Atropine Injection 600Ug	36%	T	T	T	F	F	F	F	F	F	F
Xylocaine 1%	33%	T	T	T	F	F	F	F	F	F	F
Sodium Chloride 0.9%	33%	T	T	T	F	F	F	F	F	F	F
Hypnomidate 10mL	42%	T	T	T	T	F	F	F	F	F	F
Adrenaline Injection 1mg	36%	T	T	T	F	F	F	F	F	F	F
Sterile Dopamine 200mg/5ml	42%	T	T	T	T	F	F	F	F	F	F
Suxamethonium 100mg in 2 ml	40%	T	T	T	F	F	F	F	F	F	F
Amiodarone HCL 50 mg/ml	33%	T	T	T	F	F	F	F	F	F	F
Primacor Injection 10mL	41%	T	T	T	T	F	F	F	F	F	F
Sugammadex 200 mg/2ml	37%	T	T	T	F	F	F	F	F	F	F
Rocuronium Bromide 50 mg	38%	T	T	T	F	F	F	F	F	F	F
Clonidine HCl 150 ug/1mL	36%	T	T	T	F	F	F	F	F	F	F
Cyclizine Lactate 50	43%	T	T	T	T	F	F	F	F	F	F
PITRESSIN 20 Units in 1 mL	39%	T	T	T	F	F	F	F	F	F	F
Magnesium Sulfate 2.47g	35%	T	T	T	F	F	F	F	F	F	F
Metaraminol 10mg/mL	33%	T	T	T	F	F	F	F	F	F	F
Dalacin Phosphate 600 mg/4 mL	**100%**	**T**	**T**	**T**	**T**	**T**	**T**	**T**	**T**	**T**	**F**
Pancuronium Inresa 4mg/2ml	35%	T	T	T	F	F	F	F	F	F	F
Ephedrine Hydrochloride 30mg	31%	T	T	T	F	F	F	F	F	F	F
Dexamethasone Phosphate 4mg	52%	T	T	T	T	T	F	F	F	F	F
Glycopyrronium and Neostigmine	33%	T	T	T	F	F	F	F	F	F	F
Actrapid Penfill 3mL	38%	T	T	T	F	F	F	F	F	F	F

Threshold: Pancuronium Inresa against other samples

Drug Name	Similarity Score	T10	T20	T30	T40	T50	T60	T70	T80	T90	T100
Frusemide-Claris 20mg	40%	T	T	T	F	F	F	F	F	F	F
Water For Injections 10mL	39%	T	T	T	F	F	F	F	F	F	F
Paracetamol 1000mg/100mL	29%	T	T	F	F	F	F	F	F	F	F
Fresofol 1% MCT/LCT	37%	T	T	T	F	F	F	F	F	F	F
Amoxicillin 1g	41%	T	T	T	T	F	F	F	F	F	F
Hydrocortisone sodium 100mg	42%	T	T	T	T	F	F	F	F	F	F
Cefazolin Sodium 1g	42%	T	T	T	T	F	F	F	F	F	F
Atracurium Besylate 50mg	50%	T	T	T	T	F	F	F	F	F	F
Naloxone HCl 400mg in 1mL	30%	T	T	F	F	F	F	F	F	F	F
Morphine Sulfate Injection 10mg	37%	T	T	T	F	F	F	F	F	F	F
Ondansetron Solution	41%	T	T	T	T	F	F	F	F	F	F
Protamine Sulfate 10mg/ml	44%	T	T	T	T	F	F	F	F	F	F
Vecuronium Bromide	43%	T	T	T	T	F	F	F	F	F	F
Potassium Chloride 10mmol	37%	T	T	T	F	F	F	F	F	F	F
Heparin Injection 25000IU	43%	T	T	T	T	F	F	F	F	F	F
Sugammadex 200mg/2ml	45%	T	T	T	T	F	F	F	F	F	F
Protamine Sulphate 50mg in 5ml	42%	T	T	T	T	F	F	F	F	F	F
Sodium Chloride 10ml	46%	T	T	T	T	F	F	F	F	F	F
Remifentanil-AFT 2g	40%	T	T	T	F	F	F	F	F	F	F
Sedative Midazolam 5mg	36%	T	T	T	F	F	F	F	F	F	F
Glyceryl Trinitrate 10mg in 10ml	43%	T	T	T	T	F	F	F	F	F	F
Fentanyl Citrate 785 micrograms	40%	T	T	T	F	F	F	F	F	F	F
Cefazolin-AFT 1g	41%	T	T	T	T	F	F	F	F	F	F
Dynastat 40 mg	48%	T	T	T	T	F	F	F	F	F	F
Tranexamic-AFT	38%	T	T	T	F	F	F	F	F	F	F
Calcium Chloride 1g in 10mL	38%	T	T	T	F	F	F	F	F	F	F
Provive MCT-LCT 1%	34%	T	T	T	F	F	F	F	F	F	F
METOPROLOL Mylan 5mg	43%	T	T	T	T	F	F	F	F	F	F
Noradrenaline 4mL	34%	T	T	T	F	F	F	F	F	F	F
Lidocaine-Claris 5ml	38%	T	T	T	F	F	F	F	F	F	F
Atropine Injection 600Ug	35%	T	T	T	F	F	F	F	F	F	F
Xylocaine 1%	27%	T	T	F	F	F	F	F	F	F	F
Sodium Chloride 0.9%	40%	T	T	T	F	F	F	F	F	F	F
Hypnomidate 10mL	39%	T	T	T	F	F	F	F	F	F	F
Adrenaline Injection 1mg	34%	T	T	T	F	F	F	F	F	F	F
Sterile Dopamine 200mg/5ml	32%	T	T	T	F	F	F	F	F	F	F
Suxamethonium 100mg in 2 ml	45%	T	T	T	T	F	F	F	F	F	F
Amiodarone HCL 50 mg/ml	47%	T	T	T	T	F	F	F	F	F	F
Primacor Injection 10mL	47%	T	T	T	T	F	F	F	F	F	F
Sugammadex 200 mg/2ml	46%	T	T	T	T	F	F	F	F	F	F
Rocuronium Bromide 50 mg	45%	T	T	T	T	F	F	F	F	F	F
Clonidine HCl 150 ug/1mL	34%	T	T	T	F	F	F	F	F	F	F
Cyclizine Lactate 50	36%	T	T	T	F	F	F	F	F	F	F
PITRESSIN 20 Units in 1 mL	43%	T	T	T	T	F	F	F	F	F	F
Magnesium Sulfate 2.47g	43%	T	T	T	T	F	F	F	F	F	F
Metaraminol 10mg/mL	43%	T	T	T	T	F	F	F	F	F	F
Dalacin Phosphate 600 mg/4 mL	35%	T	T	T	F	F	F	F	F	F	F
Pancuronium Inresa 4mg/2ml	**100%**	**T**	**T**	**T**	**T**	**T**	**T**	**T**	**T**	**T**	**F**
Ephedrine Hydrochloride 30mg	33%	T	T	T	F	F	F	F	F	F	F
Dexamethasone Phosphate 4mg	43%	T	T	T	T	F	F	F	F	F	F
Glycopyrronium and Neostigmine	48%	T	T	T	T	F	F	F	F	F	F
Actrapid Penfill 3mL	42%	T	T	T	T	F	F	F	F	F	F

Threshold: Ephedrine Hydrochloride against other samples

Drug Name	Similarity Score	T10	T20	T30	T40	T50	T60	T70	T80	T90	T100
Frusemide-Claris 20mg	35%	T	T	T	F	F	F	F	F	F	F
Water For Injections 10mL	39%	T	T	T	F	F	F	F	F	F	F
Paracetamol 1000mg/100mL	40%	T	T	T	F	F	F	F	F	F	F
Fresofol 1% MCT/LCT	28%	T	T	F	F	F	F	F	F	F	F
Amoxicillin 1g	36%	T	T	T	F	F	F	F	F	F	F
Hydrocortisone sodium 100mg	47%	T	T	T	T	F	F	F	F	F	F
Cefazolin Sodium 1g	39%	T	T	T	F	F	F	F	F	F	F
Atracurium Besylate 50mg	45%	T	T	T	T	F	F	F	F	F	F
Naloxone HCl 400mg in 1mL	37%	T	T	T	F	F	F	F	F	F	F
Morphine Sulfate Injection 10mg	46%	T	T	T	T	F	F	F	F	F	F
Ondansetron Solution	39%	T	T	T	F	F	F	F	F	F	F
Protamine Sulfate 10mg/ml	44%	T	T	T	T	F	F	F	F	F	F
Vecuronium Bromide	46%	T	T	T	T	F	F	F	F	F	F
Potassium Chloride 10mmol	40%	T	T	T	F	F	F	F	F	F	F
Heparin Injection 25000IU	48%	T	T	T	T	F	F	F	F	F	F
Sugammadex 200mg/2ml	45%	T	T	T	T	F	F	F	F	F	F
Protamine Sulphate 50mg in 5ml	43%	T	T	T	T	F	F	F	F	F	F
Sodium Chloride 10ml	42%	T	T	T	T	F	F	F	F	F	F
Remifentanil-AFT 2g	58%	T	T	T	T	T	F	F	F	F	F
Sedative Midazolam 5mg	32%	T	T	T	F	F	F	F	F	F	F
Glyceryl Trinitrate 10mg in 10ml	35%	T	T	T	F	F	F	F	F	F	F
Fentanyl Citrate 785 micrograms	61%	T	T	T	T	T	T	F	F	F	F
Cefazolin-AFT 1g	41%	T	T	T	T	F	F	F	F	F	F
Dynastat 40 mg	44%	T	T	T	T	F	F	F	F	F	F
Tranexamic-AFT	42%	T	T	T	T	F	F	F	F	F	F
Calcium Chloride 1g in 10mL	43%	T	T	T	T	F	F	F	F	F	F
Provive MCT-LCT 1%	26%	T	T	F	F	F	F	F	F	F	F
METOPROLOL Mylan 5mg	44%	T	T	T	T	F	F	F	F	F	F
Noradrenaline 4mL	44%	T	T	T	T	F	F	F	F	F	F
Lidocaine-Claris 5ml	54%	T	T	T	T	T	F	F	F	F	F
Atropine Injection 600Ug	50%	T	T	T	T	F	F	F	F	F	F
Xylocaine 1%	38%	T	T	T	F	F	F	F	F	F	F
Sodium Chloride 0.9%	38%	T	T	T	F	F	F	F	F	F	F
Hypnomidate 10mL	46%	T	T	T	T	F	F	F	F	F	F
Adrenaline Injection 1mg	45%	T	T	T	T	F	F	F	F	F	F
Sterile Dopamine 200mg/5ml	42%	T	T	T	T	F	F	F	F	F	F
Suxamethonium 100mg in 2 ml	40%	T	T	T	F	F	F	F	F	F	F
Amiodarone HCL 50 mg/ml	53%	T	T	T	T	T	F	F	F	F	F
Primacor Injection 10mL	40%	T	T	T	F	F	F	F	F	F	F
Sugammadex 200 mg/2ml	44%	T	T	T	T	F	F	F	F	F	F
Rocuronium Bromide 50 mg	51%	T	T	T	T	T	F	F	F	F	F
Clonidine HCl 150 ug/1mL	49%	T	T	T	T	F	F	F	F	F	F
Cyclizine Lactate 50	33%	T	T	T	F	F	F	F	F	F	F
PITRESSIN 20 Units in 1 mL	45%	T	T	T	T	F	F	F	F	F	F
Magnesium Sulfate 2.47g	44%	T	T	T	T	F	F	F	F	F	F
Metaraminol 10mg/mL	45%	T	T	T	T	F	F	F	F	F	F
Dalacin Phosphate 600 mg/4 mL	31%	T	T	T	F	F	F	F	F	F	F
Pancuronium Inresa 4mg/2ml	33%	T	T	T	F	F	F	F	F	F	F
Ephedrine Hydrochloride 30mg	**100%**	**T**	**T**	**T**	**T**	**T**	**T**	**T**	**T**	**T**	**F**
Dexamethasone Phosphate 4mg	44%	T	T	T	T	F	F	F	F	F	F
Glycopyrronium and Neostigmine	42%	T	T	T	T	F	F	F	F	F	F
Actrapid Penfill 3mL	44%	T	T	T	T	F	F	F	F	F	F

Threshold: Amoxicillin 1g against other samples

Drug Name	Similarity Score	T10	T20	T30	T40	T50	T60	T70	T80	T90	T100
Frusemide-Claris 20mg	44%	T	T	T	T	F	F	F	F	F	F
Water For Injections 10mL	39%	T	T	T	F	F	F	F	F	F	F
Paracetamol 1000mg/100mL	35%	T	T	T	F	F	F	F	F	F	F
Fresofol 1% MCT/LCT	48%	T	T	T	T	F	F	F	F	F	F
Amoxicillin 1g	**100%**	**T**	**T**	**T**	**T**	**T**	**T**	**T**	**T**	**T**	**F**
Hydrocortisone sodium 100mg	55%	T	T	T	T	T	F	F	F	F	F
Cefazolin Sodium 1g	61%	T	T	T	T	T	T	F	F	F	F
Atracurium Besylate 50mg	56%	T	T	T	T	T	F	F	F	F	F
Naloxone HCl 400mg in 1mL	28%	T	T	F	F	F	F	F	F	F	F
Morphine Sulfate Injection 10mg	35%	T	T	T	F	F	F	F	F	F	F
Ondansetron Solution	47%	T	T	T	T	F	F	F	F	F	F
Protamine Sulfate 10mg/ml	48%	T	T	T	T	F	F	F	F	F	F
Vecuronium Bromide	51%	T	T	T	T	T	F	F	F	F	F
Potassium Chloride 10mmol	46%	T	T	T	T	F	F	F	F	F	F
Heparin Injection 25000IU	45%	T	T	T	T	F	F	F	F	F	F
Sugammadex 200mg/2ml	46%	T	T	T	T	F	F	F	F	F	F
Protamine Sulphate 50mg in 5ml	49%	T	T	T	T	F	F	F	F	F	F
Sodium Chloride 10ml	46%	T	T	T	T	F	F	F	F	F	F
Remifentanil-AFT 2g	47%	T	T	T	T	F	F	F	F	F	F
Sedative Midazolam 5mg	30%	T	T	F	F	F	F	F	F	F	F
Glyceryl Trinitrate 10mg in 10ml	39%	T	T	T	F	F	F	F	F	F	F
Fentanyl Citrate 785 micrograms	42%	T	T	T	T	F	F	F	F	F	F
Cefazolin-AFT 1g	51%	T	T	T	T	T	F	F	F	F	F
Dynastat 40 mg	59%	T	T	T	T	T	F	F	F	F	F
Tranexamic-AFT	41%	T	T	T	T	F	F	F	F	F	F
Calcium Chloride 1g in 10mL	47%	T	T	T	T	F	F	F	F	F	F
Provive MCT-LCT 1%	46%	T	T	T	T	F	F	F	F	F	F
METOPROLOL Mylan 5mg	58%	T	T	T	T	T	F	F	F	F	F
Noradrenaline 4mL	39%	T	T	T	F	F	F	F	F	F	F
Lidocaine-Claris 5ml	39%	T	T	T	F	F	F	F	F	F	F
Atropine Injection 600Ug	31%	T	T	T	F	F	F	F	F	F	F
Xylocaine 1%	24%	T	T	F	F	F	F	F	F	F	F
Sodium Chloride 0.9%	45%	T	T	T	T	F	F	F	F	F	F
Hypnomidate 10mL	40%	T	T	T	F	F	F	F	F	F	F
Adrenaline Injection 1mg	42%	T	T	T	T	F	F	F	F	F	F
Sterile Dopamine 200mg/5ml	44%	T	T	T	T	F	F	F	F	F	F
Suxamethonium 100mg in 2 ml	41%	T	T	T	T	F	F	F	F	F	F
Amiodarone HCL 50 mg/ml	54%	T	T	T	T	T	F	F	F	F	F
Primacor Injection 10mL	42%	T	T	T	T	F	F	F	F	F	F
Sugammadex 200 mg/2ml	50%	T	T	T	T	F	F	F	F	F	F
Rocuronium Bromide 50 mg	35%	T	T	T	F	F	F	F	F	F	F
Clonidine HCl 150 ug/1mL	44%	T	T	T	T	F	F	F	F	F	F
Cyclizine Lactate 50	37%	T	T	T	F	F	F	F	F	F	F
PITRESSIN 20 Units in 1 mL	39%	T	T	T	F	F	F	F	F	F	F
Magnesium Sulfate 2.47g	40%	T	T	T	F	F	F	F	F	F	F
Metaraminol 10mg/mL	43%	T	T	T	T	F	F	F	F	F	F
Dalacin Phosphate 600 mg/4 mL	32%	T	T	T	F	F	F	F	F	F	F
Pancuronium Inresa 4mg/2ml	41%	T	T	T	T	F	F	F	F	F	F
Ephedrine Hydrochloride 30mg	36%	T	T	T	F	F	F	F	F	F	F
Dexamethasone Phosphate 4mg	42%	T	T	T	T	F	F	F	F	F	F
Glycopyrronium and Neostigmine	49%	T	T	T	T	F	F	F	F	F	F
Actrapid Penfill 3mL	39%	T	T	T	F	F	F	F	F	F	F

Threshold: Dexamethasone Phosphate against other samples

Drug Name	Similarity Score	T10	T20	T30	T40	T50	T60	T70	T80	T90	T100
Frusemide-Claris 20mg	48%	T	T	T	T	F	F	F	F	F	F
Water For Injections 10mL	47%	T	T	T	T	F	F	F	F	F	F
Paracetamol 1000mg/100mL	47%	T	T	T	T	F	F	F	F	F	F
Fresofol 1% MCT/LCT	58%	T	T	T	T	T	F	F	F	F	F
Amoxicillin 1g	42%	T	T	T	T	F	F	F	F	F	F
Hydrocortisone sodium 100mg	54%	T	T	T	T	T	F	F	F	F	F
Cefazolin Sodium 1g	44%	T	T	T	T	F	F	F	F	F	F
Atracurium Besylate 50mg	54%	T	T	T	T	T	F	F	F	F	F
Naloxone HCl 400mg in 1mL	45%	T	T	T	T	F	F	F	F	F	F
Morphine Sulfate Injection 10mg	58%	T	T	T	T	T	F	F	F	F	F
Ondansetron Solution	48%	T	T	T	T	F	F	F	F	F	F
Protamine Sulfate 10mg/ml	64%	T	T	T	T	T	T	F	F	F	F
Vecuronium Bromide	47%	T	T	T	T	F	F	F	F	F	F
Potassium Chloride 10mmol	37%	T	T	T	F	F	F	F	F	F	F
Heparin Injection 25000IU	51%	T	T	T	T	T	F	F	F	F	F
Sugammadex 200mg/2ml	64%	T	T	T	T	T	T	F	F	F	F
Protamine Sulphate 50mg in 5ml	61%	T	T	T	T	T	T	F	F	F	F
Sodium Chloride 10ml	69%	T	T	T	T	T	T	F	F	F	F
Remifentanil-AFT 2g	46%	T	T	T	T	F	F	F	F	F	F
Sedative Midazolam 5mg	44%	T	T	T	T	F	F	F	F	F	F
Glyceryl Trinitrate 10mg in 10ml	46%	T	T	T	T	F	F	F	F	F	F
Fentanyl Citrate 785 micrograms	47%	T	T	T	T	F	F	F	F	F	F
Cefazolin-AFT 1g	53%	T	T	T	T	T	F	F	F	F	F
Dynastat 40 mg	53%	T	T	T	T	T	F	F	F	F	F
Tranexamic-AFT	50%	T	T	T	T	F	F	F	F	F	F
Calcium Chloride 1g in 10mL	46%	T	T	T	T	F	F	F	F	F	F
Provive MCT-LCT 1%	58%	T	T	T	T	T	F	F	F	F	F
METOPROLOL Mylan 5mg	64%	T	T	T	T	T	T	F	F	F	F
Noradrenaline 4mL	37%	T	T	T	F	F	F	F	F	F	F
Lidocaine-Claris 5ml	47%	T	T	T	T	F	F	F	F	F	F
Atropine Injection 600Ug	52%	T	T	T	T	T	F	F	F	F	F
Xylocaine 1%	42%	T	T	T	T	F	F	F	F	F	F
Sodium Chloride 0.9%	38%	T	T	T	F	F	F	F	F	F	F
Hypnomidate 10mL	47%	T	T	T	T	F	F	F	F	F	F
Adrenaline Injection 1mg	49%	T	T	T	T	F	F	F	F	F	F
Sterile Dopamine 200mg/5ml	40%	T	T	T	F	F	F	F	F	F	F
Suxamethonium 100mg in 2 ml	53%	T	T	T	T	T	F	F	F	F	F
Amiodarone HCL 50 mg/ml	69%	T	T	T	T	T	T	F	F	F	F
Primacor Injection 10mL	55%	T	T	T	T	T	F	F	F	F	F
Sugammadex 200 mg/2ml	52%	T	T	T	T	T	F	F	F	F	F
Rocuronium Bromide 50 mg	56%	T	T	T	T	T	F	F	F	F	F
Clonidine HCl 150 ug/1mL	53%	T	T	T	T	T	F	F	F	F	F
Cyclizine Lactate 50	41%	T	T	T	T	F	F	F	F	F	F
PITRESSIN 20 Units in 1 mL	60%	T	T	T	T	T	F	F	F	F	F
Magnesium Sulfate 2.47g	48%	T	T	T	T	F	F	F	F	F	F
Metaraminol 10mg/mL	62%	T	T	T	T	T	T	F	F	F	F
Dalacin Phosphate 600 mg/4 mL	52%	T	T	T	T	T	F	F	F	F	F
Pancuronium Inresa 4mg/2ml	43%	T	T	T	T	F	F	F	F	F	F
Ephedrine Hydrochloride 30mg	44%	T	T	T	T	F	F	F	F	F	F
Dexamethasone Phosphate 4mg	**100%**	**T**	**T**	**T**	**T**	**T**	**T**	**T**	**T**	**T**	**F**
Glycopyrronium and Neostigmine	60%	T	T	T	T	T	F	F	F	F	F
Actrapid Penfill 3mL	49%	T	T	T	T	F	F	F	F	F	F

Threshold: Glycopyrronium and Neostigmine against other samples

Drug Name	Similarity Score	T10	T20	T30	T40	T50	T60	T70	T80	T90	T100
Frusemide-Claris 20mg	49%	T	T	T	T	F	F	F	F	F	F
Water For Injections 10mL	48%	T	T	T	T	F	F	F	F	F	F
Paracetamol 1000mg/100mL	41%	T	T	T	T	F	F	F	F	F	F
Fresofol 1% MCT/LCT	45%	T	T	T	T	F	F	F	F	F	F
Amoxicillin 1g	49%	T	T	T	T	F	F	F	F	F	F
Hydrocortisone sodium 100mg	49%	T	T	T	T	F	F	F	F	F	F
Cefazolin Sodium 1g	48%	T	T	T	T	F	F	F	F	F	F
Atracurium Besylate 50mg	57%	T	T	T	T	T	F	F	F	F	F
Naloxone HCl 400mg in 1mL	34%	T	T	T	F	F	F	F	F	F	F
Morphine Sulfate Injection 10mg	45%	T	T	T	T	F	F	F	F	F	F
Ondansetron Solution	53%	T	T	T	T	T	F	F	F	F	F
Protamine Sulfate 10mg/ml	63%	T	T	T	T	T	T	F	F	F	F
Vecuronium Bromide	67%	T	T	T	T	T	T	F	F	F	F
Potassium Chloride 10mmol	51%	T	T	T	T	T	F	F	F	F	F
Heparin Injection 25000IU	51%	T	T	T	T	T	F	F	F	F	F
Sugammadex 200mg/2ml	60%	T	T	T	T	T	F	F	F	F	F
Protamine Sulphate 50mg in 5ml	55%	T	T	T	T	T	F	F	F	F	F
Sodium Chloride 10ml	59%	T	T	T	T	T	F	F	F	F	F
Remifentanil-AFT 2g	50%	T	T	T	T	F	F	F	F	F	F
Sedative Midazolam 5mg	38%	T	T	T	F	F	F	F	F	F	F
Glyceryl Trinitrate 10mg in 10ml	42%	T	T	T	T	F	F	F	F	F	F
Fentanyl Citrate 785 micrograms	51%	T	T	T	T	T	F	F	F	F	F
Cefazolin-AFT 1g	51%	T	T	T	T	T	F	F	F	F	F
Dynastat 40 mg	54%	T	T	T	T	T	F	F	F	F	F
Tranexamic-AFT	48%	T	T	T	T	F	F	F	F	F	F
Calcium Chloride 1g in 10mL	50%	T	T	T	T	F	F	F	F	F	F
Provive MCT-LCT 1%	36%	T	T	T	F	F	F	F	F	F	F
METOPROLOL Mylan 5mg	59%	T	T	T	T	T	F	F	F	F	F
Noradrenaline 4mL	35%	T	T	T	F	F	F	F	F	F	F
Lidocaine-Claris 5ml	45%	T	T	T	T	F	F	F	F	F	F
Atropine Injection 600Ug	43%	T	T	T	T	F	F	F	F	F	F
Xylocaine 1%	33%	T	T	T	F	F	F	F	F	F	F
Sodium Chloride 0.9%	44%	T	T	T	T	F	F	F	F	F	F
Hypnomidate 10mL	48%	T	T	T	T	F	F	F	F	F	F
Adrenaline Injection 1mg	38%	T	T	T	F	F	F	F	F	F	F
Sterile Dopamine 200mg/5ml	39%	T	T	T	F	F	F	F	F	F	F
Suxamethonium 100mg in 2 ml	51%	T	T	T	T	T	F	F	F	F	F
Amiodarone HCL 50 mg/ml	56%	T	T	T	T	T	F	F	F	F	F
Primacor Injection 10mL	47%	T	T	T	T	F	F	F	F	F	F
Sugammadex 200 mg/2ml	53%	T	T	T	T	T	F	F	F	F	F
Rocuronium Bromide 50 mg	61%	T	T	T	T	T	T	F	F	F	F
Clonidine HCl 150 ug/1mL	45%	T	T	T	T	F	F	F	F	F	F
Cyclizine Lactate 50	43%	T	T	T	T	F	F	F	F	F	F
PITRESSIN 20 Units in 1 mL	48%	T	T	T	T	F	F	F	F	F	F
Magnesium Sulfate 2.47g	52%	T	T	T	T	T	F	F	F	F	F
Metaraminol 10mg/mL	56%	T	T	T	T	T	F	F	F	F	F
Dalacin Phosphate 600 mg/4 mL	33%	T	T	T	F	F	F	F	F	F	F
Pancuronium Inresa 4mg/2ml	48%	T	T	T	T	F	F	F	F	F	F
Ephedrine Hydrochloride 30mg	42%	T	T	T	T	F	F	F	F	F	F
Dexamethasone Phosphate 4mg	60%	T	T	T	T	T	F	F	F	F	F
Glycopyrronium and Neostigmine	**100%**	**T**	**T**	**T**	**T**	**T**	**T**	**T**	**T**	**T**	**F**
Actrapid Penfill 3mL	47%	T	T	T	T	F	F	F	F	F	F

Threshold: Actrapid Penfill against other samples

Drug Name	Similarity Score	T10	T20	T30	T40	T50	T60	T70	T80	T90	T100
Frusemide-Claris 20mg	39%	T	T	T	F	F	F	F	F	F	F
Water For Injections 10mL	46%	T	T	T	T	F	F	F	F	F	F
Paracetamol 1000mg/100mL	22%	T	T	F	F	F	F	F	F	F	F
Fresofol 1% MCT/LCT	28%	T	T	F	F	F	F	F	F	F	F
Amoxicillin 1g	39%	T	T	T	F	F	F	F	F	F	F
Hydrocortisone sodium 100mg	43%	T	T	T	T	F	F	F	F	F	F
Cefazolin Sodium 1g	42%	T	T	T	T	F	F	F	F	F	F
Atracurium Besylate 50mg	49%	T	T	T	T	F	F	F	F	F	F
Naloxone HCl 400mg in 1mL	41%	T	T	T	T	F	F	F	F	F	F
Morphine Sulfate Injection 10mg	49%	T	T	T	T	F	F	F	F	F	F
Ondansetron Solution	38%	T	T	T	F	F	F	F	F	F	F
Protamine Sulfate 10mg/ml	50%	T	T	T	T	F	F	F	F	F	F
Vecuronium Bromide	46%	T	T	T	T	F	F	F	F	F	F
Potassium Chloride 10mmol	43%	T	T	T	T	F	F	F	F	F	F
Heparin Injection 25000IU	53%	T	T	T	T	T	F	F	F	F	F
Sugammadex 200mg/2ml	46%	T	T	T	T	F	F	F	F	F	F
Protamine Sulphate 50mg in 5ml	48%	T	T	T	T	F	F	F	F	F	F
Sodium Chloride 10ml	42%	T	T	T	T	F	F	F	F	F	F
Remifentanil-AFT 2g	46%	T	T	T	T	F	F	F	F	F	F
Sedative Midazolam 5mg	34%	T	T	T	F	F	F	F	F	F	F
Glyceryl Trinitrate 10mg in 10ml	42%	T	T	T	T	F	F	F	F	F	F
Fentanyl Citrate 785 micrograms	40%	T	T	T	F	F	F	F	F	F	F
Cefazolin-AFT 1g	48%	T	T	T	T	F	F	F	F	F	F
Dynastat 40 mg	45%	T	T	T	T	F	F	F	F	F	F
Tranexamic-AFT	42%	T	T	T	T	F	F	F	F	F	F
Calcium Chloride 1g in 10mL	49%	T	T	T	T	F	F	F	F	F	F
Provive MCT-LCT 1%	27%	T	T	F	F	F	F	F	F	F	F
METOPROLOL Mylan 5mg	42%	T	T	T	T	F	F	F	F	F	F
Noradrenaline 4mL	37%	T	T	T	F	F	F	F	F	F	F
Lidocaine-Claris 5ml	43%	T	T	T	T	F	F	F	F	F	F
Atropine Injection 600Ug	48%	T	T	T	T	F	F	F	F	F	F
Xylocaine 1%	42%	T	T	T	T	F	F	F	F	F	F
Sodium Chloride 0.9%	39%	T	T	T	F	F	F	F	F	F	F
Hypnomidate 10mL	43%	T	T	T	T	F	F	F	F	F	F
Adrenaline Injection 1mg	50%	T	T	T	T	F	F	F	F	F	F
Sterile Dopamine 200mg/5ml	40%	T	T	T	F	F	F	F	F	F	F
Suxamethonium 100mg in 2 ml	47%	T	T	T	T	F	F	F	F	F	F
Amiodarone HCL 50 mg/ml	48%	T	T	T	T	F	F	F	F	F	F
Primacor Injection 10mL	48%	T	T	T	T	F	F	F	F	F	F
Sugammadex 200 mg/2ml	55%	T	T	T	T	T	F	F	F	F	F
Rocuronium Bromide 50 mg	51%	T	T	T	T	T	F	F	F	F	F
Clonidine HCl 150 ug/1mL	53%	T	T	T	T	T	F	F	F	F	F
Cyclizine Lactate 50	42%	T	T	T	T	F	F	F	F	F	F
PITRESSIN 20 Units in 1 mL	59%	T	T	T	T	T	F	F	F	F	F
Magnesium Sulfate 2.47g	47%	T	T	T	T	F	F	F	F	F	F
Metaraminol 10mg/mL	54%	T	T	T	T	T	F	F	F	F	F
Dalacin Phosphate 600 mg/4 mL	38%	T	T	T	F	F	F	F	F	F	F
Pancuronium Inresa 4mg/2ml	42%	T	T	T	T	F	F	F	F	F	F
Ephedrine Hydrochloride 30mg	44%	T	T	T	T	F	F	F	F	F	F
Dexamethasone Phosphate 4mg	49%	T	T	T	T	F	F	F	F	F	F
Glycopyrronium and Neostigmine	47%	T	T	T	T	F	F	F	F	F	F
Actrapid Penfill 3mL	**100%**	**T**	**T**	**T**	**T**	**T**	**T**	**T**	**T**	**T**	**F**

Appendix C -- Threshold Computation Data Summary

Frusemide-Claris

Threshold	T10	T20	T30	T40	T50	T60	T70	T80	T90	T100
No_False	0	0	2	24	45	50	51	51	51	52
No_True	52	52	50	28	7	2	1	1	1	0

Morphine Sulphate

Threshold	T10	T20	T30	T40	T50	T60	T70	T80	T90	T100
No_False	0	0	1	9	35	48	51	51	51	52
No_True	52	52	51	43	17	4	1	1	1	0

Ondansetron Solution

Threshold	T10	T20	T30	T40	T50	T60	T70	T80	T90	T100
No_False	0	0	1	20	46	50	51	51	51	52
No_True	52	52	51	32	6	2	1	1	1	0

Protamine Sulfate

Threshold	T10	T20	T30	T40	T50	T60	T70	T80	T90	T100
No_False	0	0	0	2	24	44	50	51	51	52
No_True	52	52	52	50	28	8	2	1	1	0

Vecuronium Bromide

Threshold	T10	T20	T30	T40	T50	T60	T70	T80	T90	T100
No_False	0	0	4	18	36	48	51	51	51	52
No_True	52	52	48	34	16	4	1	1	1	0

Potassium Chloride

Threshold	T10	T20	T30	T40	T50	T60	T70	T80	T90	T100
No_False	0	0	1	22	43	51	51	51	51	52
No_True	52	52	51	30	9	1	1	1	1	0

Heparin Injection

Threshold	T10	T20	T30	T40	T50	T60	T70	T80	T90	T100
No_False	0	0	1	8	34	50	51	51	51	52
No_True	52	52	51	44	18	2	1	1	1	0

Sugammadex

Threshold	T10	T20	T30	T40	T50	T60	T70	T80	T90	T100
No_False	0	0	0	6	28	44	50	50	50	52
No_True	52	52	52	46	24	8	2	2	2	0

Protamine Sulphate

Threshold	T10	T20	T30	T40	T50	T60	T70	T80	T90	T100
No_False	0	0	1	6	28	48	50	51	51	52
No_True	52	52	51	46	24	4	2	1	1	0

Sodium Chloride

Threshold	T10	T20	T30	T40	T50	T60	T70	T80	T90	T100
No_False	0	0	2	8	31	48	50	51	51	52
No_True	52	52	50	44	21	4	2	1	1	0

Remifentanil-AFT

Threshold	T10	T20	T30	T40	T50	T60	T70	T80	T90	T100
No_False	0	0	4	13	44	49	50	51	51	52
No_True	52	52	48	39	8	3	2	1	1	0

Water For Injections

Threshold	T10	T20	T30	T40	T50	T60	T70	T80	T90	T100
No_False	0	0	1	8	46	51	51	51	51	52
No_True	52	52	51	44	6	1	1	1	1	0

Sedative Midazolam

Threshold	T10	T20	T30	T40	T50	T60	T70	T80	T90	T100
No_False	0	1	9	36	50	51	51	51	51	52
No_True	52	51	43	16	2	1	1	1	1	0

Glyceryl Trinitrate

Threshold	T10	T20	T30	T40	T50	T60	T70	T80	T90	T100
No_False	0	0	1	19	51	51	51	51	51	52
No_True	52	52	51	33	1	1	1	1	1	0

Fentanyl Citrate

Threshold	T10	T20	T30	T40	T50	T60	T70	T80	T90	T100
No_False	0	0	1	14	44	48	51	51	51	52
No_True	52	52	51	38	8	4	1	1	1	0

Cefazolin-AFT

Threshold	T10	T20	T30	T40	T50	T60	T70	T80	T90	T100
No_False	0	0	1	11	33	46	49	50	50	52
No_True	52	52	51	41	19	6	3	2	2	0

Dynastat

Threshold	T10	T20	T30	T40	T50	T60	T70	T80	T90	T100
No_False	0	0	0	9	30	46	51	51	51	52
No_True	52	52	52	43	22	6	1	1	1	0

Tranexamic-AFT

Threshold	T10	T20	T30	T40	T50	T60	T70	T80	T90	T100
No_False	0	0	1	12	48	51	51	51	51	52
No_True	52	52	51	40	4	1	1	1	1	0

Calcium Chloride

Threshold	T10	T20	T30	T40	T50	T60	T70	T80	T90	T100
No_False	0	0	0	8	43	51	51	51	51	52
No_True	52	52	52	44	9	1	1	1	1	0

Proviv

Threshold	T10	T20	T30	T40	T50	T60	T70	T80	T90	T100
No_False	0	4	11	23	35	44	50	51	51	52
No_True	52	48	41	29	17	8	2	1	1	0

Noradrenaline

Threshold	T10	T20	T30	T40	T50	T60	T70	T80	T90	T100
No_False	0	0	4	37	51	51	51	51	51	52
No_True	52	52	48	15	1	1	1	1	1	0

METOPROLOL Mylan

Threshold	T10	T20	T30	T40	T50	T60	T70	T80	T90	T100
No_False	0	0	0	8	32	46	49	51	51	52
No_True	52	52	52	44	20	6	3	1	1	0

Paracetamol Kabi

Threshold	T10	T20	T30	T40	T50	T60	T70	T80	T90	T100
No_False	0	11	24	34	45	48	51	51	51	52
No_True	52	41	28	18	7	4	1	1	1	0

Lidocaine-Claris

Threshold	T10	T20	T30	T40	T50	T60	T70	T80	T90	T100
No_False	0	0	1	11	49	51	51	51	51	52
No_True	52	52	51	41	3	1	1	1	1	0

Atropine Injection

Threshold	T10	T20	T30	T40	T50	T60	T70	T80	T90	T100
No_False	0	2	4	23	46	50	51	51	51	52

No_True	52	50	48	29	6	2	1	1	1	0

Xylocaine

Threshold	T10	T20	T30	T40	T50	T60	T70	T80	T90	T100
No_False	0	3	12	39	51	51	51	51	51	52
No_True	52	49	40	13	1	1	1	1	1	0

Sodium Chloride

Threshold	T10	T20	T30	T40	T50	T60	T70	T80	T90	T100
No_False	0	1	7	45	51	51	51	51	51	52
No_True	52	51	45	7	1	1	1	1	1	0

Hypnomidate

Threshold	T10	T20	T30	T40	T50	T60	T70	T80	T90	T100
No_False	0	0	0	15	49	51	51	51	51	52
No_True	52	52	52	37	3	1	1	1	1	0

Adrenaline Injection

Threshold	T10	T20	T30	T40	T50	T60	T70	T80	T90	T100
No_False	0	1	3	17	45	47	51	51	51	52
No_True	52	51	49	35	7	5	1	1	1	0

Sterile Dopamine

Threshold	T10	T20	T30	T40	T50	T60	T70	T80	T90	T100
No_False	0	2	5	31	49	51	51	51	51	52
No_True	52	50	47	21	3	1	1	1	1	0

Suxamethonium Chloride

Threshold	T10	T20	T30	T40	T50	T60	T70	T80	T90	T100
No_False	0	0	0	6	33	49	50	51	51	52
No_True	52	52	52	46	19	3	2	1	1	0

Amiodarine Hydrochloride

Threshold	T10	T20	T30	T40	T50	T60	T70	T80	T90	T100
No_False	0	0	0	4	25	43	50	51	51	52
No_True	52	52	52	48	27	9	2	1	1	0

Primacor Injection

Threshold	T10	T20	T30	T40	T50	T60	T70	T80	T90	T100
No_False	0	0	0	4	42	51	51	51	51	52
No_True	52	52	52	48	10	1	1	1	1	0

Fresofol 1% MCT/LCT

Threshold	T10	T20	T30	T40	T50	T60	T70	T80	T90	T100

No_False	0	1	7	21	36	43	50	51	51	52
No_True	52	51	45	31	16	9	2	1	1	0

Sugammadex

Threshold	T10	T20	T30	T40	T50	T60	T70	T80	T90	T100
No_False	0	0	0	9	28	49	49	50	50	52
No_True	52	52	52	43	24	3	3	2	2	0

Rocuronium Bromide

Threshold	T10	T20	T30	T40	T50	T60	T70	T80	T90	T100
No_False	0	1	1	11	27	44	51	51	51	52
No_True	52	51	51	41	25	8	1	1	1	0

Clonidine HCI Injection

Threshold	T10	T20	T30	T40	T50	T60	T70	T80	T90	T100
No_False	0	1	1	9	32	50	51	51	51	52
No_True	52	51	51	43	20	2	1	1	1	0

Cyclizine Lactate

Threshold	T10	T20	T30	T40	T50	T60	T70	T80	T90	T100
No_False	0	1	3	31	50	51	51	51	51	52
No_True	52	51	49	21	2	1	1	1	1	0

PITRESSIN 20 Units

Threshold	T10	T20	T30	T40	T50	T60	T70	T80	T90	T100
No_False	0	1	1	10	34	50	51	51	51	52
No_True	52	51	51	42	18	2	1	1	1	0

Magnesium Sulfate

Threshold	T10	T20	T30	T40	T50	T60	T70	T80	T90	T100
No_False	0	0	1	10	41	49	51	51	51	52
No_True	52	52	51	42	11	3	1	1	1	0

Metaraminol

Threshold	T10	T20	T30	T40	T50	T60	T70	T80	T90	T100
No_False	0	0	0	8	35	47	51	51	51	52
No_True	52	52	52	44	17	5	1	1	1	0

Dalacin Phosphate

Threshold	T10	T20	T30	T40	T50	T60	T70	T80	T90	T100
No_False	0	2	5	37	50	51	51	51	51	52
No_True	52	50	47	15	2	1	1	1	1	0

Pancuronium Inresa

Threshold	T10	T20	T30	T40	T50	T60	T70	T80	T90	T100
No_False	0	0	3	25	51	51	51	51	51	52
No_True	52	52	49	27	1	1	1	1	1	0

Ephedrine Hydrochloride

Threshold	T10	T20	T30	T40	T50	T60	T70	T80	T90	T100
No_False	0	0	2	19	46	50	51	51	51	52
No_True	52	52	50	33	6	2	1	1	1	0

Amoxicillin

Threshold	T10	T20	T30	T40	T50	T60	T70	T80	T90	T100
No_False	0	0	3	18	43	50	51	51	51	52
No_True	52	52	49	34	9	2	1	1	1	0

Dexamethasone Phosphate

Threshold	T10	T20	T30	T40	T50	T60	T70	T80	T90	T100
No_False	0	0	0	4	27	44	51	51	51	52
No_True	52	52	52	48	25	8	1	1	1	0

Glycopyrronium and Neostigmine

Threshold	T10	T20	T30	T40	T50	T60	T70	T80	T90	T100
No_False	0	0	0	8	31	48	51	51	51	52
No_True	52	52	52	44	21	4	1	1	1	0

ActrapidaPenfill

Threshold	T10	T20	T30	T40	T50	T60	T70	T80	T90	T100
No_False	0	0	3	12	45	51	51	51	51	52
No_True	52	52	49	40	7	1	1	1	1	0

Appendix D – Drug Identification: Summethonium Chloride against other samples

Drug Name	Edit Distance	TSR Scores	Lev Scores	Jacc Scores	Processing Time
Primacor Injection	71	0.43	0.43	0.66	0.6155s
Cefazolin Sodium 1g	113	0.42	0.31	0.62	0.6155s
NALOXONE HCl 400mg in 1mL	44	0.42	0.32	0.50	0.6155s
Calcium Chloride 1g in 10mL	102	0.39	0.38	0.71	0.6155s
Actrapid Penfill 3ml	52	0.47	0.34	0.70	0.6155s
Vecuronium bromide	46	0.51	0.40	0.70	0.6155s
Sugammadex 200mg/2ml	60	0.52	0.43	0.75	0.6155s
Amiodarone Hydrochloride	57	0.52	0.43	0.64	0.6155s
Protamine Sulphate 50mg in 5ml	74	0.52	0.35	0.71	0.6155s
Summethonium Chloride 100mg in 2mL	**1**	**1.0**	**0.99**	**1.00**	**0.6155s**
Protamine Sulfate 10mg/ml	62	0.55	0.42	0.72	0.6155s
Glyceryl Trinitrate 1 mg/ml	82	0.45	0.34	0.68	0.6155s
Tranexamic acid	59	0.48	0.34	0.70	0.6155s
Heparin Injection 25000IU in 5 mL	58	0.52	0.43	0.65	0.6155s
Sterile Potassium Chloride	86	0.54	0.42	0.71	0.6155s
Metaraminol 10mg/ml	50	0.5	0.39	0.69	0.6155s
Cyclizine lactate	48	0.29	0.23	0.43	0.6155s
PITRESSIN argipressin	44	0.39	0.30	0.68	0.6155s
Dexamethasone phosphate 4 mg/ml	52	0.53	0.41	0.71	0.6155s
Ephedrine Hydrochloride	51	0.37	0.34	0.64	0.6155s
Ondansetron Solution	64	0.44	0.36	0.70	0.6155s
FRUSEMIDE	51	0.49	0.33	0.67	0.6155s
DALACINC PHOSPHATE	54	0.44	0.33	0.56	0.6155s
METOPROLOL Mylan	71	0.4	0.35	0.61	0.6155s
WATER FOR INJECTIONS BP	76	0.41	0.33	0.67	0.6155s
MORPHINE SULFATE	45	0.48	0.41	0.84	0.6155s
Glycopyrronium and Neostigmine	63	0.49	0.36	0.75	0.6155s
Clonidine HCl	44	0.41	0.32	0.65	0.6155s
Rocuronium Bromide 50 mg in 5 ml	54	0.54	0.47	0.68	0.6155s
Fresofol 1% MCT/LCT	332	0.41	0.19	0.59	0.6155s
Sedative Midazolam 5mg	48	0.47	0.34	0.61	0.6155s
Adrenaline Injection	61	0.34	0.29	0.58	0.6155s
Paracetamol Kabi	536	0.33	0.14	0.57	0.6155s
Provive MCT-LCT 1%	266	0.38	0.25	0.69	0.6155s
Adrenaline Injection 1mg in 10mL	61	0.34	0.29	0.58	0.6155s
Amoxicillin Sodium	125	0.36	0.30	0.67	0.6155s
Lidocain Injection	47	0.32	0.24	0.62	0.6155s
SODIUM CHLORIDE	110	0.4	0.33	0.66	0.6155s
Remifentanil-Act Injection	76	0.42	0.37	0.69	0.6155s
Sterile Dopamine	45	0.42	0.35	0.57	0.6155s
Hypnomida Etomidate 2mg	60	0.51	0.38	0.72	0.6155s
Xylocaine 1%	44	0.33	0.33	0.43	0.6155s
Fentanyl Injection	114	0.43	0.34	0.60	0.6155s
Noradrenaline acid	69	0.34	0.29	0.61	0.6155s
Magnesium Sulfate 2.47g in 5mL	70	0.43	0.32	0.54	0.6155s
Sugammadex Injection	57	0.57	0.39	0.81	0.6155s
Dynastat Powder	69	0.46	0.37	0.67	0.6155s
Hydrocortisone sodium	79	0.47	0.35	0.76	0.6155s
Atracurium Besylate	49	0.35	0.31	0.62	0.6155s
Atropine	40	0.42	0.40	0.65	0.6155s
PancuroInresa	78	0.41	0.32	0.76	0.6155s

Drug Identification: Dynastat Powder against other samples

Drug Name	Edit Distance	TSR Scores	Lev Scores	Jacc Scores	Processing Time
Primacor Injection	84	0.53	0.39	0.57	0.4608s
Cefazolin Sodium 1g	90	0.61	0.51	0.54	0.4608s
NALOXONE HCl 400mg in 1mL	78	0.34	0.30	0.57	0.4608s
Calcium Chloride 1g in 10mL	100	0.44	0.39	0.57	0.4608s
Actrapid Penfill 3ml	80	0.41	0.31	0.61	0.4608s
Vecuronium bromide	64	0.56	0.48	0.71	0.4608s
Sugammadex 200mg/2ml	72	0.51	0.42	0.70	0.4608s
Amiodarone Hydrochloride	78	0.52	0.41	0.66	0.4608s
Protamine Sulphate 50mg in 5ml	83	0.47	0.42	0.67	0.4608s
Summethonium Chloride 100mg in 2mL	69	0.46	0.37	0.67	0.4608s
Protamine Sulfate 10mg/ml	76	0.47	0.41	0.68	0.4608s
Glyceryl Trinitrate 1 mg/ml	88	0.41	0.34	0.63	0.4608s
Tranexamic acid	77	0.42	0.38	0.66	0.4608s
Heparin Injection 25000IU in 5 mL	73	0.51	0.40	0.56	0.4608s
Sterile Potassium Chloride	89	0.4	0.40	0.62	0.4608s
Metaraminol 10mg/ml	66	0.49	0.43	0.64	0.4608s
Cyclizine lactate	84	0.19	0.21	0.45	0.4608s
PITRESSIN argipressin	68	0.43	0.41	0.63	0.4608s
Dexamethasone phosphate 4 mg/ml	69	0.54	0.43	0.72	0.4608s
Ephedrine Hydrochloride	74	0.44	0.36	0.59	0.4608s
Ondansetron Solution	78	0.49	0.38	0.77	0.4608s
FRUSEMIDE	71	0.45	0.35	0.57	0.4608s
DALACINC PHOSPHATE	78	0.43	0.31	0.58	0.4608s
METOPROLOL Mylan	65	0.58	0.55	0.68	0.4608s
WATER FOR INJECTIONS BP	81	0.47	0.39	0.68	0.4608s
MORPHINE SULFATE	71	0.45	0.43	0.71	0.4608s
Glycopyrronium and Neostigmine	80	0.52	0.35	0.70	0.4608s
Clonidine HCl	75	0.44	0.33	0.50	0.4608s
Rocuronium Bromide 50 mg in 5 ml	76	0.47	0.41	0.63	0.4608s
Fresofol 1% MCT/LCT	302	0.54	0.31	0.60	0.4608s
Sedative Midazolam 5mg	78	0.33	0.30	0.58	0.4608s
Adrenaline Injection	75	0.43	0.40	0.54	0.4608s
Paracetamol Kabi	499	0.41	0.24	0.58	0.4608s
Provive MCT-LCT 1%	246	0.46	0.33	0.61	0.4608s
Adrenaline Injection 1mg in 10mL	75	0.43	0.40	0.54	0.4608s
Amoxicillin Sodium	108	0.56	0.43	0.63	0.4608s
Lidocain Injection	78	0.35	0.29	0.52	0.4608s
SODIUM CHLORIDE	111	0.38	0.34	0.67	0.4608s
Remifentanil-Act Injection	63	0.57	0.52	0.76	0.4608s
Sterile Dopamine	76	0.33	0.30	0.59	0.4608s
Hypnomida Etomidate 2mg	71	0.45	0.42	0.68	0.4608s
Xylocaine 1%	77	0.34	0.29	0.50	0.4608s
Fentanyl Injection	117	0.44	0.35	0.66	0.4608s
Noradrenaline acid	77	0.43	0.36	0.68	0.4608s
Magnesium Sulfate 2.47g in 5mL	76	0.42	0.40	0.60	0.4608s
Sugammadex Injection	61	0.49	0.46	0.69	0.4608s
Dynastat Powder	**1**	**1.0**	**0.99**	**1.00**	**0.4608s**
Hydrocortisone sodium	52	0.61	0.61	0.71	0.4608s
Atracurium Besylate	61	0.5	0.48	0.69	0.4608s
Atropine	74	0.36	0.35	0.61	0.4608s
PancuroInresa	81	0.45	0.37	0.66	0.4608s

Drug Identification: Protamine Sulphate against other samples

Drug Name	Edit Distance	TSR Scores	Lev Scores	Jacc Scores	Processing Time
Primacor Injection	71	0.55	0.41	0.67	0.5138s
Cefazolin Sodium 1g	99	0.48	0.43	0.59	0.5138s
NALOXONE HCl 400mg in 1mL	70	0.4	0.25	0.47	0.5138s
Calcium Chloride 1g in 10mL	99	0.45	0.35	0.62	0.5138s
Actrapid Penfill 3ml	67	0.51	0.36	0.66	0.5138s
Vecuronium bromide	56	0.51	0.42	0.60	0.5138s
Sugammadex 200mg/2ml	55	0.55	0.52	0.76	0.5138s
Amiodarone Hydrochloride	58	0.48	0.50	0.60	0.5138s
Protamine Sulphate 50mg in 5ml	65	0.77	0.48	0.72	0.5138s
Summethonium Chloride 100mg in 2mL	63	0.55	0.41	0.72	0.5138s
Protamine Sulphate 10mg/ml	**1**	**1.0**	**0.99**	**1.00**	**0.5138s**
Glyceryl Trinitrate 1 mg/ml	78	0.47	0.40	0.75	0.5138s
Tranexamic acid	68	0.63	0.42	0.77	0.5138s
Heparin Injection 25000IU in 5 mL	71	0.57	0.36	0.61	0.5138s
Sterile Potassium Chloride	96	0.55	0.41	0.67	0.5138s
Metaraminol 10mg/ml	45	0.66	0.58	0.77	0.5138s
Cyclizine lactate	74	0.27	0.21	0.45	0.5138s
PITRESSIN argipressin	60	0.48	0.39	0.63	0.5138s
Dexamethasone phosphate 4 mg/ml	51	0.62	0.55	0.72	0.5138s
Ephedrine Hydrochloride	67	0.32	0.30	0.48	0.5138s
Ondansetron Solution	65	0.49	0.47	0.66	0.5138s
FRUSEMIDE	67	0.44	0.32	0.57	0.5138s
DALACINC PHOSPHATE	69	0.37	0.30	0.58	0.5138s
METOPROLOL Mylan	61	0.51	0.50	0.74	0.5138s
WATER FOR INJECTIONS BP	75	0.54	0.36	0.68	0.5138s
MORPHINE SULFATE	61	0.57	0.42	0.71	0.5138s
Glycopyrronium and Neostigmine	64	0.62	0.57	0.76	0.5138s
Clonidine HCl	66	0.41	0.31	0.61	0.5138s
Rocuronium Bromide 50 mg in 5 ml	72	0.5	0.36	0.63	0.5138s
Fresofol 1% MCT/LCT	316	0.33	0.26	0.64	0.5138s
Sedative Midazolam 5mg	65	0.47	0.28	0.73	0.5138s
Adrenaline Injection	70	0.38	0.36	0.54	0.5138s
Paracetamol Kabi	515	0.4	0.20	0.58	0.5138s
Provive MCT-LCT 1%	256	0.32	0.29	0.56	0.5138s
Adrenaline Injection 1mg in 10mL	70	0.38	0.36	0.54	0.5138s
Amoxicillin Sodium	121	0.44	0.35	0.58	0.5138s
Lidocain Injection	65	0.35	0.32	0.52	0.5138s
SODIUM CHLORIDE	111	0.4	0.33	0.62	0.5138s
Remifentanil-Act Injection	73	0.48	0.44	0.59	0.5138s
Sterile Dopamine	67	0.54	0.37	0.59	0.5138s
Hypnomida Etomidate 2mg	64	0.48	0.38	0.58	0.5138s
Xylocaine 1%	63	0.43	0.36	0.55	0.5138s
Fentanyl Injection	118	0.49	0.35	0.66	0.5138s
Noradrenaline acid	67	0.42	0.37	0.62	0.5138s
Magnesium Sulfate 2.47g in 5mL	70	0.52	0.36	0.56	0.5138s
Sugammadex Injection	63	0.56	0.45	0.75	0.5138s
Dynastat Powder	76	0.47	0.41	0.68	0.5138s
Hydrocortisone sodium	84	0.46	0.39	0.66	0.5138s
Atracurium Besylate	63	0.37	0.33	0.57	0.5138s
Atropine	66	0.4	0.34	0.67	0.5138s
PancuroInresa	78	0.47	0.39	0.71	0.5138s

Drug Identification: Fresofol against other samples

Drug Name	Edit Distance	TSR Scores	Lev Scores	Jacc Scores	Processing Time
Primacor Injection	313	0.54	0.27	0.62	0.5225s
Cefazolin Sodium 1g	264	0.74	0.44	0.60	0.5225s
NALOXONE HCl 400mg in 1mL	350	0.16	0.12	0.39	0.5225s
Calcium Chloride 1g in 10mL	291	0.51	0.35	0.62	0.5225s
Actrapid Penfill 3ml	330	0.32	0.21	0.65	0.5225s
Vecuronium bromide	336	0.36	0.19	0.53	0.5225s
Sugammadex 200mg/2ml	322	0.54	0.24	0.60	0.5225s
Amiodarone Hydrochloride	317	0.4	0.27	0.56	0.5225s
Protamine Sulphate 50mg in 5ml	313	0.44	0.28	0.70	0.5225s
Summethonium Chloride 100mg in 2mL	334	0.41	0.19	0.57	0.5225s
Protamine Sulfate 10mg/ml	318	0.33	0.26	0.62	0.5225s
Glyceryl Trinitrate 1 mg/ml	317	0.31	0.26	0.55	0.5225s
Tranexamic acid	324	0.43	0.24	0.57	0.5225s
Heparin Injection 25000IU in 5 mL	323	0.36	0.24	0.65	0.5225s
Sterile Potassium Chloride	304	0.32	0.30	0.62	0.5225s
Metaraminol 10mg/ml	329	0.43	0.22	0.51	0.5225s
Cyclizine lactate	358	0.13	0.09	0.41	0.5225s
PITRESSIN argipressin	335	0.23	0.19	0.46	0.5225s
Dexamethasone phosphate 4 mg/ml	326	0.58	0.22	0.57	0.5225s
Ephedrine Hydrochloride	333	0.31	0.20	0.44	0.5225s
Ondansetron Solution	320	0.32	0.24	0.61	0.5225s
FRUSEMIDE	330	0.27	0.21	0.46	0.5225s
DALACINC PHOSPHATE	336	0.26	0.19	0.55	0.5225s
METOPROLOL Mylan	300	0.58	0.32	0.54	0.5225s
WATER FOR INJECTIONS BP	309	0.45	0.29	0.63	0.5225s
MORPHINE SULFATE	337	0.41	0.18	0.53	0.5225s
Glycopyrronium and Neostigmine	315	0.38	0.26	0.60	0.5225s
Clonidine HCl	347	0.44	0.14	0.49	0.5225s
Rocuronium Bromide 50 mg in 5 ml	317	0.52	0.26	0.42	0.5225s
Fresofol 1% MCT/LCT	**2**	**1.0**	**1.00**	**0.97**	**0.5225s**
Sedative Midazolam 5mg	337	0.21	0.18	0.55	0.5225s
Adrenaline Injection	321	0.49	0.24	0.37	0.5225s
Paracetamol Kabi	433	0.59	0.41	0.76	0.5225s
Provive MCT-LCT 1%	272	0.64	0.47	0.72	0.5225s
Adrenaline Injection 1mg in 10mL	321	0.49	0.24	0.37	0.5225s
Amoxicillin Sodium	282	0.45	0.37	0.71	0.5225s
Lidocain Injection	348	0.16	0.13	0.42	0.5225s
SODIUM CHLORIDE	304	0.37	0.29	0.78	0.5225s
Remifentanil-Act Injection	313	0.34	0.28	0.60	0.5225s
Sterile Dopamine	340	0.23	0.17	0.47	0.5225s
Hypnomida Etomidate 2mg	326	0.45	0.22	0.59	0.5225s
Xylocaine 1%	346	0.16	0.15	0.45	0.5225s
Fentanyl Injection	296	0.42	0.32	0.61	0.5225s
Noradrenaline acid	325	0.31	0.23	0.43	0.5225s
Magnesium Sulfate 2.47g in 5mL	322	0.45	0.23	0.57	0.5225s
Sugammadex Injection	321	0.69	0.25	0.55	0.5225s
Dynastat Powder	304	0.54	0.31	0.59	0.5225s
Hydrocortisone sodium	298	0.47	0.33	0.61	0.5225s
Atracurium Besylate	326	0.64	0.23	0.42	0.5225s
Atropine	347	0.46	0.14	0.49	0.5225s
PancuroInresa	311	0.34	0.27	0.57	0.5225s

Drug Identification: Tranexamic Acid against other samples

Drug Name	Edit Distance	TSR Scores	Lev Scores	Jacc Scores	Processing Time
Primacor Injection	74	0.49	0.37	0.70	0.4742s
Cefazolin Sodium 1g	114	0.45	0.30	0.62	0.4742s
NALOXONE HCl 400mg in 1mL	63	0.37	0.25	0.55	0.4742s
Calcium Chloride 1g in 10mL	104	0.44	0.33	0.65	0.4742s
Actrapid Penfill 3ml	66	0.45	0.34	0.69	0.4742s
Vecuronium bromide	61	0.41	0.28	0.58	0.4742s
Sugammadex 200mg/2ml	68	0.46	0.31	0.68	0.4742s
Amiodarone Hydrochloride	71	0.48	0.32	0.58	0.4742s
Protamine Sulphate 50mg in 5ml	81	0.45	0.33	0.60	0.4742s
Summethonium Chloride 100mg in 2mL	61	0.48	0.32	0.70	0.4742s
Protamine Sulfate 10mg/ml	69	0.63	0.41	0.77	0.4742s
Glyceryl Trinitrate 1 mg/ml	85	0.46	0.29	0.72	0.4742s
Tranexamic acid	**1**	**1.0**	**0.99**	**1.00**	**0.4742s**
Heparin Injection 25000IU in 5 mL	69	0.44	0.34	0.59	0.4742s
Sterile Potassium Chloride	95	0.46	0.32	0.65	0.4742s
Metaraminol 10mg/ml	61	0.53	0.36	0.62	0.4742s
Cyclizine lactate	63	0.3	0.27	0.43	0.4742s
PITRESSIN argipressin	61	0.36	0.32	0.50	0.4742s
Dexamethasone phosphate 4 mg/ml	65	0.55	0.38	0.76	0.4742s
Ephedrine Hydrochloride	63	0.31	0.31	0.52	0.4742s
Ondansetron Solution	62	0.54	0.47	0.74	0.4742s
FRUSEMIDE	53	0.41	0.44	0.66	0.4742s
DALACINC PHOSPHATE	64	0.41	0.30	0.61	0.4742s
METOPROLOL Mylan	73	0.44	0.31	0.55	0.4742s
WATER FOR INJECTIONS BP	80	0.5	0.37	0.66	0.4742s
MORPHINE SULFATE	59	0.39	0.36	0.75	0.4742s
Glycopyrronium and Neostigmine	74	0.5	0.29	0.62	0.4742s
Clonidine HCl	62	0.34	0.28	0.53	0.4742s
Rocuronium Bromide 50 mg in 5 ml	69	0.38	0.31	0.50	0.4742s
Fresofol 1% MCT/LCT	322	0.43	0.24	0.59	0.4742s
Sedative Midazolam 5mg	62	0.45	0.31	0.71	0.4742s
Adrenaline Injection	65	0.43	0.36	0.52	0.4742s
Paracetamol Kabi	524	0.41	0.17	0.64	0.4742s
Provive MCT-LCT 1%	263	0.32	0.26	0.59	0.4742s
Adrenaline Injection 1mg in 10mL	65	0.43	0.36	0.52	0.4742s
Amoxicillin Sodium	121	0.37	0.32	0.57	0.4742s
Lidocain Injection	60	0.34	0.29	0.55	0.4742s
SODIUM CHLORIDE	114	0.41	0.29	0.61	0.4742s
Remifentanil-Act Injection	80	0.46	0.37	0.58	0.4742s
Sterile Dopamine	59	0.39	0.30	0.57	0.4742s
Hypnomida Etomidate 2mg	70	0.47	0.32	0.56	0.4742s
Xylocaine 1%	62	0.38	0.31	0.44	0.4742s
Fentanyl Injection	117	0.45	0.30	0.59	0.4742s
Noradrenaline acid	69	0.44	0.37	0.60	0.4742s
Magnesium Sulfate 2.47g in 5mL	74	0.41	0.31	0.54	0.4742s
Sugammadex Injection	64	0.46	0.34	0.67	0.4742s
Dynastat Powder	77	0.42	0.38	0.66	0.4742s
Hydrocortisone sodium	83	0.36	0.32	0.64	0.4742s
Atracurium Besylate	58	0.41	0.37	0.61	0.4742s
Atropine	63	0.39	0.30	0.53	0.4742s
PancuroInresa	75	0.4	0.35	0.64	0.4742s

Drug Identification: Paracetamol Kabi against other samples

Drug Name	Edit Distance	TSR Scores	Lev Scores	Jacc Scores	Processing Time
Primacor Injection	508	0.41	0.21	0.69	0.5709s
Cefazolin Sodium 1g	454	0.67	0.34	0.67	0.5709s
NALOXONE HCl 400mg in 1mL	547	0.12	0.09	0.43	0.5709s
Calcium Chloride 1g in 10mL	487	0.29	0.25	0.61	0.5709s
Actrapid Penfill 3ml	525	0.2	0.16	0.60	0.5709s
Vecuronium bromide	529	0.36	0.15	0.52	0.5709s
Sugammadex 200mg/2ml	515	0.22	0.18	0.56	0.5709s
Amiodarone Hydrochloride	514	0.48	0.19	0.52	0.5709s
Protamine Sulphate 50mg in 5ml	508	0.2	0.20	0.58	0.5709s
Summethonium Chloride 100mg in 2mL	531	0.33	0.14	0.57	0.5709s
Protamine Sulfate 10mg/ml	509	0.4	0.20	0.58	0.5709s
Glyceryl Trinitrate 1 mg/ml	504	0.3	0.21	0.55	0.5709s
Tranexamic acid	522	0.41	0.16	0.64	0.5709s
Heparin Injection 25000IU in 5 mL	517	0.22	0.18	0.57	0.5709s
Sterile Potassium Chloride	496	0.25	0.23	0.58	0.5709s
Metaraminol 10mg/ml	523	0.53	0.16	0.48	0.5709s
Cyclizine lactate	557	0.08	0.06	0.38	0.5709s
PITRESSIN argipressin	527	0.19	0.15	0.43	0.5709s
Dexamethasone phosphate 4 mg/ml	523	0.47	0.16	0.57	0.5709s
Ephedrine Hydrochloride	533	0.15	0.13	0.40	0.5709s
Ondansetron Solution	511	0.36	0.20	0.60	0.5709s
FRUSEMIDE	526	0.19	0.15	0.50	0.5709s
DALACINC PHOSPHATE	534	0.16	0.13	0.55	0.5709s
METOPROLOL Mylan	499	0.54	0.23	0.47	0.5709s
WATER FOR INJECTIONS BP	509	0.45	0.20	0.70	0.5709s
MORPHINE SULFATE	536	0.2	0.13	0.52	0.5709s
Glycopyrronium and Neostigmine	517	0.37	0.18	0.56	0.5709s
Clonidine HCl	547	0.11	0.09	0.42	0.5709s
Rocuronium Bromide 50 mg in 5 ml	517	0.18	0.18	0.40	0.5709s
Fresofol 1% MCT/LCT	400	0.59	0.43	0.78	0.5709s
Sedative Midazolam 5mg	533	0.16	0.13	0.58	0.5709s
Adrenaline Injection	510	0.17	0.20	0.40	0.5709s
Paracetamol Kabi	**205**	**1.0**	**0.82**	**1.00**	**0.5709s**
Provive MCT-LCT 1%	431	0.56	0.40	0.79	0.5709s
Adrenaline Injection 1mg in 10mL	510	0.17	0.20	0.40	0.5709s
Amoxicillin Sodium	474	0.33	0.29	0.70	0.5709s
Lidocain Injection	545	0.11	0.10	0.43	0.5709s
SODIUM CHLORIDE	484	0.34	0.26	0.73	0.5709s
Remifentanil-Act Injection	497	0.24	0.23	0.56	0.5709s
Sterile Dopamine	540	0.15	0.11	0.44	0.5709s
Hypnomida Etomidate 2mg	512	0.47	0.19	0.58	0.5709s
Xylocaine 1%	545	0.11	0.10	0.39	0.5709s
Fentanyl Injection	480	0.3	0.27	0.64	0.5709s
Noradrenaline acid	508	0.24	0.20	0.47	0.5709s
Magnesium Sulfate 2.47g in 5mL	516	0.2	0.18	0.60	0.5709s
Sugammadex Injection	513	0.29	0.19	0.55	0.5709s
Dynastat Powder	492	0.41	0.25	0.58	0.5709s
Hydrocortisone sodium	491	0.35	0.25	0.64	0.5709s
Atracurium Besylate	521	0.64	0.17	0.43	0.5709s
Atropine	547	0.18	0.09	0.45	0.5709s
PancuroInresa	502	0.25	0.22	0.64	0.5709s

Drug Identification: MORPHINE SULPHATE against other samples

Drug Name	Edit Distance	TSR Scores	Lev Scores	Jacc Scores	Processing Time
Primacor Injection	72	0.44	0.38	0.65	0.5101s
Cefazolin Sodium 1g	113	0.44	0.35	0.67	0.5101s
NALOXONE HCl 400mg in 1mL	33	0.53	0.41	0.54	0.5101s
Calcium Chloride 1g in 10mL	100	0.49	0.34	0.76	0.5101s
Actrapid Penfill 3ml	52	0.53	0.32	0.69	0.5101s
Vecuronium bromide	46	0.4	0.35	0.69	0.5101s
Sugammadex 200mg/2ml	61	0.48	0.35	0.68	0.5101s
Amiodarone Hydrochloride	59	0.44	0.42	0.69	0.5101s
Protamine Sulphate 50mg in 5ml	67	0.64	0.46	0.70	0.5101s
Summethonium Chloride 100mg in 2mL	44	0.48	0.41	0.84	0.5101s
Protamine Sulfate 10mg/ml	59	0.57	0.43	0.71	0.5101s
Glyceryl Trinitrate 1 mg/ml	81	0.47	0.32	0.73	0.5101s
Tranexamic acid	58	0.39	0.36	0.75	0.5101s
Heparin Injection 25000IU in 5 mL	62	0.57	0.38	0.63	0.5101s
Sterile Potassium Chloride	93	0.39	0.35	0.70	0.5101s
Metaraminol 10mg/ml	38	0.56	0.46	0.75	0.5101s
Cyclizine lactate	39	0.3	0.26	0.46	0.5101s
PITRESSIN argipressin	39	0.57	0.47	0.67	0.5101s
Dexamethasone phosphate 4 mg/ml	45	0.61	0.51	0.77	0.5101s
Ephedrine Hydrochloride	42	0.46	0.42	0.70	0.5101s
Ondansetron Solution	64	0.37	0.35	0.63	0.5101s
FRUSEMIDE	51	0.4	0.32	0.72	0.5101s
DALACINC PHOSPHATE	46	0.4	0.40	0.60	0.5101s
METOPROLOL Mylan	70	0.5	0.36	0.65	0.5101s
WATER FOR INJECTIONS BP	78	0.51	0.36	0.66	0.5101s
MORPHINE SULFATE	**1**	**1.0**	**0.99**	**1.00**	**0.5101s**
Glycopyrronium and Neostigmine	61	0.48	0.41	0.74	0.5101s
Clonidine HCl	28	0.56	0.51	0.64	0.5101s
Rocuronium Bromide 50 mg in 5 ml	51	0.57	0.44	0.67	0.5101s
Fresofol 1% MCT/LCT	335	0.41	0.18	0.54	0.5101s
Sedative Midazolam 5mg	50	0.37	0.32	0.55	0.5101s
Adrenaline Injection	56	0.49	0.38	0.62	0.5101s
Paracetamol Kabi	537	0.2	0.14	0.52	0.5101s
Provive MCT-LCT 1%	271	0.49	0.23	0.63	0.5101s
Adrenaline Injection 1mg in 10mL	56	0.49	0.38	0.62	0.5101s
Amoxicillin Sodium	128	0.37	0.28	0.61	0.5101s
Lidocain Injection	34	0.41	0.37	0.74	0.5101s
SODIUM CHLORIDE	112	0.36	0.34	0.65	0.5101s
Remifentanil-Act Injection	78	0.42	0.33	0.68	0.5101s
Sterile Dopamine	39	0.39	0.37	0.56	0.5101s
Hypnomida Etomidate 2mg	60	0.46	0.39	0.71	0.5101s
Xylocaine 1%	36	0.52	0.44	0.46	0.5101s
Fentanyl Injection	118	0.41	0.32	0.59	0.5101s
Noradrenaline acid	61	0.36	0.37	0.65	0.5101s
Magnesium Sulfate 2.47g in 5mL	58	0.61	0.47	0.53	0.5101s
Sugammadex Injection	54	0.51	0.39	0.73	0.5101s
Dynastat Powder	70	0.45	0.43	0.71	0.5101s
Hydrocortisone sodium	76	0.45	0.44	0.75	0.5101s
Atracurium Besylate	43	0.4	0.33	0.74	0.5101s
Atropine	30	0.45	0.49	0.64	0.5101s
PancuroInresa	77	0.39	0.36	0.69	0.5101s

Drug Identification: Sugammadex against other samples

Drug Name	Edit Distance	TSR Scores	Lev Scores	Jacc Scores	Processing Time
Primacor Injection	79	0.55	0.34	0.59	0.3499s
Cefazolin Sodium 1g	110	0.51	0.37	0.56	0.3499s
NALOXONE HCl 400mg in 1mL	65	0.4	0.27	0.48	0.3499s
Calcium Chloride 1g in 10mL	103	0.53	0.35	0.59	0.3499s
Actrapid Penfill 3ml	65	0.54	0.40	0.73	0.3499s
Vecuronium bromide	52	0.46	0.45	0.62	0.3499s
Sugammadex 200mg/2ml	**1**	**1.0**	**0.99**	**1.00**	**0.3499s**
Amiodarone Hydrochloride	57	0.52	0.51	0.68	0.3499s
Protamine Sulphate 50mg in 5ml	74	0.57	0.39	0.64	0.3499s
Summethonium Chloride 100mg in 2mL	60	0.52	0.43	0.75	0.3499s
Protamine Sulfate 10mg/ml	53	0.55	0.53	0.76	0.3499s
Glyceryl Trinitrate 1 mg/ml	83	0.4	0.38	0.71	0.3499s
Tranexamic acid	67	0.46	0.33	0.68	0.3499s
Heparin Injection 25000IU in 5 mL	69	0.54	0.39	0.68	0.3499s
Sterile Potassium Chloride	91	0.49	0.34	0.64	0.3499s
Metaraminol 10mg/ml	46	0.58	0.57	0.73	0.3499s
Cyclizine lactate	70	0.25	0.18	0.37	0.3499s
PITRESSIN argipressin	58	0.52	0.40	0.65	0.3499s
Dexamethasone phosphate 4 mg/ml	43	0.53	0.55	0.63	0.3499s
Ephedrine Hydrochloride	62	0.4	0.31	0.50	0.3499s
Ondansetron Solution	69	0.47	0.38	0.73	0.3499s
FRUSEMIDE	65	0.4	0.32	0.53	0.3499s
DALACINC PHOSPHATE	69	0.37	0.32	0.55	0.3499s
METOPROLOL Mylan	54	0.51	0.53	0.64	0.3499s
WATER FOR INJECTIONS BP	76	0.46	0.36	0.60	0.3499s
MORPHINE SULFATE	61	0.48	0.35	0.68	0.3499s
Glycopyrronium and Neostigmine	65	0.55	0.52	0.79	0.3499s
Clonidine HCl	60	0.46	0.36	0.57	0.3499s
Rocuronium Bromide 50 mg in 5 ml	70	0.53	0.37	0.65	0.3499s
Fresofol 1% MCT/LCT	319	0.54	0.25	0.62	0.3499s
Sedative Midazolam 5mg	63	0.41	0.32	0.65	0.3499s
Adrenaline Injection	69	0.44	0.37	0.62	0.3499s
Paracetamol Kabi	515	0.22	0.20	0.56	0.3499s
Provive MCT-LCT 1%	256	0.46	0.28	0.58	0.3499s
Adrenaline Injection 1mg in 10mL	69	0.44	0.37	0.62	0.3499s
Amoxicillin Sodium	119	0.47	0.41	0.60	0.3499s
Lidocain Injection	61	0.37	0.34	0.54	0.3499s
SODIUM CHLORIDE	111	0.42	0.33	0.55	0.3499s
Remifentanil-Act Injection	80	0.49	0.40	0.67	0.3499s
Sterile Dopamine	64	0.41	0.32	0.61	0.3499s
Hypnomida Etomidate 2mg	65	0.49	0.36	0.59	0.3499s
Xylocaine 1%	61	0.36	0.35	0.47	0.3499s
Fentanyl Injection	121	0.47	0.31	0.68	0.3499s
Noradrenaline acid	70	0.38	0.35	0.59	0.3499s
Magnesium Sulfate 2.47g in 5mL	76	0.52	0.38	0.62	0.3499s
Sugammadex Injection	46	0.87	0.68	0.92	0.3499s
Dynastat Powder	72	0.51	0.42	0.70	0.3499s
Hydrocortisone sodium	76	0.54	0.39	0.62	0.3499s
Atracurium Besylate	65	0.35	0.33	0.59	0.3499s
Atropine	63	0.43	0.31	0.63	0.3499s
PancuroInresa	77	0.45	0.35	0.68	0.3499s

Drug Identification: Ephedrine Hydrochloride against other samples

Drug Name	Edit Distance	TSR Scores	Lev Scores	Jacc Scores	Processing Time
Primacor Injection	77	0.39	0.29	0.48	0.3773s
Cefazolin Sodium 1g	114	0.42	0.31	0.55	0.3773s
NALOXONE HCl 400mg in 1mL	40	0.33	0.30	0.46	0.3773s
Calcium Chloride 1g in 10mL	103	0.36	0.32	0.53	0.3773s
Actrapid Penfill 3ml	52	0.42	0.40	0.52	0.3773s
Vecuronium bromide	44	0.39	0.40	0.70	0.3773s
Sugammadex 200mg/2ml	60	0.4	0.33	0.50	0.3773s
Amiodarone Hydrochloride	59	0.64	0.44	0.70	0.3773s
Protamine Sulphate 50mg in 5ml	73	0.42	0.39	0.48	0.3773s
Summethonium Chloride 100mg in 2mL	50	0.37	0.34	0.64	0.3773s
Protamine Sulfate 10mg/ml	65	0.32	0.32	0.48	0.3773s
Glyceryl Trinitrate 1 mg/ml	82	0.31	0.30	0.54	0.3773s
Tranexamic acid	61	0.31	0.31	0.52	0.3773s
Heparin Injection 25000IU in 5 mL	66	0.44	0.29	0.57	0.3773s
Sterile Potassium Chloride	96	0.32	0.34	0.48	0.3773s
Metaraminol 10mg/ml	46	0.47	0.39	0.54	0.3773s
Cyclizine lactate	43	0.23	0.23	0.50	0.3773s
PITRESSIN argipressin	43	0.37	0.40	0.59	0.3773s
Dexamethasone phosphate 4 mg/ml	52	0.44	0.38	0.64	0.3773s
Ephedrine Hydrochloride	**1**	**1.0**	**0.99**	**1.00**	**0.3773s**
Ondansetron Solution	64	0.35	0.37	0.57	0.3773s
FRUSEMIDE	51	0.33	0.27	0.52	0.3773s
DALACINC PHOSPHATE	51	0.33	0.29	0.48	0.3773s
METOPROLOL Mylan	71	0.43	0.37	0.65	0.3773s
WATER FOR INJECTIONS BP	75	0.31	0.34	0.45	0.3773s
MORPHINE SULFATE	43	0.46	0.44	0.70	0.3773s
Glycopyrronium and Neostigmine	61	0.43	0.40	0.56	0.3773s
Clonidine HCl	38	0.52	0.51	0.57	0.3773s
Rocuronium Bromide 50 mg in 5 ml	61	0.46	0.36	0.59	0.3773s
Fresofol 1% MCT/LCT	331	0.31	0.20	0.45	0.3773s
Sedative Midazolam 5mg	53	0.28	0.25	0.34	0.3773s
Adrenaline Injection	58	0.48	0.35	0.62	0.3773s
Paracetamol Kabi	539	0.15	0.13	0.40	0.3773s
Provive MCT-LCT 1%	275	0.31	0.20	0.49	0.3773s
Adrenaline Injection 1mg in 10mL	58	0.48	0.35	0.62	0.3773s
Amoxicillin Sodium	124	0.35	0.31	0.50	0.3773s
Lidocain Injection	40	0.35	0.38	0.67	0.3773s
SODIUM CHLORIDE	118	0.31	0.29	0.50	0.3773s
Remifentanil-Act Injection	67	0.58	0.45	0.68	0.3773s
Sterile Dopamine	43	0.36	0.33	0.48	0.3773s
Hypnomida Etomidate 2mg	65	0.35	0.28	0.59	0.3773s
Xylocaine 1%	35	0.4	0.42	0.50	0.3773s
Fentanyl Injection	114	0.58	0.35	0.44	0.3773s
Noradrenaline acid	65	0.38	0.35	0.58	0.3773s
Magnesium Sulfate 2.47g in 5mL	74	0.46	0.29	0.42	0.3773s
Sugammadex Injection	57	0.4	0.30	0.54	0.3773s
Dynastat Powder	73	0.44	0.36	0.59	0.3773s
Hydrocortisone sodium	77	0.43	0.39	0.63	0.3773s
Atracurium Besylate	45	0.4	0.38	0.75	0.3773s
Atropine	38	0.43	0.38	0.57	0.3773s
PancuroInresa	79	0.29	0.31	0.47	0.3773s

Drug Identification: Protamine Sulphate against other samples

Drug Name	Edit Distance	TSR Scores	Lev Scores	Jacc Scores	Processing Time
Primacor Injection	75	0.52	0.45	0.71	0.4336s
Cefazolin Sodium 1g	110	0.46	0.39	0.58	0.4336s
NALOXONE HCl 400mg in 1mL	81	0.4	0.29	0.47	0.4336s
Calcium Chloride 1g in 10mL	96	0.51	0.40	0.71	0.4336s
Actrapid Penfill 3ml	73	0.52	0.38	0.65	0.4336s
Vecuronium bromide	68	0.47	0.42	0.65	0.4336s
Sugammadex 200mg/2ml	74	0.57	0.39	0.64	0.4336s
Amiodarone Hydrochloride	71	0.48	0.42	0.55	0.4336s
Protamine Sulphate 50mg in 5ml	**1**	**1.0**	**0.99**	**1.00**	**0.4336s**
Summethonium Chloride 100mg in 2mL	75	0.52	0.35	0.71	0.4336s
Protamine Sulfate 10mg/ml	65	0.77	0.49	0.72	0.4336s
Glyceryl Trinitrate 1 mg/ml	82	0.41	0.36	0.62	0.4336s
Tranexamic acid	82	0.45	0.34	0.60	0.4336s
Heparin Injection 25000IU in 5 mL	74	0.54	0.46	0.70	0.4336s
Sterile Potassium Chloride	94	0.49	0.39	0.81	0.4336s
Metaraminol 10mg/ml	71	0.64	0.41	0.63	0.4336s
Cyclizine lactate	87	0.24	0.18	0.36	0.4336s
PITRESSIN argipressin	70	0.48	0.43	0.57	0.4336s
Dexamethasone phosphate 4 mg/ml	60	0.59	0.52	0.61	0.4336s
Ephedrine Hydrochloride	75	0.42	0.38	0.48	0.4336s
Ondansetron Solution	78	0.46	0.37	0.60	0.4336s
FRUSEMIDE	78	0.39	0.29	0.56	0.4336s
DALACINC PHOSPHATE	78	0.37	0.34	0.53	0.4336s
METOPROLOL Mylan	78	0.51	0.41	0.61	0.4336s
WATER FOR INJECTIONS BP	75	0.54	0.42	0.67	0.4336s
MORPHINE SULFATE	68	0.64	0.46	0.70	0.4336s
Glycopyrronium and Neostigmine	76	0.53	0.42	0.69	0.4336s
Clonidine HCl	76	0.52	0.35	0.55	0.4336s
Rocuronium Injection 50 mg in 5 ml	69	0.52	0.43	0.57	0.4336s
Fresofol 1% MCT/LCT	313	0.44	0.28	0.72	0.4336s
Sedative Midazolam 5mg	79	0.4	0.29	0.53	0.4336s
Adrenaline Injection	69	0.43	0.41	0.48	0.4336s
Paracetamol Kabi	516	0.2	0.19	0.58	0.4336s
Provive MCT-LCT 1%	248	0.36	0.33	0.68	0.4336s
Adrenaline Injection 1mg in 10mL	69	0.43	0.41	0.48	0.4336s
Amoxicillin Sodium	118	0.42	0.40	0.71	0.4336s
Lidocain Injection	79	0.4	0.29	0.52	0.4336s
SODIUM CHLORIDE	109	0.39	0.35	0.70	0.4336s
Remifentanil-Act Injection	86	0.51	0.38	0.69	0.4336s
Sterile Dopamine	76	0.49	0.35	0.48	0.4336s
Hypnomida Etomidate 2mg	81	0.49	0.38	0.62	0.4336s
Xylocaine 1%	75	0.48	0.36	0.45	0.4336s
Fentanyl Injection	114	0.48	0.39	0.69	0.4336s
Noradrenaline acid	78	0.38	0.35	0.52	0.4336s
Magnesium Sulfate 2.47g in 5mL	76	0.54	0.47	0.59	0.4336s
Sugammadex Injection	80	0.55	0.38	0.62	0.4336s
Dynastat Powder	82	0.47	0.42	0.67	0.4336s
Hydrocortisone sodium	88	0.48	0.41	0.70	0.4336s
Atracurium Besylate	78	0.32	0.33	0.52	0.4336s
Atropine	77	0.43	0.34	0.60	0.4336s
PancuroInresa	75	0.45	0.44	0.70	0.4336s

Drug Identification: Atracurium Besylate against other samples

Drug Name	Edit Distance	TSR Scores	Lev Scores	Jacc Scores	Processing Time
Primacor Injection	72	0.33	0.36	0.47	0.5260s
Cefazolin Sodium 1g	108	0.55	0.42	0.53	0.5260s
NALOXONE HCl 400mg in 1mL	46	0.35	0.25	0.50	0.5260s
Calcium Chloride 1g in 10mL	101	0.36	0.32	0.57	0.5260s
Actrapid Penfill 3ml	52	0.34	0.34	0.55	0.5260s
Vecuronium bromide	47	0.46	0.32	0.74	0.5260s
Sugammadex 200mg/2ml	66	0.35	0.33	0.59	0.5260s
Amiodarone Hydrochloride	65	0.39	0.33	0.67	0.5260s
Protamine Sulphate 50mg in 5ml	78	0.32	0.34	0.52	0.5260s
Summethonium Chloride 100mg in 2mL	49	0.35	0.31	0.62	0.5260s
Protamine Sulfate 10mg/ml	62	0.37	0.33	0.57	0.5260s
Glyceryl Trinitrate 1 mg/ml	82	0.36	0.33	0.64	0.5260s
Tranexamic acid	58	0.41	0.37	0.61	0.5260s
Heparin Injection 25000IU in 5 mL	60	0.34	0.38	0.55	0.5260s
Sterile Potassium Chloride	92	0.38	0.33	0.57	0.5260s
Metaraminol 10mg/ml	50	0.37	0.33	0.58	0.5260s
Cyclizine lactate	50	0.24	0.21	0.55	0.5260s
PITRESSIN argipressin	43	0.43	0.41	0.64	0.5260s
Dexamethasone phosphate 4 mg/ml	57	0.37	0.29	0.62	0.5260s
Ephedrine Hydrochloride	46	0.4	0.38	0.75	0.5260s
Ondansetron Solution	66	0.35	0.36	0.67	0.5260s
FRUSEMIDE	46	0.44	0.41	0.56	0.5260s
DALACINC PHOSPHATE	50	0.35	0.31	0.52	0.5260s
METOPROLOL Mylan	62	0.47	0.46	0.70	0.5260s
WATER FOR INJECTIONS BP	79	0.33	0.33	0.53	0.5260s
MORPHINE SULFATE	44	0.4	0.33	0.74	0.5260s
Glycopyrronium and Neostigmine	65	0.39	0.34	0.65	0.5260s
Clonidine HCl	44	0.37	0.32	0.48	0.5260s
Rocuronium Bromide 50 mg in 5 ml	63	0.42	0.39	0.64	0.5260s
Fresofol 1% MCT/LCT	324	0.64	0.23	0.44	0.5260s
Sedative Midazolam 5mg	51	0.28	0.33	0.47	0.5260s
Adrenaline Injection	55	0.43	0.40	0.67	0.5260s
Paracetamol Kabi	528	0.64	0.16	0.43	0.5260s
Provive MCT-LCT 1%	266	0.55	0.26	0.51	0.5260s
Adrenaline Injection 1mg in 10mL	55	0.43	0.40	0.67	0.5260s
Amoxicillin Sodium	114	0.55	0.40	0.48	0.5260s
Lidocain Injection	45	0.34	0.31	0.57	0.5260s
SODIUM CHLORIDE	118	0.34	0.29	0.53	0.5260s
Remifentanil-Act Injection	77	0.39	0.36	0.65	0.5260s
Sterile Dopamine	44	0.36	0.35	0.58	0.5260s
Hypnomida Etomidate 2mg	65	0.33	0.29	0.57	0.5260s
Xylocaine 1%	46	0.3	0.31	0.48	0.5260s
Fentanyl Injection	120	0.33	0.31	0.52	0.5260s
Noradrenaline acid	66	0.38	0.35	0.77	0.5260s
Magnesium Sulfate 2.47g in 5mL	66	0.37	0.37	0.50	0.5260s
Sugammadex Injection	54	0.37	0.39	0.64	0.5260s
Dynastat Powder	61	0.5	0.48	0.69	0.5260s
Hydrocortisone sodium	72	0.47	0.44	0.61	0.5260s
Atracurium Besylate	**1**	**1.0**	**0.99**	**1.00**	**0.5260s**
Atropine	46	0.38	0.26	0.54	0.5260s
PancuroInresa	73	0.39	0.39	0.55	0.5260s

Drug Identification: DALACINC PHOSPHATE against other samples

Drug Name	Edit Distance	TSR Scores	Lev Scores	Jacc Scores	Processing Time
Primacor Injection	75	0.41	0.30	0.57	0.3699s
Cefazolin Sodium 1g	116	0.34	0.29	0.59	0.3699s
NALOXONE HCl 400mg in 1mL	46	0.36	0.31	0.47	0.3699s
Calcium Chloride 1g in 10mL	107	0.34	0.28	0.62	0.3699s
Actrapid Penfill 3ml	60	0.37	0.30	0.56	0.3699s
Vecuronium bromide	54	0.35	0.26	0.45	0.3699s
Sugammadex 200mg/2ml	68	0.37	0.33	0.55	0.3699s
Amiodarone Hydrochloride	66	0.37	0.31	0.60	0.3699s
Protamine Sulphate 50mg in 5ml	77	0.37	0.34	0.53	0.3699s
Summethonium Chloride 100mg in 2mL	53	0.44	0.33	0.56	0.3699s
Protamine Sulfate 10mg/ml	67	0.37	0.31	0.58	0.3699s
Glyceryl Trinitrate 1 mg/ml	85	0.39	0.27	0.58	0.3699s
Tranexamic acid	63	0.41	0.31	0.61	0.3699s
Heparin Injection 25000IU in 5 mL	62	0.44	0.34	0.61	0.3699s
Sterile Potassium Chloride	96	0.34	0.30	0.67	0.3699s
Metaraminol 10mg/ml	54	0.36	0.31	0.59	0.3699s
Cyclizine lactate	53	0.22	0.20	0.35	0.3699s
PITRESSIN argipressin	49	0.34	0.32	0.52	0.3699s
Dexamethasone phosphate 4 mg/ml	58	0.56	0.43	0.67	0.3699s
Ephedrine Hydrochloride	52	0.33	0.29	0.48	0.3699s
Ondansetron Solution	65	0.36	0.32	0.56	0.3699s
FRUSEMIDE	53	0.44	0.32	0.57	0.3699s
DALACINC PHOSPHATE	**1**	**1.0**	**0.99**	**1.00**	**0.3699s**
METOPROLOL Mylan	78	0.38	0.32	0.62	0.3699s
WATER FOR INJECTIONS BP	82	0.45	0.31	0.58	0.3699s
MORPHINE SULFATE	46	0.4	0.40	0.60	0.3699s
Glycopyrronium and Neostigmine	64	0.33	0.32	0.65	0.3699s
Clonidine HCl	48	0.31	0.33	0.55	0.3699s
Rocuronium Bromide 50 mg in 5 ml	62	0.39	0.33	0.52	0.3699s
Fresofol 1% MCT/LCT	334	0.26	0.19	0.56	0.3699s
Sedative Midazolam 5mg	52	0.41	0.35	0.58	0.3699s
Adrenaline Injection	57	0.38	0.36	0.39	0.3699s
Paracetamol Kabi	537	0.16	0.14	0.55	0.3699s
Provive MCT-LCT 1%	271	0.24	0.22	0.49	0.3699s
Adrenaline Injection 1mg in 10mL	57	0.38	0.36	0.39	0.3699s
Amoxicillin Sodium	129	0.34	0.26	0.50	0.3699s
Lidocain Injection	49	0.37	0.28	0.47	0.3699s
SODIUM CHLORIDE	119	0.32	0.26	0.58	0.3699s
Remifentanil-Act Injection	82	0.34	0.28	0.55	0.3699s
Sterile Dopamine	41	0.42	0.43	0.70	0.3699s
Hypnomida Etomidate 2mg	66	0.43	0.30	0.58	0.3699s
Xylocaine 1%	52	0.36	0.29	0.36	0.3699s
Fentanyl Injection	118	0.34	0.32	0.53	0.3699s
Noradrenaline acid	65	0.34	0.34	0.52	0.3699s
Magnesium Sulfate 2.47g in 5mL	69	0.37	0.30	0.60	0.3699s
Sugammadex Injection	59	0.42	0.32	0.58	0.3699s
Dynastat Powder	77	0.43	0.31	0.58	0.3699s
Hydrocortisone sodium	85	0.37	0.30	0.56	0.3699s
Atracurium Besylate	50	0.35	0.31	0.52	0.3699s
Atropine	45	0.4	0.40	0.61	0.3699s
PancuroInresa	79	0.36	0.32	0.56	0.3699s

Drug Identification: Dexamethasone phosphate against other samples

Drug Name	Edit Distance	TSR Scores	Lev Scores	Jacc Scores	Processing Time
Primacor Injection	73	0.55	0.33	0.66	0.4069s
Cefazolin Sodium 1g	105	0.48	0.39	0.68	0.4069s
NALOXONE HCl 400mg in 1mL	52	0.38	0.38	0.56	0.4069s
Calcium Chloride 1g in 10mL	99	0.47	0.34	0.61	0.4069s
Actrapid Penfill 3ml	58	0.49	0.39	0.65	0.4069s
Vecuronium bromide	45	0.46	0.41	0.59	0.4069s
Sugammadex 200mg/2ml	42	0.53	0.55	0.63	0.4069s
Amiodarone Hydrochloride	49	0.64	0.57	0.77	0.4069s
Protamine Sulphate 50mg in 5ml	60	0.59	0.52	0.61	0.4069s
Summethonium Chloride 100mg in 2mL	51	0.53	0.41	0.71	0.4069s
Protamine Sulfate 10mg/ml	49	0.62	0.56	0.72	0.4069s
Glyceryl Trinitrate 1 mg/ml	74	0.47	0.40	0.68	0.4069s
Tranexamic acid	64	0.55	0.39	0.76	0.4069s
Heparin Injection 25000IU in 5 mL	66	0.5	0.42	0.59	0.4069s
Sterile Potassium Chloride	91	0.37	0.37	0.61	0.4069s
Metaraminol 10mg/ml	32	0.63	0.65	0.76	0.4069s
Cyclizine lactate	60	0.25	0.20	0.48	0.4069s
PITRESSIN argipressin	49	0.49	0.42	0.62	0.4069s
Dexamethasone phosphate 4 mg/ml	**1**	**1.0**	**0.99**	**1.00**	**0.4069s**
Ephedrine Hydrochloride	54	0.44	0.36	0.64	0.4069s
Ondansetron Solution	63	0.51	0.41	0.70	0.4069s
FRUSEMIDE	58	0.46	0.30	0.67	0.4069s
DALACINC PHOSPHATE	58	0.56	0.43	0.67	0.4069s
METOPROLOL Mylan	52	0.64	0.53	0.73	0.4069s
WATER FOR INJECTIONS BP	76	0.46	0.38	0.62	0.4069s
MORPHINE SULFATE	45	0.61	0.51	0.77	0.4069s
Glycopyrronium and Neostigmine	58	0.59	0.53	0.69	0.4069s
Clonidine HCl	50	0.46	0.40	0.65	0.4069s
Rocuronium Bromide 50 mg in 5 ml	59	0.54	0.39	0.56	0.4069s
Fresofol 1% MCT/LCT	323	0.58	0.23	0.59	0.4069s
Sedative Midazolam 5mg	51	0.47	0.36	0.61	0.4069s
Adrenaline Injection	59	0.49	0.35	0.52	0.4069s
Paracetamol Kabi	523	0.47	0.18	0.57	0.4069s
Provive MCT-LCT 1%	258	0.51	0.28	0.55	0.4069s
Adrenaline Injection 1mg in 10mL	59	0.49	0.35	0.52	0.4069s
Amoxicillin Sodium	123	0.44	0.35	0.67	0.4069s
Lidocain Injection	53	0.42	0.35	0.62	0.4069s
SODIUM CHLORIDE	111	0.38	0.34	0.61	0.4069s
Remifentanil-Act Injection	80	0.5	0.38	0.69	0.4069s
Sterile Dopamine	53	0.4	0.39	0.63	0.4069s
Hypnomida Etomidate 2mg	58	0.51	0.43	0.67	0.4069s
Xylocaine 1%	50	0.42	0.39	0.54	0.4069s
Fentanyl Injection	118	0.45	0.32	0.56	0.4069s
Noradrenaline acid	69	0.35	0.32	0.67	0.4069s
Magnesium Sulfate 2.47g in 5mL	64	0.53	0.44	0.59	0.4069s
Sugammadex Injection	55	0.52	0.52	0.68	0.4069s
Dynastat Powder	68	0.54	0.43	0.72	0.4069s
Hydrocortisone sodium	79	0.55	0.42	0.70	0.4069s
Atracurium Besylate	57	0.37	0.29	0.62	0.4069s
Atropine	52	0.47	0.39	0.59	0.4069s
PancuroInresa	77	0.47	0.35	0.65	0.4069s

Drug Identification: Sterile Dopamine against other samples

Drug Name	Edit Distance	TSR Scores	Lev Scores	Jacc Scores	Processing Time
Primacor Injection	76	0.41	0.31	0.48	0.3817s
Cefazolin Sodium 1g	120	0.29	0.26	0.45	0.3817s
NALOXONE HCl 400mg in 1mL	37	0.34	0.31	0.46	0.3817s
Calcium Chloride 1g in 10mL	108	0.34	0.28	0.44	0.3817s
Actrapid Penfill 3ml	59	0.44	0.27	0.57	0.3817s
Vecuronium bromide	47	0.3	0.27	0.45	0.3817s
Sugammadex 200mg/2ml	62	0.41	0.34	0.61	0.3817s
Amiodarone Hydrochloride	61	0.47	0.34	0.56	0.3817s
Protamine Sulphate 50mg in 5ml	76	0.49	0.33	0.48	0.3817s
Summethonium Chloride 100mg in 2mL	44	0.42	0.35	0.57	0.3817s
Protamine Sulfate 10mg/ml	66	0.54	0.39	0.59	0.3817s
Glyceryl Trinitrate 1 mg/ml	81	0.37	0.32	0.54	0.3817s
Tranexamic acid	58	0.39	0.31	0.57	0.3817s
Heparin Injection 25000IU in 5 mL	60	0.42	0.36	0.62	0.3817s
Sterile Potassium Chloride	87	0.58	0.42	0.53	0.3817s
Metaraminol 10mg/ml	47	0.46	0.32	0.60	0.3817s
Cyclizine lactate	42	0.27	0.24	0.38	0.3817s
PITRESSIN argipressin	42	0.36	0.31	0.65	0.3817s
Dexamethasone phosphate 4 mg/ml	53	0.4	0.39	0.63	0.3817s
Ephedrine Hydrochloride	43	0.36	0.31	0.48	0.3817s
Ondansetron Solution	68	0.4	0.32	0.57	0.3817s
FRUSEMIDE	50	0.42	0.30	0.58	0.3817s
DALACINC PHOSPHATE	41	0.42	0.43	0.70	0.3817s
METOPROLOL Mylan	75	0.35	0.32	0.64	0.3817s
WATER FOR INJECTIONS BP	79	0.41	0.28	0.55	0.3817s
MORPHINE SULFATE	39	0.39	0.37	0.56	0.3817s
Glycopyrronium and Neostigmine	62	0.43	0.40	0.73	0.3817s
Clonidine HCl	35	0.36	0.41	0.56	0.3817s
Rocuronium Bromide 50 mg in 5 ml	55	0.38	0.43	0.58	0.3817s
Fresofol 1% MCT/LCT	338	0.23	0.17	0.49	0.3817s
Sedative Midazolam 5mg	42	0.45	0.41	0.59	0.3817s
Adrenaline Injection	57	0.31	0.33	0.42	0.3817s
Paracetamol Kabi	542	0.15	0.12	0.44	0.3817s
Provive MCT-LCT 1%	274	0.22	0.21	0.45	0.3817s
Adrenaline Injection 1mg in 10mL	57	0.31	0.33	0.42	0.3817s
Amoxicillin Sodium	130	0.34	0.25	0.46	0.3817s
Lidocain Injection	36	0.38	0.37	0.46	0.3817s
SODIUM CHLORIDE	120	0.32	0.25	0.50	0.3817s
Remifentanil-Act Injection	81	0.34	0.29	0.50	0.3817s
Sterile Dopamine	**1**	**1.0**	**0.99**	**1.00**	**0.3817s**
Hypnomida Etomidate 2mg	65	0.46	0.31	0.59	0.3817s
Xylocaine 1%	39	0.36	0.32	0.39	0.3817s
Fentanyl Injection	118	0.36	0.32	0.49	0.3817s
Noradrenaline acid	58	0.44	0.40	0.58	0.3817s
Magnesium Sulfate 2.47g in 5mL	63	0.54	0.39	0.56	0.3817s
Sugammadex Injection	56	0.46	0.39	0.65	0.3817s
Dynastat Powder	76	0.33	0.28	0.59	0.3817s
Hydrocortisone sodium	84	0.32	0.29	0.52	0.3817s
Atracurium Besylate	43	0.36	0.35	0.58	0.3817s
Atropine	34	0.34	0.39	0.56	0.3817s
PancuroInresa	80	0.35	0.26	0.57	0.3817s

Drug Identification: Calcium Chloride against other samples

Drug Name	Edit Distance	TSR Scores	Lev Scores	Jacc Scores	Processing Time
Primacor Injection	99	0.54	0.39	0.71	0.4478s
Cefazolin Sodium 1g	116	0.46	0.39	0.63	0.4478s
NALOXONE HCl 400mg in 1mL	112	0.32	0.25	0.47	0.4478s
Calcium Chloride 1g in 10mL	**1**	**1.0**	**1.00**	**1.00**	**0.4478s**
Actrapid Penfill 3ml	106	0.48	0.34	0.65	0.4478s
Vecuronium bromide	99	0.33	0.37	0.65	0.4478s
Sugammadex 200mg/2ml	104	0.53	0.34	0.59	0.4478s
Amiodarone Hydrochloride	101	0.46	0.38	0.55	0.4478s
Protamine Sulphate 50mg in 5ml	98	0.51	0.39	0.71	0.4478s
Summethonium Chloride 100mg in 2mL	103	0.39	0.38	0.71	0.4478s
Protamine Sulfate 10mg/ml	100	0.45	0.35	0.62	0.4478s
Glyceryl Trinitrate 1 mg/ml	104	0.44	0.33	0.58	0.4478s
Tranexamic acid	104	0.44	0.33	0.65	0.4478s
Heparin Injection 25000IU in 5 mL	97	0.46	0.37	0.60	0.4478s
Sterile Potassium Chloride	100	0.5	0.43	0.71	0.4478s
Metaraminol 10mg/ml	101	0.48	0.35	0.58	0.4478s
Cyclizine lactate	119	0.22	0.16	0.41	0.4478s
PITRESSIN argipressin	101	0.38	0.34	0.52	0.4478s
Dexamethasone phosphate 4 mg/ml	101	0.47	0.33	0.61	0.4478s
Ephedrine Hydrochloride	104	0.36	0.31	0.53	0.4478s
Ondansetron Solution	102	0.4	0.35	0.56	0.4478s
FRUSEMIDE	108	0.35	0.28	0.61	0.4478s
DALACINC PHOSPHATE	109	0.34	0.27	0.62	0.4478s
METOPROLOL Mylan	106	0.46	0.36	0.52	0.4478s
WATER FOR INJECTIONS BP	95	0.44	0.41	0.67	0.4478s
MORPHINE SULFATE	102	0.49	0.33	0.76	0.4478s
Glycopyrronium and Neostigmine	98	0.47	0.37	0.64	0.4478s
Clonidine HCl	107	0.44	0.29	0.50	0.4478s
Rocuronium Bromide 50 mg in 5 ml	99	0.43	0.37	0.52	0.4478s
Fresofol 1% MCT/LCT	291	0.51	0.35	0.63	0.4478s
Sedative Midazolam 5mg	111	0.34	0.26	0.49	0.4478s
Adrenaline Injection	97	0.41	0.38	0.53	0.4478s
Paracetamol Kabi	493	0.29	0.25	0.61	0.4478s
Provive MCT-LCT 1%	245	0.42	0.36	0.73	0.4478s
Adrenaline Injection 1mg in 10mL	97	0.41	0.38	0.53	0.4478s
Amoxicillin Sodium	124	0.46	0.35	0.62	0.4478s
Lidocain Injection	109	0.34	0.28	0.57	0.4478s
SODIUM CHLORIDE	114	0.46	0.38	0.70	0.4478s
Remifentanil-Act Injection	97	0.45	0.40	0.59	0.4478s
Sterile Dopamine	110	0.34	0.27	0.44	0.4478s
Hypnomida Etomidate 2mg	100	0.44	0.34	0.57	0.4478s
Xylocaine 1%	108	0.29	0.29	0.41	0.4478s
Fentanyl Injection	118	0.46	0.39	0.61	0.4478s
Noradrenaline acid	99	0.39	0.35	0.56	0.4478s
Magnesium Sulfate 2.47g in 5mL	99	0.42	0.35	0.59	0.4478s
Sugammadex Injection	100	0.53	0.37	0.62	0.4478s
Dynastat Powder	100	0.44	0.39	0.57	0.4478s
Hydrocortisone sodium	102	0.43	0.39	0.65	0.4478s
Atracurium Besylate	102	0.36	0.32	0.57	0.4478s
Atropine	109	0.38	0.27	0.60	0.4478s
PancuroInresa	100	0.4	0.39	0.65	0.4478s

Drug Identification: Cefazolin Sodium against other samples

Drug Name	Edit Distance	TSR Scores	Lev Scores	Jacc Scores	Processing Time
Primacor Injection	113	0.49	0.38	0.58	0.3963s
Cefazolin Sodium 1g	**1**	**1.0**	**1.00**	**1.00**	**0.3963s**
NALOXONE HCl 400mg in 1mL	125	0.27	0.23	0.35	0.3963s
Calcium Chloride 1g in 10mL	115	0.46	0.39	0.63	0.3963s
Actrapid Penfill 3ml	119	0.42	0.29	0.67	0.3963s
Vecuronium bromide	105	0.49	0.43	0.61	0.3963s
Sugammadex 200mg/2ml	112	0.51	0.36	0.56	0.3963s
Amiodarone Hydrochloride	108	0.45	0.38	0.61	0.3963s
Protamine Sulphate 50mg in 5ml	110	0.46	0.38	0.58	0.3963s
Summethonium Chloride 100mg in 2mL	115	0.42	0.30	0.62	0.3963s
Protamine Sulfate 10mg/ml	101	0.48	0.42	0.59	0.3963s
Glyceryl Trinitrate 1 mg/ml	118	0.4	0.32	0.55	0.3963s
Tranexamic acid	115	0.45	0.29	0.62	0.3963s
Heparin Injection 25000IU in 5 mL	109	0.51	0.36	0.62	0.3963s
Sterile Potassium Chloride	116	0.44	0.38	0.58	0.3963s
Metaraminol 10mg/ml	110	0.46	0.34	0.60	0.3963s
Cyclizine lactate	134	0.17	0.13	0.38	0.3963s
PITRESSIN argipressin	110	0.41	0.36	0.48	0.3963s
Dexamethasone phosphate 4 mg/ml	107	0.48	0.38	0.68	0.3963s
Ephedrine Hydrochloride	116	0.42	0.30	0.55	0.3963s
Ondansetron Solution	110	0.41	0.38	0.53	0.3963s
FRUSEMIDE	116	0.42	0.31	0.53	0.3963s
DALACINC PHOSPHATE	118	0.34	0.28	0.59	0.3963s
METOPROLOL Mylan	100	0.53	0.45	0.58	0.3963s
WATER FOR INJECTIONS BP	114	0.44	0.33	0.64	0.3963s
MORPHINE SULFATE	115	0.44	0.34	0.67	0.3963s
Glycopyrronium and Neostigmine	117	0.48	0.33	0.56	0.3963s
Clonidine HCl	120	0.44	0.28	0.52	0.3963s
Rocuronium Bromide 50 mg in 5 ml	113	0.43	0.36	0.44	0.3963s
Fresofol 1% MCT/LCT	262	0.74	0.44	0.61	0.3963s
Sedative Midazolam 5mg	120	0.3	0.27	0.50	0.3963s
Adrenaline Injection	101	0.61	0.46	0.55	0.3963s
Paracetamol Kabi	464	0.67	0.33	0.67	0.3963s
Provive MCT-LCT 1%	212	0.71	0.46	0.62	0.3963s
Adrenaline Injection 1mg in 10mL	101	0.61	0.46	0.55	0.3963s
Amoxicillin Sodium	112	0.61	0.45	0.69	0.3963s
Lidocain Injection	121	0.32	0.28	0.59	0.3963s
SODIUM CHLORIDE	127	0.43	0.36	0.55	0.3963s
Remifentanil-Act Injection	97	0.54	0.46	0.71	0.3963s
Sterile Dopamine	122	0.29	0.25	0.45	0.3963s
Hypnomida Etomidate 2mg	108	0.38	0.36	0.64	0.3963s
Xylocaine 1%	123	0.3	0.26	0.38	0.3963s
Fentanyl Injection	128	0.56	0.38	0.58	0.3963s
Noradrenaline acid	114	0.38	0.33	0.48	0.3963s
Magnesium Sulfate 2.47g in 5mL	111	0.42	0.35	0.57	0.3963s
Sugammadex Injection	107	0.45	0.37	0.59	0.3963s
Dynastat Powder	91	0.61	0.50	0.54	0.3963s
Hydrocortisone sodium	75	0.69	0.61	0.77	0.3963s
Atracurium Besylate	110	0.55	0.41	0.53	0.3963s
Atropine	123	0.33	0.25	0.52	0.3963s
PancuroInresa	114	0.43	0.35	0.62	0.3963s

Drug Identification: Magnesium Sulphate against other samples

Drug Name	Edit Distance	TSR Scores	Lev Scores	Jacc Scores	Processing Time
Primacor Injection	78	0.52	0.39	0.55	0.3642s
Cefazolin Sodium 1g	109	0.42	0.36	0.57	0.3642s
NALOXONE HCl 400mg in 1mL	68	0.42	0.34	0.45	0.3642s
Calcium Chloride 1g in 10mL	98	0.42	0.36	0.59	0.3642s
Actrapid Penfill 3ml	74	0.5	0.29	0.58	0.3642s
Vecuronium bromide	69	0.34	0.34	0.58	0.3642s
Sugammadex 200mg/2ml	75	0.52	0.36	0.62	0.3642s
Amiodarone Hydrochloride	73	0.55	0.41	0.58	0.3642s
Protamine Sulphate 50mg in 5ml	76	0.54	0.47	0.59	0.3642s
Summethonium Chloride 100mg in 2mL	69	0.43	0.34	0.54	0.3642s
Protamine Sulfate 10mg/ml	70	0.52	0.37	0.56	0.3642s
Glyceryl Trinitrate 1 mg/ml	85	0.42	0.36	0.51	0.3642s
Tranexamic acid	74	0.41	0.31	0.54	0.3642s
Heparin Injection 25000IU in 5 mL	76	0.51	0.37	0.54	0.3642s
Sterile Potassium Chloride	84	0.49	0.43	0.55	0.3642s
Metaraminol 10mg/ml	67	0.47	0.41	0.56	0.3642s
Cyclizine lactate	76	0.26	0.22	0.31	0.3642s
PITRESSIN argipressin	66	0.42	0.33	0.50	0.3642s
Dexamethasone phosphate 4 mg/ml	64	0.53	0.44	0.59	0.3642s
Ephedrine Hydrochloride	75	0.46	0.28	0.42	0.3642s
Ondansetron Solution	74	0.39	0.34	0.54	0.3642s
FRUSEMIDE	74	0.37	0.29	0.46	0.3642s
DALACINC PHOSPHATE	69	0.37	0.32	0.60	0.3642s
METOPROLOL Mylan	82	0.48	0.32	0.59	0.3642s
WATER FOR INJECTIONS BP	85	0.43	0.34	0.65	0.3642s
MORPHINE SULFATE	58	0.61	0.47	0.53	0.3642s
Glycopyrronium and Neostigmine	74	0.5	0.40	0.72	0.3642s
Clonidine HCl	68	0.49	0.34	0.48	0.3642s
Rocuronium Bromide 50 mg in 5 ml	58	0.56	0.47	0.55	0.3642s
Fresofol 1% MCT/LCT	319	0.45	0.24	0.58	0.3642s
Sedative Midazolam 5mg	71	0.43	0.33	0.51	0.3642s
Adrenaline Injection	67	0.5	0.42	0.47	0.3642s
Paracetamol Kabi	520	0.2	0.18	0.60	0.3642s
Provive MCT-LCT 1%	260	0.41	0.27	0.62	0.3642s
Adrenaline Injection 1mg in 10mL	67	0.5	0.42	0.47	0.3642s
Amoxicillin Sodium	124	0.37	0.32	0.53	0.3642s
Lidocain Injection	70	0.35	0.31	0.45	0.3642s
SODIUM CHLORIDE	111	0.38	0.34	0.68	0.3642s
Remifentanil-Act Injection	78	0.49	0.36	0.57	0.3642s
Sterile Dopamine	63	0.54	0.39	0.56	0.3642s
Hypnomida Etomidate 2mg	73	0.5	0.35	0.56	0.3642s
Xylocaine 1%	69	0.35	0.31	0.40	0.3642s
Fentanyl Injection	116	0.47	0.35	0.63	0.3642s
Noradrenaline acid	75	0.44	0.38	0.50	0.3642s
Magnesium Sulfate 2.47g in 5mL	**1**	**1.0**	**0.99**	**1.00**	**0.3642s**
Sugammadex Injection	64	0.54	0.43	0.66	0.3642s
Dynastat Powder	75	0.42	0.40	0.60	0.3642s
Hydrocortisone sodium	81	0.41	0.38	0.54	0.3642s
Atracurium Besylate	68	0.37	0.35	0.50	0.3642s
Atropine	69	0.38	0.31	0.44	0.3642s
PancuroInresa	84	0.44	0.36	0.58	0.3642s

Drug Identification: Amiodarone Hydrochloride against other samples

Drug Name	Edit Distance	TSR Scores	Lev Scores	Jacc Scores	Processing Time
Primacor Injection	77	0.49	0.37	0.55	0.3578s
Cefazolin Sodium 1g	106	0.45	0.39	0.61	0.3578s
NALOXONE HCl 400mg in 1mL	68	0.32	0.32	0.48	0.3578s
Calcium Chloride 1g in 10mL	99	0.46	0.38	0.55	0.3578s
Actrapid Penfill 3ml	65	0.44	0.40	0.58	0.3578s
Vecuronium bromide	59	0.4	0.41	0.63	0.3578s
Sugammadex 200mg/2ml	56	0.52	0.51	0.68	0.3578s
Amiodarone Hydrochloride	**1**	**1.0**	**0.99**	**1.00**	**0.3578s**
Protamine Sulphate 50mg in 5ml	71	0.48	0.42	0.55	0.3578s
Summethonium Chloride 100mg in 2mL	58	0.52	0.43	0.64	0.3578s
Protamine Sulfate 10mg/ml	56	0.48	0.51	0.60	0.3578s
Glyceryl Trinitrate 1 mg/ml	75	0.45	0.43	0.73	0.3578s
Tranexamic acid	72	0.48	0.32	0.58	0.3578s
Heparin Injection 25000IU in 5 mL	69	0.45	0.34	0.58	0.3578s
Sterile Potassium Chloride	86	0.51	0.43	0.55	0.3578s
Metaraminol 10mg/ml	46	0.74	0.62	0.75	0.3578s
Cyclizine lactate	75	0.2	0.17	0.41	0.3578s
PITRESSIN argipressin	62	0.4	0.42	0.60	0.3578s
Dexamethasone phosphate 4 mg/ml	50	0.64	0.57	0.77	0.3578s
Ephedrine Hydrochloride	60	0.64	0.44	0.70	0.3578s
Ondansetron Solution	69	0.46	0.38	0.63	0.3578s
FRUSEMIDE	69	0.38	0.29	0.54	0.3578s
DALACINC PHOSPHATE	67	0.37	0.31	0.60	0.3578s
METOPROLOL Mylan	67	0.59	0.46	0.79	0.3578s
WATER FOR INJECTIONS BP	76	0.36	0.38	0.47	0.3578s
MORPHINE SULFATE	59	0.44	0.42	0.69	0.3578s
Glycopyrronium and Neostigmine	61	0.55	0.49	0.68	0.3578s
Clonidine HCl	64	0.44	0.37	0.64	0.3578s
Rocuronium Bromide 50 mg in 5 ml	68	0.51	0.36	0.60	0.3578s
Fresofol 1% MCT/LCT	315	0.4	0.27	0.58	0.3578s
Sedative Midazolam 5mg	68	0.37	0.28	0.45	0.3578s
Adrenaline Injection	67	0.47	0.37	0.56	0.3578s
Paracetamol Kabi	517	0.48	0.19	0.52	0.3578s
Provive MCT-LCT 1%	250	0.48	0.32	0.58	0.3578s
Adrenaline Injection 1mg in 10mL	67	0.47	0.37	0.56	0.3578s
Amoxicillin Sodium	119	0.44	0.36	0.56	0.3578s
Lidocain Injection	66	0.35	0.32	0.60	0.3578s
SODIUM CHLORIDE	111	0.4	0.36	0.60	0.3578s
Remifentanil-Act Injection	81	0.48	0.38	0.74	0.3578s
Sterile Dopamine	62	0.47	0.34	0.56	0.3578s
Hypnomida Etomidate 2mg	69	0.49	0.37	0.66	0.3578s
Xylocaine 1%	63	0.35	0.39	0.52	0.3578s
Fentanyl Injection	114	0.46	0.35	0.59	0.3578s
Noradrenaline acid	61	0.45	0.45	0.59	0.3578s
Magnesium Sulfate 2.47g in 5mL	74	0.55	0.41	0.58	0.3578s
Sugammadex Injection	67	0.57	0.42	0.73	0.3578s
Dynastat Powder	78	0.52	0.41	0.66	0.3578s
Hydrocortisone sodium	80	0.57	0.40	0.69	0.3578s
Atracurium Besylate	65	0.39	0.33	0.67	0.3578s
Atropine	68	0.41	0.32	0.58	0.3578s
PancuroInresa	76	0.39	0.34	0.53	0.3578s

Drug Identification: Amoxicillin Sodium against other samples

Drug Name	Edit Distance	TSR Scores	Lev Scores	Jacc Scores	Processing Time
Primacor Injection	121	0.49	0.37	0.67	0.4114s
Cefazolin Sodium 1g	113	0.61	0.45	0.69	0.4114s
NALOXONE HCl 400mg in 1mL	136	0.24	0.20	0.44	0.4114s
Calcium Chloride 1g in 10mL	123	0.46	0.36	0.62	0.4114s
Actrapid Penfill 3ml	119	0.37	0.34	0.66	0.4114s
Vecuronium bromide	125	0.4	0.36	0.61	0.4114s
Sugammadex 200mg/2ml	118	0.47	0.41	0.60	0.4114s
Amiodarone Hydrochloride	119	0.44	0.35	0.56	0.4114s
Protamine Sulphate 50mg in 5ml	117	0.42	0.40	0.71	0.4114s
Summethonium Chloride 100mg in 2mL	127	0.36	0.29	0.67	0.4114s
Protamine Sulfate 10mg/ml	121	0.44	0.36	0.58	0.4114s
Glyceryl Trinitrate 1 mg/ml	126	0.35	0.32	0.50	0.4114s
Tranexamic acid	123	0.37	0.31	0.57	0.4114s
Heparin Injection 25000IU in 5 mL	120	0.45	0.36	0.71	0.4114s
Sterile Potassium Chloride	124	0.43	0.36	0.71	0.4114s
Metaraminol 10mg/ml	122	0.42	0.33	0.55	0.4114s
Cyclizine lactate	142	0.18	0.15	0.42	0.4114s
PITRESSIN argipressin	125	0.35	0.31	0.53	0.4114s
Dexamethasone phosphate 4 mg/ml	124	0.44	0.35	0.67	0.4114s
Ephedrine Hydrochloride	126	0.35	0.30	0.50	0.4114s
Ondansetron Solution	121	0.42	0.33	0.66	0.4114s
FRUSEMIDE	119	0.37	0.37	0.58	0.4114s
DALACINC PHOSPHATE	131	0.34	0.25	0.50	0.4114s
METOPROLOL Mylan	113	0.49	0.45	0.53	0.4114s
WATER FOR INJECTIONS BP	122	0.38	0.35	0.68	0.4114s
MORPHINE SULFATE	130	0.37	0.27	0.61	0.4114s
Glycopyrronium and Neostigmine	115	0.46	0.38	0.60	0.4114s
Clonidine HCl	135	0.44	0.25	0.47	0.4114s
Rocuronium Bromide 50 mg in 5 ml	123	0.39	0.32	0.44	0.4114s
Fresofol 1% MCT/LCT	280	0.45	0.37	0.72	0.4114s
Sedative Midazolam 5mg	130	0.31	0.26	0.54	0.4114s
Adrenaline Injection	120	0.42	0.36	0.45	0.4114s
Paracetamol Kabi	487	0.33	0.27	0.70	0.4114s
Provive MCT-LCT 1%	236	0.46	0.36	0.69	0.4114s
Adrenaline Injection 1mg in 10mL	120	0.42	0.36	0.45	0.4114s
Amoxicillin Sodium	**1**	**1.0**	**1.00**	**1.00**	**0.4114s**
Lidocain Injection	134	0.27	0.25	0.48	0.4114s
SODIUM CHLORIDE	131	0.43	0.36	0.62	0.4114s
Remifentanil-Act Injection	123	0.48	0.32	0.70	0.4114s
Sterile Dopamine	132	0.34	0.24	0.46	0.4114s
Hypnomida Etomidate 2mg	125	0.37	0.30	0.63	0.4114s
Xylocaine 1%	129	0.25	0.27	0.43	0.4114s
Fentanyl Injection	132	0.44	0.32	0.62	0.4114s
Noradrenaline acid	120	0.4	0.34	0.58	0.4114s
Magnesium Sulfate 2.47g in 5mL	125	0.37	0.32	0.53	0.4114s
Sugammadex Injection	124	0.43	0.32	0.59	0.4114s
Dynastat Powder	110	0.56	0.42	0.63	0.4114s
Hydrocortisone sodium	112	0.56	0.42	0.66	0.4114s
Atracurium Besylate	116	0.55	0.39	0.48	0.4114s
Atropine	136	0.26	0.21	0.52	0.4114s
PancuroInresa	125	0.4	0.32	0.71	0.4114s

Drug Identification: Primacor Injection against other samples

Drug Name	Edit Distance	TSR Scores	Lev Scores	Jacc Scores	Processing Time
Primacor Injection	**1**	**1.0**	**0.99**	**1.00**	**0.3998s**
Cefazolin Sodium 1g	112	0.49	0.38	0.58	0.3998s
NALOXONE HCl 400mg in 1mL	80	0.34	0.27	0.47	0.3998s
Calcium Chloride 1g in 10mL	99	0.54	0.38	0.71	0.3998s
Actrapid Penfill 3ml	77	0.54	0.30	0.70	0.3998s
Vecuronium bromide	73	0.41	0.35	0.55	0.3998s
Sugammadex 200mg/2ml	79	0.55	0.32	0.59	0.3998s
Amiodarone Hydrochloride	78	0.49	0.36	0.55	0.3998s
Protamine Sulphate 50mg in 5ml	74	0.52	0.45	0.71	0.3998s
Summethonium Chloride 100mg in 2mL	72	0.43	0.41	0.66	0.3998s
Protamine Sulfate 10mg/ml	71	0.55	0.41	0.67	0.3998s
Glyceryl Trinitrate 1 mg/ml	83	0.44	0.39	0.62	0.3998s
Tranexamic acid	75	0.49	0.36	0.70	0.3998s
Heparin Injection 25000IU in 5 mL	74	0.51	0.40	0.60	0.3998s
Sterile Potassium Chloride	91	0.45	0.37	0.66	0.3998s
Metaraminol 10mg/ml	73	0.53	0.35	0.63	0.3998s
Cyclizine lactate	85	0.24	0.19	0.36	0.3998s
PITRESSIN argipressin	75	0.44	0.34	0.57	0.3998s
Dexamethasone phosphate 4 mg/ml	74	0.55	0.33	0.66	0.3998s
Ephedrine Hydrochloride	78	0.39	0.28	0.48	0.3998s
Ondansetron Solution	74	0.46	0.37	0.60	0.3998s
FRUSEMIDE	74	0.41	0.34	0.67	0.3998s
DALACINC PHOSPHATE	77	0.41	0.29	0.57	0.3998s
METOPROLOL Mylan	82	0.47	0.32	0.56	0.3998s
WATER FOR INJECTIONS BP	82	0.5	0.35	0.58	0.3998s
MORPHINE SULFATE	73	0.44	0.37	0.65	0.3998s
Glycopyrronium and Neostigmine	79	0.51	0.35	0.59	0.3998s
Clonidine HCl	78	0.44	0.30	0.50	0.3998s
Rocuronium Bromide 50 mg in 5 ml	72	0.47	0.41	0.47	0.3998s
Fresofol 1% MCT/LCT	312	0.54	0.27	0.63	0.3998s
Sedative Midazolam 5mg	78	0.35	0.27	0.53	0.3998s
Adrenaline Injection	66	0.43	0.43	0.44	0.3998s
Paracetamol Kabi	514	0.41	0.20	0.69	0.3998s
Provive MCT-LCT 1%	257	0.4	0.29	0.64	0.3998s
Adrenaline Injection 1mg in 10mL	66	0.43	0.43	0.44	0.3998s
Amoxicillin Sodium	121	0.49	0.37	0.67	0.3998s
Lidocain Injection	75	0.35	0.31	0.52	0.3998s
SODIUM CHLORIDE	112	0.4	0.35	0.62	0.3998s
Remifentanil-Act Injection	78	0.53	0.43	0.59	0.3998s
Sterile Dopamine	76	0.41	0.31	0.48	0.3998s
Hypnomida Etomidate 2mg	71	0.48	0.39	0.57	0.3998s
Xylocaine 1%	77	0.35	0.29	0.45	0.3998s
Fentanyl Injection	110	0.53	0.39	0.61	0.3998s
Noradrenaline acid	77	0.4	0.36	0.52	0.3998s
Magnesium Sulfate 2.47g in 5mL	79	0.52	0.38	0.55	0.3998s
Sugammadex Injection	74	0.56	0.37	0.58	0.3998s
Dynastat Powder	84	0.53	0.38	0.57	0.3998s
Hydrocortisone sodium	89	0.48	0.36	0.65	0.3998s
Atracurium Besylate	74	0.33	0.35	0.47	0.3998s
Atropine	72	0.42	0.38	0.60	0.3998s
PancuroInresa	77	0.52	0.42	0.70	0.3998s

Drug Identification: Xylocaine against other samples

Drug Name	Edit Distance	TSR Scores	Lev Scores	Jacc Scores	Processing Time
Primacor Injection	75	0.35	0.31	0.45	0.4161s
Cefazolin Sodium 1g	121	0.3	0.27	0.38	0.4161s
NALOXONE HCl 400mg in 1mL	29	0.43	0.36	0.42	0.4161s
Calcium Chloride 1g in 10mL	107	0.29	0.29	0.41	0.4161s
Actrapid Penfill 3ml	50	0.42	0.41	0.39	0.4161s
Vecuronium bromide	41	0.4	0.37	0.41	0.4161s
Sugammadex 200mg/2ml	60	0.36	0.33	0.47	0.4161s
Amiodarone Hydrochloride	62	0.35	0.37	0.52	0.4161s
Protamine Sulphate 50mg in 5ml	74	0.48	0.36	0.45	0.4161s
Summethonium Chloride 100mg in 2mL	43	0.33	0.31	0.43	0.4161s
Protamine Sulfate 10mg/ml	61	0.43	0.37	0.55	0.4161s
Glyceryl Trinitrate 1 mg/ml	81	0.31	0.30	0.56	0.4161s
Tranexamic acid	61	0.38	0.31	0.44	0.4161s
Heparin Injection 25000IU in 5 mL	65	0.4	0.29	0.35	0.4161s
Sterile Potassium Chloride	99	0.32	0.28	0.37	0.4161s
Metaraminol 10mg/ml	41	0.45	0.40	0.56	0.4161s
Cyclizine lactate	32	0.35	0.21	0.46	0.4161s
PITRESSIN argipressin	40	0.46	0.37	0.48	0.4161s
Dexamethasone phosphate 4 mg/ml	49	0.42	0.39	0.54	0.4161s
Ephedrine Hydrochloride	37	0.4	0.40	0.50	0.4161s
Ondansetron Solution	70	0.31	0.30	0.48	0.4161s
FRUSEMIDE	50	0.29	0.25	0.38	0.4161s
DALACINC PHOSPHATE	51	0.36	0.27	0.36	0.4161s
METOPROLOL Mylan	72	0.36	0.33	0.54	0.4161s
WATER FOR INJECTIONS BP	75	0.36	0.35	0.39	0.4161s
MORPHINE SULFATE	35	0.52	0.44	0.46	0.4161s
Glycopyrronium and Neostigmine	66	0.36	0.37	0.42	0.4161s
Clonidine HCl	26	0.44	0.50	0.46	0.4161s
Rocuronium Bromide 50 mg in 5 ml	62	0.44	0.35	0.48	0.4161s
Fresofol 1% MCT/LCT	344	0.16	0.14	0.46	0.4161s
Sedative Midazolam 5mg	51	0.31	0.29	0.36	0.4161s
Adrenaline Injection	57	0.36	0.33	0.50	0.4161s
Paracetamol Kabi	549	0.11	0.10	0.39	0.4161s
Provive MCT-LCT 1%	281	0.17	0.17	0.42	0.4161s
Adrenaline Injection 1mg in 10mL	57	0.36	0.33	0.50	0.4161s
Amoxicillin Sodium	128	0.25	0.27	0.43	0.4161s
Lidocain Injection	23	0.63	0.54	0.48	0.4161s
SODIUM CHLORIDE	119	0.26	0.26	0.47	0.4161s
Remifentanil-Act Injection	81	0.34	0.31	0.47	0.4161s
Sterile Dopamine	38	0.36	0.34	0.39	0.4161s
Hypnomida Etomidate 2mg	64	0.37	0.31	0.50	0.4161s
Xylocaine 1%	**1**	**1.0**	**0.99**	**1.00**	**0.4161s**
Fentanyl Injection	126	0.27	0.24	0.42	0.4161s
Noradrenaline acid	68	0.32	0.30	0.48	0.4161s
Magnesium Sulfate 2.47g in 5mL	67	0.35	0.33	0.40	0.4161s
Sugammadex Injection	56	0.35	0.34	0.45	0.4161s
Dynastat Powder	76	0.34	0.29	0.50	0.4161s
Hydrocortisone sodium	86	0.3	0.27	0.48	0.4161s
Atracurium Besylate	45	0.3	0.29	0.48	0.4161s
Atropine	30	0.39	0.39	0.52	0.4161s
PancuroInresa	81	0.34	0.28	0.44	0.4161s

Drug Identification: Ondansetron Solution against other samples

Drug Name	Edit Distance	TSR Scores	Lev Scores	Jacc Scores	Processing Time
Primacor Injection	76	0.46	0.37	0.60	0.4204s
Cefazolin Sodium 1g	109	0.41	0.38	0.53	0.4204s
NALOXONE HCl 400mg in 1mL	71	0.31	0.26	0.55	0.4204s
Calcium Chloride 1g in 10mL	103	0.4	0.34	0.56	0.4204s
Actrapid Penfill 3ml	72	0.38	0.29	0.59	0.4204s
Vecuronium bromide	66	0.36	0.33	0.63	0.4204s
Sugammadex 200mg/2ml	71	0.47	0.37	0.73	0.4204s
Amiodarone Hydrochloride	70	0.46	0.37	0.63	0.4204s
Protamine Sulphate 50mg in 5ml	77	0.46	0.36	0.60	0.4204s
Summethonium Chloride 100mg in 2mL	66	0.44	0.34	0.70	0.4204s
Protamine Sulfate 10mg/ml	67	0.49	0.46	0.66	0.4204s
Glyceryl Trinitrate 1 mg/ml	84	0.41	0.30	0.67	0.4204s
Tranexamic acid	61	0.54	0.47	0.74	0.4204s
Heparin Injection 25000IU in 5 mL	73	0.38	0.34	0.59	0.4204s
Sterile Potassium Chloride	96	0.38	0.35	0.65	0.4204s
Metaraminol 10mg/ml	67	0.5	0.41	0.52	0.4204s
Cyclizine lactate	75	0.26	0.25	0.48	0.4204s
PITRESSIN argipressin	69	0.33	0.29	0.55	0.4204s
Dexamethasone phosphate 4 mg/ml	64	0.51	0.39	0.70	0.4204s
Ephedrine Hydrochloride	66	0.35	0.36	0.57	0.4204s
Ondansetron Solution	**1**	**1.0**	**0.99**	**1.00**	**0.4204s**
FRUSEMIDE	63	0.41	0.43	0.60	0.4204s
DALACINC PHOSPHATE	67	0.36	0.31	0.56	0.4204s
METOPROLOL Mylan	76	0.46	0.38	0.60	0.4204s
WATER FOR INJECTIONS BP	80	0.42	0.32	0.61	0.4204s
MORPHINE SULFATE	66	0.37	0.34	0.63	0.4204s
Glycopyrronium and Neostigmine	76	0.51	0.36	0.62	0.4204s
Clonidine HCl	72	0.29	0.27	0.44	0.4204s
Rocuronium Bromide 50 mg in 5 ml	74	0.36	0.33	0.50	0.4204s
Fresofol 1% MCT/LCT	318	0.32	0.24	0.62	0.4204s
Sedative Midazolam 5mg	69	0.4	0.29	0.66	0.4204s
Adrenaline Injection	68	0.34	0.35	0.52	0.4204s
Paracetamol Kabi	516	0.36	0.20	0.60	0.4204s
Provive MCT-LCT 1%	258	0.31	0.28	0.59	0.4204s
Adrenaline Injection 1mg in 10mL	68	0.34	0.35	0.52	0.4204s
Amoxicillin Sodium	120	0.42	0.34	0.66	0.4204s
Lidocain Injection	70	0.33	0.30	0.45	0.4204s
SODIUM CHLORIDE	112	0.36	0.32	0.61	0.4204s
Remifentanil-Act Injection	76	0.44	0.43	0.73	0.4204s
Sterile Dopamine	69	0.4	0.31	0.57	0.4204s
Hypnomida Etomidate 2mg	69	0.43	0.35	0.61	0.4204s
Xylocaine 1%	71	0.31	0.30	0.48	0.4204s
Fentanyl Injection	117	0.4	0.38	0.55	0.4204s
Noradrenaline acid	70	0.48	0.40	0.66	0.4204s
Magnesium Sulfate 2.47g in 5mL	75	0.39	0.33	0.54	0.4204s
Sugammadex Injection	71	0.42	0.33	0.67	0.4204s
Dynastat Powder	77	0.49	0.38	0.77	0.4204s
Hydrocortisone sodium	82	0.4	0.38	0.64	0.4204s
Atracurium Besylate	67	0.35	0.34	0.67	0.4204s
Atropine	68	0.39	0.31	0.53	0.4204s
PancuroInresa	73	0.42	0.44	0.64	0.4204s

Drug Identification: Actrapid Penfill against other samples

Drug Name	Edit Distance	TSR Scores	Lev Scores	Jacc Scores	Processing Time
Primacor Injection	76	0.54	0.31	0.70	0.5487s
Cefazolin Sodium 1g	117	0.42	0.30	0.67	0.5487s
NALOXONE HCl 400mg in 1mL	54	0.45	0.31	0.36	0.5487s
Calcium Chloride 1g in 10mL	104	0.48	0.35	0.65	0.5487s
Actrapid Penfill 3ml	**1**	**1.0**	**0.99**	**1.00**	**0.5487s**
Vecuronium bromide	57	0.42	0.34	0.58	0.5487s
Sugammadex 200mg/2ml	63	0.54	0.41	0.73	0.5487s
Amiodarone Hydrochloride	64	0.44	0.40	0.58	0.5487s
Protamine Sulphate 50mg in 5ml	71	0.52	0.39	0.65	0.5487s
Summethonium Chloride 100mg in 2mL	53	0.47	0.34	0.70	0.5487s
Protamine Sulfate 10mg/ml	65	0.51	0.38	0.66	0.5487s
Glyceryl Trinitrate 1 mg/ml	81	0.39	0.33	0.56	0.5487s
Tranexamic acid	64	0.45	0.34	0.69	0.5487s
Heparin Injection 25000IU in 5 mL	67	0.53	0.37	0.74	0.5487s
Sterile Potassium Chloride	96	0.42	0.31	0.65	0.5487s
Metaraminol 10mg/ml	53	0.56	0.45	0.68	0.5487s
Cyclizine lactate	59	0.28	0.20	0.43	0.5487s
PITRESSIN argipressin	53	0.54	0.36	0.61	0.5487s
Dexamethasone phosphate 4 mg/ml	59	0.49	0.40	0.65	0.5487s
Ephedrine Hydrochloride	52	0.42	0.40	0.52	0.5487s
Ondansetron Solution	70	0.38	0.30	0.59	0.5487s
FRUSEMIDE	58	0.41	0.27	0.60	0.5487s
DALACINC PHOSPHATE	60	0.37	0.30	0.56	0.5487s
METOPROLOL Mylan	71	0.44	0.40	0.60	0.5487s
WATER FOR INJECTIONS BP	72	0.47	0.39	0.61	0.5487s
MORPHINE SULFATE	53	0.53	0.34	0.69	0.5487s
Glycopyrronium and Neostigmine	62	0.53	0.38	0.68	0.5487s
Clonidine HCl	55	0.48	0.36	0.53	0.5487s
Rocuronium Bromide 50 mg in 5 ml	66	0.5	0.30	0.50	0.5487s
Fresofol 1% MCT/LCT	329	0.32	0.21	0.67	0.5487s
Sedative Midazolam 5mg	57	0.36	0.30	0.56	0.5487s
Adrenaline Injection	61	0.48	0.31	0.52	0.5487s
Paracetamol Kabi	530	0.2	0.15	0.60	0.5487s
Provive MCT-LCT 1%	268	0.32	0.24	0.59	0.5487s
Adrenaline Injection 1mg in 10mL	61	0.48	0.31	0.52	0.5487s
Amoxicillin Sodium	117	0.37	0.35	0.66	0.5487s
Lidocain Injection	57	0.4	0.32	0.55	0.5487s
SODIUM CHLORIDE	115	0.42	0.27	0.61	0.5487s
Remifentanil-Act Injection	83	0.45	0.30	0.62	0.5487s
Sterile Dopamine	60	0.44	0.28	0.57	0.5487s
Hypnomida Etomidate 2mg	65	0.49	0.33	0.61	0.5487s
Xylocaine 1%	48	0.42	0.43	0.39	0.5487s
Fentanyl Injection	123	0.46	0.28	0.69	0.5487s
Noradrenaline acid	69	0.37	0.33	0.50	0.5487s
Magnesium Sulfate 2.47g in 5mL	75	0.5	0.30	0.58	0.5487s
Sugammadex Injection	60	0.55	0.36	0.72	0.5487s
Dynastat Powder	79	0.41	0.32	0.61	0.5487s
Hydrocortisone sodium	85	0.42	0.32	0.64	0.5487s
Atracurium Besylate	52	0.34	0.34	0.55	0.5487s
Atropine	54	0.4	0.33	0.59	0.5487s
PancuroInresa	81	0.47	0.32	0.64	0.5487s

Drug Identification: METOPROLOL Mylan against other samples

Drug Name	Edit Distance	TSR Scores	Lev Scores	Jacc Scores	Processing Time
Primacor Injection	83	0.47	0.33	0.56	0.3672s
Cefazolin Sodium 1g	98	0.53	0.46	0.58	0.3672s
NALOXONE HCl 400mg in 1mL	80	0.25	0.21	0.39	0.3672s
Calcium Chloride 1g in 10mL	105	0.46	0.36	0.52	0.3672s
Actrapid Penfill 3ml	73	0.44	0.39	0.60	0.3672s
Vecuronium bromide	67	0.44	0.39	0.65	0.3672s
Sugammadex 200mg/2ml	55	0.51	0.53	0.64	0.3672s
Amiodarone Hydrochloride	68	0.59	0.46	0.79	0.3672s
Protamine Sulphate 50mg in 5ml	79	0.51	0.41	0.61	0.3672s
Summethonium Chloride 100mg in 2mL	71	0.4	0.35	0.61	0.3672s
Protamine Sulfate 10mg/ml	60	0.51	0.50	0.74	0.3672s
Glyceryl Trinitrate 1 mg/ml	88	0.48	0.38	0.69	0.3672s
Tranexamic acid	74	0.44	0.31	0.55	0.3672s
Heparin Injection 25000IU in 5 mL	75	0.44	0.35	0.60	0.3672s
Sterile Potassium Chloride	96	0.37	0.35	0.56	0.3672s
Metaraminol 10mg/ml	57	0.6	0.50	0.78	0.3672s
Cyclizine lactate	84	0.22	0.16	0.48	0.3672s
PITRESSIN argipressin	71	0.38	0.36	0.70	0.3672s
Dexamethasone phosphate 4 mg/ml	53	0.64	0.53	0.73	0.3672s
Ephedrine Hydrochloride	73	0.43	0.35	0.65	0.3672s
Ondansetron Solution	76	0.46	0.40	0.60	0.3672s
FRUSEMIDE	68	0.46	0.38	0.56	0.3672s
DALACINC PHOSPHATE	79	0.38	0.30	0.62	0.3672s
METOPROLOL Mylan	**1**	**1.0**	**0.99**	**1.00**	**0.3672s**
WATER FOR INJECTIONS BP	80	0.42	0.37	0.53	0.3672s
MORPHINE SULFATE	71	0.5	0.36	0.65	0.3672s
Glycopyrronium and Neostigmine	67	0.58	0.52	0.77	0.3672s
Clonidine HCl	75	0.44	0.30	0.60	0.3672s
Rocuronium Bromide 50 mg in 5 ml	78	0.51	0.35	0.62	0.3672s
Fresofol 1% MCT/LCT	298	0.58	0.32	0.55	0.3672s
Sedative Midazolam 5mg	74	0.41	0.30	0.52	0.3672s
Adrenaline Injection	76	0.51	0.36	0.52	0.3672s
Paracetamol Kabi	504	0.54	0.23	0.47	0.3672s
Provive MCT-LCT 1%	243	0.47	0.34	0.51	0.3672s
Adrenaline Injection 1mg in 10mL	76	0.51	0.36	0.52	0.3672s
Amoxicillin Sodium	112	0.49	0.45	0.53	0.3672s
Lidocain Injection	76	0.31	0.27	0.50	0.3672s
SODIUM CHLORIDE	115	0.37	0.31	0.57	0.3672s
Remifentanil-Act Injection	84	0.5	0.44	0.70	0.3672s
Sterile Dopamine	76	0.35	0.32	0.64	0.3672s
Hypnomida Etomidate 2mg	73	0.45	0.37	0.62	0.3672s
Xylocaine 1%	73	0.36	0.34	0.54	0.3672s
Fentanyl Injection	117	0.46	0.35	0.61	0.3672s
Noradrenaline acid	80	0.41	0.31	0.62	0.3672s
Magnesium Sulfate 2.47g in 5mL	83	0.48	0.34	0.59	0.3672s
Sugammadex Injection	71	0.51	0.45	0.69	0.3672s
Dynastat Powder	65	0.58	0.55	0.68	0.3672s
Hydrocortisone sodium	68	0.58	0.51	0.66	0.3672s
Atracurium Besylate	62	0.47	0.46	0.70	0.3672s
Atropine	76	0.35	0.29	0.67	0.3672s
PancuroInresa	78	0.44	0.41	0.60	0.3672s

Drug Identification: Sterile Potassium Chloride against other samples

Drug Name	Edit Distance	TSR Scores	Lev Scores	Jacc Scores	Processing Time
Primacor Injection	94	0.46	0.37	0.64	0.4826s
Cefazolin Sodium 1g	118	0.44	0.37	0.57	0.4826s
NALOXONE HCl 400mg in 1mL	102	0.34	0.27	0.50	0.4826s
Calcium Chloride 1g in 10mL	102	0.5	0.42	0.69	0.4826s
Actrapid Penfill 3ml	100	0.42	0.31	0.63	0.4826s
Vecuronium bromide	99	0.42	0.31	0.58	0.4826s
Sugammadex 200mg/2ml	93	0.48	0.34	0.62	0.4826s
Amiodarone Hydrochloride	89	0.52	0.43	0.53	0.4826s
Protamine Sulphate 50mg in 5ml	95	0.48	0.37	0.79	0.4826s
Summethonium Chloride 100mg in 2mL	88	0.53	0.42	0.69	0.4826s
Protamine Sulfate 10mg/ml	97	0.55	0.42	0.65	0.4826s
Glyceryl Trinitrate 1 mg/ml	102	0.41	0.34	0.61	0.4826s
Tranexamic acid	98	0.46	0.31	0.63	0.4826s
Heparin Injection 25000IU in 5 mL	93	0.51	0.36	0.73	0.4826s
Sterile Potassium Chloride	**3**	**1.0**	**0.99**	**0.97**	**0.4826s**
Metaraminol 10mg/ml	99	0.45	0.31	0.56	0.4826s
Cyclizine lactate	112	0.24	0.15	0.35	0.4826s
PITRESSIN argipressin	95	0.41	0.34	0.50	0.4826s
Dexamethasone phosphate 4 mg/ml	95	0.36	0.36	0.59	0.4826s
Ephedrine Hydrochloride	98	0.32	0.33	0.47	0.4826s
Ondansetron Solution	99	0.37	0.35	0.63	0.4826s
FRUSEMIDE	102	0.36	0.28	0.55	0.4826s
DALACINC PHOSPHATE	99	0.34	0.30	0.65	0.4826s
METOPROLOL Mylan	97	0.37	0.33	0.55	0.4826s
WATER FOR INJECTIONS BP	97	0.43	0.31	0.65	0.4826s
MORPHINE SULFATE	97	0.39	0.33	0.68	0.4826s
Glycopyrronium and Neostigmine	95	0.44	0.39	0.67	0.4826s
Clonidine HCl	101	0.35	0.28	0.53	0.4826s
Rocuronium Bromide 50 mg in 5 ml	88	0.39	0.39	0.55	0.4826s
Fresofol 1% MCT/LCT	302	0.32	0.30	0.62	0.4826s
Sedative Midazolam 5mg	101	0.37	0.30	0.60	0.4826s
Adrenaline Injection	95	0.35	0.34	0.47	0.4826s
Paracetamol Kabi	499	0.25	0.23	0.57	0.4826s
Provive MCT-LCT 1%	246	0.38	0.32	0.59	0.4826s
Adrenaline Injection 1mg in 10mL	95	0.35	0.34	0.47	0.4826s
Amoxicillin Sodium	124	0.44	0.35	0.69	0.4826s
Lidocain Injection	101	0.33	0.28	0.50	0.4826s
SODIUM CHLORIDE	112	0.47	0.38	0.60	0.4826s
Remifentanil-Act Injection	97	0.46	0.37	0.62	0.4826s
Sterile Dopamine	91	0.58	0.40	0.52	0.4826s
Hypnomida Etomidate 2mg	98	0.4	0.33	0.56	0.4826s
Xylocaine 1%	102	0.32	0.27	0.36	0.4826s
Fentanyl Injection	112	0.46	0.40	0.68	0.4826s
Noradrenaline acid	89	0.41	0.41	0.55	0.4826s
Magnesium Sulfate 2.47g in 5mL	88	0.49	0.41	0.54	0.4826s
Sugammadex Injection	97	0.44	0.33	0.61	0.4826s
Dynastat Powder	90	0.4	0.40	0.60	0.4826s
Hydrocortisone sodium	97	0.42	0.36	0.63	0.4826s
Atracurium Besylate	95	0.38	0.33	0.55	0.4826s
Atropine	104	0.32	0.25	0.53	0.4826s
PancuroInresa	99	0.39	0.35	0.68	0.4826s

Drug Identification: Sugammadex Injection against other samples

Drug Name	Edit Distance	TSR Scores	Lev Scores	Jacc Scores	Processing Time
Primacor Injection	73	0.56	0.39	0.58	0.4521s
Cefazolin Sodium 1g	107	0.45	0.37	0.59	0.4521s
NALOXONE HCl 400mg in 1mL	59	0.38	0.29	0.52	0.4521s
Calcium Chloride 1g in 10mL	99	0.53	0.38	0.62	0.4521s
Actrapid Penfill 3ml	61	0.55	0.35	0.72	0.4521s
Vecuronium bromide	55	0.46	0.44	0.67	0.4521s
Sugammadex 200mg/2ml	48	0.87	0.67	0.92	0.4521s
Amiodarone Hydrochloride	68	0.57	0.40	0.73	0.4521s
Protamine Sulphate 50mg in 5ml	80	0.55	0.37	0.62	0.4521s
Summethonium Chloride 100mg in 2mL	57	0.57	0.38	0.81	0.4521s
Protamine Sulfate 10mg/ml	62	0.56	0.47	0.75	0.4521s
Glyceryl Trinitrate 1 mg/ml	78	0.46	0.38	0.70	0.4521s
Tranexamic acid	64	0.46	0.36	0.67	0.4521s
Heparin Injection 25000IU in 5 mL	65	0.54	0.39	0.67	0.4521s
Sterile Potassium Chloride	94	0.44	0.33	0.62	0.4521s
Metaraminol 10mg/ml	48	0.56	0.52	0.79	0.4521s
Cyclizine lactate	64	0.26	0.19	0.39	0.4521s
PITRESSIN argipressin	55	0.5	0.37	0.71	0.4521s
Dexamethasone phosphate 4 mg/ml	57	0.52	0.50	0.68	0.4521s
Ephedrine Hydrochloride	59	0.4	0.28	0.54	0.4521s
Ondansetron Solution	70	0.42	0.35	0.67	0.4521s
FRUSEMIDE	60	0.4	0.32	0.57	0.4521s
DALACINC PHOSPHATE	59	0.42	0.31	0.58	0.4521s
METOPROLOL Mylan	73	0.51	0.44	0.69	0.4521s
WATER FOR INJECTIONS BP	78	0.49	0.34	0.64	0.4521s
MORPHINE SULFATE	55	0.51	0.39	0.73	0.4521s
Glycopyrronium and Neostigmine	72	0.54	0.38	0.85	0.4521s
Clonidine HCl	55	0.49	0.38	0.62	0.4521s
Rocuronium Bromide 50 mg in 5 ml	60	0.55	0.42	0.71	0.4521s
Fresofol 1% MCT/LCT	319	0.69	0.25	0.56	0.4521s
Sedative Midazolam 5mg	60	0.42	0.30	0.63	0.4521s
Adrenaline Injection	62	0.41	0.41	0.67	0.4521s
Paracetamol Kabi	521	0.29	0.18	0.55	0.4521s
Provive MCT-LCT 1%	258	0.52	0.28	0.61	0.4521s
Adrenaline Injection 1mg in 10mL	62	0.41	0.41	0.67	0.4521s
Amoxicillin Sodium	123	0.43	0.31	0.59	0.4521s
Lidocain Injection	56	0.35	0.34	0.58	0.4521s
SODIUM CHLORIDE	114	0.41	0.31	0.58	0.4521s
Remifentanil-Act Injection	69	0.5	0.43	0.66	0.4521s
Sterile Dopamine	57	0.46	0.39	0.65	0.4521s
Hypnomida Etomidate 2mg	64	0.53	0.38	0.63	0.4521s
Xylocaine 1%	58	0.35	0.32	0.45	0.4521s
Fentanyl Injection	114	0.48	0.35	0.67	0.4521s
Noradrenaline acid	69	0.35	0.36	0.63	0.4521s
Magnesium Sulfate 2.47g in 5mL	64	0.54	0.42	0.66	0.4521s
Sugammadex Injection	**1**	**1.0**	**0.99**	**1.00**	**0.4521s**
Dynastat Powder	61	0.49	0.46	0.69	0.4521s
Hydrocortisone sodium	71	0.47	0.41	0.67	0.4521s
Atracurium Besylate	55	0.37	0.38	0.64	0.4521s
Atropine	58	0.44	0.33	0.68	0.4521s
PancuroInresa	77	0.44	0.35	0.72	0.4521s

Drug Identification: Lidocain Injection against other samples

Drug Name	Edit Distance	TSR Scores	Lev Scores	Jacc Scores	Processing Time
Primacor Injection	75	0.35	0.31	0.55	0.3668s
Cefazolin Sodium 1g	120	0.32	0.28	0.57	0.3668s
NALOXONE HCl 400mg in 1mL	31	0.42	0.30	0.61	0.3668s
Calcium Chloride 1g in 10mL	106	0.34	0.30	0.60	0.3668s
Actrapid Penfill 3ml	57	0.4	0.29	0.53	0.3668s
Vecuronium bromide	42	0.37	0.33	0.52	0.3668s
Sugammadex 200mg/2ml	61	0.37	0.33	0.52	0.3668s
Amiodarone Hydrochloride	65	0.35	0.32	0.58	0.3668s
Protamine Sulphate 50mg in 5ml	79	0.4	0.30	0.55	0.3668s
Summethonium Chloride 100mg in 2mL	46	0.32	0.24	0.59	0.3668s
Protamine Sulfate 10mg/ml	65	0.35	0.32	0.50	0.3668s
Glyceryl Trinitrate 1 mg/ml	84	0.33	0.26	0.56	0.3668s
Tranexamic acid	58	0.34	0.31	0.53	0.3668s
Heparin Injection 25000IU in 5 mL	65	0.4	0.29	0.59	0.3668s
Sterile Potassium Chloride	97	0.34	0.29	0.55	0.3668s
Metaraminol 10mg/ml	44	0.4	0.34	0.62	0.3668s
Cyclizine lactate	30	0.34	0.28	0.46	0.3668s
PITRESSIN argipressin	37	0.42	0.37	0.54	0.3668s
Dexamethasone phosphate 4 mg/ml	52	0.42	0.35	0.59	0.3668s
Ephedrine Hydrochloride	40	0.35	0.35	0.64	0.3668s
Ondansetron Solution	68	0.33	0.32	0.44	0.3668s
FRUSEMIDE	46	0.35	0.31	0.54	0.3668s
DALACINC PHOSPHATE	48	0.37	0.27	0.45	0.3668s
METOPROLOL Mylan	75	0.31	0.27	0.48	0.3668s
WATER FOR INJECTIONS BP	80	0.32	0.29	0.56	0.3668s
MORPHINE SULFATE	33	0.41	0.37	0.71	0.3668s
Glycopyrronium and Neostigmine	70	0.34	0.28	0.57	0.3668s
Clonidine HCl	25	0.47	0.47	0.65	0.3668s
Rocuronium Bromide 50 mg in 5 ml	60	0.39	0.35	0.54	0.3668s
Fresofol 1% MCT/LCT	345	0.16	0.14	0.46	0.3668s
Sedative Midazolam 5mg	48	0.38	0.29	0.41	0.3668s
Adrenaline Injection	57	0.36	0.33	0.57	0.3668s
Paracetamol Kabi	549	0.11	0.10	0.45	0.3668s
Provive MCT-LCT 1%	283	0.18	0.17	0.54	0.3668s
Adrenaline Injection 1mg in 10mL	57	0.36	0.33	0.57	0.3668s
Amoxicillin Sodium	133	0.27	0.26	0.52	0.3668s
Lidocain Injection	**2**	**1.0**	**0.97**	**0.95**	**0.3668s**
SODIUM CHLORIDE	117	0.28	0.29	0.51	0.3668s
Remifentanil-Act Injection	81	0.35	0.29	0.57	0.3668s
Sterile Dopamine	35	0.38	0.37	0.44	0.3668s
Hypnomida Etomidate 2mg	64	0.35	0.34	0.61	0.3668s
Xylocaine 1%	25	0.63	0.51	0.46	0.3668s
Fentanyl Injection	126	0.26	0.25	0.46	0.3668s
Noradrenaline acid	66	0.35	0.30	0.48	0.3668s
Magnesium Sulfate 2.47g in 5mL	69	0.35	0.31	0.48	0.3668s
Sugammadex Injection	55	0.35	0.36	0.56	0.3668s
Dynastat Powder	77	0.35	0.29	0.50	0.3668s
Hydrocortisone sodium	87	0.31	0.24	0.64	0.3668s
Atracurium Besylate	44	0.34	0.31	0.54	0.3668s
Atropine	28	0.45	0.39	0.52	0.3668s
PancuroInresa	81	0.33	0.31	0.53	0.3668s

Drug Identification: WATER FOR INJECTIONS BP against other samples

Drug Name	Edit Distance	TSR Scores	Lev Scores	Jacc Scores	Processing Time
Primacor Injection	84	0.5	0.35	0.56	0.4934s
Cefazolin Sodium 1g	112	0.44	0.34	0.62	0.4934s
NALOXONE HCl 400mg in 1mL	87	0.31	0.22	0.47	0.4934s
Calcium Chloride 1g in 10mL	96	0.44	0.41	0.65	0.4934s
Actrapid Penfill 3ml	74	0.47	0.39	0.59	0.4934s
Vecuronium bromide	74	0.4	0.36	0.64	0.4934s
Sugammadex 200mg/2ml	78	0.46	0.36	0.58	0.4934s
Amiodarone Hydrochloride	77	0.36	0.38	0.46	0.4934s
Protamine Sulphate 50mg in 5ml	76	0.54	0.42	0.65	0.4934s
Summethonium Chloride 100mg in 2mL	78	0.41	0.32	0.65	0.4934s
Protamine Sulfate 10mg/ml	76	0.54	0.36	0.66	0.4934s
Glyceryl Trinitrate 1 mg/ml	90	0.42	0.33	0.49	0.4934s
Tranexamic acid	81	0.5	0.37	0.64	0.4934s
Heparin Injection 25000IU in 5 mL	74	0.47	0.36	0.64	0.4934s
Sterile Potassium Chloride	96	0.43	0.31	0.65	0.4934s
Metaraminol 10mg/ml	75	0.51	0.37	0.53	0.4934s
Cyclizine lactate	89	0.28	0.17	0.45	0.4934s
PITRESSIN argipressin	78	0.39	0.33	0.52	0.4934s
Dexamethasone phosphate 4 mg/ml	76	0.46	0.37	0.60	0.4934s
Ephedrine Hydrochloride	77	0.31	0.34	0.44	0.4934s
Ondansetron Solution	80	0.42	0.33	0.59	0.4934s
FRUSEMIDE	83	0.39	0.28	0.56	0.4934s
DALACINC PHOSPHATE	84	0.45	0.30	0.57	0.4934s
METOPROLOL Mylan	79	0.42	0.37	0.51	0.4934s
WATER FOR INJECTIONS BP	**2**	**1.0**	**0.99**	**0.97**	**0.4934s**
MORPHINE SULFATE	80	0.51	0.36	0.64	0.4934s
Glycopyrronium and Neostigmine	79	0.46	0.38	0.68	0.4934s
Clonidine HCl	80	0.38	0.29	0.46	0.4934s
Rocuronium Bromide 50 mg in 5 ml	82	0.43	0.34	0.52	0.4934s
Fresofol 1% MCT/LCT	308	0.45	0.29	0.63	0.4934s
Sedative Midazolam 5mg	80	0.39	0.30	0.66	0.4934s
Adrenaline Injection	74	0.42	0.40	0.48	0.4934s
Paracetamol Kabi	511	0.45	0.21	0.68	0.4934s
Provive MCT-LCT 1%	253	0.34	0.29	0.68	0.4934s
Adrenaline Injection 1mg in 10mL	74	0.42	0.40	0.48	0.4934s
Amoxicillin Sodium	123	0.38	0.35	0.66	0.4934s
Lidocain Injection	82	0.32	0.29	0.52	0.4934s
SODIUM CHLORIDE	114	0.38	0.32	0.69	0.4934s
Remifentanil-Act Injection	89	0.47	0.36	0.58	0.4934s
Sterile Dopamine	80	0.41	0.29	0.53	0.4934s
Hypnomida Etomidate 2mg	82	0.52	0.38	0.61	0.4934s
Xylocaine 1%	77	0.36	0.36	0.38	0.4934s
Fentanyl Injection	119	0.48	0.36	0.56	0.4934s
Noradrenaline acid	82	0.43	0.31	0.51	0.4934s
Magnesium Sulfate 2.47g in 5mL	85	0.43	0.34	0.63	0.4934s
Sugammadex Injection	79	0.49	0.35	0.62	0.4934s
Dynastat Powder	81	0.47	0.38	0.66	0.4934s
Hydrocortisone sodium	89	0.43	0.37	0.64	0.4934s
Atracurium Besylate	80	0.33	0.32	0.52	0.4934s
Atropine	79	0.4	0.34	0.55	0.4934s
PancuroInresa	81	0.43	0.39	0.74	0.4934s

Drug Identification: Remifentanil-Act Injection against other samples

Drug Name	Edit Distance	TSR Scores	Lev Scores	Jacc Scores	Processing Time
Primacor Injection	79	0.53	0.44	0.59	0.4999s
Cefazolin Sodium 1g	95	0.54	0.47	0.71	0.4999s
NALOXONE HCl 400mg in 1mL	83	0.32	0.29	0.43	0.4999s
Calcium Chloride 1g in 10mL	96	0.45	0.40	0.59	0.4999s
Actrapid Penfill 3ml	84	0.45	0.30	0.62	0.4999s
Vecuronium bromide	69	0.51	0.46	0.74	0.4999s
Sugammadex 200mg/2ml	82	0.49	0.39	0.67	0.4999s
Amiodarone Hydrochloride	82	0.48	0.38	0.74	0.4999s
Protamine Sulphate 50mg in 5ml	85	0.51	0.38	0.69	0.4999s
Summethonium Chloride 100mg in 2mL	77	0.42	0.36	0.69	0.4999s
Protamine Sulfate 10mg/ml	74	0.48	0.44	0.59	0.4999s
Glyceryl Trinitrate 1 mg/ml	89	0.44	0.35	0.60	0.4999s
Tranexamic acid	81	0.46	0.37	0.58	0.4999s
Heparin Injection 25000IU in 5 mL	80	0.46	0.36	0.62	0.4999s
Sterile Potassium Chloride	97	0.46	0.37	0.64	0.4999s
Metaraminol 10mg/ml	76	0.44	0.36	0.61	0.4999s
Cyclizine lactate	90	0.21	0.18	0.41	0.4999s
PITRESSIN argipressin	75	0.42	0.38	0.59	0.4999s
Dexamethasone phosphate 4 mg/ml	81	0.5	0.37	0.69	0.4999s
Ephedrine Hydrochloride	68	0.58	0.45	0.68	0.4999s
Ondansetron Solution	74	0.44	0.43	0.73	0.4999s
FRUSEMIDE	83	0.34	0.30	0.53	0.4999s
DALACINC PHOSPHATE	83	0.34	0.28	0.55	0.4999s
METOPROLOL Mylan	85	0.5	0.44	0.70	0.4999s
WATER FOR INJECTIONS BP	88	0.47	0.36	0.60	0.4999s
MORPHINE SULFATE	79	0.42	0.33	0.68	0.4999s
Glycopyrronium and Neostigmine	81	0.47	0.38	0.61	0.4999s
Clonidine HCl	82	0.44	0.30	0.52	0.4999s
Rocuronium Bromide 50 mg in 5 ml	74	0.42	0.39	0.54	0.4999s
Fresofol 1% MCT/LCT	311	0.34	0.28	0.62	0.4999s
Sedative Midazolam 5mg	83	0.31	0.26	0.46	0.4999s
Adrenaline Injection	70	0.51	0.43	0.56	0.4999s
Paracetamol Kabi	501	0.24	0.23	0.56	0.4999s
Provive MCT-LCT 1%	247	0.34	0.33	0.67	0.4999s
Adrenaline Injection 1mg in 10mL	70	0.51	0.43	0.56	0.4999s
Amoxicillin Sodium	121	0.48	0.33	0.70	0.4999s
Lidocain Injection	83	0.35	0.28	0.59	0.4999s
SODIUM CHLORIDE	111	0.41	0.35	0.59	0.4999s
Remifentanil-Act Injection	**1**	**1.0**	**1.00**	**1.00**	**0.4999s**
Sterile Dopamine	82	0.34	0.30	0.50	0.4999s
Hypnomida Etomidate 2mg	78	0.42	0.36	0.76	0.4999s
Xylocaine 1%	83	0.34	0.29	0.47	0.4999s
Fentanyl Injection	99	0.57	0.50	0.63	0.4999s
Noradrenaline acid	79	0.45	0.35	0.59	0.4999s
Magnesium Sulfate 2.47g in 5mL	79	0.49	0.36	0.57	0.4999s
Sugammadex Injection	69	0.5	0.43	0.66	0.4999s
Dynastat Powder	64	0.57	0.52	0.76	0.4999s
Hydrocortisone sodium	73	0.51	0.47	0.86	0.4999s
Atracurium Besylate	78	0.39	0.36	0.65	0.4999s
Atropine	78	0.43	0.35	0.63	0.4999s
PancuroInresa	81	0.44	0.38	0.58	0.4999s

Drug Identification: Cyclizine lactate against other samples

Drug Name	Edit Distance	TSR Scores	Lev Scores	Jacc Scores	Processing Time
Primacor Injection	83	0.24	0.21	0.36	0.4218s
Cefazolin Sodium 1g	132	0.17	0.14	0.38	0.4218s
NALOXONE HCl 400mg in 1mL	26	0.27	0.23	0.42	0.4218s
Calcium Chloride 1g in 10mL	117	0.22	0.17	0.41	0.4218s
Actrapid Penfill 3ml	58	0.28	0.20	0.43	0.4218s
Vecuronium bromide	49	0.24	0.21	0.41	0.4218s
Sugammadex 200mg/2ml	69	0.25	0.18	0.37	0.4218s
Amiodarone Hydrochloride	74	0.2	0.17	0.41	0.4218s
Protamine Sulphate 50mg in 5ml	85	0.24	0.20	0.36	0.4218s
Summethonium Chloride 100mg in 2mL	46	0.29	0.26	0.43	0.4218s
Protamine Sulfate 10mg/ml	72	0.27	0.19	0.45	0.4218s
Glyceryl Trinitrate 1 mg/ml	91	0.26	0.19	0.44	0.4218s
Tranexamic acid	62	0.3	0.27	0.43	0.4218s
Heparin Injection 25000IU in 5 mL	71	0.24	0.20	0.39	0.4218s
Sterile Potassium Chloride	108	0.24	0.17	0.36	0.4218s
Metaraminol 10mg/ml	50	0.28	0.23	0.44	0.4218s
Cyclizine lactate	**1**	**1.0**	**0.98**	**1.00**	**0.4218s**
PITRESSIN argipressin	44	0.23	0.25	0.48	0.4218s
Dexamethasone phosphate 4 mg/ml	59	0.25	0.20	0.48	0.4218s
Ephedrine Hydrochloride	42	0.23	0.23	0.50	0.4218s
Ondansetron Solution	73	0.26	0.25	0.48	0.4218s
FRUSEMIDE	51	0.3	0.22	0.48	0.4218s
DALACINC PHOSPHATE	51	0.22	0.22	0.35	0.4218s
METOPROLOL Mylan	82	0.22	0.18	0.48	0.4218s
WATER FOR INJECTIONS BP	87	0.28	0.18	0.47	0.4218s
MORPHINE SULFATE	38	0.3	0.26	0.46	0.4218s
Glycopyrronium and Neostigmine	73	0.22	0.21	0.41	0.4218s
Clonidine HCl	26	0.26	0.26	0.35	0.4218s
Rocuronium Bromide 50 mg in 5 ml	71	0.22	0.18	0.31	0.4218s
Fresofol 1% MCT/LCT	355	0.13	0.09	0.42	0.4218s
Sedative Midazolam 5mg	50	0.36	0.27	0.40	0.4218s
Adrenaline Injection	65	0.25	0.19	0.38	0.4218s
Paracetamol Kabi	560	0.08	0.07	0.38	0.4218s
Provive MCT-LCT 1%	294	0.12	0.10	0.42	0.4218s
Adrenaline Injection 1mg in 10mL	65	0.25	0.19	0.38	0.4218s
Amoxicillin Sodium	141	0.18	0.15	0.42	0.4218s
Lidocain Injection	29	0.34	0.25	0.48	0.4218s
SODIUM CHLORIDE	126	0.23	0.20	0.47	0.4218s
Remifentanil-Act Injection	88	0.21	0.20	0.41	0.4218s
Sterile Dopamine	40	0.27	0.24	0.38	0.4218s
Hypnomida Etomidate 2mg	69	0.32	0.24	0.45	0.4218s
Xylocaine 1%	30	0.35	0.25	0.46	0.4218s
Fentanyl Injection	134	0.17	0.16	0.33	0.4218s
Noradrenaline acid	73	0.21	0.21	0.48	0.4218s
Magnesium Sulfate 2.47g in 5mL	75	0.26	0.22	0.31	0.4218s
Sugammadex Injection	62	0.26	0.22	0.39	0.4218s
Dynastat Powder	83	0.19	0.21	0.45	0.4218s
Hydrocortisone sodium	94	0.18	0.16	0.43	0.4218s
Atracurium Besylate	49	0.24	0.18	0.55	0.4218s
Atropine	25	0.31	0.27	0.46	0.4218s
PancuroInresa	85	0.25	0.22	0.43	0.4218s

Drug Identification: Noradrenaline acid against other samples

Drug Name	Edit Distance	TSR Scores	Lev Scores	Jacc Scores	Processing Time
Primacor Injection	78	0.4	0.35	0.52	0.4658s
Cefazolin Sodium 1g	114	0.38	0.33	0.48	0.4658s
NALOXONE HCl 400mg in 1mL	70	0.3	0.28	0.56	0.4658s
Calcium Chloride 1g in 10mL	98	0.39	0.35	0.56	0.4658s
Actrapid Penfill 3ml	71	0.37	0.32	0.50	0.4658s
Vecuronium bromide	68	0.32	0.29	0.59	0.4658s
Sugammadex 200mg/2ml	70	0.38	0.33	0.59	0.4658s
Amiodarone Hydrochloride	62	0.45	0.43	0.59	0.4658s
Protamine Sulphate 50mg in 5ml	78	0.38	0.34	0.52	0.4658s
Summethonium Chloride 100mg in 2mL	70	0.34	0.29	0.61	0.4658s
Protamine Sulfate 10mg/ml	67	0.42	0.37	0.62	0.4658s
Glyceryl Trinitrate 1 mg/ml	82	0.36	0.37	0.57	0.4658s
Tranexamic acid	68	0.44	0.38	0.60	0.4658s
Heparin Injection 25000IU in 5 mL	70	0.36	0.33	0.50	0.4658s
Sterile Potassium Chloride	86	0.41	0.41	0.56	0.4658s
Metaraminol 10mg/ml	68	0.36	0.32	0.58	0.4658s
Cyclizine lactate	75	0.21	0.23	0.48	0.4658s
PITRESSIN argipressin	66	0.35	0.37	0.62	0.4658s
Dexamethasone phosphate 4 mg/ml	69	0.35	0.30	0.67	0.4658s
Ephedrine Hydrochloride	67	0.38	0.33	0.58	0.4658s
Ondansetron Solution	68	0.48	0.42	0.66	0.4658s
FRUSEMIDE	69	0.37	0.28	0.56	0.4658s
DALACINC PHOSPHATE	66	0.34	0.32	0.52	0.4658s
METOPROLOL Mylan	81	0.41	0.31	0.62	0.4658s
WATER FOR INJECTIONS BP	81	0.43	0.30	0.53	0.4658s
MORPHINE SULFATE	63	0.36	0.35	0.65	0.4658s
Glycopyrronium and Neostigmine	73	0.38	0.32	0.64	0.4658s
Clonidine HCl	67	0.28	0.29	0.48	0.4658s
Rocuronium Bromide 50 mg in 5 ml	72	0.35	0.33	0.62	0.4658s
Fresofol 1% MCT/LCT	323	0.31	0.22	0.44	0.4658s
Sedative Midazolam 5mg	68	0.36	0.28	0.52	0.4658s
Adrenaline Injection	57	0.46	0.53	0.58	0.4658s
Paracetamol Kabi	516	0.24	0.20	0.47	0.4658s
Provive MCT-LCT 1%	259	0.31	0.27	0.51	0.4658s
Adrenaline Injection 1mg in 10mL	57	0.46	0.53	0.58	0.4658s
Amoxicillin Sodium	118	0.4	0.34	0.58	0.4658s
Lidocain Injection	68	0.35	0.29	0.50	0.4658s
SODIUM CHLORIDE	111	0.38	0.35	0.53	0.4658s
Remifentanil-Act Injection	80	0.45	0.35	0.59	0.4658s
Sterile Dopamine	60	0.44	0.38	0.58	0.4658s
Hypnomida Etomidate 2mg	72	0.38	0.32	0.52	0.4658s
Xylocaine 1%	69	0.32	0.30	0.48	0.4658s
Fentanyl Injection	115	0.41	0.36	0.51	0.4658s
Noradrenaline acid	**1**	**1.0**	**0.99**	**1.00**	**0.4658s**
Magnesium Sulfate 2.47g in 5mL	75	0.44	0.38	0.50	0.4658s
Sugammadex Injection	69	0.35	0.35	0.63	0.4658s
Dynastat Powder	78	0.43	0.36	0.68	0.4658s
Hydrocortisone sodium	86	0.34	0.33	0.55	0.4658s
Atracurium Besylate	67	0.38	0.33	0.77	0.4658s
Atropine	71	0.27	0.26	0.54	0.4658s
PancuroInresa	80	0.38	0.33	0.55	0.4658s

Drug Identification: Vecuronium bromide against other samples

Drug Name	Edit Distance	TSR Scores	Lev Scores	Jacc Scores	Processing Time
Primacor Injection	71	0.41	0.36	0.55	0.5211s
Cefazolin Sodium 1g	103	0.49	0.44	0.61	0.5211s
NALOXONE HCl 400mg in 1mL	43	0.33	0.32	0.43	0.5211s
Calcium Chloride 1g in 10mL	97	0.33	0.38	0.65	0.5211s
Actrapid Penfill 3ml	56	0.42	0.34	0.58	0.5211s
Vecuronium bromide	**1**	**1.0**	**0.99**	**1.00**	**0.5211s**
Sugammadex 200mg/2ml	52	0.46	0.45	0.62	0.5211s
Amiodarone Hydrochloride	60	0.4	0.41	0.63	0.5211s
Protamine Sulphate 50mg in 5ml	69	0.47	0.42	0.65	0.5211s
Summethonium Chloride 100mg in 2mL	45	0.51	0.40	0.70	0.5211s
Protamine Sulfate 10mg/ml	54	0.51	0.43	0.60	0.5211s
Glyceryl Trinitrate 1 mg/ml	80	0.29	0.33	0.55	0.5211s
Tranexamic acid	59	0.41	0.29	0.58	0.5211s
Heparin Injection 25000IU in 5 mL	59	0.46	0.37	0.58	0.5211s
Sterile Potassium Chloride	95	0.43	0.33	0.59	0.5211s
Metaraminol 10mg/ml	41	0.46	0.44	0.56	0.5211s
Cyclizine lactate	50	0.24	0.23	0.41	0.5211s
PITRESSIN argipressin	39	0.45	0.45	0.54	0.5211s
Dexamethasone phosphate 4 mg/ml	46	0.46	0.41	0.59	0.5211s
Ephedrine Hydrochloride	45	0.39	0.40	0.70	0.5211s
Ondansetron Solution	64	0.36	0.34	0.63	0.5211s
FRUSEMIDE	52	0.34	0.31	0.48	0.5211s
DALACINC PHOSPHATE	53	0.35	0.28	0.45	0.5211s
METOPROLOL Mylan	66	0.44	0.39	0.65	0.5211s
WATER FOR INJECTIONS BP	74	0.4	0.37	0.66	0.5211s
MORPHINE SULFATE	46	0.4	0.35	0.69	0.5211s
Glycopyrronium and Neostigmine	68	0.46	0.41	0.68	0.5211s
Clonidine HCl	41	0.37	0.39	0.46	0.5211s
Rocuronium Bromide 50 mg in 5 ml	57	0.53	0.47	0.60	0.5211s
Fresofol 1% MCT/LCT	333	0.36	0.19	0.54	0.5211s
Sedative Midazolam 5mg	48	0.32	0.31	0.45	0.5211s
Adrenaline Injection	57	0.36	0.35	0.62	0.5211s
Paracetamol Kabi	530	0.36	0.16	0.52	0.5211s
Provive MCT-LCT 1%	268	0.26	0.23	0.63	0.5211s
Adrenaline Injection 1mg in 10mL	57	0.36	0.35	0.62	0.5211s
Amoxicillin Sodium	126	0.4	0.37	0.61	0.5211s
Lidocain Injection	43	0.37	0.33	0.48	0.5211s
SODIUM CHLORIDE	113	0.31	0.32	0.60	0.5211s
Remifentanil-Act Injection	68	0.51	0.46	0.74	0.5211s
Sterile Dopamine	48	0.3	0.29	0.45	0.5211s
Hypnomida Etomidate 2mg	57	0.38	0.41	0.60	0.5211s
Xylocaine 1%	41	0.4	0.40	0.41	0.5211s
Fentanyl Injection	122	0.39	0.28	0.59	0.5211s
Noradrenaline acid	67	0.32	0.30	0.59	0.5211s
Magnesium Sulfate 2.47g in 5mL	69	0.34	0.34	0.58	0.5211s
Sugammadex Injection	54	0.46	0.46	0.67	0.5211s
Dynastat Powder	63	0.56	0.48	0.71	0.5211s
Hydrocortisone sodium	71	0.49	0.44	0.69	0.5211s
Atracurium Besylate	47	0.46	0.32	0.74	0.5211s
Atropine	44	0.4	0.33	0.58	0.5211s
PancuroInresa	74	0.42	0.40	0.63	0.5211s

Drug Identification: SODIUM CHLORIDE against other samples

Drug Name	Edit Distance	TSR Scores	Lev Scores	Jacc Scores	Processing Time
Primacor Injection	151	0.35	0.29	0.41	0.5734s
Cefazolin Sodium 1g	149	0.38	0.31	0.39	0.5734s
NALOXONE HCl 400mg in 1mL	161	0.22	0.20	0.31	0.5734s
Calcium Chloride 1g in 10mL	139	0.4	0.36	0.46	0.5734s
Actrapid Penfill 3ml	157	0.34	0.23	0.42	0.5734s
Vecuronium bromide	156	0.25	0.23	0.38	0.5734s
Sugammadex 200mg/2ml	153	0.35	0.25	0.39	0.5734s
Amiodarone Hydrochloride	150	0.33	0.31	0.41	0.5734s
Protamine Sulphate 50mg in 5ml	150	0.32	0.29	0.46	0.5734s
Summethonium Chloride 100mg in 2mL	155	0.33	0.28	0.42	0.5734s
Protamine Sulfate 10mg/ml	153	0.34	0.27	0.43	0.5734s
Glyceryl Trinitrate 1 mg/ml	148	0.34	0.27	0.40	0.5734s
Tranexamic acid	155	0.36	0.26	0.42	0.5734s
Heparin Injection 25000IU in 5 mL	153	0.34	0.27	0.40	0.5734s
Sterile Potassium Chloride	153	0.41	0.32	0.41	0.5734s
Metaraminol 10mg/ml	155	0.3	0.23	0.37	0.5734s
Cyclizine lactate	167	0.17	0.15	0.30	0.5734s
PITRESSIN argipressin	155	0.28	0.25	0.33	0.5734s
Dexamethasone phosphate 4 mg/ml	155	0.31	0.25	0.42	0.5734s
Ephedrine Hydrochloride	158	0.25	0.23	0.31	0.5734s
Ondansetron Solution	153	0.31	0.28	0.40	0.5734s
FRUSEMIDE	155	0.31	0.24	0.34	0.5734s
DALACINC PHOSPHATE	158	0.26	0.21	0.40	0.5734s
METOPROLOL Mylan	154	0.31	0.27	0.39	0.5734s
WATER FOR INJECTIONS BP	143	0.35	0.31	0.47	0.5734s
MORPHINE SULFATE	158	0.29	0.23	0.41	0.5734s
Glycopyrronium and Neostigmine	152	0.35	0.27	0.46	0.5734s
Clonidine HCl	161	0.26	0.20	0.35	0.5734s
Rocuronium Bromide 50 mg in 5 ml	151	0.3	0.30	0.33	0.5734s
Fresofol 1% MCT/LCT	307	0.35	0.28	0.56	0.5734s
Sedative Midazolam 5mg	158	0.26	0.21	0.38	0.5734s
Adrenaline Injection	150	0.26	0.29	0.27	0.5734s
Paracetamol Kabi	500	0.32	0.22	0.52	0.5734s
Provive MCT-LCT 1%	252	0.41	0.29	0.53	0.5734s
Adrenaline Injection 1mg in 10mL	150	0.26	0.29	0.27	0.5734s
Amoxicillin Sodium	152	0.38	0.29	0.42	0.5734s
Lidocain Injection	161	0.22	0.21	0.31	0.5734s
SODIUM CHLORIDE	**102**	**0.96**	**0.89**	**0.93**	**0.5734s**
Remifentanil-Act Injection	150	0.34	0.31	0.39	0.5734s
Sterile Dopamine	159	0.26	0.22	0.35	0.5734s
Hypnomida Etomidate 2mg	151	0.34	0.27	0.43	0.5734s
Xylocaine 1%	161	0.2	0.20	0.30	0.5734s
Fentanyl Injection	154	0.38	0.30	0.43	0.5734s
Noradrenaline acid	150	0.32	0.29	0.34	0.5734s
Magnesium Sulfate 2.47g in 5mL	151	0.33	0.26	0.47	0.5734s
Sugammadex Injection	151	0.35	0.28	0.40	0.5734s
Dynastat Powder	149	0.32	0.30	0.43	0.5734s
Hydrocortisone sodium	155	0.38	0.27	0.42	0.5734s
Atracurium Besylate	157	0.28	0.24	0.33	0.5734s
Atropine	165	0.22	0.17	0.33	0.5734s
PancuroInresa	153	0.34	0.27	0.40	0.5734s

Drug Identification: Provive MCT-LCT against other samples

Drug Name	Edit Distance	TSR Scores	Lev Scores	Jacc Scores	Processing Time
Primacor Injection	256	0.4	0.29	0.64	0.4913s
Cefazolin Sodium 1g	212	0.71	0.46	0.62	0.4913s
NALOXONE HCl 400mg in 1mL	286	0.16	0.15	0.43	0.4913s
Calcium Chloride 1g in 10mL	246	0.42	0.37	0.73	0.4913s
Actrapid Penfill 3ml	269	0.32	0.23	0.59	0.4913s
Vecuronium bromide	270	0.26	0.23	0.63	0.4913s
Sugammadex 200mg/2ml	258	0.46	0.28	0.58	0.4913s
Amiodarone Hydrochloride	252	0.48	0.31	0.58	0.4913s
Protamine Sulphate 50mg in 5ml	250	0.36	0.32	0.68	0.4913s
Summethonium Chloride 100mg in 2mL	268	0.38	0.24	0.69	0.4913s
Protamine Sulfate 10mg/ml	257	0.32	0.28	0.56	0.4913s
Glyceryl Trinitrate 1 mg/ml	252	0.33	0.30	0.57	0.4913s
Tranexamic acid	265	0.32	0.25	0.59	0.4913s
Heparin Injection 25000IU in 5 mL	259	0.36	0.29	0.55	0.4913s
Sterile Potassium Chloride	248	0.38	0.31	0.60	0.4913s
Metaraminol 10mg/ml	264	0.59	0.26	0.53	0.4913s
Cyclizine lactate	296	0.12	0.10	0.42	0.4913s
PITRESSIN argipressin	269	0.27	0.24	0.51	0.4913s
Dexamethasone phosphate 4 mg/ml	260	0.51	0.27	0.55	0.4913s
Ephedrine Hydrochloride	276	0.31	0.20	0.49	0.4913s
Ondansetron Solution	259	0.31	0.27	0.59	0.4913s
FRUSEMIDE	265	0.3	0.25	0.56	0.4913s
DALACINC PHOSPHATE	273	0.24	0.21	0.49	0.4913s
METOPROLOL Mylan	245	0.47	0.34	0.51	0.4913s
WATER FOR INJECTIONS BP	255	0.34	0.29	0.69	0.4913s
MORPHINE SULFATE	273	0.49	0.22	0.63	0.4913s
Glycopyrronium and Neostigmine	259	0.34	0.27	0.62	0.4913s
Clonidine HCl	285	0.44	0.16	0.46	0.4913s
Rocuronium Bromide 50 mg in 5 ml	261	0.46	0.28	0.47	0.4913s
Fresofol 1% MCT/LCT	271	0.64	0.47	0.74	0.4913s
Sedative Midazolam 5mg	275	0.24	0.20	0.49	0.4913s
Adrenaline Injection	265	0.3	0.25	0.44	0.4913s
Paracetamol Kabi	424	0.56	0.40	0.79	0.4913s
Provive MCT-LCT 1%	**1**	**1.0**	**1.00**	**1.00**	**0.4913s**
Adrenaline Injection 1mg in 10mL	265	0.3	0.25	0.44	0.4913s
Amoxicillin Sodium	236	0.46	0.36	0.69	0.4913s
Lidocain Injection	282	0.18	0.17	0.51	0.4913s
SODIUM CHLORIDE	249	0.44	0.32	0.82	0.4913s
Remifentanil-Act Injection	248	0.34	0.33	0.67	0.4913s
Sterile Dopamine	276	0.22	0.20	0.45	0.4913s
Hypnomida Etomidate 2mg	258	0.48	0.28	0.69	0.4913s
Xylocaine 1%	283	0.17	0.17	0.42	0.4913s
Fentanyl Injection	246	0.42	0.33	0.63	0.4913s
Noradrenaline acid	260	0.31	0.27	0.51	0.4913s
Magnesium Sulfate 2.47g in 5mL	261	0.41	0.27	0.62	0.4913s
Sugammadex Injection	259	0.52	0.28	0.61	0.4913s
Dynastat Powder	247	0.46	0.33	0.61	0.4913s
Hydrocortisone sodium	242	0.47	0.35	0.72	0.4913s
Atracurium Besylate	268	0.55	0.25	0.51	0.4913s
Atropine	284	0.17	0.16	0.54	0.4913s
PancuroInresa	257	0.35	0.28	0.68	0.4913s

Drug Identification: Adrenaline Injection against other samples

Drug Name	Edit Distance	TSR Scores	Lev Scores	Jacc Scores	Processing Time
Primacor Injection	66	0.43	0.44	0.44	0.4678s
Cefazolin Sodium 1g	100	0.61	0.47	0.55	0.4678s
NALOXONE HCl 400mg in 1mL	58	0.44	0.36	0.52	0.4678s
Calcium Chloride 1g in 10mL	96	0.41	0.38	0.53	0.4678s
Actrapid Penfill 3ml	62	0.48	0.31	0.52	0.4678s
Vecuronium bromide	58	0.36	0.35	0.62	0.4678s
Sugammadex 200mg/2ml	68	0.44	0.37	0.62	0.4678s
Amiodarone Hydrochloride	67	0.47	0.37	0.56	0.4678s
Protamine Sulphate 50mg in 5ml	68	0.43	0.41	0.48	0.4678s
Summethonium Chloride 100mg in 2mL	61	0.34	0.29	0.58	0.4678s
Protamine Sulfate 10mg/ml	69	0.38	0.36	0.54	0.4678s
Glyceryl Trinitrate 1 mg/ml	78	0.43	0.36	0.48	0.4678s
Tranexamic acid	65	0.43	0.36	0.52	0.4678s
Heparin Injection 25000IU in 5 mL	61	0.45	0.43	0.52	0.4678s
Sterile Potassium Chloride	91	0.36	0.35	0.48	0.4678s
Metaraminol 10mg/ml	61	0.45	0.36	0.54	0.4678s
Cyclizine lactate	66	0.25	0.19	0.38	0.4678s
PITRESSIN argipressin	56	0.48	0.38	0.52	0.4678s
Dexamethasone phosphate 4 mg/ml	60	0.49	0.35	0.52	0.4678s
Ephedrine Hydrochloride	59	0.48	0.35	0.62	0.4678s
Ondansetron Solution	66	0.34	0.36	0.52	0.4678s
FRUSEMIDE	60	0.36	0.28	0.41	0.4678s
DALACINC PHOSPHATE	58	0.38	0.36	0.39	0.4678s
METOPROLOL Mylan	76	0.51	0.35	0.52	0.4678s
WATER FOR INJECTIONS BP	73	0.42	0.41	0.50	0.4678s
MORPHINE SULFATE	56	0.49	0.38	0.62	0.4678s
Glycopyrronium and Neostigmine	69	0.45	0.35	0.56	0.4678s
Clonidine HCl	60	0.48	0.34	0.50	0.4678s
Rocuronium Bromide 50 mg in 5 ml	59	0.48	0.43	0.67	0.4678s
Fresofol 1% MCT/LCT	319	0.49	0.24	0.38	0.4678s
Sedative Midazolam 5mg	61	0.33	0.31	0.39	0.4678s
Adrenaline Injection	**1**	**1.0**	**0.99**	**1.00**	**0.4678s**
Paracetamol Kabi	516	0.17	0.20	0.40	0.4678s
Provive MCT-LCT 1%	264	0.3	0.25	0.44	0.4678s
Adrenaline Injection 1mg in 10mL	1	1.0	0.99	1.00	0.4678s
Amoxicillin Sodium	118	0.42	0.37	0.45	0.4678s
Lidocain Injection	58	0.36	0.33	0.59	0.4678s
SODIUM CHLORIDE	109	0.32	0.36	0.42	0.4678s
Remifentanil-Act Injection	69	0.51	0.43	0.56	0.4678s
Sterile Dopamine	58	0.31	0.33	0.42	0.4678s
Hypnomida Etomidate 2mg	66	0.37	0.31	0.43	0.4678s
Xylocaine 1%	58	0.36	0.35	0.50	0.4678s
Fentanyl Injection	102	0.61	0.48	0.53	0.4678s
Noradrenaline acid	56	0.46	0.53	0.58	0.4678s
Magnesium Sulfate 2.47g in 5mL	66	0.5	0.42	0.47	0.4678s
Sugammadex Injection	61	0.41	0.42	0.67	0.4678s
Dynastat Powder	75	0.43	0.40	0.54	0.4678s
Hydrocortisone sodium	74	0.61	0.46	0.57	0.4678s
Atracurium Besylate	55	0.43	0.40	0.67	0.4678s
Atropine	57	0.39	0.34	0.57	0.4678s
PancuroInresa	72	0.36	0.40	0.52	0.4678s

Drug Identification: Hydrocortisone sodium against other samples

Drug Name	Edit Distance	TSR Scores	Lev Scores	Jacc Scores	Processing Time
Primacor Injection	89	0.48	0.37	0.65	0.3596s
Cefazolin Sodium 1g	73	0.69	0.62	0.77	0.3596s
NALOXONE HCl 400mg in 1mL	87	0.33	0.26	0.45	0.3596s
Calcium Chloride 1g in 10mL	101	0.43	0.39	0.65	0.3596s
Actrapid Penfill 3ml	86	0.42	0.32	0.64	0.3596s
Vecuronium bromide	72	0.49	0.44	0.69	0.3596s
Sugammadex 200mg/2ml	76	0.54	0.39	0.62	0.3596s
Amiodarone Hydrochloride	80	0.57	0.40	0.69	0.3596s
Protamine Sulphate 50mg in 5ml	89	0.48	0.42	0.70	0.3596s
Summethonium Chloride 100mg in 2mL	79	0.47	0.35	0.76	0.3596s
Protamine Sulfate 10mg/ml	85	0.46	0.40	0.66	0.3596s
Glyceryl Trinitrate 1 mg/ml	94	0.41	0.36	0.67	0.3596s
Tranexamic acid	84	0.36	0.32	0.64	0.3596s
Heparin Injection 25000IU in 5 mL	83	0.47	0.38	0.59	0.3596s
Sterile Potassium Chloride	96	0.42	0.37	0.65	0.3596s
Metaraminol 10mg/ml	74	0.47	0.44	0.68	0.3596s
Cyclizine lactate	95	0.18	0.17	0.43	0.3596s
PITRESSIN argipressin	79	0.43	0.38	0.61	0.3596s
Dexamethasone phosphate 4 mg/ml	80	0.55	0.42	0.70	0.3596s
Ephedrine Hydrochloride	78	0.43	0.39	0.63	0.3596s
Ondansetron Solution	82	0.4	0.38	0.64	0.3596s
FRUSEMIDE	80	0.44	0.35	0.60	0.3596s
DALACINC PHOSPHATE	86	0.37	0.30	0.56	0.3596s
METOPROLOL Mylan	68	0.58	0.51	0.66	0.3596s
WATER FOR INJECTIONS BP	90	0.43	0.38	0.66	0.3596s
MORPHINE SULFATE	77	0.45	0.44	0.75	0.3596s
Glycopyrronium and Neostigmine	87	0.5	0.33	0.62	0.3596s
Clonidine HCl	82	0.44	0.34	0.59	0.3596s
Rocuronium Bromide 50 mg in 5 ml	81	0.45	0.39	0.55	0.3596s
Fresofol 1% MCT/LCT	296	0.47	0.33	0.62	0.3596s
Sedative Midazolam 5mg	88	0.31	0.27	0.51	0.3596s
Adrenaline Injection	73	0.61	0.46	0.57	0.3596s
Paracetamol Kabi	498	0.35	0.25	0.64	0.3596s
Provive MCT-LCT 1%	241	0.47	0.36	0.72	0.3596s
Adrenaline Injection 1mg in 10mL	73	0.61	0.46	0.57	0.3596s
Amoxicillin Sodium	110	0.56	0.43	0.66	0.3596s
Lidocain Injection	88	0.31	0.26	0.67	0.3596s
SODIUM CHLORIDE	115	0.45	0.35	0.65	0.3596s
Remifentanil-Act Injection	72	0.51	0.47	0.86	0.3596s
Sterile Dopamine	85	0.32	0.29	0.52	0.3596s
Hypnomida Etomidate 2mg	79	0.45	0.40	0.83	0.3596s
Xylocaine 1%	87	0.3	0.27	0.48	0.3596s
Fentanyl Injection	112	0.53	0.40	0.69	0.3596s
Noradrenaline acid	87	0.34	0.33	0.55	0.3596s
Magnesium Sulfate 2.47g in 5mL	82	0.41	0.38	0.54	0.3596s
Sugammadex Injection	72	0.47	0.41	0.67	0.3596s
Dynastat Powder	51	0.61	0.61	0.71	0.3596s
Hydrocortisone sodium	**1**	**1.0**	**1.00**	**1.00**	**0.3596s**
Atracurium Besylate	73	0.47	0.44	0.61	0.3596s
Atropine	81	0.34	0.36	0.64	0.3596s
PancuroInresa	87	0.41	0.35	0.64	0.3596s

Drug Identification: Glycopyrronium Bromide and Neostigmine against other samples

Drug Name	Edit Distance	TSR Scores	Lev Scores	Jacc Scores	Processing Time
Primacor Injection	78	0.51	0.36	0.59	0.4810s
Cefazolin Sodium 1g	115	0.48	0.34	0.56	0.4810s
NALOXONE HCl 400mg in 1mL	71	0.33	0.28	0.54	0.4810s
Calcium Chloride 1g in 10mL	97	0.47	0.38	0.64	0.4810s
Actrapid Penfill 3ml	62	0.53	0.38	0.68	0.4810s
Vecuronium bromide	67	0.46	0.41	0.68	0.4810s
Sugammadex 200mg/2ml	63	0.55	0.53	0.79	0.4810s
Amiodarone Hydrochloride	60	0.55	0.49	0.68	0.4810s
Protamine Sulphate 50mg in 5ml	75	0.53	0.43	0.69	0.4810s
Summethonium Chloride 100mg in 2mL	64	0.49	0.36	0.75	0.4810s
Protamine Sulfate 10mg/ml	62	0.62	0.59	0.76	0.4810s
Glyceryl Trinitrate 1 mg/ml	85	0.39	0.35	0.66	0.4810s
Tranexamic acid	74	0.5	0.30	0.62	0.4810s
Heparin Injection 25000IU in 5 mL	76	0.5	0.34	0.73	0.4810s
Sterile Potassium Chloride	93	0.44	0.40	0.69	0.4810s
Metaraminol 10mg/ml	64	0.59	0.50	0.73	0.4810s
Cyclizine lactate	75	0.22	0.19	0.41	0.4810s
PITRESSIN argipressin	66	0.45	0.35	0.72	0.4810s
Dexamethasone phosphate 4 mg/ml	56	0.59	0.54	0.69	0.4810s
Ephedrine Hydrochloride	61	0.43	0.40	0.56	0.4810s
Ondansetron Solution	75	0.51	0.37	0.62	0.4810s
FRUSEMIDE	68	0.42	0.28	0.59	0.4810s
DALACINC PHOSPHATE	65	0.33	0.32	0.65	0.4810s
METOPROLOL Mylan	65	0.58	0.53	0.77	0.4810s
WATER FOR INJECTIONS BP	78	0.46	0.38	0.70	0.4810s
MORPHINE SULFATE	62	0.48	0.41	0.74	0.4810s
Glycopyrronium Bromide and Neostigmine	**1**	**1.0**	**0.99**	**1.00**	**0.4810s**
Clonidine HCl	70	0.51	0.34	0.63	0.4810s
Rocuronium Bromide 50 mg in 5 ml	66	0.6	0.41	0.72	0.4810s
Fresofol 1% MCT/LCT	313	0.38	0.26	0.62	0.4810s
Sedative Midazolam 5mg	70	0.42	0.32	0.65	0.4810s
Adrenaline Injection	68	0.45	0.35	0.56	0.4810s
Paracetamol Kabi	520	0.37	0.18	0.56	0.4810s
Provive MCT-LCT 1%	258	0.34	0.27	0.62	0.4810s
Adrenaline Injection 1mg in 10mL	68	0.45	0.35	0.56	0.4810s
Amoxicillin Sodium	113	0.46	0.39	0.60	0.4810s
Lidocain Injection	71	0.34	0.30	0.54	0.4810s
SODIUM CHLORIDE	113	0.41	0.32	0.69	0.4810s
Remifentanil-Act Injection	82	0.47	0.38	0.61	0.4810s
Sterile Dopamine	63	0.43	0.40	0.73	0.4810s
Hypnomida Etomidate 2mg	69	0.49	0.38	0.65	0.4810s
Xylocaine 1%	64	0.36	0.38	0.42	0.4810s
Fentanyl Injection	115	0.49	0.35	0.63	0.4810s
Noradrenaline acid	73	0.38	0.33	0.64	0.4810s
Magnesium Sulfate 2.47g in 5mL	75	0.5	0.40	0.72	0.4810s
Sugammadex Injection	72	0.54	0.40	0.85	0.4810s
Dynastat Powder	80	0.52	0.36	0.70	0.4810s
Hydrocortisone sodium	86	0.5	0.33	0.62	0.4810s
Atracurium Besylate	66	0.39	0.34	0.65	0.4810s
Atropine	69	0.4	0.31	0.63	0.4810s
PancuroInresa	79	0.44	0.36	0.73	0.4810s

Drug Identification: Metaraminol against other samples

Drug Name	Edit Distance	TSR Scores	Lev Scores	Jacc Scores	Processing Time
Primacor Injection	73	0.53	0.35	0.63	0.6332s
Cefazolin Sodium 1g	108	0.46	0.35	0.60	0.6332s
NALOXONE HCl 400mg in 1mL	47	0.39	0.33	0.46	0.6332s
Calcium Chloride 1g in 10mL	99	0.48	0.36	0.58	0.6332s
Actrapid Penfill 3ml	54	0.56	0.43	0.68	0.6332s
Vecuronium bromide	41	0.46	0.44	0.56	0.6332s
Sugammadex 200mg/2ml	46	0.58	0.57	0.73	0.6332s
Amiodarone Hydrochloride	47	0.74	0.62	0.75	0.6332s
Protamine Sulphate 50mg in 5ml	71	0.64	0.41	0.63	0.6332s
Summethonium Chloride 100mg in 2mL	49	0.5	0.39	0.69	0.6332s
Protamine Sulfate 10mg/ml	43	0.66	0.60	0.77	0.6332s
Glyceryl Trinitrate 1 mg/ml	70	0.47	0.45	0.79	0.6332s
Tranexamic acid	59	0.53	0.38	0.62	0.6332s
Heparin Injection 25000IU in 5 mL	59	0.52	0.40	0.57	0.6332s
Sterile Potassium Chloride	95	0.46	0.32	0.58	0.6332s
Metaraminol 10mg/ml	**1**	**1.0**	**0.99**	**1.00**	**0.6332s**
Cyclizine lactate	51	0.28	0.20	0.44	0.6332s
PITRESSIN argipressin	40	0.47	0.44	0.73	0.6332s
Dexamethasone phosphate 4 mg/ml	32	0.63	0.65	0.76	0.6332s
Ephedrine Hydrochloride	47	0.47	0.37	0.54	0.6332s
Ondansetron Solution	67	0.5	0.42	0.52	0.6332s
FRUSEMIDE	50	0.44	0.34	0.64	0.6332s
DALACINC PHOSPHATE	54	0.36	0.29	0.59	0.6332s
METOPROLOL Mylan	57	0.6	0.50	0.78	0.6332s
WATER FOR INJECTIONS BP	73	0.51	0.37	0.55	0.6332s
MORPHINE SULFATE	38	0.56	0.46	0.75	0.6332s
Glycopyrronium and Neostigmine	65	0.59	0.49	0.73	0.6332s
Clonidine HCl	43	0.53	0.37	0.70	0.6332s
Rocuronium Bromide 50 mg in 5 ml	62	0.56	0.38	0.65	0.6332s
Fresofol 1% MCT/LCT	327	0.43	0.22	0.53	0.6332s
Sedative Midazolam 5mg	51	0.36	0.34	0.53	0.6332s
Adrenaline Injection	61	0.45	0.36	0.54	0.6332s
Paracetamol Kabi	525	0.53	0.17	0.48	0.6332s
Provive MCT-LCT 1%	262	0.59	0.27	0.53	0.6332s
Adrenaline Injection 1mg in 10mL	61	0.45	0.36	0.54	0.6332s
Amoxicillin Sodium	121	0.42	0.33	0.55	0.6332s
Lidocain Injection	45	0.4	0.34	0.65	0.6332s
SODIUM CHLORIDE	115	0.37	0.31	0.54	0.6332s
Remifentanil-Act Injection	75	0.44	0.36	0.61	0.6332s
Sterile Dopamine	47	0.46	0.32	0.60	0.6332s
Hypnomida Etomidate 2mg	61	0.45	0.36	0.64	0.6332s
Xylocaine 1%	42	0.45	0.40	0.56	0.6332s
Fentanyl Injection	120	0.45	0.32	0.62	0.6332s
Noradrenaline acid	66	0.36	0.34	0.58	0.6332s
Magnesium Sulfate 2.47g in 5mL	67	0.47	0.41	0.56	0.6332s
Sugammadex Injection	46	0.56	0.54	0.79	0.6332s
Dynastat Powder	65	0.49	0.43	0.64	0.6332s
Hydrocortisone sodium	73	0.47	0.44	0.68	0.6332s
Atracurium Besylate	50	0.37	0.33	0.58	0.6332s
Atropine	42	0.43	0.43	0.70	0.6332s
PancuroInresa	78	0.5	0.36	0.68	0.6332s

Drug Identification: PITRESSIN argipressin against other samples

Drug Name	Edit Distance	TSR Scores	Lev Scores	Jacc Scores	Processing Time
Primacor Injection	74	0.44	0.36	0.57	0.4105s
Cefazolin Sodium 1g	108	0.41	0.37	0.48	0.4105s
NALOXONE HCl 400mg in 1mL	39	0.38	0.39	0.44	0.4105s
Calcium Chloride 1g in 10mL	99	0.38	0.35	0.52	0.4105s
Actrapid Penfill 3ml	52	0.54	0.36	0.61	0.4105s
Vecuronium bromide	40	0.45	0.45	0.54	0.4105s
Sugammadex 200mg/2ml	58	0.52	0.40	0.65	0.4105s
Amiodarone Hydrochloride	62	0.4	0.42	0.60	0.4105s
Protamine Sulphate 50mg in 5ml	69	0.48	0.43	0.57	0.4105s
Summethonium Chloride 100mg in 2mL	44	0.39	0.30	0.68	0.4105s
Protamine Sulfate 10mg/ml	58	0.48	0.40	0.63	0.4105s
Glyceryl Trinitrate 1 mg/ml	79	0.4	0.34	0.58	0.4105s
Tranexamic acid	60	0.36	0.33	0.50	0.4105s
Heparin Injection 25000IU in 5 mL	59	0.55	0.42	0.61	0.4105s
Sterile Potassium Chloride	92	0.41	0.36	0.52	0.4105s
Metaraminol 10mg/ml	39	0.47	0.44	0.73	0.4105s
Cyclizine lactate	45	0.23	0.25	0.48	0.4105s
PITRESSIN argipressin	**1**	**1.0**	**0.99**	**1.00**	**0.4105s**
Dexamethasone phosphate 4 mg/ml	48	0.49	0.42	0.62	0.4105s
Ephedrine Hydrochloride	43	0.37	0.40	0.59	0.4105s
Ondansetron Solution	68	0.33	0.31	0.55	0.4105s
FRUSEMIDE	47	0.41	0.36	0.62	0.4105s
DALACINC PHOSPHATE	50	0.34	0.32	0.52	0.4105s
METOPROLOL Mylan	70	0.38	0.36	0.70	0.4105s
WATER FOR INJECTIONS BP	76	0.39	0.34	0.53	0.4105s
MORPHINE SULFATE	38	0.57	0.47	0.67	0.4105s
Glycopyrronium and Neostigmine	66	0.45	0.35	0.72	0.4105s
Clonidine HCl	39	0.5	0.43	0.54	0.4105s
Rocuronium Bromide 50 mg in 5 ml	59	0.48	0.37	0.64	0.4105s
Fresofol 1% MCT/LCT	333	0.23	0.19	0.47	0.4105s
Sedative Midazolam 5mg	50	0.34	0.30	0.47	0.4105s
Adrenaline Injection	55	0.48	0.38	0.52	0.4105s
Paracetamol Kabi	531	0.19	0.16	0.43	0.4105s
Provive MCT-LCT 1%	267	0.27	0.24	0.51	0.4105s
Adrenaline Injection 1mg in 10mL	55	0.48	0.38	0.52	0.4105s
Amoxicillin Sodium	123	0.35	0.32	0.53	0.4105s
Lidocain Injection	38	0.42	0.37	0.57	0.4105s
SODIUM CHLORIDE	115	0.34	0.31	0.53	0.4105s
Remifentanil-Act Injection	74	0.42	0.38	0.59	0.4105s
Sterile Dopamine	41	0.36	0.33	0.65	0.4105s
Hypnomida Etomidate 2mg	60	0.4	0.36	0.63	0.4105s
Xylocaine 1%	41	0.46	0.37	0.48	0.4105s
Fentanyl Injection	118	0.35	0.31	0.47	0.4105s
Noradrenaline acid	64	0.35	0.39	0.62	0.4105s
Magnesium Sulfate 2.47g in 5mL	65	0.42	0.33	0.50	0.4105s
Sugammadex Injection	53	0.5	0.39	0.71	0.4105s
Dynastat Powder	67	0.43	0.41	0.63	0.4105s
Hydrocortisone sodium	78	0.43	0.38	0.61	0.4105s
Atracurium Besylate	43	0.43	0.41	0.64	0.4105s
Atropine	37	0.46	0.41	0.68	0.4105s
PancuroInresa	75	0.47	0.37	0.67	0.4105s

Drug Identification: Clonidine HCl against other samples

Drug Name	Edit Distance	TSR Scores	Lev Scores	Jacc Scores	Processing Time
Primacor Injection	75	0.53	0.33	0.50	0.4680s
Cefazolin Sodium 1g	117	0.43	0.30	0.52	0.4680s
NALOXONE HCl 400mg in 1mL	20	0.57	0.52	0.54	0.4680s
Calcium Chloride 1g in 10mL	104	0.43	0.32	0.50	0.4680s
Actrapid Penfill 3ml	54	0.54	0.34	0.53	0.4680s
Vecuronium bromide	39	0.37	0.40	0.46	0.4680s
Sugammadex 200mg/2ml	60	0.46	0.36	0.57	0.4680s
Amiodarone Hydrochloride	64	0.53	0.36	0.64	0.4680s
Protamine Sulphate 50mg in 5ml	75	0.54	0.37	0.55	0.4680s
Summethonium Chloride 100mg in 2mL	44	0.48	0.34	0.65	0.4680s
Protamine Sulfate 10mg/ml	64	0.44	0.33	0.61	0.4680s
Glyceryl Trinitrate 1 mg/ml	84	0.36	0.31	0.62	0.4680s
Tranexamic acid	61	0.38	0.31	0.53	0.4680s
Heparin Injection 25000IU in 5 mL	61	0.53	0.37	0.59	0.4680s
Sterile Potassium Chloride	97	0.37	0.31	0.55	0.4680s
Metaraminol 10mg/ml	42	0.55	0.39	0.70	0.4680s
Cyclizine lactate	28	0.3	0.25	0.35	0.4680s
PITRESSIN argipressin	38	0.49	0.42	0.54	0.4680s
Dexamethasone phosphate 4 mg/ml	49	0.53	0.42	0.65	0.4680s
Ephedrine Hydrochloride	40	0.51	0.48	0.57	0.4680s
Ondansetron Solution	70	0.29	0.29	0.44	0.4680s
FRUSEMIDE	51	0.33	0.23	0.48	0.4680s
DALACINC PHOSPHATE	45	0.35	0.37	0.55	0.4680s
METOPROLOL Mylan	74	0.53	0.32	0.60	0.4680s
WATER FOR INJECTIONS BP	80	0.39	0.29	0.47	0.4680s
MORPHINE SULFATE	28	0.56	0.50	0.64	0.4680s
Glycopyrronium and Neostigmine	68	0.43	0.32	0.63	0.4680s
Clonidine HCl	**2**	**0.98**	**0.97**	**1.00**	**0.4680s**
Rocuronium Bromide 50 mg in 5 ml	56	0.56	0.42	0.76	0.4680s
Fresofol 1% MCT/LCT	343	0.53	0.15	0.50	0.4680s
Sedative Midazolam 5mg	48	0.35	0.34	0.50	0.4680s
Adrenaline Injection	58	0.47	0.35	0.50	0.4680s
Paracetamol Kabi	550	0.12	0.10	0.42	0.4680s
Provive MCT-LCT 1%	282	0.53	0.17	0.46	0.4680s
Adrenaline Injection 1mg in 10mL	58	0.47	0.35	0.50	0.4680s
Amoxicillin Sodium	132	0.43	0.24	0.47	0.4680s
Lidocain Injection	27	0.46	0.47	0.68	0.4680s
SODIUM CHLORIDE	121	0.31	0.24	0.51	0.4680s
Remifentanil-Act Injection	81	0.43	0.31	0.52	0.4680s
Sterile Dopamine	33	0.41	0.42	0.56	0.4680s
Hypnomida Etomidate 2mg	62	0.51	0.37	0.55	0.4680s
Xylocaine 1%	28	0.44	0.49	0.46	0.4680s
Fentanyl Injection	125	0.53	0.27	0.55	0.4680s
Noradrenaline acid	65	0.28	0.31	0.48	0.4680s
Magnesium Sulfate 2.47g in 5mL	67	0.53	0.35	0.48	0.4680s
Sugammadex Injection	52	0.53	0.42	0.62	0.4680s
Dynastat Powder	74	0.43	0.33	0.50	0.4680s
Hydrocortisone sodium	80	0.43	0.35	0.59	0.4680s
Atracurium Besylate	43	0.36	0.34	0.48	0.4680s
Atropine	24	0.48	0.47	0.46	0.4680s
PancuroInresa	79	0.34	0.30	0.48	0.4680s

Drug Identification: Sedative Midazolam against other samples

Drug Name	Edit Distance	TSR Scores	Lev Scores	Jacc Scores	Processing Time
Primacor Injection	77	0.35	0.28	0.53	0.4517s
Cefazolin Sodium 1g	118	0.3	0.28	0.50	0.4517s
NALOXONE HCl 400mg in 1mL	51	0.29	0.26	0.47	0.4517s
Calcium Chloride 1g in 10mL	109	0.34	0.27	0.49	0.4517s
Actrapid Penfill 3ml	58	0.36	0.30	0.56	0.4517s
Vecuronium bromide	48	0.32	0.29	0.45	0.4517s
Sugammadex 200mg/2ml	62	0.41	0.30	0.65	0.4517s
Amiodarone Hydrochloride	67	0.37	0.28	0.45	0.4517s
Protamine Sulphate 50mg in 5ml	79	0.4	0.29	0.53	0.4517s
Summethonium Chloride 100mg in 2mL	50	0.47	0.34	0.61	0.4517s
Protamine Sulfate 10mg/ml	65	0.47	0.29	0.73	0.4517s
Glyceryl Trinitrate 1 mg/ml	83	0.38	0.31	0.58	0.4517s
Tranexamic acid	63	0.45	0.30	0.71	0.4517s
Heparin Injection 25000IU in 5 mL	65	0.38	0.31	0.56	0.4517s
Sterile Potassium Chloride	97	0.37	0.31	0.62	0.4517s
Metaraminol 10mg/ml	51	0.36	0.32	0.53	0.4517s
Cyclizine lactate	52	0.36	0.24	0.40	0.4517s
PITRESSIN argipressin	51	0.34	0.30	0.47	0.4517s
Dexamethasone phosphate 4 mg/ml	51	0.47	0.36	0.61	0.4517s
Ephedrine Hydrochloride	54	0.28	0.24	0.34	0.4517s
Ondansetron Solution	67	0.4	0.29	0.66	0.4517s
FRUSEMIDE	53	0.41	0.28	0.57	0.4517s
DALACINC PHOSPHATE	52	0.41	0.35	0.58	0.4517s
METOPROLOL Mylan	73	0.41	0.30	0.52	0.4517s
WATER FOR INJECTIONS BP	79	0.39	0.30	0.68	0.4517s
MORPHINE SULFATE	52	0.37	0.32	0.55	0.4517s
Glycopyrronium and Neostigmine	70	0.42	0.32	0.65	0.4517s
Clonidine HCl	51	0.31	0.30	0.50	0.4517s
Rocuronium Bromide 50 mg in 5 ml	65	0.43	0.33	0.47	0.4517s
Fresofol 1% MCT/LCT	335	0.21	0.18	0.56	0.4517s
Sedative Midazolam 5mg	**1**	**1.0**	**0.99**	**1.00**	**0.4517s**
Adrenaline Injection	60	0.33	0.31	0.39	0.4517s
Paracetamol Kabi	536	0.16	0.14	0.58	0.4517s
Provive MCT-LCT 1%	273	0.24	0.20	0.49	0.4517s
Adrenaline Injection 1mg in 10mL	60	0.33	0.31	0.39	0.4517s
Amoxicillin Sodium	128	0.31	0.26	0.54	0.4517s
Lidocain Injection	50	0.38	0.29	0.42	0.4517s
SODIUM CHLORIDE	119	0.32	0.25	0.54	0.4517s
Remifentanil-Act Injection	82	0.31	0.26	0.46	0.4517s
Sterile Dopamine	44	0.45	0.41	0.59	0.4517s
Hypnomida Etomidate 2mg	62	0.44	0.34	0.49	0.4517s
Xylocaine 1%	52	0.31	0.27	0.36	0.4517s
Fentanyl Injection	118	0.33	0.31	0.53	0.4517s
Noradrenaline acid	69	0.36	0.29	0.52	0.4517s
Magnesium Sulfate 2.47g in 5mL	71	0.43	0.33	0.51	0.4517s
Sugammadex Injection	59	0.42	0.32	0.63	0.4517s
Dynastat Powder	77	0.33	0.28	0.58	0.4517s
Hydrocortisone sodium	87	0.31	0.27	0.51	0.4517s
Atracurium Besylate	52	0.28	0.33	0.47	0.4517s
Atropine	50	0.34	0.31	0.45	0.4517s
PancuroInresa	80	0.38	0.29	0.66	0.4517s

Drug Identification: NALOXONE HCl against other samples

Drug Name	Edit Distance	TSR Scores	Lev Scores	Jacc Scores	Processing Time
Primacor Injection	78	0.34	0.27	0.47	0.2967s
Cefazolin Sodium 1g	123	0.27	0.24	0.35	0.2967s
NALOXONE HCl 400mg in 1mL	**1**	**1.0**	**0.98**	**1.00**	**0.2967s**
Calcium Chloride 1g in 10mL	110	0.32	0.26	0.47	0.2967s
Actrapid Penfill 3ml	53	0.45	0.31	0.36	0.2967s
Vecuronium bromide	42	0.33	0.32	0.43	0.2967s
Sugammadex 200mg/2ml	63	0.4	0.29	0.48	0.2967s
Amiodarone Hydrochloride	67	0.32	0.32	0.48	0.2967s
Protamine Sulphate 50mg in 5ml	80	0.4	0.29	0.47	0.2967s
Summethonium Chloride 100mg in 2mL	42	0.42	0.34	0.50	0.2967s
Protamine Sulfate 10mg/ml	68	0.4	0.26	0.47	0.2967s
Glyceryl Trinitrate 1 mg/ml	85	0.33	0.27	0.52	0.2967s
Tranexamic acid	62	0.37	0.26	0.55	0.2967s
Heparin Injection 25000IU in 5 mL	64	0.42	0.32	0.45	0.2967s
Sterile Potassium Chloride	98	0.34	0.29	0.52	0.2967s
Metaraminol 10mg/ml	47	0.39	0.33	0.46	0.2967s
Cyclizine lactate	27	0.27	0.19	0.42	0.2967s
PITRESSIN argipressin	38	0.38	0.39	0.44	0.2967s
Dexamethasone phosphate 4 mg/ml	51	0.38	0.38	0.56	0.2967s
Ephedrine Hydrochloride	40	0.33	0.30	0.46	0.2967s
Ondansetron Solution	69	0.31	0.28	0.55	0.2967s
FRUSEMIDE	53	0.31	0.24	0.44	0.2967s
DALACINC PHOSPHATE	45	0.36	0.31	0.47	0.2967s
METOPROLOL Mylan	79	0.25	0.23	0.39	0.2967s
WATER FOR INJECTIONS BP	85	0.31	0.22	0.48	0.2967s
MORPHINE SULFATE	32	0.53	0.41	0.54	0.2967s
Glycopyrronium and Neostigmine	70	0.33	0.28	0.54	0.2967s
Clonidine HCl	20	0.58	0.53	0.54	0.2967s
Rocuronium Bromide 50 mg in 5 ml	59	0.47	0.38	0.57	0.2967s
Fresofol 1% MCT/LCT	347	0.16	0.13	0.40	0.2967s
Sedative Midazolam 5mg	50	0.29	0.26	0.47	0.2967s
Adrenaline Injection	57	0.44	0.36	0.52	0.2967s
Paracetamol Kabi	552	0.12	0.09	0.43	0.2967s
Provive MCT-LCT 1%	284	0.16	0.16	0.43	0.2967s
Adrenaline Injection 1mg in 10mL	57	0.44	0.36	0.52	0.2967s
Amoxicillin Sodium	134	0.24	0.22	0.44	0.2967s
Lidocain Injection	30	0.42	0.30	0.57	0.2967s
SODIUM CHLORIDE	124	0.27	0.21	0.49	0.2967s
Remifentanil-Act Injection	82	0.32	0.29	0.43	0.2967s
Sterile Dopamine	36	0.34	0.33	0.46	0.2967s
Hypnomida Etomidate 2mg	64	0.35	0.29	0.42	0.2967s
Xylocaine 1%	28	0.43	0.39	0.42	0.2967s
Fentanyl Injection	125	0.3	0.26	0.39	0.2967s
Noradrenaline acid	68	0.3	0.30	0.56	0.2967s
Magnesium Sulfate 2.47g in 5mL	67	0.42	0.34	0.45	0.2967s
Sugammadex Injection	57	0.38	0.31	0.52	0.2967s
Dynastat Powder	77	0.34	0.30	0.57	0.2967s
Hydrocortisone sodium	86	0.33	0.26	0.45	0.2967s
Atracurium Besylate	45	0.35	0.25	0.50	0.2967s
Atropine	26	0.4	0.42	0.42	0.2967s
PancuroInresa	81	0.33	0.28	0.50	0.2967s

Drug Identification: Atropine Injection against other samples

Drug Name	Edit Distance	TSR Scores	Lev Scores	Jacc Scores	Processing Time
Primacor Injection	70	0.42	0.40	0.60	0.4063s
Cefazolin Sodium 1g	121	0.33	0.26	0.52	0.4063s
NALOXONE HCl 400mg in 1mL	26	0.4	0.42	0.42	0.4063s
Calcium Chloride 1g in 10mL	107	0.38	0.29	0.60	0.4063s
Actrapid Penfill 3ml	53	0.4	0.31	0.59	0.4063s
Vecuronium bromide	45	0.4	0.33	0.58	0.4063s
Sugammadex 200mg/2ml	62	0.43	0.31	0.63	0.4063s
Amiodarone Hydrochloride	67	0.41	0.32	0.58	0.4063s
Protamine Sulphate 50mg in 5ml	75	0.43	0.36	0.60	0.4063s
Summethonium Chloride 100mg in 2mL	39	0.42	0.40	0.65	0.4063s
Protamine Sulfate 10mg/ml	64	0.4	0.35	0.67	0.4063s
Glyceryl Trinitrate 1 mg/ml	86	0.3	0.26	0.56	0.4063s
Tranexamic acid	61	0.39	0.32	0.53	0.4063s
Heparin Injection 25000IU in 5 mL	64	0.38	0.34	0.53	0.4063s
Sterile Potassium Chloride	101	0.32	0.26	0.55	0.4063s
Metaraminol 10mg/ml	41	0.43	0.43	0.70	0.4063s
Cyclizine lactate	25	0.31	0.27	0.46	0.4063s
PITRESSIN argipressin	36	0.46	0.41	0.68	0.4063s
Dexamethasone phosphate 4 mg/ml	52	0.47	0.39	0.59	0.4063s
Ephedrine Hydrochloride	37	0.43	0.35	0.57	0.4063s
Ondansetron Solution	66	0.39	0.33	0.53	0.4063s
FRUSEMIDE	49	0.34	0.26	0.54	0.4063s
DALACINC PHOSPHATE	46	0.4	0.40	0.61	0.4063s
METOPROLOL Mylan	75	0.35	0.29	0.67	0.4063s
WATER FOR INJECTIONS BP	77	0.4	0.34	0.56	0.4063s
MORPHINE SULFATE	29	0.45	0.49	0.64	0.4063s
Glycopyrronium and Neostigmine	68	0.4	0.31	0.63	0.4063s
Clonidine HCl	25	0.48	0.44	0.46	0.4063s
Rocuronium Bromide 50 mg in 5 ml	61	0.38	0.33	0.54	0.4063s
Fresofol 1% MCT/LCT	345	0.46	0.14	0.50	0.4063s
Sedative Midazolam 5mg	50	0.34	0.31	0.45	0.4063s
Adrenaline Injection	56	0.39	0.34	0.57	0.4063s
Paracetamol Kabi	551	0.18	0.09	0.45	0.4063s
Provive MCT-LCT 1%	282	0.17	0.17	0.54	0.4063s
Adrenaline Injection 1mg in 10mL	56	0.39	0.34	0.57	0.4063s
Amoxicillin Sodium	134	0.26	0.22	0.52	0.4063s
Lidocain Injection	28	0.45	0.40	0.54	0.4063s
SODIUM CHLORIDE	123	0.28	0.23	0.51	0.4063s
Remifentanil-Act Injection	76	0.43	0.37	0.63	0.4063s
Sterile Dopamine	33	0.34	0.39	0.56	0.4063s
Hypnomida Etomidate 2mg	65	0.42	0.32	0.61	0.4063s
Xylocaine 1%	30	0.39	0.39	0.52	0.4063s
Fentanyl Injection	120	0.37	0.31	0.50	0.4063s
Noradrenaline acid	69	0.27	0.28	0.54	0.4063s
Magnesium Sulfate 2.47g in 5mL	68	0.38	0.31	0.44	0.4063s
Sugammadex Injection	56	0.44	0.35	0.68	0.4063s
Dynastat Powder	72	0.36	0.37	0.61	0.4063s
Hydrocortisone sodium	80	0.34	0.36	0.64	0.4063s
Atracurium Besylate	45	0.38	0.28	0.54	0.4063s
Atropine	**1**	**1.0**	**0.98**	**1.00**	**0.4063s**
PancuroInresa	78	0.31	0.31	0.64	0.4063s

Drug Identification: Hypnomida Etomidate against other samples

Drug Name	Edit Distance	TSR Scores	Lev Scores	Jacc Scores	Processing Time
Primacor Injection	70	0.48	0.39	0.57	0.5239s
Cefazolin Sodium 1g	106	0.38	0.36	0.64	0.5239s
NALOXONE HCl 400mg in 1mL	65	0.35	0.29	0.42	0.5239s
Calcium Chloride 1g in 10mL	98	0.44	0.34	0.57	0.5239s
Actrapid Penfill 3ml	64	0.49	0.33	0.61	0.5239s
Vecuronium bromide	58	0.38	0.41	0.60	0.5239s
Sugammadex 200mg/2ml	65	0.49	0.36	0.59	0.5239s
Amiodarone Hydrochloride	68	0.49	0.37	0.66	0.5239s
Protamine Sulphate 50mg in 5ml	80	0.49	0.38	0.62	0.5239s
Summethonium Chloride 100mg in 2mL	61	0.51	0.38	0.72	0.5239s
Protamine Sulfate 10mg/ml	65	0.48	0.39	0.58	0.5239s
Glyceryl Trinitrate 1 mg/ml	78	0.47	0.39	0.63	0.5239s
Tranexamic acid	71	0.47	0.34	0.56	0.5239s
Heparin Injection 25000IU in 5 mL	68	0.4	0.36	0.56	0.5239s
Sterile Potassium Chloride	95	0.41	0.34	0.57	0.5239s
Metaraminol 10mg/ml	61	0.45	0.36	0.64	0.5239s
Cyclizine lactate	70	0.32	0.24	0.45	0.5239s
PITRESSIN argipressin	61	0.4	0.36	0.63	0.5239s
Dexamethasone phosphate 4 mg/ml	59	0.51	0.43	0.67	0.5239s
Ephedrine Hydrochloride	66	0.35	0.28	0.59	0.5239s
Ondansetron Solution	67	0.43	0.36	0.61	0.5239s
FRUSEMIDE	68	0.45	0.30	0.62	0.5239s
DALACINC PHOSPHATE	67	0.43	0.30	0.58	0.5239s
METOPROLOL Mylan	74	0.45	0.37	0.62	0.5239s
WATER FOR INJECTIONS BP	81	0.52	0.38	0.63	0.5239s
MORPHINE SULFATE	61	0.46	0.38	0.71	0.5239s
Glycopyrronium and Neostigmine	70	0.49	0.38	0.65	0.5239s
Clonidine HCl	64	0.47	0.34	0.55	0.5239s
Rocuronium Bromide 50 mg in 5 ml	65	0.44	0.38	0.52	0.5239s
Fresofol 1% MCT/LCT	323	0.45	0.22	0.60	0.5239s
Sedative Midazolam 5mg	62	0.44	0.34	0.49	0.5239s
Adrenaline Injection	67	0.37	0.31	0.43	0.5239s
Paracetamol Kabi	519	0.47	0.19	0.58	0.5239s
Provive MCT-LCT 1%	257	0.48	0.28	0.69	0.5239s
Adrenaline Injection 1mg in 10mL	67	0.37	0.31	0.43	0.5239s
Amoxicillin Sodium	125	0.37	0.30	0.63	0.5239s
Lidocain Injection	63	0.35	0.35	0.63	0.5239s
SODIUM CHLORIDE	108	0.41	0.34	0.67	0.5239s
Remifentanil-Act Injection	77	0.42	0.36	0.76	0.5239s
Sterile Dopamine	66	0.46	0.31	0.59	0.5239s
Hypnomida Etomidate 2mg	**1**	**1.0**	**0.99**	**1.00**	**0.5239s**
Xylocaine 1%	65	0.37	0.31	0.50	0.5239s
Fentanyl Injection	116	0.46	0.35	0.57	0.5239s
Noradrenaline acid	71	0.38	0.33	0.52	0.5239s
Magnesium Sulfate 2.47g in 5mL	73	0.5	0.35	0.56	0.5239s
Sugammadex Injection	65	0.53	0.39	0.63	0.5239s
Dynastat Powder	70	0.45	0.42	0.68	0.5239s
Hydrocortisone sodium	78	0.45	0.40	0.83	0.5239s
Atracurium Besylate	66	0.33	0.29	0.57	0.5239s
Atropine	66	0.42	0.32	0.61	0.5239s
PancuroInresa	84	0.42	0.36	0.61	0.5239s

Drug Identification: Fentanyl Injection against other samples

Drug Name	Edit Distance	TSR Scores	Lev Scores	Jacc Scores	Processing Time
Primacor Injection	109	0.53	0.39	0.61	0.5067s
Cefazolin Sodium 1g	126	0.56	0.38	0.58	0.5067s
NALOXONE HCl 400mg in 1mL	127	0.3	0.24	0.39	0.5067s
Calcium Chloride 1g in 10mL	117	0.46	0.39	0.61	0.5067s
Actrapid Penfill 3ml	124	0.46	0.27	0.69	0.5067s
Vecuronium bromide	123	0.39	0.27	0.59	0.5067s
Sugammadex 200mg/2ml	123	0.47	0.31	0.68	0.5067s
Amiodarone Hydrochloride	115	0.46	0.34	0.59	0.5067s
Protamine Sulphate 50mg in 5ml	115	0.48	0.38	0.69	0.5067s
Summethonium Chloride 100mg in 2mL	116	0.43	0.33	0.60	0.5067s
Protamine Sulfate 10mg/ml	118	0.49	0.35	0.66	0.5067s
Glyceryl Trinitrate 1 mg/ml	118	0.42	0.36	0.62	0.5067s
Tranexamic acid	118	0.45	0.31	0.59	0.5067s
Heparin Injection 25000IU in 5 mL	112	0.46	0.38	0.59	0.5067s
Sterile Potassium Chloride	114	0.46	0.40	0.69	0.5067s
Metaraminol 10mg/ml	122	0.45	0.31	0.62	0.5067s
Cyclizine lactate	136	0.17	0.15	0.33	0.5067s
PITRESSIN argipressin	120	0.35	0.30	0.47	0.5067s
Dexamethasone phosphate 4 mg/ml	120	0.45	0.31	0.56	0.5067s
Ephedrine Hydrochloride	116	0.58	0.34	0.44	0.5067s
Ondansetron Solution	118	0.4	0.39	0.55	0.5067s
FRUSEMIDE	125	0.35	0.25	0.47	0.5067s
DALACINC PHOSPHATE	120	0.34	0.31	0.53	0.5067s
METOPROLOL Mylan	118	0.46	0.34	0.61	0.5067s
WATER FOR INJECTIONS BP	118	0.48	0.36	0.57	0.5067s
MORPHINE SULFATE	120	0.41	0.31	0.59	0.5067s
Glycopyrronium and Neostigmine	116	0.49	0.34	0.63	0.5067s
Clonidine HCl	128	0.44	0.25	0.55	0.5067s
Rocuronium Bromide 50 mg in 5 ml	109	0.46	0.39	0.56	0.5067s
Fresofol 1% MCT/LCT	294	0.42	0.32	0.63	0.5067s
Sedative Midazolam 5mg	120	0.33	0.30	0.53	0.5067s
Adrenaline Injection	104	0.61	0.47	0.53	0.5067s
Paracetamol Kabi	492	0.3	0.25	0.64	0.5067s
Provive MCT-LCT 1%	244	0.42	0.34	0.63	0.5067s
Adrenaline Injection 1mg in 10mL	104	0.61	0.47	0.53	0.5067s
Amoxicillin Sodium	132	0.44	0.32	0.62	0.5067s
Lidocain Injection	128	0.26	0.24	0.47	0.5067s
SODIUM CHLORIDE	129	0.44	0.35	0.61	0.5067s
Remifentanil-Act Injection	99	0.57	0.50	0.63	0.5067s
Sterile Dopamine	120	0.36	0.31	0.49	0.5067s
Hypnomida Etomidate 2mg	117	0.46	0.34	0.57	0.5067s
Xylocaine 1%	128	0.27	0.23	0.42	0.5067s
Fentanyl Injection	**1**	**1.0**	**1.00**	**1.00**	**0.5067s**
Noradrenaline acid	116	0.41	0.36	0.51	0.5067s
Magnesium Sulfate 2.47g in 5mL	118	0.47	0.34	0.63	0.5067s
Sugammadex Injection	116	0.48	0.34	0.67	0.5067s
Dynastat Powder	118	0.44	0.35	0.66	0.5067s
Hydrocortisone sodium	114	0.53	0.40	0.69	0.5067s
Atracurium Besylate	121	0.33	0.30	0.52	0.5067s
Atropine	122	0.37	0.30	0.50	0.5067s
PancuroInresa	114	0.42	0.36	0.55	0.5067s

Drug Identification: Ondansetron Solution against other samples

Drug Name	Edit Distance	TSR Scores	Lev Scores	Jacc Scores	Processing Time
Primacor Injection	83	0.43	0.33	0.63	0.3491s
Cefazolin Sodium 1g	102	0.5	0.41	0.51	0.3491s
NALOXONE HCl 400mg in 1mL	84	0.3	0.21	0.48	0.3491s
Calcium Chloride 1g in 10mL	109	0.38	0.32	0.58	0.3491s
Actrapid Penfill 3ml	83	0.44	0.26	0.57	0.3491s
Vecuronium bromide	74	0.36	0.35	0.52	0.3491s
Sugammadex 200mg/2ml	74	0.42	0.35	0.56	0.3491s
Amiodarone Hydrochloride	79	0.44	0.32	0.52	0.3491s
Protamine Sulphate 50mg in 5ml	82	0.4	0.31	0.50	0.3491s
Summethonium Chloride 100mg in 2mL	74	0.45	0.33	0.62	0.3491s
Protamine Sulfate 10mg/ml	75	0.44	0.37	0.59	0.3491s
Glyceryl Trinitrate 1 mg/ml	89	0.41	0.29	0.65	0.3491s
Tranexamic acid	62	0.5	0.49	0.77	0.3491s
Heparin Injection 25000IU in 5 mL	78	0.41	0.35	0.49	0.3491s
Sterile Potassium Chloride	97	0.39	0.33	0.54	0.3491s
Metaraminol 10mg/ml	74	0.44	0.34	0.50	0.3491s
Cyclizine lactate	82	0.27	0.22	0.47	0.3491s
PITRESSIN argipressin	77	0.36	0.32	0.48	0.3491s
Dexamethasone phosphate 4 mg/ml	76	0.45	0.31	0.62	0.3491s
Ephedrine Hydrochloride	77	0.28	0.29	0.50	0.3491s
Ondansetron Solution	**67**	**0.91**	**0.98**	**0.89**	**0.3491s**
FRUSEMIDE	41	0.6	0.71	0.75	0.3491s
DALACINC PHOSPHATE	81	0.37	0.27	0.50	0.3491s
METOPROLOL Mylan	72	0.45	0.40	0.48	0.3491s
WATER FOR INJECTIONS BP	84	0.41	0.32	0.59	0.3491s
MORPHINE SULFATE	79	0.35	0.28	0.67	0.3491s
Glycopyrronium and Neostigmine	85	0.45	0.29	0.56	0.3491s
Clonidine HCl	84	0.24	0.20	0.42	0.3491s
Rocuronium Bromide 50 mg in 5 ml	80	0.36	0.30	0.44	0.3491s
Fresofol 1% MCT/LCT	311	0.43	0.27	0.57	0.3491s
Sedative Midazolam 5mg	77	0.42	0.31	0.64	0.3491s
Adrenaline Injection	80	0.31	0.32	0.41	0.3491s
Paracetamol Kabi	510	0.36	0.21	0.67	0.3491s
Provive MCT-LCT 1%	251	0.37	0.32	0.66	0.3491s
Adrenaline Injection 1mg in 10mL	80	0.31	0.32	0.41	0.3491s
Amoxicillin Sodium	119	0.42	0.36	0.59	0.3491s
Lidocain Injection	78	0.29	0.26	0.48	0.3491s
SODIUM CHLORIDE	114	0.44	0.34	0.63	0.3491s
Remifentanil-Act Injection	87	0.39	0.37	0.51	0.3491s
Sterile Dopamine	80	0.38	0.28	0.50	0.3491s
Hypnomida Etomidate 2mg	78	0.43	0.33	0.59	0.3491s
Xylocaine 1%	80	0.29	0.25	0.42	0.3491s
Fentanyl Injection	121	0.4	0.30	0.54	0.3491s
Noradrenaline acid	79	0.4	0.29	0.58	0.3491s
Magnesium Sulfate 2.47g in 5mL	83	0.37	0.30	0.49	0.3491s
Sugammadex Injection	80	0.43	0.30	0.55	0.3491s
Dynastat Powder	77	0.5	0.37	0.64	0.3491s
Hydrocortisone sodium	82	0.44	0.37	0.57	0.3491s
Atracurium Besylate	71	0.39	0.37	0.59	0.3491s
Atropine	81	0.31	0.24	0.42	0.3491s
PancuroInresa	83	0.44	0.33	0.62	0.3491s

Drug Identification: PancuroInresa against other samples

Drug Name	Edit Distance	TSR Scores	Lev Scores	Jacc Scores	Processing Time
Primacor Injection	77	0.52	0.44	0.70	0.4817s
Cefazolin Sodium 1g	113	0.43	0.35	0.62	0.4817s
NALOXONE HCl 400mg in 1mL	83	0.33	0.26	0.50	0.4817s
Calcium Chloride 1g in 10mL	100	0.4	0.39	0.65	0.4817s
Actrapid Penfill 3ml	82	0.47	0.32	0.64	0.4817s
Vecuronium bromide	74	0.42	0.39	0.63	0.4817s
Sugammadex 200mg/2ml	77	0.45	0.35	0.68	0.4817s
Amiodarone Hydrochloride	77	0.39	0.34	0.53	0.4817s
Protamine Sulphate 50mg in 5ml	75	0.45	0.43	0.70	0.4817s
Summethonium Chloride 100mg in 2mL	79	0.41	0.32	0.76	0.4817s
Protamine Sulfate 10mg/ml	78	0.47	0.39	0.71	0.4817s
Glyceryl Trinitrate 1 mg/ml	86	0.39	0.34	0.61	0.4817s
Tranexamic acid	76	0.4	0.35	0.64	0.4817s
Heparin Injection 25000IU in 5 mL	74	0.47	0.40	0.64	0.4817s
Sterile Potassium Chloride	98	0.39	0.36	0.70	0.4817s
Metaraminol 10mg/ml	78	0.5	0.34	0.68	0.4817s
Cyclizine lactate	87	0.25	0.20	0.43	0.4817s
PITRESSIN argipressin	75	0.47	0.37	0.67	0.4817s
Dexamethasone phosphate 4 mg/ml	78	0.47	0.34	0.65	0.4817s
Ephedrine Hydrochloride	81	0.29	0.30	0.47	0.4817s
Ondansetron Solution	71	0.42	0.45	0.64	0.4817s
FRUSEMIDE	78	0.46	0.33	0.66	0.4817s
DALACINC PHOSPHATE	80	0.36	0.32	0.56	0.4817s
METOPROLOL Mylan	78	0.44	0.41	0.60	0.4817s
WATER FOR INJECTIONS BP	81	0.43	0.39	0.76	0.4817s
MORPHINE SULFATE	79	0.39	0.34	0.69	0.4817s
Glycopyrronium and Neostigmine	80	0.44	0.35	0.73	0.4817s
Clonidine HCl	81	0.33	0.29	0.48	0.4817s
Rocuronium Bromide 50 mg in 5 ml	73	0.51	0.43	0.55	0.4817s
Fresofol 1% MCT/LCT	309	0.34	0.28	0.59	0.4817s
Sedative Midazolam 5mg	82	0.38	0.28	0.66	0.4817s
Adrenaline Injection	72	0.36	0.40	0.52	0.4817s
Paracetamol Kabi	505	0.25	0.22	0.64	0.4817s
Provive MCT-LCT 1%	256	0.35	0.28	0.68	0.4817s
Adrenaline Injection 1mg in 10mL	72	0.36	0.40	0.52	0.4817s
Amoxicillin Sodium	124	0.4	0.33	0.71	0.4817s
Lidocain Injection	82	0.33	0.29	0.50	0.4817s
SODIUM CHLORIDE	116	0.4	0.30	0.61	0.4817s
Remifentanil-Act Injection	82	0.44	0.38	0.58	0.4817s
Sterile Dopamine	81	0.35	0.26	0.57	0.4817s
Hypnomida Etomidate 2mg	84	0.42	0.36	0.61	0.4817s
Xylocaine 1%	82	0.34	0.30	0.44	0.4817s
Fentanyl Injection	113	0.42	0.36	0.55	0.4817s
Noradrenaline acid	80	0.38	0.34	0.55	0.4817s
Magnesium Sulfate 2.47g in 5mL	84	0.44	0.35	0.58	0.4817s
Sugammadex Injection	78	0.44	0.35	0.72	0.4817s
Dynastat Powder	81	0.45	0.37	0.66	0.4817s
Hydrocortisone sodium	88	0.41	0.35	0.64	0.4817s
Atracurium Besylate	74	0.39	0.39	0.55	0.4817s
Atropine	80	0.31	0.29	0.64	0.4817s
PancuroInresa	**1**	**1.0**	**0.99**	**1.00**	**0.4817s**

Appendix E – Drug Identification in Varied Conditions

Sample 1

s1_noisy Vs others					s1_noisy enhanced Vs others				
Drug Name	Edit Distance	TSR Scores	Lev Scores	Jacc Scores	Drug Name	Edit Distance	TSR Scores	Lev Scores	Jacc Scores
s1	60	0.98	0.94	1.00	s1_noisy_enhanced Vs others	141	0.97	0.86	1.00
s1_noisy	**0**	**1.0**	**1.00**	**1.00**	s1	86	0.98	0.92	1.00
s1_noisy_en	86	0.98	0.92	1.00	s1_noisy	**0**	**1.0**	**1.00**	**1.00**
s1_3x3	85	0.99	0.92	1.00	**s1_noisy_en**	15	0.97	0.99	1.00
s1_3x3_en	86	0.98	0.92	1.00	s1_3x3	0	1.0	1.00	1.00
s1_5x5	93	0.97	0.91	0.97	s1_3x3_en	19	0.97	0.98	0.97
s1_5x5_en	482	0.35	0.29	0.64	s1_5x5	476	0.34	0.29	0.64
s1_7x7	133	0.95	0.86	0.97	s1_5x5_en	63	0.94	0.94	0.97
s1_7x7_en	122	1.0	0.88	1.00	s1_7x7	51	0.99	0.95	1.00
s1_3x3 Vs others					s1_3x3_enhanced Vs Vs others				
s1	132	0.98	0.87	1.00	s1_3x3_en_enhanced Vs others	141	0.97	0.86	1.00
s1_noisy	85	0.99	0.92	1.00	s1	86	0.98	0.92	1.00
s1_noisy_en	15	0.97	0.99	1.00	s1_noisy	0	1.0	1.00	1.00
s1_3x3	**0**	**1.0**	**1.00**	**1.00**	s1_noisy_en	15	0.97	0.99	1.00
s1_3x3_en	15	0.97	0.99	1.00	s1_3x3	**0**	**1.0**	**1.00**	**1.00**
s1_5x5	24	0.97	0.98	0.97	**s1_3x3_en**	19	0.97	0.98	0.97
s1_5x5_en	483	0.35	0.28	0.64	s1_5x5	476	0.34	0.29	0.64
s1_7x7	68	0.95	0.93	0.97	s1_5x5_en	63	0.94	0.94	0.97
s1_7x7_en	54	0.98	0.95	1.00	s1_7x7	51	0.99	0.95	1.00
s1_5x5 Vs others					s1_5x5_enhanced Vs others				
s1	145	0.96	0.86	0.97	s1	499	0.35	0.29	0.64
s1_noisy	93	0.97	0.91	0.97	s1_noisy	482	0.35	0.29	0.64
s1_noisy_en	19	0.97	0.98	0.97	s1_noisy_en	476	0.34	0.29	0.64
s1_3x3	24	0.97	0.98	0.97	s1_3x3	483	0.35	0.28	0.64
s1_3x3_en	19	0.97	0.98	0.97	s1_3x3_en	476	0.34	0.29	0.64
s1_5x5	**0**	**1.0**	**1.00**	**1.00**	s1_5x5	467	0.35	0.29	0.66
s1_5x5_en	467	0.35	0.29	0.66	**s1_5x5_en**	**0**	**1.0**	**1.00**	**1.00**
s1_7x7	53	0.95	0.94	1.00	s1_7x7	427	0.37	0.30	0.66
s1_7x7_en	59	0.97	0.94	0.97	s1_7x7_en	482	0.35	0.28	0.64
s1_7x7 Vs others					s1_7x7_enhanced Vs others				
s1	178	0.93	0.81	0.97	s1	96	0.97	0.91	1.00
s1_noisy	133	0.95	0.86	0.97	s1_noisy	122	1.0	0.88	1.00
s1_noisy_en	63	0.94	0.94	0.97	s1_noisy_en	51	0.99	0.95	1.00
s1_3x3	68	0.95	0.93	0.97	s1_3x3	54	0.98	0.95	1.00
s1_3x3_en	63	0.94	0.94	0.97	s1_3x3_en	51	0.99	0.95	1.00
s1_5x5	53	0.95	0.94	1.00	s1_5x5	59	0.97	0.94	0.97
s1_5x5_en	427	0.37	0.30	0.66	s1_5x5_en	482	0.35	0.28	0.64
s1_7x7	**0**	**1.0**	**1.00**	**1.00**	s1_7x7	101	0.95	0.89	0.97
s1_7x7_en	101	0.95	0.89	0.97	**s1_7x7_en**	**0**	**1.0**	**1.00**	**1.00**

Sample 2

Drug Name	Edit Distance	TSR Scores	Lev Scores	Jacc Scores	Drug Name	Edit Distance	TSR Scores	Lev Scores	Jacc Scores
s2_noisy Vs others					s2_noisy enhanced Vs others				
s2	5	0.99	0.99	1.00	s2	7	1.0	0.98	1.00
s2_noisy	**0**	**1.0**	**1.00**	**1.00**	s2_noisy	2	1.0	0.99	1.00
s2_noisy_en	2	1.0	0.99	1.00	**s2_noisy_en**	**0**	**1.0**	**1.00**	**1.00**
s2_3x3	2	1.0	0.99	1.00	s2_3x3	0	1.0	1.00	1.00
s2_3x3_en	3	1.0	0.99	1.00	s2_3x3_en	1	1.0	1.00	1.00
s2_5x5	7	0.96	0.98	1.00	s2_5x5	5	0.97	0.98	1.00
s2_5x5_en	2	1.0	0.99	1.00	s2_5x5_en	0	1.0	1.00	1.00
s2_7x7	6	0.94	0.98	1.00	s2_7x7	4	0.94	0.98	1.00
s2_7x7_en	2	1.0	0.99	1.00	s2_7x7_en	0	1.0	1.00	1.00
s2_3x3 Vs others					s2_3x3_enhanced Vs others				
s2	7	1.0	0.98	1.00	s2	8	1.0	0.98	1.00
s2_noisy	2	1.0	0.99	1.00	s2_noisy	3	1.0	0.99	1.00
s2_noisy_en	0	1.0	1.00	1.00	s2_noisy_en	1	1.0	1.00	1.00
s2_3x3	**0**	**1.0**	**1.00**	**1.00**	s2_3x3	1	1.0	1.00	1.00
s2_3x3_en	1	1.0	1.00	1.00	**s2_3x3_en**	**0**	**1.0**	**1.00**	**1.00**
s2_5x5	5	0.97	0.98	1.00	s2_5x5	4	0.97	0.98	1.00
s2_5x5_en	0	1.0	1.00	1.00	s2_5x5_en	1	1.0	1.00	1.00
s2_7x7	4	0.94	0.98	1.00	s2_7x7	3	0.94	0.99	1.00
s2_7x7_en	0	1.0	1.00	1.00	s2_7x7_en	1	1.0	1.00	1.00
s2_5x5 Vs others					s2_5x5_en Vs others				
s2	12	0.96	0.96	1.00	s2	7	1.0	0.98	1.00
s2_noisy	7	0.96	0.98	1.00	s2_noisy	2	1.0	0.99	1.00
s2_noisy_en	5	0.97	0.98	1.00	s2_noisy_en	0	1.0	1.00	1.00
s2_3x3	5	0.97	0.98	1.00	s2_3x3	0	1.0	1.00	1.00
s2_3x3_en	4	0.97	0.98	1.00	s2_3x3_en	1	1.0	1.00	1.00
s2_5x5	**0**	**1.0**	**1.00**	**1.00**	s2_5x5	5	0.97	0.98	1.00
s2_5x5_en	5	0.97	0.98	1.00	**s2_5x5_en**	**0**	**1.0**	**1.00**	**1.00**
s2_7x7	3	0.98	0.99	1.00	s2_7x7	4	0.94	0.98	1.00
s2_7x7_en	5	0.97	0.98	1.00	s2_7x7_en	0	1.0	1.00	1.00
s2_7x7 Vs others					s2_7x7_enhanced Vs others				
s2	11	0.92	0.96	1.00	**s2**	**7**	**1.0**	**0.98**	**1.00**
s2_noisy	6	0.94	0.98	1.00	s2_noisy	2	1.0	0.99	1.00
s2_noisy_en	4	0.94	0.98	1.00	s2_noisy_en	0	1.0	1.00	1.00
s2_3x3	4	0.94	0.98	1.00	s2_3x3	0	1.0	1.00	1.00
s2_3x3_en	3	0.94	0.99	1.00	s2_3x3_en	1	1.0	1.00	1.00
s2_5x5	3	0.98	0.99	1.00	s2_5x5	5	0.97	0.98	1.00
s2_5x5_en	4	0.94	0.98	1.00	s2_5x5_en	0	1.0	1.00	1.00
s2_7x7	**0**	**1.0**	**1.00**	**1.00**	s2_7x7	4	0.94	0.98	1.00
s2_7x7_en	4	0.94	0.98	1.00	s2_7x7_en	0	1.0	1.00	1.00

Sample 3

Drug Name	Edit Distance	TSR Scores	Lev Scores	Jacc Scores	Drug Name	Edit Distance	TSR Scores	Lev Scores	Jacc Scores
s3_noisy Vs others					s3_noisy_enhanced Vs others				
s3	1	0.99	0.99	1.00	s3	1	0.99	0.99	1.00
s3_noisy	**0**	**1.0**	**1.00**	**1.00**	s3_noisy	0	1.0	1.00	1.00
s3_noisy_en	0	1.0	1.00	1.00	**s3_noisy_en**	**0**	**1.0**	**1.00**	**1.00**
s3_3x3	0	1.0	1.00	1.00	s3_3x3	0	1.0	1.00	1.00
s3_3x3_en	0	1.0	1.00	1.00	s3_3x3_en	0	1.0	1.00	1.00
s3_5x5	1	0.98	0.98	1.00	s3_5x5	1	0.98	0.98	1.00
s3_5x5_en	0	1.0	1.00	1.00	s3_5x5_en	0	1.0	1.00	1.00
s3_7x7	2	0.97	0.97	1.00	s3_7x7	2	0.97	0.97	1.00
s3_7x7_en	2	0.97	0.97	1.00	s3_7x7_en	2	0.97	0.97	1.00
s3_3x3 Vs others					s3_3x3_enhanced Vs others				
s3	1	0.99	0.99	1.00	s3	1	0.99	0.99	1.00
s3_noisy	0	1.0	1.00	1.00	**s3_noisy**	**0**	**1.0**	**1.00**	**1.00**
s3_noisy_en	0	1.0	1.00	1.00	s3_noisy_en	0	1.0	1.00	1.00
s3_3x3	**0**	**1.0**	**1.00**	**1.00**	s3_3x3	0	1.0	1.00	1.00
s3_3x3_en	0	1.0	1.00	1.00	s3_3x3_en	0	1.0	1.00	1.00
s3_5x5	1	0.98	0.98	1.00	s3_5x5	1	0.98	0.98	1.00
s3_5x5_en	0	1.0	1.00	1.00	s3_5x5_en	0	1.0	1.00	1.00
s3_7x7	2	0.97	0.97	1.00	s3_7x7	2	0.97	0.97	1.00
s3_7x7_en	2	0.97	0.97	1.00	s3_7x7_en	2	0.97	0.97	1.00
s3_5x5 vs Others					s3_5x5 enhanced Vs Others				
s3	2	0.97	0.97	1.00	s3	1	0.99	0.99	1.00
s3_noisy	1	0.98	0.98	1.00	s3_noisy	0	1.0	1.00	1.00
s3_noisy_en	1	0.98	0.98	1.00	s3_noisy_en	0	1.0	1.00	1.00
s3_3x3	1	0.98	0.98	1.00	s3_3x3	0	1.0	1.00	1.00
s3_3x3_en	1	0.98	0.98	1.00	s3_3x3_en	0	1.0	1.00	1.00
s3_5x5	**0**	**1.0**	**1.00**	**1.00**	s3_5x5	1	0.98	0.98	1.00
s3_5x5_en	1	0.98	0.98	1.00	**s3_5x5_en**	**0**	**1.0**	**1.00**	**1.00**
s3_7x7	1	0.99	0.99	1.00	s3_7x7	2	0.97	0.97	1.00
s3_7x7_en	1	0.99	0.99	1.00	s3_7x7_en	2	0.97	0.97	1.00
s3_7x7 Vs others					s3_7x7 enhanced Vs others				
s3	3	0.97	0.97	1.00	s3	3	0.97	0.97	1.00
s3_noisy	2	0.97	0.97	1.00	s3_noisy	2	0.97	0.97	1.00
s3_noisy_en	2	0.97	0.97	1.00	s3_noisy_en	2	0.97	0.97	1.00
s3_3x3	2	0.97	0.97	1.00	s3_3x3	2	0.97	0.97	1.00
s3_3x3_en	2	0.97	0.97	1.00	s3_3x3_en	2	0.97	0.97	1.00
s3_5x5	1	0.99	0.99	1.00	s3_5x5	1	0.99	0.99	1.00
s3_5x5_en	2	0.97	0.97	1.00	s3_5x5_en	2	0.97	0.97	1.00
s3_7x7	**0**	**1.0**	**1.00**	**1.00**	s3_7x7	0	1.0	1.00	1.00
s3_7x7_en	0	1.0	1.00	1.00	**s3_7x7_en**	**0**	**1.0**	**1.00**	**1.00**

Sample 4

s4_noisy					s4_noisy_enhanced				
Drug Name	Edit Distance	TSR Scores	Lev Scores	Jacc Scores	Drug Name	Edit Distance	TSR Scores	Lev Scores	Jacc Scores
s4	1	0.99	1.00	1.00	s4	0	1.0	1.00	1.00
s4_noisy	**0**	**1.0**	**1.00**	**1.00**	s4_noisy	1	0.99	1.00	1.00
s4_noisy_en	1	0.99	1.00	1.00	**s4_noisy_en**	**0**	**1.0**	**1.00**	**1.00**
s4_3x3	1	0.99	1.00	1.00	s4_3x3	0	1.0	1.00	1.00
s4_3x3_en	1	0.99	1.00	1.00	s4_3x3_en	0	1.0	1.00	1.00
s4_5x5	1	0.99	1.00	1.00	s4_5x5	0	1.0	1.00	1.00
s4_5x5_en	1	0.99	1.00	1.00	s4_5x5_en	0	1.0	1.00	1.00
s4_7x7	16	0.99	0.93	1.00	s4_7x7	15	1.0	0.94	1.00
s4_7x7_en	16	0.99	0.93	1.00	s4_7x7_en	15	1.0	0.94	1.00
s4_3x3					s4_3x3_enhanced				
s4	0	1.0	1.00	1.00	s4	0	1.0	1.00	1.00
s4_noisy	1	0.99	1.00	1.00	s4_noisy	1	0.99	1.00	1.00
s4_noisy_en	0	1.0	1.00	1.00	s4_noisy_en	0	1.0	1.00	1.00
s4_3x3	**0**	**1.0**	**1.00**	**1.00**	s4_3x3	0	1.0	1.00	1.00
s4_3x3_en	0	1.0	1.00	1.00	**s4_3x3_en**	**0**	**1.0**	**1.00**	**1.00**
s4_5x5	0	1.0	1.00	1.00	s4_5x5	0	1.0	1.00	1.00
s4_5x5_en	0	1.0	1.00	1.00	s4_5x5_en	0	1.0	1.00	1.00
s4_7x7	15	1.0	0.94	1.00	s4_7x7	15	1.0	0.94	1.00
s4_7x7_en	15	1.0	0.94	1.00	s4_7x7_en	15	1.0	0.94	1.00
s4_5x5					s4_5x5_enhanced				
s4	0	1.0	1.00	1.00	**s4**	**0**	**1.0**	**1.00**	**1.00**
s4_noisy	1	0.99	1.00	1.00	s4_noisy	1	0.99	1.00	1.00
s4_noisy_en	0	1.0	1.00	1.00	s4_noisy_en	0	1.0	1.00	1.00
s4_3x3	0	1.0	1.00	1.00	s4_3x3	0	1.0	1.00	1.00
s4_3x3_en	0	1.0	1.00	1.00	s4_3x3_en	0	1.0	1.00	1.00
s4_5x5	**0**	**1.0**	**1.00**	**1.00**	s4_5x5	0	1.0	1.00	1.00
s4_5x5_en	0	1.0	1.00	1.00	**s4_5x5_en**	**0**	**1.0**	**1.00**	**1.00**
s4_7x7	15	1.0	0.94	1.00	s4_7x7	15	1.0	0.94	1.00
s4_7x7_en	15	1.0	0.94	1.00	s4_7x7_en	15	1.0	0.94	1.00
s4_7x7					s4_7x7_enhanced				
s4	15	1.0	0.94	1.00	s4	15	1.0	0.94	1.00
s4_noisy	16	0.99	0.93	1.00	s4_noisy	16	0.99	0.93	1.00
s4_noisy_en	15	1.0	0.94	1.00	s4_noisy_en	15	1.0	0.94	1.00
s4_3x3	15	1.0	0.94	1.00	s4_3x3	15	1.0	0.94	1.00
s4_3x3_en	15	1.0	0.94	1.00	s4_3x3_en	15	1.0	0.94	1.00
s4_5x5	15	1.0	0.94	1.00	s4_5x5	15	1.0	0.94	1.00
s4_5x5_en	15	1.0	0.94	1.00	s4_5x5_en	15	1.0	0.94	1.00
s4_7x7	**0**	**1.0**	**1.00**	**1.00**	s4_7x7	0	1.0	1.00	1.00
s4_7x7_en	0	1.0	1.00	1.00	**s4_7x7_en**	**0**	**1.0**	**1.00**	**1.00**

Sample 5

s5_noisy Vs others					s5_noisy enhanced Vs others				
Drug Name	Edit Distance	TSR Scores	Lev Scores	Jacc Scores	Drug Name	Edit Distance	TSR Scores	Lev Scores	Jacc Scores
s5	1	0.99	0.99	0.96	**s5**	**1**	**1.0**	**0.99**	**1.00**
s5_noisy	**0**	**1.0**	**1.00**	**1.00**	s5_noisy	2	0.99	0.98	0.96
s5_noisy_en	2	0.99	0.98	0.96	**s5_noisy_en**	**0**	**1.0**	**1.00**	**1.00**
s5_3x3	2	0.99	0.98	0.96	s5_3x3	0	1.0	1.00	1.00
s5_3x3_en	2	0.99	0.98	0.96	s5_3x3_en	0	1.0	1.00	1.00
s5_5x5_en	2	0.99	0.98	0.96	s5_5x5_en	0	1.0	1.00	1.00
s5_5x5	1	0.99	0.99	0.96	s5_5x5	1	1.0	0.99	1.00
s5_7x7	15	0.99	0.90	0.96	s5_7x7	14	1.0	0.91	1.00
s5_7x7_en	1	0.99	0.99	0.96	s5_7x7_en	1	1.0	0.99	1.00
s5_3x3 Vs others					s5_3x3_enhanced Vs others				
s5	1	1.0	0.99	1.00	s5	1	1.0	0.99	1.00
s5_noisy	2	0.99	0.98	0.96	s5_noisy	2	0.99	0.98	0.96
s5_noisy_en	0	1.0	1.00	1.00	s5_noisy_en	0	1.0	1.00	1.00
s5_3x3	**0**	**1.0**	**1.00**	**1.00**	s5_3x3	0	1.0	1.00	1.00
s5_3x3_en	0	1.0	1.00	1.00	**s5_3x3_en**	**0**	**1.0**	**1.00**	**1.00**
s5_5x5_en	0	1.0	1.00	1.00	s5_5x5_en	0	1.0	1.00	1.00
s5_5x5	1	1.0	0.99	1.00	s5_5x5	1	1.0	0.99	1.00
s5_7x7	14	1.0	0.91	1.00	s5_7x7	14	1.0	0.91	1.00
s5_7x7_en	1	1.0	0.99	1.00	s5_7x7_en	1	1.0	0.99	1.00
s5_5x5_enhanced Vs others					s5_5x5 Vs others				
s5	0	1.0	1.00	1.00	s5	1	1.0	0.99	1.00
s5_noisy	1	0.99	0.99	0.96	s5_noisy	2	0.99	0.98	0.96
s5_noisy_en	1	1.0	0.99	1.00	s5_noisy_en	0	1.0	1.00	1.00
s5_3x3	1	1.0	0.99	1.00	s5_3x3	0	1.0	1.00	1.00
s5_3x3_en	1	1.0	0.99	1.00	s5_3x3_en	0	1.0	1.00	1.00
s5_5x5_en	**1**	**1.0**	**0.99**	**1.00**	s5_5x5_en	0	1.0	1.00	1.00
s5_5x5	0	1.0	1.00	1.00	**s5_5x5**	**1**	**1.0**	**0.99**	**1.00**
s5_7x7	14	1.0	0.91	1.00	s5_7x7	14	1.0	0.91	1.00
s5_7x7_en	0	1.0	1.00	1.00	s5_7x7_en	1	1.0	0.99	1.00
s5_7x7 Vs others					s5_7x7_enhanced Vs others				
s5	14	1.0	0.91	1.00	s5	0	1.0	1.00	1.00
s5_noisy	15	0.99	0.90	0.96	s5_noisy	1	0.99	0.99	0.96
s5_noisy_en	14	1.0	0.91	1.00	s5_noisy_en	1	1.0	0.99	1.00
s5_3x3	14	1.0	0.91	1.00	s5_3x3	1	1.0	0.99	1.00
s5_3x3_en	14	1.0	0.91	1.00	s5_3x3_en	1	1.0	0.99	1.00
s5_5x5_en	14	1.0	0.91	1.00	s5_5x5_en	1	1.0	0.99	1.00
s5_5x5	14	1.0	0.91	1.00	s5_5x5	0	1.0	1.00	1.00
s5_7x7	**0**	**1.0**	**1.00**	**1.00**	s5_7x7	14	1.0	0.91	1.00
s5_7x7_en	14	1.0	0.91	1.00	**s5_7x7_en**	**0**	**1.0**	**1.00**	**1.00**

Sample 6

s6_noisy Vs others					s6_noisy_enhanced Vs others				
Drug Name	Edit Distance	TSR Scores	Lev Scores	Jacc Scores	Drug Name	Edit Distance	TSR Scores	Lev Scores	Jacc Scores
s6	0	1.0	1.00	1.00	s6	2	1.0	0.99	1.00
s6_noisy	**0**	**1.0**	**1.00**	**1.00**	s6_noisy	2	1.0	0.99	1.00
s6_noisy_en	2	1.0	0.99	1.00	**s6_noisy_en**	**0**	**1.0**	**1.00**	**1.00**
s6_3x3	2	1.0	0.99	1.00	s6_3x3	0	1.0	1.00	1.00
s6_3x3_en	2	1.0	0.99	1.00	s6_3x3_en	0	1.0	1.00	1.00
s6_5x5	2	1.0	0.99	1.00	s6_5x5	0	1.0	1.00	1.00
s6_5x5_en	2	1.0	0.99	1.00	s6_5x5_en	0	1.0	1.00	1.00
s6_7x7	5	0.96	0.97	0.96	s6_7x7	3	0.96	0.98	0.96
s6_7x7_en	5	0.96	0.97	0.96	s6_7x7_en	3	0.96	0.98	0.96
s6_3x3 Vs others					s6_3x3_enhanced Vs others				
s6	2	1.0	0.99	1.00	s6	2	1.0	0.99	1.00
s6_noisy	2	1.0	0.99	1.00	s6_noisy	2	1.0	0.99	1.00
s6_noisy_en	0	1.0	1.00	1.00	s6_noisy_en	0	1.0	1.00	1.00
s6_3x3	**0**	**1.0**	**1.00**	**1.00**	s6_3x3	0	1.0	1.00	1.00
s6_3x3_en	0	1.0	1.00	1.00	**s6_3x3_en**	**0**	**1.0**	**1.00**	**1.00**
s6_5x5	0	1.0	1.00	1.00	s6_5x5	0	1.0	1.00	1.00
s6_5x5_en	0	1.0	1.00	1.00	s6_5x5_en	0	1.0	1.00	1.00
s6_7x7	3	0.96	0.98	0.96	s6_7x7	3	0.96	0.98	0.96
s6_7x7_en	3	0.96	0.98	0.96	s6_7x7_en	3	0.96	0.98	0.96
s6_5x5 Vs others					s6_5x5_enhanced Vs others				
s6	2	1.0	0.99	1.00	s6	2	1.0	0.99	1.00
s6_noisy	2	1.0	0.99	1.00	s6_noisy	2	1.0	0.99	1.00
s6_noisy_en	0	1.0	1.00	1.00	s6_noisy_en	0	1.0	1.00	1.00
s6_3x3	0	1.0	1.00	1.00	s6_3x3	0	1.0	1.00	1.00
s6_3x3_en	0	1.0	1.00	1.00	s6_3x3_en	0	1.0	1.00	1.00
s6_5x5	**0**	**1.0**	**1.00**	**1.00**	s6_5x5	0	1.0	1.00	1.00
s6_5x5_en	0	1.0	1.00	1.00	**s6_5x5_en**	**0**	**1.0**	**1.00**	**1.00**
s6_7x7	3	0.96	0.98	0.96	s6_7x7	3	0.96	0.98	0.96
s6_7x7_en	3	0.96	0.98	0.96	s6_7x7_en	3	0.96	0.98	0.96
s6_7x7					s6_7x7_enhanced				
s6	5	0.96	0.97	0.96	s6	5	0.96	0.97	0.96
s6_noisy	5	0.96	0.97	0.96	s6_noisy	5	0.96	0.97	0.96
s6_noisy_en	3	0.96	0.98	0.96	s6_noisy_en	3	0.96	0.98	0.96
s6_3x3	3	0.96	0.98	0.96	s6_3x3	3	0.96	0.98	0.96
s6_3x3_en	3	0.96	0.98	0.96	s6_3x3_en	3	0.96	0.98	0.96
s6_5x5	3	0.96	0.98	0.96	s6_5x5	3	0.96	0.98	0.96
s6_5x5_en	3	0.96	0.98	0.96	s6_5x5_en	3	0.96	0.98	0.96
s6_7x7	**0**	**1.0**	**1.00**	**1.00**	s6_7x7	0	1.0	1.00	1.00
s6_7x7_en	0	1.0	1.00	1.00	s6_7x7_en	**0**	**1.0**	**1.00**	**1.00**

Sample 7

s7_noisy Vs others					s7_noisy_enhanced Vs others				
Drug Name	Edit Distance	TSR Scores	Lev Scores	Jacc Scores	Drug Name	Edit Distance	TSR Scores	Lev Scores	Jacc Scores
s7	3	0.96	0.98	1.00	s7	4	0.97	0.98	0.96
s7_noisy	**0**	**1.0**	**1.00**	**1.00**	s7_noisy	3	0.97	0.98	0.96
s7_noisy_en	3	0.97	0.98	0.96	**s7_noisy_en**	**0**	**1.0**	**1.00**	**1.00**
s7_3x3	4	0.97	0.98	0.96	s7_3x3	2	0.99	0.99	1.00
s7_3x3_en	3	0.97	0.98	0.96	s7_3x3_en	0	1.0	1.00	1.00
s7_5x5	5	0.97	0.97	0.93	s7_5x5	3	0.99	0.98	0.96
s7_5x5_en	3	0.98	0.98	0.96	s7_5x5_en	1	0.99	0.99	1.00
s7_7x7	7	0.94	0.95	0.93	s7_7x7	7	0.92	0.94	0.96
s7_7x7_en	6	0.95	0.95	0.93	s7_7x7_en	4	0.97	0.97	0.96
s7_3x3 Vs others					s7_3x3_enhanced Vs others				
s7	4	0.97	0.98	0.96	s7	4	0.97	0.98	0.96
s7_noisy	4	0.97	0.98	0.96	s7_noisy	3	0.97	0.98	0.96
s7_noisy_en	2	0.99	0.99	1.00	s7_noisy_en	0	1.0	1.00	1.00
s7_3x3	**0**	**1.0**	**1.00**	**1.00**	s7_3x3	2	0.99	0.99	1.00
s7_3x3_en	2	0.99	0.99	1.00	**s7_3x3_en**	**0**	**1.0**	**1.00**	**1.00**
s7_5x5	3	0.99	0.98	0.96	s7_5x5	3	0.99	0.98	0.96
s7_5x5_en	1	0.99	0.99	1.00	s7_5x5_en	1	0.99	0.99	1.00
s7_7x7	8	0.92	0.94	0.96	s7_7x7	7	0.92	0.94	0.96
s7_7x7_en	5	0.97	0.97	0.96	s7_7x7_en	4	0.97	0.97	0.96
s7_5x5 Vs others					s7_5x5_enhanced Vs others				
s7	7	0.96	0.96	0.93	s7	5	0.97	0.97	0.96
s7_noisy	5	0.97	0.97	0.93	s7_noisy	3	0.98	0.98	0.96
s7_noisy_en	3	0.99	0.98	0.96	s7_noisy_en	1	0.99	0.99	1.00
s7_3x3	3	0.99	0.98	0.96	s7_3x3	1	0.99	0.99	1.00
s7_3x3_en	3	0.99	0.98	0.96	s7_3x3_en	1	0.99	0.99	1.00
s7_5x5	**0**	**1.0**	**1.00**	**1.00**	s7_5x5	2	0.99	0.99	0.96
s7_5x5_en	2	0.99	0.99	0.96	**s7_5x5_en**	**0**	**1.0**	**1.00**	**1.00**
s7_7x7	5	0.93	0.96	1.00	s7_7x7	7	0.92	0.95	0.96
s7_7x7_en	2	0.98	0.98	1.00	s7_7x7_en	4	0.98	0.97	0.96
s7_7x7 Vs others					s7_7x7_enhanced Vs others				
s7	10	0.92	0.93	0.93	s7	8	0.94	0.95	0.93
s7_noisy	7	0.94	0.95	0.93	s7_noisy	6	0.95	0.95	0.93
s7_noisy_en	7	0.92	0.94	0.96	s7_noisy_en	4	0.97	0.97	0.96
s7_3x3	8	0.92	0.94	0.96	s7_3x3	5	0.97	0.97	0.96
s7_3x3_en	7	0.92	0.94	0.96	s7_3x3_en	4	0.97	0.97	0.96
s7_5x5	5	0.93	0.96	1.00	s7_5x5	2	0.98	0.98	1.00
s7_5x5_en	7	0.92	0.95	0.96	s7_5x5_en	4	0.98	0.97	0.96
s7_7x7	**0**	**1.0**	**1.00**	**1.00**	s7_7x7	4	0.94	0.96	1.00
s7_7x7_en	4	0.94	0.96	1.00	**s7_7x7_en**	**0**	**1.0**	**1.00**	**1.00**

Sample 8

s8_noisy Vs others					s8_noisy_enhanced Vs others				
Drug Name	Edit Distance	TSR Scores	Lev Scores	Jacc Scores	Drug Name	Edit Distance	TSR Scores	Lev Scores	Jacc Scores
s8	1	1.0	1.00	1.00	s8	1	1.0	1.00	1.00
s8_noisy	**0**	**1.0**	**1.00**	**1.00**	s8_noisy	0	1.0	1.00	1.00
s8_noisy_en	0	1.0	1.00	1.00	**s8_noisy_en**	**0**	**1.0**	**1.00**	**1.00**
s8_3x3	0	1.0	1.00	1.00	s8_3x3	0	1.0	1.00	1.00
s8_3x3_en	0	1.0	1.00	1.00	s8_3x3_en	0	1.0	1.00	1.00
s8_5x5	0	1.0	1.00	1.00	s8_5x5	0	1.0	1.00	1.00
s8_5x5_en	0	1.0	1.00	1.00	s8_5x5_en	0	1.0	1.00	1.00
s8_7x7	5	0.96	0.97	0.97	s8_7x7	5	0.96	0.97	0.97
s8_7x7_en	7	0.97	0.96	0.93	s8_7x7_en	7	0.97	0.96	0.93
s8_3x3 Vs others					s8_3x3_enhanced Vs others				
s8	1	1.0	1.00	1.00	s8	1	1.0	1.00	1.00
s8_noisy	0	1.0	1.00	1.00	s8_noisy	0	1.0	1.00	1.00
s8_noisy_en	0	1.0	1.00	1.00	s8_noisy_en	0	1.0	1.00	1.00
s8_3x3	**0**	**1.0**	**1.00**	**1.00**	s8_3x3	0	1.0	1.00	1.00
s8_3x3_en	0	1.0	1.00	1.00	**s8_3x3_en**	**0**	**1.0**	**1.00**	**1.00**
s8_5x5	0	1.0	1.00	1.00	s8_5x5	0	1.0	1.00	1.00
s8_5x5_en	0	1.0	1.00	1.00	s8_5x5_en	0	1.0	1.00	1.00
s8_7x7	5	0.96	0.97	0.97	s8_7x7	5	0.96	0.97	0.97
s8_7x7_en	7	0.97	0.96	0.93	s8_7x7_en	7	0.97	0.96	0.93
s8_5x5 Vs others					s8_5x5_enhanced Vs others				
s8	1	1.0	1.00	1.00	s8	1	1.0	1.00	1.00
s8_noisy	0	1.0	1.00	1.00	s8_noisy	0	1.0	1.00	1.00
s8_noisy_en	0	1.0	1.00	1.00	s8_noisy_en	0	1.0	1.00	1.00
s8_3x3	0	1.0	1.00	1.00	s8_3x3	0	1.0	1.00	1.00
s8_3x3_en	0	1.0	1.00	1.00	s8_3x3_en	0	1.0	1.00	1.00
s8_5x5	**0**	**1.0**	**1.00**	**1.00**	s8_5x5	0	1.0	1.00	1.00
s8_5x5_en	0	1.0	1.00	1.00	**s8_5x5_en**	**0**	**1.0**	**1.00**	**1.00**
s8_7x7	5	0.96	0.97	0.97	s8_7x7	5	0.96	0.97	0.97
s8_7x7_en	7	0.97	0.96	0.93	s8_7x7_en	7	0.97	0.96	0.93
s8_7x7 Vs others					s8_7x7_enhanced Vs others				
s8	6	0.97	0.97	0.97	s8	8	0.96	0.96	0.93
s8_noisy	5	0.96	0.97	0.97	s8_noisy	7	0.97	0.96	0.93
s8_noisy_en	5	0.96	0.97	0.97	s8_noisy_en	7	0.97	0.96	0.93
s8_3x3	5	0.96	0.97	0.97	s8_3x3	7	0.97	0.96	0.93
s8_3x3_en	5	0.96	0.97	0.97	s8_3x3_en	7	0.97	0.96	0.93
s8_5x5	5	0.96	0.97	0.97	s8_5x5	7	0.97	0.96	0.93
s8_5x5_en	5	0.96	0.97	0.97	s8_5x5_en	7	0.97	0.96	0.93
s8_7x7	**0**	**1.0**	**1.00**	**1.00**	s8_7x7	3	0.98	0.98	0.97
s8_7x7_en	3	0.98	0.98	0.97	**s8_7x7_en**	**0**	**1.0**	**1.00**	**1.00**

Sample 9

s9_noisy Vs others					s9_noisy_enhanced Vs others				
Drug Name	Edit Distance	TSR Scores	Lev Scores	Jacc Scores	Drug Name	Edit Distance	TSR Scores	Lev Scores	Jacc Scores
s9	0	1.0	1.00	1.00	s9	0	1.0	1.00	1.00
s9_noisy	**0**	**1.0**	**1.00**	**1.00**	s9_noisy	0	1.0	1.00	1.00
s9_noisy_en	0	1.0	1.00	1.00	**s9_noisy_en**	**0**	**1.0**	**1.00**	**1.00**
s9_3x3	0	1.0	1.00	1.00	s9_3x3	0	1.0	1.00	1.00
s9_3x3_en	0	1.0	1.00	1.00	s9_3x3_en	0	1.0	1.00	1.00
s9_5x5	0	1.0	1.00	1.00	s9_5x5	0	1.0	1.00	1.00
s9_5x5_en	0	1.0	1.00	1.00	s9_5x5_en	0	1.0	1.00	1.00
s9_7x7	0	1.0	1.00	1.00	s9_7x7	0	1.0	1.00	1.00
s9_7x7_en	0	1.0	1.00	1.00	s9_7x7_en	0	1.0	1.00	1.00
s9_3x3 Vs others					s9_3x3_enhanced Vs others				
s9	0	1.0	1.00	1.00	s9	0	1.0	1.00	1.00
s9_noisy	0	1.0	1.00	1.00	s9_noisy	0	1.0	1.00	1.00
s9_noisy_en	0	1.0	1.00	1.00	s9_noisy_en	0	1.0	1.00	1.00
s9_3x3	**0**	**1.0**	**1.00**	**1.00**	s9_3x3	0	1.0	1.00	1.00
s9_3x3_en	0	1.0	1.00	1.00	**s9_3x3_en**	**0**	**1.0**	**1.00**	**1.00**
s9_5x5	0	1.0	1.00	1.00	s9_5x5	0	1.0	1.00	1.00
s9_5x5_en	0	1.0	1.00	1.00	s9_5x5_en	0	1.0	1.00	1.00
s9_7x7	0	1.0	1.00	1.00	s9_7x7	0	1.0	1.00	1.00
s9_7x7_en	0	1.0	1.00	1.00	s9_7x7_en	0	1.0	1.00	1.00
s9_5x5 Vs others					s9_5x5_enhanced Vs others				
s9	0	1.0	1.00	1.00	s9	0	1.0	1.00	1.00
s9_noisy	0	1.0	1.00	1.00	s9_noisy	0	1.0	1.00	1.00
s9_noisy_en	0	1.0	1.00	1.00	s9_noisy_en	0	1.0	1.00	1.00
s9_3x3	0	1.0	1.00	1.00	s9_3x3	0	1.0	1.00	1.00
s9_3x3_en	0	1.0	1.00	1.00	s9_3x3_en	0	1.0	1.00	1.00
s9_5x5	**0**	**1.0**	**1.00**	**1.00**	s9_5x5	0	1.0	1.00	1.00
s9_5x5_en	0	1.0	1.00	1.00	**s9_5x5_en**	**0**	**1.0**	**1.00**	**1.00**
s9_7x7	0	1.0	1.00	1.00	s9_7x7	0	1.0	1.00	1.00
s9_7x7_en	0	1.0	1.00	1.00	s9_7x7_en	0	1.0	1.00	1.00
s9_7x7 Vs others					s9_7x7_enhanced Vs others				
s9	0	1.0	1.00	1.00	s9	0	1.0	1.00	1.00
s9_noisy	0	1.0	1.00	1.00	s9_noisy	0	1.0	1.00	1.00
s9_noisy_en	0	1.0	1.00	1.00	s9_noisy_en	0	1.0	1.00	1.00
s9_3x3	0	1.0	1.00	1.00	s9_3x3	0	1.0	1.00	1.00
s9_3x3_en	0	1.0	1.00	1.00	s9_3x3_en	0	1.0	1.00	1.00
s9_5x5	0	1.0	1.00	1.00	s9_5x5	0	1.0	1.00	1.00
s9_5x5_en	0	1.0	1.00	1.00	s9_5x5_en	0	1.0	1.00	1.00
s9_7x7	**0**	**1.0**	**1.00**	**1.00**	s9_7x7	0	1.0	1.00	1.00
s9_7x7_en	0	1.0	1.00	1.00	**s9_7x7_en**	**0**	**1.0**	**1.00**	**1.00**

Sample 10

s10_noisy Vs others					s10_noisy_enhanced Vs others				
Drug Name	Edit Distance	TSR Scores	Lev Scores	Jacc Scores	Drug Name	Edit Distance	TSR Scores	Lev Scores	Jacc Scores
s10	**1**	**1.0**	**0.99**	**0.95**	**s10**	**0**	**1.0**	**1.00**	**1.00**
s10_noisy	0	1.0	1.00	1.00	s10_noisy	1	1.0	0.99	0.95
s10_noisy_en	1	1.0	0.99	0.95	s10_noisy_en	0	1.0	1.00	1.00
s10_3x3	1	1.0	0.99	0.95	s10_3x3	0	1.0	1.00	1.00
s10_3x3_en	1	1.0	0.99	0.95	s10_3x3_en	0	1.0	1.00	1.00
s10_5x5	1	1.0	0.99	0.95	s10_5x5	0	1.0	1.00	1.00
s10_5x5_en	2	1.0	0.97	0.95	s10_5x5_en	1	1.0	0.99	1.00
s10_7x7	1	1.0	0.99	0.95	s10_7x7	0	1.0	1.00	1.00
s10_7x7_en	1	1.0	0.99	0.95	s10_7x7_en	0	1.0	1.00	1.00
s10_3x3 Vs others					s10_3x3_enhanced Vs others				
s10	**0**	**1.0**	**1.00**	**1.00**	**s10**	**0**	**1.0**	**1.00**	**1.00**
s10_noisy	1	1.0	0.99	0.95	s10_noisy	1	1.0	0.99	0.95
s10_noisy_en	0	1.0	1.00	1.00	s10_noisy_en	0	1.0	1.00	1.00
s10_3x3	0	1.0	1.00	1.00	s10_3x3	0	1.0	1.00	1.00
s10_3x3_en	0	1.0	1.00	1.00	s10_3x3_en	0	1.0	1.00	1.00
s10_5x5	0	1.0	1.00	1.00	s10_5x5	0	1.0	1.00	1.00
s10_5x5_en	1	1.0	0.99	1.00	s10_5x5_en	1	1.0	0.99	1.00
s10_7x7	0	1.0	1.00	1.00	s10_7x7	0	1.0	1.00	1.00
s10_7x7_en	0	1.0	1.00	1.00	s10_7x7_en	0	1.0	1.00	1.00
s10_5x5 Vs others					s10_5x5_enhanced Vs others				
s10	**0**	**1.0**	**1.00**	**1.00**	**s10**	**1**	**1.0**	**0.99**	**1.00**
s10_noisy	1	1.0	0.99	0.95	s10_noisy	2	1.0	0.97	0.95
s10_noisy_en	0	1.0	1.00	1.00	s10_noisy_en	1	1.0	0.99	1.00
s10_3x3	0	1.0	1.00	1.00	s10_3x3	1	1.0	0.99	1.00
s10_3x3_en	0	1.0	1.00	1.00	s10_3x3_en	1	1.0	0.99	1.00
s10_5x5	0	1.0	1.00	1.00	s10_5x5	1	1.0	0.99	1.00
s10_5x5_en	1	1.0	0.99	1.00	s10_5x5_en	0	1.0	1.00	1.00
s10_7x7	0	1.0	1.00	1.00	s10_7x7	1	1.0	0.99	1.00
s10_7x7_en	0	1.0	1.00	1.00	s10_7x7_en	1	1.0	0.99	1.00
s10_7x7 Vs others					s10_7x7_enhanced Vs others				
s10	**0**	**1.0**	**1.00**	**1.00**	**s10**	**0**	**1.0**	**1.00**	**1.00**
s10_noisy	1	1.0	0.99	0.95	s10_noisy	1	1.0	0.99	0.95
s10_noisy_en	0	1.0	1.00	1.00	s10_noisy_en	0	1.0	1.00	1.00
s10_3x3	0	1.0	1.00	1.00	s10_3x3	0	1.0	1.00	1.00
s10_3x3_en	0	1.0	1.00	1.00	s10_3x3_en	0	1.0	1.00	1.00
s10_5x5	0	1.0	1.00	1.00	s10_5x5	0	1.0	1.00	1.00
s10_5x5_en	1	1.0	0.99	1.00	s10_5x5_en	1	1.0	0.99	1.00
s10_7x7	0	1.0	1.00	1.00	s10_7x7	0	1.0	1.00	1.00
s10_7x7_en	0	1.0	1.00	1.00	s10_7x7_en	0	1.0	1.00	1.00